

Biomimetische Semisynthesen von terpenoiden Naturstoffen

Von der Naturwissenschaftlichen Fakultät der
Gottfried Wilhelm Leibniz Universität Hannover

zur Erlangung des Grades
Doktor der Naturwissenschaften (Dr. rer. nat.)

genehmigte Dissertation
von
Mykhaylo Alekseychuk, M.Sc.

2023

Referent: Prof. Dr. rer. nat. Philipp Heretsch

Korreferent: Prof. Dr. rer. nat. Markus Kalesse

Korreferent: Prof. Dr. rer. nat. Christian Stark

Tag der Promotion: 11.08.2023

Kurzzusammenfassung

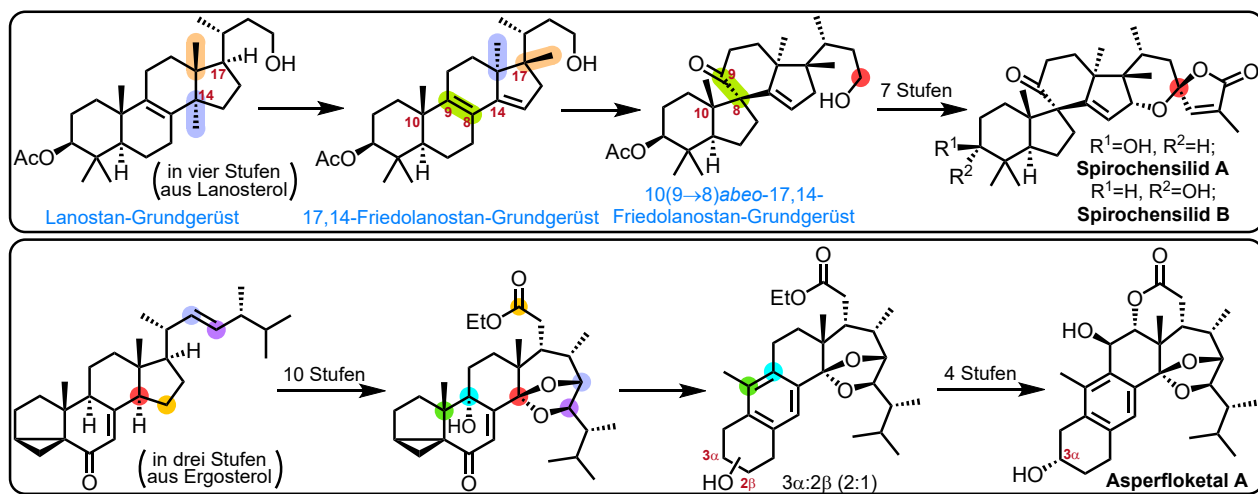
Schlagwörter: Spirochensilide A und B, Asperflokal A, Naturstoffsynthese, biomimetische Semisynthese, Anthrasteroid, Meinwald-Umlagerung, Biogeneseraum-geleitete Analyse

Diese Dissertation befasst sich mit der Weiterentwicklung eines Biogeneseraum-geleiteten Synthesekonzepts, welches angewandt wurde, um die Spirochensilide A und B, das Asperflokal A und den synthetischen Vorläufer des Asperflokal B in effizienten Semisynthesen herzustellen.

Bei der Biogeneseraum-geleiteten Analyse handelt es sich um eine im Rahmen dieser Arbeit weiterentwickelte Methode biomimetische Synthesen für terpenoide Naturstoffe mit steroidalen Vorläufern zu planen. Dabei werden zuerst coisolierte Naturstoffe aus demselben Organismus, aus dem der Naturstoff isoliert wurde, und anschließend Naturstoffe welche aus derselben Gattung isoliert wurden, betrachtet. Strukturell verwandte Moleküle werden in Gruppen zusammengefasst (z. B. selbes Grundgerüst, jedoch verschiedene funktionelle Gruppen) und anschließend nach einer logischen biosynthetischen Verknüpfung untersucht. Weiterführend können Naturstoffe anderer Gattungen mit ähnlicher Struktur herangezogen werden, um intrinsische Reaktivität vorherzusagen.

Die Spirochensilide A und B wurden beide im Jahr 2015 aus den Ästen und Nadeln der chinesischen Schensi-Tanne *Abies chensiensis* isoliert. Es handelt sich bei den Naturstoffen um Epimere des Alkohols, welche jeweils sechs Ringe, neun sterogene Zentren, ein Spiro[4.5]decan-Motiv (zwischen B- und C-Ring) und ein 1,6-Dioxaspiro[4.5]decen-Motiv (E- und F-Ring) besitzen. Eine Analyse strukturell verwandter Verbindungen machte uns auf weitere $10(9 \rightarrow 8)$ abeo-17,14-Friedolanostane aufmerksam und deutete darauf hin, dass diese biosynthetisch aus Lanostenanen entstehen. Diese müssen dabei zu 17,14-Friedolanostanen umlagern, bevor sie in einer Meinwald-Umlagerung das Spiro[4.5]decan bilden können. Beide Spirochensilide konnten im Laufe dieser Arbeit in jeweils 13 und 15 Schritten hergestellt werden. Gleichzeitig konnte durch synthetische Intermediate ein potentieller Zugang zu weiteren strukturell verwandten Naturstoffen (z. B. Abifarine) erhalten werden.

Die Asperflokalale A und B gehören zu den Anthrasteroiden und wurde 2020 aus dem Pilz *Aspergillus flocculosus 16D-1* isoliert. Sie besitzen neun aufeinanderfolgende stereogene Zentren (insgesamt zehn), ein intramolekulares Ketal und eine für Anthrasteroide außergewöhnliche geschnittene C14-C15 Bindung. Bei den Naturstoffen handelt es sich um Regioisomere des Alkohols am A-Ring, wobei es sich beim Asperflokal B um das erste isolierte Anthrasteroid handelt, welches einen 2β -Alkohol besitzt. Mittels historischer Ergebnisse und einer Strukturanalyse verwandter Naturstoffe, konnte im Laufe dieser Arbeit eine plausible, divergente Biogenese formuliert werden und diese angewandt werden, um Asperflokal A in 18 Schritten, zusammen mit dem synthetischen Vorläufer des Asperflokal B, herzustellen.



Abstract

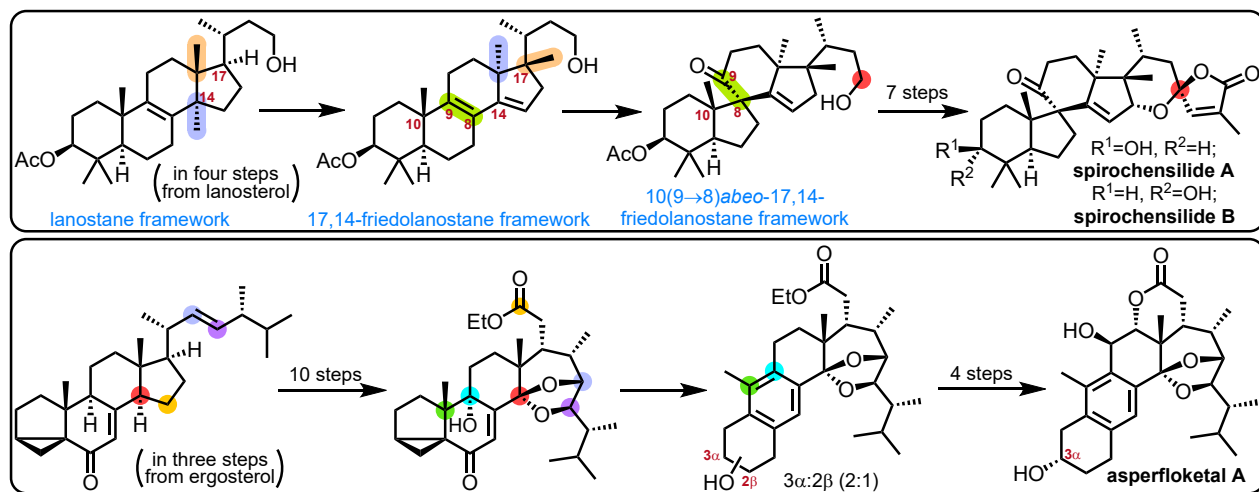
Keywords: spirochensilide A and B, asperfloketal A, natural product synthesis, biomimetic semisynthesis, anthrasteroid, Meinwald-rearrangement, biogenetic space-guided analysis

This dissertation describes the further development of a biogenetic space-guided synthesis strategy, which was used to synthesise spirochensilide A and B, asperfloketal A and a synthetic precursor of asperfloketal B in an efficient semisynthetic manner.

Biogenetic space-guided analysis is a concept, which was further developed in this work, to plan biomimetic syntheses of terpenoid natural products from steroidal precursors. Said concept is applied by first analysing coisolated natural products from the same producing organism from which the natural product was isolated, and afterwards at natural products from the same genus. Structurally related molecules are sorted into groups (e.g. same carbon framework with different functional groups) and afterwards analysed to find logical biosynthetic connections which could shed light on intrinsic reactivity. Furthermore, other structurally related natural products from other genera can be used for further analysis.

Spirochensilides A and B were isolated in 2015 from the branches and needles of the Chinese fir *Abies chensiensis*. These natural products are epimers at the alcohol and feature six rings, nine stereogenic centres, a spiro[4.5]decane motif (between the B- and C-ring) and a 1,6-dioxaspiro[4.5]decene motif (between the E- and F-ring). An analysis of structurally related compounds made us aware of other 10(9 \rightarrow 8)abeo-17,14-friedolanostanes and indicated, that those may biosynthetically originate from classic lanostanes. The latter have to first rearrange to the corresponding 17,14-friedolanostanes before they are able to form the spiro[4.5]decane through a Meinwald rearrangement. Both natural products could be synthesised in this thesis in 13 and 15 steps respectively, while, at the same time, giving access to other structurally related natural products (e.g. the abifarins) from synthetic intermediates.

Asperfloketal A and B are anthrasteroids which were isolated in 2020 from *Aspergillus flocculosus* 16D-1. They feature nine contiguous stereogenic centres (ten in total), an intramolecular ketal and a (for anthrasteroids) unique cleaved C14-C15 bond. These natural products are regioisomers with the connectivity of the alcohol in the A-ring being different, making asperfloketal B the first isolated anthrasteroid with an 2 β -alcohol. Intrigued by their unknown biogenesis, this dissertation describes the development of a divergent, biomimetic synthesis of asperfloketal A in 18 steps and of the synthetic precursor for asperfloketal B. In addition to the biogenetic space-guided analysis, inspiration from historical research into the class of anthrasteroids was taken to accomplish the synthesis.



Diese Dissertation wurde unter der Leitung von Prof. Dr. Philipp Heretsch im Zeitraum von Oktober 2020 bis März 2023 zuerst am Institut für Chemie und Biochemie der Freien Universität Berlin und später am Institut für Organische Chemie der Gottfried Wilhelm Leibniz Universität Hannover angefertigt.

In Erinnerung an

Олександр Сергійович Юшин

Familie, Freund und große Inspiration

Danksagungen

An dieser Stelle möchte ich meinen Dank für diejenigen Aussprechen, die mir im Laufe der Promotion hilfreich zur Seite standen.

An erster Stelle möchte ich mich bei meinem Betreuer Prof. Dr. Philipp Heretsch für die interessanten Themen bedanken, an welchen ich über den Zeitraum meines Studiums und meiner Promotion in seiner Arbeitsgruppe mitwirken durfte. Die Betreuung war stets exzellent und im Fall von spontanen Ideen nahezu rund um die Uhr zu erhalten. Über die Jahre habe ich viel gelernt und könnte mir rückblickend keinen besseren Ort für meine Promotion vorstellen.

Weiterhin gilt mein Dank Prof. Dr. Markus Kalesse und Prof. Dr. Christian B. W. Stark für die Übernahme des Zweit- und Drittgutachtens dieser Arbeit. Zusätzlich möchte ich mich bei Herrn Kalesse für die problemlose Integration unserer Arbeitsgruppe nach unserem Umzug aus Berlin bedanken.

Herrn Prof. Dr. Jürgen Caro gilt mein Dank für die Bereitschaft als Prüfer an meiner Disputation teilzunehmen.

Für das Korrekturlesen der Dissertation danke ich Marius Saxarra, Maximilian Bauer und Sinan Adrian.

Für moralische Unterstützung möchte ich meine Eltern und besonders meinen Großeltern danken.

Ich möchte Linda Hermanns und Ines-Britta Roloff für ihre Hilfe bei der Bewältigung der teils übermäßigen Bürokratie an dieser Universität danken und ihre Bereitschaft bei jeglichen Fragen auszuhelfen.

Auch Dr. Reinhold Zimmer und Luise Schefzig gilt mein besonderer Dank. Sie haben mich im Rahmen meines Schülerpraktikums in der Arbeitsgruppe von Prof. Dr. Hans-Ulrich Reißig betreut und mir somit einen ersten Einblick in die Synthesechemie gewährt. Auch viele Jahre später, während meines Studiums, erinnerten sie sich noch an mich und baten mir im Rahmen eines Forschungspraktikums die Möglichkeit wieder mit ihnen im Labor zu stehen.

Ich danke allen ehemaligen und aktuellen Mitgliedern der AG Heretsch, der AG Christmann und der AG Kalesse. Besonderer Dank gilt hierbei Sinan Adrian, welcher mich durch die Schulzeit, das Studium und später in der Promotion als Laborpartner, begleitet hat.

Bei Gregor Drendel, Anja Peuker, Bettina Zeisig, Xuan Pham, Monika Rettstadt, Sabine Ohlrogge, Dagmer Körtje und Dr. Linn Müggenburg möchte ich mich für die Aufnahme meiner NMR-Spektren bedanken. Bei Christiane Groneberg und bei Sabine Ohlrogge möchte ich mich für die Aufnahme meiner IR-Spektren bedanken. Bei Gregor Drendel, Xuan Pham, Fabian Klautzsch und Dr. Gerald Dräger möchte ich mich für die Aufnahme meiner MS-Spektren bedanken.

Zuletzt möchte ich noch dem Europäischen Forschungsrat für die Finanzierung meiner Arbeit danken.

Abkürzungsverzeichnis

<i>m</i> CPBA	<i>meta</i> -Chlorperbenzoësäure
<i>p</i> TsOH	<i>para</i> -Toluolsulfonsäure
Ac	Acetat
CAS	Cycloartenolsynthase
d.r.	Diastereomerenverhältnis
DMAPP	Dimethylallylpyrophosphat
FAD	Flavin-Adenin-Dinukleotid
FDA	Food and Drug Administration
FPPS	Farnesylpyrophosphatsynthase
Glc	Glucose
IPP	Isopentenylpyrophosphat
LSS	Lanosterinsynthase
Man	Mannose
NADPH	Nicotinsäureamid-Adenin-Dinukleotid-Phosphat
OSC	Oxidosqualencyclase
PCC	Pyridiniumchlorochromat
SQE	Squalenepoxidase
SQS	Squalensynthase
TMS	Trimethylsilyl-
UV	Ultraviolett
VIS	visible; deutsch = sichtbar
z. B.	zum Beispiel

Inhaltsverzeichnis

Kurzzusammenfassung	iii
Abstract	iv
Vorwort	v
Widmung	vi
Danksagungen	vii
Abkürzungsverzeichnis	viii
1. Einleitung	1
1.1. Steroidbiosynthese	3
1.2. Secosteroide und <i>abeo</i> -Steroide	4
1.3. Friedolanostane	5
1.3.1. Erste Semisynthese von Friedolanostanen	6
1.3.2. Die Spirochensilide A und B	7
1.3.2.1. Erste Synthese des Spirochensilids A	8
1.3.2.2. Planung einer biomimetischen Semisynthese der Spirochensilide	9
1.4. Anthrasteroide	10
1.4.1. Die Geschichte der Anthrasteroide	10
1.4.2. Überlegungen zur biomimetischen Synthese von Asperfloketal A und B	14
2. Biogeneseraum-geleitete Analyse	17
2.1. Überlegungen zum Asperfloketal	19

3. Einordnung der Ergebnisse dieser Arbeit	21
Literaturverzeichnis	23
Anhang	27
Anhang A	28
Anhang B	100
Anhang C	171
Lebenslauf	187
Veröffentlichte Publikationen	188

1. Einleitung

In der Medizin werden heutzutage synthetische Wirkstoffe für die Bekämpfung einer großen Anzahl an Erkrankungen eingesetzt. Diese Wirkstoffe basieren oft auf isolierten Molekülen aus der Natur oder deren synthetischen Derivaten. Eine Klasse von Naturstoffen welche aufgrund ihres natürlichen Vorhandenseins im menschlichen Körper bereits seit den 1940er Jahren als sogenannte Leitstrukturen einen besonderen Fokus in der pharmazeutischen Forschung genießt, sind die Steroide.^[1] Diese gehören zur übergeordneten Klasse der Terpenoide und sind Produkte des sekundären Metabolismus.^[2]

Während Steroide in der Natur eine wichtige Rolle als Botenstoffe (Hormone) und zur Stabilisierung der Zellmembran spielen, sind sie in der allgemeinen Bevölkerung eher bekannt als leistungssteigernden Substanzen, welche im Profisport missbraucht werden.^[3,4] Diese sogenannten anabolen Steroide sind Derivate des männlichen Sexualhormons Testosteron (**8**) und wurden bereits zu Zeiten des Zweiten Weltkrieges in größeren Mengen synthetisch hergestellt.^[5]

Heutzutage spielen diese in der Medizin jedoch nur eine untergeordnete Rolle, wenn sie mit anderen biologisch aktiven Vertretern dieser Klasse verglichen werden. Einige pharmakologisch eingesetzte Steroide dienen hierbei zur Behandlung postpartaler Stimmungskrisen, langanhaltendem Status Epilepticus, entzündlicher Erkrankungen, von Krebs und anderen Erkrankungen.^[6] Derivate der Steroide machten somit im Jahr 2021 zwölf der 200 umsatzstärksten Wirkstoffe (kleine Moleküle) in der Medizin aus.^[7] Bis heute wurden mehr als 100 Medikamente auf Steroidbasis von der U.S. Food and Drug Administration (FDA) zugelassen und einige davon, wie zum Beispiel Dexamethason (**1**), welches ein synthetisches Derivat des körpereigenen Cortisons (**9**) ist und rund 25-mal stärker wirkt, in die „Liste der unentbehrlichen Arzneimittel der Weltgesundheitsorganisation“ aufgenommen (Abb. 1.1).^[8,9]

Die biologische Aktivität der Steroide ist neben ihrer funktionellen Gruppen unter anderem auch auf ihre charakteristische Struktur zurückzuführen.^[10] Sie sind aus drei anellierten Cyclohexanringen (Ring A, B, C) und einem an dem C-Ring anellierten Cyclopentanring (Ring D) aufgebaut. Die Ringe sind meistens vollständig *trans*-verknüpft und bilden damit eine starre, planare Struktur (Abb. 1.1).^[11] Dieses sogenannte Steran-Grundgerüst ist im einfachsten Fall im 5α -Gonan (**6**) zu sehen. Eine Unterscheidung der Substituenten im Ringsystem kann über die Halbräume oberhalb und unterhalb der steroidalen Ebene geschehen. Liegen die Substituenten unter der Ebene (zeigen nach hinten in der Skelettformel) so sind sie α -ständig, liegen sie hingegen über der Ebene (zeigen nach vorne in der Skelettformel) so sind sie β -ständig.^[12] Bei den meisten Steroiden handelt es sich aufgrund ihrer Biosynthese um 5α -Steroide (A- und B- Ring sind *trans*-verknüpft),^[13] jedoch gibt es auch Beispiele für 5β -Steroide, wie die Cholsäure (**10**), in denen die Ringe *cis*-verknüpft sind und das Grundgerüst nicht mehr planar ist. Steroide besitzen zusätzlich zum Ringsystem meistens eine oder zwei anguläre Methylgruppe (C18, C19) welche an C10 und C13 gebunden sind und eine aus der Biosynthese resultierende Seitenkette (*vide infra*), welche an C17 gebunden

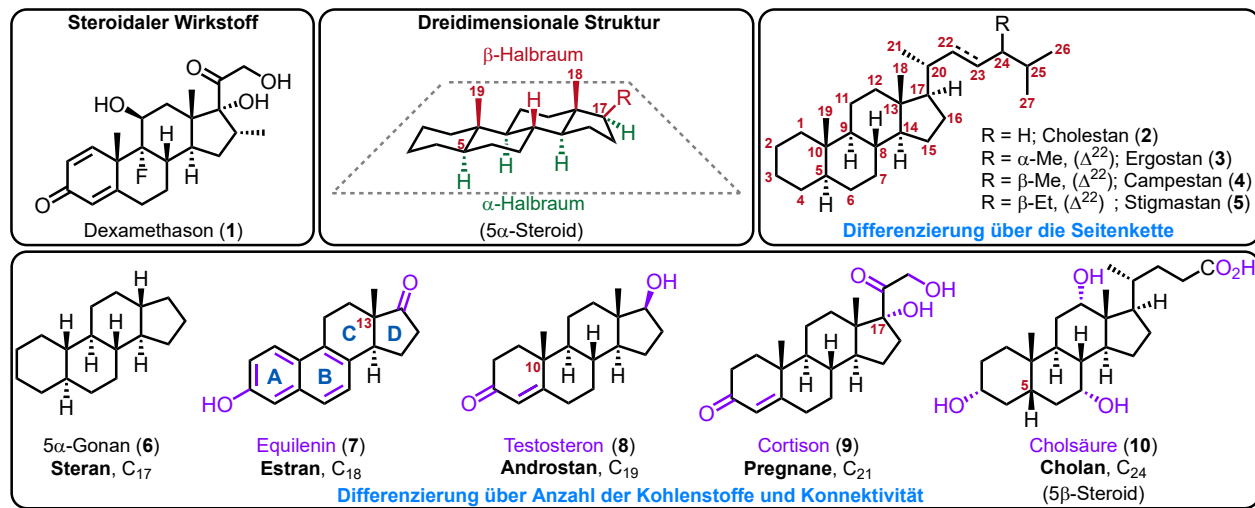


Abbildung 1.1. Übersicht zur Struktur von Steroiden und deren Differenzierung nach Seitenkette oder Anzahl von Kohlenstoffen.

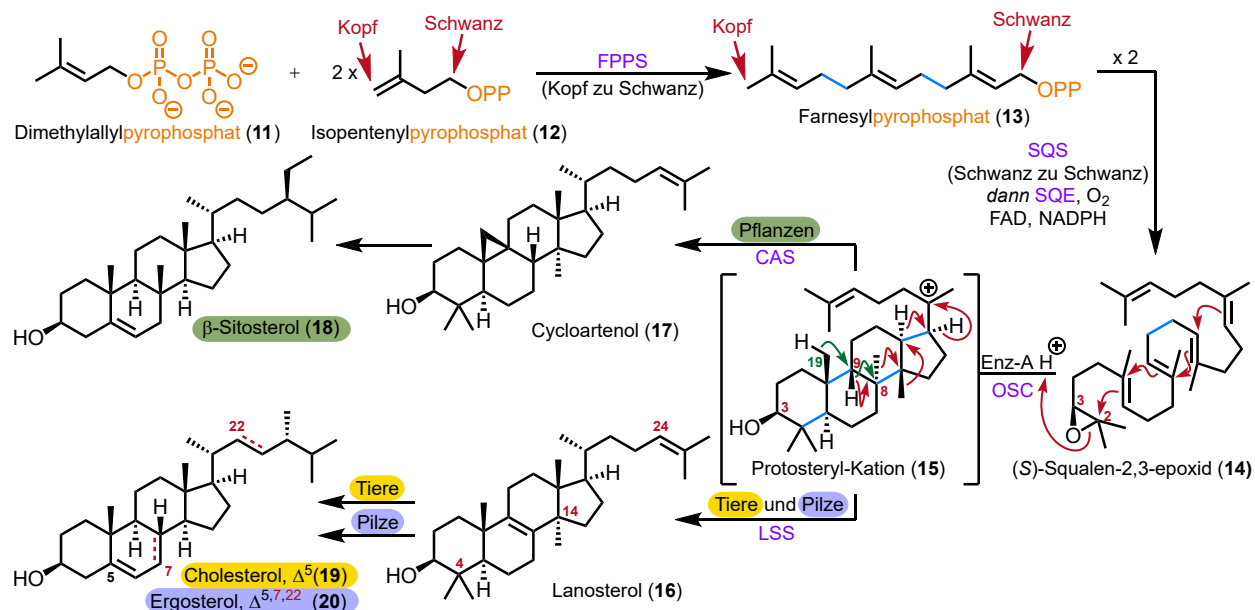
ist. Sowohl die Methylgruppen, als auch die Seitenkette sind meistens β -ständig.^[11]

Eine Einteilung von klassischen Steroiden in Untergruppen kann über strukturelle Eigenschaften in der Seitenkette, über die Anzahl der Kohlenstoffe oder den Saturierungsgrad des A-Rings erfolgen. Wird die Seitenkette betrachtet, so kann Cholestan (2), das Grundgerüst des Cholesterols (19), als Beispiel herangezogen werden. Wird die Seitenkette an C24 um eine α -ständige Methylgruppe ergänzt, wird daraus ein Ergostan (3), mit einer β -ständigen Methylgruppe ein Campestanen (4) und im Fall einer β -Ethylgruppe an C24 ein Stigmastan (5). Zusätzlich können Naturstoffe welche diese Grundgerüste besitzen auch eine Doppelbindung zwischen C22 und C23 haben (Δ^{22}).^[12]

Ist keine Seitenkette vorhanden, so kann eine Einteilung über die Anzahl der Kohlenstoffatome vorgenommen werden. Die Sterane (C₁₇-Grundgerüst, z. B. 5 α -Gonan (6)) bilden hierbei die einfachste Gruppe. Besitzt das Steroid ein zusätzliches Kohlenstoffatom, meist in Form einer angulären Methylgruppe an C13, so handelt es sich um ein Estran (C₁₈-Grundgerüst, z. B. Equilenin (7)). Kommt eine zweite anguläre Methylgruppe an C10 hinzu, gehört das Steroid zu den Androstanen (C₁₉-Grundgerüst, z. B. Testosteron (8)). Dieses Schema kann weitergeführt werden, was folgende Gruppen ergibt: Prenane (C₂₁-Grundgerüst, z. B. Cortison (9)), Cholane (C₂₄-Grundgerüst, z. B. Cholsäure (10)), Cholestane (C₂₇-Grundgerüst, z. B. Cholesterin (19)) und Lanostane (C₃₀-Grundgerüst, z. B. Lanosterol (16)). Besitzt ein Naturstoff mehr als 30 Kohlenstoffatome und ein steroidales Grundgerüst, so wird er nicht mehr den Steroiden, sondern den übergeordneten Terpenoiden zugeordnet.^[12,14]

1.1. Steroidbiosynthese

Ihre Vielfalt verdanken die Steroide ihrer Biosynthese, welche in Pflanzen, Tieren und Pilzen abläuft und jeweils verschiedene Triterpenoide als Endprodukte liefert. Als biosynthetisches Startmaterial der Terpensynthesen dient in der Regel das „aktivierte“ C₅-Isopren Isopentenylpyrophosphat (IPP, **12**) und dessen Isomer, das Dimethylallylpyrophosphat (DMAPP, **11**) (Schema 1.1).^[15,16] Durch enzymatische Entfernung des Pyrophosphats in DMAPP (**11**) entsteht das entsprechende allylische Kation, welches anschließend durch die terminale Doppelbindung des IPP (**12**) nukleophil angegriffen werden kann und somit die beiden Moleküle miteinander verknüpft.^[17] Bei dieser Art Verknüpfung handelt es sich um eine Kopf-zu-Schwanz-Verknüpfung, welche wiederholt werden kann, um Farnesylpyrophosphat (**13**, C₁₅) zu erhalten. Während diese Kettenverlängerung weitergeführt werden kann für entsprechende C₂₀ und C₂₅-Einheiten, werden in der Steroidbiosynthese zwei FPP-Einheiten (**13**) mittels der Squalensynthase (SQS) in einer Schwanz-zu-Schwanz-Verknüpfung zum Triterpen Squalen (C₃₀) verknüpft.



Schema 1.1. Biosynthese von Steroiden ausgehend von IPP (**12**) und DMPP (**11**).

Dieses wird anschließend mittels der Squalenepoxidase (SQE) in Gegenwart von Sauerstoff und den Co-faktoren Flavin-Adenin-Dinukleotid (FAD) und Nicotinsäureamid-Adenin-Dinukleotid-Phosphat (NADPH) an der endständigen Doppelbindung epoxidiert und liefert (S)-Squalen-2,3-epoxid (**14**).^[15] Das (S)-Squalen-2,3-epoxid (**14**) wird dann zuerst auf der Oxidosqualencyclase (OSC) präorganisiert und anschließend in einer kationischen Cyclisierungskaskade in das Protosteryl-Kation (**15**) umgewandelt.^[13] Dieses kann in Tieren und Pilzen durch die Lanosterinsynthase (LSS) in einer Reihe von Wagner-Meerwein-Umlagerungen und Hydrid-Shifts, mit abschließender Eliminierung des Wasserstoffs an C9, in Lanosterol (**16**) umgewandelt werden (rote Pfeile). In Pflanzen, in Gegenwart der Cycloartenolsynthase (CAS), wandert hingegen der C9 Wasserstoff zum C8 und die C19-Methylgruppe bildet das im Cycloartenol (**17**) zu sehende Cyclopropan-Motiv (grüne Pfeile und rote Pfeile).

Sowohl Cycloartenol (**17**, C₃₀) als auch Lanosterol (**16**, C₃₀) können enzymatisch weiterreagieren und in einer Reihe von Demethylierungsreaktionen (C4, C14), Seitenketten-Modifikationen (C24, Δ^{22}) und Desaturierungen (Δ^5 , Δ^7) in die jeweiligen steroidalen Grundbausteine umgewandelt werden. In Pflanzen ist dies β -Sitosterol (**18**, C₂₉), in Pilzen Ergosterol (**20**, C₂₈), und in Tieren Cholesterin (**19**, C₂₇).^[15,16] Die Namen aller dieser Verbindungen enden aufgrund der C3-Hydroxyfunktion, welche aus dem Epoxid entstanden ist, auf „-ol“. Liegt wie im Testosteron (**8**) oder Cortison (**9**) eine C3-Oxofunktion vor, so ist die Endung typischerweise „-on“.^[12] Es wird vermutet, dass die fünf Steroide (**16–20**) die biosynthetischen Vorläufer der meisten derzeit isolierten steroidalen Naturstoffe sind.

1.2. Secosteroide und *abeo*-Steroide

Organismen sind in der Lage, die Komplexität von Steroiden in ihren jeweiligen Metabolismen weiter zu modifizieren und diese somit in ihrer Funktion zu verändern. Dies kann z. B. durch Funktionalisierung/Oxidation des Ringsystems oder durch Modifikation der Seitenkette passieren. Enzyme sind jedoch auch in der Lage, Bindungen im Steroid zu spalten, die Konnektivität zwischen Kohlenstoffen zu verändern und Kohlenstoffe hinzuzufügen oder herauszuschneiden. Weicht das Grundgerüst eines Steroids von der klassischen Ringstruktur des Sterans ab, muss eine weitere Spezifizierung der Struktur durch Verwendung von Präfixen und/oder Suffixen durchgeführt werden.

Ist eine Bindung im Grundgerüst geschnitten und dadurch ein Ring geöffnet worden, so handelt es sich um ein Secosteroïd.^[12] Erwähnenswerterweise besitzen Secosteroide oftmals eine signifikante biologische Aktivität. Diese kann unter anderem entzündungshemmend, cytotoxisch, antiproliferativ, antimikrobiell oder antiviral sein.^[6,18,19]

Eins der bekanntesten Secosteroide ist wahrscheinlich Vitamin D₃ (**21**) (Abb. 1.2). Es handelt sich hierbei um ein 9,10-Secocolesterol, welches durch eine photoinduzierte elektrocyclische Ringöffnung aus 7-Dehydrocholesterol entsteht.^[20] Die Zahlen geben dabei an, welche Bindung im Steroid gespalten wurde. Wurden wie im Sarocladiolone (**22**) zwei Bindungen gespalten, so handelt es sich um ein Disecosteroïd.^[21] Die gespaltenen Bindungen werden in der Nomenklatur durch einen Doppelpunkt von einander getrennt (5,10:8,9-Disecosteroïd).

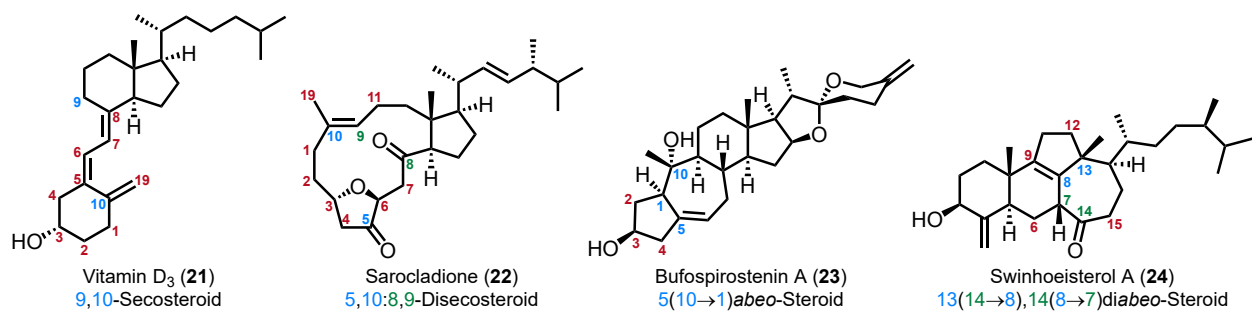


Abbildung 1.2. Beispiele für Secosteroide und *abeo*-Steroide.

Hat eine Bindungsmigration im Ringsystem stattgefunden, so handelt es sich um ein *abeo*-Steroid.^[12] Das Bufospiostenin A (**23**) gehört mit seinem besonderen „5-7-6-5“-Ringsystem (Zahlen beschreiben die

Ringgrößen vom A-, B-, C- und D-Ring) zu dieser Klasse.^[22] Es handelt sich dabei um ein sogenanntes 5(10→1)*abeo*-Steroid. Die Nomenklatur 5(10→1) beschreibt hierbei, dass C5, welches vor der Migration mit C10 verbunden war, jetzt an C1 gebunden ist. Haben, wie im Swinhoeisterol A (24), zwei Bindungsmigrationen stattgefunden, so handelt es sich um ein di*abeo*-Steroid [13(14→8),14(8→7)*diabeo*-Motiv].^[23] Wenn sowohl eine Bindung geöffnet wurde, als auch eine Bindung migriert ist, werden die Präfixe in alphabetischer Reihenfolge verwendet.^[12]

Weiterhin werden die Deskriptoren *nor* und *homo* verwendet. Bei einem Norsteroid fehlt dabei ein Kohlenstoffatom, bei einem Homosteroid ist hingegen ein zusätzliches Kohlenstoffatom angefügt worden.^[12] Hierbei kann eine allgemeine Angabe gemacht werden, wie z. B. ein „6-6-5-6“-Steroid als C-*nor*-D-*homo*-Steroid bezeichnet werden oder wie im Fall von 19-*nor*-Testosteron eine genau Angabe darüber gemacht werden, welches Kohlenstoffatom fehlt.^[24] Im Fall von 19-*nor*-Testosteron fehlt die 19 β -Methylgruppe, an deren Stelle ein β -ständiger Wasserstoff an C10 gebunden ist.

1.3. Friedolanostane

Ähnlich zur *abeo*-Nomenklatur beschreibt das Präfix „Friedo“ auch eine Bindungsmigration im Molekül und findet besonders bei Lanostanen und seinen Derivaten Anwendung. Dabei geht es speziell um die Migration von einer oder mehreren angulärer Methylgruppen im steroidalen Grundgerüst.^[25] Ein Beispiel für solche Friedolanostane sind Abiesatrin A (25) und Abifarin B (26)(Abb. 1.3).^[26,27] Beide sind aus Bäumen der *Abies* Gattung isoliert worden und sind Vertreter größerer Naturstofffamilien mit gleichem Grundgerüst. Beim Abiesatrin A (25) handelt es sich um ein so genanntes 17,13-Friedolanostan. Während die erste Zahl die Position angibt an welcher die gewanderte Methylgruppe nach der Umlagerung gebunden ist, macht die zweite Zahl eine Aussage über die ursprüngliche Position, an welcher die Methylgruppe gebunden war. Somit ist im Abiesatrin A (25) die 18-Methylgruppe von C13 nach C17 gewandert. Da meistens Wagner–Meerwein-Umlagerungen für solche Friedolanostane verantwortlich sind, liegt ein stereospezifischer Verlauf vor. Wenn es wie im Fall von Abifarin B (26) dazu kommt, dass zwei Methylgruppen sich aufgrund einer sukzessiven Migration in ihrer Position zum klassischen Lanostan-Grundgerüst unterscheiden, so wird der Endpunkt der ersten Umlagerung und der Startpunkt der Zweiten angegeben. Es handelt sich also hierbei um ein 17,14-Friedolanostan.

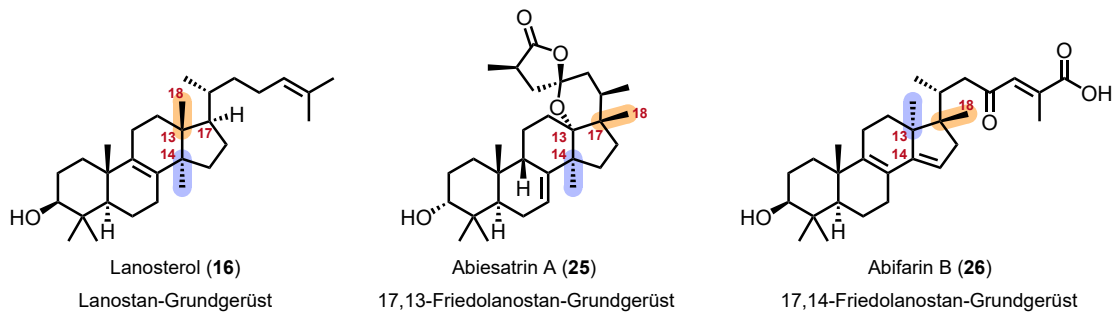
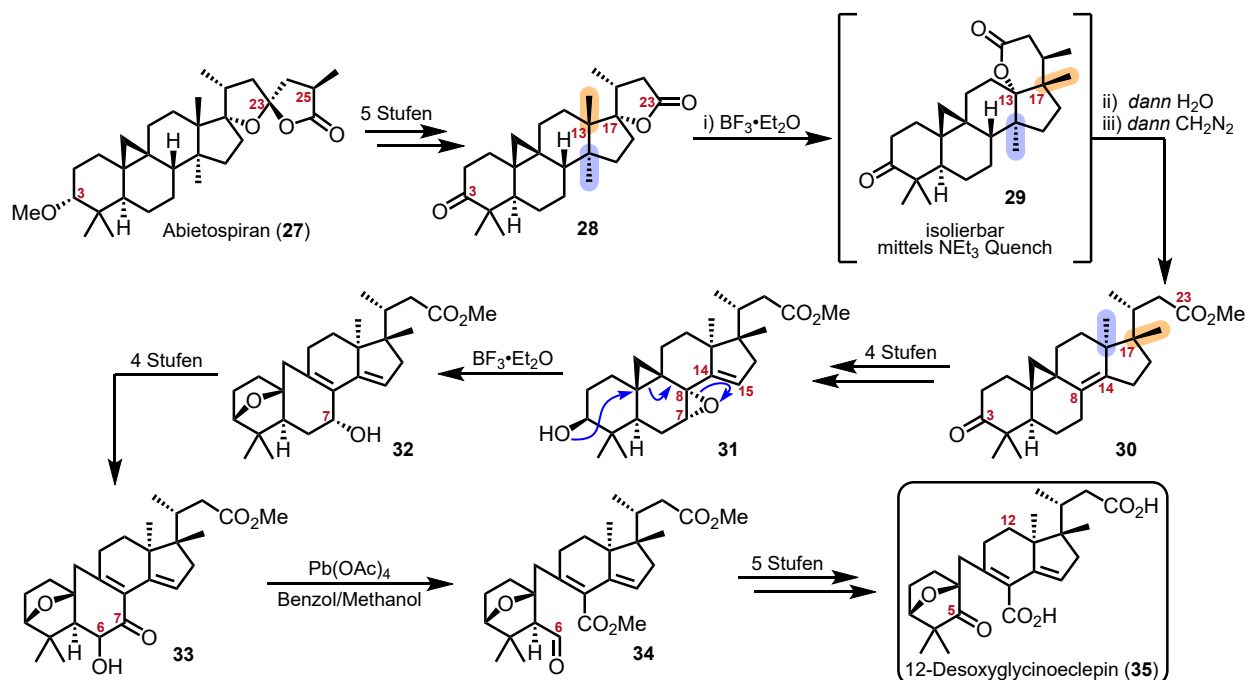


Abbildung 1.3. Beispiele für Friedolanostane im Vergleich zum klassischen Lanostan-Grundgerüst.

1.3.1. Erste Semisynthese von Friedolanostanen

Die einzige bekannte Synthese solcher Friedolanostane war lange Zeit Coreys Semisynthese von 12-Desoxyglycinoeclepin (35), welche er 1994 publiziert hat.^[28] Die Struktur des 12-Desoxyglycinoeclepins (35) deutet auf einen biosynthetischen Ursprung aus der Gruppe der Cycloartenole hin und bewegte Corey dazu, eine Semisynthese ausgehend von Abietospiran (27) zu planen. Dieses ist mit einem Anteil von bis zu 1% in der Rinde der Weiß-Tanne *Abies alba* zu finden, welche als Abfallprodukt in der Holzindustrie entsteht und zu der Zeit im Multitonnen-Maßstab zur Verfügung stand (Schema 1.2).^[29]

Die Synthese begann mit einer vierstufigen Reaktionssequenz bestehend aus α -Hydroxylierung der C25-Position, Mesylierung, Eliminierung und anschließender Lemieux-von Rudloff-Oxidation, um das [5,5]-Oxaspirolacton in ein Lacton zu überführen. Darauffolgende selektive oxidative Spaltung der C3-Methoxygruppe gab Keton 28. Bei diesem handelte es sich um das für die Wagner–Meerwein-Kaskade abgeleitete Startmaterial. Wenn dieses mit $\text{BF}_3\cdot\text{Et}_2\text{O}$ umgesetzt, langsam mit Wasser gequenched und dann mit Diazomethan versetzt wurde, konnte 17,14-Friedolanostan 30 isoliert werden.



Schema 1.2. Coreys Semisynthese von 12-Desoxyglycinoeclepin (35), dem ersten synthetisch hergestellten Naturstoff mit 17,14-Friedolanostan-Grundgerüst.^[28]

Um eine genauere Vorstellung über die Umlagerungssequenz zu bekommen, wurde die Reaktion statt mit Wasser mit Triethylamin gequenched. Die Isolation des δ -Lactons 29, welches ein 17,13-Friedolanostan-Grundgerüst besitzt, konnte zeigen, dass die Wagner–Meerwein-Umlagerungen sequenziell stattfindet. Hierbei wird durch Zugabe der Lewis-Säure zuerst ein C17-Kation generiert, welches durch die erste Wagner–Meerwein-Umlagerung der C18-Methylgruppe (orange), auf die C13-Position wandert. Dieses C13-Kation kann dann durch das Carboxylat in der Seitenkette abgefangen werden, was zum δ -Lacton 29 führt. Langsame Zugabe von Wasser unter Brønsted-sauren Bedingungen initiiert dann die zweite Wagner–Meerwein-

Umlagerung und bildet das entsprechende 17,14-Friedolanostan (**30**-23-COOH).

Die Synthese wurde fortgesetzt durch Epoxidierung der $\Delta^{8(14)}$ -Bindung, Öffnung und Eliminierung dieses Epoxids unter leicht sauren Bedingungen zum $\Delta^{7,14}$ -Dien, Reduktion der C3-Oxofunktion und anschließender regio- und stereoselektiver Epoxidierung der reaktivierten Δ^7 -Bindung. Epoxid **31** wurde daraufhin durch Zugabe von $\text{BF}_3 \cdot \text{Et}_2\text{O}$ aktiviert und reagierte in einer $\text{S}_{\text{N}}2'$ -Reaktion zu Tetrahydrofuran **32**, welches dann in vier Schritten in α -Ketol **33** umgewandelt wurde. Zugabe von Blei(IV)-acetat in Benzol/Methanol zu α -Ketol **33** führte anschließend zu einer 6,7-Bindungsspaltung und gab Dimethylester **34** mit einem C6-Aldehyd. Dieser wurde zur Säure oxidiert, mittels Bartons Decarboxyhydroxylierung in den C5-Alkohol überführt, welcher dann zum Keton oxidiert wurde. Abschließende Verseifung der beiden Methylester gab 12-Desoxyglycinoeclepin (**35**) in 21 Stufen.

Seit der Publikation dieser Synthese wurden mehrere Totalsynthesen, unter anderem auch aus der Gruppe um Corey, für das Glycinoeclepin publiziert.^[30–32] Was diese Synthese, so wie einige andere Semisynthesen, so besonders macht, ist das gewonnene Verständnis über intrinsische Reaktivität, welche auf ähnliche Systeme übertragen werden kann. Während der Naturstoff ohne Zweifel das Ziel einer Synthese darstellt, kann eine Semisynthese gleichzeitig das Ziel verfolgen, ganze Strukturklassen auf eine divergente Art und Weise zugänglich zu machen, wie es hier mit den 17,13-Friedolanostanen und den 17,14-Friedolanostanen der Fall war.

1.3.2. Die Spirochensilide A und B

Über die Jahre wurden weitere 17,14-Friedolanostane gefunden, welche ein zusätzliche Stufe an Komplexität aufwiesen. Es handelt sich hierbei um die Gruppe der 10(9 \rightarrow 8)abeo-17,14-Friedolanostane. Während bereits 2004 ein Reihe unbenannter 10(9 \rightarrow 8)abeo-17,14-Friedolanostane mit unterschiedlichen Seitenketten isoliert wurden, wie z. B. Verbindung **36**,^[33,34] sind zwei der heutzutage bekanntesten Vertreter die Spirochensilide A (**37**) und B (**38**) (Abb. 1.4). Beide Moleküle wurden 2015 durch die Gruppe um Gao aus den Ästen und Nadeln der chinesischen Schensi-Tanne *Abies chensiensis* isoliert und sind C3-Epimere.^[35] Eine vollständige Strukturaufklärung gelang den Isolatoren über Infrarotspektroskopie, Kernresonanzspektroskopie, Einkristall-Röntgendiffraktometrie und Massenspektrometrie.

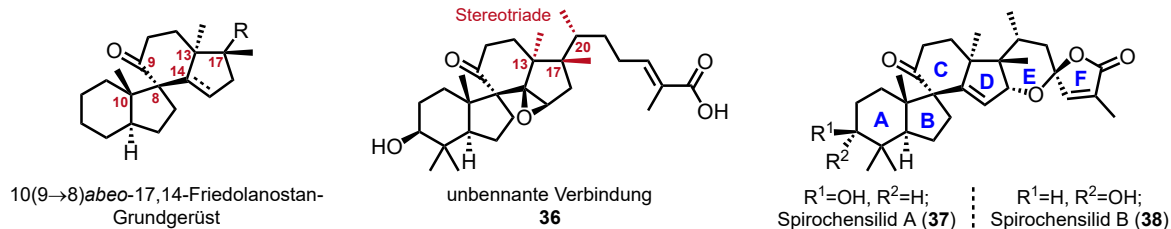


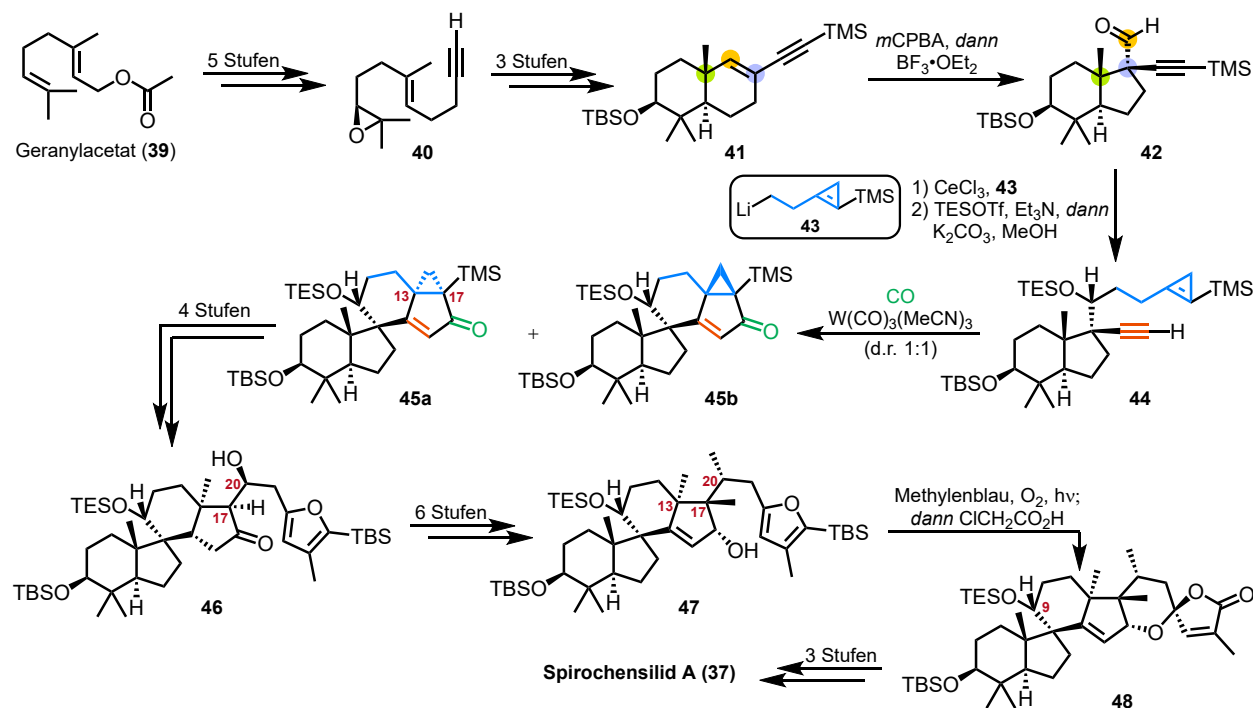
Abbildung 1.4. 10(9 \rightarrow 8)abeo-17,14-Friedolanostan-Grundgerüst und Beispiele für Naturstoffe.

Die beiden Spirochensilide besitzen jeweils sechs Ringe, zwei namensgebende Spirozentren (das Spiro[4.5]-decan zwischen B- und C-Ring und das 1,6-Dioxaspiro[4.5]decen, welches den E- und F-Ring verbindet) und neun stereogene Zentren. Zusätzlich besitzen die Spirochensilide die für 17,14-Friedolanostane typische Methylgruppen-Stereotriade (C14, C17, C20).

1.3.2.1. Erste Synthese des Spirochensilids A

Erstmals synthetisiert wurde Spirochensilid A (**37**) durch die Gruppe um Yang im Frühjahr 2020.^[36] Ihre Totalsynthese ging von Geranylacetat (**39**) aus, welches in fünf literaturbekannten Stufen in Epoxid **40** umgewandelt wurde (Schema 1.3). Anschließende kationische Cyclisierung in das entsprechende vinylische Bromid gab nach Sonogashira-Reaktion Enin **41** über drei Stufen. Das Enin **41** wurde epoxidiert und dann unter Lewis-sauren Bedingungen in einer Meinwald-Umlagerung, dem ersten Schlüsselschritt der Synthese, in Aldehyd **42** überführt. Diese Reaktion diente dem Aufbau des stereogenen Zentrums des späteren Spiro[4.5]decans zwischen B- und C-Ring und der Ringkontraktion des B-Rings. Addition des Li-Nukleophils **43** an Aldehyd **42**, Schützung des entstandenen Alkohols und Entfernung der TMS-Gruppe am Alkin ergab das Cyclopropen-Derivat **44**.

Der zweite Schlüsselschritt, eine Pauson–Khand-Reaktion, baute unter Verwendung von **44** den C- und D-Ring des Spirochensilid-Grundgerüstes auf, lieferte jedoch selbst nach extensiver Optimierung nur ein 1:1 Diastereomerengemisch der 13,17-Cyclopropane **45a** und **45b**, von welchen nur **45a** für die weitere Synthese verwendet werden konnte. Die Einführung der Seitenkette gab anschließend Furan **46** über vier Stufen. In den nächsten sechs Stufen der Synthese wurde die Stereotriade der Methylgruppen aufgebaut (Eliminierung des C20-Alkohols, 1,4-Methylierung mit Me₂CuLi, Methylierung) und der allylische Alkohol **47** durch oxidative Manipulationen am Grundgerüst gewonnen.



Schema 1.3. Totalsynthese von Spirochensilid A (**37**) über 27 Stufen aus der Gruppe Yang.

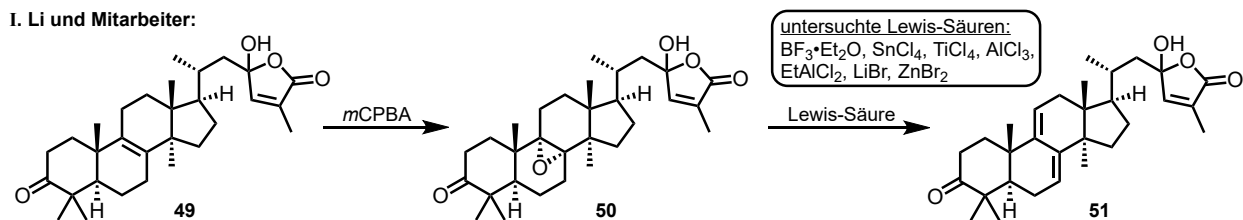
Der E- und F-Ring konnten im dritten Schlüsselschritt der Synthese aus dem allylischen Alkohol **47** in einer Furan-basierten oxidativen Cyclisierung (Kornblum–DeLaMare-artig) aufgebaut werden. Das erhaltene Oxaspirolacton **48** wurde abschließend durch Spaltung der Schutzgruppen und Oxidation des C9-

Alkohols in Spirochensilide A (37) umgewandelt. Mit 27 Stufen in der längsten linearen Sequenz handelt es sich um eine relativ lange Synthese, was jedoch durch die Komplexität des Naturstoffes gerechtfertigt ist.

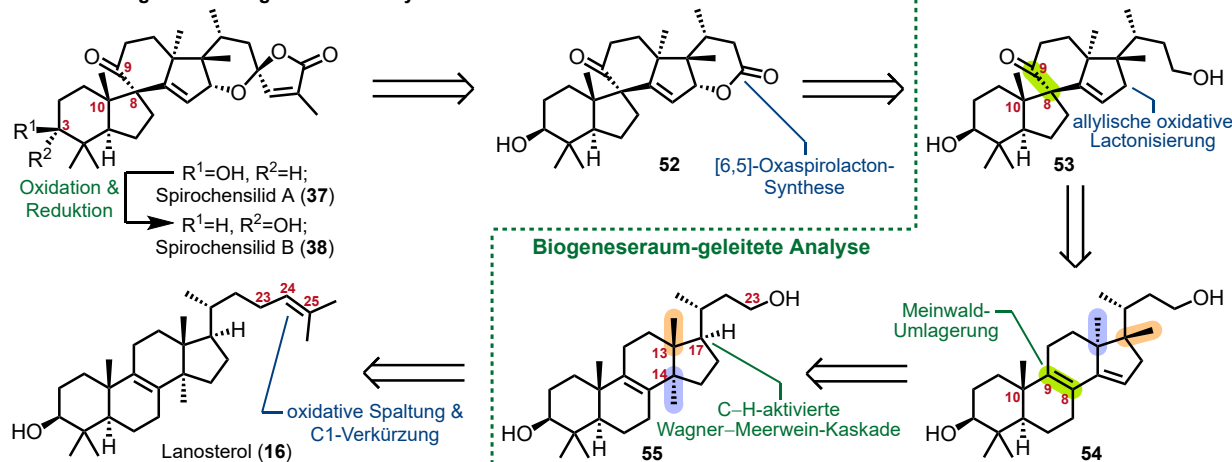
1.3.2.2. Planung einer biomimetischen Semisynthese der Spirochensilide

Die Spirochensilide A (37) und B (38) fielen uns aufgrund ihres 17,14-Friedolanostan-Grundgerüstes ins Auge und bewegten uns dazu, Überlegungen zu einem semisynthetischen Zugang einzuleiten. Die von Li und Mitarbeitern vorgeschlagene Biosynthese baute auf dem coisolierten Keton **49** auf (Schema 1.4, I). Dessen Epoxidierung und Meinwald-Umlagerung sollte zuerst das Spiro[4.5]decan aufbauen, gefolgt von einer Methylgruppen-Migration. Um ihre Hypothese zu untersuchen, führten sie ausführliche Studien mit Epoxid **50** durch, konnten jedoch unabhängig von der eingesetzten Lewis-Säure immer nur Dien **51** isolieren.^[35]

I. Li und Mitarbeiter:



II. Unsere Biogeneseraum-geleitete Retrosynthese:



Schema 1.4. I. Untersuchungen einer Meinwald-Reaktion in Lanostan **50** als Ursprung des $10(9 \rightarrow 8)abeo$ -Motivs durch Li und Mitarbeiter, **II:** Unser Biogeneseraum-geleiteter Retrosyntheseplan für Spirochensilid A (37) und B (38) ausgehend von Lanosterol (16).

Diese Ergebnisse bewegten uns dazu, den Strukturraum der aus der *abies*-Gattung isolierten Naturstoffe genauer zu analysieren.^[26,27,37–40] Was dabei auffiel, war, dass es keine $10(9 \rightarrow 8)abeo$ -Steroide gab, welche nicht zusätzlich 17,14-Friedolanostane waren. Aufgrund der großen Menge an Naturstoffen mit Lanosten-, 17,13-Friedolanostan-, 17,14-Friedolanostan- und $10(9 \rightarrow 8)abeo$ -17,14-Friedolanostan-Grundgerüst, konnten wir eine Biogeneseraum-geleitete Retrosynthese von Spirochensilid A (37) und B (38) entwickeln (siehe Kapitel 2, Biogeneseraum-geleitete Analyse).

Wir gingen davon aus, dass Spirochensilid B (**38**) durch Oxidation und Reduktion aus Spirochensilid A (**37**) entsteht (Schema 1.4). Spirochensilid A (**37**) könnte dabei aus Lacton **52** in einer Oxaspirolacton-Synthese hergestellt werden. Oxaspirolactone sind bekannte Motive und in vielen Naturstoffen anzutreffen, sodass Methoden wie die Dreiding–Schmidt-Reaktion (einstufig) oder weitere zweistufige Ansätze ausgehend von Lactonen verfügbar sind.^[41] Lacton **52** könnte durch eine allylische oxidative Lactonisierung aus 10(9→8)*abeo*-Alkohol **53** entstehen. Dieser sollte durch eine selektive Epoxidierung und Meinwald-Umlagerung aus 17,14-Friedolanostan **54** herstellbar sein. 17,14-Friedolanostan **54** könnte wiederum in einer C-H-aktivierten Wagner–Meerwein-Umlagerungskaskade aus C23-Alkohol **55** entstehen, welcher in einer teils-literaturbekannten Synthese, durch oxidative Spaltung und Decarboxylierung, auf Lanosterol **16** zurückzuführen ist.^[42]

Die Syntheseplanung stellte sich am Ende als erfolgreich heraus und erlaubte uns eine Synthese von Spirochensilid A (**37**) und B (**38**) in 13 Stufen bzw. 15 Stufen, ausgehend von Lanosterol (**16**), zu entwickeln (siehe Anhang A).^[43] Es konnte somit nicht nur die Anzahl der Schritte im Vergleich zur Totalsynthese halbiert werden, sondern es ist uns zudem gelungen, einen eleganten Zugang zu den 17,13-Friedolanostanen und den 17,14-Friedolanostanen mit leicht modifizierbarer Seitenkette aus einem leicht zugänglichen Startmaterial zu entwickeln. Die synthetischen Intermediate können darüber hinaus verwendet werden um weitere Naturstoffklassen, wie z. B. die Abifarne, herzustellen, was wir mit der Synthese von Abifarin B (**26**) noch einmal veranschaulicht haben (siehe Anhang A).

Einige Monate nachdem wir unsere Ergebnisse publiziert hatten, erschien eine zweite Semisynthese aus der Gruppe um Deng.^[44] Sie stimmten unserem Rational bezüglich der sich von den Isolatoren unterscheidenden Reihenfolge der Wagner–Meerwein-Umlagerung und der anschließenden Meinwald-Umlagerung zu und zeigten einen leicht variierten Syntheseansatz [1) Epoxidierung der Δ^8 -Bindung, 2) C17-Kation initiierte Wagner–Meerwein-Kaskade 3) Meinwald-Umlagerung]. Auch in ihrem Fall konnten sie mit 17 Schritten ausgehend von Lanosterol (**16**) eine effiziente Synthese des Spirochensilids A (**37**) entwickeln.

1.4. Anthrasteroide

Die Anthrasteroide sind eine kleine Gruppe von terpenoiden Naturstoffen, welche ein *diabeo*-Motiv besitzen. Im Gegensatz zur klassischen steroidalen Ringverknüpfung, sind hier der A-, B- und C-Ring linear miteinander anelliert, wobei der B-Ring aromatisch ist (Abb. 1.5). Mit Ausnahme von Asperflokal A (**64**) und B (**65**) ist der D-Ring bei den Anthrasteroiden intakt und mit dem C-Ring anelliert.^[45]

1.4.1. Die Geschichte der Anthrasteroide

Bei den Anthrasteroiden handelt es sich um eine Klasse von Naturstoffen, welche untypischerweise zuerst chemisch erschlossen wurde. Erst 34 Jahre später konnten Vertreter natürlichen Ursprungs isoliert und charakterisiert werden.^[46]

Erste Veröffentlichungen zeigen, dass Nes und Mosettig bereits 1954 zum ersten Mal Dehydroergosterolace-

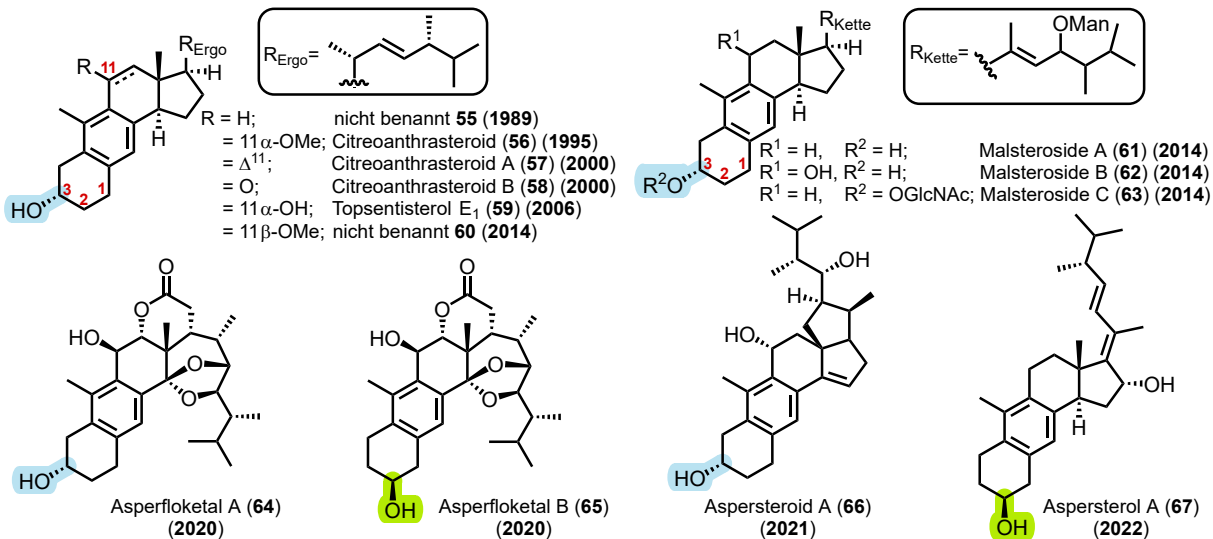


Abbildung 1.5. Übersicht aller 13 bis heute isolierten Vertreter der Anthrasteroide.^[46–54]

tat (**68**) unter saueren Bedingungen in ein Anthrasteroid umgelagert haben (Abb. 1.6 und Schema 1.5).^[45] Mit den limitierten analytischen Methoden ihrer Zeit konnten grundlegende Aussagen über das Molekül getroffen werden. Zum einen besaß es einen aromatischen Ring dessen UV/Vis-Spektrum nicht mit dem von Cook und Haslewood charakterisierten Neoergosterol (**69**) übereinstimmte und zum anderen schlossen sie ein Steroid-Grundgerüst durch den Vergleich des Drehwertes mit verschiedenen bekannten Steroiden aus (Abb. 1.6).^[55] Stattdessen zeigte ein Vergleich des UV/Vis-Spektrums eine gute Deckung mit dem von 1,2,3,4,5,6,7,8-Octahydroanthracen (**70**) und deutete darauf hin, dass eine Methylgruppe am aromatischen Ring gebunden sein muss. Der Name „Anthrasteroid“ setzte sich entsprechend aus dieser Erkenntnis und dem steroidalen Vorläufer zusammen.

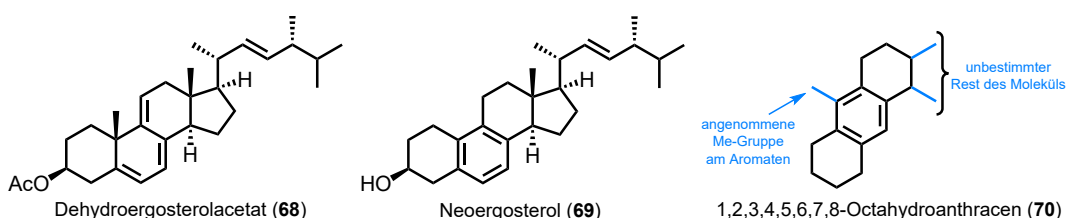


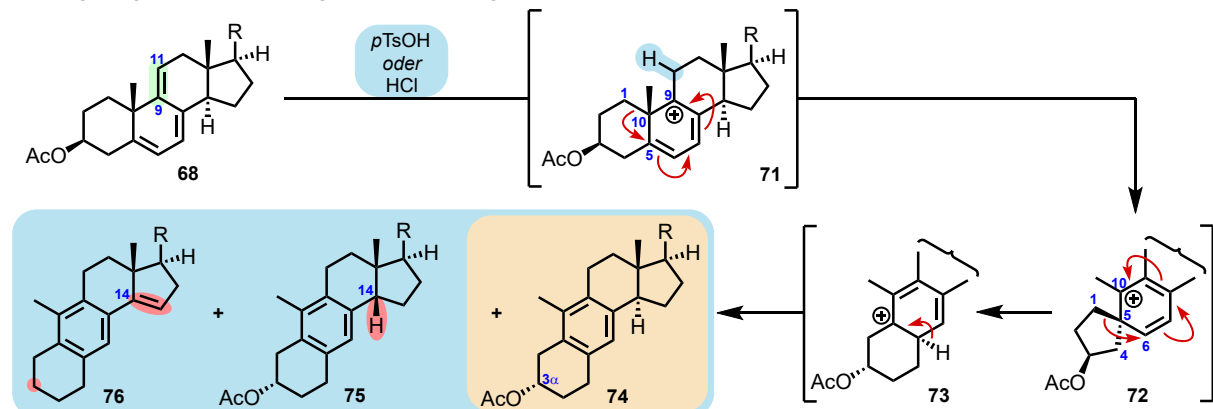
Abbildung 1.6. Für die Untersuchungen zu Anthrasteroiden relevante Strukturen.^[45,55]

Während ihrer Untersuchungen wurden Nes und Mosettig auf die Ergebnisse von Cook und Haslewood aufmerksam, welche die kanzerogenen Eigenschaften verschiedener Kohlenwasserstoffe, darunter auch von Anthracen-Derivaten, untersucht hatten und eine entsprechende Korrelation entdecken konnten.^[56] Diese Ergebnisse bewegten Nes und Mosettig vermutlich dazu, zu postulieren, dass Steroide, welche in Form von Hormonen im menschlichen Körper vorkommen, möglicherweise unter *in vivo* Bedingungen in Anthrasteroide umgewandelt werden können und somit zu Krebs bei Menschen führen könnten. Um diese Theorie zu untersuchen, publizierten sie über die nächsten neun Jahre eine elfteilige Serie an Forschungsarbeiten, welche sich mit der Struktur dieser Molekülklasse und ihrer Derivate, der Anthrasteroid-Umlagerung und der physiologischen Eigenschaften der Anthrasteroide beschäftigte. Weitere Gruppen griffen diese For-

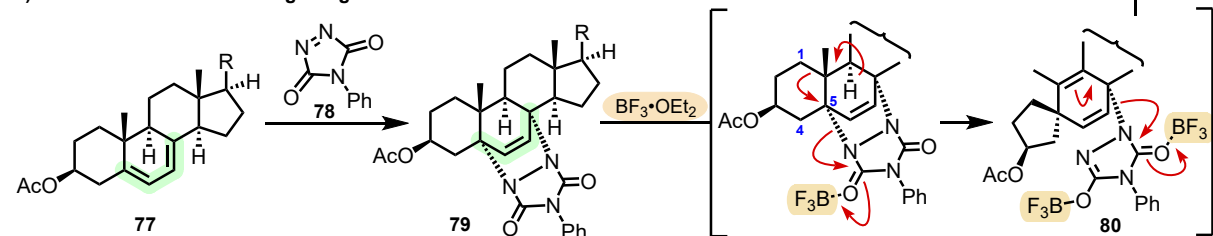
schung auf und führten eigene Untersuchungen durch. Die Idee der Umwandlung von Steroiden unter *in vivo* Bedingungen konnte nicht realisiert werden und fehlende kanzerogene Eigenschaften der Moleküle widersprachen der ursprünglich aufgestellten Hypothese.^[45,57–66]

Nes und Mosettig gingen davon aus, dass die chemisch geführte Anthrasteroid-Umlagerung durch eine Protonierung der $\Delta^{9(11)}$ -Bindung in Dehydroergosterolacetat (**68**) mittels einer starken Brønsted-Säure, typischerweise konzentrierte Salzsäure oder *p*-Toluolsulfonsäure, initiiert wird und C9-Kation **71** gebildet wird (Schema 1.5).

I) Umlagerung durch Protonierung der $\Delta^{9(11)}$ Bindung:



II) Lewis-Säure initiierte Umlagerung des Triazol-Addukts:



Schema 1.5. Mechanismus der Anthrasteroid-Umlagerung initiiert I) durch Brønsted-Säure und II) durch Lewis-Säure.

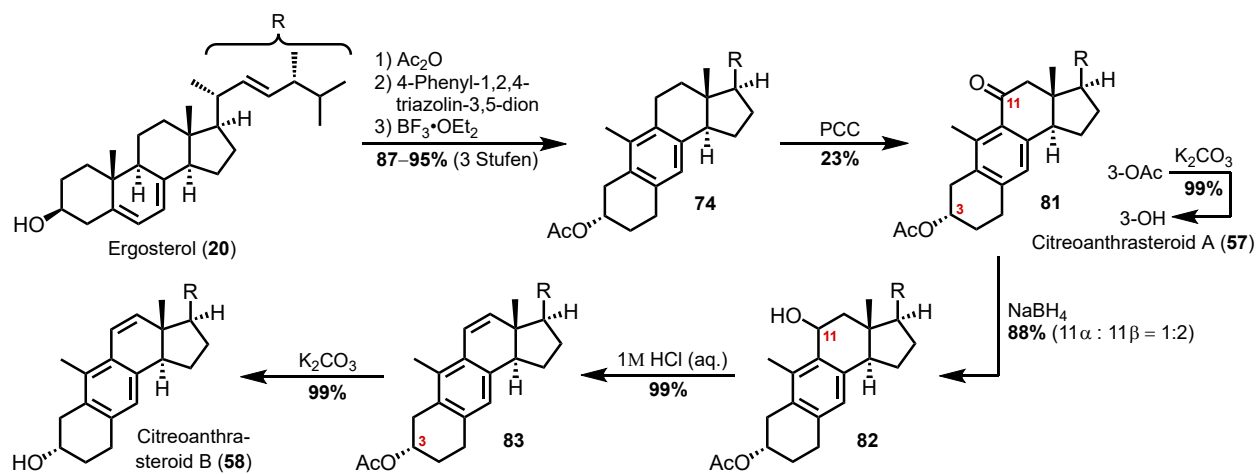
Eine erste Wagner–Meerwein-Umlagerung führt dann zur Bildung eines 1(10 \rightarrow 5)*abeo*-Intermediates **72**, welches sofort in einer zweiten Wagner–Meerwein-Umlagerung zum 1(10 \rightarrow 5),1(5 \rightarrow 6)*diabeo*-Grundgerüst **73** der Anthrasteroide umlagern kann. Eliminierung eines Protons führt zuletzt zur Aromatisierung des B-Rings. Unter den eingesetzten Reaktionsbedingungen konnte nur die Bildung des 3 α -Produkts **74** (Nummerierung unterscheidet sich von der klassischen Steroidnummerierung) beobachtet werden.

Mehrere Probleme traten jedoch aufgrund der aggressiven Reaktionsbedingungen auf. Zum einen konnten nur geringe Mengen des 3 α -Produktes **74** isoliert werden und zum anderen kam es oftmals zu einem Verlust von Funktionalität im A-Ring **76** und/oder zum Verlust der stereogenen Information an C14 **75/76**. Diese Probleme wurden alle 1974 von den Gruppen um Ferguson, Whalley und Midgley durch einen neuen Umlagerungsansatz gelöst. Sie gingen von Ergosterolacetat (**77**) als Startmaterial aus und setzten dieses mit 4-Phenyl-1,2,4-triazolin-3,5-dion (**78**) in einer [4+2]-Cycloaddition um. Zugabe eines Überschusses von $\text{BF}_3\cdot\text{Et}_2\text{O}$ zum Triazol-Addukt **79**, führte dann in einer Wagner–Meerwein-Umlagerung zum 1(10 \rightarrow 5)*abeo*-Intermediat **80**, welches weiter zur literaturbekannten kationischen Spezies **72** reagieren konnte.^[67,68] Von

hier aus deckt sich der Rest des Mechanismus mit dem, welcher bereits von Nes und Mosettig vorgeschlagen wurde. Durch die milden Bedingungen zur Initiierung der Umlagerung kam es zu quantitativen Ausbeuten, keinem Verlust von Funktionalität oder stereogener Information, jedoch auch nur zur Bildung des 3α -Produktes **74**.

Neun Jahre später wurde zum ersten Mal ein Anthrasteroid aus Sedimentschichten der Tiefsee isoliert. Dabei handelte es sich laut der Autoren jedoch eher um ein Artefakt aus Diageneseprozessen, als um einen echten Naturstoff.^[69] Erst fünf Jahre später, im Jahr 1988, wurde der erste Naturstoff mit Anthrasteroid-Grundgerüst **55** aus dem Pilz *Epichloe typhina* isoliert.^[46] Bei diesem unbenannten Naturstoff handelt es sich um das selbe Moleköl, welches bereits 14 Jahre zuvor von den Gruppen um Ferguson, Whalley und Midgley in ihrer Triazol-basierten Umlagerung hergestellt wurde (nach Verseifung).

Diese Methode wurde im Jahr 2000 von Nakada und Yamamura aufgegriffen, um die von ihnen isolierten Anthrasteroide Citreanthrasteroid A (**57**) und B (**58**) herzustellen (Schema 1.6).^[48]



Schema 1.6. Synthese von Citreanthrasteroid A (**57**) und B (**58**) von Nakada und Yamamura.

Ausgehend von Ergosterol (**20**) bildeten sie Anthrasteroid **74** durch Acetylierung des C3-Alkohols, Bildung des Triazol-Adukts **79** und anschließende $\text{BF}_3\cdot\text{Et}_2\text{O}$ induzierte Umlagerung. Oxidation der C11-Position gelang ihnen daraufhin durch Reaktion mit Pyridiniumchlorochromat (PCC). Während Verseifung des C3-Acetats zum Citreanthrasteroid A (**57**) führte, musste für Citreanthrasteroid B (**58**) zuerst das Keton zu Alkohol **81** reduziert und der generierte Alkohol zum Δ^{11} -Anthrasteroid **83** eliminiert werden. Anschließende Verseifung gab dann das gewünschte Produkt **58**.

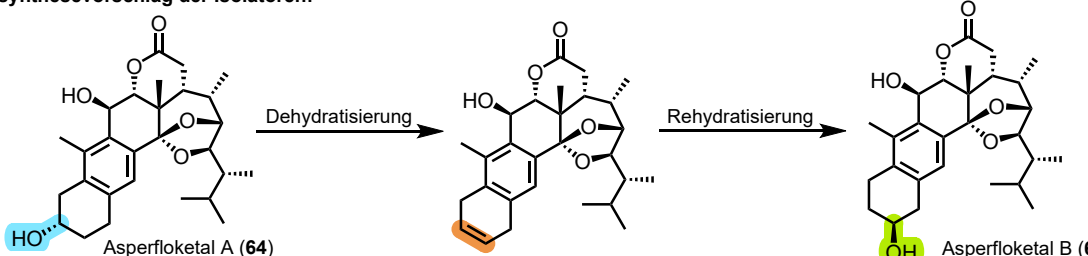
Bis heute wurden insgesamt 13 Anthrasteroide aus diversen Organismen isoliert (Abb. 1.5).^[46–54]

1.4.2. Überlegungen zur biomimetischen Synthese von Asperfloketal A und B

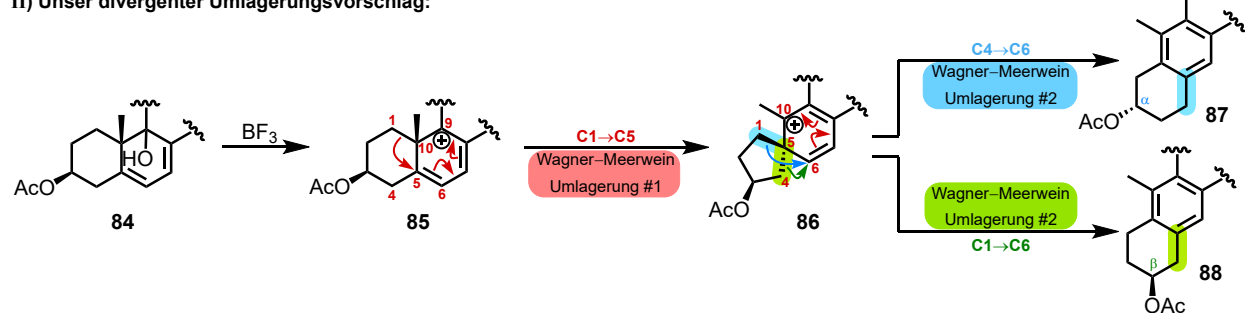
Unter den 13 Anthrasteroiden befinden sich auch die vor kurzem isolierten Asperfloketale A (**64**) und B (**65**). Sie wurden beide im Jahr 2020 in gleichen Mengen aus dem Pilz *Aspergillus Flocculosus 16D-1* isoliert, welcher auf dem Tiefseeschwamm *Phakellia Fusca* entdeckt wurde und später für die Isolation in größeren Mengen kultiviert wurde.^[52] Beide Naturstoffe besitzen neun aufeinanderfolgende stereogene Zentren (insgesamt zehn), ein intramolekulares Ketal und eine geschnittene C14-C15 Bindung. Bei den Naturstoffen handelt es sich um Regioisomere des Alkohols im A-Ring. Während im Asperfloketal A (**64**) ein 3α -Alkohol vorliegt, wie bei allen bis zu dem Zeitpunkt isolierten Anthrasteroiden, befindet sich der Alkohol im Asperfloketal B (**65**) in der 2β -Position (Schema 1.7). Dies machte sie in unseren Augen für die Aufklärung der Biogenese und für die anschließende Entwicklung einer biomimetischen divergenten Synthese besonders interessant.

Während die Isolatoren von einer Dehydratisierung und anschließender Rehydratisierung ausgingen^[52] (Schema 1.7, I), vermuteten wir, dass der Mechanismus identisch zu dem ist, welcher bereits von Nes und Mosettig formuliert wurde, jedoch die aggressiven Reaktionsbedingungen in ihren Experimenten dazu führten, dass sich der 2β -Alkohol **88** nicht bildete, eliminierte oder sich zersetzte. Dessen Bildung könnte jedoch durch eine C4-C5 Bindungsmigration in **86** (grün) während der zweiten Wagner-Meerwein-Umlagerung, statt einer C1-C5 Bindungsmigration (blau) erklärt werden (Schema 1.7, II).

I) Biosynthesevorschlag der Isolatoren:

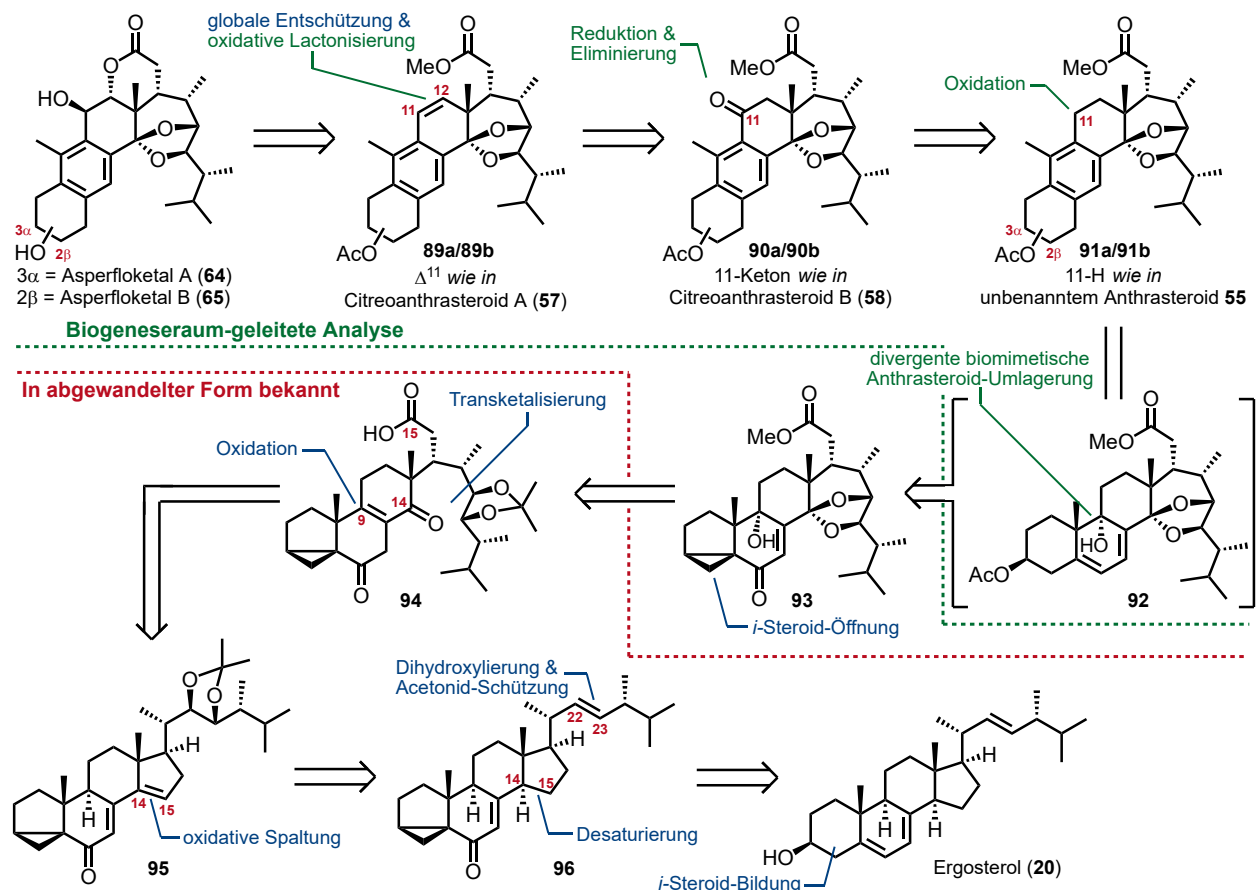


II) Unser divergenter Umlagerungsvorschlag:



Schema 1.7. Vergleich der Biosynthesevorschläge für die Asperfloketale A (**64**) und B (**65**) I) Vorschlag der Isolatoren^[52] II) unser Vorschlag.

Zwar wurde eine solche Migration ursprünglich aufgrund von vermuteten destabilisierenden Effekten des C3-Alkohols ausgeschlossen, jedoch auch nie weiter untersucht.^[70] Wir vermuteten, dass die Generierung eines C9-Kations **85**, z. B. aus Alkohol **84**, unter milden Bedingungen zu einer solchen Umlagerung führen könnte, was unsere Forschung zu einem semisynthetischen Zugang zu den Asperfloketalen A (**64**) und B (**65**) einleitete (Schema 1.8).



Schema 1.8. Biogeneseraum-geleiteter Retrosyntheseplan für Asperfloketal A (64) und B (65).

Ein Vergleich der C11-Substitution der bereits zuvor isolierten Naturstoffe deutete darauf hin, dass Asperfloketal A (64) und B (65) mittels oxidativer Lactonisierung auf Δ¹¹-Anthrasteroide 89a/89b zurückzuführen sind (siehe Kapitel 2.1, Überlegungen zum Asperfloketal). Diese könnten in der Natur entweder direkt aus den Anthrasterolen 91a/91b entstehen, oder, hergeleitet von weiteren isolierten Anthrasteroiden, durch Oxidation von 91a/91b zu Keton 90a/90b und anschließender Reduktion und Eliminierung hergestellt werden. Die Anthrasteroide 91a/91b sollten beide in einer divergenten Anthrasteroid-Umlagerung aus dem C9-Alkohol 92 entstehen. Da jedoch das Dien im C9-Alkohol 92 sehr reaktiv ist, müsste dieses zuvor aus *i*-Steroid 93 generiert werden. Beim *i*-Steroid handelt es sich in diesem Fall um eine Schutzgruppe, welche am Anfang der Synthese erzeugt werden muss und mittels BF₃·Et₂O/AcOH entfernt werden kann. Da es sich hierbei um Lewis-Saure Bedingungen handelt, welche das gewünschte C9-Kation aus 92 generieren könnten, wurde *i*-Steroid 93 als Ausgangspunkt der Anthrasteroid-Umlagerung anvisiert. Das *i*-Steroid 93 sollte mittels intramolekularer Transketalisierung, C9-Oxidation und Veresterung aus 14,15-Secosteroidenon 94 synthetisiert werden können. Die Synthese eines solchen 14,15-Secosteroidenons war uns in abgewandelter Form bereits aus der Synthese von Strophasterol A bekannt und konnte zurückgeführt werden auf Δ¹⁴-Steroid 95, in welchem die 14,15-Doppelbindung oxidativ gespalten werden kann.^[71] Das Δ¹⁴-Steroid 95 sollte hierbei aus *i*-Steroid 96 durch Desaturierung und syn-Oxidation der Δ²²-Doppelbindung hergestellt werden. Die Synthese von *i*-Steroid 96 über drei Stufen ausgehend von Ergosterol (20) ist literatur-

bekannt.^[72] Wie zuvor erwähnt dient das *i*-Steroid einerseits dazu, das reaktive Diensystem im B-Ring zu schützen, jedoch zusätzlich auch dazu, um mithilfe des generierten Enons die allylische C14-Position für die Desaturierung zu aktivieren.

Ausgehend von Ergosterol (**20**) gelang uns mit dem zuvor beschriebenen Plan die Synthese von Asperfloketal A (**64**) in 18 Schritten und die divergente Synthese von 2β -**91b**, welches als Startmaterial für eine Synthese von Asperfloketal B (**65**) verwendet werden kann.^[73] Das 2β -**91b** konnte wie zuvor vermutet zusammen mit 3α -**91a** in zwei Schritten aus C9-Alkohol **93** in einem Verhältnis von 2:1 (3α : 2β) hergestellt werden. Während unserer Untersuchungen zur Anthrasteroid-Umlagerung und der darauffolgenden C11-Funktionalisierungen fielen zwei Sachen auf, welche unsere Biogeneseraum-geleitete Analyse unterstützen (siehe Kapitel 2.1, Überlegungen zum Asperfloketal).

Um die C11-Oxidation im Anthrasteroid zu umgehen, haben wir versucht, bereits vor der Umlagerung eine Oxo-Funktion an C11 einzubauen (siehe Anhang B). Eliminierung des C9-Alkohols in **93** und anschließende Epoxidierung gab uns das $9\alpha,11$ -Epoxid (nicht gezeigt). Dieses stellte sich jedoch als nicht reaktiv heraus. Es konnte weder zum 1,2-*trans*-Diol noch zum α -Ketol geöffnet werden. Auch eine Lewis-Säure initiierte Anthrasteroid-Umlagerung mit dem Epoxid führte nur zur Zersetzung des Startmaterials. Die Tatsache, dass in der Natur Anthrasteroide ohne funktionelle Gruppe in C11 existieren, deutet darauf hin, dass diese erst später durch benzylyche Oxidation eingeführt wird.

Der zweite Punkt, welcher für die gezeigte Reihenfolge in der Biosynthese spricht, ist, dass die C12 Position in keinem unserer Versuche direkt funktionalisiert werden konnte. Selbst als sie durch das Keton in **90a** aktiviert wurde, konnte keine Reaktion beobachtet werden. Nur Eliminierung des Alkohols zu **89a** ermöglichte anschließende Epoxidierung. Bei dem Epoxid handelte es sich jedoch um ein α -ständiges Epoxid, welches unter Säure- und Lewis-Säure-Aktivierung keine Reaktion oder nur Zersetzung zeigte. Umsetzung mit einer Hydroxid-Basis hingegen öffnete das Epoxid durch Angriff an C11 zum $11\beta,12\alpha$ -Diol, welches mit der freien Säure zum Asperfloketal A (**64**) reagieren konnte (siehe Anhang B).

2. Biogeneseraum-geleitete Analyse

Bei der Biogeneseraum-geleiteten Analyse handelt es sich um eine von uns weiterentwickelte Methode, biomimetische Synthesen terpenoider Naturstoffe aus steroidalen Vorläufern zu planen. Der Grundgedanke hinter diesem Konzept ist zwar nicht neu, wird jedoch in dieser Form eher oberflächlich und nicht systematisch angewandt.

Zwei Beispiele wie diese Art von Planung retrosynthetische Überlegungen unterstützen kann, wurden bereits zuvor bei der Synthese von Spirochensilid A (**37**) und B (**38**) und der Synthese von Asperfloketal A (**64**) angesprochen. Am Beispiel der Spirochensilide soll an dieser Stelle der Prozess hinter der Biogeneseraum-geleitete Analyse nochmal vertieft werden.

Zunächst wird für das Zielmolekül nach einem logischen biosynthetischen Startmaterial gesucht. Die Unterschiede in der Konnektivität der Kohlenstoffe von diesem zur Zielverbindung können für die spätere Bestimmung der biosynthetischen Reihenfolge relevant sein. Für das Spirochensilid deuteten die zwei Methylgruppen an C4, die Anzahl der Kohlenstoffe und die Tatsache, dass es aus einem Baum isoliert wurde, auf eine Ursprung aus Cycloartenol (**17**) hin. Die Abwesenheit des Cyclopropans (und die Anwesenheit der C19 Methylgruppe) können auch auf Lanosterol (**16**) als Startmaterial hindeuten, da dieses strukturell anderweitig identisch ist. Während bereits entdeckt wurde, dass einige Pflanzen in der Lage sind Lanosterol (**16**) direkt aus (*S*)-Squalen-2,3-epoxid (**14**) herzustellen, kann schlussendlich keine genauere Aussage über den biosynthetischen Ursprung getroffen werden, ohne nähere biosynthetische Studien durchzuführen.^[74-76]

Im ersten Schritt der Analyse werden coisierte Naturstoffe aus demselben Organismus, aus welchem auch die Zielverbindung isoliert wurde, betrachtet. Die Anzahl der Verbindungen hängt hierbei stark davon ab, wie ausführlich die Spezies untersucht wurde. Im Fall der Spirochensilide sind mehrere Isolationsberichte aus der *Abies chensiensis* publiziert.^[35,37,39,40] Werden nicht relevante Moleküle (z. B. kleinere Terpene) aussortiert, so können bereits mehrere interessante Verbindungen mit einem Lanostan-Grundgerüst und einem 17,14-Friedolanostan-Grundgerüst gefunden werden (ausgewählte Beispiele in Abb. 2.1).

Im zweiten Schritt der Analyse wird das Suchfeld auf Verbindungen der selben Gattung (*Abies*) erweitert. Bei *Abies recurvata* und *Abies forrestii var. georgei* handelt es sich wie bei der *Abies chensiensis* um chinesische Tannen, welche in einem geographisch nahen Umfeld in Zentralchina zu finden sind.^[26,27,38] Aus beiden Arten konnten weitere interessante Triterpenoide isoliert werden, von denen ausgewählte Beispiele in Abb. 2.1 gezeigt sind. Einerseits wurden nicht umgelagerte Moleküle mit einem Cyclopropan isoliert (Cycloartan-Grundgerüst), was den biologischen Ursprung aus Cycloartenol (**17**) bekräftigt und andererseits sind strukturell verwandte Vertreter der 17,13-Friedolanostane und 17,14-Friedolanostane mit nahezu identischer Seitenkette zum Cycloartan, jedoch mit einer C19 Methylgruppe statt des Cyclopropans, gefunden worden. Das deutet darauf hin, dass das Cyclopropan vor oder nach der Umlagerung geöffnet und das Lanostan- bzw. 17,13-Friedolanostan-Grundgerüst gebildet wird.

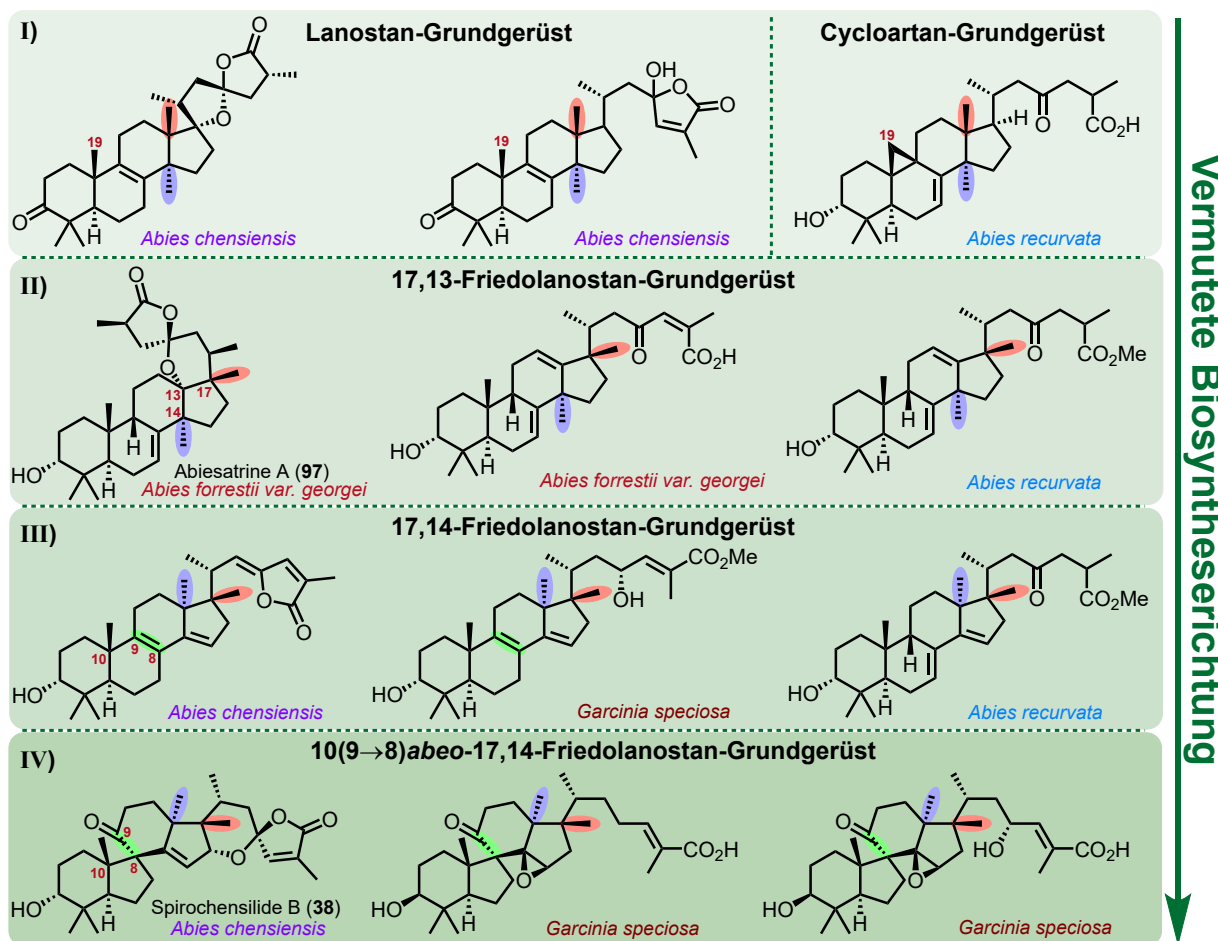


Abbildung 2.1. Analyse der Biosyntheserichtung von $10(9 \rightarrow 8)$ abeo-Steroiden durch Vergleich strukturell ähnlicher Steroide aus Pflanzen der *Abies*- und *Garcinia*-Gattung.

Zuletzt wird die Sphäre an betrachteten Verbindungen ein weiteres Mal erweitert und es werden strukturell ähnliche Naturstoffe unabhängig von der produzierenden Gattung betrachtet. Hierbei muss die Molekülstruktur im Vergleich zum Naturstoff oftmals deutlich vereinfacht werden, um relevante Resultate zu erhalten. Wird nur das A-D-Ringsystem des Spirochensilids betrachtet, so können mehrere unbenannte Verbindungen mit $10(9 \rightarrow 8)$ abeo-17,14-Friedolanostan-Grundgerüst und einige Vertreter der 17,14-Friedolanostane, welche aus der *Garcinia speciosa* isoliert wurden, identifiziert werden (ausgewählte Beispiele in Abb. 2.1).^[33,34] Strukturell ähnliche Moleküle werden nun in Gruppen zusammengefasst (z. B. selbes Grundgerüst, jedoch verschiedene funktionelle Gruppen). Für das Spirochensilid sind diese Gruppen in Abb. 2.1 zusammengefasst: I) keine Methylgruppe ist gewandert, II) eine Methylgruppe ist von C13 nach C17 gewandert, III) zusätzlich zur ersten Methylgruppe ist die zweite von C14 nach C13 gewandert, IV) beide Methylgruppen sind gewandert und zwischen B- und C-Ring besteht ein Spiro[4.5]decan-Motiv. Unterschiede zwischen diesen Gruppen können dann analysiert werden, um eine mögliche Biosynthese zu formulieren und entsprechende intrinsische Reaktivität der Moleküle vorherzusagen. Anhand der gezeigten Beispiele zeigt sich: 1) die Methylgruppen wandern nacheinander und stereospezifisch, 2) ein für die Wagner-Meerwein Umlagerung nötiges Kation an C17 könnte durch eine funktionelle Gruppen in der Seitenkette entstehen, 3)

nach der ersten Wagner-Meerwein Umlagerung kann das C13-Kation durch die Seitenkette abgefangen werden oder durch Eliminierung zur Δ^{12} -Doppelbindung abreagieren, 4) es existieren nur Beispiele für 10(9 \rightarrow 8)*abeo*-Steroide in denen beide Methylgruppen gewandert sind, was darauf hindeutet, dass dies eine Voraussetzung für die Umlagerung ist.

2.1. Überlegungen zum Asperfloketal

Für die Asperfloketale kann aufgrund von fehlender Literatur keine ausführliche Analyse durchgeführt werden, welche auf einen strukturellen Vorläufer für die Anthrasteroid-Umlagerung hindeuten könnte. Die bekannten Anthrasteroide (siehe Abb. 1.5)^[45,57–66] können jedoch verwendet werden, um eine Vorhersage über die Reihenfolge der C11 und C12-Funktionalisierung zu machen. Vereinfacht kann hierbei nur der C-Ring betrachtet werden.

Unter den Anthrasteroiden gibt es mehrere Beispiele für Verbindungen, welche keine Funktionalität in C11 besitzen (Abb. 2.2). Das deutet darauf hin, dass vor der Anthrasteroid-Umlagerung auch keine Funktionalität in dieser Position vorliegt, was typisch für die meisten klassischen Steroide ist. Eine benzylike Oxidation könnte anschließend zu einem C11-Oxoanthrasteroid führen (Alkohol, Ether oder Keton). Bis auf Citreoanthrasteroid A (57) und Asperfloketal A (64) und B (65) besitzt keiner der bekannten Anthrasteroide eine C12-Funktionalität. Die Δ^{11} -Doppelbindung im Citreoanthrasteroid A (57) könnte durch Eliminierung einer C11-Oxoverbindung entstehen und dann durch *trans*-Dihydroxylierung einen möglichen Vorläufer für die Asperfloketale bilden (unter der Annahme, dass die 14,15-Bindung gespalten ist und die C15-Säure mit dem C12-Alkohol reagieren kann).

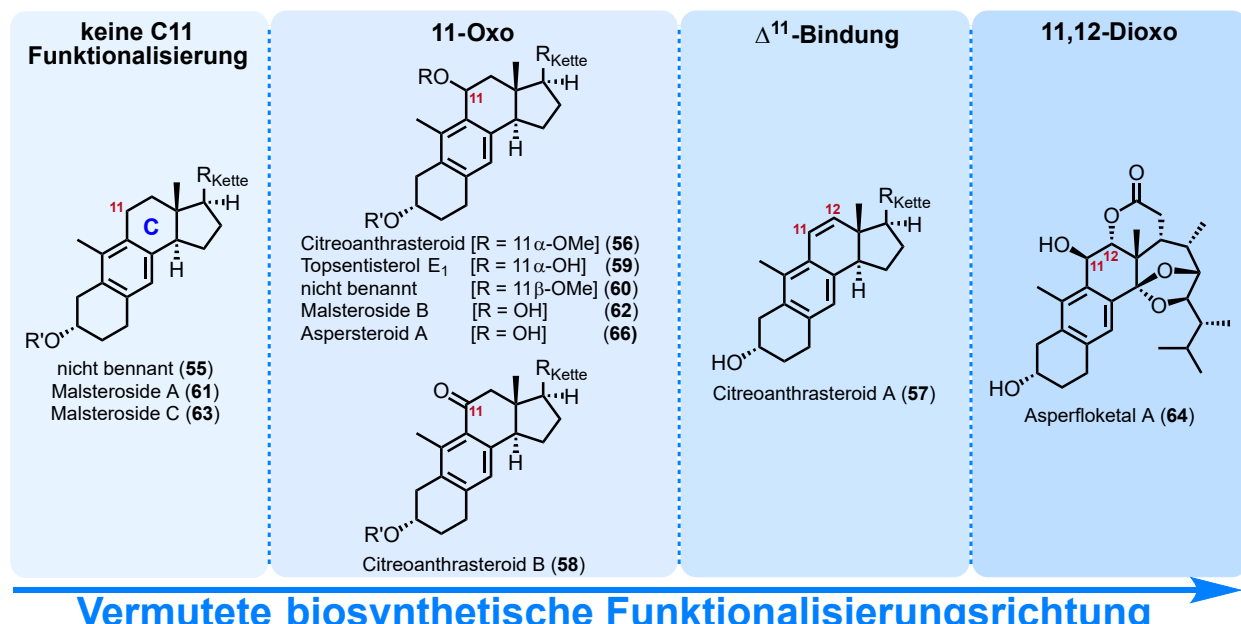


Abbildung 2.2. Vermutete biosynthetische Funktionalisierungsrichtung anhand von bekannten Anthrasteroiden.

Die tatsächliche Synthese bestätigte die vorgeschlagene Reihenfolge und zeigte, dass z. B. die Δ^{11} -Doppelbindung nicht mit bekannten Reaktionen in einem Schritt vom unfunktionalisierten Anthrasteroid hergestellt werden konnte (siehe Anhang B).

Schlussendlich ist die Biogeneseraum-geleitete Analyse nicht in der Lage eine garantiert erfolgreiche Synthese vorherzusagen. Die Qualität der Aussage hängt zum einen stark davon ab, wie intensiv die Art und die Gattung des entsprechenden Naturstoffs untersucht wurde und wie viele Isolationsberichte vorliegen und zum anderen kann nur eine Vermutung über die intrinsische Reaktivität einer Verbindung gemacht werden. Die Natur besitzt mit Enzymen Werkzeuge, welche oftmals nicht mit den uns bekannten Reaktionen im Labor nachgeahmt werden können. Im Fall der Spirochensilide und des Asperflokets war es jedoch möglich, entscheidende Schritte durch diese Art von Planung vorherzusagen und anschließend zu realisieren. Mit der steigenden Anzahl an isolierten Naturstoffen sollte in Zukunft gleichzeitig die Qualität der Vorhersagen steigen und dementsprechend auch die Qualität von biomimetischen Semisynthesen.

3. Einordnung der Ergebnisse dieser Arbeit

Die Naturstoffsynthese ist eine historisch stark geprägte chemische Disziplin. Über die Jahre konnte sie stets weiterentwickelt werden und ist heutzutage durch drei, sich teils überlappende Disziplinen (Totalsynthese, Semisynthese und Biotechnologie), in der organischen Chemie vertreten.

Während der Fokus in der Vergangenheit oftmals darin lag, ein Molekül herzustellen um einen Beweis für dessen Struktur zu liefern oder um neu entwickelte Reaktionen an Praxisbeispielen zu untersuchen, waren diese Synthesen nach heutigen Maßstäben häufig wenig elegant. Das hing ohne Zweifel auch mit einem geringeren Repertoire an bekannten Reaktionen zusammen.

Heutzutage hat sich das Interesse, auch aufgrund besserer analytischer Methoden und komplexerer Reaktionen, von der „Synthese um jeden Preis“ auf nachhaltige, ökonomische und schritteffiziente Synthesen verlagert.^[77] Wie Lowe bereits zur klassischen Totalsynthese gesagt hat: „*We have so many synthetic techniques now, compared to the Woodward days, that most molecules can be banged out one way or another if you're willing to throw enough post-docs at them.*“^[78] Das Feld der Totalsynthese hat sich jedoch auch weiterentwickelt und unter Naturstoffchemikern keineswegs an Relevanz verloren. Wie Stork bereits 1978 kommentierte: „*We have travelled far since 1828, and the interest attached to total synthesis has disappeared.*“
Thus spoke the leading organic chemist of the time in his Pedler Lecture in 1936. „This statement was not really true in 1936. It will still not be true in a hundred years.“^[79] Hierbei rücken in der modernen Naturstoffsynthese oftmals divergente Synthesekonzepte, welche große Strukturklassen z. B. ausgehend von synthetischen Intermediate erschließen können, im Vergleich zu langen Synthesen von einzelnen komplexen, jedoch anderweitig uninteressanten Molekülen, in den Fokus.

Wie ein Vergleich der Totalsynthese von Spirochensilid A (37) durch Yang (Kapitel 1.3.2.1) mit unserer Semisynthese (siehe Anhang A) zeigt, können Semisynthesen diese Kriterien, welche für „interessante“ Totalsynthesen gestellt wurden, erfüllen und signifikante Einsparungen in der Schrittzahl und Ökonomie erreichen. Gleichzeitig können biosynthetisch nahe Intermediate generiert werden, welche als Ausgangspunkte für weitere Naturstoffsynthesen genutzt oder für die Untersuchung von „structure-activity-relationships“ (SARs) verwendet werden können. Ein guter Syntheseplan ist dabei jedoch essenziell. Ein solcher kann, wie in dieser Arbeit gezeigt, durch Inspiration von der vermuteten Biogenese und coisolierten Molekülen (Biogeneseraum-geleitete Analyse) formuliert werden. Ein Umdenken zur klassischen Annahme der vollständig polaren Biogenese muss zusätzlich geschehen, um neue effiziente Transformationen auf Basis von intrinsischer Reaktivität zu planen und umzusetzen.

Während die in dieser Arbeit gezeigte Synthese des Asperfloketals A (64)^[73] oder die neulich publizierte Synthese des Penicillitons (98)^[80] gute Beispiele für biomimetische polare Reaktionen sind, können weitere Synthesen aus der Gruppe um Heretsch zeigen, dass auch radikalische Transformationen plausible biomimetische Umlagerungen zur Generierung von *abeo*-Steroiden liefern können (Abb. 3.1). Einige

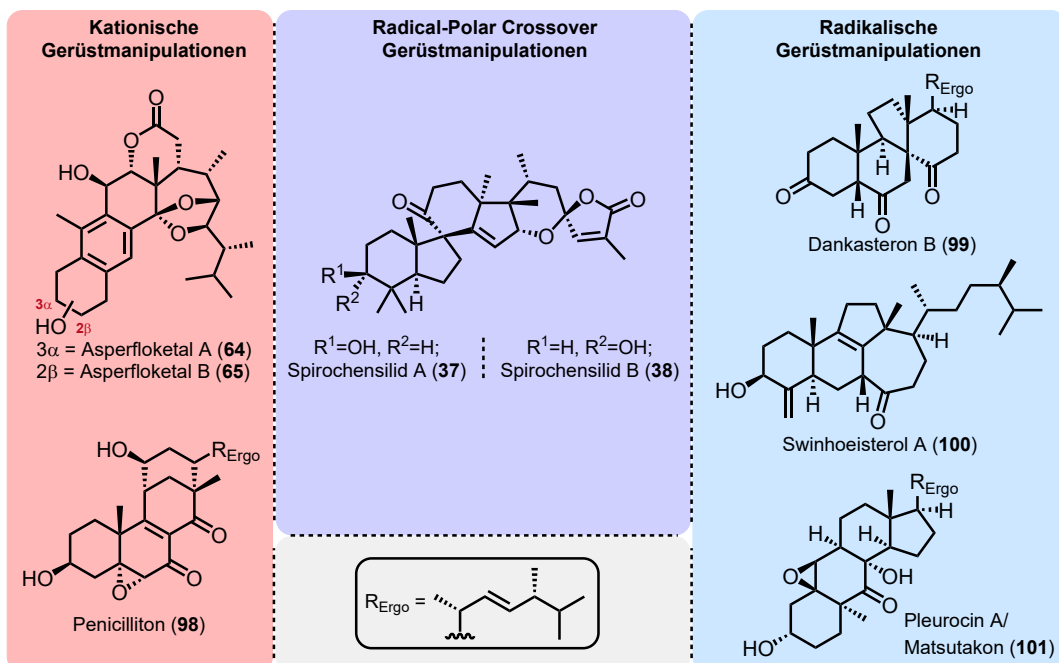


Abbildung 3.1. Beispiele für umgelagerte terpenoide Naturstoffe die in der Gruppe um Heretsch mittels kationischer, radikalischer und radical-polar crossover-Gerüstmanipulationen aufgebaut wurden.

Beispiele hierfür sind die Synthesen von Dankasteron B (99),^[81] Swinhoeosterol A (100)^[81] und Pleurocin A/Matsutakon (101)^[82](siehe Anhang C).

Die Kombination aus radikalischen und polaren Mechanismen war zuvor nahezu ausschließlich in der Photo-Redox-Chemie, unter Verwendung von Elektronentransferkatalysatoren^[83–85] und der Elektrochemie^[86] anzutreffen. Mit der in dieser Arbeit gezeigten Synthese der Spirochensilide, konnte nun auch ein Beispiel für eine biomimetische Synthese mit einem sogenannten „Radical-Polar Crossover“-Event gezeigt werden.^[43] Dieser Schlüsselschritt der Synthese führte somit beide Mechanismen zusammen und erlaubte es eine kationische Umlagerung durch Initiierung unter milden H-Atom Transfer-Bedingungen (HAT) durchzuführen. Die Verbindung von polaren und radikalischen Mechanismen kann in Zukunft, zusammen mit der Biogeneseraum-geleitete Analyse, zur Realisierung von zuvor im Labor für nicht möglich gehaltenen Umlagerungen führen, ein besseres Verständnis von biosynthetischen Vorgängen liefern und damit das Feld der Naturstoffsynthese, besonders der von terpenoiden Naturstoffen, weiterentwickeln.

Literaturverzeichnis

- [1] A. G. Atanasov, S. B. Zotchev, V. M. Dirsch, C. T. Supuran, *Nat. Rev. Drug Discov.* **2021**, *20*, 200–216.
- [2] A. Sultan, *Med. chem.* **2015**, *5*, 310–317.
- [3] G. Habermehl, P. E. Hammann, H. C. Krebs, W. Ternes, *Naturstoffchemie: Eine Einführung*, Springer-Lehrbuch, 3. Aufl., Springer, Berlin und Heidelberg, **2008**.
- [4] R. Calfee, P. Fadale, *Pediatrics* **2006**, *117*, 577–589.
- [5] E. R. Freeman, D. A. Bloom, E. J. McGuire, *J. Urol.* **2001**, *165*, 371–373.
- [6] D. Sica, D. Musumeci, *Steroids* **2004**, *69*, 743–756.
- [7] N. A. McGrath, M. Brichacek, J. T. Njardarson, *J. Chem. Educ.* **2010**, *87*, 1348–1349.
- [8] L. Parente, *BMC Pharmacol. Toxicol.* **2017**, *18*, 1–8.
- [9] *The selection and use of essential medicines: Report of the WHO Expert Committee, 2017 (including the 20th WHO Model List of Essential Medicines and the 6th WHO ModelList of Essential Medicines for Children)*, Bd. 1006 von WHO technical report series, WHO, Geneva, **2017**.
- [10] M. Bohl, *Molecular Structure and Biological Activity of Steroids*, 1. Aufl., CRC Press, Milton, **2018**.
- [11] E. Breitmaier, *Terpene: Aromen, Düfte, Pharmaka, Pheromone*, 2. Aufl., Wiley-VCH, Weinheim, **2005**.
- [12] G. P. Moss, *Pure and Applied Chemistry* **1989**, *61*, 1783–1822.
- [13] M. W. Huff, D. E. Telford, *Trends Pharmacol. Sci.* **2005**, *26*, 335–340.
- [14] A. Zorea, *Steroids*, Health and Medical Issues Today Ser, ABC-CLIO, Santa Barbara, **2014**.
- [15] L. J. Mulheirn, P. J. Ramm, *Chem. Soc. Rev.* **1972**, *1*, 259–291.
- [16] G. D. Brown, *Nat. Prod. Rep.* **1998**, *15*, 653–696.
- [17] M. K. Dhar, A. Koul, S. Kaul, *N. Biotechnol.* **2013**, *30*, 114–123.
- [18] M. V. D'Auria, L. Minale, R. Riccio, *Chem. Rev.* **1993**, *93*, 1839–1895.
- [19] K. Gasi, M. Sakac, S. Jovanovic-Santa, E. Djurendic, *Curr. Org. Chem.* **2014**, *18*, 216–259.
- [20] A. W. Norman, *Am. J. Clin. Nutr.* **2008**, *88*, 491–499.
- [21] S.-Q. Fan, C.-L. Xie, J.-M. Xia, C.-P. Xing, Z.-H. Luo, Z. Shao, X.-J. Yan, S. He, X.-W. Yang, *Org. Biomol. Chem.* **2019**, *17*, 5925–5928.
- [22] H.-Y. Tian, L.-J. Ruan, T. Yu, Q.-F. Zheng, N.-H. Chen, R.-B. Wu, X.-Q. Zhang, L. Wang, R.-W. Jiang, W.-C. Ye, *J. Nat. Prod.* **2017**, *80*, 1182–1186.
- [23] J. Gong, P. Sun, N. Jiang, R. Riccio, G. Lauro, G. Bifulco, T.-J. Li, W. H. Gerwick, W. Zhang, *Org. Lett.* **2014**, *16*, 2224–2227.

- [24] P. Heretsch, S. Rabe, A. Giannis, *J. Am. Chem. Soc.* **2010**, *132*, 9968–9969.
- [25] IUPAC Commission on the Nomenclature of Organic Chemistry, *Eur. J. Biochem.* **1978**, *86*, 1–8.
- [26] X.-W. Yang, S.-M. Li, L. Wu, Y.-L. Li, L. Feng, Y.-H. Shen, J.-M. Tian, J. Tang, N. Wang, Y. Liu, W.-D. Zhang, *Org. Biomol. Chem.* **2010**, *8*, 2609–2616.
- [27] W. Wu, X. Chen, Y. Liu, Y. Wang, T. Tian, X. Zhao, J. Li, H. Ruan, *Phytochemistry* **2016**, *130*, 301–312.
- [28] E. J. Corey, B. Hong, *J. Am. Chem. Soc.* **1994**, *116*, 3149–3150.
- [29] W. Steglich, M. Klaar, L. Zechlin, H. J. Hecht, *Angew. Chem. Int. Ed.* **1979**, *18*, 698.
- [30] A. Murai, N. Tanimoto, N. Sakamoto, T. Masamune, *J. Am. Chem. Soc.* **1988**, *110*, 1985–1986.
- [31] E. J. Corey, I. N. Houpis, *J. Am. Chem. Soc.* **1990**, *112*, 8997–8998.
- [32] Y. Shiina, Y. Tomata, M. Miyashita, K. Tanino, *Chem. Lett.* **2010**, *39*, 835–837.
- [33] L. M. M. Vieira, A. Kijjoa, R. Wilairat, M. S. J. Nascimento, L. Gales, A. M. Damas, A. M. S. Silva, I.-O. Mondranondra, W. Herz, *J. Nat. Prod.* **2004**, *67*, 2043–2047.
- [34] L. M. M. Vieira, A. Kijjoa, R. Wilairat, M. S. J. Nascimento, L. Gales, A. M. Damas, A. M. S. Silva, I.-O. Mondranondra, W. Herz, *J. Nat. Prod.* **2005**, *68*, 969–970.
- [35] Q.-Q. Zhao, Q.-Y. Song, K. Jiang, G.-D. Li, W.-J. Wei, Y. Li, K. Gao, *Org. Lett.* **2015**, *17*, 2760–2763.
- [36] X.-T. Liang, J.-H. Chen, Z. Yang, *J. Am. Chem. Soc.* **2020**, *142*, 8116–8121.
- [37] Y.-L. Li, X.-W. Yang, S.-M. Li, Y.-H. Shen, H.-W. Zeng, X.-H. Liu, J. Tang, W.-D. Zhang, *J. Nat. Prod.* **2009**, *72*, 1065–1068.
- [38] Y.-L. Li, Y.-X. Gao, X.-W. Yang, H.-Z. Jin, J. Ye, L. Simmons, N. Wang, A. Steinmetz, W.-D. Zhang, *Phytochemistry* **2012**, *81*, 159–164.
- [39] Q.-Q. Zhao, S.-F. Wang, Y. Li, Q.-Y. Song, K. Gao, *Fitoterapia* **2016**, *111*, 87–94.
- [40] W.-J. Wei, Q.-Y. Song, J.-C. Ying, H.-Y. Li, K.-L. Ma, Y. Li, Y. Li, K. Gao, *J. Nat. Prod.* **2019**, *82*, 2859–2869.
- [41] S. S. Thorat, R. Kontham, *Org. Biomol. Chem.* **2019**, *17*, 7270–7292.
- [42] X. Chen, X. Shao, W. Li, X. Zhang, B. Yu, *Angew. Chem. Int. Ed.* **2017**, *56*, 7648–7652.
- [43] M. Alekseychuk, S. Adrian, R. C. Heinze, P. Heretsch, *J. Am. Chem. Soc.* **2022**, *144*, 11574–11579.
- [44] X. Long, J. Li, F. Gao, H. Wu, J. Deng, *J. Am. Chem. Soc.* **2022**, *144*, 16292–16297.
- [45] W. Nes, E. Mosettig, *J. Am. Chem. Soc.* **1954**, *76*, 3182–3186.
- [46] H. Koshino, T. Yoshihara, S. Sakamura, T. Shimanuki, T. Sato, A. Tajimi, *Phytochemistry* **1989**, *28*, 771–772.
- [47] S. Kosemura, S. Uotsu, S. Yamamura, *Tetrahedron Lett.* **1995**, *36*, 7481–7482.
- [48] T. Nakada, S. Yamamura, *Tetrahedron* **2000**, *56*, 2595–2602.
- [49] X. Luo, F. Li, P. B. Shinde, J. Hong, C.-O. Lee, K. S. Im, J. H. Jung, *J. Nat. Prod.* **2006**, *69*, 1760–1768.
- [50] X.-H. Liu, F.-P. Miao, X.-R. Liang, N.-Y. Ji, *Nat. Prod. Rep.* **2014**, *28*, 1182–1186.

- [51] D. Wakana, T. Itabashi, K.-I. Kawai, T. Yaguchi, K. Fukushima, Y. Goda, T. Hosoe, *J. Antibiot.* **2014**, *67*, 585–588.
- [52] F.-R. Jiao, B.-B. Gu, H.-R. Zhu, Y. Zhang, K.-C. Liu, W. Zhang, H. Han, S.-H. Xu, H.-W. Lin, *J. Org. Chem.* **2021**, *86*, 10954–10961.
- [53] L. Liu, F.-F. Duan, Y. Gao, X.-G. Peng, J.-L. Chang, J. Chen, H.-L. Ruan, *Org. Lett.* **2021**, *23*, 9620–9624.
- [54] A. van Cao, J.-H. Kwon, J. S. Kang, H.-S. Lee, C.-S. Heo, H. J. Shin, *J. Nat. Prod.* **2022**, *85*, 2177–2183.
- [55] J. W. Cook, G. A. D. Haslewood, *Chem. Ind.-Lond.* **1934**, *53*, 507–508.
- [56] G. Barry, J. W. Cook, G. A. D. Haslewood, C. L. Hewett, I. Hieger, E. L. Kennaway, *Proc. R. Soc. Lond. B* **1934**, *117*, 318–351.
- [57] W. R. Nes, E. Mosettig, *J. Am. Chem. Soc.* **1954**, *76*, 3186–3188.
- [58] W. R. Nes, *J. Am. Chem. Soc.* **1956**, *78*, 193–198.
- [59] W. R. Nes, R. B. Kostic, E. Mosettig, *J. Am. Chem. Soc.* **1956**, *78*, 436–440.
- [60] W. R. Nes, J. A. Steele, E. Mosettig, *J. Am. Chem. Soc.* **1958**, *80*, 5230–5232.
- [61] W. R. Nes, J. A. Steele, E. Mosettig, *J. Am. Chem. Soc.* **1958**, *80*, 5233–5235.
- [62] W. R. Nes, D. L. Ford, *J. Am. Chem. Soc.* **1961**, *83*, 4811–4815.
- [63] K. Tsuda, R. Hayatsu, J. A. Steele, O. Tanaka, E. Mosettig, *J. Am. Chem. Soc.* **1963**, *85*, 1126–1131.
- [64] O. Tanaka, E. Mosettig, *J. Am. Chem. Soc.* **1963**, *85*, 1131–1133.
- [65] J. A. Steele, L. A. Cohen, E. Mosettig, *J. Am. Chem. Soc.* **1963**, *85*, 1134–1138.
- [66] W. R. Nes, D. L. Ford, *J. Am. Chem. Soc.* **1963**, *85*, 2137–2141.
- [67] N. Bosworth, J. M. Midgley, C. J. Moore, W. B. Whalley, G. Ferguson, W. C. Marsh, *J. Chem. Soc., Chem. Commun.* **1974**, 719.
- [68] N. Bosworth, A. Emke, J. M. Midgley, C. J. Moore, W. B. Whalley, G. Ferguson, W. C. Marsh, *J. Chem. Soc., Perkin Trans. 1* **1977**, 805–809.
- [69] G. Hussler, P. Albrecht, *Nature* **1983**, *304*, 262–263.
- [70] R. B. Woodward, T. Singh, *J. Am. Chem. Soc.* **1950**, *72*, 494–500.
- [71] R. C. Heinze, D. Lentz, P. Heretsch, *Angew. Chem. Int. Ed.* **2016**, *55*, 11656–11659.
- [72] T. C. McMorris, P. A. Patil, *J. Org. Chem.* **1993**, *58*, 2338–2339.
- [73] M. Alekseychuk, P. Heretsch, *J. Am. Chem. Soc.* **2022**, *144*, 21867–21871.
- [74] M. D. Kolesnikova, Q. Xiong, S. Lodeiro, L. Hua, S. P. T. Matsuda, *Arch. Biochem. Biophys.* **2006**, *447*, 87–95.
- [75] M. Suzuki, T. Xiang, K. Ohyama, H. Seki, K. Saito, T. Muranaka, H. Hayashi, Y. Katsume, T. Kushiro, M. Shibuya, Y. Ebizuka, *Plant Cell Physiol.* **2006**, *47*, 565–571.
- [76] K. Ohyama, M. Suzuki, J. Kikuchi, K. Saito, T. Muranaka, *Proc. Natl. Acad. Sci. U.S.A.* **2009**, *106*, 725–730.
- [77] J. Mulzer, *Nat. Prod. Rep.* **2014**, *31*, 595–603.

- [78] D. Lowe, *How Healthy is the Field of Total Synthesis?* In *the pipeline 2015*, <https://www.science.org/content/blog-post/healthy-field-total-synthesis>, zuletzt eingesehen am 05.03.2023.
- [79] G. Stork, Roussel Prize Award Adress, Institute Scientific, Paris, France **1978**.
- [80] M. Bauer, P. Heretsch, *Synthesis* **2023**, DOI: 10.1055/s-0042-1751422.
- [81] F. L. Duecker, R. C. Heinze, P. Heretsch, *J. Am. Chem. Soc.* **2020**, *142*, 104–108.
- [82] R. C. Heinze, P. Heretsch, *J. Am. Chem. Soc.* **2019**, *141*, 1222–1226.
- [83] L. Pitzer, J. L. Schwarz, F. Glorius, *Chem. Sci.* **2019**, *10*, 8285–8291.
- [84] S. Sharma, J. Singh, A. Sharma, *Adv. Synth. Catal.* **2021**, *363*, 3146–3169.
- [85] R. J. Wiles, G. A. Molander, *Isr. J. Chem.* **2020**, *60*, 281–293.
- [86] Y.-F. Tan, D. Yang, Y.-N. Zhao, J.-F. Lv, Z. Guan, Y.-H. He, *Green Chem.* **2023**, *25*, 1540–1545.

Anhang

Berechtigungen für die Verwendung der Publikationen

Biogenesis-Inspired, Divergent Synthesis of Spirochensilide A, Spirochensilide B, and Abifarane B Employing a Radical-Polar Crossover Rearrangement Strategy



Author: Mykhaylo Alekseychuk, Sinan Adrian, Robert C. Heinze, et al

Publication: Journal of the American Chemical Society

Publisher: American Chemical Society

Date: Jul 1, 2022

Copyright © 2022, American Chemical Society

PERMISSION/LICENSE IS GRANTED FOR YOUR ORDER AT NO CHARGE

This type of permission/license, instead of the standard Terms and Conditions, is sent to you because no fee is being charged for your order. Please note the following:

- Permission is granted for your request in both print and electronic formats, and translations.
- If figures and/or tables were requested, they may be adapted or used in part.
- Please print this page for your records and send a copy of it to your publisher/graduate school.
- Appropriate credit for the requested material should be given as follows: "Reprinted (adapted) with permission from {COMPLETE REFERENCE CITATION}. Copyright {YEAR} American Chemical Society." Insert appropriate information in place of the capitalized words.
- One-time permission is granted only for the use specified in your RightsLink request. No additional uses are granted (such as derivative works or other editions). For any uses, please submit a new request.

If credit is given to another source for the material you requested from RightsLink, permission must be obtained from that source.

[BACK](#)

[CLOSE WINDOW](#)

Chemical Emulation of the Biosynthetic Route to Anthrasteroids: Synthesis of Asperfloketal A



Author: Mykhaylo Alekseychuk, Philipp Heretsch

Publication: Journal of the American Chemical Society

Publisher: American Chemical Society

Date: Dec 1, 2022

Copyright © 2022, American Chemical Society

PERMISSION/LICENSE IS GRANTED FOR YOUR ORDER AT NO CHARGE

This type of permission/license, instead of the standard Terms and Conditions, is sent to you because no fee is being charged for your order. Please note the following:

- Permission is granted for your request in both print and electronic formats, and translations.
- If figures and/or tables were requested, they may be adapted or used in part.
- Please print this page for your records and send a copy of it to your publisher/graduate school.
- Appropriate credit for the requested material should be given as follows: "Reprinted (adapted) with permission from {COMPLETE REFERENCE CITATION}. Copyright {YEAR} American Chemical Society." Insert appropriate information in place of the capitalized words.
- One-time permission is granted only for the use specified in your RightsLink request. No additional uses are granted (such as derivative works or other editions). For any uses, please submit a new request.

If credit is given to another source for the material you requested from RightsLink, permission must be obtained from that source.

[BACK](#)

[CLOSE WINDOW](#)

Title:

Biogenesis-Inspired, Divergent Synthesis of Spirochensilide A, Spirochensilide B, and Abifarine B Employing a Radical-Polar Crossover Rearrangement Strategy

Type of authorship:

First Author

Type of article:

Communication

Share of work:

40% Mykhaylo Alekseychuk
40% Sinan Adrian
10% Robert C. Heinze
10% Philipp Heretsch

Contribution to the publication:

This project was designed by Mykhaylo Alekseychuk, Sinan Adrian, Robert C. Heinze and Philipp Heretsch.

The synthetic work and analytical characterizations were carried out by Mykhaylo Alekseychuk, Sinan Adrian and Robert C. Heinze.

The manuscript was prepared by Mykhaylo Alekseychuk, Sinan Adrian and Philipp Heretsch.

Journal:

Journal of the American Chemical Society

5-Year-impact factor:

14.690 (Academic Accelerator)

Date of publication:

21.06.2022

Number of citations:

5

DOI:

10.1021/jacs.2c05358

PubMed-ID:

35729679

Reprinted with permission from M. Alekseychuk, S. Adrian, R. C. Heinze and P. Heretsch, *J. Am. Chem. Soc.* **2022** 144, 11574-11579. Copyright 2023 American Chemical Society.

Biogenesis-Inspired, Divergent Synthesis of Spirochensilide A, Spirochensilide B, and Abifarane B Employing a Radical-Polar Crossover Rearrangement Strategy

Mykhaylo Alekseychuk,[†] Sinan Adrian,[†] Robert C. Heinze, and Philipp Heretsch*



Cite This: *J. Am. Chem. Soc.* 2022, 144, 11574–11579



Read Online

ACCESS |

Metrics & More

Article Recommendations

Supporting Information

ABSTRACT: Triterpenoids and related *abeo*-steroids are of interest to the scientific community for their potent and varied biological activities as well as their unique structures. Within this large and diverse family of natural products, the fir metabolites (−)-spirochensilide A and B are particularly noteworthy for their controversial biogenesis. We herein report the chemical synthesis of the spirochensilides, which involves a concerted sequence of bioinspired rearrangements contributing to its resolution. Points of divergence after each rearrangement step also allow for an approach to the abifarane family of natural products with abifarane B as a synthetic target. Key to this strategy is a radical-polar crossover event to initiate the first rearrangement without the need for a sacrificial functionality to be introduced beforehand.

The design of efficient and selective synthetic strategies toward complex natural products has always been a showcase for the maturity of organic chemistry.¹ The development of novel methods and the access of previously elusive chemical entities with novel reactivity have been indispensable tools toward this goal. On the other hand, the almost overwhelming complexity of terpenoid natural products is accessed by nature with a rather small armament of transformations. As such, the enzymatically orchestrated cyclization and rearrangement cascades in the biogenesis of triterpenoids and steroids are exceptional examples. Thus, cation polyene cyclizations in combination with Wagner–Meerwein methanide and hydride shifts create these topologically complex, polycyclic structures. Consequentially and where validated intermediates and enzymes are unknown, biogenesis proposals typically invoke polar mechanisms involving ionic intermediates to account for topology-changing steps.

To investigate divergent innate reactivity for potentially biomimetic triterpenoid synthesis, we have been probing the propensity of coisolated precursors and related species to undergo radical-mediated processes and came to the realization that highly efficient and selective radical rearrangements can indeed provide access to this class of natural products. As such and reported for our routes to swinhoeisterol A, dankasterones A and B, and periconiastone A, an alkoxy radical-initiated Dowd–Beckwith rearrangement was employed.² In our efforts toward strophasterol A,³ pleurocine A/matsukatone, and pleurocine B,⁴ radical cyclization was key to forge complex topologies with complete stereoselectivity.

However, building solely upon radical processes for skeletal rearrangements toward complex triterpenoids unnecessarily confines our chemical room to maneuver since powerful cationic rearrangements are no longer accessible.

Hence, we now started to investigate radical-initiated processes, which involve a radical-polar crossover event and, thus, unlock cationic rearrangements under mild hydrogen atom transfer (HAT) conditions. This strategy may provide a relay and unify polar and radical-mediated entries.

Within this respect, the spirochensilide class of natural products with their $10(9 \rightarrow 8)abeo$ -17,14-friedolanostane framework struck our attention (**Scheme 1**). These plant metabolites were first isolated and structurally elucidated in 2015 from the fir *Abies chensiensis*. NMR-spectroscopic, MS, and X-ray crystallographic analyses combined with computational methods were used to elucidate the structure and absolute configuration of spirochensilide A (**1**).⁵ Li and co-workers⁵ also reported spirochensilide B (**2**), the 3-epimer of **1**. Structurally, the spirochensilide natural products exhibit two eponymous spirocyclic motifs, one spiro[4.5]decane and one 1,6-dioxaspiro[4.5]decene. Besides, two methyl groups have formally shifted to C14 and C17 (17,14-friedolanostane type)⁶ from their respective C13 and C14 positions in lanosterol, pointing at the latter as a plausible biogenetic precursor, which has been proven to be possible for other phytosterols.⁷

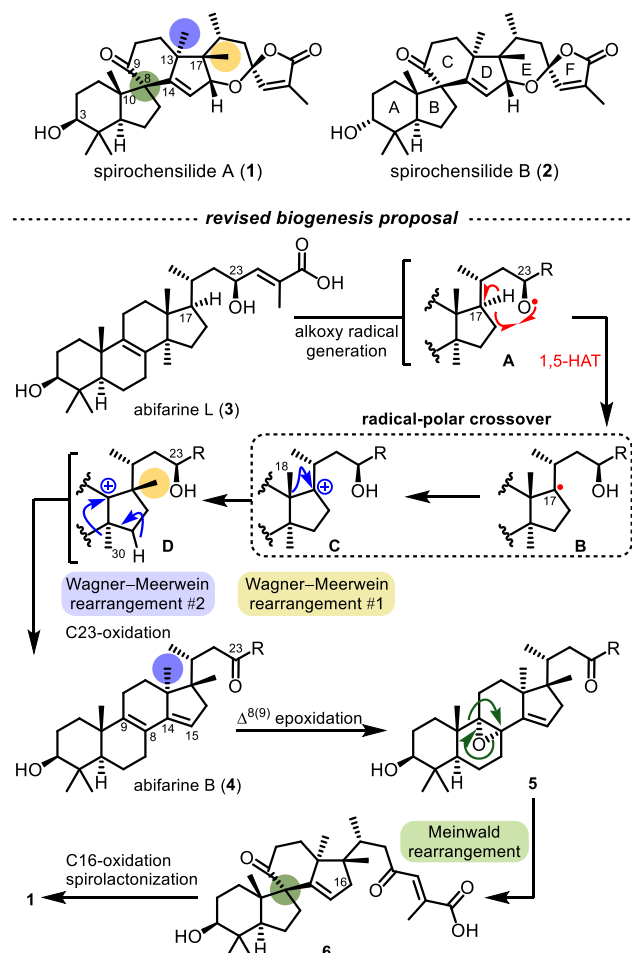
A biosynthesis proposal was put forward by the isolation team consisting of a Meinwald rearrangement of a coisolated lanostane epoxide to give the $10(9 \rightarrow 8)abeo$ -motif, followed by two Wagner–Meerwein methanide shifts to install the 17,14-friedo-motif (see structures **C** and **D**, **Scheme 1**). Further oxidation and cyclization steps would then be necessary to yield the spirochensilides. Interestingly and in

Received: May 20, 2022

Published: June 21, 2022



Scheme 1. Structures of Spirochensilide A and B and Revised Biogenesis Proposal^a



^aHAT: hydrogen atom transfer.

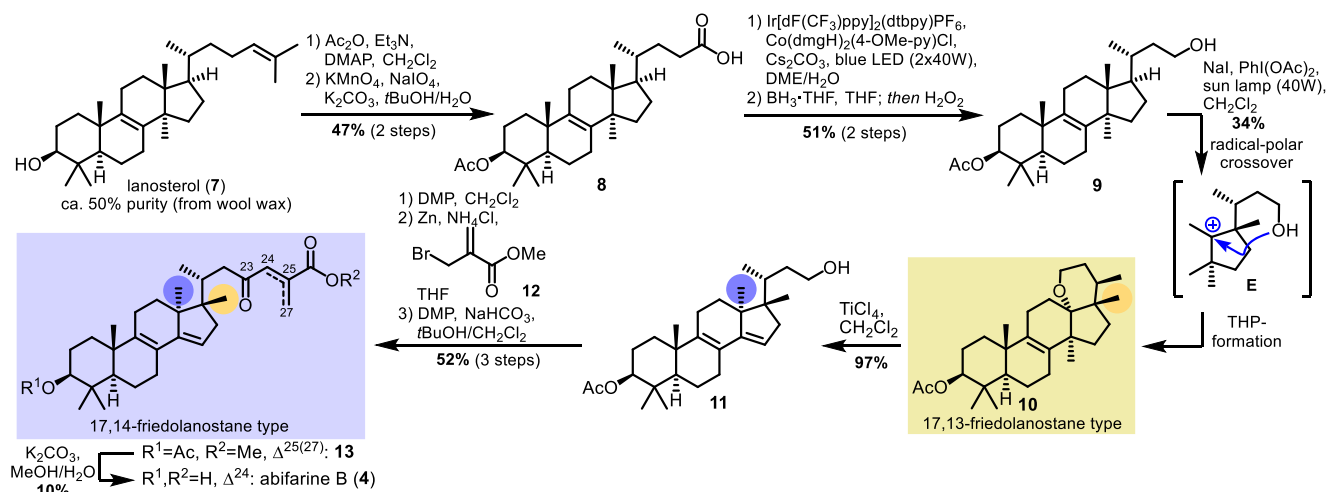
contrast to this proposal, Li and Gao investigated the Meinwald rearrangement of a lanosterol epoxide with the result of disproving its feasibility under a variety of conditions.⁵

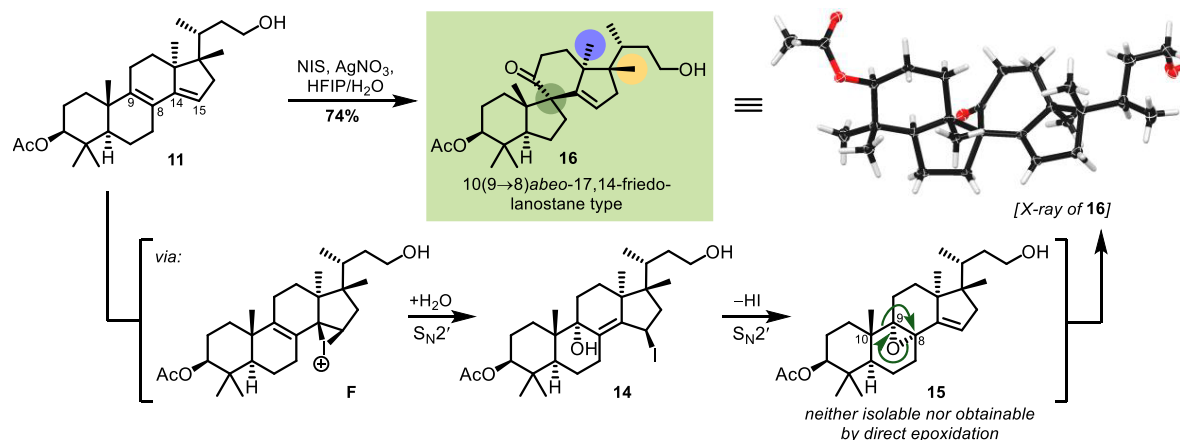
When searching for potential biogenetically related natural products to the spirochensilides, we identified the rather large class of abifarnes⁸ and neoabiestrines⁹ as well as several, yet unnamed, compounds isolated from *Garcinia* species.¹⁰ While for the abifarnes and neoabiestrines [e.g., abifarane B (4)] only 17,13- (18-Me shifted to C17) and 17,14-friedolanostane structures have been reported, the unnamed *Garcinia* metabolites also, and only in addition to 17,14-friedolanostanes, possess the 10(9 → 8)abeo-motif. Notably, no examples for 10(9 → 8)abeo-lanostane or 10(9 → 8)abeo-17,13-friedolanostane metabolites could be found. We, thus, reasoned that the biosynthetic order of rearrangement events may be reverse to the original proposal; i.e., the Wagner–Meerwein methanide shifts precede the Meinwald rearrangement in a consecutive fashion and not as a cascade event. Since Wagner–Meerwein shifts in triterpenoid biosynthesis are known to be energetically “uphill”,¹¹ the stepwise character is in agreement with this realization. Thus and as depicted in Scheme 1, a potential precursor for the spirochensilides is abifarane L (3). Enzymatically orchestrated Wagner–Meerwein shifts lead to abifarane B (4), which in turn undergoes a Meinwald rearrangement (5 → 6).

To initiate this process, activation of C17 and formation of a carbenium ion in this position is necessary. While hydroxylation of C17 presents an option, we reasoned that the proximal hydroxyl at C23 in abifarane L (3) may play a role in this process. Thus and returning to our original rationale, a 1,5-HAT by an initial alkoxy radical A at C23 could, in a radical–polar crossover event (B → C), furnish the desired carbenium ion for the required methanide shifts via D.¹² The C23 hydroxy moiety may or may not be oxidized in the process, as examples for 23-oxo metabolites (e.g., abifarane B)⁸ as well as for 23-hydroxy metabolites (unnamed natural products from *Garcinia* species) are known.¹⁰

A primary alcohol (structure A, Scheme 1, R = H) was chosen to chemically probe and emulate this proposal and,

Scheme 2. Chemical Emulation of the Wagner–Meerwein Rearrangements and Synthesis of Abifarane B^a



Scheme 3. Chemical Emulation of the Meinwald Rearrangement^a

^aNIS: *N*-iodosuccinimide; HFIP: hexafluoro-2-propanol.

thereby, also allow for access to other members of this family of natural products by late-stage side-chain manipulation. Starting from the literature known carboxylic acid **8**,¹³ we briefly revisited its efficient preparation from technical grade lanosterol (7, 50% purity); the results showed that a modified protocol for the acetylation/Lemieux–von Rudloff oxidative scission could remove the main impurities agnosterol and 24,25-dihydrolanosterol on sufficiently large scale (Scheme 2). The use of Ritter's photocatalytic decarboxylative olefination protocol¹⁴ then resulted in a clean conversion into a terminal olefin (structure not shown) without the need of stoichiometric heavy metal oxidants [e.g., Pb(OAc)₄/Cu(OAc)₂.¹³] Hydroboration/oxidation of the latter gave model substrate **9** in 24% yield over 4 steps. The switch to other boranes (e.g., 9-BBN, Si₂BH, Thexyl₂BH) did not improve the yield.

Toward a viable radical-polar crossover event, we then studied several conditions for the generation of primary alkoxy radicals, among them HgO, Pb(OAc)₄, PhI(OAc)₂, or PhI(CF₃COO)₂ with I₂, as well as (photocatalytic) protocols after derivatization of the alcohol moiety.¹⁵ Eventually, only the combination of PhI(OAc)₂ with NaI as an additive gave,¹⁶ under carefully controlled irradiation conditions (45 W white spectrum lamp, 10 °C, 4 h), an appreciable amount of a methanide shifted product.

Further NMR-spectroscopic analysis revealed its 17,13-friedolanostane structure **10** and, additionally, the presence of a tetrahydropyran. Thus, the intermediary C13 carbonium ion **E** was intercepted by the primary hydroxy moiety at C23. The application of Lewis acid (TiCl₄) then initiated the second methanide shift¹⁷ to 17,14-friedolanostane **11** in almost quantitative yield.

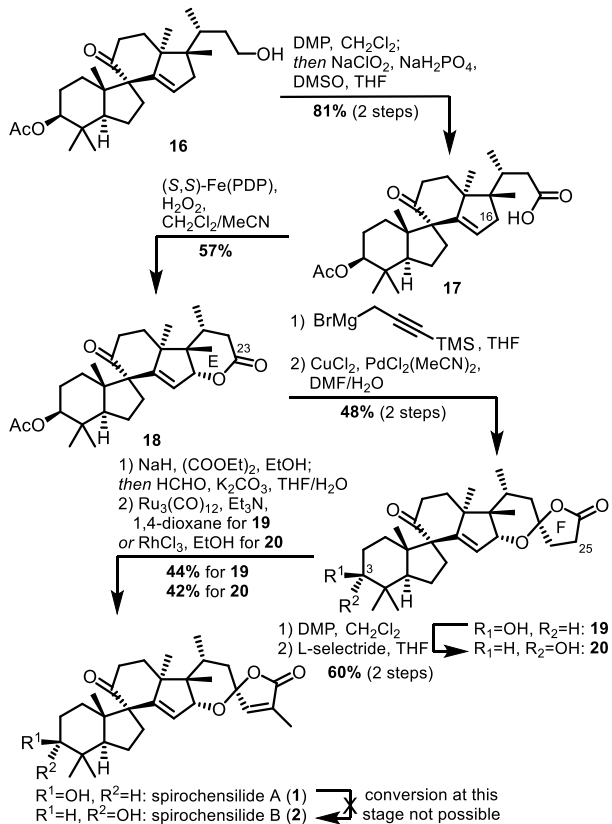
To access abifarine B (**4**) from **11**, oxidation with Dess–Martin periodinane and addition of the allylzinc reagent generated from methyl bromo methacrylate (**12**) gave an inconsequential 1:1 mixture of epimers at C23, the further oxidation of which (DMP, buffered with NaHCO₃) furnished ketone **13**. Treatment of the latter with aqueous base (K₂CO₃) then led to isomerization of the Δ²⁵⁽²⁷⁾ bond into the 24,25-position under concomitant cleavage of the methyl ester and the acetyl group and accomplished the first synthesis of abifarine B (**4**) in 7 steps from the previously described terminal alkene.¹³

We went on to study the Meinwald rearrangement on 17,14-friedolanostane **11**. Toward this goal, selective formation of an α-8,9-epoxide of type **15** was necessary since only this epoxide possesses the stereoelectronic prerequisites for the desired Meinwald rearrangement to occur (Scheme 3). The initial epoxidation experiments employing a wide range of reagents (e.g., *m*CPBA, MMPP, DMDO, or trifluoroperacetic acid) revealed the innate reactivity of diene **11** to form a β-14,15-epoxide instead (displaying both the undesired regio- and stereoselectivity), which upon exposure to air, immediately formed a hydroperoxide (for details, see the Supporting Information). Utilizing this reactivity, we started investigating the propensity of diene **11** for halohydrin formation. We rationalized the initial formation of an iodonium species **F** (displaying the identical regio- and stereoselectivity as for our direct epoxidation experiments), followed by the attack of water in a vinylogous manner to give halohydrin **14**. Upon prolonged reaction time, the latter only transformed into a complex mixture of undesired products (for more details, see the Supporting Information), and only minute amounts (<5%) of a 10(9 → 8)abeo-lanostane could be isolated. Hence, the desired α-8,9-epoxide **15** only formed in small amounts from **14**, a notion that led us to search for reaction conditions more strongly favoring an intramolecular S_N2' pathway for displacement of the iodide in **14**. After extensive experimentation, using aqueous AgNO₃ in hexafluoroisopropanol (HFIP) as the main solvent resulted in the almost exclusive formation of the desired 10(9 → 8)abeo-17,14-friedolanostane **16** in 74% isolated yield. These conditions may also allow for a direct formation of **16** from **14** through vinylogous semipinacol rearrangement. The absolute configuration of **16** was then unequivocally established by X-ray crystallographic analysis.

Having established these three consecutive rearrangements and demonstrated the validity of our biogenetic hypothesis, we finally aimed at the completion of the synthesis of the spirochensilides (Scheme 4).

Thus, allylic oxidation of the 16-position followed by E ring formation had to be achieved next. Initially, the introduction of a hydroxy group in this position was studied. Although under most conditions [e.g., Mn(OAc)₃/tBuOOH, Rh₂(cap)₄/tBuOOH, PDC, or CrO₃·3,5-dimethylpyrazole] C16 oxidation products could be isolated, both the yield and the selectivity fell short of our expectations (for details, see the Supporting

Scheme 4. Completion of the Synthesis of Spirochensilide A and B^a



^a Fe(PDP): *N,N'*-bis(2-pyridylmethyl)-2,2'-bipyrrolidine-bis(acetonitrile)iron(II); TMS: trimethylsilyl.

Information. We then turned our attention toward a direct allylic oxidative lactonization and, for this purpose, oxidized the primary alcohol **16** under standard conditions to carboxylic acid **17**. Treatment of the latter with Rh₂(esp)₄/tBuOOH indeed gave up to 36% of lactone **18**. Further experimentation could then identify the White–Chen catalytic system¹⁸ [Fe(PDP) and H₂O₂] to provide the desired lactone **18** in a superior and reproducible yield. Notably, the use of the (*S,S*)-enantiomer of the catalyst provided **18** in 57% yield, while the (*R,R*)-enantiomer only gave 33% yield. From lactone **18**, a wide spectrum of methods for the introduction of the remaining 1,6-dioxaspiro[4.5]decene (F ring) was investigated. Among the conditions studied, a direct approach by the Dreiding–Schmidt reaction¹⁹ with the allylzinc species of methyl bromo methacrylate (**12**) failed, as did all olefination attempts or the addition of 2-methylallylmagnesium bromide and other sterically demanding metal organyls (for details, see the Supporting Information).

Since both methylmagnesium bromide and allylmagnesium bromide could be successfully introduced and led to a single hemiacetal product without any double addition or reaction with the sterically hindered oxo moiety at C9, we sought for a Grignard reagent that would allow for a straightforward lactone formation. Toward this end, silylated propargylmagnesium bromide was identified to give the hemiacetal product in almost quantitative yield under concomitant removal of the acetate at position 3. Treatment with PdCl₂/CuCl₂ then resulted in the direct formation of spiro-lactone **19** in a

combined yield of 48% over 2 steps.²⁰ Notably, this method has not been applied for the synthesis of 1,6-dioxaspiro[4.5]-decanes before. The introduction of the missing carbon in position 25 as methylene²¹ [NaH, (COOEt)₂; then HCHO] and isomerization of the so-obtained double bond [Ru₃(CO)₁₂] completed the synthesis of spirochensilide A (**1**) in 10 steps and 1% overall yield from the known alkene.¹³ This route compares well to Chen and co-workers' total synthesis of **1** from geranyl acetate (27 steps, 1.4% overall yield).²²

Spirochensilide B (**2**) was then obtained by treatment of spiro-lactone **19** with DMP, followed by diastereoselective reduction with L-selectride to give 3*α*-hydroxy lactone **20** in 60% yield. The subjection of the latter to similar conditions as in the case of **1** yielded spirochensilide B (**2**) in 42% yield over 2 steps. All analytical data for **1** and **2** were in agreement with those reported. Minor misassignments in the original NMR report of **2** could be corrected by extensive 2D NMR experiments (for details, see the Supporting Information). Direct conversion of spirochensilide A (**1**) into spirochensilide B (**2**) by oxidation/reduction protocols only resulted in decomposition, presumably due to the labile character of the butenolide moiety toward these conditions.

In summary, we here describe a divergent approach to 17,13-friedo-, 17,14-friedo-, and 10(9 → 8)abeo-17,14-friedolanostane natural products through three orchestrated rearrangements and applied it to the synthesis of spirochensilide A (**1**), spirochensilide B (**2**), and abifarine B (**4**), thereby delivering a conclusive biogenesis hypothesis.

For this purpose, we provided a radical-polar crossover approach for the direct activation of the C17 position in a lanostane derivative without the need for prior introduction of a sacrificial functional group. One or two consecutive Wagner–Meerwein methanide shifts gave either 17,13-friedolanostane or 17,14-friedolanostane. An in-depth innate reactivity analysis and mechanistic investigation guided fine-tuning of the reaction outcome toward a Meinwald rearrangement and concluded with access to 10(9 → 8)abeo-17,14-friedolanostanes. Finally, a novel 2-step method for the formation of the key 1,6-dioxaspiro[4.5]undecane motif was discovered.

ASSOCIATED CONTENT

Supporting Information

The Supporting Information is available free of charge at <https://pubs.acs.org/doi/10.1021/jacs.2c05358>.

General methods; detailed experimental studies; experimental procedures and spectral data; comparison of synthetic and natural spirochensilide A, spirochensilide B, and abifarine B; ¹H and ¹³C NMR spectra; X-ray crystallographic data (PDF)

Accession Codes

CCDC 2115191 contains the supplementary crystallographic data for this paper. These data can be obtained free of charge via www.ccdc.cam.ac.uk/data_request/cif, or by emailing data_request@ccdc.cam.ac.uk, or by contacting The Cambridge Crystallographic Data Centre, 12 Union Road, Cambridge CB2 1EZ, UK; fax: +44 1223 336033.

AUTHOR INFORMATION

Corresponding Author

Philipp Heretsch – Institute of Organic Chemistry, Leibniz Universität Hannover, 30167 Hannover, Germany;

 orcid.org/0000-0002-9967-3541
Email: philipp.heretsch@oci.uni-hannover.de

Authors

Mykhaylo Alekseychuk — Institute of Organic Chemistry, Leibniz Universität Hannover, 30167 Hannover, Germany
Sinan Adrian — Institute of Organic Chemistry, Leibniz Universität Hannover, 30167 Hannover, Germany
Robert C. Heinze — Institute of Organic Chemistry, Leibniz Universität Hannover, 30167 Hannover, Germany

Complete contact information is available at:
<https://pubs.acs.org/10.1021/jacs.2c05358>

Author Contributions

[†]M.A. and S.A. contributed equally.

Notes

The authors declare no competing financial interest.

ACKNOWLEDGMENTS

Financial support for this work was provided by the European Research Council (ERC Consolidator Grant “RadCrossSyn”, agreement no. 101043353), Deutsche Forschungsgemeinschaft (Heisenberg-Program HE 7133/8-1), and Boehringer Ingelheim Stiftung (plus3 perspectives program).

REFERENCES

- (1) For reviews, see: (a) de la Torre, M. C.; Sierra, M. A. Comments on Recent Achievements in Biomimetic Organic Synthesis. *Angew. Chem., Int. Ed.* **2004**, *43*, 160–181. (b) Razzak, M.; De Brabander, J. K. Lessons and revelations from biomimetic syntheses. *Nat. Chem. Biol.* **2011**, *7*, 865–875. (c) Baunach, M.; Franke, J.; Hertweck, C. Terpenoid Biosynthesis Off the Beaten Track: Unconventional Cyclases and Their Impact on Biomimetic Synthesis. *Angew. Chem., Int. Ed.* **2015**, *54*, 2604–2626. (d) Brown, P. D.; Lawrence, A. L. The importance of asking “how and why?” in natural product structure elucidation. *Nat. Prod. Rep.* **2017**, *34*, 1193–1202. For recent examples see: (e) Giannis, A.; Heretsch, P.; Sarli, V.; Stössel, A. Synthesis of Cyclopamine Using a Biomimetic and Diastereoselective Approach. *Angew. Chem., Int. Ed.* **2009**, *48*, 7911–7914. (f) Hong, A. Y.; Stoltz, B. M. Biosynthesis and Chemical Synthesis of Presilphiperfolanol Natural Products. *Angew. Chem., Int. Ed.* **2014**, *53*, 5248–5260. (g) Schmid, M.; Trauner, D. Biomimetic Synthesis of Complex Flavonoids Isolated from *Daemonorops* “Dragon’s Blood”. *Angew. Chem., Int. Ed.* **2017**, *56*, 12332–12335. (h) Xu, G.; Elkin, M.; Tantillo, D. J.; Newhouse, T. R.; Maimone, T. J. Traversing Biosynthetic Carbocation Landscapes in the Total Synthesis of Andrastin and Terretonin Meroterpenes. *Angew. Chem., Int. Ed.* **2017**, *56*, 12498–12502. (i) Liffert, R.; Linden, A.; Gademann, K. Total Synthesis of the Sesquiterpenoid Periconianone A Based on a Postulated Biogenesis. *J. Am. Chem. Soc.* **2017**, *139*, 16096–16099. (j) Bartels, F.; Hong, Y. J.; Ueda, D.; Weber, M.; Sato, T.; Tantillo, D. J.; Christmann, M. Bioinspired synthesis of pentacyclic onocerane triterpenoids. *Chem. Sci.* **2017**, *8*, 8285–8290. (k) Wang, Y.; Ju, W.; Tian, H.; Tian, W.; Gui, J. Scalable Synthesis of Cyclocitinol. *J. Am. Chem. Soc.* **2018**, *140*, 9413–9416.
- (2) (a) Duecker, F. L.; Heinze, R. C.; Heretsch, P. Synthesis of Swinhoeosterol A, Dankasterone A and B, and Periconianone A by Radical Framework Reconstruction. *J. Am. Chem. Soc.* **2020**, *142*, 104–108. (b) Duecker, F. L.; Heinze, R. C.; Steinhauer, S.; Heretsch, P. Discoveries and Challenges en Route to Swinhoeosterol A. *Chem. Eur. J.* **2020**, *26*, 9971–9981.
- (3) Heinze, R. C.; Lentz, D.; Heretsch, P. Synthesis of Strophasterol A Guided by a Proposed Biosynthesis and Innate Reactivity. *Angew. Chem., Int. Ed.* **2016**, *55*, 11656–11659.
- (4) Heinze, R. C.; Heretsch, P. Translation of a Polar Biogenesis Proposal into a Radical Synthetic Approach: Synthesis of Pleurocin A/Matsutakone and Pleurocin B. *J. Am. Chem. Soc.* **2019**, *141*, 1222–1226.
- (5) Zhao, Q.-Q.; Song, Q.-Y.; Jiang, K.; Li, G.-D.; Wie, W.-J.; Li, Y.; Gao, K. Spirochensilides A and B, Two New Rearranged Triterpenoids from *Abies chensiensis*. *Org. Lett.* **2015**, *17*, 2760–2763.
- (6) IUPAC Commission on the Nomenclature of Organic Chemistry. Nomenclature of Organic Chemistry. Section F: Natural Products and Related Compounds. *Eur. J. Biochem.* **1978**, *86*, 1–8.
- (7) (a) Ohyama, K.; Suzuki, M.; Kikuchi, J.; Saito, K.; Muranaka, T. Dual biosynthetic pathways to phytosterol via cycloartenol and lanosterol in *Arabidopsis*. *Proc. Natl. Acad. Sci. U.S.A.* **2009**, *106*, 725–730.
- (8) Wu, W.; Chen, X.; Liu, Y.; Wang, Y.; Tian, T.; Zhao, X.; Li, J.; Ruan, H. Triterpenoids from the branch and leaf of *Abies fargesii*. *Phytochemistry* **2016**, *130*, 301–312.
- (9) Li, Y. L.; Gao, Y. X.; Yang, X. W.; Jin, H. Z.; Ye, J.; Simmons, L.; Wang, N.; Steinmetz, A.; Zhang, W. D. Cytotoxic triterpenoids from *Abies recurvata*. *Phytochemistry* **2012**, *81*, 159–164.
- (10) (a) Vieira, L. M. M.; Kijjoa, A.; Wilirat, R.; Nascimento, M. S.; Gales, L.; Damas, A. M.; Silva, A. M. S.; Mondranondra, I.-O.; Herz, W. Bioactive Friedolanostanes and 11(10→8)-Abeolanostanes from the Bark of *Garcinia speciosa*. *J. Nat. Prod.* **2004**, *67*, 2043–2047; (b) **2005**, *68*, 969–970. (c) Vieira, L. M. M.; Kijjoa, A.; Silva, A. M. S.; Mondranondra, I.-O.; Kengthong, S.; Gales, L.; Damas, A. M.; Herz, W. Lanostanes and friedolanostanes from the bark of *Garcinia speciosa*. *Phytochemistry* **2004**, *65*, 393–398.
- (11) Eschenmoser, A.; Arigoni, D. Revisited after 50 Years: The ‘Stereochemical Interpretation of the Biogenetic Isoprene Rule for the Triterpenes’. *Helv. Chim. Acta* **2005**, *88*, 3011–3050.
- (12) Fan, R.; Pu, D.; Wen, F.; Wu, J. δ and α SP³ C–H Bond Oxidation of Sulfonamides with PhI(OAc)₂/I₂ under Metal-Free Conditions. *J. Org. Chem.* **2007**, *72*, 8994–8997.
- (13) Chen, X.; Shao, X.; Li, W.; Zhang, X.; Yu, B. Total Synthesis of Echinoside A, a Representative Triterpene Glycoside of Sea Cucumbers. *Angew. Chem., Int. Ed.* **2017**, *56*, 7648–7652.
- (14) Sun, X.; Chen, J.; Ritter, T. Catalytic dehydrogenative decarboxyolefination of carboxylic acids. *Nat. Chem.* **2018**, *10*, 1229–1233.
- (15) (a) Chen, M. S.; Prabagaran, N.; Labenz, N. A.; White, M. C. Serial Ligand Catalysis: A Highly Selective Allylic C–H Oxidation. *J. Am. Chem. Soc.* **2005**, *127*, 6970–6971. (b) Ye, Q.; Qu, P.; Snyder, S. A. Total Syntheses of Scaparvins B, C, and D Enabled by a Key C–H Functionalization. *J. Am. Chem. Soc.* **2017**, *139*, 18428–18431. (c) de Armas, P.; Concepción, J. I.; Francisco, C. G.; Hernández, R.; Salazar, J. A.; Suárez, E. Intramolecular hydrogen abstraction. Hypervalent organoiodine compounds, convenient reagents for alkoxy radical generation. *J. Chem. Soc., Perkin Trans.* **1989**, *1*, 405–411. (d) Short, M. A.; Blackburn, J. M.; Roizen, J. L. Sulfamate Esters Guide Selective Radical-Mediated Chlorination of Aliphatic C–H Bonds. *Angew. Chem., Int. Ed.* **2018**, *57*, 296–299.
- (16) Wappes, E. A.; Fosu, S. C.; Chopko, T. C.; Nagib, D. A. Triiodide-Mediated δ -Amination of Secondary C–H Bonds. *Angew. Chem., Int. Ed.* **2016**, *55*, 9974–9978.
- (17) Corey, E. J.; Hong, B.-c. Chemical Emulation of the Biosynthetic Route to Glycinoclepin from a Cycloartenol Derivative. *J. Am. Chem. Soc.* **1994**, *116*, 3149–3150.
- (18) Chen, M. S.; White, M. C. A Predictably Selective Aliphatic C–H Oxidation Reaction for Complex Molecule Synthesis. *Science* **2007**, *318*, 783–787.
- (19) Csuk, R.; Schröder, C.; Hutter, S.; Mohr, K. Enantioselective Dreiding-Schmidt reactions: asymmetric synthesis and analysis of α -methylene- γ -butyrolactones. *Tetrahedron Asymmetry* **1997**, *8*, 1411–1429.
- (20) (a) Complain, P.; Vafèle, J. M.; Goré, J. A New Synthesis of γ -Butyrolactones via Palladium(II)-Catalyzed Cyclisation of Trimethylsilylalkynes. *Synlett* **1994**, *1994*, 943–945. (b) Complain, P.; Vafèle, J. M.; Goré, J. Palladium(II)-Catalyzed Formation of 7-Butyrolactones from 4-Trimethylsilyl-3-alkyn-1-ols: Synthetic and Mechanistic Aspects. *Tetrahedron* **1996**, *52*, 10405–10416.

- (21) Tanaka, A.; Yamashita, K. A Simple Procedure for α -Methylenation or γ - and δ -Lactones. *Agric. Biol. Chem.* **1978**, *42*, 1585–1588.
- (22) (a) Liang, X.-T.; Chen, J.-H.; Yang, Z. Asymmetric Total Synthesis of (−)-Spirochensilide A. *J. Am. Chem. Soc.* **2020**, *142*, 8116–8121. (b) Liang, X.-T.; Sun, B.-C.; Liu, C.; Li, Y.-H.; Zhang, N.; Xu, Q.-Q.; Zhang, Z.-C.; Han, Y.-X.; Chen, J.-H.; Yang, Z. Asymmetric Total Synthesis of (−)-Spirochensilide A, Part 1: Diastereoselective Synthesis of the ABCD Ring and Stereoselective Total Synthesis of 13(R)-Demethyl Spirochensilide A. *J. Org. Chem.* **2021**, *86*, 2135–2157. (c) Liang, X.-T.; Sun, B.-C.; Zhang, N.; Zhang, Z.-C.; Li, Y.-H.; Xu, Q.-Q.; Liu, C.; Chen, J.-H.; Yang, Z. Asymmetric Total Synthesis of (−)-Spirochensilide A, Part 2: The Final Phase and Completion. *J. Org. Chem.* **2021**, *86*, 2158–2172.

□ Recommended by ACS

Chemical Emulation of the Biosynthetic Route to Anthrasteroids: Synthesis of Asperfloketal A

Mykhaylo Alekseychuk and Philipp Heretsch

NOVEMBER 21, 2022

JOURNAL OF THE AMERICAN CHEMICAL SOCIETY

[READ ▶](#)

General Synthetic Approach to Diverse Taxane Cores

Melecio A. Perea, Richmond Sarpong, et al.

NOVEMBER 08, 2022

JOURNAL OF THE AMERICAN CHEMICAL SOCIETY

[READ ▶](#)

Chemical Degradation-Inspired Total Synthesis of the Antibiotic Macrodiolide, Luminamicin

Aoi Kimishima, Toshiaki Sunazuka, et al.

DECEMBER 09, 2022

JOURNAL OF THE AMERICAN CHEMICAL SOCIETY

[READ ▶](#)

Total Synthesis of Atrachinenins A and B

Sarah A. French, Jonathan H. George, et al.

DECEMBER 12, 2022

JOURNAL OF THE AMERICAN CHEMICAL SOCIETY

[READ ▶](#)

[Get More Suggestions >](#)

Biogenesis-Inspired, Divergent Synthesis of Spirochensilide A, Spirochensilide B, and Abifarane B employing a Radical-Polar Crossover Rearrangement Strategy

Mykhaylo Alekseychuk, Sinan Adrian, Robert C. Heinze,
Philipp Heretsch*

Institute of Organic Chemistry, Leibniz Universität Hannover, Schneiderberg 1B, 30167 Hannover, Germany

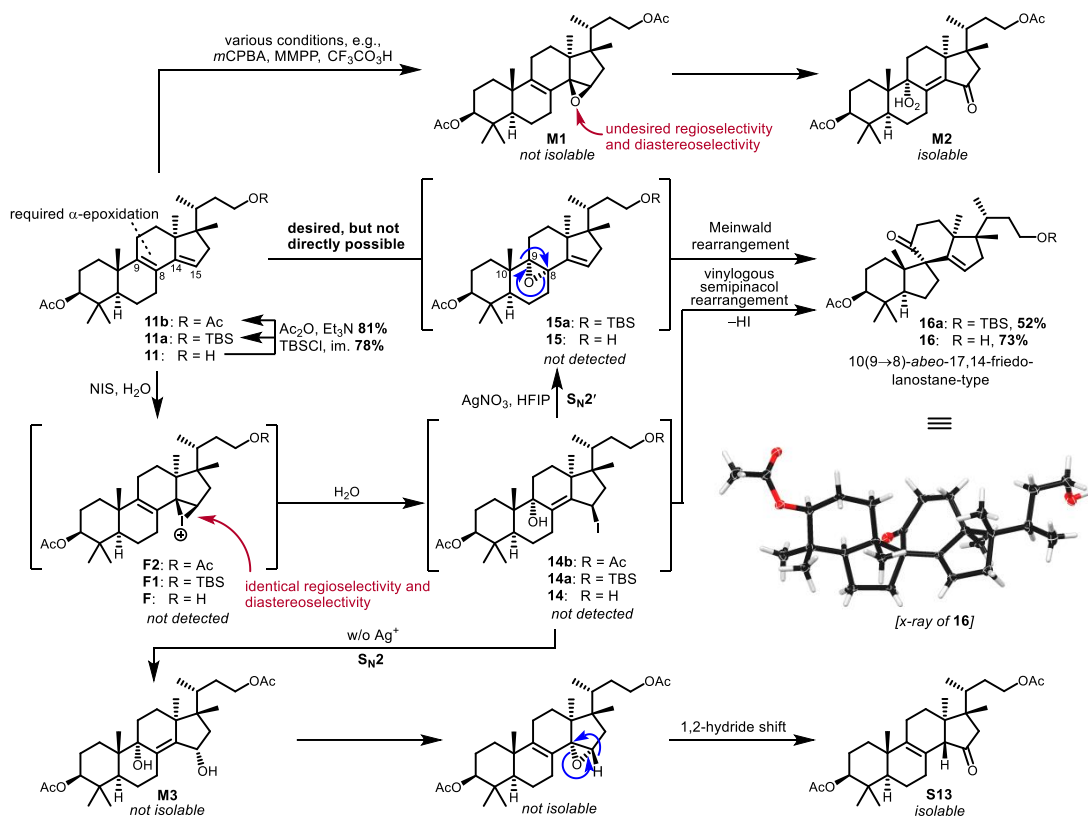
*Correspondence to: philipp.heretsch@oci.uni-hannover.de

Supporting Information

Table of Contents

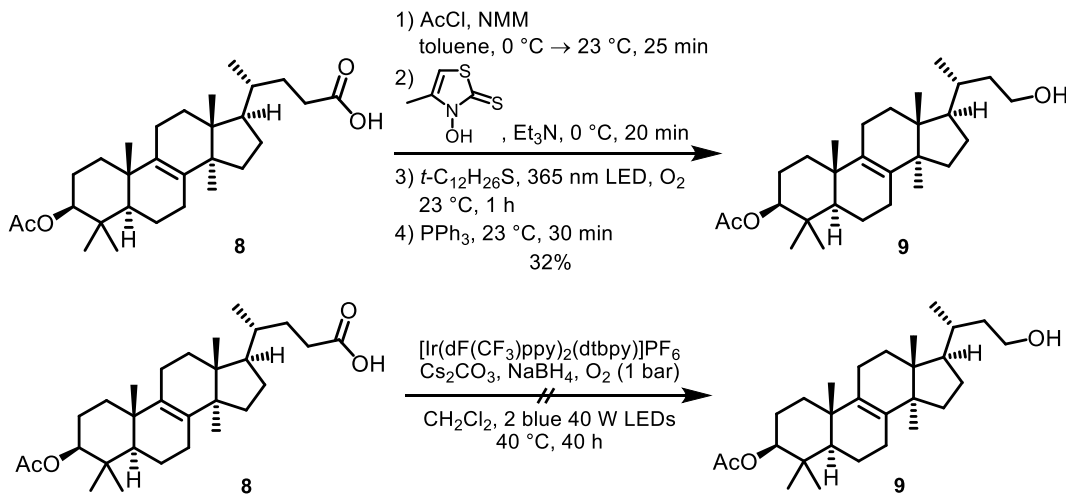
1 Mechanistic insights towards the chemical emulation of the Meinwald rearrangement.....	2
2 Failed strategies towards abifarane B and spirochensilides A&B	2
3 The final route towards abifarane B and spirochensilides A&B.....	8
4 General Methods	9
5 Experimental Procedures and Characterization Data	10
6 X-Ray Crystallographic Data.....	28
7 NMR Comparisons.....	29
References	35
NMR Spectra.....	36

1 Mechanistic insights towards the chemical emulation of the Meinwald rearrangement



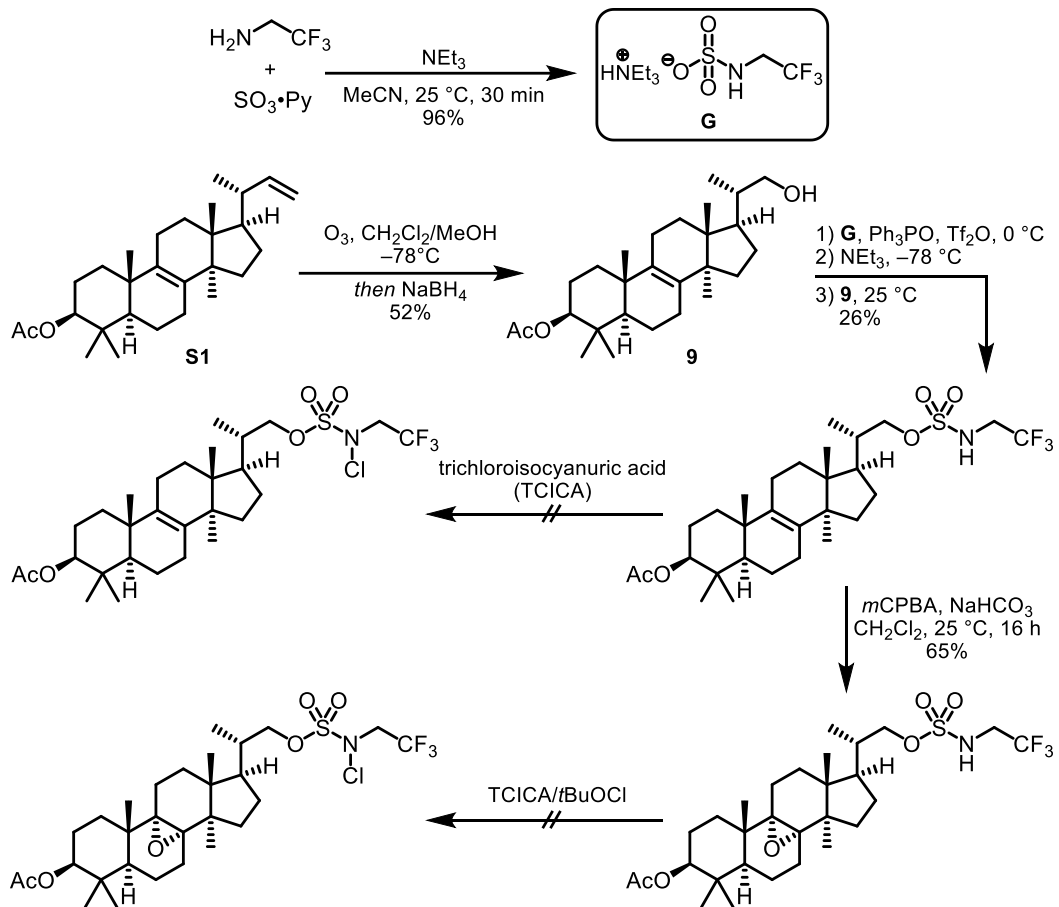
2 Failed strategies towards abifarane B and spirochensilides A&B

2.1 Attempts at decarboxylative hydroxylation

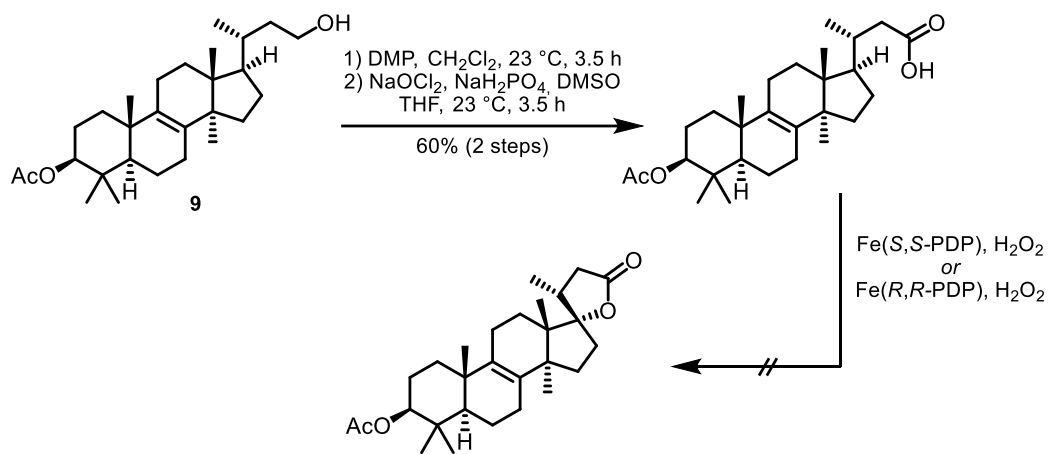


2.2 Attempts at C17 oxidation

2.2.1 Sulfamate ester directed^[1]

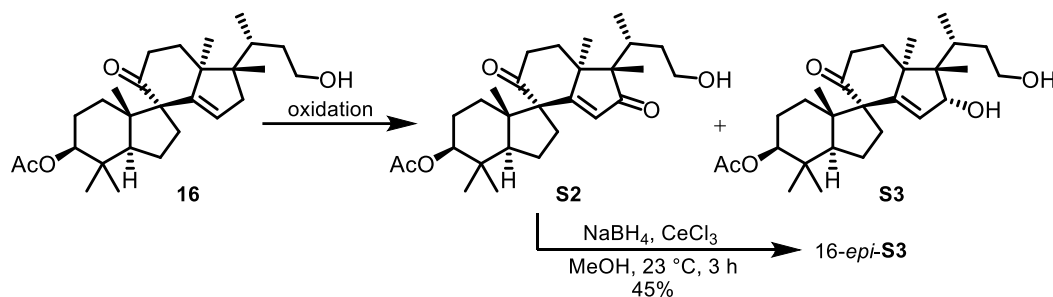


2.2.2 Carboxylic acid directed



2.3 Attempts at C16 oxidation

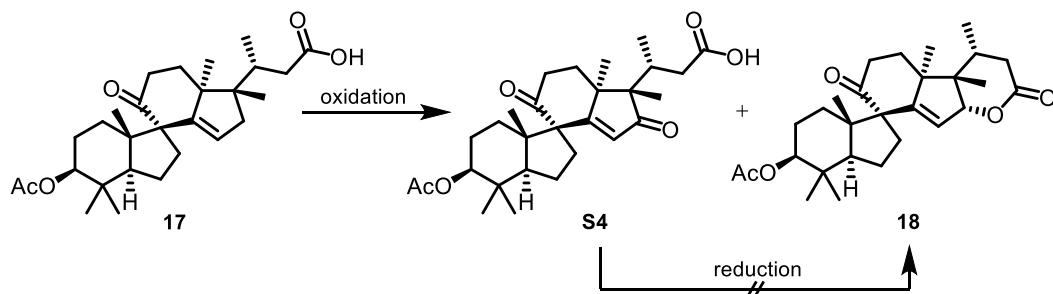
2.3.1 Substrate with truncated side chain



- 9-oxo functionality has shown no reaction with hydride donors

oxidation: • O₂, TPP/[Ru(bpy)₃]Cl, CHCl₃/MeOH, 23 °C, Hg-lamp (300 W)/violet LED/CFL, 0 °C/23 °C (7 protocols, no reaction)

- NBS, DBPO, MeCN, 85 °C, 2.5 h (decomp.)
- SeO₂, tBuOOH (70% aq.), CH₂Cl₂, 40 °C, 4 h (no reaction)
- Rh₂(cap)₄, K₂CO₃, tBuOOH (5.5 M dec./70% aq.), CH₂Cl₂/1,2-DCE, 23 °C, 3 h (4 protocols, **S2** = 33%, **S3** = 24%)
- Mn(OAc)₃, tBuOOH (5.5 M dec.), 4 Å MS, EtOAc, 23 °C, 48 h (**S2** = 29%, **S3** = 25%)
- Pd(OAc)₂, K₂CO₃, tBuOOH (70%), CH₂Cl₂, 23 °C, 72 h (**S2** = 37%, **S3** = 30%)
- CrO₃·3,5-DMP, CH₂Cl₂, -20 °C, 30 min (16,23-dioxo-16 = 27%)



oxidation: a) White-catalyst, 1,4-benzoquinone, CH₂Cl₂, 45 °C, 4 d (decomp.).

b) Rh₂(cap)₄, tBuOOH (70% aq.), DCE, 40 °C, 27 h (**S4** = 24%; **18** = 21%).

c) Rh₂(esp)₂, tBuOOH (70% aq.), DCE, 40 °C, 41 h (**17** = 18%; **S4** = 25%; **18** = 36%).

d) Fe(R,R-PDP), H₂O₂, CH₂Cl₂, MeCN, 23 °C, 2 h (**18** = 33%).

e) Fe(S,S-PDP), H₂O₂, CH₂Cl₂, MeCN, 23 °C, 2 h (**18** = 57%).

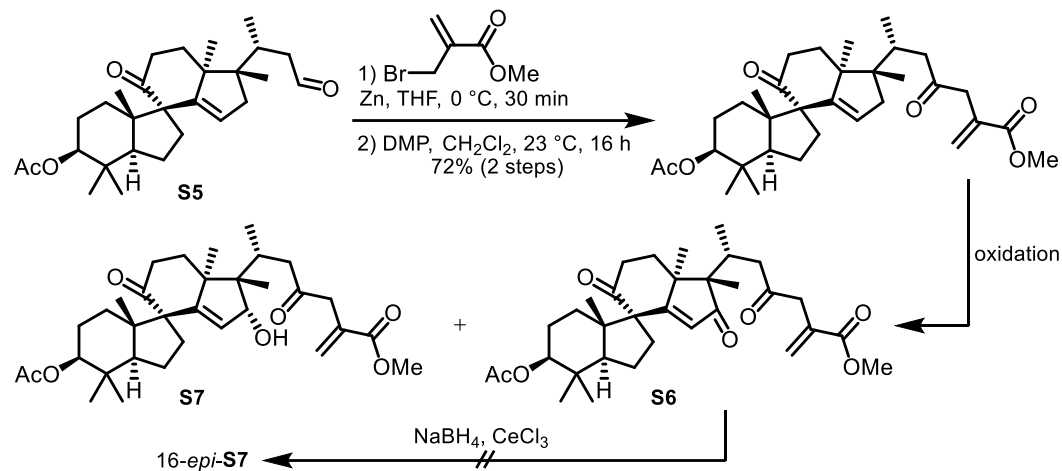
reduction: a) DIBAL, THF, -78 °C → -20 °C → 0 °C (decomp.).

b) DIBAL, THF, -78 °C (decomp.).

c) NaBH₄, CeCl₃, MeOH, 23 °C (decomp.).

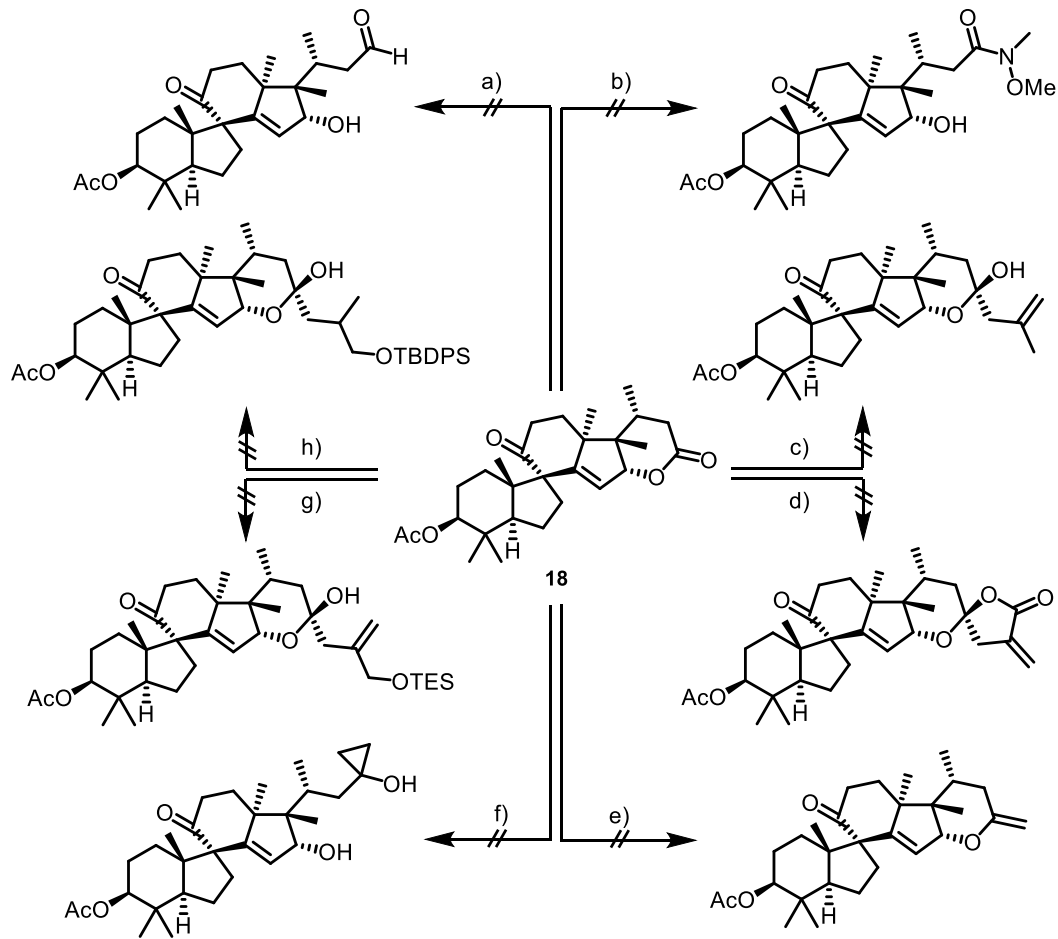
d) LiBH₄, MeOH, 0 °C → 23 °C (decomp.).

2.3.2 Substrate with complete side chain



oxidation: • Rh₂(cap)₄, tBuOOH (70% aq.), 1,2-DCE, 23 °C, 24 h (**S6** = 35%)
 • Mn(OAc)₃, tBuOOH (5.5 M dec.), 4 Å MS, EtOAc, 23 °C, 48 h (**S6** = 21%, **S7** = 21%)
 • CrO₃•3,5-DMP, CH₂Cl₂, -20 °C, 1.5 h (**S6** = 23%)
 • Pd(OAc)₂, K₂CO₃, tBuOOH (70%), CH₂Cl₂, 23 °C, 48 h (**S6** = 29%, **S7** = 15%)
 • Pd(OAc)₂, 1,4-BQ, AcOH, 50 °C, 2 h (oxidation at C27)

2.4 Attempts at C23 additions



conditions: a) DIBAL, toluene, $-78\text{ }^{\circ}\text{C}$ (decomp.).

b) i) $\text{MeO}(\text{Me})\text{NH}\cdot\text{HCl}$, $\text{EDC}\cdot\text{HCl}$, DMAP , NEt_3 , THF , $23\text{ }^{\circ}\text{C}$ (SM reisolated); ii) $\text{MeO}(\text{Me})\text{NH}\cdot\text{HCl}$, AlMe_3 , DMAP , NEt_3 , THF , $-78\text{ }^{\circ}\text{C} \rightarrow 0\text{ }^{\circ}\text{C}$ (64% SM, 21% 3-OI-lactone); iii) $i\text{PrMgCl}$, $\text{MeO}(\text{Me})\text{NH}\cdot\text{HCl}$, THF , $-78\text{ }^{\circ}\text{C} \rightarrow 23\text{ }^{\circ}\text{C}$ (decomp.).

c) $\text{BrMg}-\text{CH}=\text{CH}$ or $\text{ClMg}-\text{CH}=\text{CH}$, THF , $-78\text{ }^{\circ}\text{C}$ (decomp.).

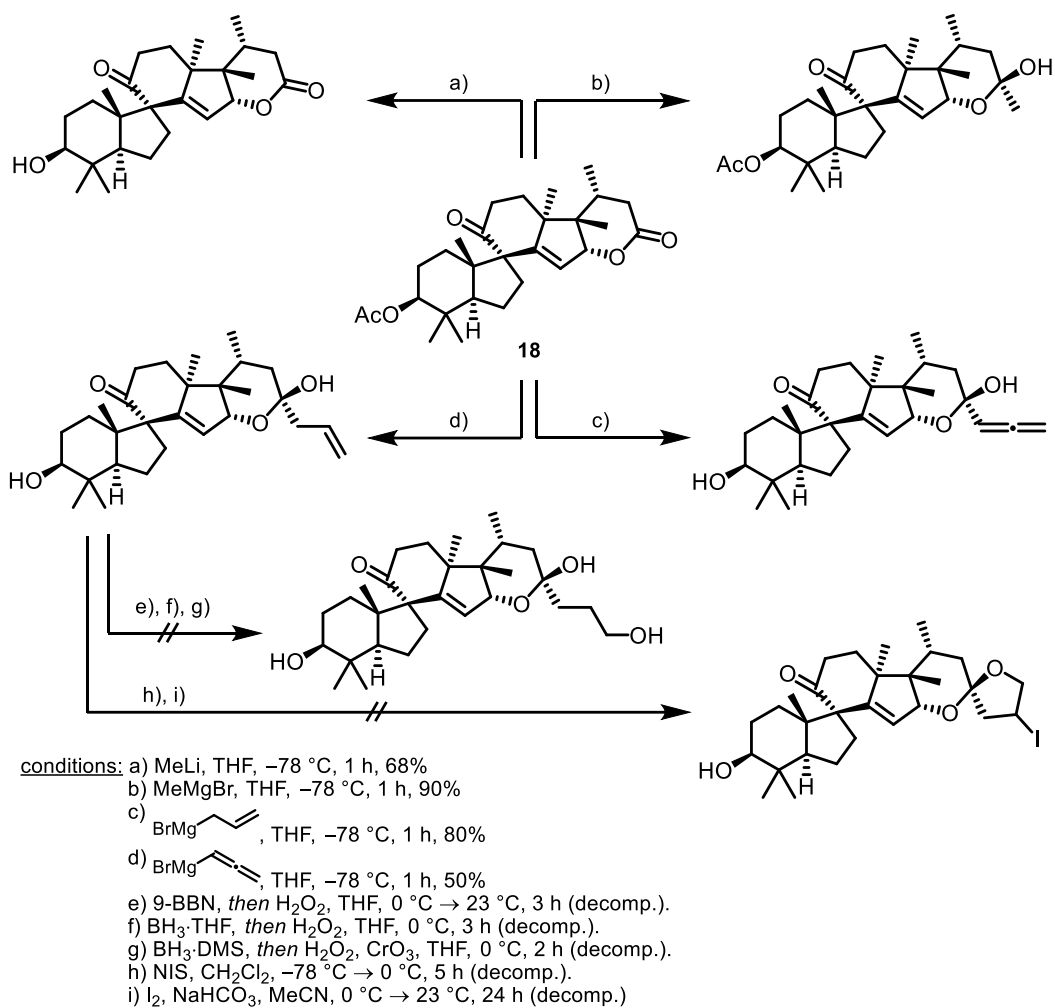
d) $\text{CH}_2=\text{CH}-\text{C}(=\text{O})-\text{OMe}$, Zn , THF or $1,4\text{-dioxane}$, $45\text{ }^{\circ}\text{C}$ (decomp.).

e) $\text{Ti}(\text{Cp})_2\text{Me}_2$, pyridine, toluene, $110\text{ }^{\circ}\text{C}$ (decomp.).

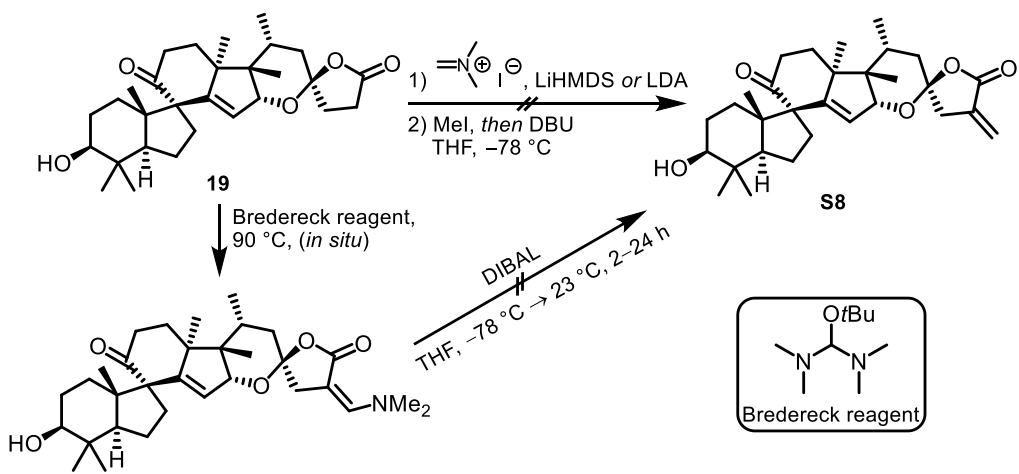
f) $\text{Ti}(\text{O}i\text{Pr})_4$, EtMgBr , THF , $0\text{ }^{\circ}\text{C} \rightarrow 23\text{ }^{\circ}\text{C}$ (decomp.).

g) i) $\text{BrMg}-\text{CH}=\text{CH}-\text{OTES}$, THF , $-78\text{ }^{\circ}\text{C}$ (decomp.); ii) $\text{I}-\text{CH}=\text{CH}-\text{OTES}$, $t\text{BuLi}$, THF , $-78\text{ }^{\circ}\text{C}$ (decomp.).

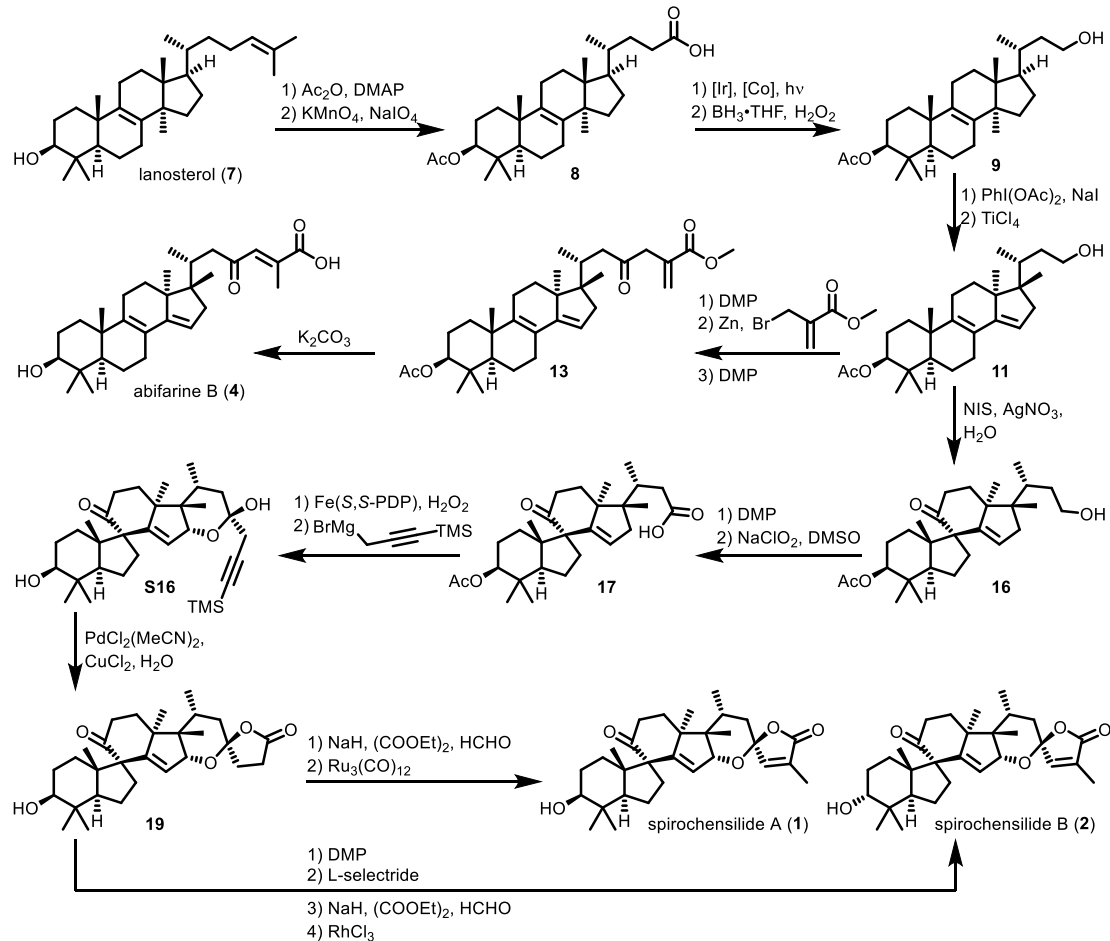
h) $\text{I}-\text{CH}=\text{CH}-\text{OTBDPS}$, $t\text{BuLi}$, THF , $-78\text{ }^{\circ}\text{C}$ (decomp.).



2.5 Attempts at C25 methylenation



3 The final route towards abifarine B and spirochensilides A&B



4 General Methods

All reactions sensitive to moisture and/or air were carried out using heat gun-dried glassware, under an atmosphere of argon, and anhydrous solvents. Anhydrous dichloromethane, toluene, tetrahydrofuran, and diethyl ether were taken from a M. Braun GmbH MB SPS-800 solvent purification system and were stored over 4 Å molecular sieves. Ethyl acetate and *n*-hexane were purified by distillation on a rotary evaporator. Magnesium turnings were activated by stirring in 1 M HCl solution for 2 min, washing three times with ethanol, then three times with diethyl ether, followed by exposure to high vacuum (10^{-3} mbar) at 25 °C. Activated magnesium turnings were stored under an atmosphere of argon. NaI was dried overnight under high vacuum (10^{-3} mbar) at 90 °C and stored under argon. Lanosterol was acquired from TCI in >50.0% (GC) purity. All other solvents (HPLC quality) and commercially available reagents were used without further purification unless otherwise stated.

Concentration under reduced pressure was performed by rotary evaporation at 45 °C and appropriate pressure, followed by exposure to high vacuum (10^{-3} mbar) at 25 °C.

Chromatography and TLC: Reactions were monitored by thin-layer chromatography (TLC) carried out on Merck Silica Gel 60 F₂₅₄-plates and visualized by fluorescence quenching under UV-light, or staining with an aqueous solution of cerium sulfate and phosphomolybdic acid and heat. Column chromatographic purification was performed on Macherey-Nagel Silica Gel 60 M (40–60 µm). Preparative TLC was performed on 20x20 cm Merck Silica Gel 60 F₂₅₄-glass plates.

NMR: NMR spectra were recorded on either a Jeol ECX400 (400 MHz), a Bruker Ultrashield 400 (400 MHz), a Jeol ECP500 (500 MHz), a Bruker AVANCE III 500 (500 MHz), a Bruker Ascend 600 (600 MHz, with CryoProbe), a Varian INOVA600 (600 MHz), or a Bruker AVANCE III 700 (700 MHz, with CryoProbe) spectrometer. Chemical shifts δ are reported in parts per million (ppm) and are referenced using residual undeuterated solvent (CDCl_3 : δ_H = 7.26 ppm, δ_C = 77.16 ppm; unless otherwise stated) as an internal reference at 298 K. The given multiplicities are phenomenological; thus, the actual appearance of the signals is stated and not the theoretically expected one. The following abbreviations are used to designate multiplicities: s = singlet, d = doublet, t = triplet, q = quartet, p = pentet, br = broad, and combinations thereof. In case no multiplicity could be identified, the chemical shift range of the signal is given (m = multiplet).

Infrared spectroscopy: Infrared (IR) spectra were measured on a Jasco FT/IR-4100 Type A spectrometer with a TGS detector or a SHIMADZU FT-IR Affinity-1S spectrometer. Wavenumbers ν are given in cm^{-1} and intensities are as follows: s = strong, m = medium, w = weak, b = broad.

Mass spectrometry: High-resolution mass spectra (HRMS) were recorded using an Agilent 6210 ESI-TOF, an Ionspec QFT-7 ESI-TOF or a Waters QTof Premier (with an Acquity UPLC system) spectrometer.

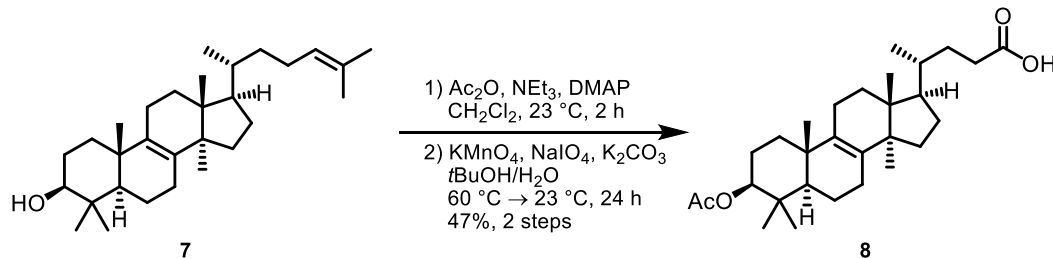
Optical rotation: Optical rotations were measured on a JASCO P-2000 polarimeter or a Krüss P3000 at 589 nm using 100 mm cells and the solvent and concentration (g/100 mL) indicated.

Melting Point: Melting points were measured on a Büchi B-545.

Lamps: CFL lamps used were 45 W lamps from HWAMART with a colour temperature of 5500 K. Blue LED lamps used were two A160WE 40 W lamps from Kessil.

5 Experimental Procedures and Characterization Data

4,4,14 α -Trimethyl-3 β -acetoxy-5 α -chola-8-ene-24-oic acid (**8**)



To a solution of lanosterol (**7**) (app. 50% purity, 20.0 g, 23.4 mmol, 1.0 eq.), triethylamine (19.6 mL, 141 mmol, 6.0 eq.) and *N,N*-dimethyl-4-aminopyridine (286 mg, 2.34 mmol, 0.1 eq.) in anhydrous CH₂Cl₂ (60.0 mL) was added acetic anhydride (8.86 mL, 93.8 mmol, 4.0 eq.) over the course of 10 min. After stirring for 2 h, NaHCO₃ (sat. aq., 50 mL) was carefully added and the phases were separated. The aqueous phase was extracted with CH₂Cl₂ (3 x 120 mL), the combined organic phases were dried over MgSO₄, and all volatiles were removed under reduced pressure. The crude product and K₂CO₃ (9.72 g, 70.3 mmol, 3.0 eq.) were dissolved in tBuOH (500 mL) and heated to 60 °C. A slurry of NaIO₄ (24.1 g, 113 mmol, 4.8 eq.) and KMnO₄ (1.48 g, 9.37 mmol, 0.4 eq.) in H₂O (300 mL) was added to the solution which was stirred for 2 h at 60 °C, then cooled to 23 °C, and stirred for an additional 22 h. An aqueous solution of NaHSO₃ (w = 10%, 500 mL) was added until the solution changed from purple to yellow. tBuOH was removed under reduced pressure and the pH-value of the remaining aqueous solution was adjusted to pH = 2. The aqueous phase was extracted with CH₂Cl₂ (4 x 700 mL), the combined organic phases were dried over MgSO₄, and all volatiles were removed under reduced pressure. Column chromatography (SiO₂, nhexane/EtOAc 4:1 → 2:1, v/v) and subsequent recrystallization from EtOAc gave carboxylic acid **8** (5.54 g, 11.0 mmol, 47%; corrected yield using ¹H-NMR spectroscopy based on 5% impurity) as colourless crystals.

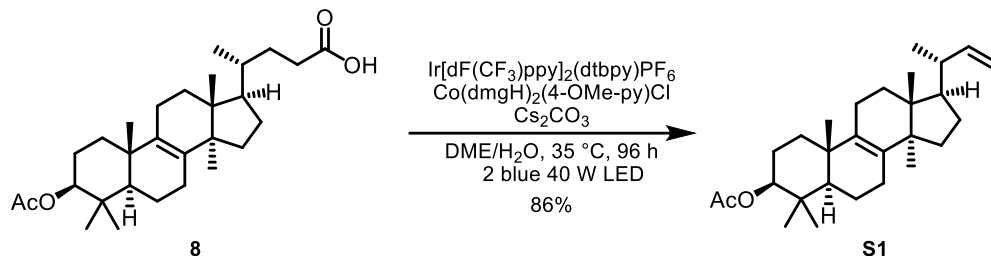
TLC: R_f = 0.45 (nhexane/EtOAc 2:1, v/v).

¹H-NMR: (700 MHz, CDCl₃): δ [ppm] = 4.50 (dd, J = 11.9, 4.4 Hz, 1H), 2.41 (ddd, J = 15.6, 10.2, 5.3 Hz, 1H), 2.27 (ddd, J = 16.0, 9.9, 6.5 Hz, 1H), 2.06 (d, J = 3.2 Hz, 1H), 2.05 (s, 3H), 2.04 – 1.92 (m, 4H), 1.83 (dddd, J = 13.1, 9.6, 6.5, 2.6 Hz, 1H), 1.77 – 1.53 (m, 8H), 1.53 – 1.39 (m, 3H), 1.38 – 1.28 (m, 3H), 1.19 (ddd, J = 11.9, 9.1, 2.0 Hz, 1H), 1.15 (dd, J = 12.7, 2.2 Hz, 1H), 1.00 (s, 3H), 0.91 (d, J = 6.3 Hz, 3H), 0.88 (s, 3H), 0.88 (s, 3H), 0.87 (d, J = 1.0 Hz, 3H), 0.69 (d, J = 0.7 Hz, 3H).

¹³C-NMR: (176 MHz, CDCl₃): δ [ppm] = 179.9, 170.7, 134.6, 134.4, 81.1, 50.6, 50.4, 50.0, 44.7, 38.0, 37.0, 36.2, 35.4, 31.2, 31.2, 31.1, 30.9, 28.2, 28.1, 26.5, 24.4, 24.3, 21.5, 21.1, 19.3, 18.4, 18.3, 16.7, 15.9.

All characterization data was consistent with previously reported data.^[2]

4,4,14 α -Trimethyl-24-nor-5 α -chola-8,22-diene-3 β -ylacetate (S1**)**



To a mixture of acid **8** (2.00 g, 4.36 mmol, 1.0 eq.), $\text{Ir}[\text{dF}(\text{CF}_3)\text{ppy}]_2(\text{dtbpy})\text{PF}_6$ (49.0 mg, 43.6 μmol , 0.01 eq.), $\text{Co}(\text{dmgH})_2(4\text{-OMe-py})\text{Cl}$ (94.6 mg, 218 μmol , 0.05 eq.), and Cs_2CO_3 (281 mg, 872 μmol , 0.2 eq.) was added a degassed mixture of DME (43.6 mL) and H_2O (2.4 mL). Two blue LEDs (Kessil A160WE) were placed opposite and at a distance of 2 cm from the reaction vessel and the reaction was stirred under irradiation for 96 h. A 120 mm cooling fan ensured a reaction temperature of approximately 35 °C during that time. After completion of the reaction as indicated by TLC, all volatiles were removed under reduced pressure. Column chromatography (SiO_2 , *n*hexane/EtOAc 29:1, *v/v*) gave alkene **S1** (1.55 g, 3.75 mmol, 86%) as a colourless solid.

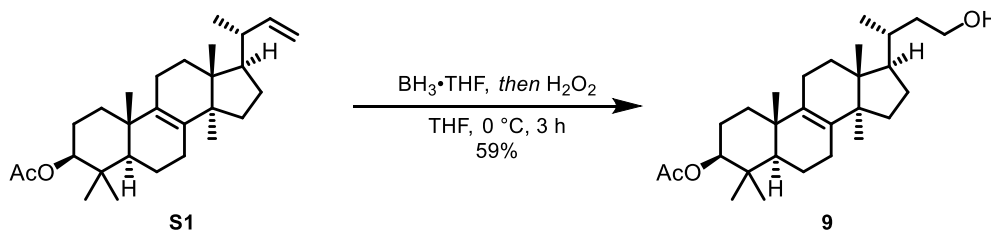
TLC: $R_f = 0.27$ (*n*hexane/EtOAc 29:1, *v/v*).

¹H-NMR: (500 MHz, CDCl_3): δ [ppm] = 5.67 (ddd, $J = 17.0, 10.2, 8.3$ Hz, 1H), 4.92 (ddd, $J = 17.1, 2.1, 0.9$ Hz, 1H), 4.82 (dd, $J = 10.2, 2.1$ Hz, 1H), 4.50 (dd, $J = 11.6, 4.5$ Hz, 1H), 2.05 (s, 1H), 2.05 (s, 3H), 2.05 – 2.01 (m, 3H), 1.83 – 1.69 (m, 4H), 1.68 (d, $J = 2.9$ Hz, 1H), 1.68 – 1.64 (m, 2H), 1.64 – 1.60 (m, 1H), 1.58 (dd, $J = 12.2, 4.6$ Hz, 1H), 1.55 – 1.53 (m, 1H), 1.50 (dd, $J = 9.3, 3.1$ Hz, 1H), 1.36 – 1.28 (m, 2H), 1.15 (dd, $J = 12.7, 2.3$ Hz, 2H), 1.02 (d, $J = 6.3$ Hz, 3H), 1.01 (s, 3H), 0.89 – 0.87 (m, 9H), 0.72 (s, 3H).

¹³C-NMR: (126 MHz, CDCl_3): δ [ppm] = 171.1, 145.7, 134.7, 134.4, 111.7, 81.1, 50.7, 50.0, 49.9, 44.6, 42.0, 38.0, 37.1, 35.4, 31.1, 31.0, 28.4, 28.1, 26.5, 24.4, 24.3, 21.5, 21.1, 20.2, 19.3, 18.3, 16.7, 16.1.

All characterization data was consistent with previously reported data.^[2]

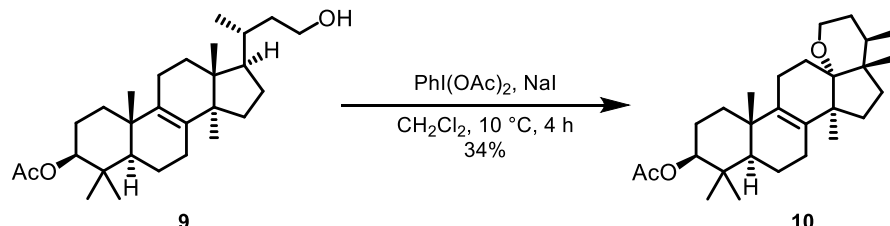
23-Hydroxy-4,4,14 α -trimethyl-24-nor-5 α -chola-8-ene-3 β -yl acetate (9**)**



To a stirred solution of alkene **S1** (651 mg, 1.58 mmol, 1.0 eq.) in THF was added $\text{BH}_3\text{-THF}$ (1 M in THF, 4.72 mmol, 3.0 eq.) at 0 °C. After stirring for 2 h at 0 °C, the solution was quenched at 0 °C with a mixture of H_2O_2 ($w = 35\%$, 4.8 mL) and phosphate buffer (pH = 7, 7.9 mL), warmed to 23 °C, and stirred for 30 min. The phases were separated and the aqueous phase was extracted with EtOAc (3 x 40 mL). The combined organic phases were washed with brine (100 mL), dried over MgSO_4 , and all volatiles were removed under reduced pressure. Column chromatography (SiO_2 , *n*hexane/EtOAc 3:1) gave primary alcohol **9** (403 mg, 936 μmol , 59%) as a colourless solid.

m.p.: 160–161 °C (EtOAc).
TLC: $R_f = 0.27$ (*n*hexane/EtOAc 3:1, *v/v*).
 $^1\text{H-NMR}$: (600 MHz, CDCl₃); δ [ppm] = 4.49 (dd, $J = 11.8, 4.4$ Hz, 1H), 3.72 (ddd, $J = 10.3, 8.1, 4.7$ Hz, 1H), 3.65 (dt, $J = 10.4, 7.6$ Hz, 1H), 2.05 (s, 3H), 2.04 – 1.93 (m, 4H), 1.76 – 1.62 (m, 7H), 1.60 – 1.49 (m, 6H), 1.34 – 1.22 (m, 3H), 1.18 (ddd, $J = 11.9, 9.3, 2.1$ Hz, 1H), 1.14 (dd, $J = 12.6, 2.2$ Hz, 1H), 1.00 (s, 3H), 0.93 (d, $J = 6.0$ Hz, 3H), 0.88 – 0.86 (m, 9H), 0.69 (s, 3H).
 $^{13}\text{C-NMR}$: (151 MHz, CDCl₃); δ [ppm] = 171.2, 134.5, 134.4, 81.0, 61.1, 50.8, 50.6, 49.9, 44.6, 39.4, 37.9, 37.0, 35.3, 33.5, 31.1, 30.9, 28.4, 28.0, 26.4, 24.3, 24.2, 21.4, 21.1, 19.3, 18.9, 18.2, 16.6, 15.8.
IR: $\tilde{\nu}$ [cm⁻¹] = 3324 (br, w), 2952 (m), 2923 (s), 2853 (m), 1735 (w), 1715 (w), 1457 (w), 1372 (m), 1266 (m), 1247 (m), 1037 (m), 1009 (w).
HRMS: (ESI-TOF); *m/z* calcd. for C₂₈H₄₆O₃Na⁺ [M+Na]⁺: 453.3339, found: 453.3339.
Opt. act.: $[\alpha]_D^{21} = +58.7$ (*c* = 1.0, CHCl₃).

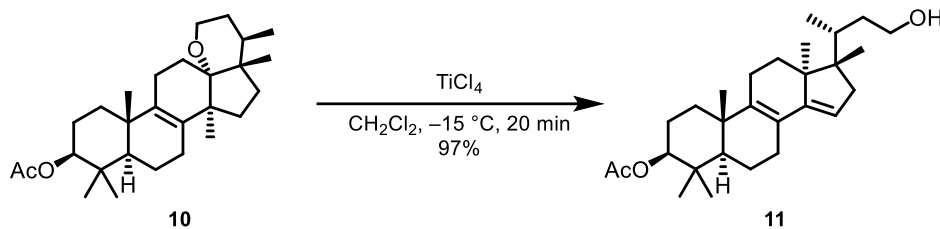
13 α ,23-Epoxy-4,4,14 α ,17 β -tetramethyl-18,24-dinor-5 α -chola-8-ene-3 β -yl acetate (**10**)



The reaction was carried out in multiple batches of 100 mg, which were combined after the Na₂S₂O₃ solution was added. A flame dried 10 mL Schlenk tube was charged with alcohol **9** (90% purity, 100 mg, 209 μmol , 1.0 eq.) dissolved in CH₂Cl₂ (4.7 mL). Using a water bath, the solution was cooled to 10 °C and subsequently charged with phenyliodine(III) diacetate (299 mg, 928 μmol , 4.0 eq.) and NaI (139 mg, 928 μmol , 4.0 eq.). The solution was irradiated by a compact fluorescent lamp (45 W) at a distance of 2 cm for 4 h at 10 °C. After this time, Na₂S₂O₃ (sat. aq., 5 mL) and EtOAc (5 mL) were added and the mixture was stirred at 23 °C for 30 min. The phases were separated and the aqueous phase was extracted with EtOAc (3 x 40 mL). The combined organic phases were dried over MgSO₄ and all volatiles were removed under reduced pressure. Column chromatography (SiO₂, *n*hexane/EtOAc 12:1) gave tetrahydropyran **10** (30.8 mg, 71.9 μmol , 34%) as colourless crystals.

m. p.: 188–190 °C (EtOAc).
TLC: $R_f = 0.5$ (*n*hexane/EtOAc 6:1, *v/v*).
 $^1\text{H-NMR}$: (700 MHz, CDCl₃); δ [ppm] = 4.48 (dd, $J = 11.9, 4.6$ Hz, 1H), 3.66 (ddd, $J = 11.8, 10.7, 5.6$ Hz, 1H), 3.59 (ddd, $J = 11.7, 9.1, 5.8$ Hz, 1H), 2.13 – 2.07 (m, 1H), 2.04 (s, 3H), 2.02 – 1.95 (m, 2H), 1.93 – 1.86 (m, 2H), 1.76 – 1.63 (m, 6H), 1.62 – 1.59 (m, 1H), 1.58 – 1.54 (m, 1H), 1.43 – 1.37 (m, 2H), 1.33 – 1.25 (m, 2H), 1.23 – 1.18 (m, 1H), 1.16 – 1.09 (m, 2H), 1.04 (s, 3H), 0.97 (s, 3H), 0.87 (s, 3H), 0.87 (s, 3H), 0.86 (d, $J = 7.1$ Hz, 3H), 0.78 (s, 3H).
 $^{13}\text{C-NMR}$: (176 MHz, CDCl₃); δ [ppm] = 171.1, 137.1, 133.4, 83.2, 81.1, 57.4, 52.2, 50.9, 45.2, 39.1, 37.7, 37.6, 36.2, 35.4, 33.9, 28.2, 27.7, 27.5, 26.0, 24.2, 21.5, 21.2, 21.0, 19.4, 18.8, 16.9, 16.7, 16.2.
IR: (film); $\tilde{\nu}$ [cm⁻¹] = 2952 (m), 2920 (s), 2852 (m), 1739 (w), 1458 (w), 1377 (w), 1243 (w).
HRMS: (ESI-TOF); *m/z* calcd. for C₂₈H₄₄O₃Na⁺ [M+Na]⁺: 451.3183, found: 451.3175.
Opt. act.: $[\alpha]_D^{24} = +67.8$ (*c* = 0.68, CHCl₃).

23-Hydroxy-4,4,17 β -trimethyl-24-nor-5 α ,13 α -chola-8,14-diene-3 β -yl acetate (10**)**



A solution of tetrahydropyran **10** (122 mg, 285 μmol , 1.0 eq.) in CH_2Cl_2 (19 mL) was cooled to -15°C and TiCl_4 (0.31 mL, 2.82 mmol, 10 eq.) was added dropwise. After stirring at -15°C for 20 min, the solution was neutralized with NaHCO_3 (sat. aq., 15 mL), allowed to warm to 23°C over 20 min, and the aqueous phase was extracted with EtOAc (3 x 20 mL). The combined organic phases were dried over MgSO_4 and concentrated under reduced pressure. Column chromatography (SiO_2 , *n*hexane/ EtOAc 3:1) gave diene **11** (119 mg, 278 μmol , 97%) as a light yellow amorphous solid.

TLC: $R_f = 0.24$ (*n*hexane/ EtOAc 3:1, *v/v*).

$^1\text{H-NMR}$: (700 MHz, CDCl_3); δ [ppm] = 5.30 – 5.26 (m, 1H), 4.50 (dd, $J = 11.8, 4.6$ Hz, 1H), 3.74 (ddd, $J = 10.2, 8.4, 4.5$ Hz, 1H), 3.64 (dt, $J = 10.3, 7.6$ Hz, 1H), 2.40 – 2.35 (m, 1H), 2.28 (d, $J = 16.7$ Hz, 1H), 2.08 – 2.07 (m, 1H), 2.05 (s, 3H), 1.98 – 1.92 (m, 2H), 1.87 – 1.82 (m, 1H), 1.82 – 1.77 (m, 1H), 1.77 – 1.70 (m, 2H), 1.70 – 1.59 (m, 3H), 1.55 – 1.47 (m, 1H), 1.36 – 1.24 (m, 4H), 1.22 (dd, $J = 12.4, 1.9$ Hz, 1H), 1.03 (s, 3H), 0.99 – 0.95 (m, 1H), 0.90 (s, 3H), 0.90 (s, 3H), 0.87 (d, $J = 6.7$ Hz, 3H), 0.85 (s, 3H), 0.77 (s, 3H).

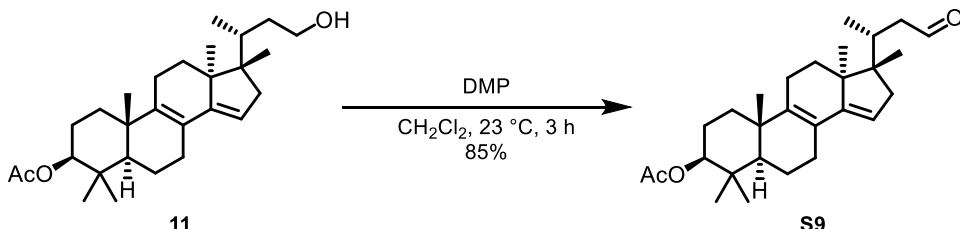
$^{13}\text{C-NMR}$: (176 MHz, CDCl_3); δ [ppm] = 171.2, 148.6, 141.9, 123.2, 116.4, 81.0, 62.1, 50.8, 50.3, 48.2, 45.5, 37.9 (2C), 35.9, 34.5, 34.4, 30.1, 28.1, 27.1, 24.1, 22.9, 21.4, 19.3, 18.3, 17.3, 16.8, 15.8, 15.8.

IR: (film); $\tilde{\nu}$ [cm^{-1}] = 3416 (br, w), 2922 (s), 2852 (m), 1735 (m), 1458 (m), 1376 (w), 1244 (m), 1028 (w), 759 (s).

HRMS: (ESI-TOF); m/z calcd. for $\text{C}_{28}\text{H}_{44}\text{O}_3\text{Na}^+ [\text{M}+\text{Na}]^+$: 451.3183, found: 451.3185.

Opt. act.: $[\alpha]_D^{24} = +40.0$ ($c = 0.82$, CHCl_3).

4,4,17 β -Trimethyl-23-oxo-24-nor-5 α ,13 α -chola-8,14-diene-3 β -yl acetate (S9**)**



To a solution of alcohol **11** (60.5 mg, 141 μmol , 1.0 eq.) in CH_2Cl_2 (1.4 mL) was added Dess–Martin periodinane (77.8 mg, 183 μmol , 1.3 eq.) at 0°C . After 15 min, the solution was warmed to 23°C and stirred for 3 h at this temperature. Sat. aq. $\text{Na}_2\text{S}_2\text{O}_3$ (3 mL) was added and the mixture was stirred for an additional 15 min. The aqueous phase was extracted with CH_2Cl_2 (3 x 4 mL), the combined organic phases were washed sequentially with sat. aq. NaHCO_3 (2 x 4 mL) and brine (4 mL), dried over MgSO_4 , and all volatiles were removed under reduced pressure. Column chromatography (SiO_2 , *n*hexane/ EtOAc 14:1) gave aldehyde **S9** (51.0 mg, 120 μmol , 85%) as colourless crystals.

TLC: $R_f = 0.46$ (nhexane/EtOAc 6:1, v/v).

¹H-NMR: (400 MHz, CDCl₃); δ [ppm] = 9.76 (d, $J = 3.5$ Hz, 1H), 5.33 – 5.27 (m, 1H), 4.49 (dd, $J = 11.6, 4.7$ Hz, 1H), 2.52 (d, $J = 15.1$ Hz, 1H), 2.39 – 2.31 (m, 2H), 2.26 – 2.16 (m, 2H), 2.11 – 2.09 (m, 1H), 2.05 (s, 3H), 1.97 (dd, $J = 16.4, 3.6$ Hz, 1H), 1.83 (dt, $J = 13.1, 3.6$ Hz, 1H), 1.76 – 1.69 (m, 2H), 1.67 – 1.59 (m, 3H), 1.57 – 1.44 (m, 3H), 1.37 – 1.28 (m, 2H), 1.03 (s, 3H), 0.93 – 0.88 (m, 9H), 0.86 (s, 3H), 0.78 (s, 3H).

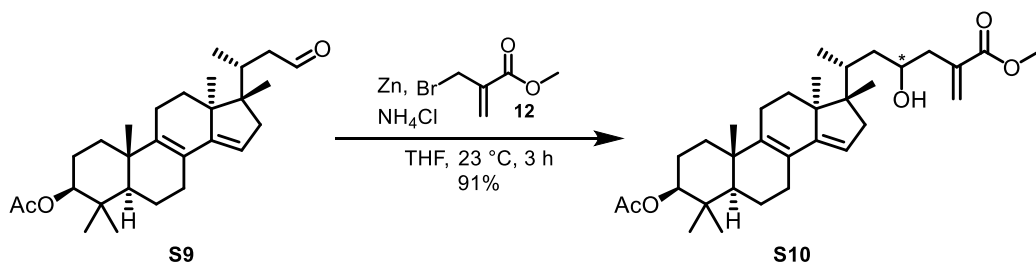
¹³C-NMR: (101 MHz, CDCl₃); δ [ppm] = 203.2, 171.1, 148.3, 141.9, 123.2, 116.4, 80.9, 50.8, 49.8, 48.1, 47.8, 45.2, 37.9, 37.9, 34.5, 32.5, 30.1, 28.1, 27.0, 24.1, 22.9, 21.5, 19.4, 18.3, 17.4, 16.8, 16.8, 16.1.

IR: (film); $\tilde{\nu}$ [cm⁻¹] = 2962 (m), 2941 (m), 2877 (m), 1728 (s), 1456 (m), 1367 (m), 1242 (s), 1089 (m), 1028 (m), 975 (m), 902 (w), 867 (w), 796 (w), 751 (m), 665 (w).

HRMS: (ESI-TOF); m/z calcd. for C₂₈H₄₂O₃Na⁺ [M+Na]⁺: 449.3026, found: 449.3030.

Opt. act.: $[\alpha]_D^{20} = +51.2$ ($c = 0.93$, CHCl₃).

Methyl 4,4,17 β -trimethyl-23-hydroxy-5 α ,13 α -cholestane-8,14,25(27)-triene-26-carboxylate (**S10**)



Aldehyde **S9** (17.5 mg, 41.0 μ mol, 1.0 eq.) was dissolved in THF (0.9 mL) and zinc powder (26.8 mg, 410 μ mol, 10 eq.) was added. Bromomethyl acrylate **12** (15.8 μ L, 132 μ mol, 3.2 eq.) and NH₄Cl (sat. aq., 17.5 μ L) were simultaneously added and the solution was stirred for 3 h at 23 °C. After addition of phosphate buffer (pH = 7, 2 mL) the aqueous phase was extracted with EtOAc (3 x 5 mL), the combined organic phases were dried over MgSO₄, and all volatiles were removed under reduced pressure. Column chromatography (SiO₂, nhexane/EtOAc 4:1) gave secondary alcohol **S10** as a separable mixture of epimers at C23 (19.6 mg, 37.2 μ mol, 91%) as a colourless oil.

S10a:

TLC: $R_f = 0.29$ (nhexane/EtOAc 4:1, v/v).

¹H-NMR: (400 MHz, CDCl₃); δ [ppm] = 6.28 (d, $J = 1.5$ Hz, 1H), 5.72 – 5.68 (m, 1H), 5.30 – 5.26 (m, 1H), 4.50 (dd, $J = 11.6, 4.7$ Hz, 1H), 3.88 – 3.80 (m, 1H), 3.78 (s, 3H), 2.80 (ddd, $J = 13.8, 2.7, 1.2$ Hz, 1H), 2.42 – 2.34 (m, 1H), 2.29 (d, $J = 16.2$ Hz, 1H), 2.21 – 2.14 (m, 1H), 2.11 – 2.06 (m, 2H), 2.06 (s, 3H), 2.02 – 1.90 (m, 3H), 1.85 (dt, $J = 13.1, 3.5$ Hz, 1H), 1.77 – 1.70 (m, 2H), 1.68 – 1.57 (m, 4H), 1.53 – 1.41 (m, 2H), 1.37 – 1.27 (m, 1H), 1.25 – 1.19 (m, 2H), 1.03 (s, 3H), 0.95 (d, $J = 6.6$ Hz, 3H), 0.90 (s, 3H), 0.90 (s, 3H), 0.84 (s, 3H), 0.78 (s, 3H).

S10b:

TLC: $R_f = 0.22$ (nhexane/EtOAc 4:1, v/v).

¹H-NMR: (400 MHz, CDCl₃); δ [ppm] = 6.25 (d, $J = 1.5$ Hz, 1H), 5.68 (d, $J = 1.3$ Hz, 1H), 5.30 – 5.25 (m, 1H), 4.50 (dd, $J = 11.6, 4.7$ Hz, 1H), 3.85 – 3.80 (m, 1H), 3.77 (s, 3H), 2.54 (ddd, $J = 13.9, 3.7, 1.1$ Hz, 1H), 2.42 – 2.28 (m, 3H), 2.24 – 2.17 (m, 1H), 2.13 – 2.06 (m, 2H), 2.05 (s, 3H), 2.05 – 2.00 (m, 1H), 1.99 – 1.89 (m, 2H), 1.84 (dt, $J = 13.1, 3.5$ Hz, 1H), 1.77 – 1.70 (m, 2H), 1.68 – 1.57 (m, 3H),

1.53 – 1.46 (m, 1H), 1.36 – 1.29 (m, 1H), 1.27 – 1.14 (m, 3H), 1.03 (s, 3H), 0.92 – 0.86 (m, 12H), 0.75 (s, 3H).

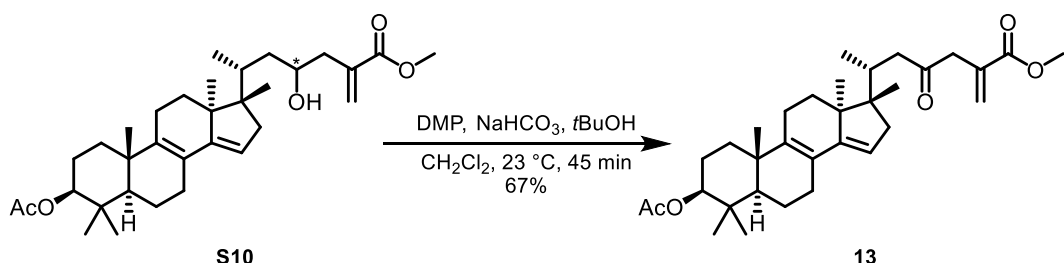
S10a/b:

¹³C-NMR: (101 MHz, CDCl₃); δ [ppm] = 171.2, 171.2, 186.3, 186.1, 148.7, 148.6, 141.9, 141.8, 137.8, 137.7, 128.2, 127.9, 123.2, 123.1, 116.5, 116.4, 81.0 (2C), 70.1, 68.5, 52.2 (2C), 50.8, 50.8, 50.6, 50.2, 48.1, 48.1, 45.7, 45.6, 40.4 (2C), 40.0, 37.9 (4C), 35.5, 34.5, 34.4, 33.8, 30.1, 30.0, 28.1 (2C), 27.0 (2C), 24.1, 22.9, 22.9, 21.5 (2C), 19.3, 19.3, 18.3 (2C), 17.3, 17.2, 16.8 (2C), 15.9 (2C), 15.8 (2C), 15.4 (2C).

HRMS:

(ESI-TOF); *m/z* calcd. for C₃₃H₅₁O₅⁺ [M+H]⁺: 527.3731, found: 527.3739.

Methyl 4,4,17β-trimethyl-23-oxo-5α,13α-cholestane-8,14,25(27)-triene-26-carboxylate (**13**)



To a solution of secondary alcohols **S10** (16.5 mg, 30.5 μmol, 1.0 eq.) and *t*BuOH (5 μL) in CH₂Cl₂ (1.0 mL) was added NaHCO₃ (19.4 mg, 231 μmol, 7.6 eq.) and Dess–Martin periodinane (49.6 mg, 117 μmol, 3.8 eq.) at 23 °C. The solution was stirred for 45 min at this temperature. Sat. aq. Na₂S₂O₃ (2 mL) and NaHCO₃ (sat. aq., 2 mL) were added and the mixture was stirred for an additional 15 min. The aqueous phase was extracted with CH₂Cl₂ (3 × 4 mL), the combined organic phases were dried over MgSO₄, and all volatiles were removed under reduced pressure. Column chromatography (SiO₂, *n*hexane/EtOAc 6:1) gave ketone **13** (10.8 mg, 20.6 μmol, 67%) as colourless crystals.

TLC: *R*_f = 0.35 (*n*hexane/EtOAc 6:1, *v/v*).

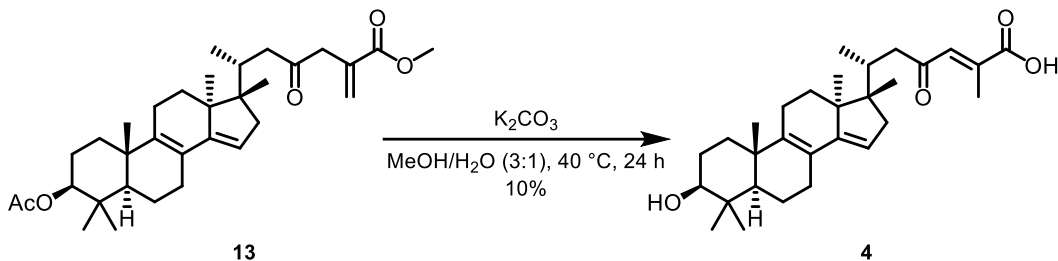
¹H-NMR: (400 MHz, CDCl₃); δ [ppm] = 6.34 (s, 1H), 5.64 (s, 1H), 5.32 – 5.26 (m, 1H), 4.49 (dd, *J* = 11.6, 4.7 Hz, 1H), 3.75 (s, 3H), 3.45 (d, *J* = 16.8 Hz, 1H), 3.36 (d, *J* = 16.9 Hz, 1H), 2.57 (d, *J* = 15.8 Hz, 1H), 2.53 – 2.45 (m, 1H), 2.39 – 2.26 (m, 3H), 2.14 – 2.08 (m, 2H), 2.05 (s, 3H), 1.95 (dd, *J* = 16.4, 3.5 Hz, 1H), 1.83 (dt, *J* = 13.1, 3.5 Hz, 1H), 1.78 – 1.59 (m, 5H), 1.52 – 1.44 (m, 2H), 1.36 – 1.29 (m, 1H), 1.23 – 1.20 (m, 1H), 1.03 (s, 3H), 0.90 (s, 3H), 0.90 (s, 3H), 0.86 (d, *J* = 7.2 Hz, 3H), 0.85 (s, 3H), 0.77 (s, 3H).

¹³C-NMR: (101 MHz, CDCl₃); δ [ppm] = 207.3, 171.1, 167.0, 148.2, 141.8, 134.4, 128.8, 123.3, 116.6, 80.9, 52.2, 50.8, 49.9, 48.1, 46.6, 46.5, 45.3, 37.9 (2C), 34.5, 33.9, 30.2, 28.1, 27.0, 24.1, 22.9, 21.5, 19.4, 18.3, 17.4, 16.8, 16.5, 16.1.

HRMS: (ESI-TOF); *m/z* calcd. for C₃₃H₄₈O₅Na⁺ [M+Na]⁺: 547.3394, found: 547.3396.

Opt. act.: [α]_D²⁰ = +40.0 (c = 1.00, CHCl₃).

Abifarine B (4)



To a solution of methylester **13** (8.0 mg, 15.2 μmol , 1.0 eq.) in a mixture of MeOH and H₂O (1.52 mL, 3:1 v/v) was added K₂CO₃ (10.5 mg, 76.0 μmol , 5.0 eq.). After stirring at 40 °C for 24 h the solution was diluted with water (2 mL) and acidified with HCl (0.1 M) to pH = 2, leading to the formation of a colourless precipitate. The aqueous phase was extracted with CH₂Cl₂ (4 x 3 mL), the combined organic phases were dried over Na₂SO₄, and all volatiles were removed under reduced pressure. Preparative TLC (SiO₂, CH₂Cl₂/MeOH 16.5/1) gave abifarine B (**4**) (0.7 mg, 1.5 μmol , 10%) as a colourless solid.

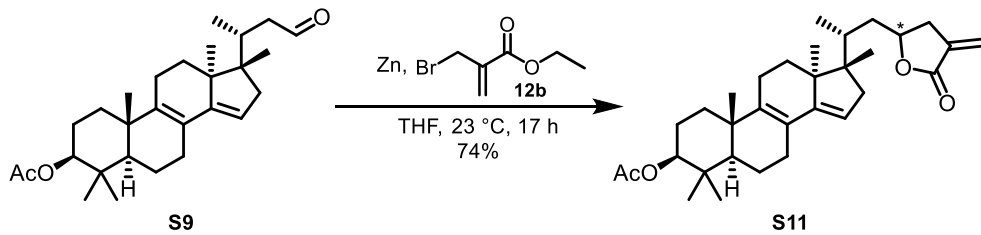
TLC: R_f = 0.22 (CH₂Cl₂/MeOH 20:1, v/v).

¹H-NMR: (600 MHz, pyridin-d₅); δ [ppm] = 7.65 (d, J = 1.6 Hz, 1H), 5.43 – 5.41 (m, 1H), 3.47 (dd, J = 9.2, 6.9 Hz, 1H), 2.84 (d, J = 15.8 Hz, 1H), 2.80 – 2.73 (m, 1H), 2.62 (d, J = 1.6 Hz, 3H), 2.56 (dd, J = 15.9, 11.3 Hz, 1H), 2.48 – 2.45 (m, 1H), 2.39 (d, J = 16.3 Hz, 1H), 2.18 (d, J = 8.3 Hz, 2H), 2.11 – 2.08 (m, 1H), 1.98 (dd, J = 16.2, 3.5 Hz, 1H), 1.94 – 1.90 (m, 2H), 1.84 – 1.82 (m, 1H), 1.79 – 1.77 (m, 1H), 1.74 – 1.70 (m, 1H), 1.60 – 1.56 (m, 1H), 1.54 – 1.50 (m, 1H), 1.25 (s, 3H), 1.25 – 1.24 (m, 1H), 1.22 – 1.20 (m, 1H), 1.08 (s, 3H), 1.08 (s, 3H), 1.07 (s, 3H), 0.97 (d, J = 6.6 Hz, 3H), 0.86 (s, 3H).

¹³C-NMR: (151 MHz, pyridin-d₅); δ [ppm] = 202.4, 170.4, 148.8, 143.0, 142.3, 132.8, 123.1, 116.5, 77.9, 51.0, 50.1, 48.7, 48.3, 45.3, 39.4, 38.2, 35.1, 34.2, 30.2, 28.6, 28.5, 27.4, 23.1, 19.3, 18.7, 17.6, 16.7, 16.4, 16.2, 15.0.

HRMS: (ESI-TOF); *m/z* calcd. for C₃₀H₄₃O₄⁻ [M]⁻: 467.3221, found: 467.3232.

3 β -Acetoxy-4,4,17 β -trimethyl-5 α ,13 α -cholestane-8,14,25(27)-triene-26,23-lactone (S11**)**



To a solution of aldehyde **S9** (70.0 mg, 164 μmol , 1.0 eq.) in THF (1.75 mL) was added activated zinc dust (63 mg, 963 μmol , 5.9 eq.) and bromoethyl acrylate (35 μL , 272 μmol , 1.7 eq.). After stirring for 17 h at 23 °C, the reaction was quenched with NH₄Cl (sat. aq., 2 mL), the phases were separated, and the aqueous phase was extracted with EtOAc (3 x 4 mL). The combined organic phases were dried over MgSO₄ and all volatiles were removed under reduced pressure. Column chromatography (SiO₂, nhexane/EtOAc 6:1) gave lactone **S11** (mixture of epimers at C23, 65.2 mg, 121 μmol , 74%) as a colourless amorphous solid.

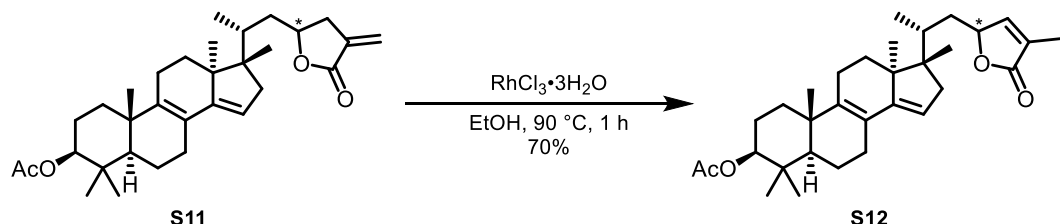
S11a/b:

TLC: $R_f = 0.61$ (*n*hexane/EtOAc 3:1, *v/v*).

¹H-NMR: (400 MHz, CDCl₃); δ [ppm] = 6.27 – 6.18 (m, 2H), 5.67 – 5.58 (m, 2H), 5.27 (s, 2H), 4.65 – 4.54 (m, 2H), 4.52 – 4.44 (m, 2H), 3.15 – 3.00 (m, 2H), 2.67 – 2.59 (m, 1H), 2.57 – 2.50 (m, 1H), 2.38 – 2.24 (m, 5H), 2.05 – 2.03 (m, 6H), 2.01 – 1.90 (m, 4H), 1.85 – 1.55 (m, 15H), 1.53 – 1.43 (m, 4H), 1.43 – 1.14 (m, 8H), 1.02 (s, 3H), 1.01 (s, 3H), 0.94 (s, 3H), 0.92 (s, 3H), 0.91 – 0.86 (m, 12H), 0.84 (s, 3H), 0.82 (s, 3H), 0.78 (s, 3H), 0.75 (s, 3H).

HRMS: (ESI-TOF); *m/z* calcd. for C₃₂H₄₆O₄Na⁺ [M+Na]⁺: 517.3288, found: 517.3281.

3 β -Acetoxy-4,4,17 β -trimethyl-5 α ,13 α -cholestane-8,14,24-triene-26,23-lactone (**S12**)



To a solution of lactones **S11** (32.5 mg, 65.7 μ mol, 1.0 eq.) in EtOH (4.5 mL) was added RuCl₃·3H₂O (3.0 mg, 11.4 μ mol, 0.17 eq.). The solution was stirred at 90 °C for 1 h. After the solution was cooled to 23 °C, all volatiles were removed under reduced pressure and the crude product was purified by column chromatography (SiO₂, *n*hexane/EtOAc 6:1) to yield butenolide **S12** (mixture of epimers at C23, 22.9 mg, 46.3 μ mol, 70%) as a colourless amorphous solid.

S12a/b:

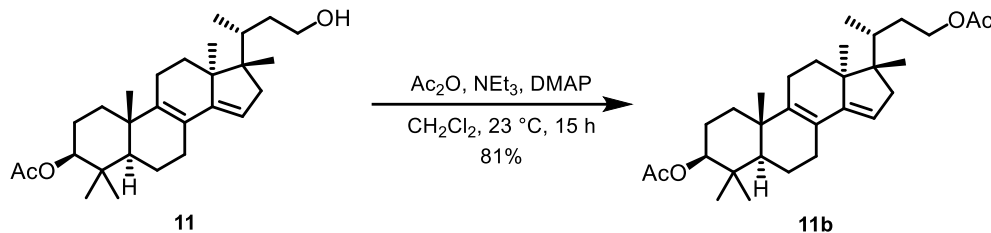
TLC: $R_f = 0.58$ (*n*hexane/EtOAc 3:1, *v/v*).

¹H-NMR: (400 MHz, CDCl₃); δ [ppm] = 7.18 – 7.14 (m, 1H), 7.02 – 7.00 (m, 1H), 5.30 – 5.24 (m, 2H), 4.98 – 4.90 (m, 2H), 4.52 – 4.46 (m, 2H), 2.39 – 2.25 (m, 5H), 2.05 (s, 3H), 2.04 (s, 3H), 2.01 – 1.94 (m, 3H), 1.94 – 1.91 (m, 6H), 1.85 – 1.78 (m, 2H), 1.76 – 1.39 (m, 20H), 1.33 – 1.19 (m, 6H), 1.02 (s, 3H), 1.01 (s, 3H), 0.99 (d, *J* = 6.6 Hz, 3H), 0.97 (d, *J* = 6.6 Hz, 3H), 0.91 – 0.87 (m, 12H), 0.83 (s, 3H), 0.79 – 0.76 (m, 6H), 0.75 (s, 3H).

¹³C-NMR: (101 MHz, CDCl₃); δ [ppm] = 174.4, 174.3, 171.1, 171.1, 149.8, 148.7, 148.5, 148.3, 142.0, 141.9, 130.1, 129.6, 123.1, 123.1, 116.2, 116.2, 81.0, 80.9, 80.8, 79.8, 77.4, 50.8, 50.7, 50.5, 50.2, 48.1, 48.0, 45.5, 45.4, 37.9, 37.9 (2C), 37.9, 37.5, 37.1, 35.3, 34.6, 34.5, 34.4, 30.1, 30.0, 28.1 (2C), 27.0, 24.1, 22.9, 22.8, 21.4, 21.4, 19.3, 19.3, 18.3, 18.2, 17.4, 17.3, 16.8, 16.8, 16.3, 15.6 (4C), 10.9, 10.8.

HRMS: (ESI-TOF); *m/z* calcd. for C₃₂H₄₆O₄Na⁺ [M+Na]⁺: 517.3288, found: 517.3281.

4,4,17 β -Trimethyl-24-nor-5 α ,13 α -chola-8,14-diene-3 β ,23-yl diacetate (11b**)**



To a stirred solution of diene **11** (14.0 mg, 32.7 μmol , 1.0 eq.), *N,N*-dimethyl-4-aminopyridine (0.2 mg, 1.63 μmol , 0.05 eq.), and NEt_3 (13.6 μL , 98.0 μmol , 3.0 eq.) in CH_2Cl_2 (100 μL) was added Ac_2O (6.2 μL , 65.3 μmol , 2.0 eq.) and the resulting mixture was stirred at 25 °C for 15 h. The reaction mixture was then diluted with CH_2Cl_2 (1 mL), sat. aq. NaHCO_3 (0.5 mL) was added, and the mixture was stirred for an additional 20 min. The aqueous phase was extracted with CH_2Cl_2 (3 \times 1 mL), the combined organic phases were dried over MgSO_4 , and all volatiles were removed under reduced pressure. Column chromatography (SiO_2 , *n*hexane/EtOAc 6:1, v/v) gave diacetate **11b** (12.5 mg, 26.6 μmol , 81%) as a colourless crystalline solid.

TLC: $R_f = 0.55$ (*n*hexane/EtOAc 4:1, v/v).

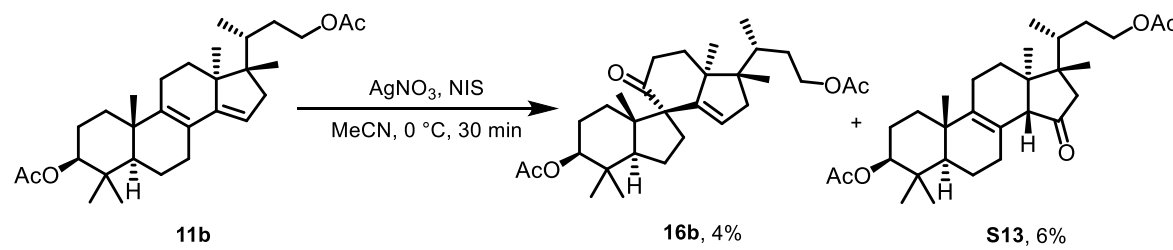
$^1\text{H-NMR}$: (400 MHz, CDCl_3) δ [ppm] = 5.30 – 5.24 (m, 1H), 4.49 (dd, $J = 11.6, 4.7$ Hz, 1H), 4.19 – 4.13 (m, 1H), 4.08 – 4.02 (m, 1H), 2.40 – 2.26 (m, 2H), 2.05 (s, 3H), 2.04 (s, 3H), 1.99 – 1.80 (m, 5H), 1.76 – 1.46 (m, 8H), 1.35 – 1.27 (m, 2H), 1.24 – 1.20 (m, 1H), 1.03 (s, 3H), 0.90 (s, 3H), 0.90 (s, 3H), 0.88 (d, $J = 6.7$ Hz, 3H), 0.83 (s, 3H), 0.76 (s, 3H).

$^{13}\text{C-NMR}$: (101 MHz, CDCl_3) δ [ppm] = 171.4, 171.1, 148.5, 141.9, 123.2, 116.4, 80.9, 63.7, 50.8, 50.3, 48.1, 45.5, 37.9 (2C), 34.6, 34.5, 31.8, 30.1, 28.1, 27.0, 24.1, 23.0, 21.4, 21.2, 19.3, 18.3, 17.1, 16.8, 15.7, 15.6.

HRMS: (ESI-TOF); m/z calcd. for $\text{C}_{30}\text{H}_{46}\text{O}_4\text{Na}^+$ [$\text{M}+\text{Na}]^+$: 493.3288, found: 493.3290.

Opt. Act.: $[\alpha]_D^{24} = +51.0$ ($c = 1.00$, CHCl_3).

10(9 \rightarrow 8)abeo-4,4,17 β -trimethyl-24-nor-5 α ,13 α -chola-14-ene-3 β ,23-yl diacetate (16b**)**

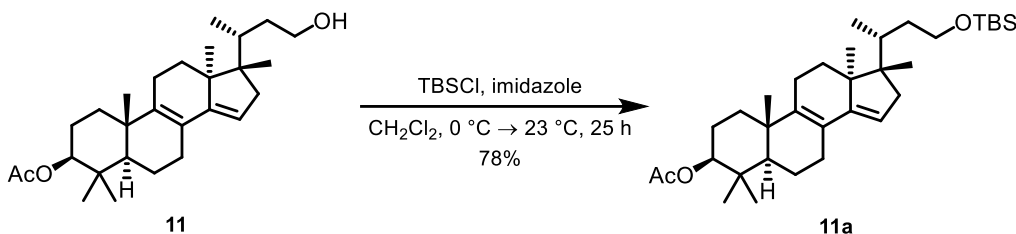


To a stirred solution of diene **11b** (12.5 mg, 26.6 μmol , 1.0 eq.) in acetonitrile (760 μL) were added NIS (8.9 mg, 39.5 μmol , 1.5 eq.) and a solution of AgNO_3 (0.45 mg, 2.66 μmol , 0.1 eq.) in H_2O (143 μL) at 0 °C under exclusion of light. After stirring for 30 min at this temperature, sat. aq. $\text{Na}_2\text{S}_2\text{O}_3$ (2 mL) was added, the solution was warmed to 23 °C, and stirred for an additional 20 min. The aqueous phase was extracted with EtOAc (3 \times 5 mL), the combined organic phases were washed with brine (10 mL), dried over MgSO_4 , and all volatiles were removed under reduced pressure. Column chromatography (SiO_2 , *n*hexane/EtOAc 6:1 → 3:1, v/v) and subsequent preparative TLC (developed twice in *n*hexane/EtOAc 2:1) gave spiro-compound **16b** (0.5 mg, 1.03 μmol , 4%) and 15-ketone **S13** (0.8 mg, 1.64 μmol , 6%) as yellow oils.

Spectroscopically homogeneous compound for full analysis could be synthesised from spiro-alcohol **16** by acetylation of the alcohol using the same procedure as for the synthesis of **11b**.

Mp.:	121–123 °C (CHCl ₃).
TLC:	R _f = 0.36 (nhexane/EtOAc 3:1, v/v).
¹H-NMR:	(500 MHz, CDCl ₃) δ [ppm] = 5.35 – 5.30 (m, 1H), 4.41 – 4.34 (m, 1H), 4.15 (ddd, J = 10.9, 7.6, 4.4 Hz, 1H), 4.03 (ddd, J = 10.9, 8.5, 6.7 Hz, 1H), 2.54 (ddd, J = 20.1, 12.8, 7.5 Hz, 1H), 2.37 (dd, J = 19.9, 7.0 Hz, 1H), 2.33 – 2.24 (m, 2H), 2.11 – 1.99 (m, 8H), 1.94 (ddd, J = 11.4, 6.7, 2.1 Hz, 1H), 1.87 (dt, J = 14.8, 10.2 Hz, 1H), 1.72 – 1.59 (m, 7H), 1.53 – 1.43 (m, 1H), 1.39 – 1.31 (m, 2H), 1.04 (s, 3H), 0.94 (s, 3H), 0.91 – 0.87 (m, 6H), 0.84 (s, 3H), 0.82 (s, 3H).
¹³C-NMR:	(151 MHz, CDCl ₃) δ [ppm] = 215.8, 171.4, 171.2, 151.1, 125.0, 80.7, 67.2, 63.4, 51.8, 50.6, 50.6, 48.6, 45.7, 38.2, 37.8, 35.7, 34.7, 32.7, 31.5, 29.0, 27.0, 25.3, 21.4, 21.2, 20.7, 19.2, 18.4, 16.9, 16.1, 15.5.
IR:	ν [cm ⁻¹] = 2961 (m), 2926 (m), 2878 (w), 2840 (w), 1737 (s), 1695 (m), 1457 (w), 1442 (w), 1417 (w), 1371 (w), 1244 (s), 1073 (w), 1048 (w), 1027 (w), 993 (w), 983 (w), 799 (w).
HRMS:	(ESI-TOF); m/z calcd. for C ₃₀ H ₄₆ O ₅ Na ⁺ [M+Na] ⁺ : 509.3237, found: 509.3226.
Opt. Act.:	[α] _D ²⁵ = -9.9 (c = 0.5, CHCl ₃).

23-(*tert*-Butyldimethylsilyl)oxy-4,4,17β-trimethyl-24-nor-5α,13α-chola-8,14-diene-3β-yl acetate (**11a**)

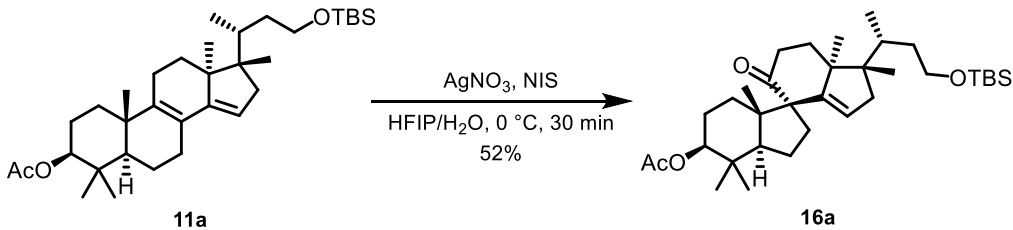


To a stirred solution of diene **11** (53.7 mg, 125 μmol, 1.0 eq.) in CH₂Cl₂ (210 μL) were added TBSCl (28.3 mg, 188 μmol, 1.5 eq.) and imidazole (12.8 mg, 188 μmol, 1.5 eq.) at 0 °C. After addition, the solution was warmed to 23 °C and stirred at this temperature for 25 h. Phosphate buffer (pH = 7, 5.0 mL) was added, the aqueous phase was extracted with CH₂Cl₂ (3 × 15 mL), the combined organic phases were washed with brine (30 mL), dried over MgSO₄, and all volatiles were removed under reduced pressure. Column chromatography (SiO₂, nhexane/EtOAc 29:1, v/v) gave diacetate **11a** (54.1 mg, 99.6 μmol, 78%) as a colourless oil.

TLC:	R _f = 0.27 (nhexane/EtOAc 29:1, v/v).
¹H-NMR:	(600 MHz, CDCl ₃) δ [ppm] = 5.27 (s, 1H), 4.50 (dd, J = 11.8, 4.6 Hz, 1H), 3.68 (ddd, J = 10.1, 8.0, 4.2 Hz, 1H), 3.59 (ddd, J = 10.1, 8.2, 6.8 Hz, 1H), 2.41 – 2.34 (m, 1H), 2.27 (d, J = 16.3 Hz, 1H), 2.09 – 2.04 (m, 6H), 1.94 (ddd, J = 16.1, 8.2, 2.5 Hz, 2H), 1.84 (dt, J = 13.2, 3.6 Hz, 1H), 1.79 – 1.71 (m, 3H), 1.69 – 1.61 (m, 4H), 1.50 (qd, J = 12.5, 6.7 Hz, 1H), 1.33 (td, J = 13.4, 3.9 Hz, 3H), 1.23 – 1.15 (m, 3H), 1.03 (s, 3H), 1.00 – 0.91 (m, 2H), 0.89 (s, 9H), 0.85 (s, 3H), 0.84 (s, 3H), 0.76 (s, 3H), 0.05 (s, 6H).
¹³C-NMR:	(151 MHz, CDCl ₃) δ [ppm] = 171.2, 148.4, 141.9, 123.1, 116.4, 82.2, 62.1, 50.8, 50.3, 48.2, 45.6, 37.9, 36.0, 34.5, 34.2, 30.1, 29.8, 28.1, 27.1, 26.1, 24.1, 23.0, 21.5, 19.3, 18.5, 18.3, 17.3, 16.8, 15.9, 15.7, -5.1, -5.2.
IR:	ν [cm ⁻¹] = 2954 (s), 2926 (s), 2855 (m), 1737 (m), 1463 (w), 1376 (w), 1245 (s), 1090 (m), 1030 (w), 900 (w), 833 (m), 776 (w).
HRMS:	(ESI-TOF); m/z calcd. for C ₃₄ H ₅₈ O ₃ SiNa ⁺ [M+Na] ⁺ : 565.4047, found: 565.4046.

Opt. Act.: $[\alpha]_D^{23} = +25.8$ ($c = 0.98$, CHCl_3).

23-(*tert*-Butyldimethylsilyl)oxy-10(9→8)abeo-4,4,17β-trimethyl-24-nor-5α,13α-chola-14-ene-3β-yl acetate (**16a**)



To a stirred solution of diene **11a** (22.3 mg, 41.1 μmol , 1.0 eq.) in hexafluoroisopropanol (1.2 mL) were added *N*-Iodosuccinimide (13.9 mg, 61.7 μmol , 1.5 eq.) and a solution of AgNO_3 (0.7 mg, 4.11 μmol , 0.1 eq.) in H_2O (220 μL) at 0 °C under exclusion of light. After stirring for 30 min at this temperature, sat. aq. $\text{Na}_2\text{S}_2\text{O}_3$ (3 mL) was added, the solution was warmed to 23 °C, and stirred for an additional 20 min. The aqueous phase was extracted with CH_2Cl_2 (4 × 10 mL), the combined organic phases were washed with brine (10 mL), dried over MgSO_4 , and all volatiles were removed under reduced pressure. Column chromatography (SiO_2 , nhexane/EtOAc 3:2, v/v) gave spiro-compound **16a** (12.1 mg, 21.3 μmol , 52%) as a yellow oil.

TLC: $R_f = 0.19$ (nhexane/EtOAc 14:1, v/v).

$^1\text{H-NMR}$: (600 MHz, CDCl_3) δ [ppm] = 5.31 (dd, $J = 3.5, 1.8$ Hz, 1H), 4.40 – 4.36 (m, 1H), 3.67 (ddd, $J = 9.9, 7.3, 4.0$ Hz, 1H), 3.58 (ddd, $J = 10.0, 8.7, 6.0$ Hz, 1H), 2.53 (ddd, $J = 20.1, 12.9, 7.5$ Hz, 1H), 2.39 – 2.25 (m, 3H), 2.09 – 2.04 (m, 2H), 2.03 (s, 3H), 2.01 (dd, $J = 16.3, 3.6$ Hz, 2H), 1.76 (ddt, $J = 21.4, 13.6, 7.7$ Hz, 2H), 1.70 (dq, $J = 5.6, 3.0$ Hz, 2H), 1.68 – 1.58 (m, 5H), 1.47 (tdd, $J = 14.1, 11.0, 4.4$ Hz, 1H), 1.36 (td, $J = 11.9, 6.1$ Hz, 1H), 1.19 (dddd, $J = 13.0, 10.9, 6.0, 4.0$ Hz, 2H), 1.04 (s, 3H), 0.94 (s, 3H), 0.88 (s, 9H), 0.86 (s, 3H), 0.85 (s, 3H), 0.84 (s, 3H), 0.04 (s, 6H).

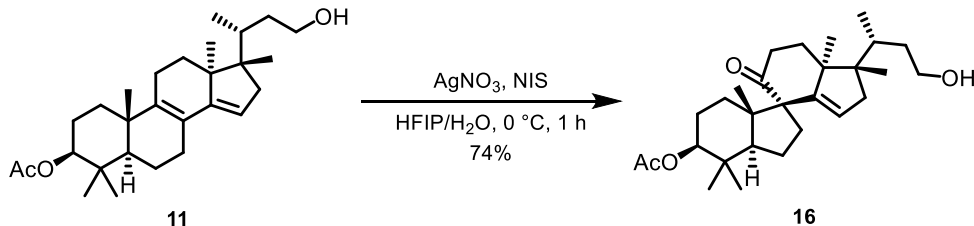
$^{13}\text{C-NMR}$: (151 MHz, CDCl_3) δ [ppm] = 216.1, 171.2, 151.2, 125.0, 80.7, 67.2, 61.7, 51.8, 50.7, 50.5, 48.6, 45.8, 38.3, 37.8, 35.8, 35.7, 34.2, 32.7, 29.0, 27.0, 26.1, 25.3, 21.4, 20.7, 19.3, 18.5, 18.4, 16.9, 16.2, 15.5, –5.1, –5.2.

IR: $\tilde{\nu}$ [cm^{-1}] = 2952 (m), 2925 (m), 2853 (w), 1737 (s), 1697 (w), 1460 (w), 1373 (m), 1217 (m), 1090 (w), 1028 (w), 836 (w), 754 (s).

HRMS: (ESI-TOF); m/z calcd. for $\text{C}_{34}\text{H}_{58}\text{O}_4\text{SiNa}^+$ [M+Na] $^+$: 581.3996, found: 581.4011.

Opt. Act.: $[\alpha]_D^{24} = -20.4$ ($c = 0.1$, CHCl_3).

23-Hydroxy-10(9→8)abeo-4,4,17β-trimethyl-24-nor-5α,13α-chola-14-ene-3β-yl acetate (**16**)

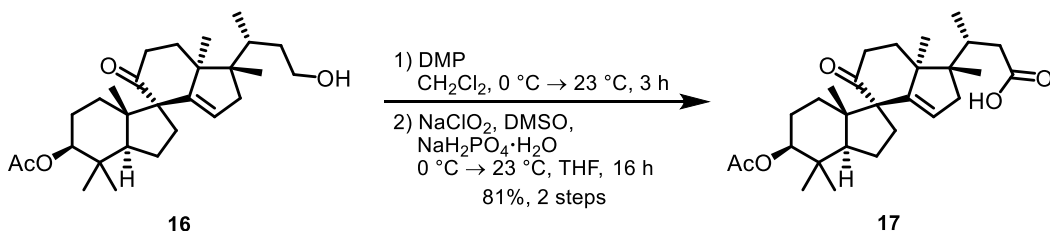


To a stirred solution of diene **11** (53.3 mg, 124 μmol , 1.0 eq.) in hexafluoroisopropanol (3.7 mL) were added *N*-Iodosuccinimide (42.0 mg, 187 μmol , 1.5 eq.) and a solution of AgNO_3 (2.1 mg, 12.4 μmol , 0.1 eq.) in H_2O (670 μL) at 0 °C under exclusion of light. After stirring for 1 h at this temperature, sat. aq. $\text{Na}_2\text{S}_2\text{O}_3$ (4 mL) was added, the solution was warmed to 23 °C, and

stirred for an additional 20 min. The aqueous phase was extracted with CH_2Cl_2 ($4 \times 5 \text{ mL}$), the combined organic phases were washed with brine (15 mL), dried over MgSO_4 , and all volatiles were removed under reduced pressure. Column chromatography (SiO_2 , *n*hexane/EtOAc 3:2, *v/v*) gave spiro-alcohol **16** (40.7 mg, 91.5 μmol , 74%) as a colourless crystalline solid.

- m.p.:** 202–203 °C (EtOAc).
- TLC:** $R_f = 0.27$ (*n*hexane/EtOAc 3:2, *v/v*).
- $^1\text{H-NMR}$:** (700 MHz, CDCl_3) δ [ppm] = 5.32 (dd, $J = 3.6, 1.8 \text{ Hz}$, 1H), 4.39 – 4.35 (m, 1H), 3.74 (ddd, $J = 10.4, 8.1, 4.4 \text{ Hz}$, 1H), 3.62 (ddd, $J = 10.3, 8.1, 7.1 \text{ Hz}$, 1H), 2.52 (ddd, $J = 20.1, 12.8, 7.5 \text{ Hz}$, 1H), 2.35 (ddd, $J = 19.8, 7.2, 1.0 \text{ Hz}$, 1H), 2.33 – 2.25 (m, 2H), 2.09 – 2.01 (m, 5H), 1.97 (dqd, $J = 11.1, 6.7, 2.2 \text{ Hz}$, 1H), 1.80 (td, $J = 13.3, 8.1, 2.3 \text{ Hz}$, 1H), 1.75 – 1.71 (m, 1H), 1.69 (ddd, $J = 8.6, 3.5, 1.2 \text{ Hz}$, 2H), 1.66 – 1.58 (m, 4H), 1.51 – 1.42 (m, 2H), 1.38 – 1.28 (m, 2H), 1.04 (s, 3H), 0.94 (s, 3H), 0.88 (s, 3H), 0.88 (d, $J = 6.6 \text{ Hz}$, 3H), 0.84 (s, 3H), 0.84 (s, 3H).
- $^{13}\text{C-NMR}$:** (176 MHz, CDCl_3) δ [ppm] = 215.9, 171.1, 151.1, 125.0, 80.7, 67.2, 61.8, 51.8, 50.6, 50.6, 48.6, 45.8, 38.2, 37.8, 35.7, 35.6, 34.5, 32.7, 29.0, 27.0, 25.3, 21.3, 20.7, 19.3, 18.4, 16.9, 16.2, 15.6.
- IR:** $\tilde{\nu}$ [cm^{-1}] = 2956 (m), 2926 (s), 2858 (w), 1736 (s), 1694 (w), 1543 (w), 1374 (m), 1242 (m), 1215 (m), 1021 (w), 789 (w), 716 (w).
- HRMS:** (ESI-TOF); m/z calcd. for $\text{C}_{28}\text{H}_{44}\text{O}_4\text{Na}^+ [\text{M}+\text{Na}]^+$: 467.3132, found: 467.3113.
- Opt. act.:** $[\alpha]_D^{24} = -54.0$ ($c = 1.0$, CHCl_3).

3 β -Acetoxy-9-oxo-10(9→8)abeo-4,4,17 β -trimethyl-24-nor-5 α ,13 α -chola-14-ene-23-oic acid (17)



To a solution of spiro-alcohol **16** (100 mg, 225 μmol , 1.0 eq.) in CH_2Cl_2 (2.3 mL) was added Dess–Martin periodinane (124 mg, 292 μmol , 1.3 eq.) at 0 °C. After 15 min, the solution was warmed to 23 °C and stirred for 3 h at this temperature. Sat. aq. $\text{Na}_2\text{S}_2\text{O}_3$ (3 mL) was added and the mixture was stirred for an additional 15 min. The aqueous phase was extracted with CH_2Cl_2 ($3 \times 4 \text{ mL}$), the combined organic phases were washed sequentially with sat. aq. NaHCO_3 ($2 \times 4 \text{ mL}$) and brine (4 mL), dried over MgSO_4 , and all volatiles were removed under reduced pressure. Column chromatography (SiO_2 , *n*hexane/EtOAc 4:1, *v/v*) gave the aldehyde which was immediately dissolved in THF (2.3 mL) and cooled to 0 °C. NaClO_2 (80 wt%, 38.2 mg, 338 μmol , 1.5 eq.), NaH_2PO_4 (68.1 mg, 495 μmol , 2.2 eq.), and DMSO (48.0 μL , 675 μmol , 3.0 eq.) were added, the mixture was stirred for 30 min and then warmed to 23 °C. After stirring for 16 h at this temperature, 1 M HCl (4 mL) was added, the aqueous phase was extracted with CH_2Cl_2 ($4 \times 5 \text{ mL}$), the combined organic phases were dried over Na_2SO_4 , and all volatiles were removed under reduced pressure. Column chromatography (SiO_2 , *n*hexane/EtOAc/AcOH 3:2 + 1% AcOH, *v/v/v*) gave spiro-acid **17** (83.3 mg, 182 μmol , 81%) as colourless cubic crystals.

- m.p.:** decomp. at 231 °C (CHCl_3).
- TLC:** $R_f = 0.38$ (*n*hexane/EtOAc/AcOH 3:2 + 1% AcOH, *v/v/v*).
- $^1\text{H-NMR}$:** (600 MHz, CDCl_3) δ [ppm] = 5.35 – 5.32 (m, 1H), 4.37 (dd, $J = 10.5, 5.9 \text{ Hz}$, 1H), 2.58 – 2.49 (m, 2H), 2.43 – 2.33 (m, 3H), 2.29 (ddd, $J = 13.8, 9.0, 4.2 \text{ Hz}$,

1H), 2.12 – 2.01 (m, 7H), 1.71 – 1.67 (m, 2H), 1.67 – 1.57 (m, 5H), 1.51 – 1.44 (m, 1H), 1.35 (td, J = 11.9, 5.6 Hz, 1H), 1.03 (s, 3H), 0.96 (d, J = 6.8 Hz, 3H), 0.94 (s, 3H), 0.89 (s, 3H), 0.87 (s, 3H), 0.84 (s, 3H).

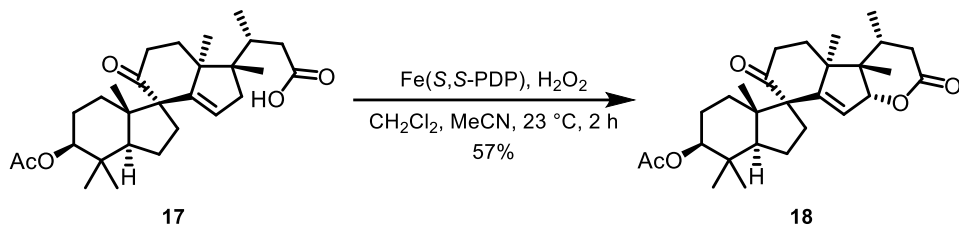
$^{13}\text{C-NMR}$: (151 MHz, CDCl_3) δ [ppm] = 215.6, 178.9, 171.2, 150.9, 125.0, 80.7, 67.1, 51.8, 50.5, 50.1, 48.7, 45.4, 38.1, 37.9, 37.8, 35.7, 35.0, 32.7, 29.0, 27.0, 25.3, 21.4, 20.7, 19.3, 18.4, 16.9, 16.3, 16.2.

IR: $\tilde{\nu}$ [cm^{-1}] = 2958 (m), 2924 (s), 2853 (w), 1732 (s), 1705 (s), 1457 (w), 1416 (w), 1373 (m), 1244 (s), 1073 (w), 1027 (w), 983 (w), 948 (w), 911 (w), 876 (w), 821 (w), 803 (w), 756 (m).

HRMS: (ESI-TOF); m/z calcd. for $\text{C}_{28}\text{H}_{42}\text{O}_5\text{Na}^+$ $[\text{M}+\text{Na}]^+$: 481.2924, found: 481.2921.

Opt. act.: $[\alpha]_D^{24} = -14.6$ (c = 0.27, CHCl_3).

3 β -Acetoxy-9-oxo-10(9 \rightarrow 8)abeo-4,4,17 β -trimethyl-24-nor-5 α ,13 α -chola-14-ene-23,16 α -lactone (**18**)



To a solution of spiro-acid **17** (81.9 mg, 179 μmol , 1.0 eq.) in CH_2Cl_2 (1.8 mL) was added a solution of $[\text{Fe}(\text{II})(\text{S},\text{S-PDP})(\text{CH}_3\text{CN})_2](\text{SbF}_6)_2$ (8.3 mg, 8.9 μmol , 0.05 eq.) in MeCN (41.0 μL), followed by dropwise addition of a solution of H_2O_2 (50 wt% in H_2O , 12.2 μL , 179 μmol , 1.0 eq.) in MeCN (410 μL). After 10 min of stirring at 23 °C, another portion of $[\text{Fe}(\text{II})(\text{S},\text{S-PDP})(\text{CH}_3\text{CN})_2](\text{SbF}_6)_2$ (8.3 mg, 8.9 μmol , 0.05 eq.) in MeCN (41.0 μL) was added, followed by dropwise addition of H_2O_2 (50 wt% in H_2O , 12.2 μL , 179 μmol , 1.0 eq.) in MeCN (410 μL). This was repeated for a total of 5 times with 10 min in between additions, and the resulting mixture was stirred for another hour after the last addition. Sat. aq. NaHCO_3 (5 mL) was then added, the aqueous phase was extracted with CH_2Cl_2 (4 \times 5 mL), the combined organic phases were washed with brine, dried over MgSO_4 , and all volatiles were removed under reduced pressure. Column chromatography (SiO_2 , *n*hexane/EtOAc 1:1, v/v) gave spiro-lactone **18** (46.3 mg, 101 μmol , 57%) as a yellowish amorphous solid.

TLC: R_f = 0.33 (*n*hexane/EtOAc 1:1, v/v).

$^1\text{H-NMR}$: (600 MHz, CDCl_3) δ [ppm] = 5.59 (d, J = 3.2 Hz, 1H), 4.84 (d, J = 3.2 Hz, 1H), 4.36 (dd, J = 11.3, 5.2 Hz, 1H), 2.66 – 2.54 (m, 2H), 2.49 – 2.38 (m, 2H), 2.36 (ddd, J = 13.6, 7.7, 3.5 Hz, 1H), 2.27 – 2.19 (m, 1H), 2.10 – 2.04 (m, 1H), 2.03 (s, 3H), 1.77 – 1.72 (m, 1H), 1.72 – 1.63 (m, 5H), 1.58 – 1.48 (m, 2H), 1.36 (td, J = 12.4, 4.7 Hz, 1H), 1.18 (d, J = 7.1 Hz, 3H), 1.14 (s, 3H), 1.06 (s, 3H), 1.05 (s, 3H), 0.95 (s, 3H), 0.86 (s, 3H).

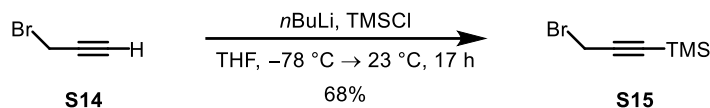
$^{13}\text{C-NMR}$: (151 MHz, CDCl_3) δ [ppm] = 213.7, 171.1, 170.5, 160.5, 123.2, 93.5, 80.4, 66.8, 51.7, 51.2, 49.5, 44.7, 37.8, 37.5, 36.1, 35.8, 35.4, 32.7, 29.1, 26.4, 25.9, 25.2, 25.0, 21.3, 21.0, 18.7, 17.0, 16.3.

IR: $\tilde{\nu}$ [cm^{-1}] = 2954 (m), 2924 (s), 2853 (m), 1731 (s), 1697 (m), 1625 (w), 1459 (m), 1375 (m), 1247 (s), 1208 (w), 1078 (w), 1026 (w), 908 (m), 732 (s).

HRMS: (ESI-TOF); m/z calcd. for $\text{C}_{28}\text{H}_{40}\text{O}_5\text{Na}^+$ $[\text{M}+\text{Na}]^+$: 479.2768, found: 479.2776.

Opt. act.: $[\alpha]_D^{22} = -10.9$ (c = 0.47, CHCl_3).

3-(Trimethylsilyl)propargyl bromide (**S15**)



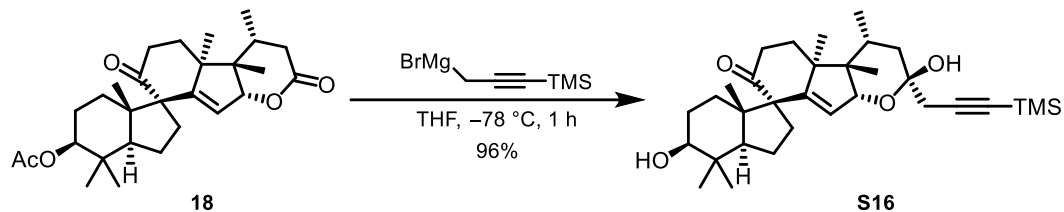
To a solution of propargyl bromide (**S14**) (4.7 mL, 42.2 mmol, 1.25 eq.) in THF (88 mL) was added *n*BuLi (2.4 M in hexane, 14.1 mL, 33.8 mmol, 1.0 eq.) dropwise at -78 °C. The solution was stirred for 10 min at this temperature, then, trimethylsilyl chloride (4.3 mL, 33.8 mmol, 1.0 eq.) was added dropwise, and the reaction was warmed to 23 °C. After stirring for 17 h, aq. sat. NH₄Cl (40 mL) was added, the aqueous phase was extracted with CH₂Cl₂ (2 × 50 mL), the combined organic phases were dried over MgSO₄, and concentrated under reduced pressure. Column chromatography (SiO₂, *n*-pentane) gave 3-(trimethylsilyl)propargyl bromide (**S15**) (4.36 g, 22.8 mmol, 68%) as a colourless oil.

TLC: $R_f = 0.66$ (pentane).

¹H-NMR: (500 MHz, CDCl₃) δ = 3.91 (s, 2H), 0.18 (s, 9H).

All characterization data was consistent with previously reported data.^[3]

9-Oxo-10(9→8)abeo-4,4,17β-trimethyl-24-nor-5α,13α-chola-14-ene-16α,23-epoxy-23α-(trimethylsilyl)propagyl-3β,23β-diol (**S16**)



A mixture of activated Mg (253 mg, 10.4 mmol, 2.0 eq.) and ZnBr₂ (25.0 mg, 110 µmol, 0.02 eq.) was briefly heated (~90 °C) under vacuum and, after cooling to 23 °C, suspended in Et₂O (3 mL). To this suspension was added dropwise 1 mL of a solution of 3-(trimethylsilyl)propargyl bromide **S15** (1.00 g, 5.23 mmol, 1.0 eq.) in Et₂O (4 mL). The suspension was heated to boiling and immediately cooled to 0 °C. The rest of the 3-(trimethylsilyl)propargyl bromide solution was then added dropwise over a period of 30 min, and the suspension was stirred for 2 h at this temperature afterwards. To determine the concentration of the Grignard reagent, it was titrated against (–)-menthol and 1,10-phenanthroline and used immediately afterwards.^[4]

To a solution of spirolactone **18** (28.0 mg, 61.3 μmol , 1.0 eq.) in THF (620 μL) was added freshly prepared TMS-propargylmagnesium bromide (0.41 M in Et₂O, 1.21 mL, 491 μmol , 8.0 eq.) dropwise at -78 °C and the resulting mixture was stirred for 30 min. Phosphate buffer (pH = 7, 3 mL) was added at -78 °C, the reaction was allowed to warm to 23 °C, the aqueous phase was extracted with CH₂Cl₂ (3 \times 4 mL), the combined organic phases were dried over MgSO₄, and all volatiles were removed under reduced pressure. Column chromatography (SiO₂, nhexane/EtOAc 1:1, v/v) gave hemiacetal **S16** (30.9 mg, 58.7 μmol , 96%) as a colourless amorphous solid.

TLC: $R_f = 0.55$ (*n*hexane/EtOAc 1:1, *v/v*).

¹H-NMR: (600 MHz, CDCl₃) δ = 5.53 (d, *J* = 3.3 Hz, 1H), 4.42 (d, *J* = 3.2 Hz, 1H), 3.16 (dd, *J* = 10.7, 5.6 Hz, 1H), 2.61 – 2.57 (m, 1H), 2.56 (s, 2H), 2.53 (d, *J* = 4.6 Hz, 1H), 2.36 – 2.30 (m, 2H), 2.25 (ddd, *J* = 13.2, 7.4, 5.6 Hz, 1H), 2.08 – 2.01 (m, 1H), 1.84 (t, *J* = 13.6 Hz, 1H), 1.76 (ddd, *J* = 13.5, 10.9, 3.8 Hz, 1H), 1.71 – 1.64

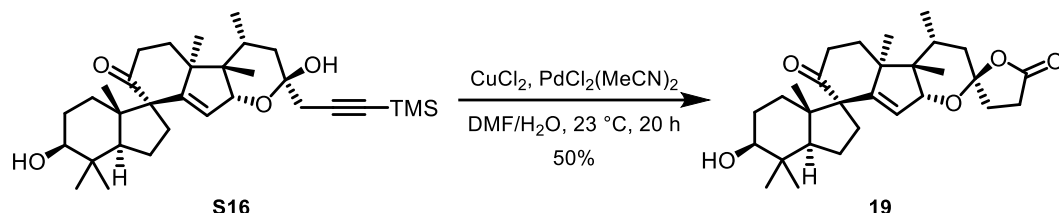
(m, 4H), 1.61 (dd, $J = 13.7, 5.4$ Hz, 1H), 1.58 – 1.56 (m, 2H), 1.51 (dd, $J = 11.7, 5.4$ Hz, 1H), 1.31 – 1.26 (m, 2H), 1.18 (s, 3H), 1.14 (d, $J = 7.3$ Hz, 3H), 1.03 (s, 3H), 1.02 (s, 3H), 0.95 (s, 3H), 0.89 (s, 3H), 0.14 (s, 9H).

$^{13}\text{C-NMR}$: (151 MHz, CDCl_3) $\delta = 215.6, 158.6, 125.1, 101.4, 95.7, 88.8, 83.2, 79.1, 67.1, 51.8, 51.3, 49.4, 45.2, 38.8, 38.6, 37.8, 36.0, 35.4, 33.8, 33.1, 29.2, 29.0, 26.4, 25.7, 25.0, 21.1, 18.5, 16.7, 16.0, 0.2.$

HRMS: (ESI-TOF); m/z calcd. for $\text{C}_{32}\text{H}_{50}\text{O}_4\text{SiNa}^+ [\text{M}+\text{Na}]^+$: 549.3371, found: 549.3390.

Opt. act.: $[\alpha]_D^{20} = -25.1$ ($c = 0.94$, CHCl_3).

9-Oxo-3 β -hydroxy-16 α ,23-epoxy-10(9→8)*abeo*-4,4,17 β -trimethyl-27-nor-5 α ,13 α -chola-14-ene-26,23 β -lactone (**19**)



To a solution of hemiacetal **S16** (30.9 mg, 58.7 μmol , 1.0 eq.) in $\text{DMF}/\text{H}_2\text{O}$ (99:1, 590 μL) was added anhydrous CuCl_2 (11.8 mg, 88.0 μmol , 1.5 eq.) and $\text{PdCl}_2(\text{MeCN})_2$ (3.0 mg, 11.7 μmol , 0.2 eq.), and the resulting mixture was stirred at 25 °C for 15 h. The reaction mixture was then diluted with CH_2Cl_2 (5 mL), the organic phase was washed with water (5 x 3 mL), dried over MgSO_4 , and all volatiles were removed under reduced pressure. Column chromatography (SiO_2 , nhexane/EtOAc 1:1, v/v) gave oxaspirolactone **19** (13.7 mg, 29.1 μmol , 50%) as a colourless amorphous solid.

TLC: $R_f = 0.34$ (nhexane/EtOAc 1:1, v/v).

$^1\text{H-NMR}$: (600 MHz, CDCl_3) $\delta = 5.50$ (d, $J = 3.3$ Hz, 1H), 4.38 (d, $J = 3.3$ Hz, 1H), 3.16 (dd, $J = 10.5, 5.7$ Hz, 1H), 2.79 (ddd, $J = 17.7, 10.7, 9.4$ Hz, 1H), 2.57 (ddd, $J = 20.1, 12.5, 7.8$ Hz, 1H), 2.50 (ddd, $J = 17.7, 9.5, 2.2$ Hz, 1H), 2.39 – 2.32 (m, 2H), 2.27 (ddd, $J = 13.1, 7.3, 5.6$ Hz, 1H), 2.24 – 2.19 (m, 1H), 2.10 – 2.03 (m, 3H), 1.95 (t, $J = 13.8$ Hz, 1H), 1.76 – 1.64 (m, 7H), 1.29 (dd, $J = 11.9, 5.2$ Hz, 2H), 1.17 (s, 3H), 1.15 (d, $J = 7.3$ Hz, 3H), 1.04 (s, 3H), 1.03 (s, 3H), 0.96 (s, 3H), 0.89 (s, 3H).

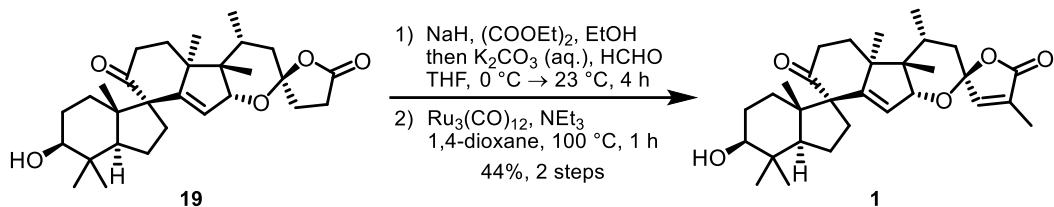
$^{13}\text{C-NMR}$: (101 MHz, CDCl_3) $\delta = 215.2, 176.8, 159.8, 124.4, 108.4, 84.7, 79.1, 67.1, 51.9, 51.4, 49.6, 45.3, 39.7, 38.8, 37.7, 36.2, 34.6, 34.4, 33.1, 29.2, 28.9, 28.3, 26.4, 25.4, 24.9, 21.1, 18.5, 16.5, 16.0.$

IR: $\tilde{\nu}$ [cm^{-1}] = 3487 (w), 2955 (m), 2936 (m), 2882 (w), 1749 (s), 1692 (s), 1456 (w), 1416 (w), 1369 (m), 1302 (m), 1271 (w), 1225 (s), 1204 (m), 1188 (m), 1072 (s), 1024 (s), 968 (s), 918 (s), 907 (s), 691 (w), 656 (m), 631 (s).

HRMS: (ESI-TOF); m/z calcd. for $\text{C}_{29}\text{H}_{42}\text{O}_5\text{Na}^+ [\text{M}+\text{Na}]^+$: 493.2924, found: 493.2937.

Opt. act.: $[\alpha]_D^{20} = 11.7$ ($c = 0.43$, CHCl_3).

Spirochensilide A (**1**)



To a suspension of NaH (60 wt% dispersion in mineral oil, 1.6 mg, 66.9 µmol, 2.5 eq.) in THF (110 µL) was added a solution of oxaspirolactone **19** (12.6 mg, 26.8 µmol, 1.0 eq.) and diethyl oxalate (11.0 µL, 81.7 µmol, 3.05 eq.) in THF (120 µL) dropwise at 0 °C. After complete addition, EtOH (7.0 µL) was added, the solution was warmed to 23 °C, and stirred for 4 h. After cooling the reaction mixture to 0 °C, a solution of K₂CO₃ (10.2 mg) in H₂O (15.0 µL) and formaldehyde (37 wt% aq. solution, 22.0 µL) were added, followed by stirring for 15 min at this temperature. Brine (3 mL) was added, the aqueous phase was extracted with CH₂Cl₂ (3 × 5 mL), the combined organic phases were dried over MgSO₄, and all volatiles were removed under reduced pressure. The residue was filtered over SiO₂ (*n*hexane/EtOAc 1:2, v/v) to give crude exomethylenelactone, which was redissolved in 1,4-dioxane (340 µL). To this solution, Ru₃(CO)₁₂ (2.2 mg, 3.44 µmol, 0.13 eq.) and NEt₃ (3.2 µL) were added. After stirring at 100 °C for 1 h, the reaction was cooled to 23 °C, all volatiles were removed under reduced pressure, and the crude product was purified by preparative TLC (SiO₂, *n*hexane/EtOAc 2:3, v/v). Spirochensilide A (**1**) (5.7 mg, 11.8 µmol, 44%) was obtained as colourless cubic crystals.

TLC: $R_f = 0.35$ (*n*hexane/EtOAc 2:3, *v/v*).

¹H-NMR: (600 MHz, CDCl₃) δ = 6.74 (q, *J* = 1.6 Hz, 1H), 5.52 (d, *J* = 3.3 Hz, 1H), 4.50 (d, *J* = 3.3 Hz, 1H), 3.16 (dd, *J* = 10.5, 5.8 Hz, 1H), 2.58 (ddd, *J* = 20.0, 12.6, 7.7 Hz, 1H), 2.39 – 2.36 (m, 1H), 2.36 – 2.30 (m, 2H), 2.11 – 2.04 (m, 1H), 2.05 (t, *J* = 13.7 Hz, 1H), 1.91 (d, *J* = 1.6 Hz, 3H), 1.75 – 1.63 (m, 5H), 1.58 (s, 1H), 1.55 (d, *J* = 3.0 Hz, 2H), 1.52 (dd, *J* = 11.8, 5.1 Hz, 1H), 1.30 (dd, *J* = 12.1, 5.4 Hz, 1H), 1.21 (s, 3H), 1.17 (d, *J* = 7.3 Hz, 3H), 1.07 (s, 3H), 1.03 (s, 3H), 0.96 (s, 3H), 0.89 (s, 3H).

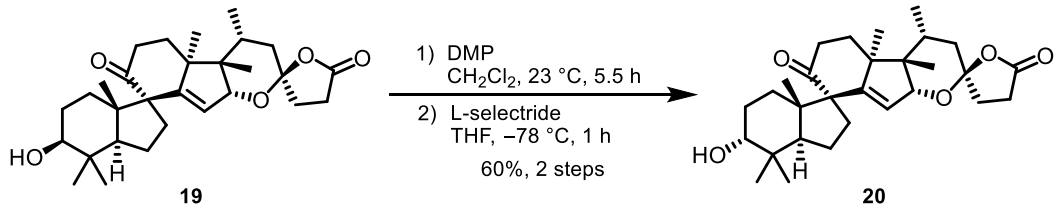
¹³C-NMR: (151 MHz, CDCl₃) δ = 215.0, 172.1, 160.4, 147.3, 132.2, 124.1, 105.5, 86.2, 79.1, 67.1, 51.9, 51.5, 49.7, 45.2, 38.8, 37.8, 37.7, 36.2, 34.3, 33.1, 29.2, 28.9, 26.4, 25.4, 25.0, 21.1, 18.6, 16.5, 16.0, 10.7.

IR: $\tilde{\nu}$ [cm⁻¹] = 3497 (br w), 2955 (m), 2922 (s), 2880 (m), 2853 (m), 1744 (s), 1692 (s), 1458 (m), 1420 (w), 1382 (m), 1371 (m), 1319 (w), 1302 (w), 1261 (m), 1244 (m), 1179 (m), 1163 (m), 1067 (s), 976 (s), 939 (m), 883 (m), 868 (m), 854 (m), 762 (s), 725 (w), 611 (m).

HRMS: (ESI-TOF); m/z calcd. for $C_{30}H_{42}O_5Na^+$ [M+Na] $^+$: 505.2924, found: 505.2917.

Opt. act.: $[\alpha]_D^{28} = -7.9$ ($c = 0.51$, CHCl_3), [ref. [5]: $[\alpha]_D^{20} = -10.0$ ($c = 0.2$, CHCl_3)].

9-Oxo-10(9→8)abeo-4,4,17 β -trimethyl-24-nor-5 α ,13 α -chola-14-ene-16 α ,23-epoxy-3 α -hydroxy-26,23 β -lactone (**20**)



To a solution of oxaspirolactone **19** (4.8 mg, 10.2 µmol, 1.0 eq.) in CH₂Cl₂ (120 µL) was added Dess–Martin periodinane (6.2 mg, 14.6 µmol, 1.4 eq.) at 0 °C. After 10 min the solution was warmed to 23 °C and stirred for 5.5 h at this temperature. Sat. aq. Na₂S₂O₃ (1 mL) was added and the mixture stirred for an additional 15 min. The aqueous phase was extracted with CH₂Cl₂ (3 × 2 mL), the combined organic phases were washed sequentially with sat. aq. NaHCO₃ (2 × 2 mL) and brine (2 mL), dried over MgSO₄, and all volatiles were removed under reduced pressure. Column chromatography (SiO₂, *n*hexane/EtOAc 2:1, *v/v*) gave the ketone which was dissolved in THF (100 µL) and cooled to –78 °C.

L-Selectride (9.7 μ L, 9.73 μ mol, 1.2 eq.) was added dropwise, the mixture was stirred for 1 h, sat. aq. NH₄Cl (1 mL) was added at –78 °C, and the mixture was warmed to 23 °C. The mixture was diluted with CH₂Cl₂ (1 mL), the aqueous phase was extracted with CH₂Cl₂ (3 \times 1.5 mL), the combined organic phases were dried over MgSO₄, and all volatiles were removed under reduced pressure. Preparative TLC (SiO₂, nhexane/EtOAc 1:1, v/v) gave 3-epi-oxaspirolactone **20** (2.9 mg, 6.1 μ mol, 60%) as colourless crystals.

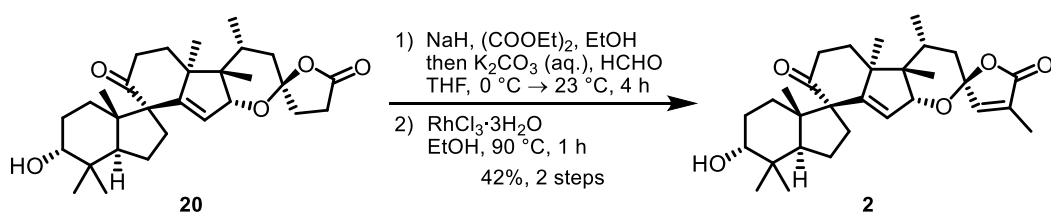
TLC: $R_f = 0.35$ (*n*hexane/EtOAc 1:1, *v/v*).

¹H-NMR: (600 MHz, CDCl₃) δ = 5.49 (d, *J* = 3.3 Hz, 1H), 4.38 (d, *J* = 3.3 Hz, 1H), 3.39 (t, *J* = 2.7 Hz, 1H), 2.79 (ddd, *J* = 17.7, 10.7, 9.4 Hz, 1H), 2.60 – 2.54 (m, 1H), 2.49 (ddd, *J* = 17.7, 9.5, 2.2 Hz, 1H), 2.42 (dd, *J* = 19.9, 7.2 Hz, 1H), 2.36 – 2.31 (m, 1H), 2.27 (ddd, *J* = 13.0, 7.3, 5.5 Hz, 1H), 2.22 (ddd, *J* = 13.2, 9.4, 2.2 Hz, 1H), 2.14 – 2.09 (m, 1H), 2.09 – 2.05 (m, 1H), 1.96 (t, *J* = 13.8 Hz, 1H), 1.93 – 1.89 (m, 2H), 1.74 (dd, *J* = 14.3, 5.5 Hz, 1H), 1.70 (dd, *J* = 13.6, 7.7 Hz, 1H), 1.66 – 1.61 (m, 4H), 1.47 (dd, *J* = 12.6, 5.5 Hz, 1H), 1.34 (dd, *J* = 9.3, 3.8 Hz, 1H), 1.18 (s, 3H), 1.16 (d, *J* = 7.3 Hz, 3H), 1.05 (s, 3H), 0.99 (s, 3H), 0.92 (s, 3H), 0.91 (s, 3H).

¹³C-NMR: (151 MHz, CDCl₃) δ = 215.0, 176.9, 160.1, 124.1, 108.5, 84.8, 74.6, 67.6, 51.4, 49.6, 45.3, 45.2, 39.7, 38.2, 37.7, 34.8, 34.6, 34.4, 28.8, 28.3, 28.1, 27.1, 26.4, 25.4, 24.9, 21.9, 21.2, 17.9, 16.5

HRMS: (ESI-TOF): m/z calcd. for $C_{29}H_{42}O_5Na^+ [M+Na]^+$: 493.2924; found: 493.2931.

Spirochensilide B (2)



To a suspension of NaH (60 wt% dispersion in mineral oil, 0.6 mg, 14.9 µmol, 5.0 eq.) in THF (60 µL) was added a solution of oxaspirolactone **20** (1.4 mg, 2.98 µmol, 1.0 eq.) and diethyl oxalate (2.5 µL, 18.2 µmol, 6.1 eq.) in THF (60 µL) dropwise at 0 °C. After complete addition, EtOH (1.2 µL) was added, the solution was warmed to 23 °C, and stirred for 4 h. After cooling the reaction mixture to 0 °C, a solution of K₂CO₃ (1.4 mg) in H₂O (2.0 µL) and formaldehyde (37 wt% aq. solution, 2.6 µL) were added, followed by stirring for 15 min at this temperature. Brine (3 mL) was added, the aqueous phase was extracted with CH₂Cl₂ (3 × 5 mL), the combined organic phases were dried over MgSO₄, and all volatiles were removed under reduced pressure. The residue was filtered over SiO₂ (*n*-hexane/EtOAc 1:2, v/v) to give crude exomethylenelactone, which was redissolved in EtOH (300 µL). To this solution, RhCl₃·3H₂O (0.3 mg, 1.15 µmol, 0.36 eq.) was added. After stirring at 90 °C for 1 h the reaction was cooled to 23 °C, all volatiles were removed under reduced pressure, and the crude product was purified by preparative TLC (SiO₂, *n*-hexane/EtOAc 1:2, v/v). Spirochensilide B (**2**) (0.6 mg, 1.24 µmol, 42%) was obtained as a colourless solid.

TLC: $R_f = 0.54$ (*n*hexane/EtOAc 1:2, *v/v*).

¹H-NMR: (600 MHz, CDCl₃) δ = 6.74 (d, *J* = 1.7 Hz, 1H), 5.52 (d, *J* = 3.3 Hz, 1H), 4.50 (d, *J* = 3.3 Hz, 1H), 3.39 (t, *J* = 2.7 Hz, 1H), 2.58 (ddd, *J* = 20.0, 12.4, 7.8 Hz, 1H), 2.44 (dd, *J* = 19.7, 7.4 Hz, 1H), 2.37 – 2.30 (m, 2H), 2.16 – 2.09 (m, 1H), 2.06 (t, *J* = 13.7 Hz, 1H), 1.92 (d, *J* = 1.7 Hz, 3H), 1.96 – 1.90 (m, 2H), 1.72 (dd, *J* = 13.4, 7.6 Hz, 1H), 1.65 – 1.62 (m, 3H), 1.60 (dd, *J* = 10.6, 3.0 Hz, 1H), 1.56 (dd, *J* = 14.0, 5.3 Hz, 1H), 1.47 (dd, *J* = 12.3, 5.5 Hz, 1H), 1.35 – 1.34 (m, 1H), 1.22 (s, 3H), 1.18 (d, *J* = 7.2 Hz, 3H), 1.08 (s, 3H), 0.99 (s, 3H), 0.92 (s, 3H), 0.91 (s, 3H).

¹³C-NMR: (151 MHz, CDCl₃) δ = 214.8, 172.1, 160.7, 147.4, 132.2, 123.8, 105.6, 86.3, 74.6, 67.6, 51.5, 49.7, 45.24, 45.19, 38.2, 37.8, 37.7, 34.9, 34.4, 28.8, 28.1, 27.1, 26.4, 25.5, 25.1, 21.9, 21.2, 18.0, 16.5, 10.7.

HRMS: (ESI-TOF); *m/z* calcd. for C₃₀H₄₂O₅Na⁺ [M+Na]⁺: 505.2924, found: 505.2918.

6 X-Ray Crystallographic Data

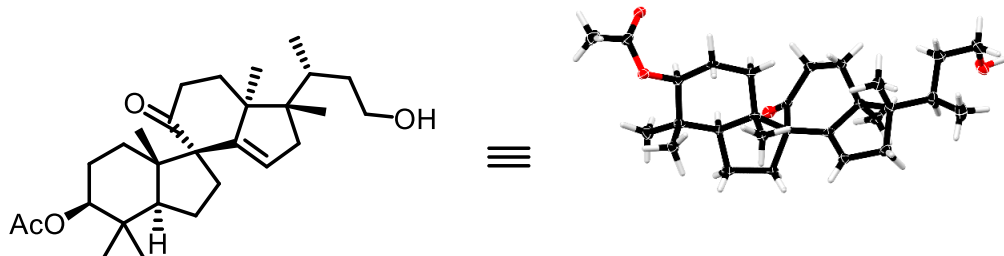


Table 1. Crystal data and structure refinement for **16**.

Identification code	2115191
Empirical formula	C ₂₈ H ₄₄ O ₄
Formula weight	444.66
Temperature/K	100
Crystal system	orthorhombic
Space group	P ₂ 1P ₂ 12 ₁
a/Å	7.24317(5)
b/Å	12.15925(7)
c/Å	28.85806(18)
α/°	90
β/°	90
γ/°	90
Volume/Å	2541.57(3)
Z	4
P _{calc} g/cm ³	1.162
μ/mm ⁻¹	0.592
F(000)	976.0
Crystal size/mm	1.0 x 0.7 x 0.1
Radiation	Cu Kα ($\lambda = 1.54178$)
2θ range for data collection/°	to 136.694
Index ranges	-8 ≤ h ≤ 8, -14 ≤ k ≤ 14, -34 ≤ l ≤ 34
Reflections collected	54715
Independent reflections	4644 [R _{int} = 0.0457, R _{sigma} = 0.0192]
Goodness-of-fit on F ²	1.076
Final R indexes [all data]	R ₁ = 0.0300, wR ₂ = 0.0772
Largest diff. peak/hole / e Å ⁻³	0.32/-0.16
Flack parameter	0.018(167)

7 NMR Comparisons

Table 2. NMR comparison of natural spirochensilide A (**1**) and synthetic material.

#	¹ H-NMR		¹³ C-NMR	
	natural	synthetic	natural	synthetic
1	1.56 m, 1.30 m	1.56 m, 1.31 dd (12.1, 5.4)	32.9	33.0
2	1.67 m	1.70 m	28.8	28.8
3	3.17 dd (10.2, 6.0)	3.17 dd (10.5, 5.8)	78.9	78.9
4	-	-	38.6	38.6
5	1.58 m	1.59 m	51.7	51.7
6	2.37 m, 1.70 m	2.35 m, 1.70 m	36.0	36.0
7	1.69 m, 1.55 m	1.70 m, 1.53 dd (11.9, 5.1)	20.9	21.0
8	-	-	66.9	67.0
9	-	-	214.9	214.8
10	-	-	49.5	49.5
11	2.58 m, 2.39 m	2.59 ddd (20.1, 12.6, 7.7), 2.39 m	37.6	37.7
12	1.72 m, 2.08 m	1.70 m, 2.08 m	26.2	26.2
13	-	-	51.3	51.3
14	-	-	160.2	160.2
15	5.53 d (3.6)	5.53 d (3.3)	123.9	124.0
16	4.51 d (3.0)	4.51 d (3.3)	86.1	86.1
17	-	-	44.9	45.0
18	1.08 s	1.08 s	25.3	25.3
19	1.04 s	1.04 s	18.4	18.4
20	2.35 m	2.35 m	34.2	34.2
21	1.19 d (7.2)	1.18 d (7.3)	16.3	16.3
22	1.57 m, 2.07 m	1.56 m, 2.06 t (13.7)	37.6	37.6
23	-	-	105.4	105.4
24	6.75 brs	6.75 q (1.6)	147.2	147.2
25	-	-	132.0	132.0
26	-	-	171.9	171.9
27	1.92 s	1.92 d (1.7)	10.5	10.5
28	0.96 s	0.97 s	29.0	29.0
29	0.90 s	0.90 s	15.8	15.8
30	1.22 s	1.22 s	24.9	24.9

All chemical shifts are reported in ppm. Coupling constants are given in parentheses and are reported in Hz. m = centered multiplet. All spectra were measured in CDCl₃ and are referenced to the residual solvent peak at δ_H = 7.27 ppm and δ_C = 77.00 ppm as done in the original isolation report. ¹H-NMR spectra were recorded at 600 MHz. ¹³C-NMR spectra were recorded at 151 MHz.

Table 3. NMR comparison of natural spirochensilide B (**2**) and synthetic material.

#	¹ H-NMR		¹³ C-NMR	
	natural	synthetic	natural	synthetic
1	2.12 m, 1.72 m	1.65 m, 1.35 m	26.9	28.7
2	1.91 m, 1.66 m	1.93 m, 1.65 m	27.9	26.9
3	3.38 brs	3.40 t (2.7)	74.5	74.4
4	-	-	38.0	38.0
5	1.94 m	1.93 m	44.7	45.1
6	1.61 m	1.65 m, 1.48 dd (12.3, 5.5)	34.7	21.1
7	1.62 m, 1.52 m	2.34 m, 1.61 dd (10.6, 3.0)	22.7	34.7
8	-	-	67.6	67.4
9	-	-	214.6	214.6
10	-	-	49.6	49.5
11	2.58 m, 2.44 m	2.59 ddd (20.0, 12.5, 7.8), 2.45 dd (19.7, 7.4)	37.8	37.5
12	2.15 m, 1.74 m	2.13 m, 1.73 dd (13.4, 7.6)	26.2	26.3
13	-	-	51.2	51.4
14	-	-	160.5	160.6
15	5.51 s	5.53 d (3.3)	123.4	123.7
16	4.50 s	4.51 d (3.3)	86.0	86.1
17	-	-	45.0	45.0
18	1.09 s	1.09 s	25.3	25.3
19	1.00 s	1.00 s	17.8	17.8
20	2.33 m	2.34 m	34.1	34.2
21	1.18 d (6.6)	1.19 d (7.2)	16.3	16.3
22	2.08 m, 1.60 m	2.07 t (13.7), 1.57 dd (14.0, 5.3)	37.6	37.7
23	-	-	105.7	105.4
24	6.75 brs	6.75 d (1.7)	147.4	147.2
25	-	-	132.3	132.0
26	-	-	171.9	172.0
27	1.91 s	1.93 d (1.7)	10.6	10.5
28	0.91 s	0.92 s	21.7	21.8
29	0.92 s	0.93 s	28.8	27.9
30	1.22 s	1.23 s	24.9	25.0

All chemical shifts are reported in ppm. Coupling constants are given in parentheses and are reported in Hz. m = centered multiplet. All spectra were measured in CDCl₃ and are referenced to the residual solvent peak at δ_H = 7.27 ppm and δ_C = 77.00 ppm as done in the original isolation report. ¹H-NMR spectra were recorded at 600 MHz.

¹³C-NMR spectra were recorded at 151 MHz.

Some assignments of signals in the original isolation report and our analysis differ slightly. The assignment of 29-CH₃ in the ¹³C-NMR spectrum can be supported by DEPT-135 experiment which indicates, that the originally assigned signal of 28.8 ppm corresponds to a CH₂ carbon while the signal at 27.9 ppm corresponds either to a CH or CH₃ carbon. HSQC analysis shows that the ¹³C signal correlates with a singlet with the integral of 3 in the ¹H-NMR spectrum, thus proving that the signal at 27.9 ppm has to be the 29-CH₃ group. All other assignments for CH₃-groups are identical to the original isolation report.

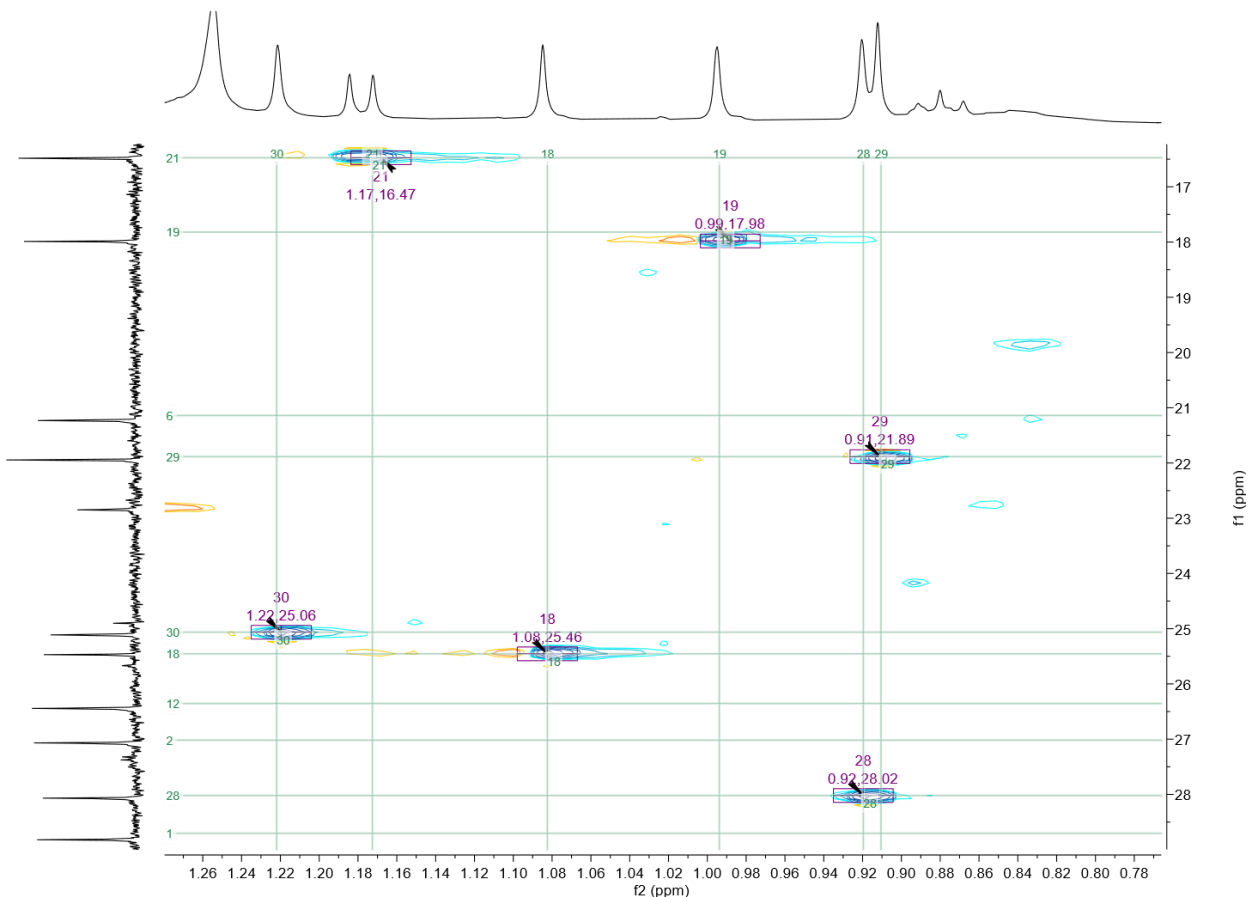


Figure 1: ¹H-¹³C-HMDS spectrum of spirochensilide B (2) (detail).

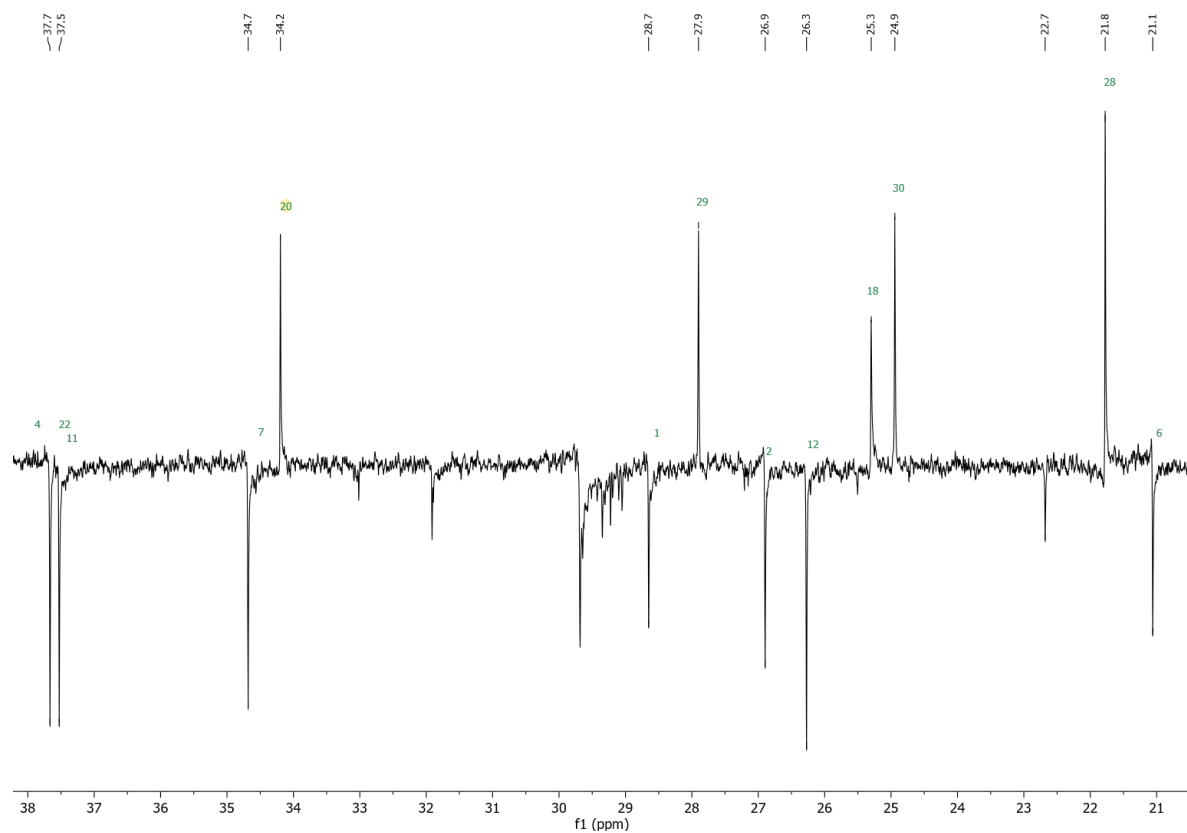


Figure 2: DEPT-135 spectrum of spirochensilide B (2) (detail).

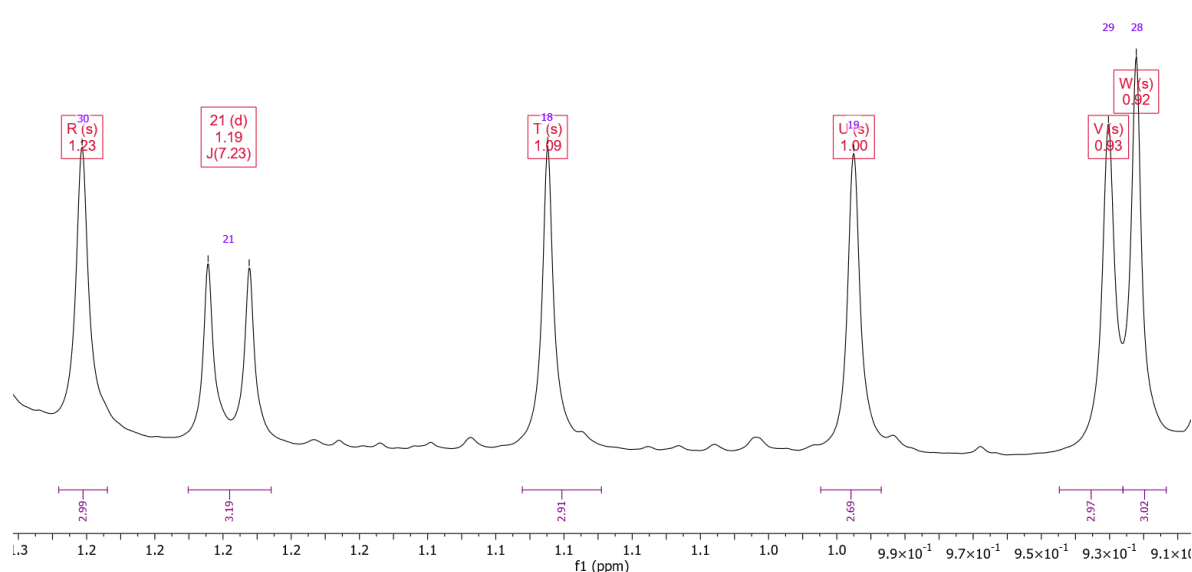


Figure 3: ^1H -NMR spectrum of spirochensilide B (2) (detail).

The assignments of the CH₂-groups of carbons 1,2,6, and 7 can be explained by COSY and HMQC analysis. 3-CH correlates with only two other protons in the COSY spectrum which must be the 2-CH₂ protons. Both signals are part of overlapping multiplets containing signals for 1-CH₂, 5-CH, 6-CH₂, and 7-CH₂, which makes an assignment difficult, but possible by the process of elimination. 5-CH can only correlate with 6-CH₂, which only correlates with 7-CH₂. Neither of those signal sets correlates with 1-CH₂, while the signals of 1-CH₂ correlate with signals of 2-CH₂ and no other. A HMQC assignment using the before mentioned rationale gives the results shown in the comparison table. Calculated spectra using the prediction plug-in of the MestReNova NMR analysis software show a good match with the new assignment of 6-CH₂ and 7-CH₂ in the ¹³C-NMR spectra, indicating that the assignment in spirochensilide A (**1**) is also switched. Due to signal overlapping, it is not possible to verify this, but it being the case for spirochensilide B (**2**) is a strong argument in favour of this assumption.

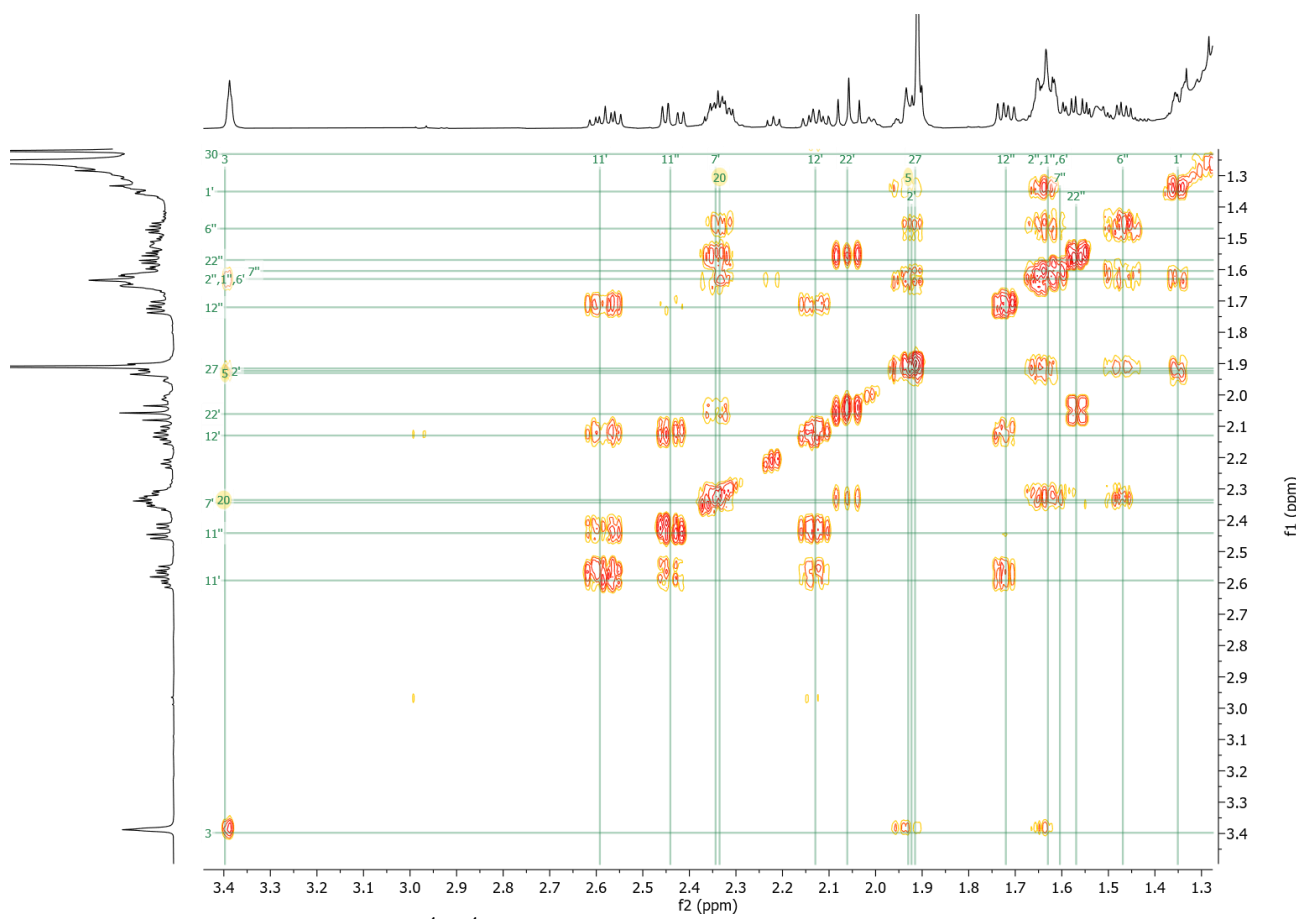


Figure 4: ^1H - ^1H -COSY of spirochensilide B (**2**) (detail).

Table 4. NMR comparison of natural abifarine B (**4**) and synthetic material.

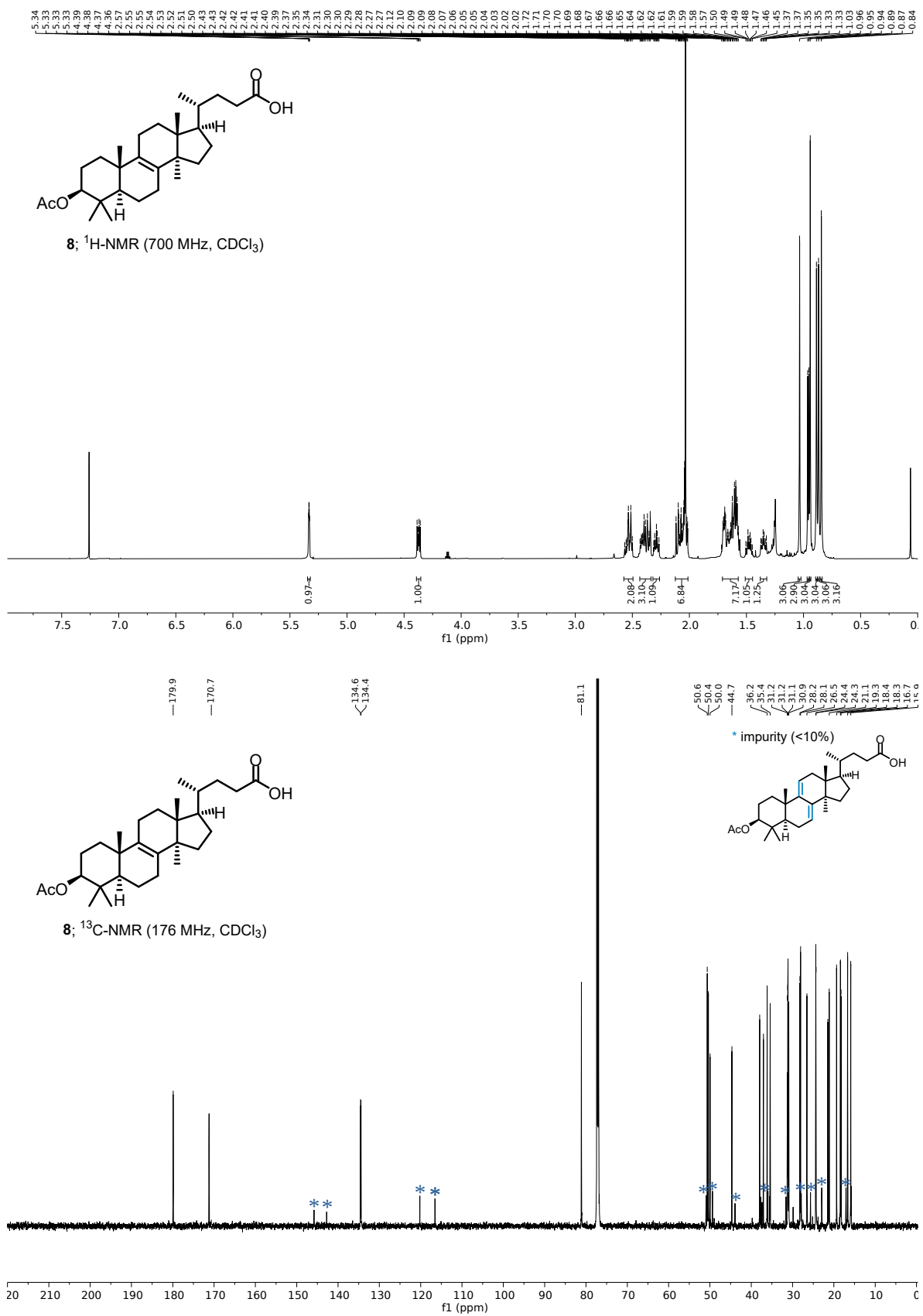
#	¹ H-NMR		¹³ C-NMR	
	natural	synthetic	natural	synthetic
1	1.82 m 1.24 m	1.83 m 1.24 m	35.1	35.1
2	1.71 m 1.57 m	1.72 m 1.58 m	30.3	30.2
3	3.46 dd (7.0, 9.0)	3.47 dd (6.9, 9.2)	77.9	77.9
4	-	-	39.4	39.4
5	1.19 m	1.21 m	51.0	51.0
6	1.76 m 1.52 m	1.78 m 1.52 m	18.7	18.7
7	2.47 dd (5.9 17.3) 2.09 m	2.47 m 2.09 m	27.4	27.4
8	-	-	123.0	123.1
9	-	-	143.0	143.0
10	-	-	38.2	38.2
11	2.17 d (6.4)	2.18 d (6.5)	23.1	23.1
12	1.91 m	1.91 m	28.5	28.5
13	-	-	50.1	50.1
14	-	-	148.8	148.8
15	5.41 m	5.42 m	116.5	116.5
16	2.38 d (16.5) 1.97 dd (3.5 16.5)	2.39 d (16.4) 1.98 dd (3.6, 16.2)	45.4	45.3
17	-	-	48.4	48.3
18	0.84 s	0.86 s	16.2	16.2
19	1.06 s	1.07 s	16.4	16.4
20	2.74 dt (6.6, 13.6)	2.76 m	34.3	34.2
21	0.96 d (6.6)	0.97 d (6.6)	16.7	16.7
22	2.82 d (15.7) 2.54 m	2.84 d (15.8) 2.56 dd (15.9, 11.3)	48.7	48.7
23	-	-	202.4	202.4
24	7.63 d (1.3)	7.65 d (1.6)	132.8	132.8
25	-	-	142.4	142.3
26	-	-	170.5	170.4
27	2.60 d (1.3)	2.62 d (1.6)	15.0	15.0
28	1.24 s	1.25 s	28.6	28.6
29	1.07 s	1.08 s	19.4	19.3
30	1.06 s	1.08 s	17.6	17.6

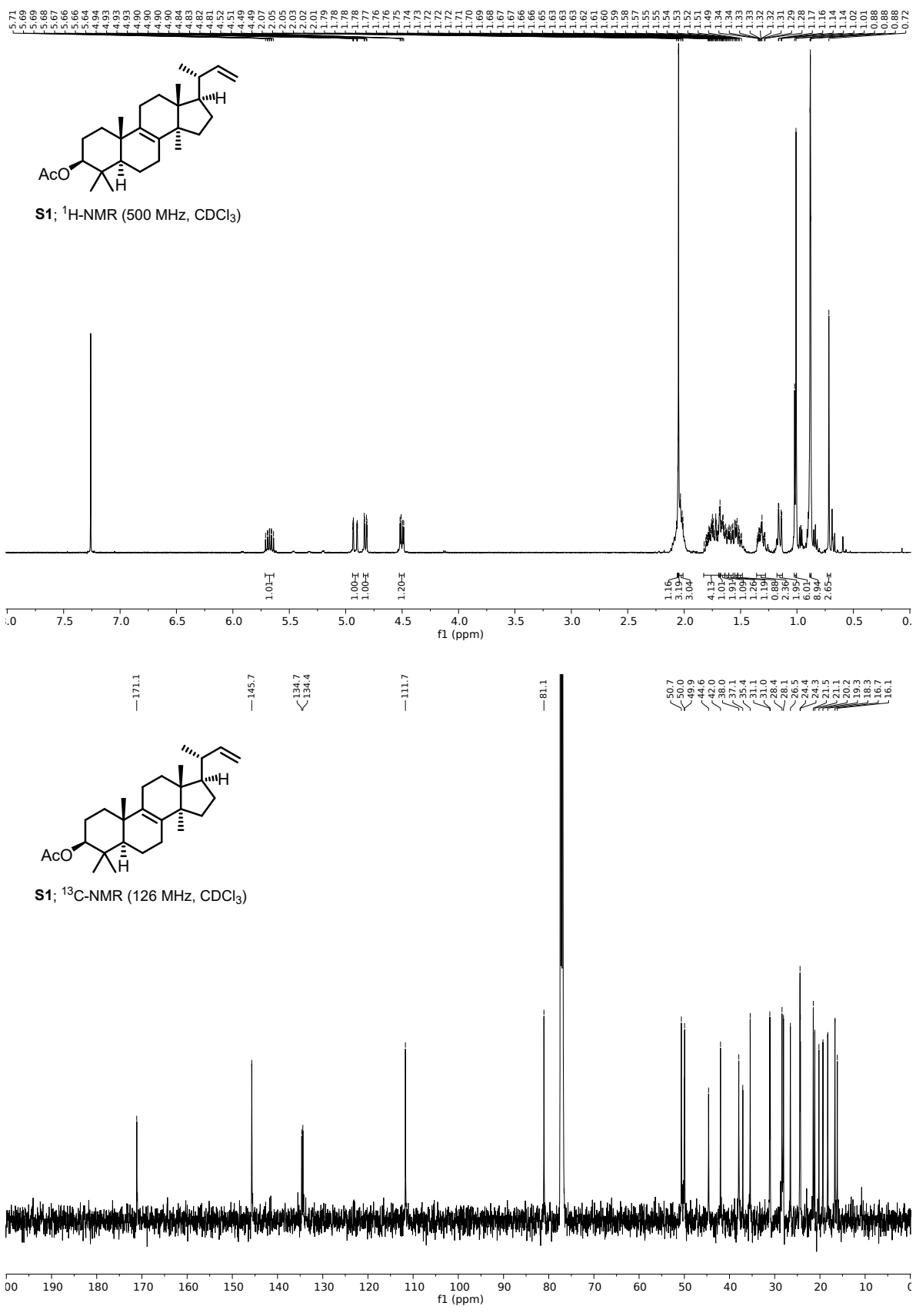
All chemical shifts are reported in ppm. Coupling constants are given in parentheses and are reported in Hz. m = centered multiplet. All spectra were measured in pyridine-d₅ and are referenced to the residual solvent peak at δ_H = 7.21 ppm and δ_C = 123.5 ppm as done in the original isolation report. ¹H-NMR spectra were recorded at 600 MHz. ¹³C-NMR spectra were recorded at 151 MHz.

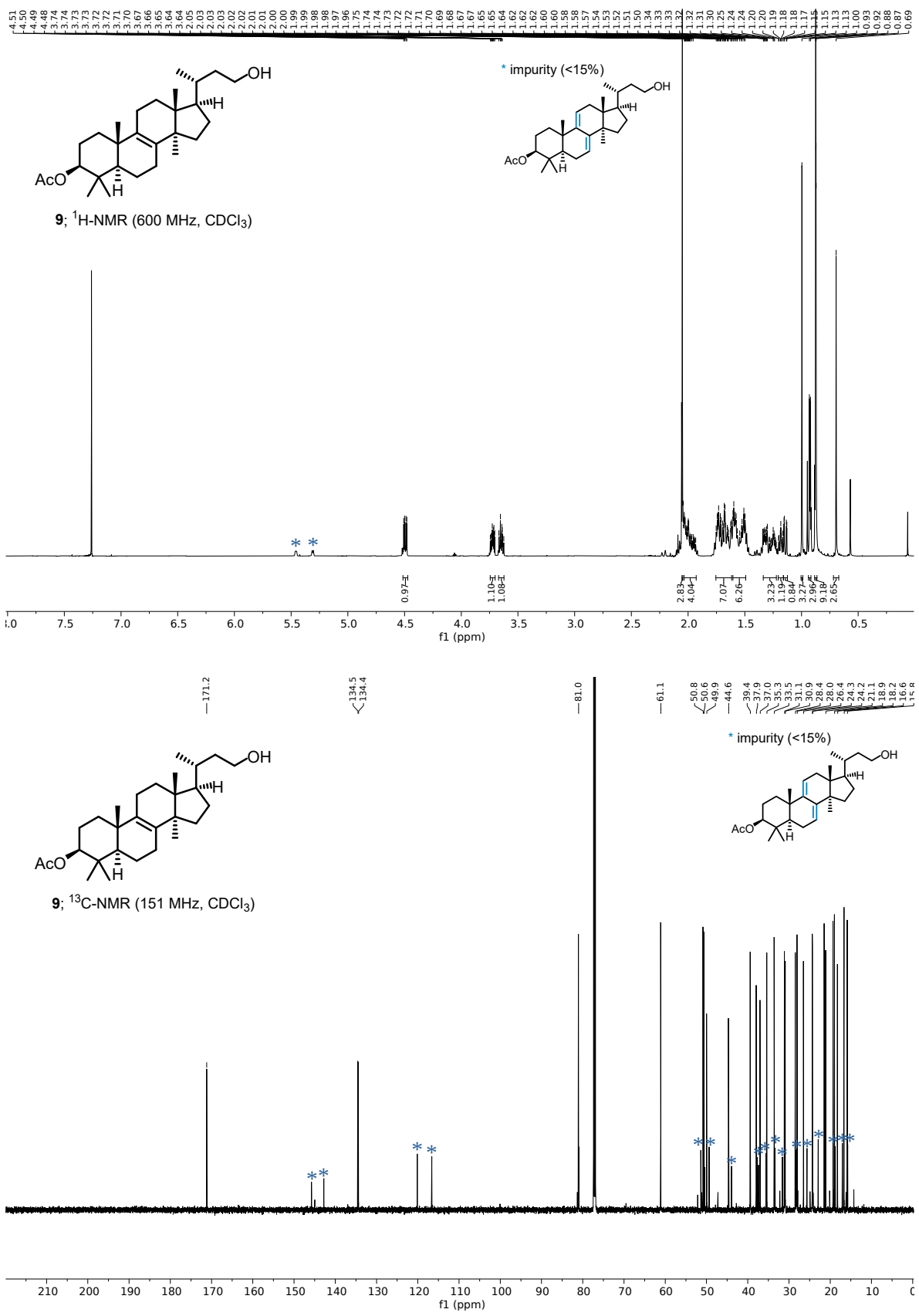
References

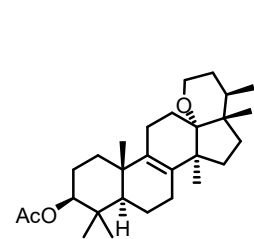
- [1] M.A. Short, J.M. Blackburn, J.L. Roizen, Sulfamate Esters Guide Selective Radical-Mediated Chlorination of Aliphatic C–H Bonds, *Angew. Chem. Int. Ed.* **2018**, *130*, 296–299.
- [2] X. Chen, X. Shao, W. Li, X. Zhang, B. Yu, Total Synthesis of Echinoside A, a Representative Triterpene Glycoside of Sea Cucumbers, *Angew. Chem. Int. Ed.* **2017**, *56*, 7648–7652.
- [3] H.D. Verkruisze, L. Brandsma, Trimethylsilylation of Propargyl Chloride and Propargyl Bromide, *Synth. Commun.* **1990**, *20*, 3375–3378.
- [4] H.S. Lin, L.A. Paquette, A Convenient Method for Determining the Concentration of Grignard Reagents, *Synth. Commun.* **1994**, *24*, 2503–2506.
- [5] Q. Zhao, Q. Song, K. Jiang, G. Li, W. Wei, Y. Li, K. Gao, Spirochensilides A and B, Two New Rearranged Triterpenoids from *Abies chensiensis*, *Org. Lett.* **2015**, *17*, 2760–2763.

NMR Spectra

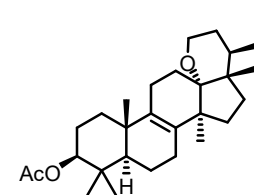
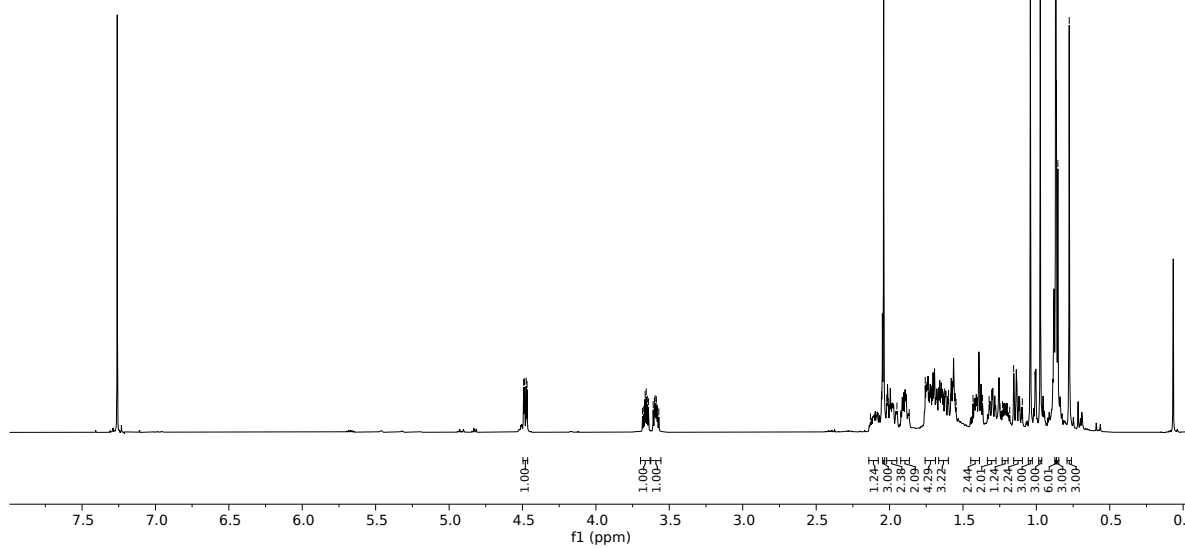




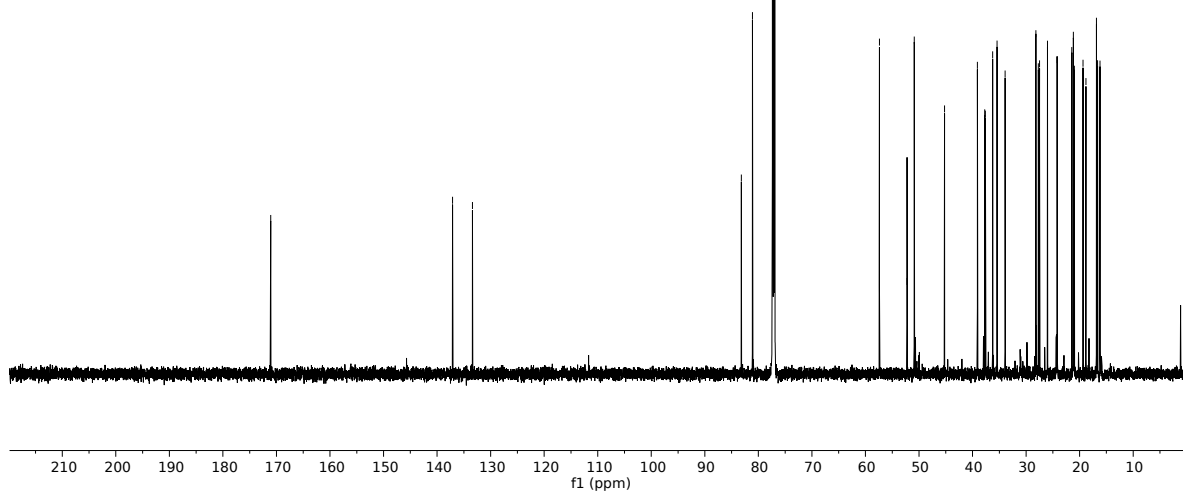


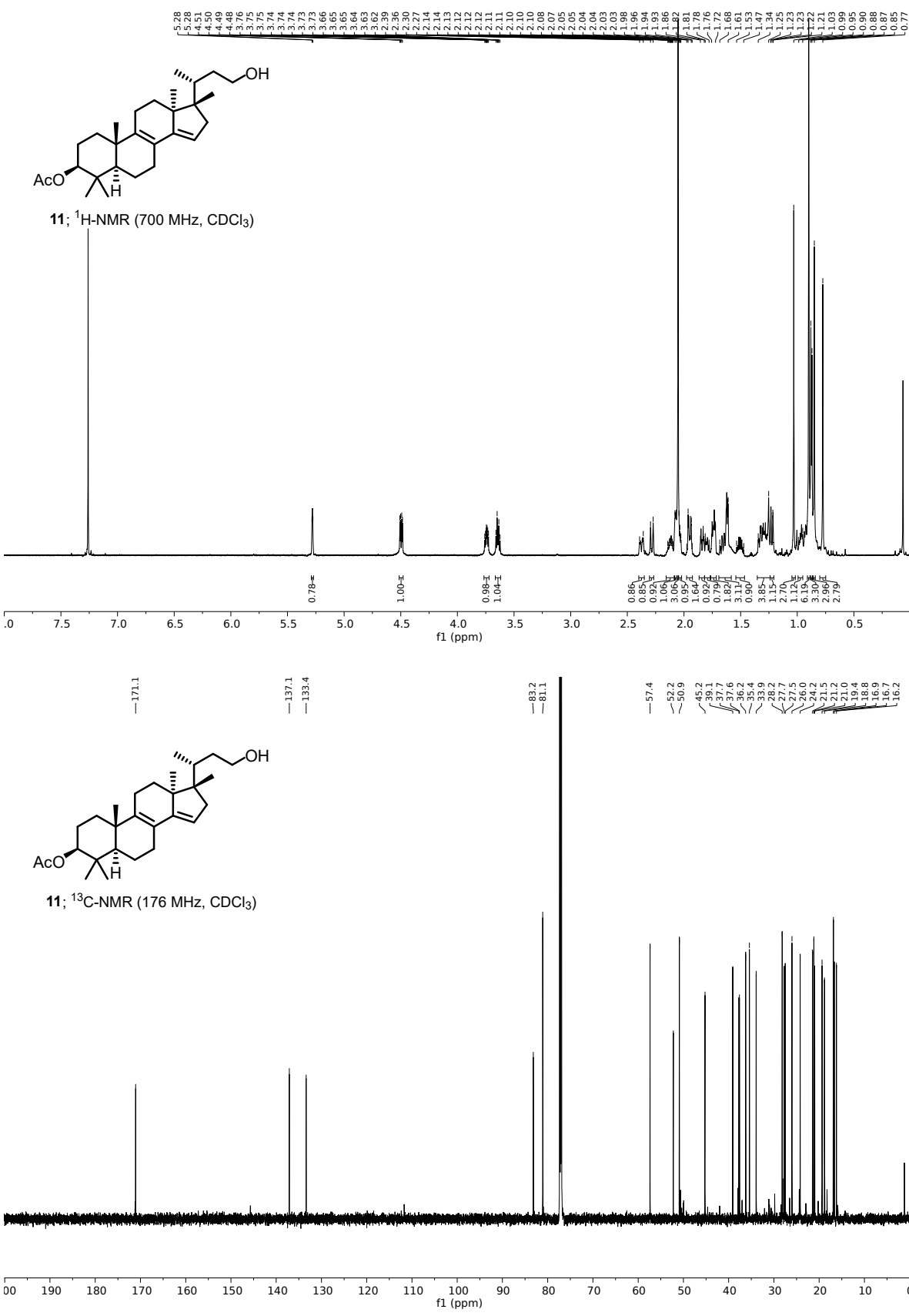


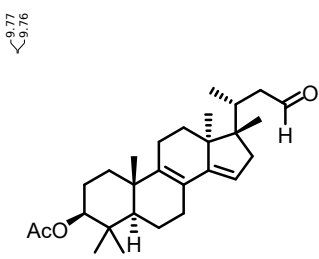
10; $^1\text{H-NMR}$ (700 MHz, CDCl_3)



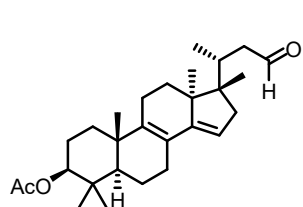
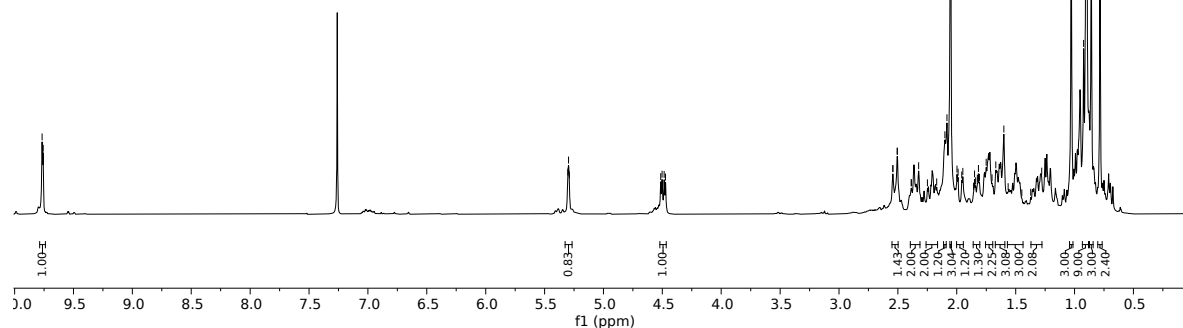
10; ^{13}C -NMR (176 MHz, CDCl_3)



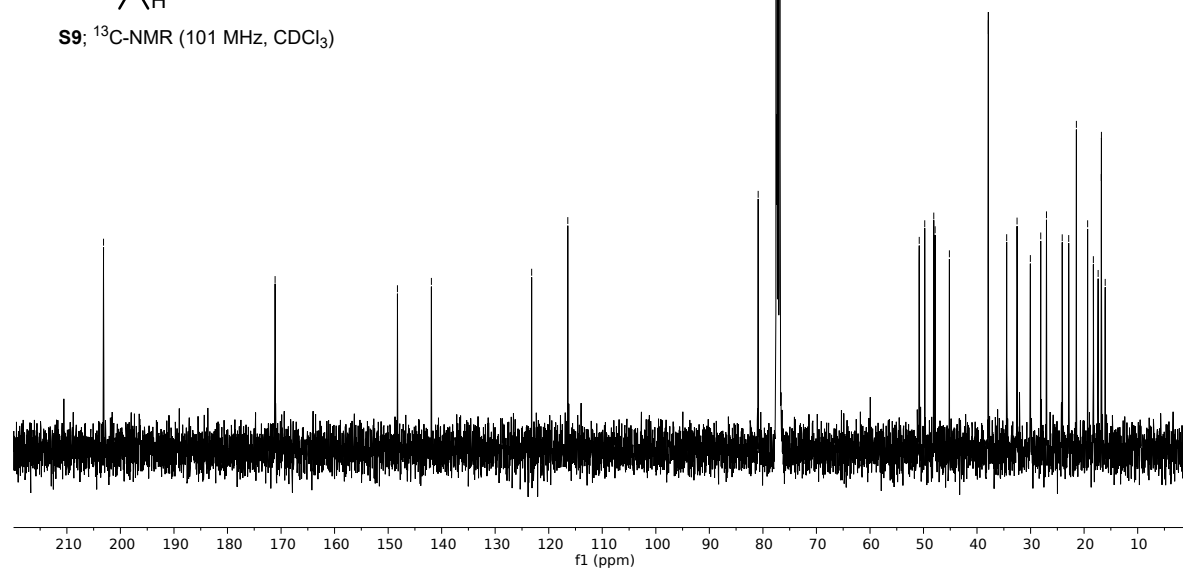


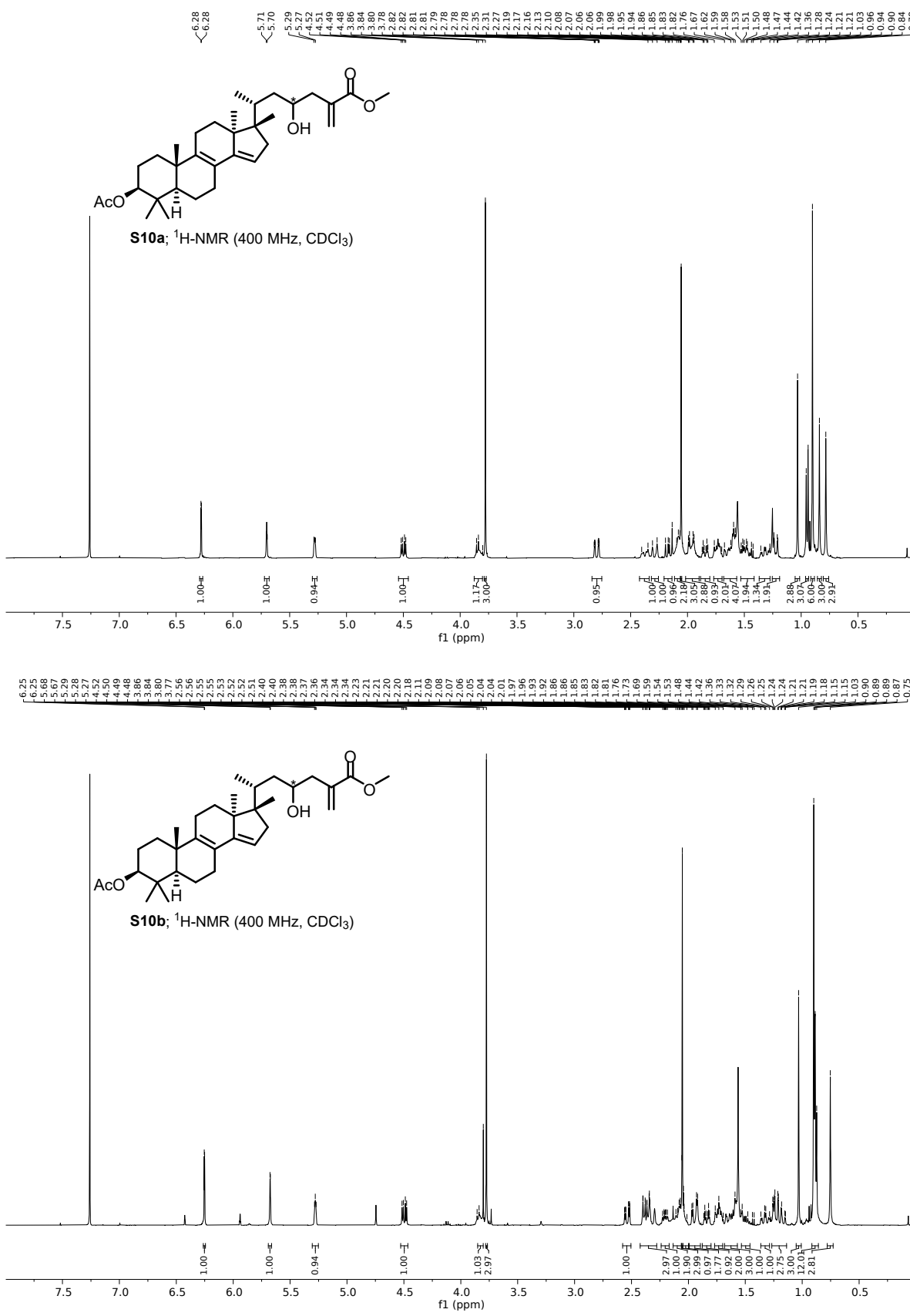


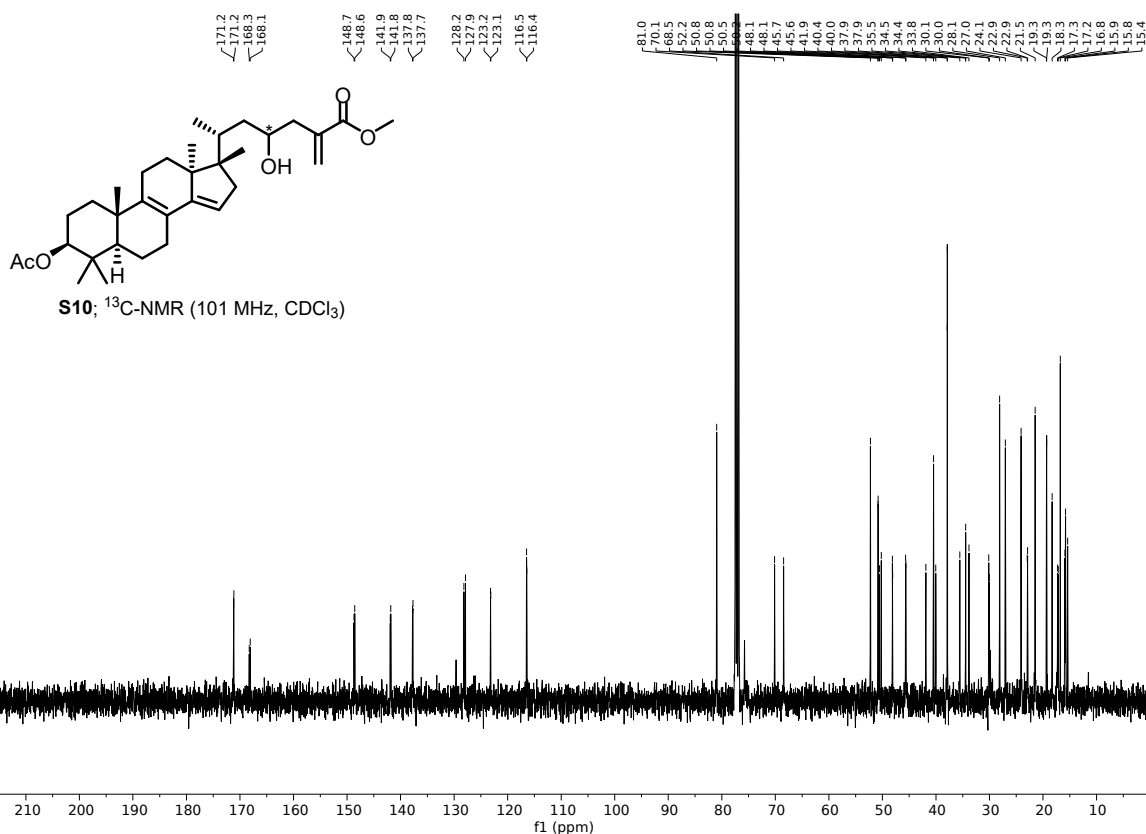
S9; ^1H -NMR (400 MHz, CDCl_3)

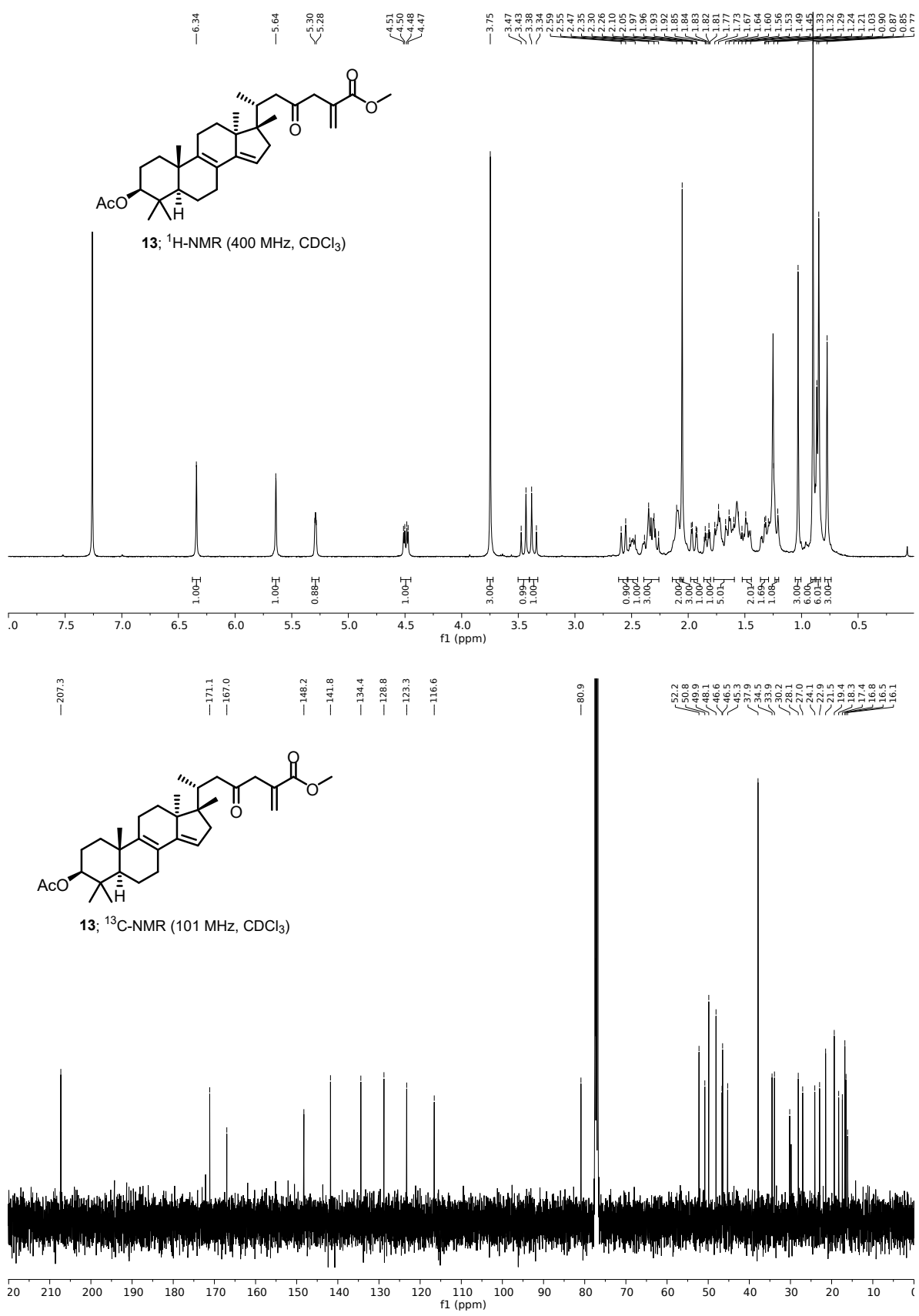


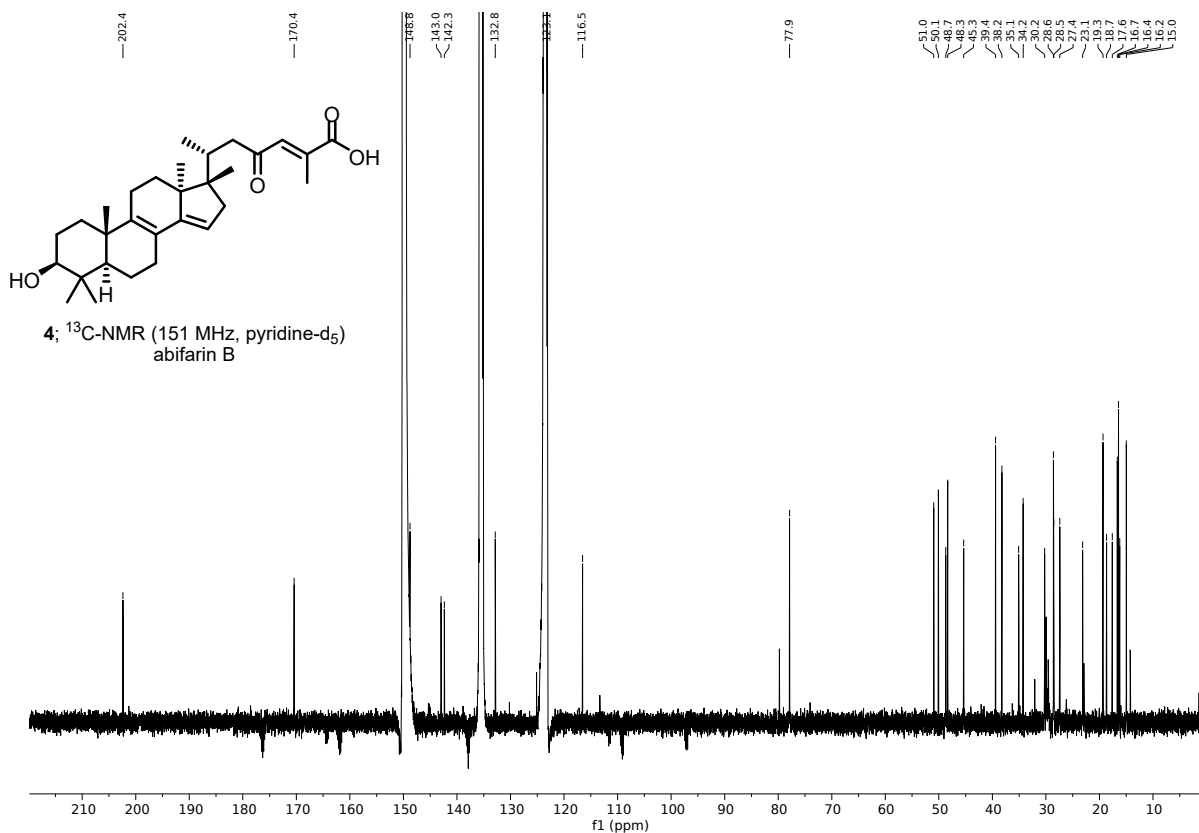
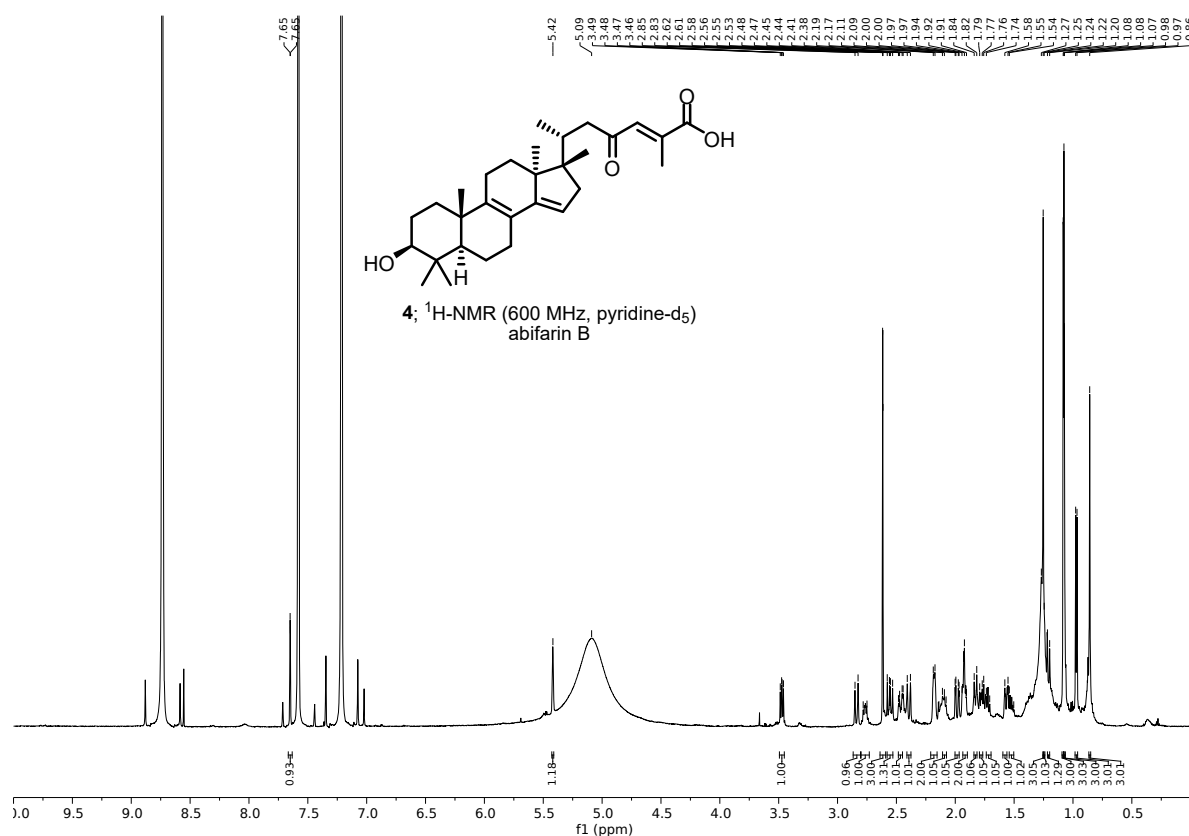
S9: ^{13}C -NMR (101 MHz, CDCl_3)

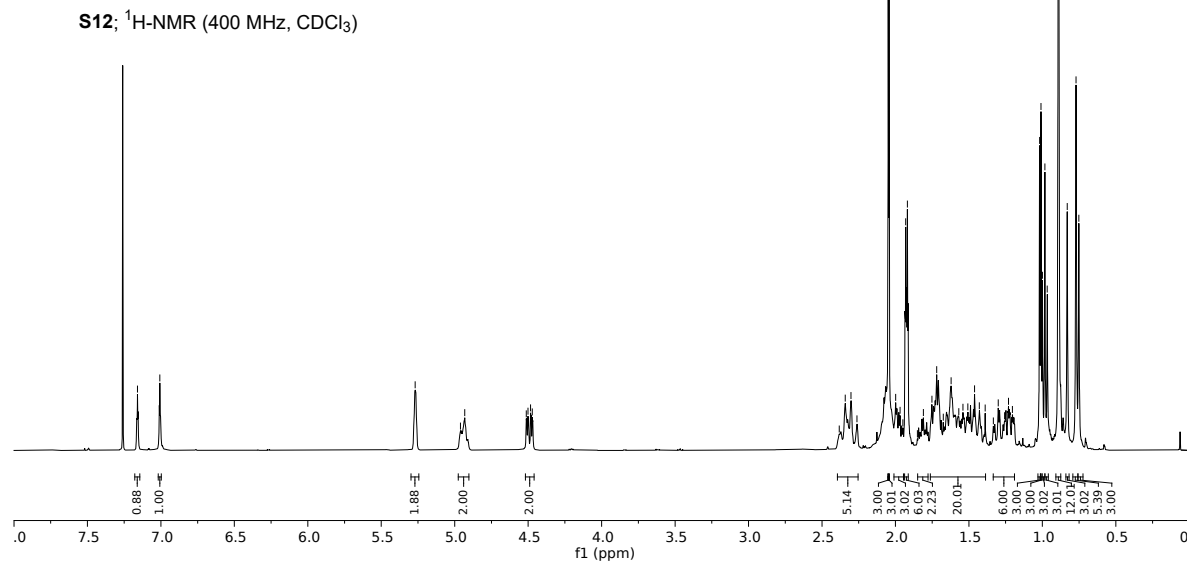
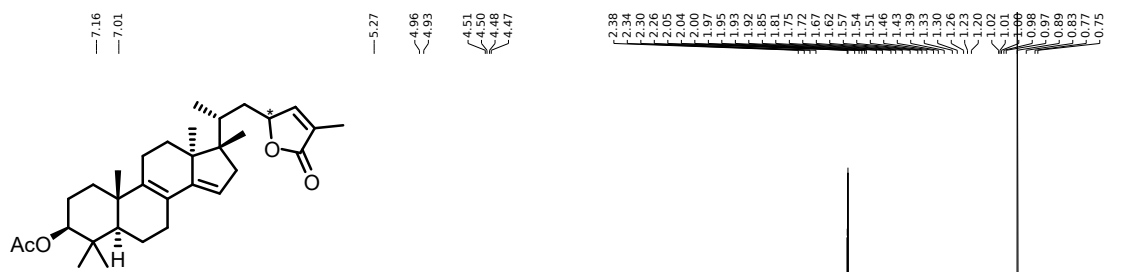
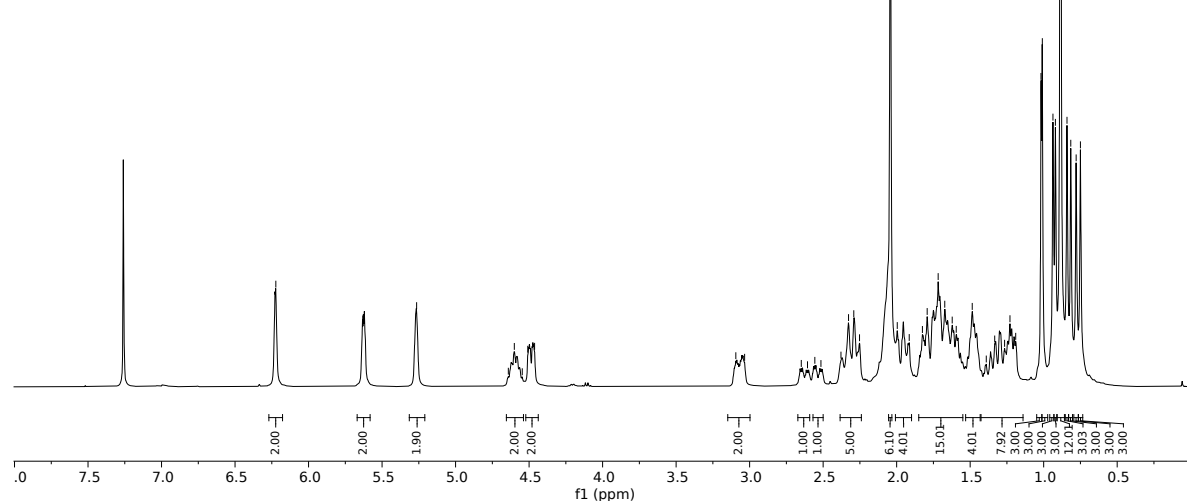
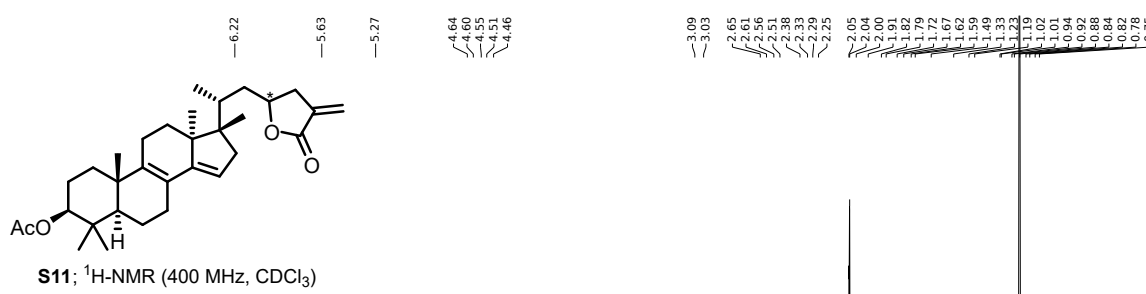


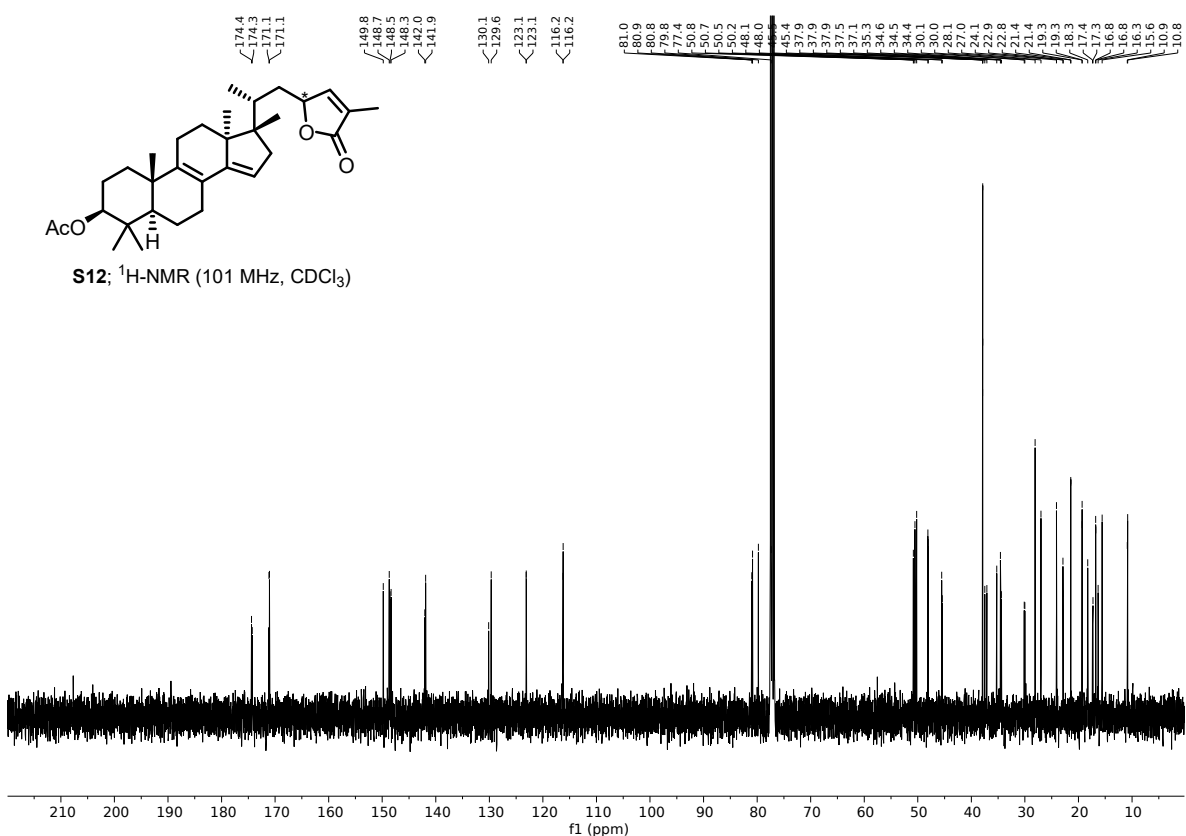


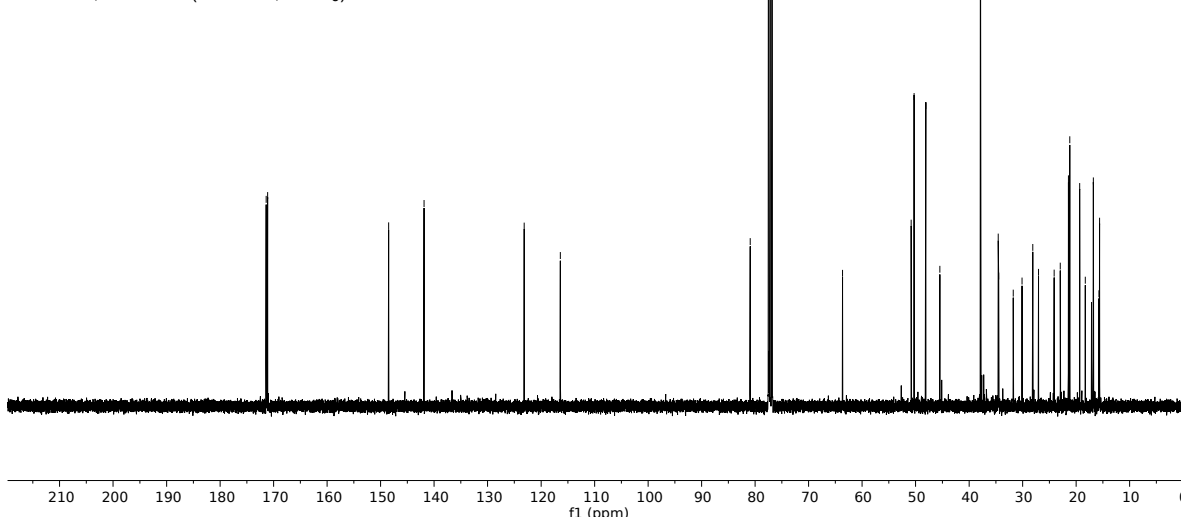
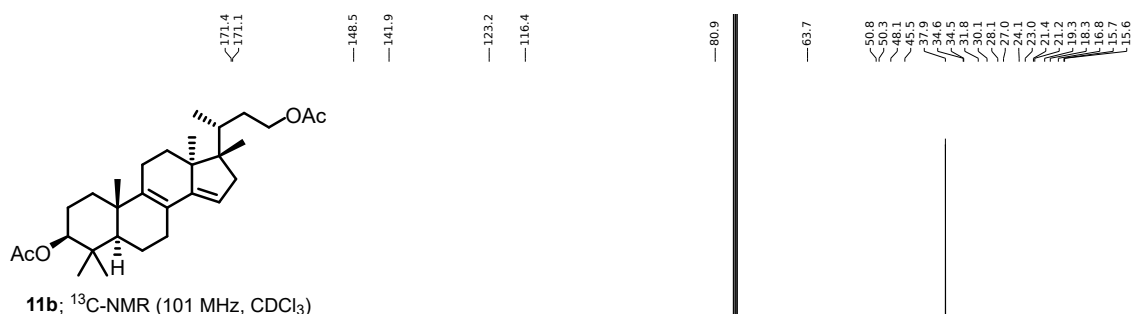
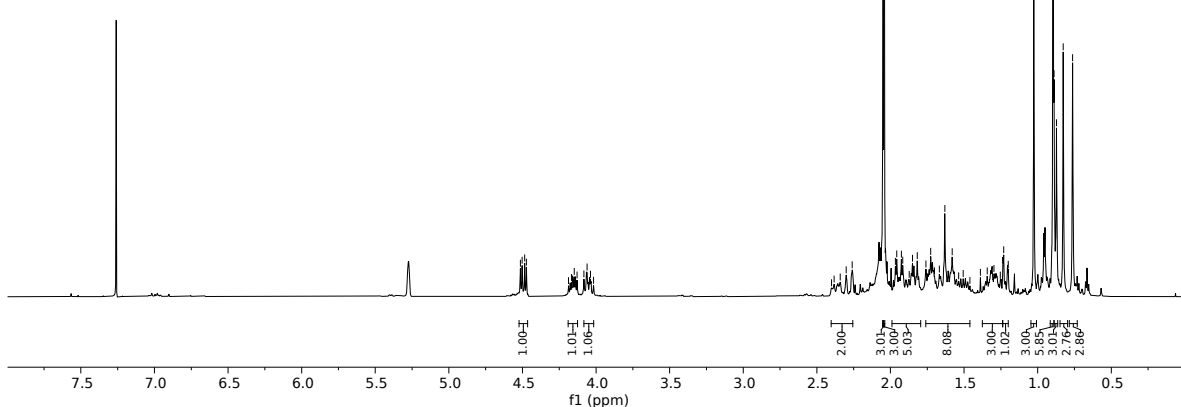
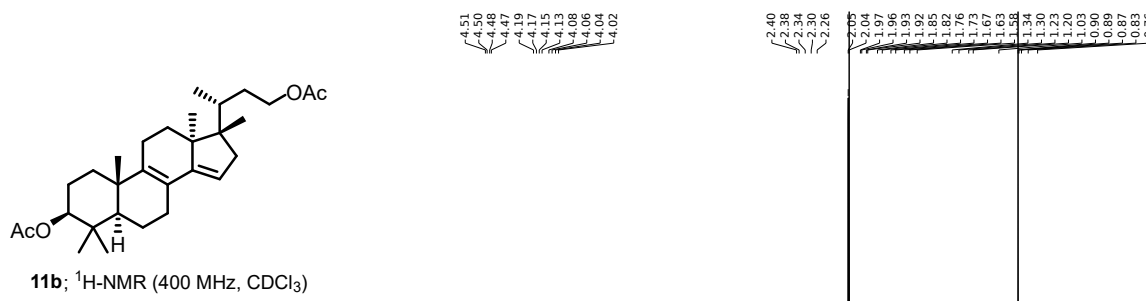


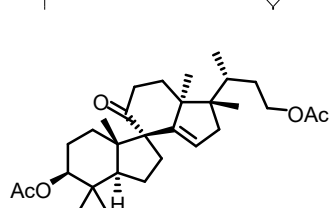
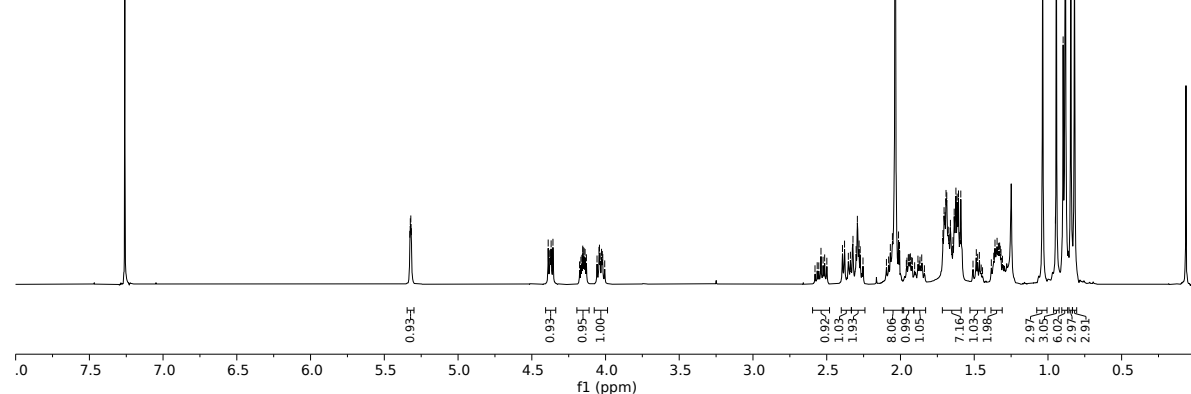
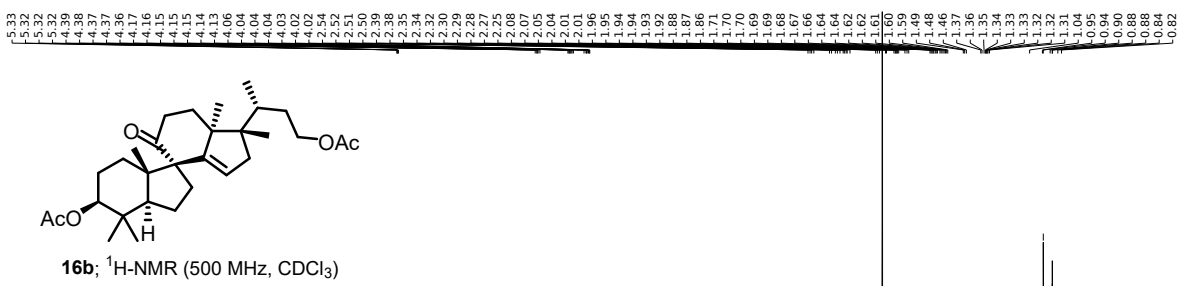




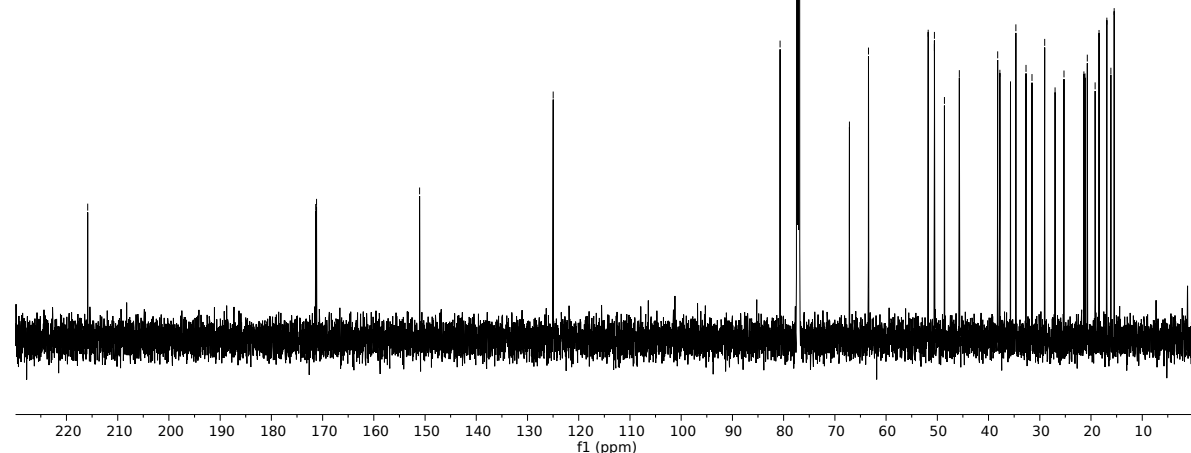


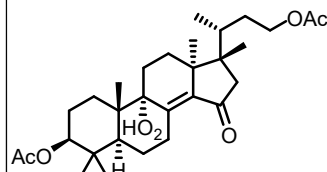
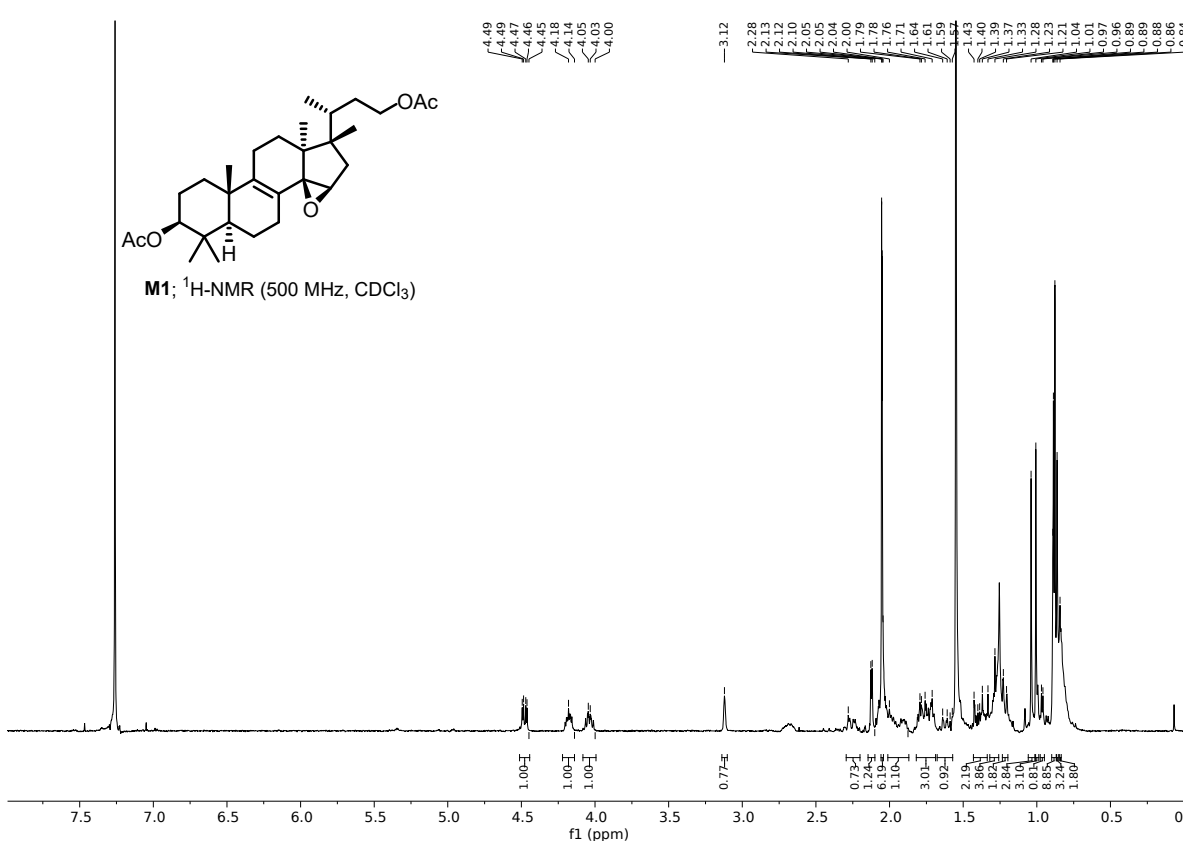




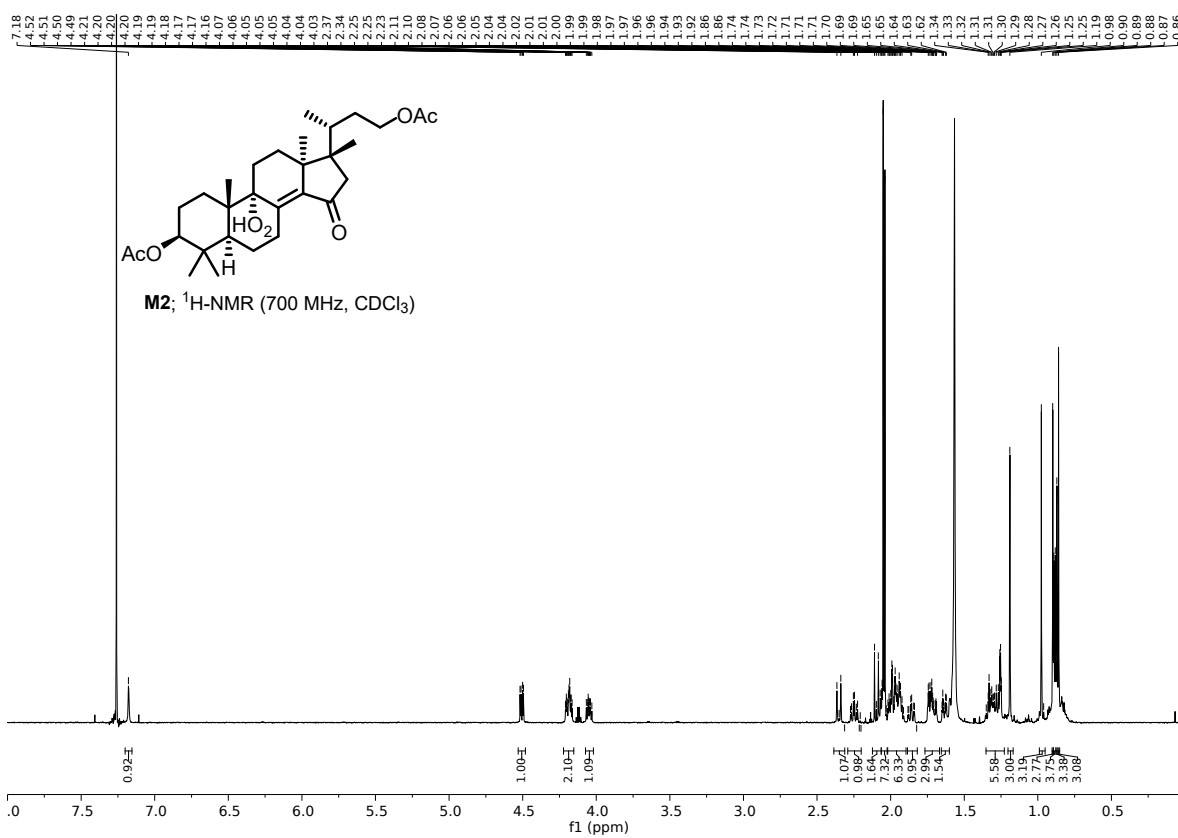


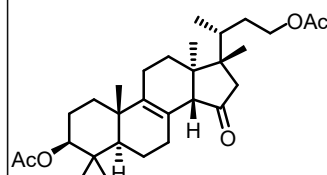
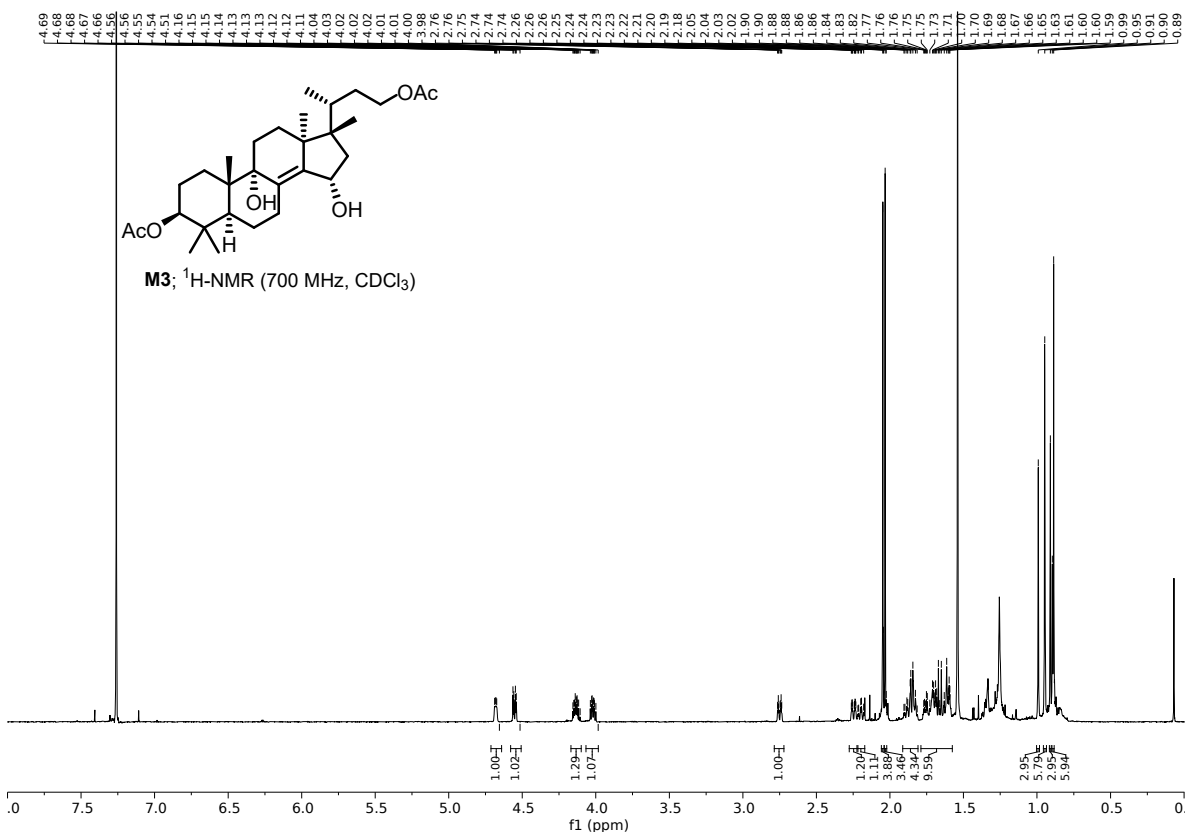
16b; ^{13}C -NMR (151 MHz, CDCl_3)



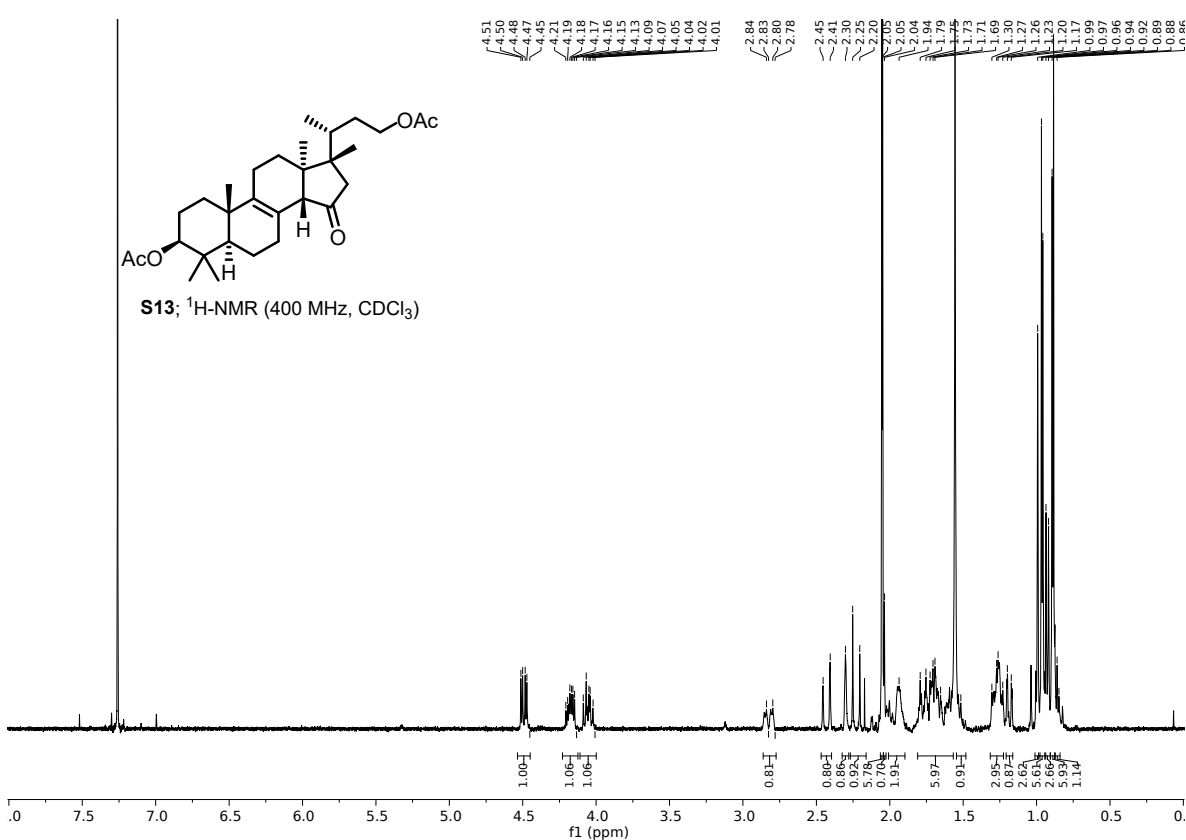


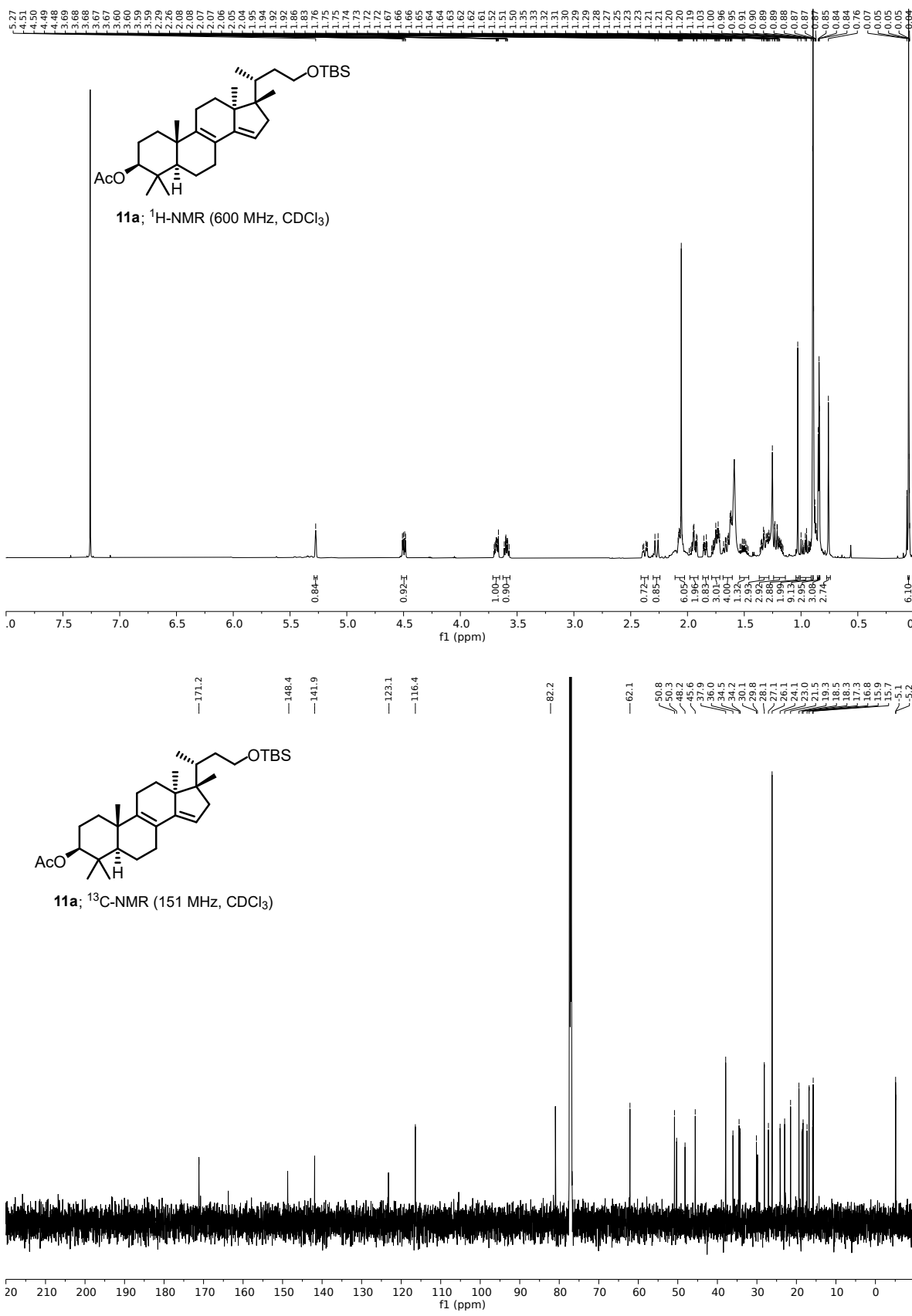
M2; $^1\text{H-NMR}$ (700 MHz, CDCl_3)

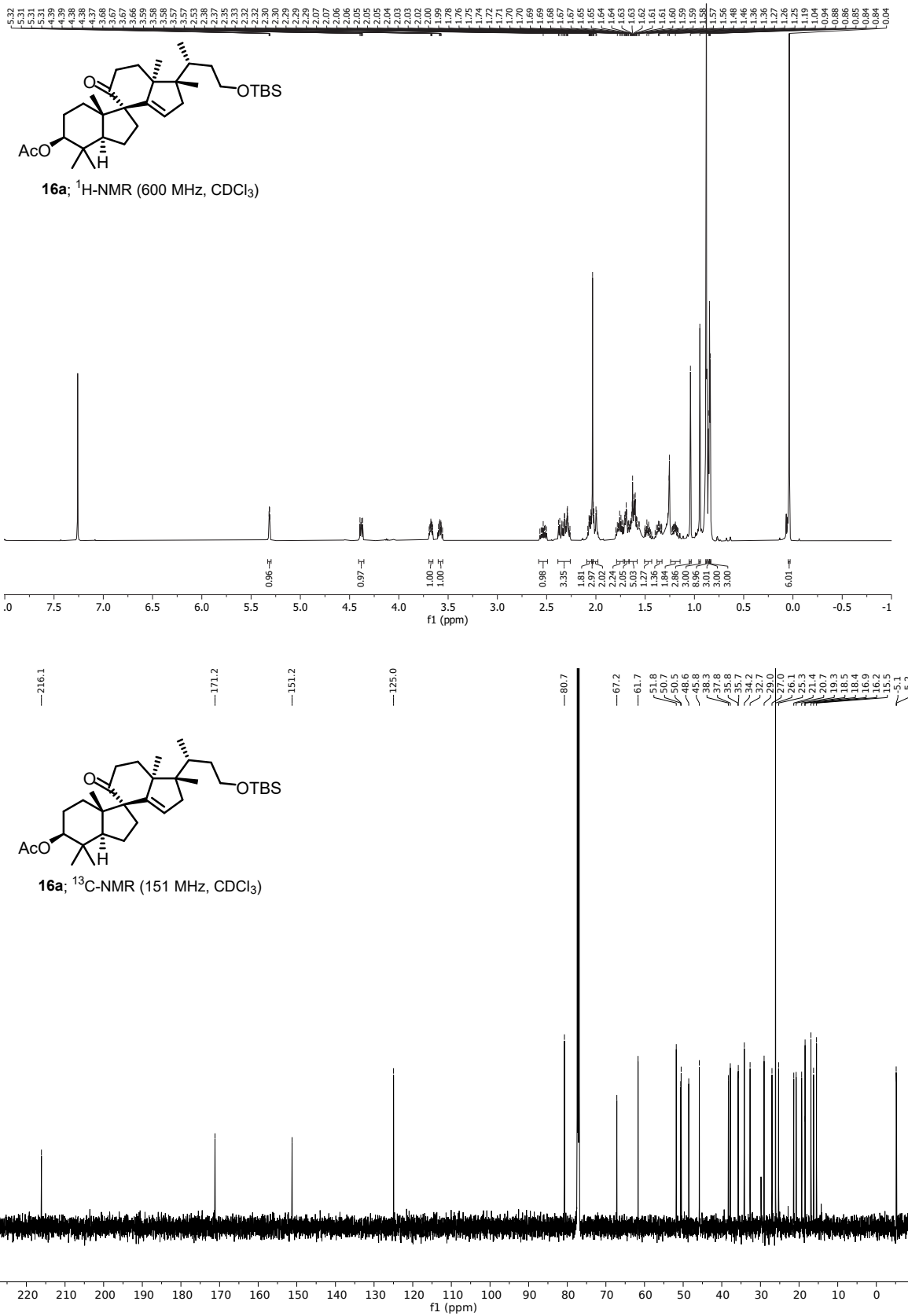


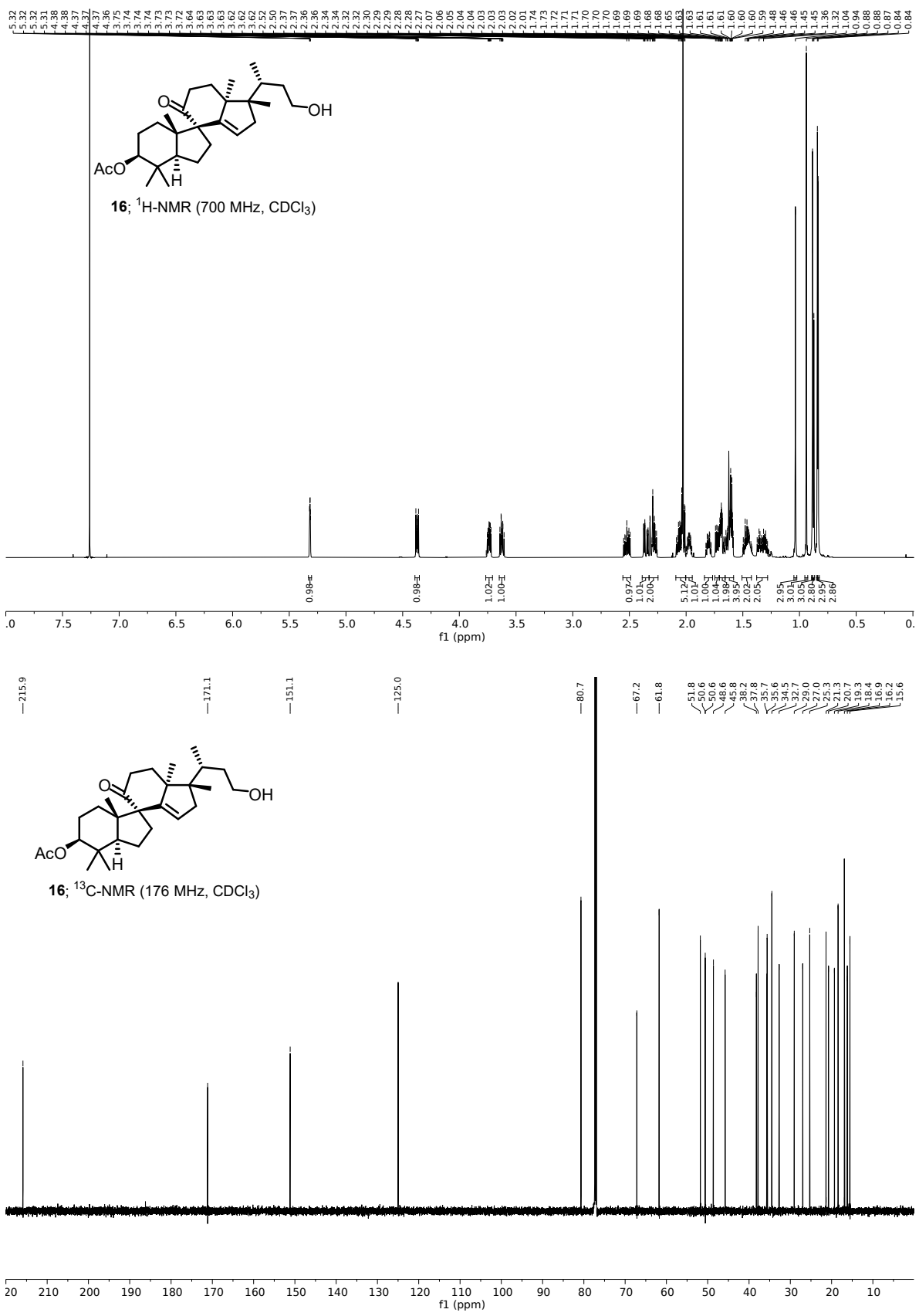


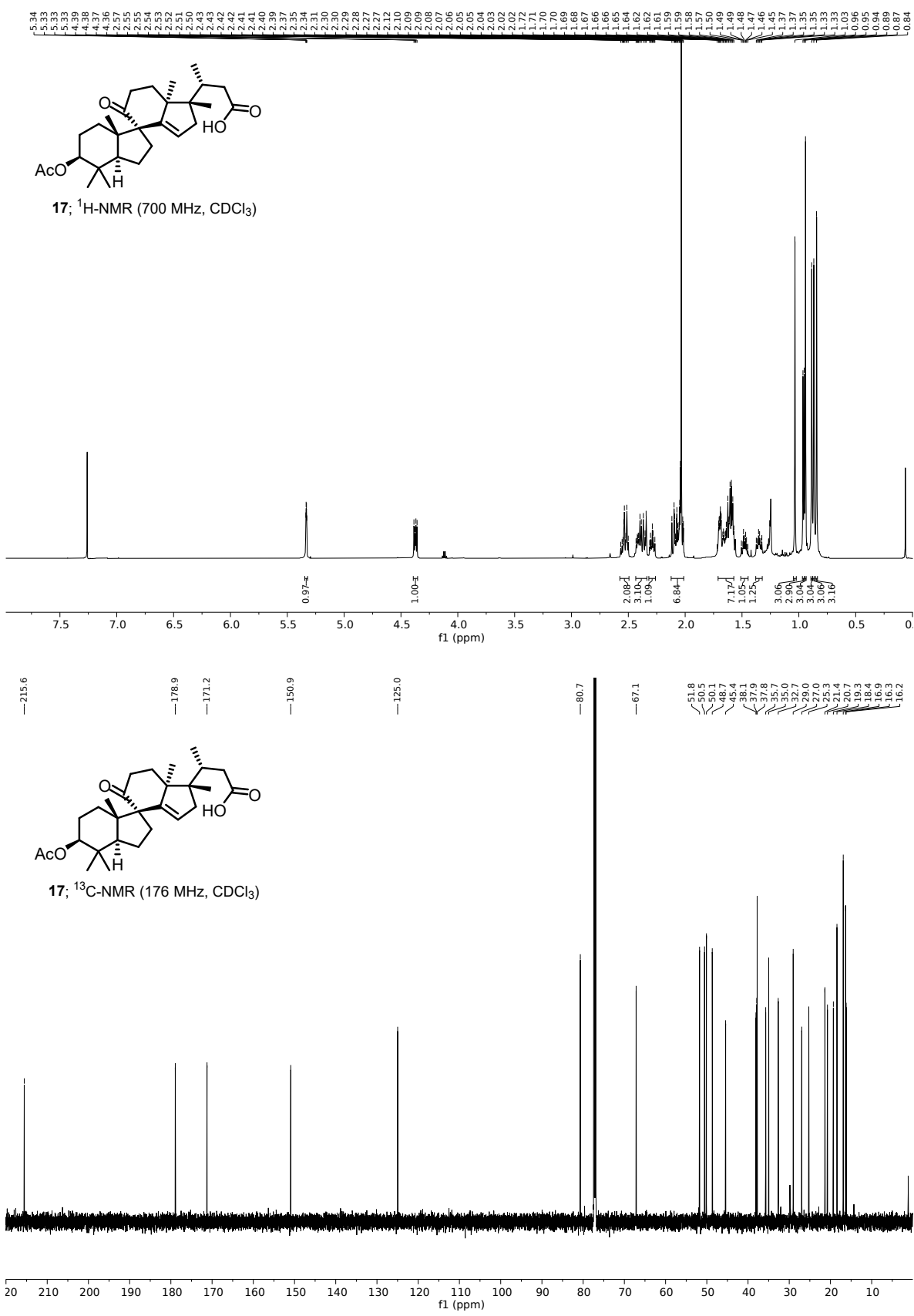
S13; ^1H -NMR (400 MHz, CDCl_3)

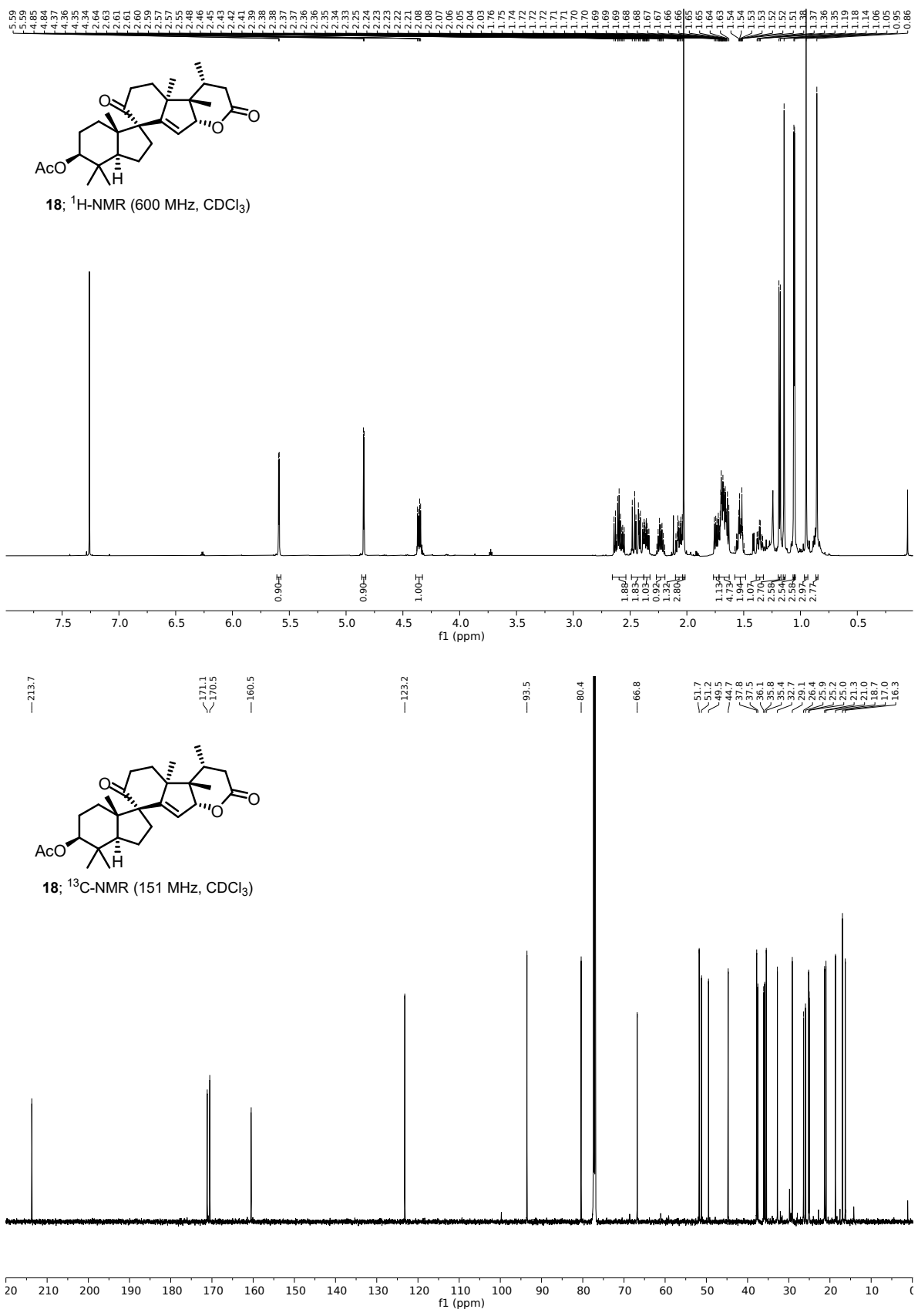


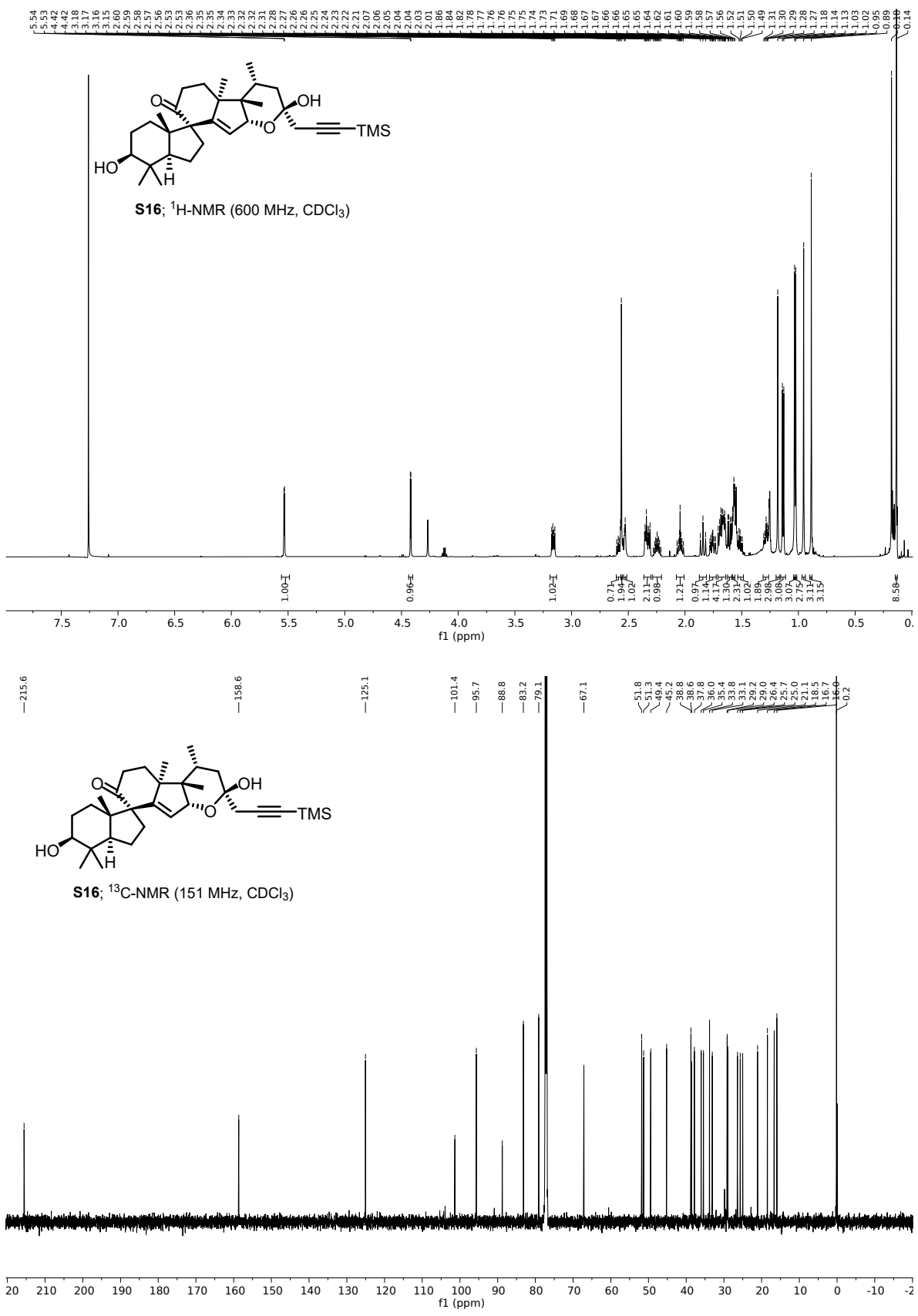


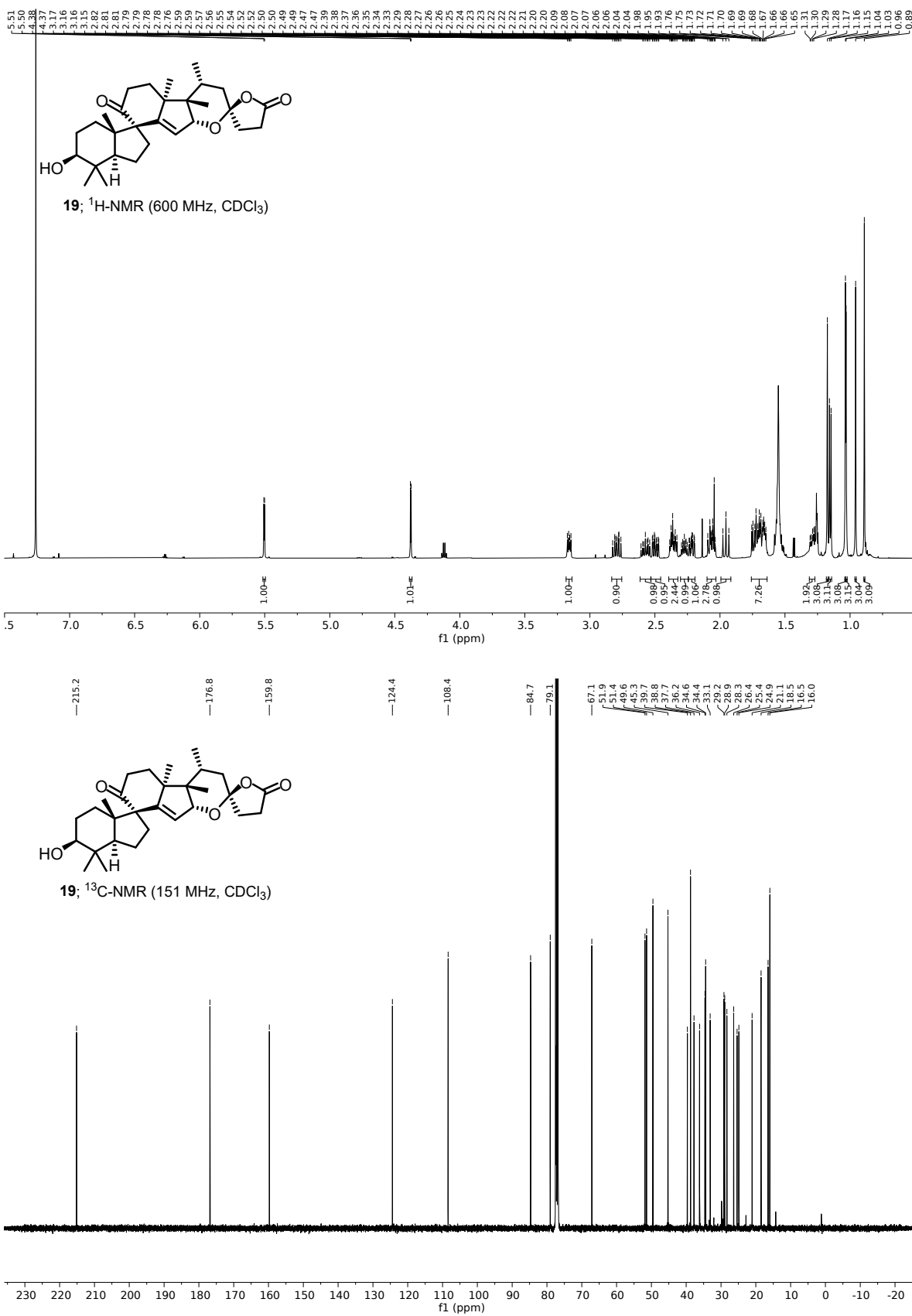


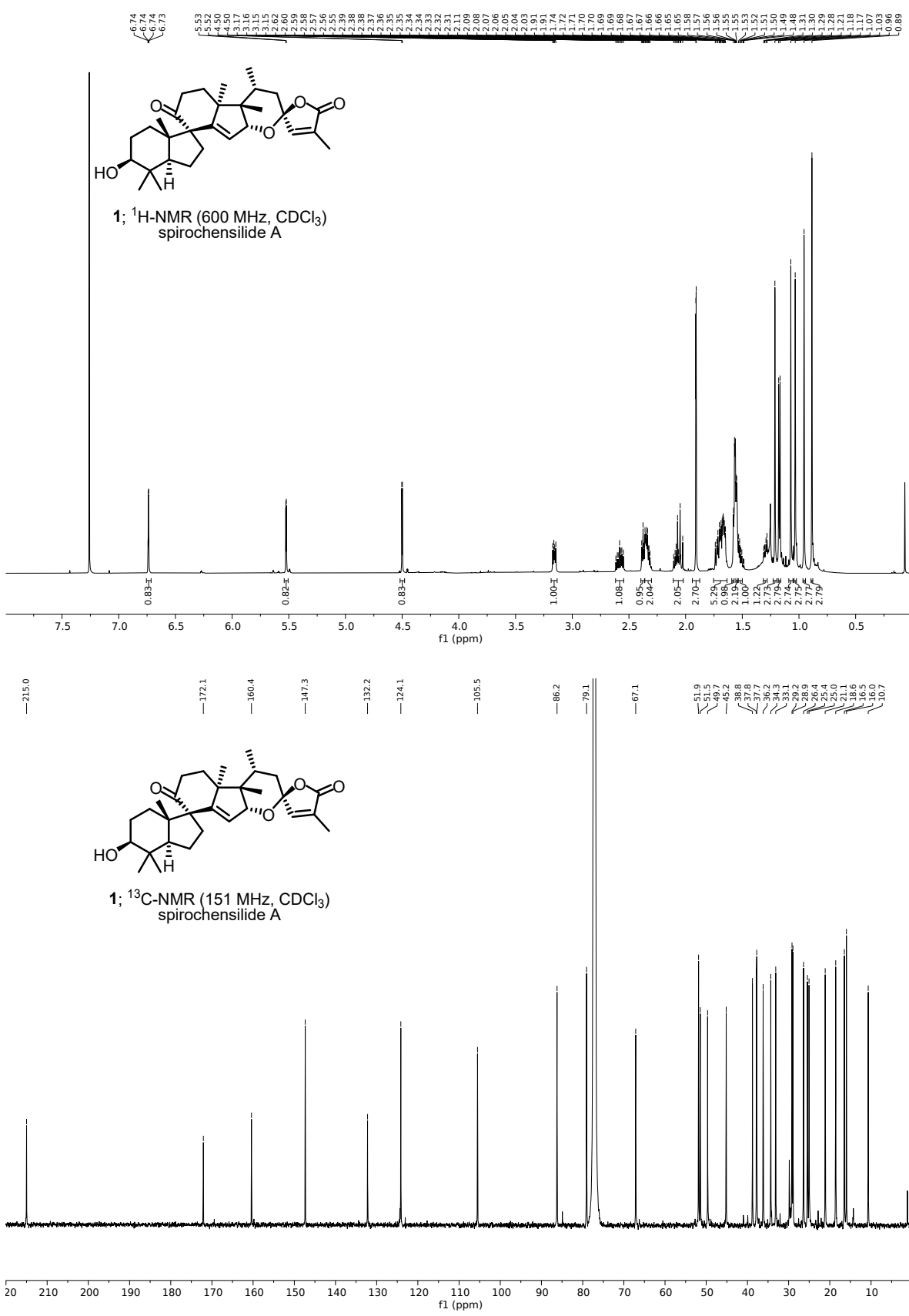


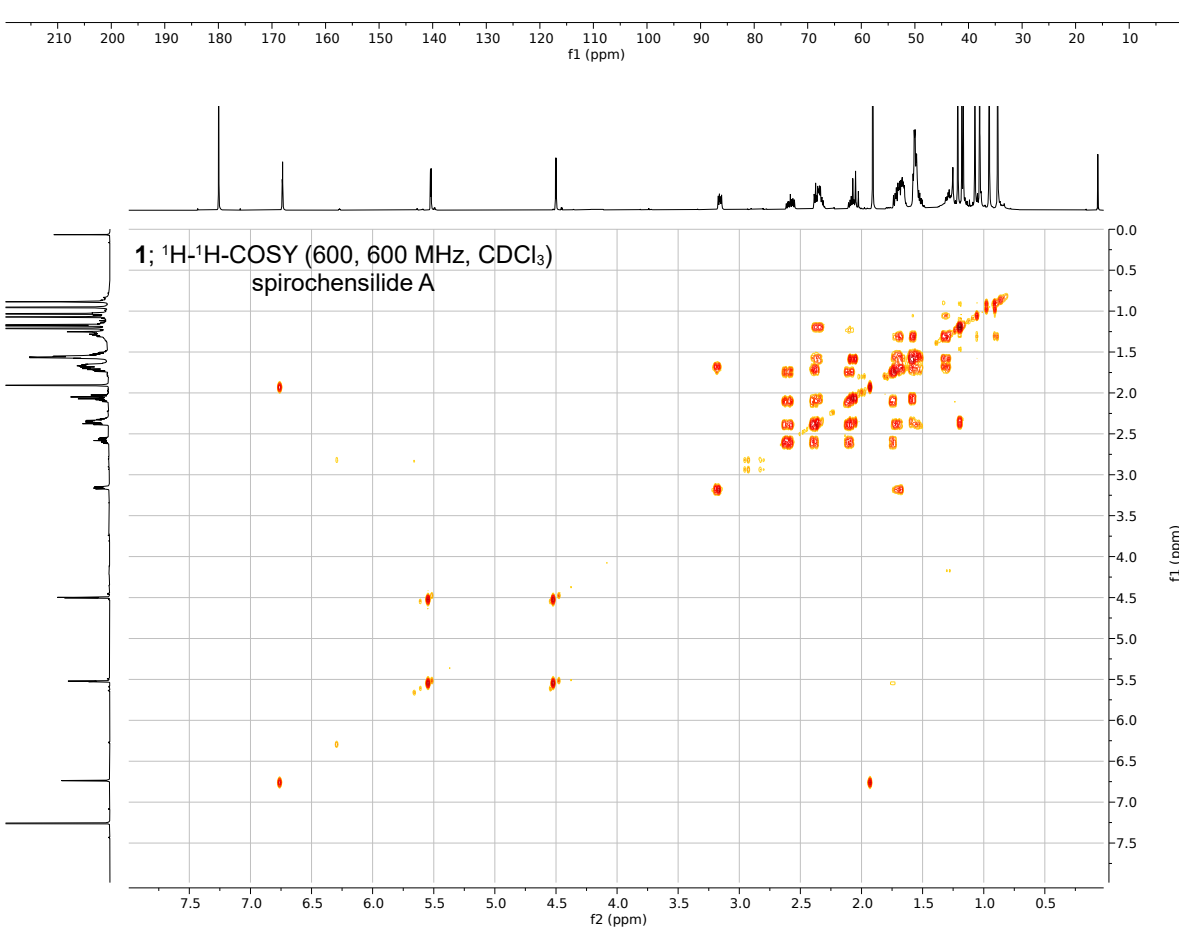
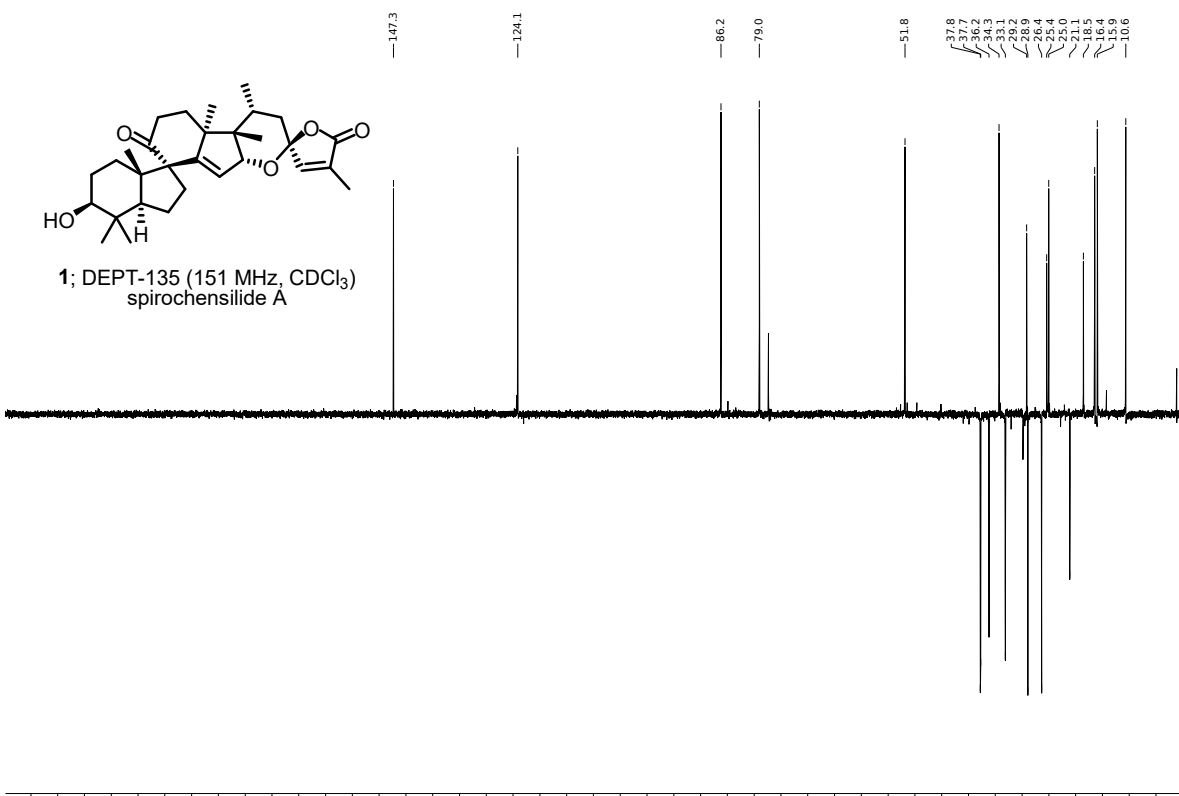


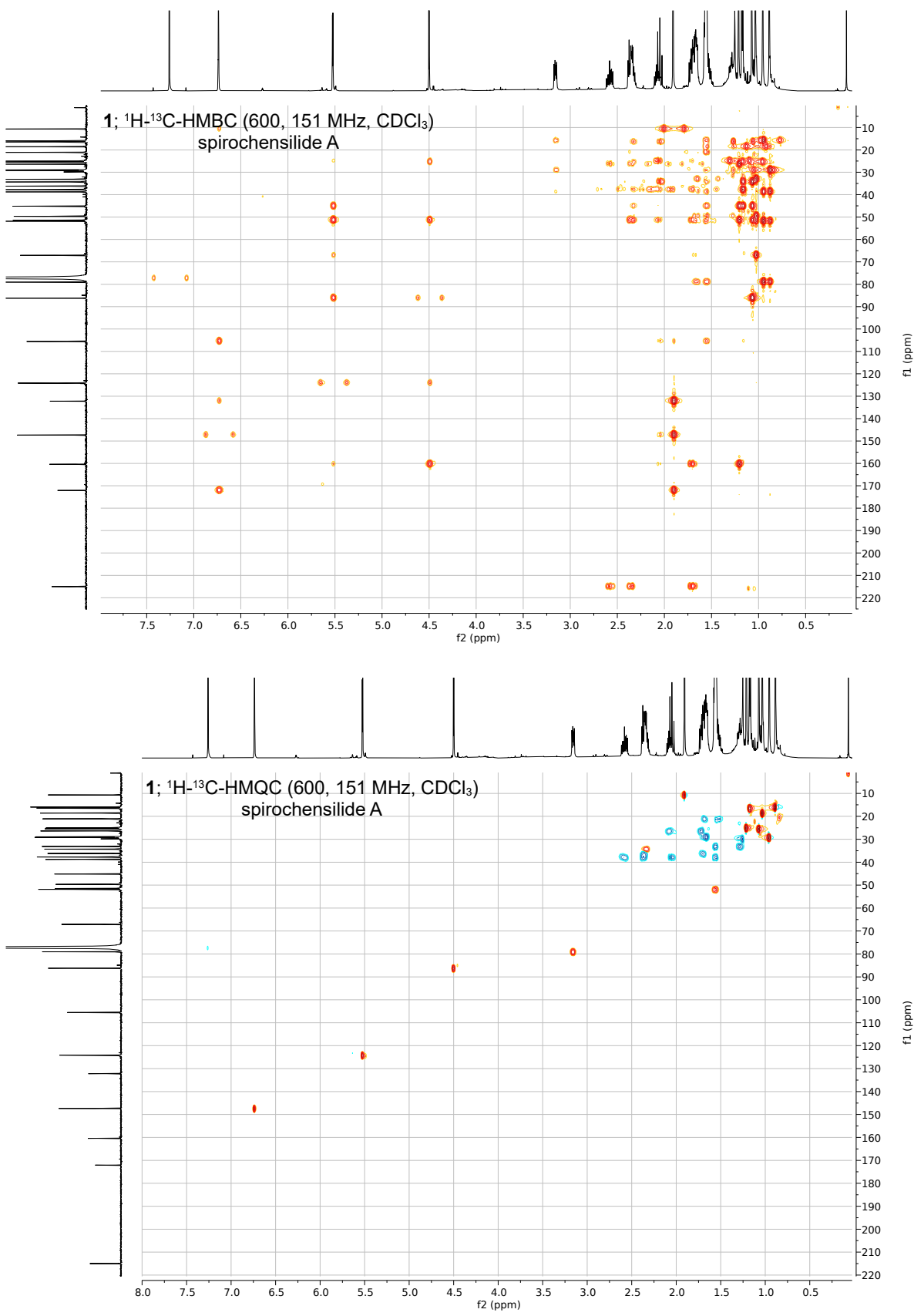


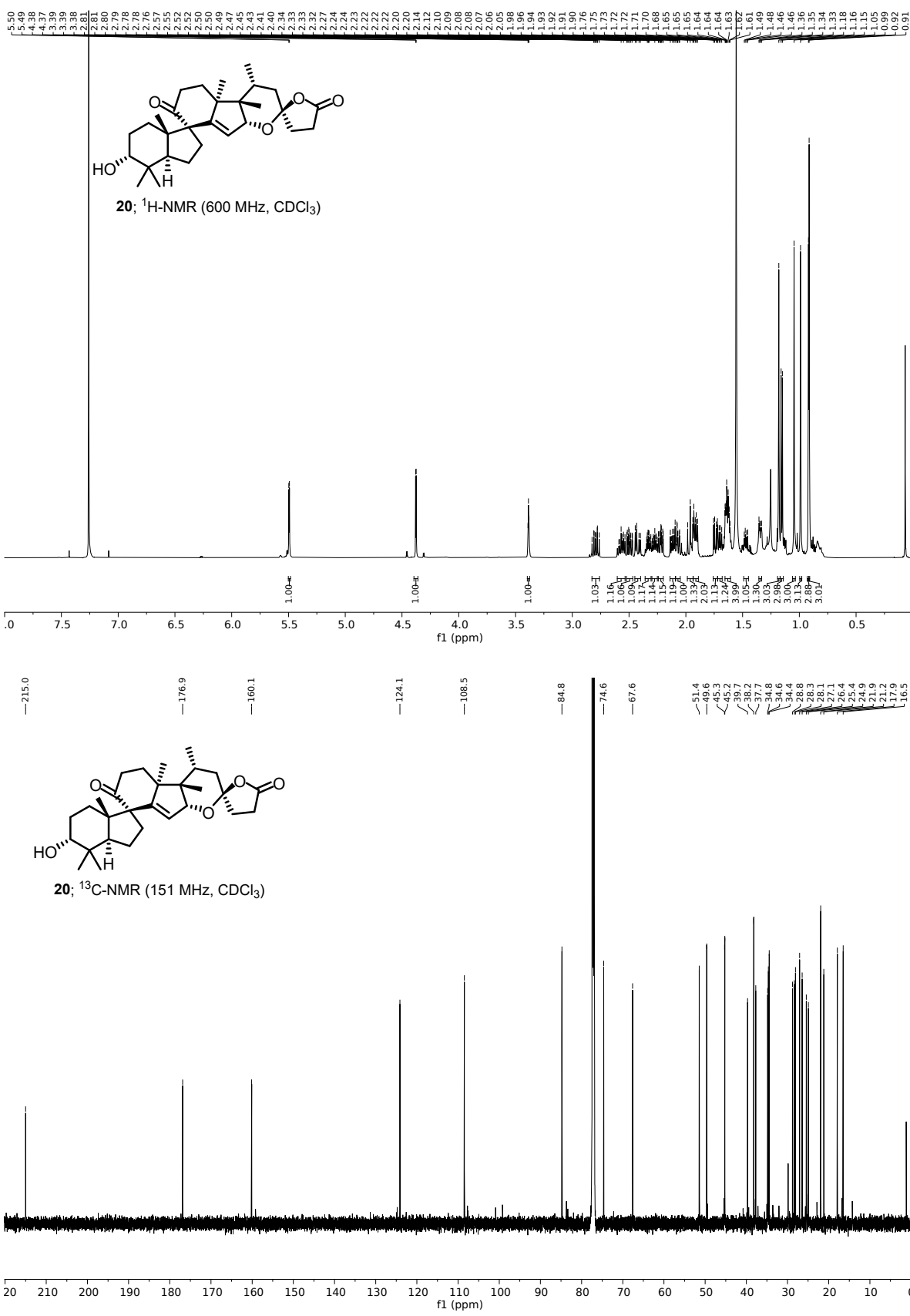


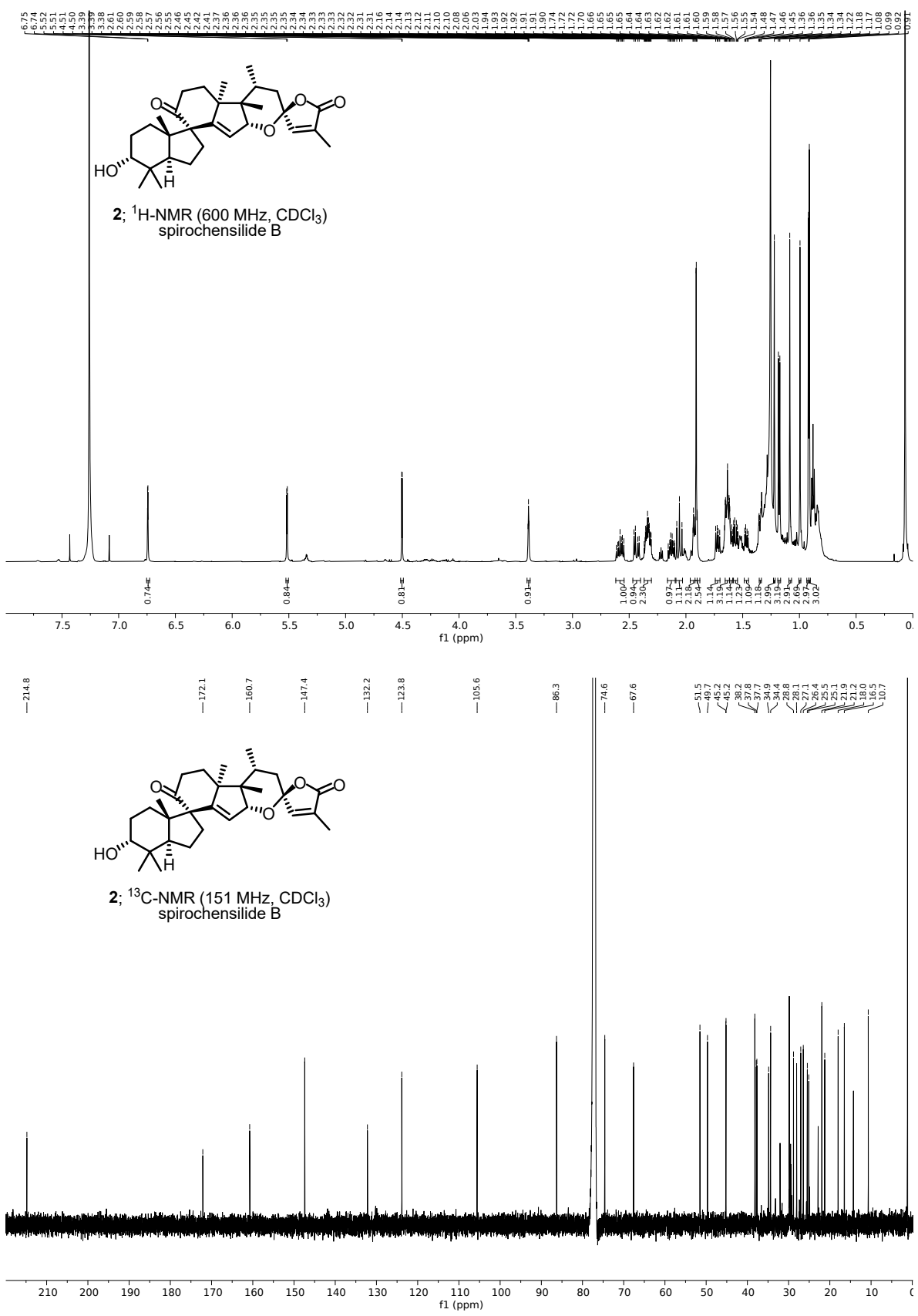


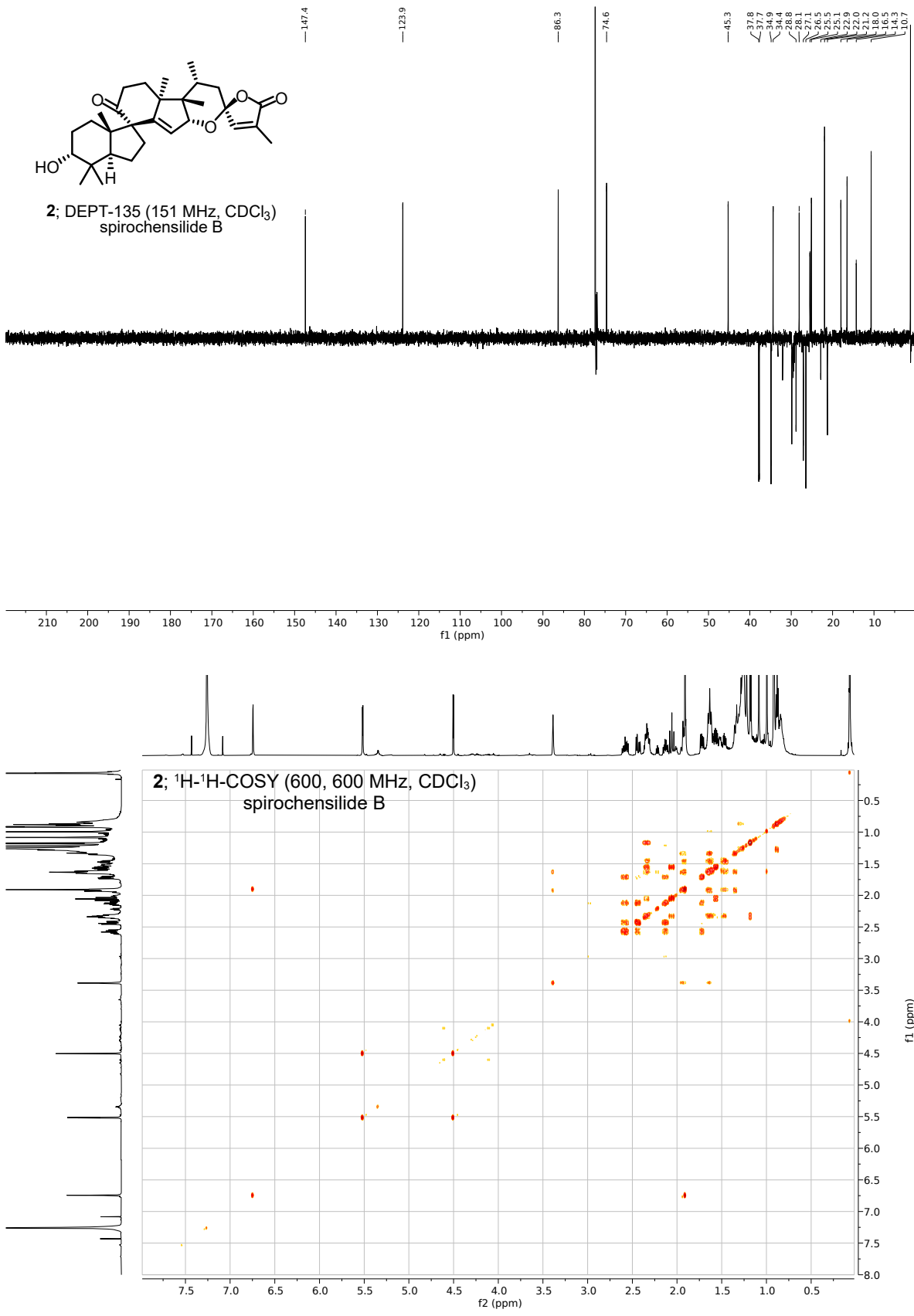


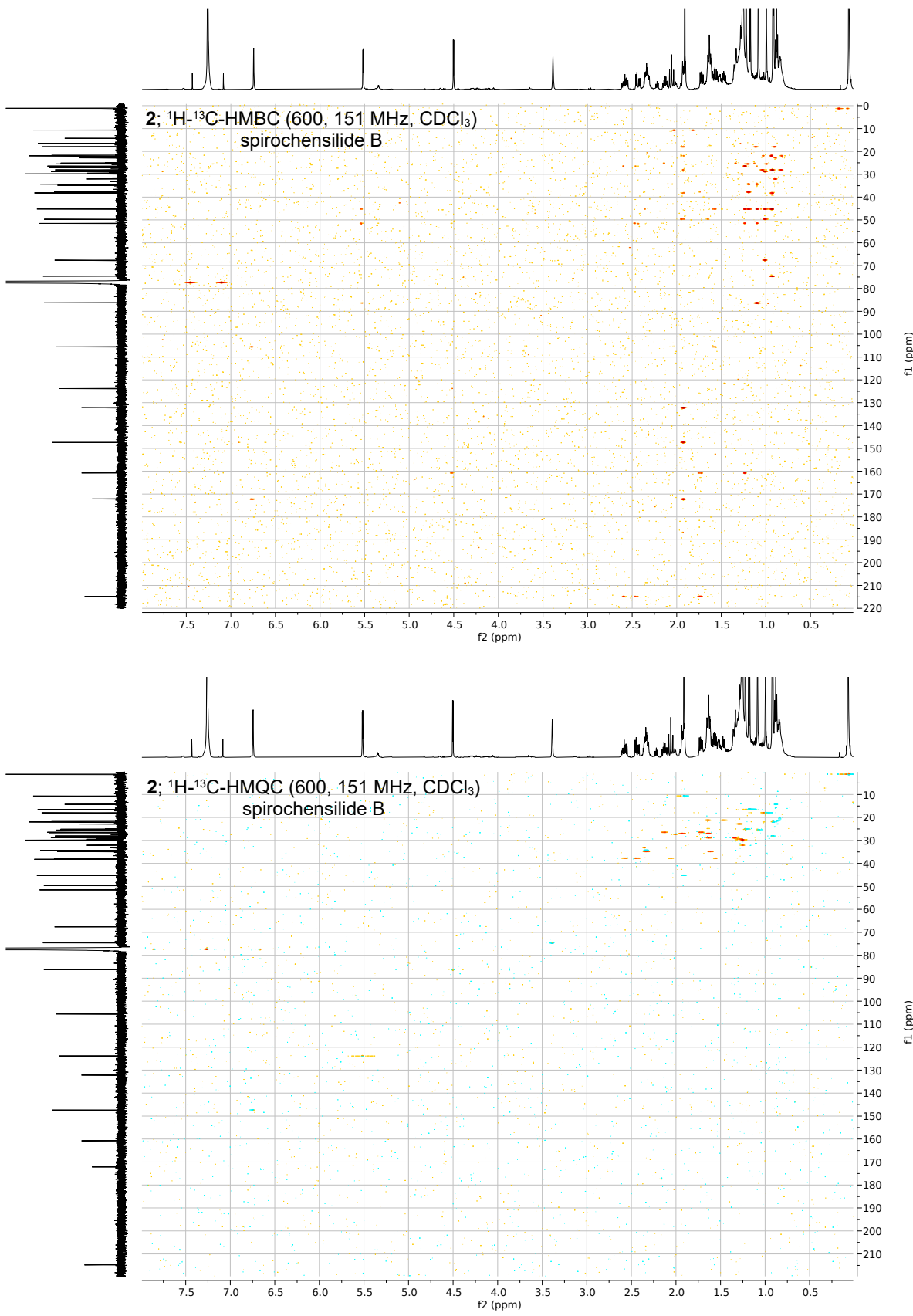












Title:

Chemical Emulation of the Biosynthetic Route to Anthrasteroids: Synthesis of Asperfloketal A

Type of authorship:

First Author

Type of article:

Communication

Share of work:

90% Mykhaylo Alekseychuk

10% Philipp Heretsch

Contribution to the publication:

This project was designed by Mykhaylo Alekseychuk and Philipp Heretsch.

The synthetic work and analytical characterizations were carried out by Mykhaylo Alekseychuk.

The manuscript was prepared by Mykhaylo Alekseychuk and Philipp Heretsch.

Journal:

Journal of the American Chemical Society

5-Year-impact factor:

14.690 (Academic Accelerator)

Date of publication:

21.11.2022

Number of citations:

2

DOI:

10.1021/jacs.2c10735

PubMed-ID:

36410736

Reprinted with permission from M. Alekseychuk, and P. Heretsch, *J. Am. Chem. Soc.* 2022, 144, 48, 21867–21871.

Copyright 2023 American Chemical Society.

Chemical Emulation of the Biosynthetic Route to Anthrasteroids: Synthesis of Asperfloketal A

Mykhaylo Alekseychuk and Philipp Heretsch*



Cite This: *J. Am. Chem. Soc.* 2022, 144, 21867–21871



Read Online

ACCESS |

Metrics & More

Article Recommendations

Supporting Information

ABSTRACT: The anthrasteroid rearrangement has been discussed for the formation of the eponymous substance class since its discovery. We here report its chemical emulation from a plausible biogenetic precursor and show how it accounts for the formation of asperfloketals A and B through a mechanistic bifurcation event. As a result, these natural products arise from double Wagner–Meerwein rearrangements and, thus, are $1(10 \rightarrow 5),1(5 \rightarrow 6)$ - and $1(10 \rightarrow 5),4(5 \rightarrow 6)$ diabeo-14,15-seco steroids, respectively. To establish an efficient route to a bioinspired precursor, we devised a sequence of orchestrated oxidative activation and rearrangement from ergosterol.

Anthrasteroids constitute a compound class of steroidal descendants with an aromatic B ring, attached in linear fashion to saturated, six-membered A and C rings, forming their eponymous anthracene framework (for an example, see Scheme 1, structure 6).¹

The first members of the class were obtained by chemical means, i.e., through acid treatment of unsaturated steroid precursors.² Early after isolation and structural elucidation of the products from these reactions, hypotheses on their possible occurrence as natural products, especially on their *in vivo* formation and further processing into polycyclic aromatic carcinogens, were discussed.³

The first anthrasteroids isolated from nature were obtained from sediments and investigated as markers for the stage of diagenesis.⁴ Later, the first anthrasteroid isolated from a living source was confirmed.⁵ Several more isolation reports followed, leading to a low two-digit number of naturally occurring anthrasteroids known today (see Supporting Information (SI)).⁶

The mechanism of rearrangement furnishing their aromatic core has remained controversial, though.⁷ Thus, cationic intermediates of type A (Scheme 1A) are thought to initiate the required Wagner–Meerwein rearrangement of C1 from C10 to C6, proposedly through the intermediacy of spirocyclic D. A second Wagner–Meerwein rearrangement then gives the anthrasteroid framework via Wheland intermediate E. This course of events renders possible a bifurcation from D; i.e., either C4 or C1 migrates in the second Wagner–Meerwein rearrangement (see red vs green pathway from G). Although both lead to the same framework, a different connectivity of the original carbons is obtained, with either a $1(10 \rightarrow 5),1(5 \rightarrow 6)$ - or a $1(10 \rightarrow 5),4(5 \rightarrow 6)$ diabeo-steroid as a result. When C3 is substituted as in precursor 3, regiosomeric products can arise, with the resulting substituent residing in either the 3α - or 2β -position (anthrasteroid differs from steroid numbering).

Contrarily to these thoughts, all anthrasteroids isolated from nature until very recently have been 3α -hydroxylated. We got interested in this anomaly when, in 2020, two novel natural

products, asperfloketals A (1) and B (2), were isolated from the sponge-associated fungus *Aspergillus flocculosus* 16D-1 by the group of Han, Xu, and Lin.⁸ The asperfloketals A and B are regiosomeric 3α - and 2β -hydroxy-anthrasteroids which additionally exhibit a 14,15-seco motif accompanied by a high degree of oxidation. Thus, asperflokal B (2) is the first example of a 2β -anthrasteroid, and only very recently, aspersterol A was reported as a second example.⁹ The biosynthesis hypothesis by the isolation team (see Supporting Information (SI)) does not invoke the anthrasteroid rearrangement and entails a dehydration/rehydration event to convert 1 into 2.

Here, we contribute to resolving the remaining controversy around the anthrasteroid rearrangement using the example of asperfloketals A (1) and B (2) by devising an efficient and selective synthetic strategy toward these complex natural products, and we provide chemical proof for the occurrence of a bifurcation event between the two Wagner–Meerwein rearrangements.

A close examination of reported protocols to chemically initiate the anthrasteroid rearrangement revealed 2β -anthrasteroids never to be isolated and structurally elucidated. Early attempts by Tsuda, Tanaka, and Mosettig to convert $\Delta^{5,7,9(11)}$ -ergosta-triene 3 (Scheme 1A) under strongly acidic conditions furnished anthrasteroid products but led to elimination (see compound 4), loss of stereointegrity at C14 (as in compound 5), and only low yields of 3α -product 6.² Spectroscopic methods or isolation attempts did not indicate the formation of the 2β -regioisomer in these reactions.¹⁰

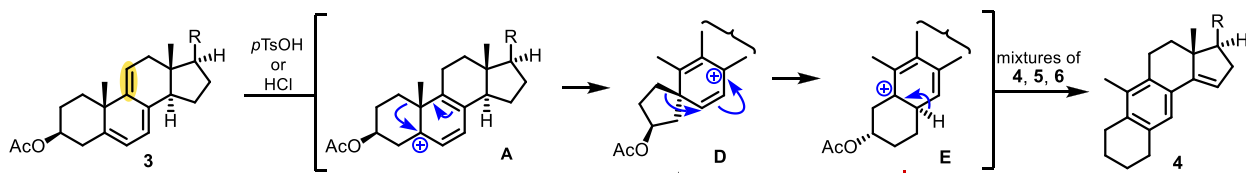
Received: October 10, 2022

Published: November 21, 2022

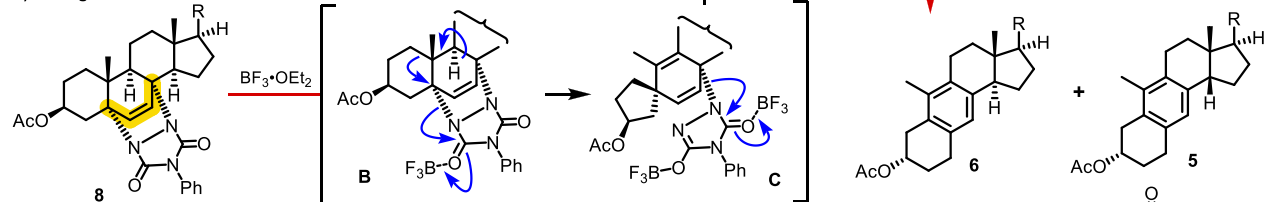


Scheme 1. (A, B) Previous Studies in the Anthrasteroid Rearrangement, (C) Structures of Asperfloketals A and B and Revised Biogenesis Proposal, and (D) Chemical Emulation

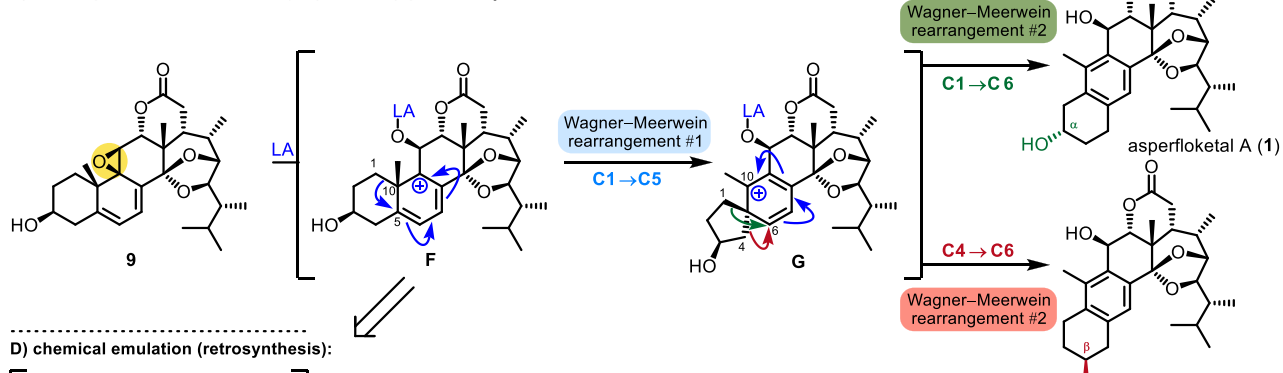
A) anthrasteroid formation through protonation of $\Delta^{9(11)}$ steroids:



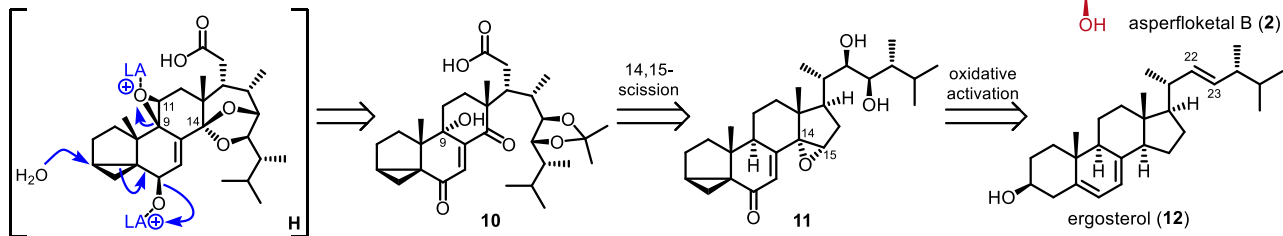
B) through Lewis-activation of diazo adducts:



C) our biogenesis proposal employing a leaving group at C9:



D) chemical emulation (retrosynthesis):



The other known chemical method for initiating the anthrasteroid rearrangement chemically entails the addition of artificial dienophiles such as 4-phenyl-1,2,4-triazoline-3,5-dione to steroidal $\Delta^{5,7}$ -dienes (see adduct 8, Scheme 1B), followed by their Lewis-acidic conversion (see structure B), again likely traversing spirocyclic intermediates C and D.¹¹ This method is advantageous in terms of yield, and it preserves stereointegrity at C14, but it obviously is not biomimetic and, most importantly, only leads to the formation of the 3 α -regioisomer 6.¹² This was later explained by different migration tendencies of C1 and C4 in D, attributed to destabilizing effects of the 3-hydroxyl in the case of C4-migration.¹³ Although related endoperoxides to 8 have been proposed to initiate the anthrasteroid rearrangement in a similar fashion,^{6b} a chemical emulation remains elusive.

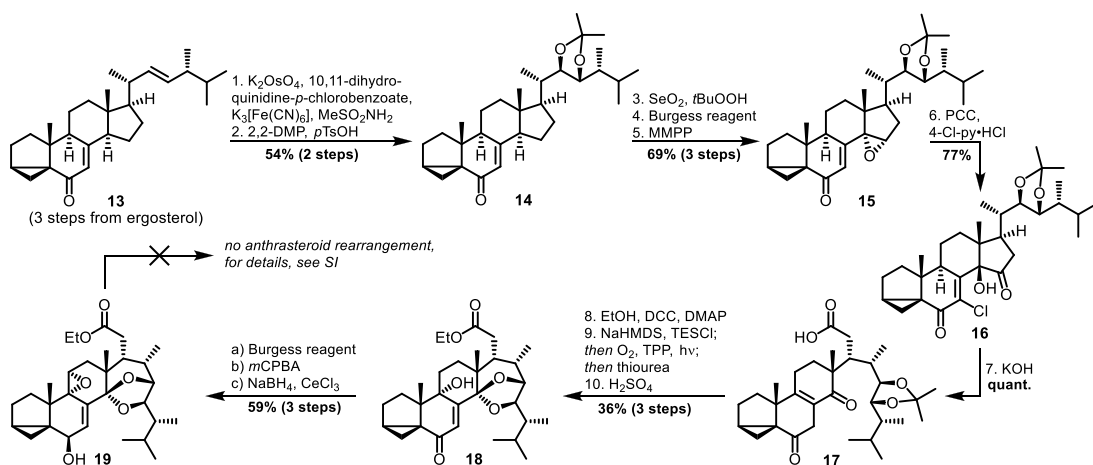
Key to our biogenesis proposal was a leaving group at C9 to access the desired carbonium ion (Scheme 1C). In this context, the hydroxy group at C11 in 1 and 2 hinted at β -epoxide 9 to provide access to intermediate F and, simultaneously, to access a β -hydroxy group at C11. We assumed that, after the first Wagner–Meerwein shift, intermediate G would further

rearrange to give both asperfloketals A (1) and B (2), thereby providing conclusive evidence for the bifurcation event.

Our retrosynthetic analysis is emulating plausible biosynthesis intermediate F by activating *i*-steroid diol H under Lewis-acidic conditions to engage in the rearrangement (Scheme 1D). The *i*-steroid was chosen to mask the highly reactive $\Delta^{5,7}$ -diene-9,11-epoxide until the rearrangement is attempted. In the retrosynthetic direction, intermediate H can be obtained from 14,15-secoesteroid 10, available through a route reminiscent of our synthesis of 14,15-secoesteroid strophasterol A.¹⁴ The required 14,15-epoxide 11 was eventually planned to be synthesized from commercial ergosterol (12) by an orchestrated sequence of oxidation events.

Starting from literature-known *i*-steroid 13, available in 3 steps and 58% yield from ergosterol (12),¹⁵ application of a modified Sharpless protocol with 10,11-dihydroquinidine-*p*-chlorobenzoate as a superior ligand¹⁶ led to the formation of the desired (22*R*,23*R*)-diol, with no detectable formation of the respective (22*S*,23*S*)-diastereomer and only small quantities of 22,23-dione obtained from overoxidation (Scheme 2).

Scheme 2. Preparation of Bioinspired Precursors for the Anthrasteroid Rearrangement



Acetonide protection then gave enone **14** in a yield of 54% over 2 steps. Introduction of a 14*α*,15-epoxide was accomplished through Riley oxidation (catalytic SeO_2 , stoichiometric $t\text{BuOOH}$), Burgess elimination,¹⁷ and treatment with magnesium monoperoxyphthalate (MMPP) to give **15** in 69% yield over 3 steps. With this intermediate, we attempted a two-step sequence toward 14,15-secoacid **17**. We had previously observed similar reactivity in our synthesis of strophasterol A, but its applicability to other substrates remained unclear. Thus, treatment with pyridinium chlorochromate (PCC) and 4-chloro-pyridinium chloride as a chloride source led to the formation of α -chloro- γ -hydroxy- δ -oxo enone **16** in 77% yield. This process is thought to proceed through an S_N2' epoxide opening by chloride as a nucleophile, followed by oxidation of C15.

α -Hydroxylation through a cyclic chromate ester is believed to yield **16**. When treated with KOH in $t\text{BuOH}$, this material quantitatively rearranges to 14,15-secoacid **17**. A possible mechanistic rationale for this transformation is given in the SI and entails a retro-Dieckmann condensation, double keto-enol tautomerization, followed by chloride elimination, and double bond isomerization into the thermodynamically favored $\Delta^{8(9)}$ position. From **17**, the pivotal rearrangement precursor **19** was accessible: esterification, formation of a silyl enol ether, its [4+2] addition to O_2 under irradiation (tetraphenylporphyrin as a photosensitizer), followed by reduction with thiourea and, eventually, transketolization, aided by the combined use of hexafluoroisopropanol (HFIP) and H_2SO_4 , gave the 9-hydroxy compound **18**.

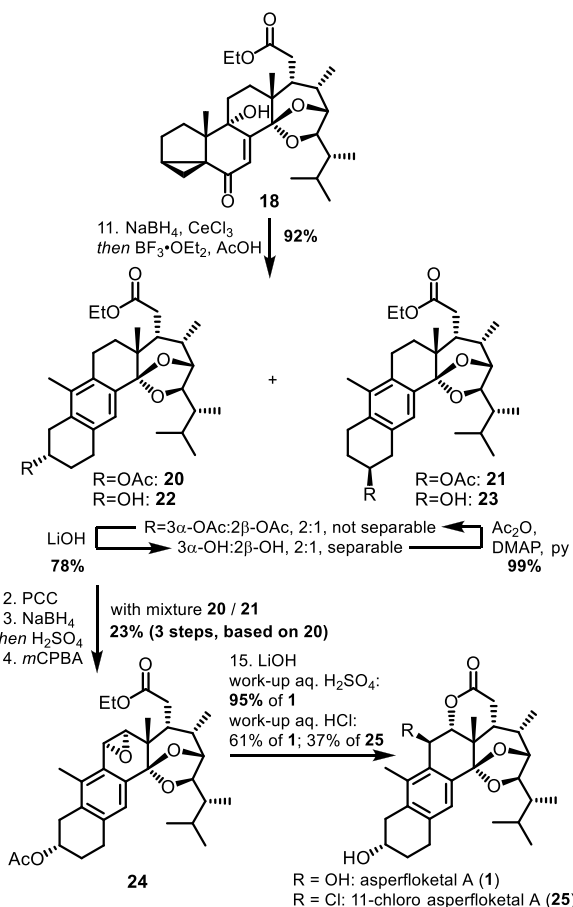
To put our biosynthetic hypothesis to test, we eliminated the alcohol in **18** and epoxidized the so obtained $\Delta^{9(11)}$ bond. Among the few reagents to effect this transformation, *m*-chloroperbenzoic acid (*m*CPBA) gave the best yield (66%), but 2D NMR analysis clearly indicated the exclusive formation of the α -epoxide. Although an attempted anthrasteroid rearrangement would yield the undesired stereoconfiguration at C11, we still reduced the 6-oxo moiety under mild conditions (NaBH_4 , CeCl_3) to activate the *i*-steroid toward opening. A screening of Brønsted and Lewis acids then failed to identify conditions to effect the rearrangement, with either no reaction or complete decomposition as a result.

At this point, it was unclear whether the epoxide as a leaving group or its presumably unnatural stereoconfiguration in a concerted mechanism led to this result. We thus narrowed

down the problem by next employing only a hydroxyl moiety at C9. Thus, intermediate **18** was directly reduced at C6 to activate the *i*-steroid toward opening (Scheme 3). When employing $\text{BF}_3 \cdot \text{OEt}_2$ in glacial acetic acid, we could observe a fast (75 min) and almost quantitative transformation (92% yield over 2 steps).

Chromatographic methods could not separate what seemed to be a single product, judged by thin-layer chromatography

Scheme 3. Anthrasteroid Rearrangement and Synthesis of Asperflokal A



(TLC). NMR spectroscopic analysis, though, clearly indicated the presence of two very similar compounds in an approximately 2:1 ratio. Since 2D NMR experiments gave first evidence that these might be the desired regioisomeric products **20** and **21**, we decided to selectively remove the acetyl groups in both molecules (LiOH) to allow separation at this stage. The resulting mixture of **22** and **23** was obtained in the same ratio and could, indeed, be separated by preparative TLC (eluent toluene/Et₂O, 3:1). Extensive NMR analysis of the purified products clearly proved the so obtained **22** to be the 3 α -regioisomeric anthrasteroid, while **23** was identified as the 2 β -isomer. Separate acetylation of the two gave pure **20** from **22**, as well as **21** from **23**, indicating that the major product in the rearrangement was the 3 α -isomer. These results clearly prove an α -oriented oxygen-containing leaving group at C9 to be competent in initiating the anthrasteroid rearrangement upon Lewis acid activation. Furthermore, both 2 β - and 3 α -regioisomeric products were obtained, with only moderate preference for the 3 α -product, a result pointing at a mechanistic bifurcation. Based on these findings, the formation of asperflokets A (**1**) and B (**2**) can now be rationalized effortlessly and without invoking selective dehydration/rehydration, as assumed in the isolation report (see SI). The 1:1 isolation ratio of **1** and **2** from the natural source additionally supports this conclusion.⁸ The failure in isolating and identifying any 2 β -product in earlier reports may, in this context, be attributed to the reaction conditions employed for the anthrasteroid rearrangement, which included treatment with a strong Brønsted or Lewis acid (typically in combination with several hours of heating), while the 9 α -alcohol **18** could be transformed at 0 °C in only 75 min.

Since we deemed the detour consisting of deacetylation/acetylation impractical for accessing the asperflokets, we decided to use the mixture obtained from the rearrangement step, without attempting separation of the regioisomers. To close the lactone ring and install the 11-hydroxy group, we explored methods to generate an 11 β ,12-epoxide or a related functionality. Furthermore, desaturation, oxidative lactonization, as well as benzylic oxidations were explored but remained unsuccessful (see SI).

Eventually, the use of PCC was found to effect C11 oxidation,¹⁸ and the 11-oxo product could be obtained in acceptable amounts after two additional reaction cycles with re-isolated starting material. Interestingly, when analyzing the byproducts obtained from this reaction, no trace of the 2 β -acetoxy (or related 11-oxo) products could be found. Indeed, the 2 β -isomer **21** apparently is not oxidized under these conditions. Another example for its lower reactivity is the treatment of the mixture of **20** and **21** with 2,3-dichloro-5,6-dicyano-1,4-benzoquinone (DDQ), which leads to the isolation of a product with an aromatized, unfunctionalized A ring (see SI) as well as the unchanged 2 β -isomer.

No traces of remaining 3 α -material (**20** or **22**) could be found, indicating the higher reactivity of the 3 α -compound under several conditions. Continuing with the oxidation product from the PCC reaction, its reduction (NaBH₄) and elimination under acidic conditions (H₂SO₄) led to the introduction of the desired Δ¹¹ bond. Epoxidation attempts using a variety of reagents again furnished only the 11 α ,12-epoxide **24** in 23% yield over 3 steps. No β-epoxide could be obtained in any of these reactions, the only diastereomer we initially deemed competent in forging the lactone ring and the 11-hydroxy group with correct stereoconfiguration directly. To

utilize the so obtained diastereomer **24**, we subjected it to basic conditions (LiOH) to effect deprotection. Instead, and potentially through a benzylic S_N2 mechanism and the intermediacy of an 11 β ,12 α -diol, followed by transesterification, we observed the direct formation of asperfloketal A (**1**) in almost quantitative yield, thereby completing the first synthesis of asperfloketal A (**1**) in 15 steps and 2% overall yield from the known *i*-steroid **13**. All analytical data were in agreement with those reported. Minor misassignments in the original NMR report could be corrected by extensive 2D NMR experiments (see SI). Interestingly, when hydrochloric instead of sulfuric acid was employed for workup, 11-chloroasperfloketal A (**25**) could be obtained as a byproduct, hinting at epoxide opening and transesterification happening only upon acidic workup and not during basic deacetylation.

In summary, we here describe the biomimetic emulation of the anthrasteroid rearrangement which allows, for the first time, the generation and isolation of pure 2 β - and 3 α -regioisomeric products. This study confirms two consecutive Wagner–Meerwein shifts to give rise to what are indeed 1(10→5),1(5→6)- and 1(10→5),4(5→6)diabeo-steroids, through a mechanistic bifurcation event of a spiro intermediate. We applied our method to the synthesis of asperfloketal A (**1**), thereby delivering chemical evidence for the feasibility of our biogenesis hypothesis, also for asperfloketal B (**2**). For this purpose, we developed a route from ergosterol making use of an oxidative activation/rearrangement strategy. Key transformations are a base-driven rearrangement of an α -chloro- γ -hydroxy- δ -oxo enone, furnishing a 14,15-secosteroid platform, C9-functionalization by [4+2] addition of ¹O₂ to an extended silylenol ether, and installation of the eponymous ketal by HFIP-facilitated transketolization. We expect these results to be applicable to the synthesis of other anthrasteroids, and related research is currently being conducted in our laboratory.

ASSOCIATED CONTENT

SI Supporting Information

The Supporting Information is available free of charge at <https://pubs.acs.org/doi/10.1021/jacs.2c10735>.

General methods; detailed experimental studies; experimental procedures and spectral data; comparison of synthetic and natural asperfloketal A; ¹H and ¹³C NMR spectra; and additional references (PDF)

AUTHOR INFORMATION

Corresponding Author

Philipp Heretsch – Institute of Organic Chemistry, Leibniz Universität Hannover, 30167 Hannover, Germany;
orcid.org/0000-0002-9967-3541;
 Email: philipp.heretsch@oci.uni-hannover.de

Author

Mykhaylo Alekseychuk – Institute of Organic Chemistry, Leibniz Universität Hannover, 30167 Hannover, Germany

Complete contact information is available at:
<https://pubs.acs.org/10.1021/jacs.2c10735>

Notes

The authors declare no competing financial interest.

ACKNOWLEDGMENTS

Financial support for this work was provided by the European Research Council (ERC Consolidator Grant “RadCrossSyn”), Deutsche Forschungsgemeinschaft (Heisenberg-Program HE 7133/8-1), and Boehringer Ingelheim Stiftung (plus3 perspectives program).

REFERENCES

- (1) (a) Nes, W. R.; Mosettig, E. The Rearrangement of Dehydroergosteryl acetate to a *s*-Octahydroanthracene Derivative. *J. Am. Chem. Soc.* **1953**, *75*, 2787. (b) Nes, W. R.; Mosettig, E. The Anthrasteroid Rearrangement. I. The Formation and Proof of Structure of Anthraergostapentaene. *J. Am. Chem. Soc.* **1954**, *76*, 3182–3186.
- (2) (a) Tsuda, K.; Hayatsu, R.; Steele, J. A.; Tanaka, O.; Mosettig, E. The Anthrasteroid Rearrangement. VIII. The Rearrangement of Dehydroergosterol and $\Delta^{5,7,9(11)}$ -cholestatriene- 3β -ol to $\Delta^{5,7,9,22}$ -anthraergostatetraen-x-ols and $\Delta^{5,7,9}$ -anthracholestatrien-x-ols. *J. Am. Chem. Soc.* **1963**, *85*, 1126–1131. (b) Tanaka, O.; Mosettig, E. The Anthrasteroid Rearrangement. IX. The Acid-catalyzed Rearrangement of $\Delta^{5,7,9(11),22}$ -Ergostatetraene and $\Delta^{5,8(14),9(11)}$ -Ergostatrien- 3β -ol. *J. Am. Chem. Soc.* **1963**, *85*, 1131–1133.
- (3) Nes, W. R.; Ford, D. L. The Anthrasteroid Rearrangement. XI. The Conversion of $\Delta^{5,7,9}$ -Anthrapregnatrien-20-one to 4',10-Dimethyl-1,2-benzanthracene by a Model of a Biochemical Route. *J. Am. Chem. Soc.* **1963**, *85*, 2137–2141.
- (4) (a) Hussler, G.; Albrecht, P. C₂₇–C₂₉ Monoaromatic anthrasteroid hydrocarbons in Cretaceous black shales. *Nature* **1983**, *304*, 262–263. (b) Curiale, J. A. Steroidal hydrocarbons of the Kishenehn Formation, northwest Montana. *Org. Geochem.* **1987**, *11*, 233–244.
- (5) Koshino, H.; Yoshihara, T.; Sakamura, S.; Shimanuki, T.; Sato, T.; Tajimi, A. A ring B aromatic sterol from stromata of *Epichloe typhina*. *Phytochemistry* **1989**, *28*, 771–772.
- (6) (a) Kosemura, S.; Uotsu, S.; Yamamura, S. Citreoanthrasteroid, a new metabolite of a hybrid strain KO 0011 derived from *Penicillium citreo-viride* B. IFO 6200 and 4692. *Tetrahedron Lett.* **1995**, *36*, 7481–7482. (b) Nakada, T.; Yamamura, S. Three New Metabolites of Hybrid Strain KO 0231, Derived from *Penicillium citreo-viride* IFO 6200 and 4692. *Tetrahedron* **2000**, *56*, 2595–2602. (c) Luo, X.; Li, F.; Shinde, P. B.; Hong, J.; Lee, C.-O.; Im, K. S.; Jung, J. H. 26,27-Cyclosterols and Other Polyoxygenated Sterols from a Marine Sponge *Topsentia* sp. *J. Nat. Prod.* **2006**, *69*, 1760–1768. (d) Wakana, D.; Itabashi, T.; Kawai, K.-i.; Yaguchi, T.; Fukushima, K.; Goda, Y.; Hosoe, T. Cytotoxic anthrasteroid glycosides, malsterosides A–C, from *Malbranchea filamentosa*. *J. Antibiot.* **2014**, *67*, 585–588. (e) Liu, L.; Duan, F.-F.; Gao, Y.; Peng, X.-G.; Chang, J.-L.; Chen, J.; Ruan, H.-L. Aspersteroids A–C, Three Rearranged Ergostane-type Steroids from *Aspergillus ustus* NRRL 275. *Org. Lett.* **2021**, *23*, 9620–9624.
- (7) (a) Burgstahler, A. W. A Contribution to the Anthrasteroid Problem. The Location of the Aromatic C-Methyl Group and the Position of the Conjugated Double Bond. *J. Am. Chem. Soc.* **1957**, *79*, 6047–6050. (b) Nes, W. R.; Steele, J. A.; Mosettig, E. The Anthrasteroid Rearrangement. V. The Preparation of an Analog of Progesterone. *J. Am. Chem. Soc.* **1958**, *80*, 5230–5232.
- (8) Jiao, F.-R.; Gu, B.-B.; Zhu, H.-R.; Zhang, Y.; Liu, K.-C.; Zhang, W.; Han, H.; Xu, S.-H.; Lin, H.-W. Asperfloketals A and B, the First Two Ergostanes with Rearranged A and D Rings: From the Sponge-Associated *Aspergillus flocculosus* 16D-1. *J. Org. Chem.* **2021**, *86*, 10954–10961.
- (9) Cao, V. A.; Kwon, J.-H.; Kang, J. S.; Lee, H.-S.; Heo, C.-S.; Shin, H. J. Aspersterols A–D, Ergostane-Type Sterols with an Unusual Unsaturated Side Chain from the Deep-Sea-Derived Fungus *Aspergillus unguis*. *J. Nat. Prod.* **2022**, *85*, 2177–2183.
- (10) Steele, J. A.; Cohen, L. A.; Mosettig, E. The Anthrasteroid Rearrangement. X. Elucidation of the Stereochemistry of the C/D Ring Fusion from Chemical Transformation and N.m.r. Data. *J. Am. Chem. Soc.* **1963**, *85*, 1134–1138.
- (11) (a) van der Gen, A.; Lakeman, J.; Gras, M. A. M. P.; Huisman, H. O. Addition to Steroid Polyenes—I Reaction of 7-dehydrocholesteryl acetate with diethyl diazodicarboxylate. *Tetrahedron* **1964**, *20*, 2521–2530. (b) de Nijs, H.; Speckamp, W. N. Skeletal rearrangements of 4,4-dimethyl- $\Delta^{5,8(9)}$ steroidal azoester adducts. *Tetrahedron Lett.* **1973**, *14*, 813–816.
- (12) (a) Bosworth, N.; Midgley, J. M.; Moore, C. J.; Whalley, W. B.; Ferguson, G.; Marsh, W. C. A novel route to anthrasteroids: X-ray crystal structure of 1(10→6)abeo-cholesta-5,7,9-trien-3-yl *p*-bromobenzoate. *J. Chem. Soc., Chem. Commun.* **1974**, 719. (b) Bosworth, N.; Emke, A.; Midgley, J. M.; Moore, C. J.; Whalley, W. B.; Ferguson, G.; Marsh, W. C. Unsaturated Steroids. Part 2. A Novel Route to Anthrasteroids: X-Ray Crystal Structure of 1(10→6)abeo-Cholesta-5,7,9-trien-3-yl *p*-Bromobenzoate. *J. Chem. Soc., Perkin Trans. 1* **1977**, 805–809. (c) Emke, A.; Midgley, J. M.; Whalley, W. B. Unsaturated Steroids. Part 10. The Mechanism of the Anthrasteroid Rearrangement: The Conformation of Anthrasteroids. *J. Chem. Soc., Perkin Trans. 1* **1980**, 1779–1781.
- (13) Woodward, R. B.; Singh, T. Synthesis and Rearrangement of Cyclohexadienones. *J. Am. Chem. Soc.* **1950**, *72*, 494–500.
- (14) Heinze, R. C.; Lentz, D.; Heretsch, P. Synthesis of Strophasterol A Guided by a Proposed Biosynthesis and Innate Reactivity. *Angew. Chem., Int. Ed.* **2016**, *55*, 11656–11659.
- (15) McMorris, T. C.; Patil, P. A. Improved synthesis of 24-epibrassinolide from ergosterol. *J. Org. Chem.* **1993**, *58*, 2338–2339.
- (16) (a) Jacobsen, E. N.; Markó, I.; Mungall, W. S.; Schroder, G.; Sharpless, K. B. Asymmetric Dihydroxylation via Ligand-Accelerated Catalysis. *J. Am. Chem. Soc.* **1988**, *110*, 1968–1970. (b) Litvinovskaya, R. P.; Aver'kova, M. A.; Baranovskii, A. V.; Khripach, V. A. Synthesis of 6-deoxo-24-epiteasterone and its analogs. *Russ. J. Org. Chem.* **2006**, *42*, 1325–1332.
- (17) Burgess, E. M.; Penton, H. R., Jr.; Taylor, E. A. Synthetic applications of *N*-carboalkoxysulfamate esters. *J. Am. Chem. Soc.* **1970**, *92*, 5224–5226.
- (18) (a) Nakada, T.; Yamamura, S. Three New Metabolites of Hybrid Strain KO 0231, Derived from *Penicillium citreo-viride* IFO 6200 and 4692. *Tetrahedron* **2000**, *56*, 2595–2602. (b) Sennari, G.; Gardner, K. E.; Wiesler, S.; Haider, M.; Eggert, A.; Sarpong, R. Unified Total Syntheses of Benzenoid Cephalotane-Type Norditerpenoids: Cephanolides and Ceforalides. *J. Am. Chem. Soc.* **2022**, *144*, 19173–19185.

Chemical Emulation of the Biosynthetic Route to Anthrasteroids – Synthesis of Asperfloketal A

Mykhaylo Alekseychuk and Philipp Heretsch*

Institute of Organic Chemistry, Leibniz Universität Hannover,
Schneiderberg 1B, 30167 Hannover, Germany

*Correspondence to: philipp.heretsch@oci.uni-hannover.de

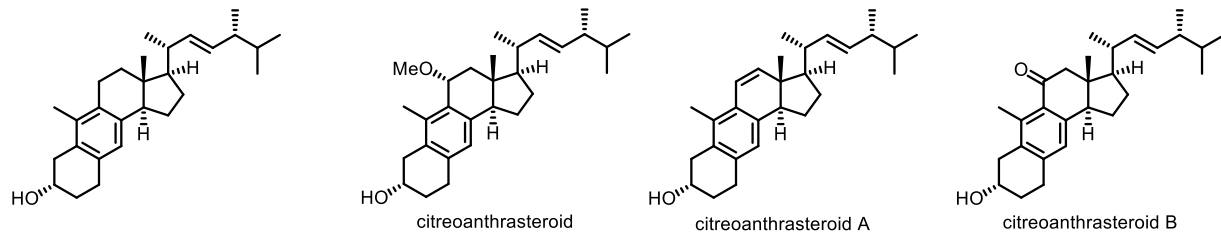
Supporting Information

Table of Contents

1 Failed reactions and detours	4
2 General Methods	14
3 Experimental Section	15
4 NMR Comparison.....	28
5 Correction of original ^{13}C-NMR assignments from isolation report	29
6 Characterization of mixture 20/21	32
7 NMR Spectra	46

All isolated anthrasteroids from natural origin.

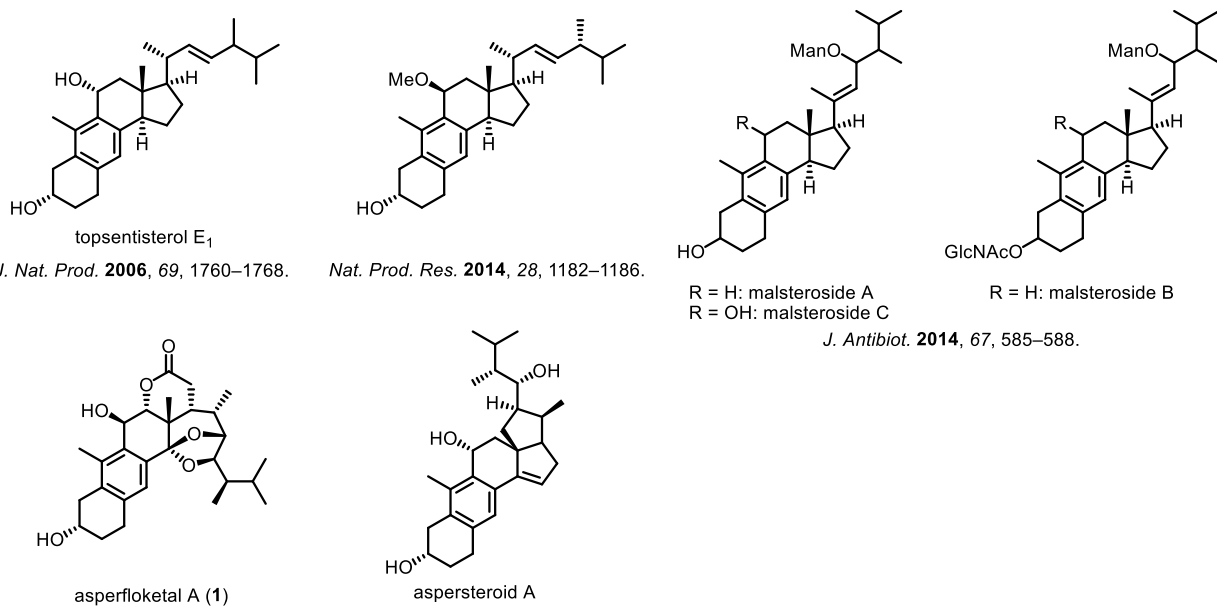
3α -hydroxy-anthrasteroids



Phytochemistry **1989**, *28*, 771–772.

Tetrahedron Lett. **1995**, *36*, 7481–7482.

Tetrahedron **2000**, *56*, 2595–2602.



J. Nat. Prod. **2006**, *69*, 1760–1768.

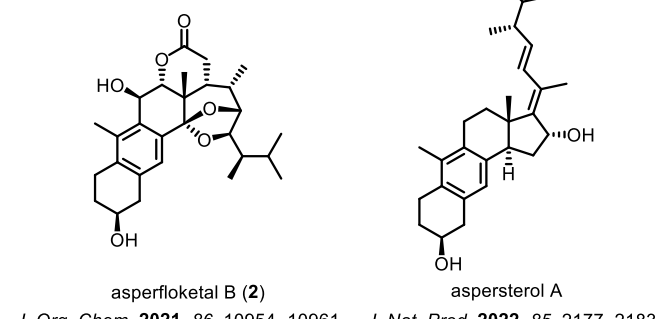
Nat. Prod. Res. **2014**, *28*, 1182–1186.

R = H: malsteroside A
R = OH: malsteroside C

J. Antibiot. **2014**, *67*, 585–588.

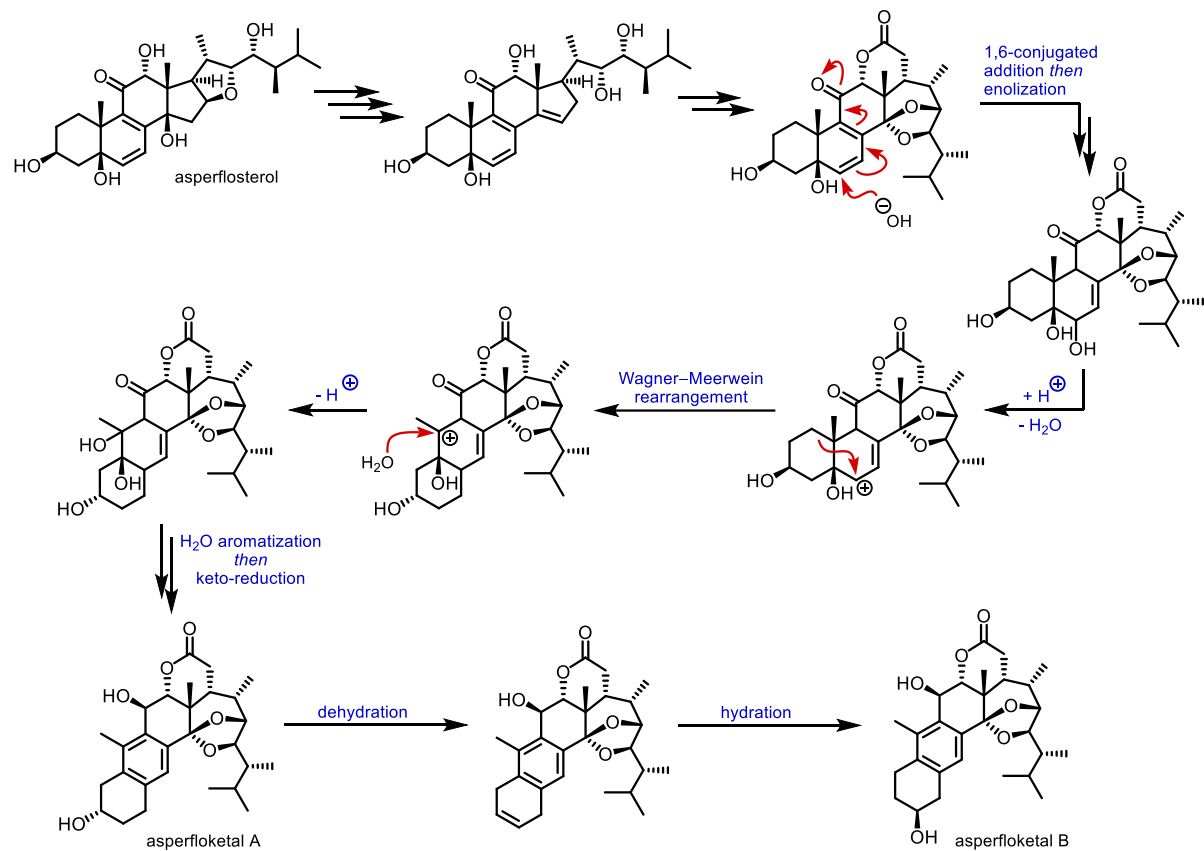
asperflokal A (1)
J. Org. Chem. **2021**, *86*, 10954–10961. *Org. Lett.* **2021**, *23*, 9620–9624.

2β -hydroxy-anthrasteroids

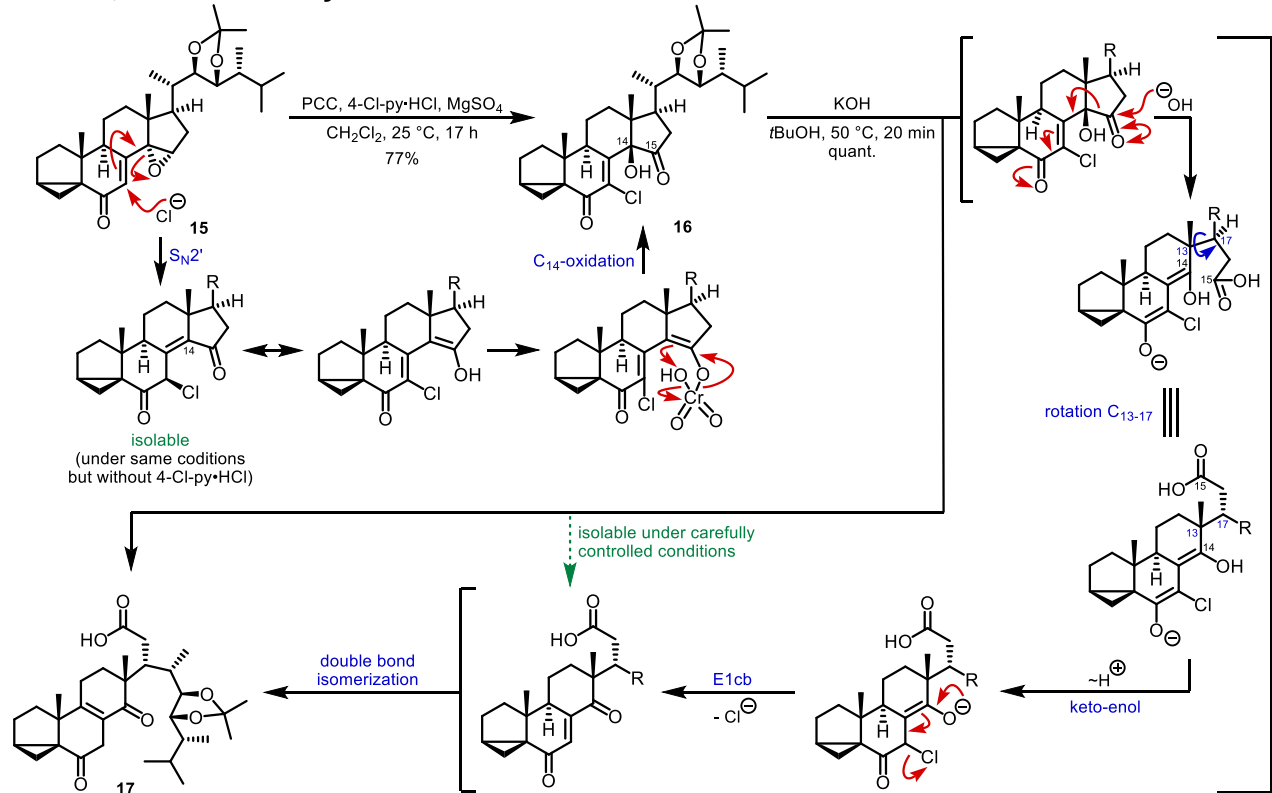


asperflokal B (2)
J. Org. Chem. **2021**, *86*, 10954–10961. *J. Nat. Prod.* **2022**, *85*, 2177–2183.

Original biosynthetic hypothesis by Han, Xu, and Lin.^[1]

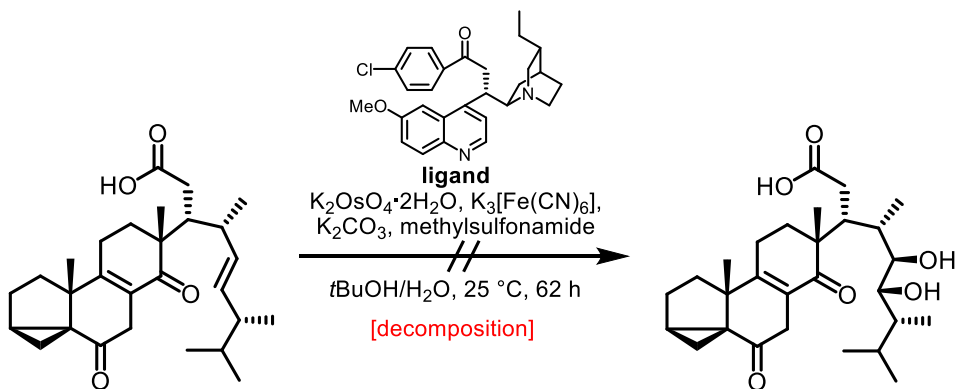


Mechanistic proposal for the formation of α -chloro- γ -hydroxy- δ -oxo enone 16 and 14,15-scission by retro-Dieckmann and keto-enol tautomerizations.

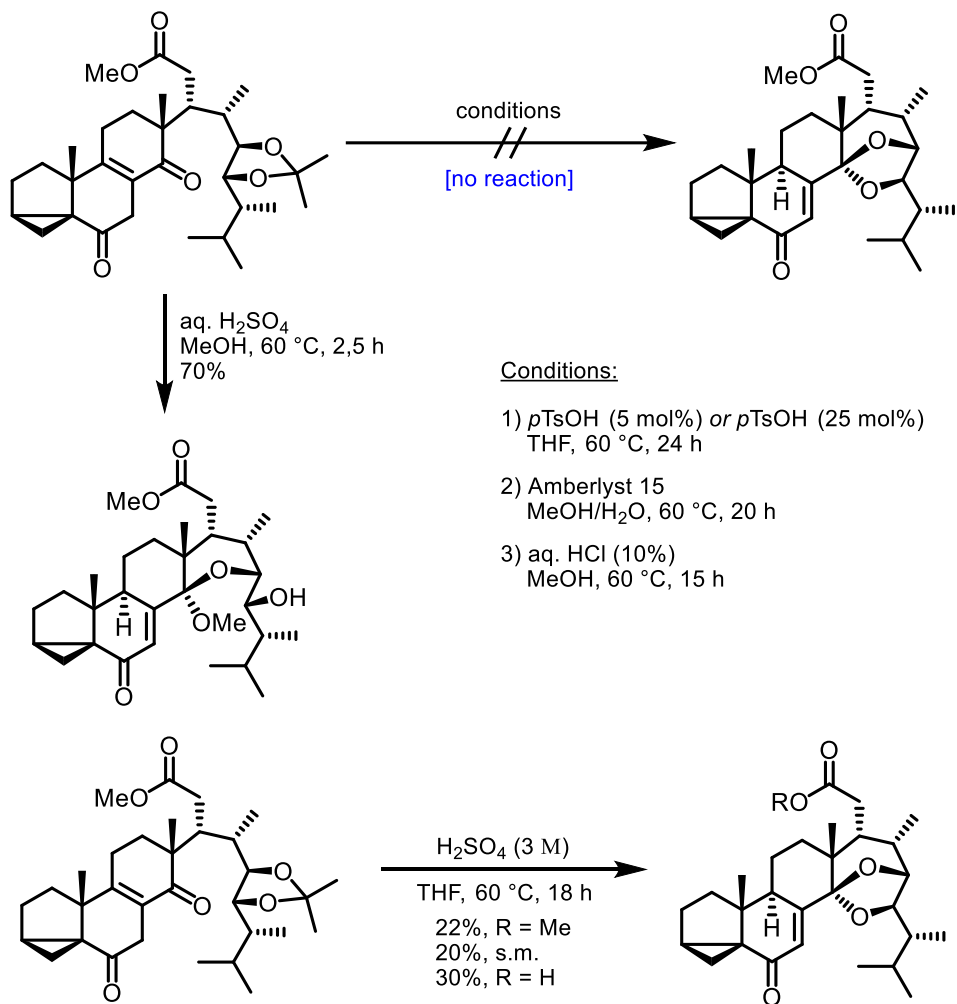


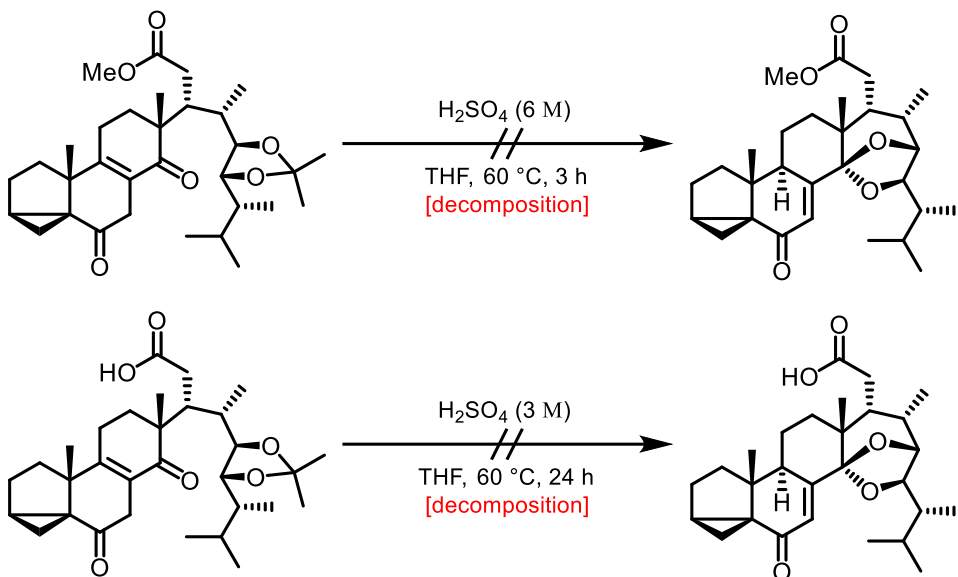
1 Failed reactions and detours

Late-stage dihydroxylation attempt

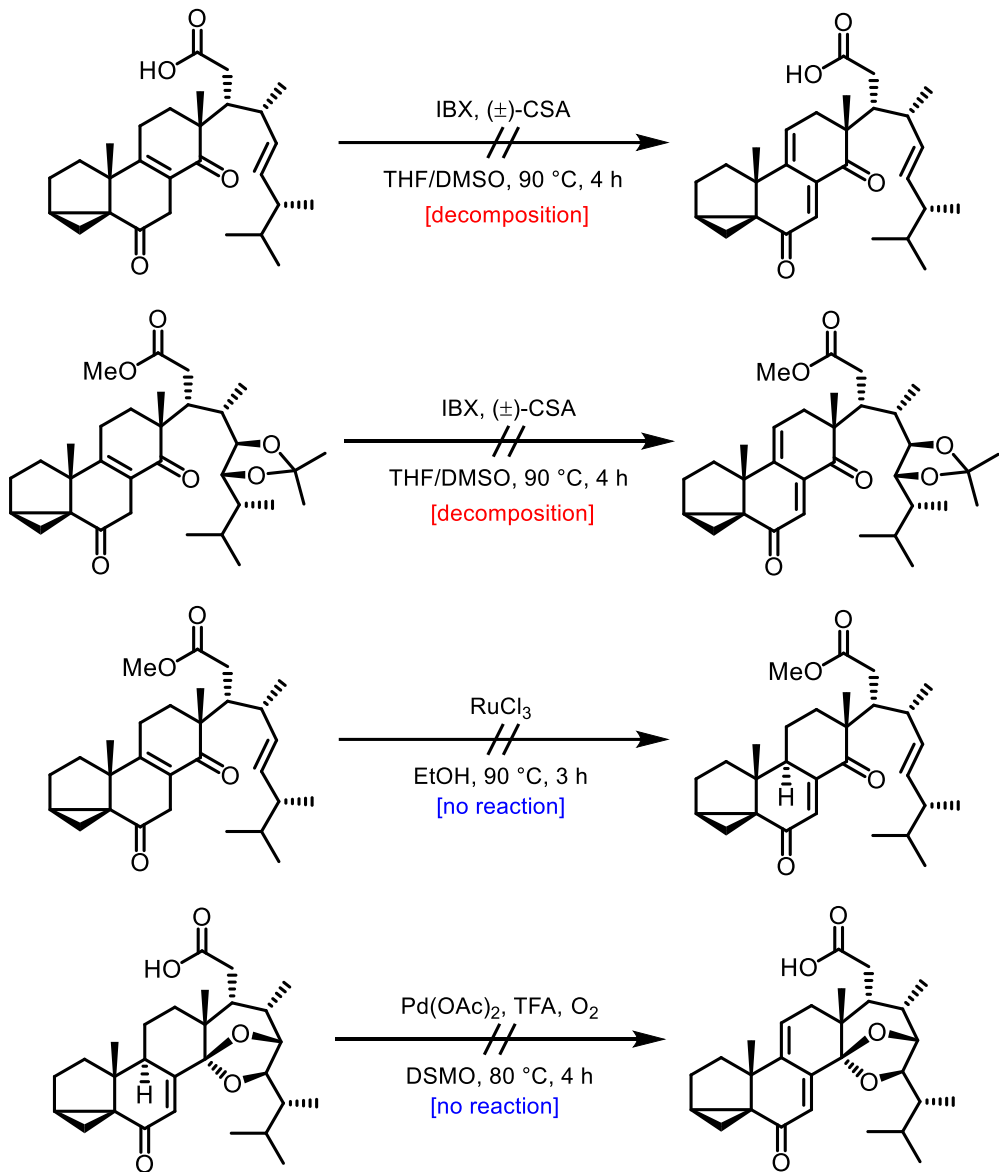


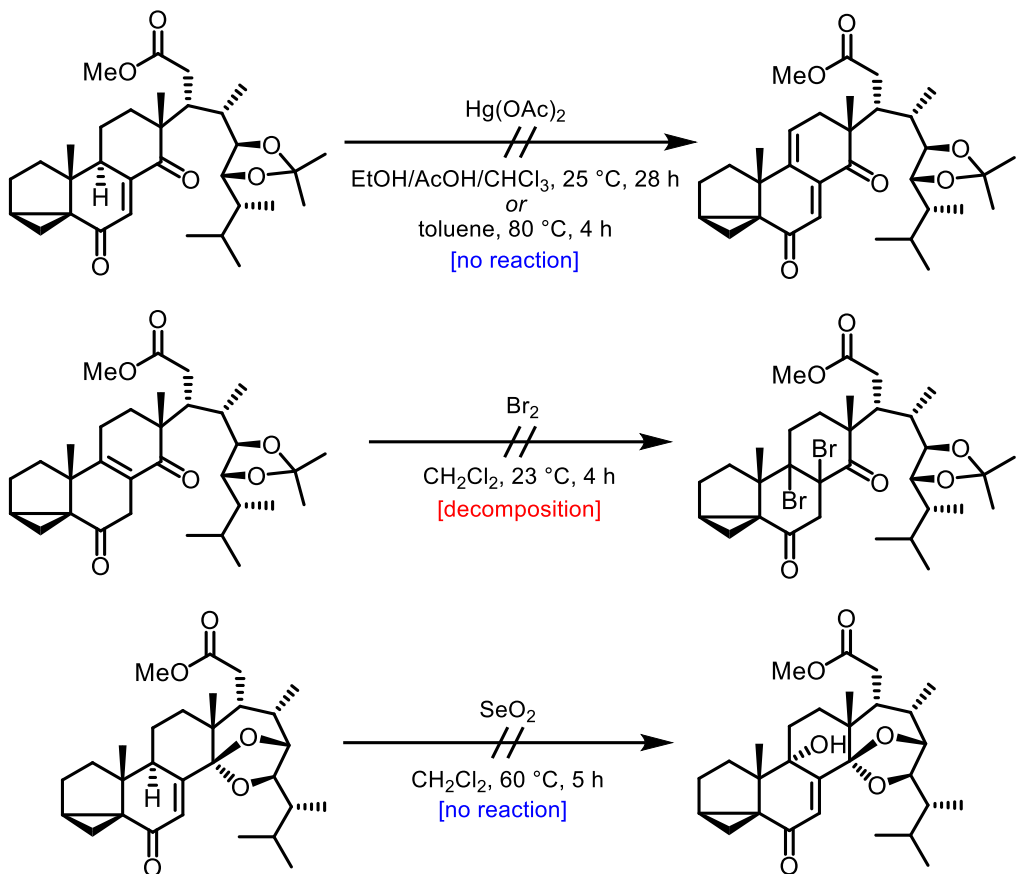
Transketalization studies



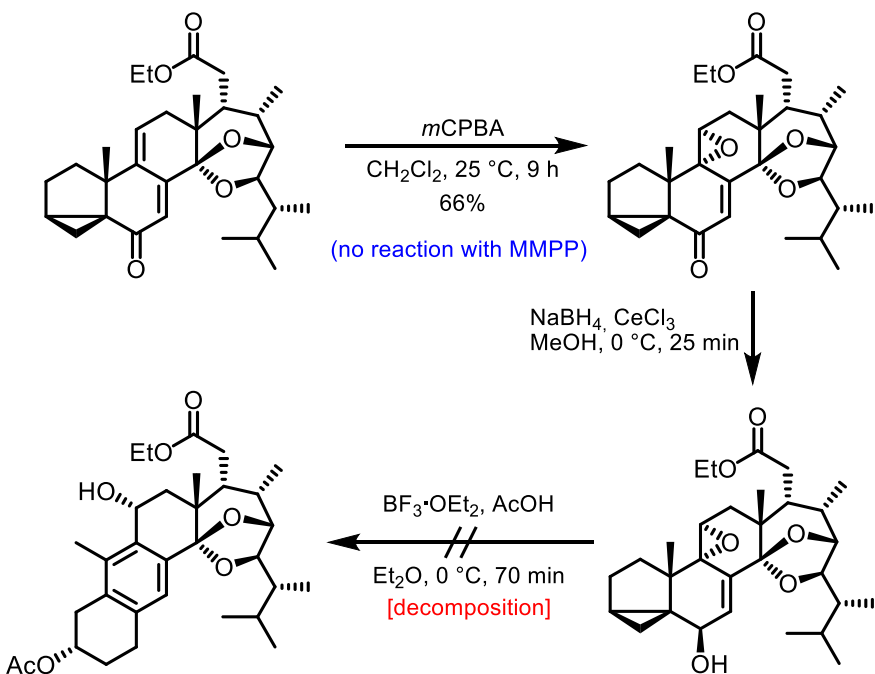


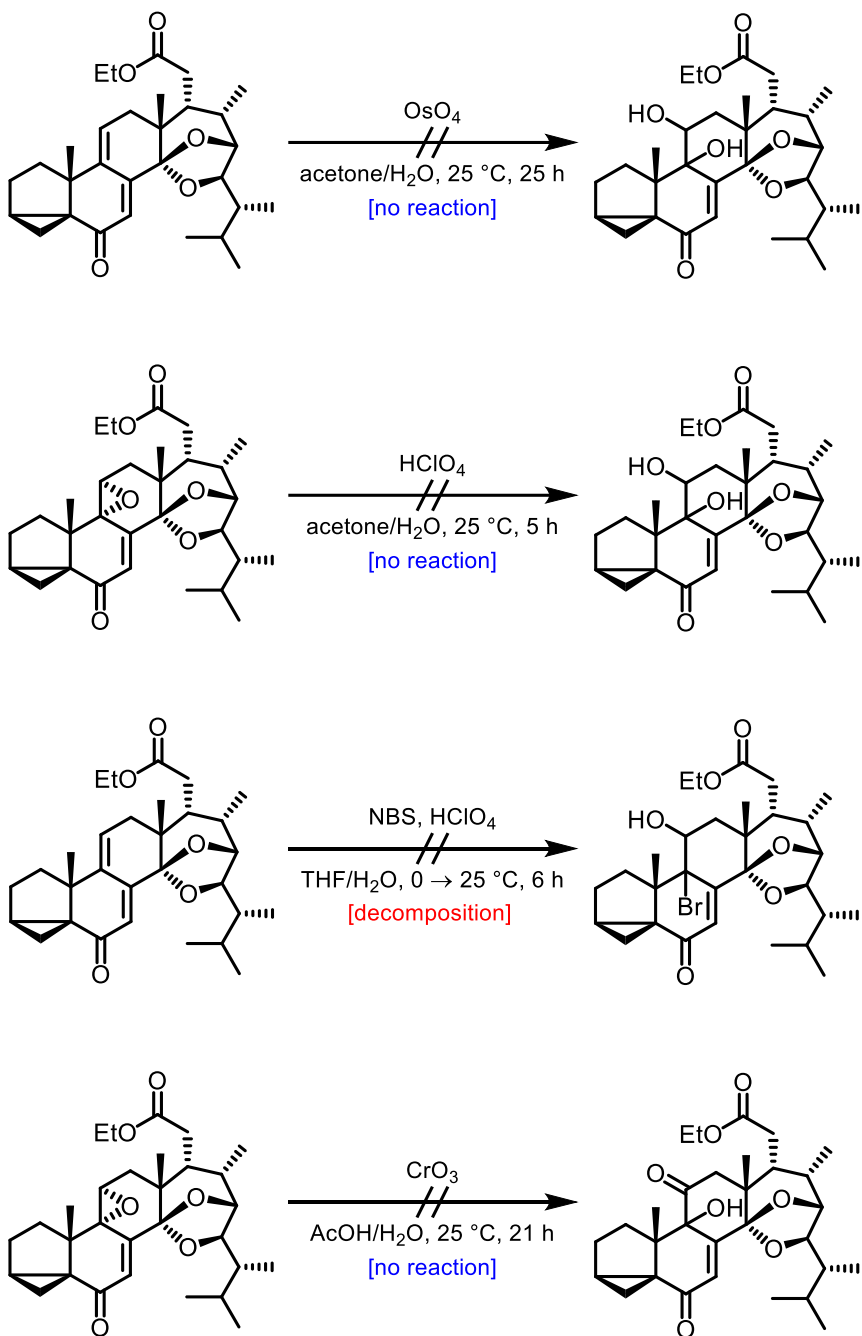
Functionalization of 14,15-seco-framework



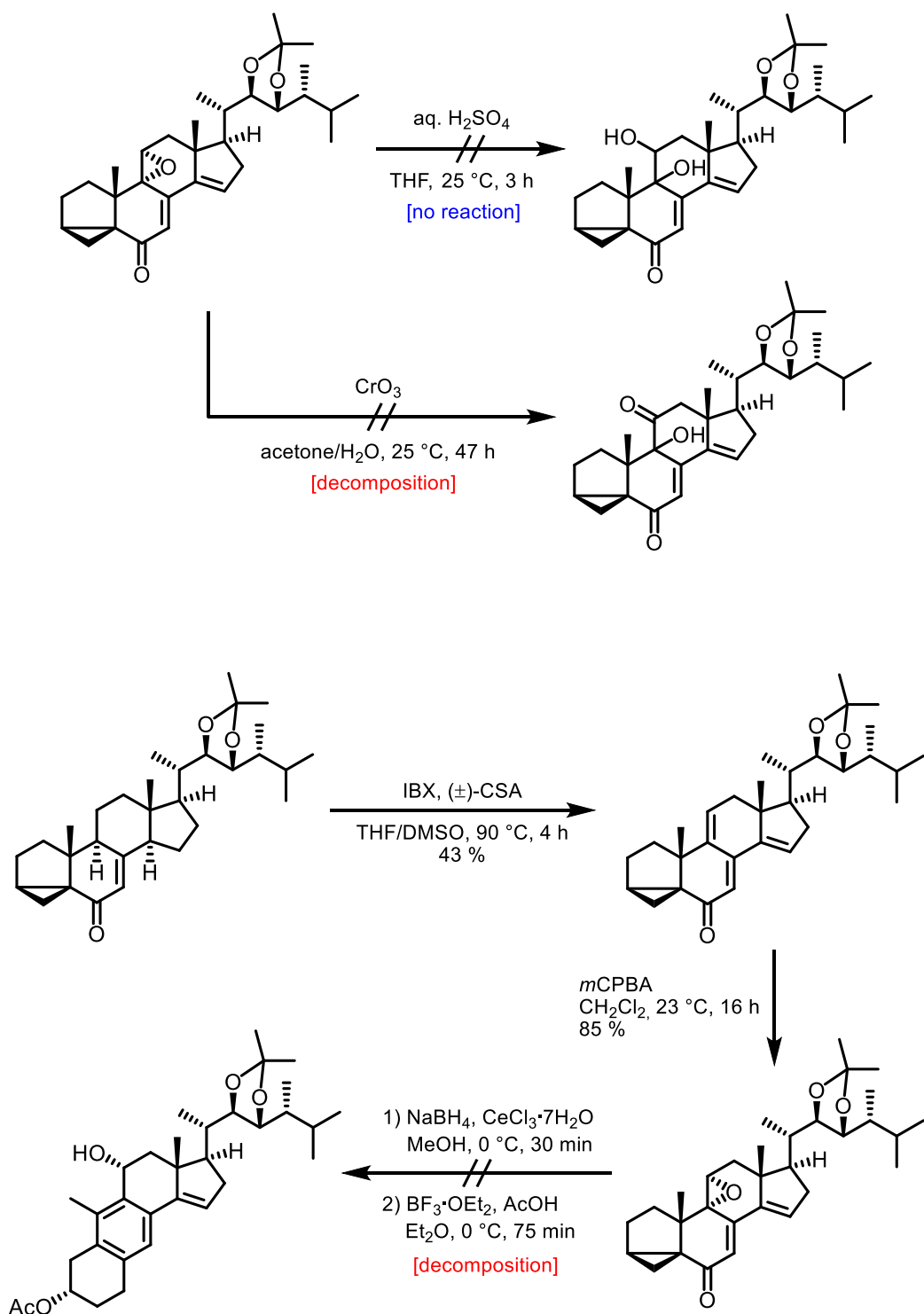


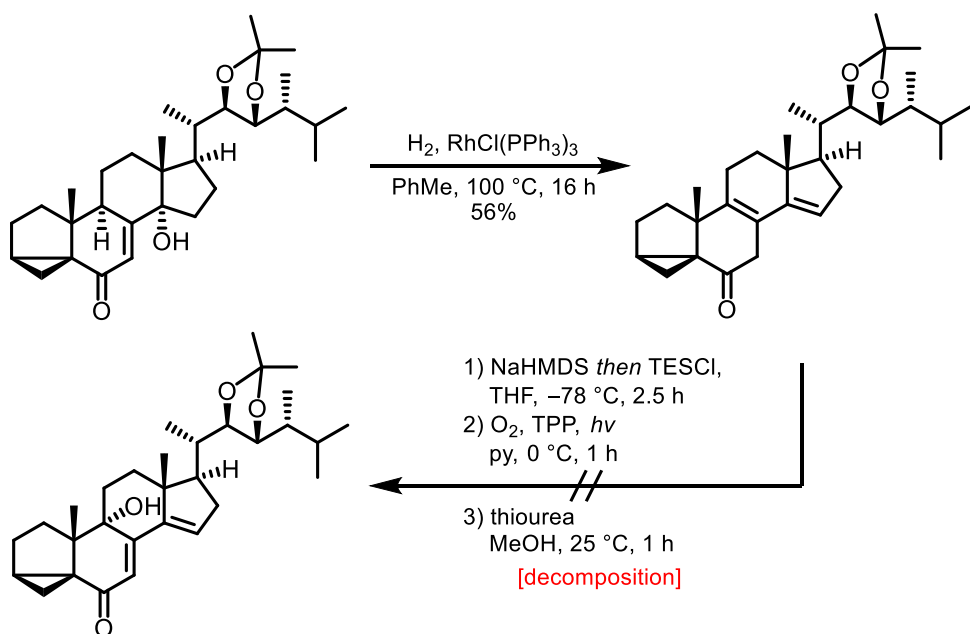
Functionalization of the 9,11-double bond for a Wagner–Meerwein rearrangement



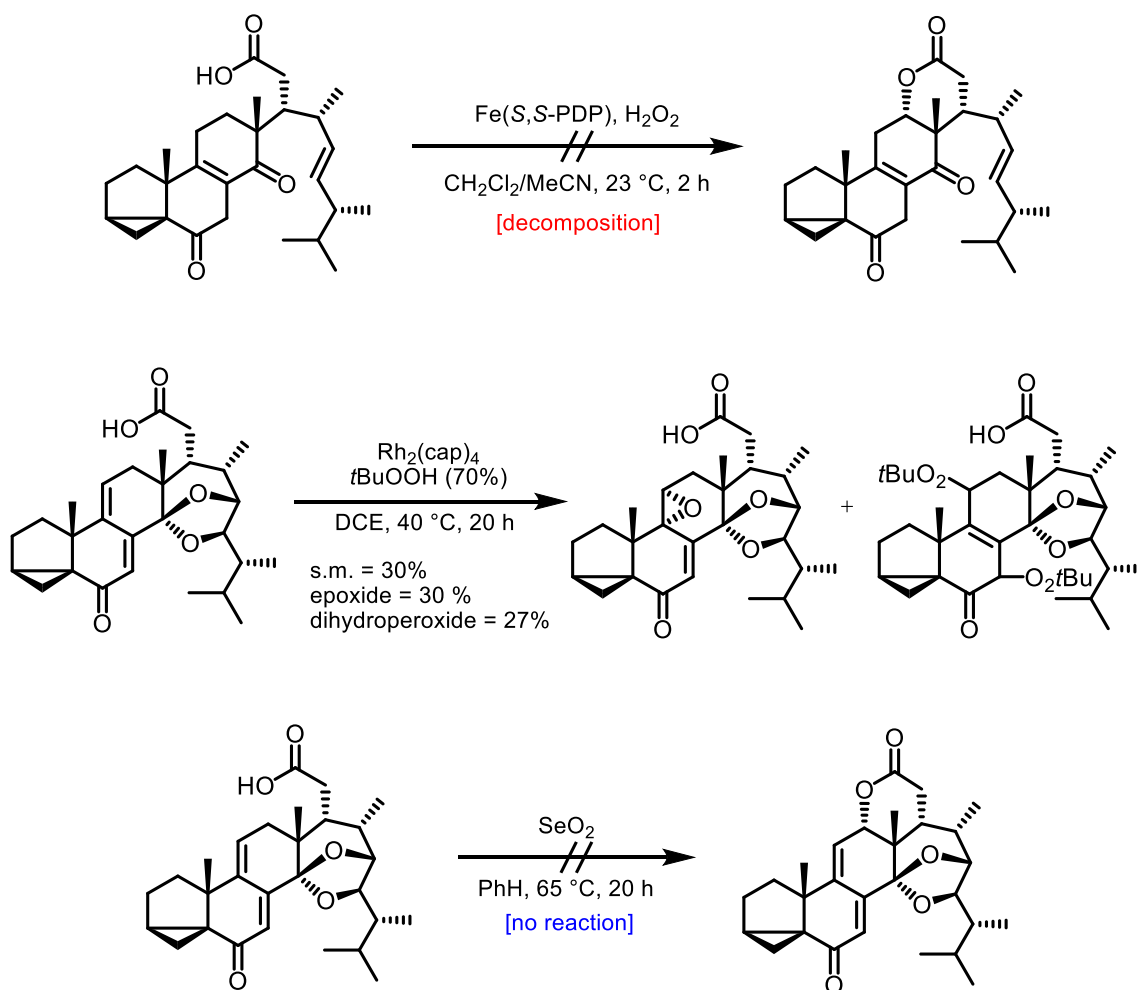


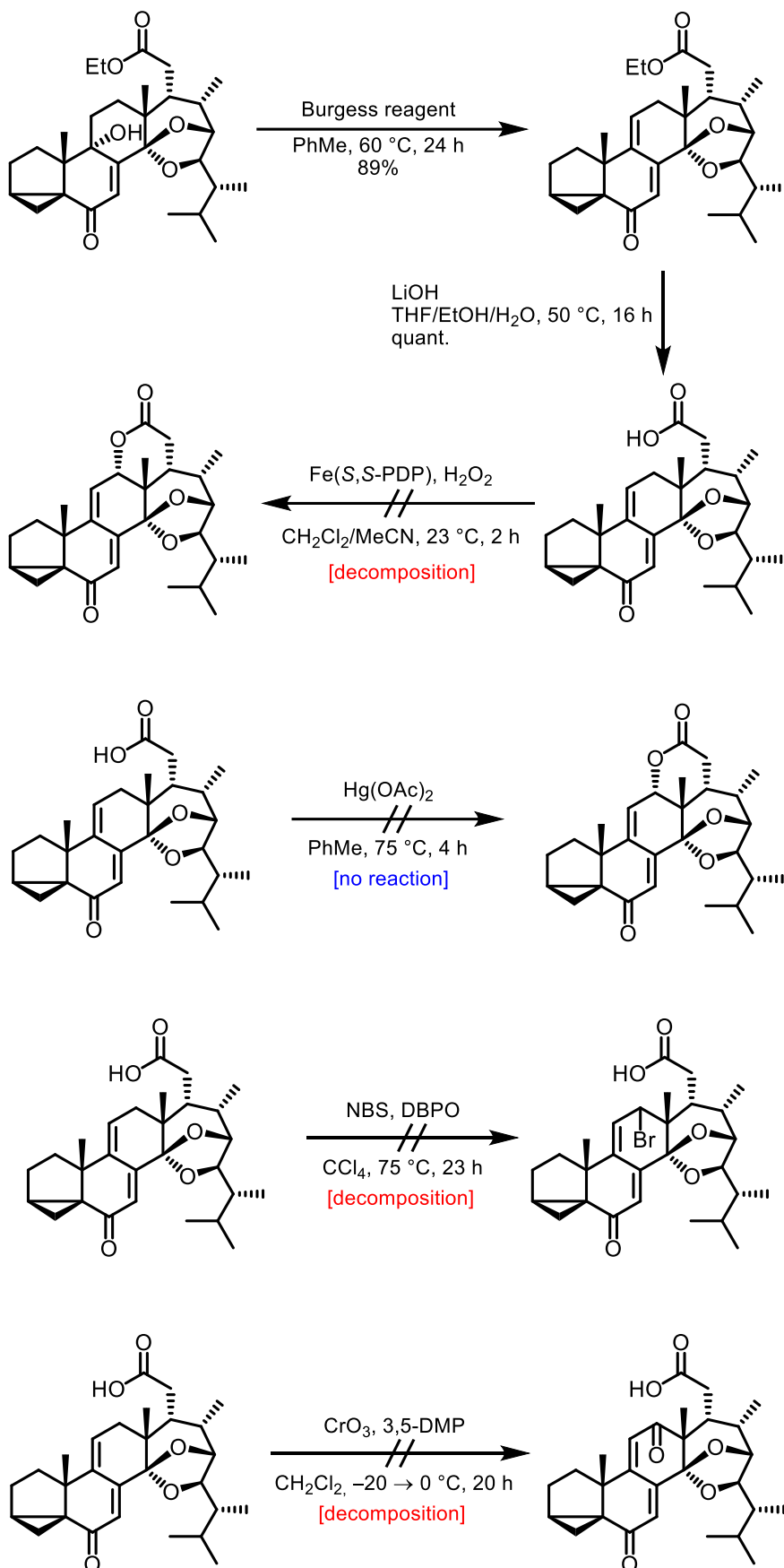
Other early stage attempts to introduce functionality at C9

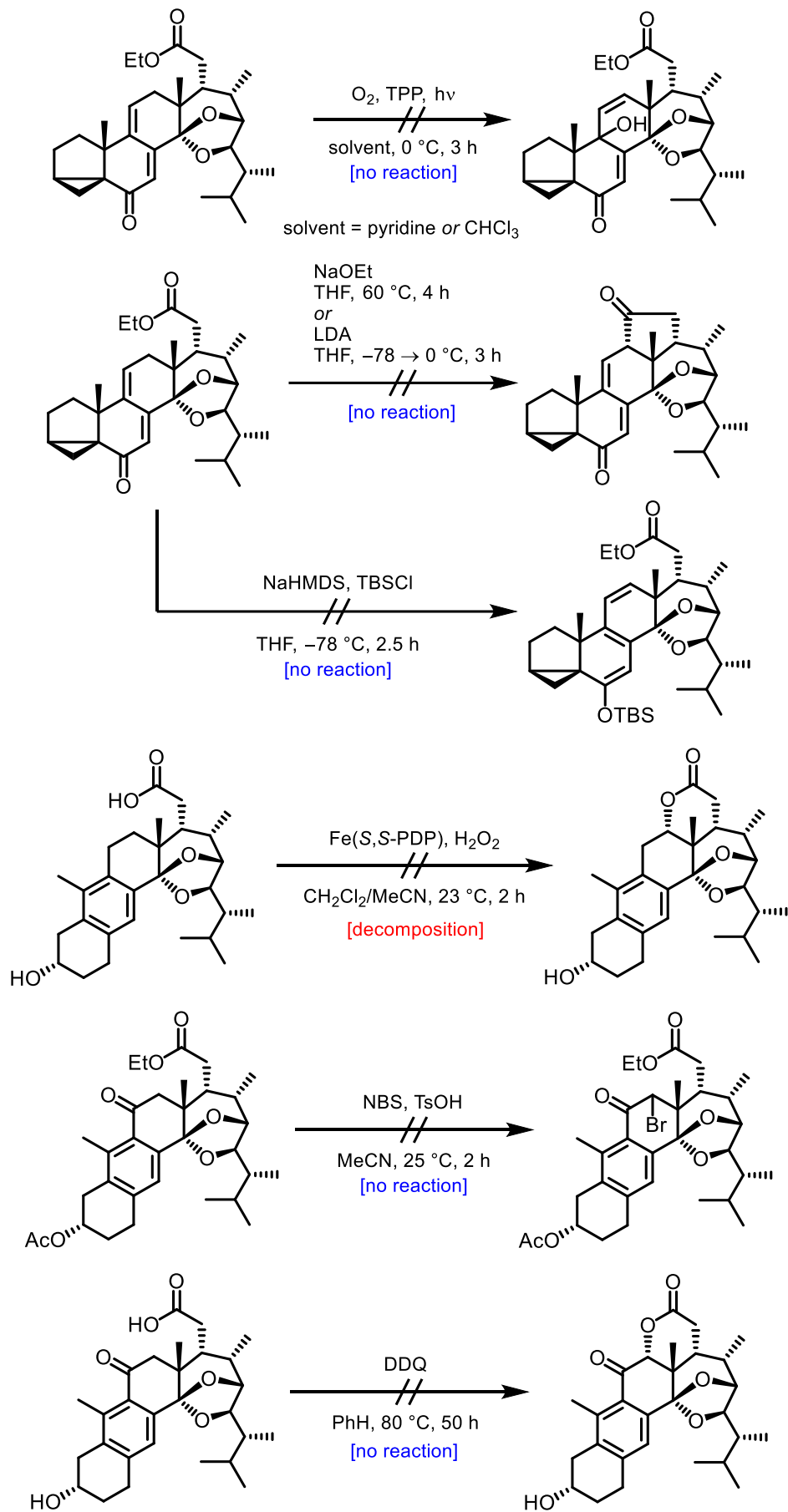


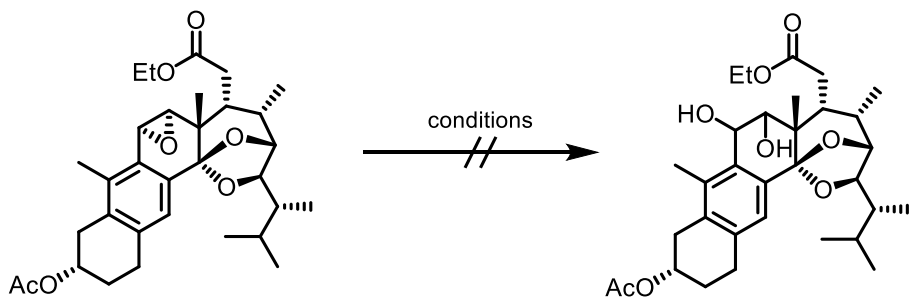
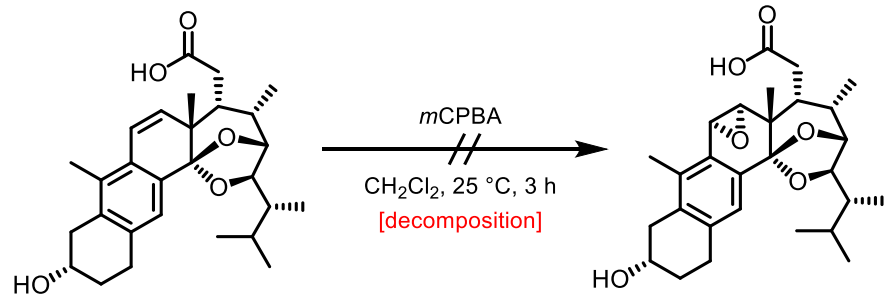
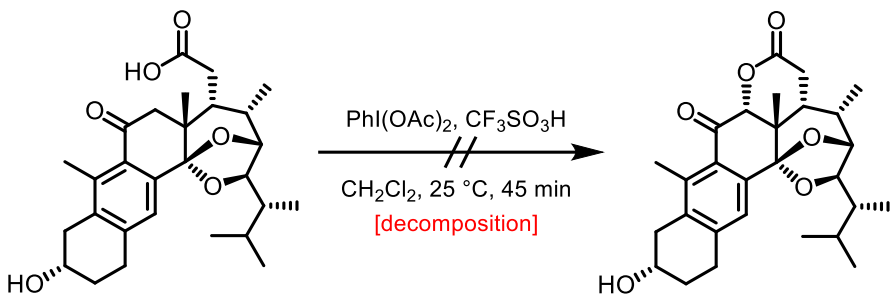


Attempts at oxidative lactonization or C12 functionalization







Conditions:

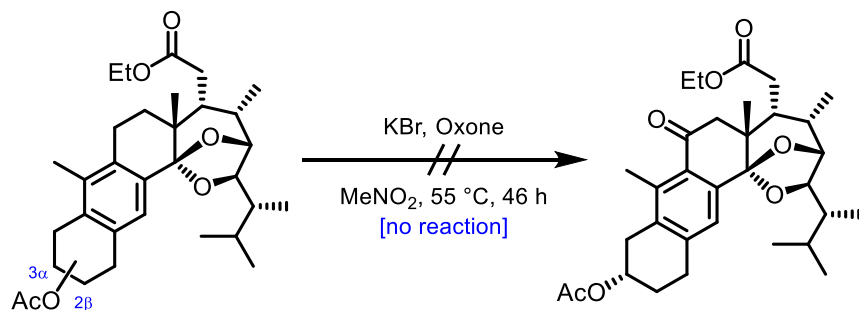
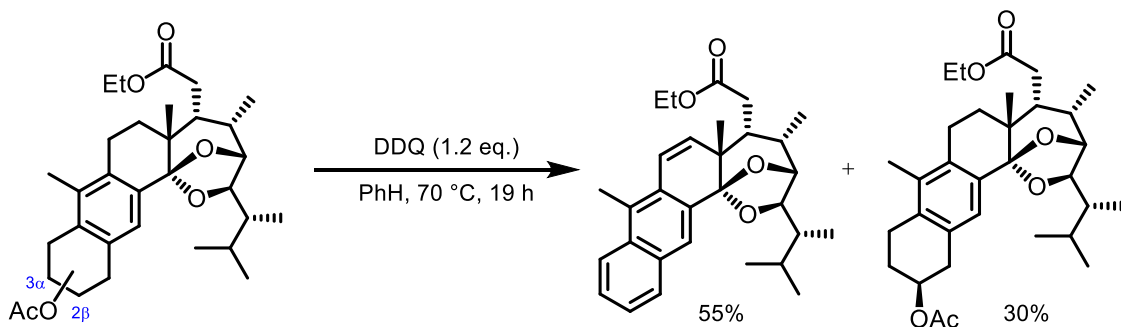
1) ZnCl₂
CH₂Cl₂, 25 °C, 7 h

3) BF₃·OEt₂
CH₂Cl₂, 0 → 25 °C, 10.5 h

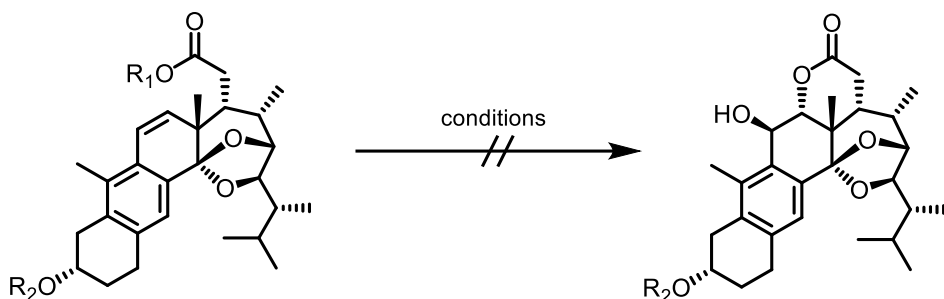
2) TFA
CH₂Cl₂, 25 °C, 12 h

[decomposition]

[no reaction]



Halolactonization attempts



- | | |
|--|---|
| 1) NIS, AgNO_3
HFIP/ H_2O , 0 °C, 2 h ($\text{R}_1 = \text{H}, \text{R}_2 = \text{H}$) | 5) NIS, AgNO_3
HFIP/ H_2O , 0 °C, 2 h ($\text{R}_1 = \text{Et}, \text{R}_2 = \text{Ac}$) |
| 2) NIS, NaHCO_3
THF/ H_2O , 0 → 23 °C, 2 h ($\text{R}_1 = \text{H}, \text{R}_2 = \text{H}$) | 6) NBS, AcOH
THF/ H_2O , 50 °C, 2.5 h ($\text{R}_1 = \text{Et}, \text{R}_2 = \text{Ac}$) |
| 3) NIS, AgNO_3
THF/ H_2O , 0 → 23 °C, 2 h ($\text{R}_1 = \text{H}, \text{R}_2 = \text{H}$) | 7) NCS, AcOH
HFIP/ H_2O , 0 °C, 1.5 h ($\text{R}_1 = \text{Et}, \text{R}_2 = \text{Ac}$) |
| 4) NBS, AgNO_3
HFIP/ H_2O , 0 °C, 2 h ($\text{R}_1 = \text{H}, \text{R}_2 = \text{H}$) | |

2 General Methods

All reactions sensitive to moisture and/or air were carried out under an atmosphere of argon using heat gun-dried glassware, and anhydrous solvents. Anhydrous dichloromethane, toluene, and tetrahydrofuran were taken from a M. Braun GmbH MB SPS-800 solvent purification system and were stored over 4 Å molecular sieves. Anhydrous methanol and benzene were acquired from Sigma Aldrich. Ethyl acetate and *n*-hexane were purified by distillation on a rotary evaporator. Ergosterol was acquired from TCI in >95.0% (GC) purity. All other solvents (HPLC quality) and commercially available reagents were used without further purification unless otherwise stated.

Concentration under reduced pressure was performed by rotary evaporation at 45 °C and appropriate pressure, followed by exposure to high vacuum (10^{-3} mbar) at 25 °C.

Chromatography and TLC: Reactions were monitored by thin-layer chromatography (TLC) carried out on Merck Silica Gel 60 F₂₅₄-plates and visualized by fluorescence quenching under UV-light or an aqueous solution of cerium sulfate and phosphomolybdic acid and heat as developing agent. Column chromatographic purification was performed on Macherey-Nagel Silica Gel 60 M (40–60 µm). Preparative TLC was performed on 20x20 cm Merck Silica Gel 60 F₂₅₄-glass plates.

NMR: NMR spectra were recorded on either a Bruker Ultrashield 400 (400 MHz), a Bruker AVANCE III 500 (500 MHz), or a Bruker Ascend 600 (600 MHz, with CryoProbe) spectrometer. Chemical shifts δ are reported in parts per million (ppm) and are referenced using residual undeuterated solvent (CDCl_3 : $\delta_{\text{H}} = 7.26$ ppm, $\delta_{\text{C}} = 77.16$ ppm; unless otherwise stated) as an internal reference at 298 K. The given multiplicities are phenomenological; thus, the actual appearance of the signals is stated and not the theoretically expected one. The following abbreviations are used to designate multiplicities: s = singlet, d = doublet, t = triplet, q = quartet, p = quintet, br = broad, and combinations thereof. In case no multiplicity could be identified, the chemical shift range of the signal is given (m = multiplet).

Infrared spectroscopy: Infrared (IR) spectra were measured on a SHIMADZU FT-IR Affinity-1S spectrometer. Wavenumbers $\tilde{\nu}$ are given in cm^{-1} and intensities are indicated as follows: s = strong, m = medium, w = weak, b = broad.

Mass spectrometry: High-resolution mass spectra (HRMS) were recorded using an Waters QToF Premier (with an Acquity UPLC system) spectrometer.

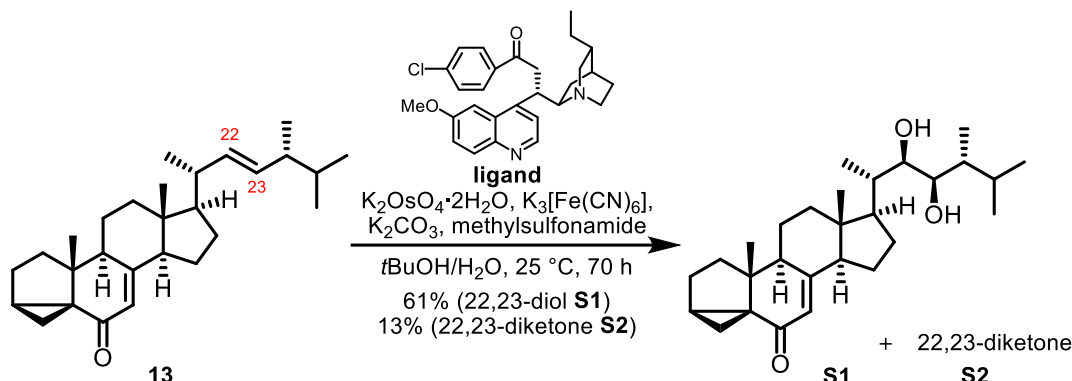
Optical rotation: Optical rotations were measured on a Krüss P3000 at 589 nm using 100 mm cells and the solvent and concentration (g/100 mL) indicated.

Melting Point: Melting points were measured on an OptiMelt MPA 100 instrument (Stanford Research System).

Lamps: For irradiation, a 300 W high pressure mercury lamp was used.

3 Experimental Section

(22*R*,23*R*)-3 α ,5 α -Cyclo-5 α -ergost-7-en-6-one-22,23-diol (**S1**)



To a suspension of $K_2OsO_4 \cdot 2H_2O$ (187 mg, 507 μ mol, 0.04 eq.), ligand^[2] (471 mg, 1.01 mmol, 0.08 eq.), $K_3[Fe(CN)_6]$ (25.0 g, 76.0 mmol, 6.0 eq.), K_2CO_3 (10.5 g, 76.0 mmol, 6.0 eq.) and methylsulfonamide (7.23 g, 76.0 mmol, 6.0 eq.) in a mixture of $tBuOH/H_2O$ (1:1, 520 mL) was added enone **13** (5.00 g, 12.7 mmol, 1.0 eq.). After vigorous stirring at 25 °C for 70 h, sat. aq. $Na_2S_2O_3$ (250 mL) was added, the mixture was stirred for an additional 30 min, and subsequently diluted with H_2O (150 mL). The aqueous phase was extracted with CH_2Cl_2 (3 × 500 mL), the combined organic phases dried over $MgSO_4$, and all volatiles were removed under reduced pressure. Column chromatography (SiO_2 , *n*hexane/EtOAc 9:1 → 3:2, *v/v*) gave diol **S1** (3.32 g, 7.75 mmol, 61%) as colourless crystals and diketone **S2** (700 mg, 1.65 mmol, 13%) as a yellow crystalline solid.

(22*R*,23*R*)-3 α ,5 α -Cyclo-5 α -ergost-7-en-6-one-22,23-diol (**S1**)

m.p.:	149–151 °C ($CHCl_3$).
TLC:	$R_f = 0.31$ (<i>n</i> hexane/EtOAc 1.5:1, <i>v/v</i>).
1H-NMR:	(400 MHz, $CDCl_3$); δ [ppm] = 5.80 (t, $J = 2.3$ Hz, 1H), 3.71 (d, $J = 5.0$ Hz, 1H), 3.42 (q, $J = 5.0$ Hz, 1H), 2.26 (ddd, $J = 10.9, 7.5, 2.4$ Hz, 1H), 2.19 – 2.06 (m, 5H), 1.97 (ddd, $J = 11.8, 7.7, 4.2$ Hz, 1H), 1.90 (qd, $J = 6.9, 3.8$ Hz, 1H), 1.81 – 1.68 (m, 8H), 1.58 – 1.37 (m, 5H), 1.17 – 1.10 (m, 1H), 1.09 (s, 3H), 1.01 (d, $J = 6.8$ Hz, 3H), 0.93 (d, $J = 6.9$ Hz, 3H), 0.87 (d, $J = 6.8$ Hz, 3H), 0.86 (d, $J = 7.0$ Hz, 3H), 0.75 (t, $J = 4.6$ Hz, 1H), 0.68 (s, 3H).
^{13}C-NMR:	(101 MHz, $CDCl_3$); δ [ppm] = 197.3, 164.1, 123.8, 76.5, 72.6, 56.1, 52.9, 45.2, 44.4, 43.8, 42.1, 41.6, 40.8, 39.2, 35.1, 33.9, 27.6, 27.2, 26.9, 23.3, 22.8, 22.3, 19.6, 17.4, 13.3, 12.8, 12.5, 11.0.
IR:	$\tilde{\nu}$ [cm^{-1}] = 3509 (w), 3478 (w), 2955 (m), 2870 (m), 1639 (s), 1609 (m), 1460 (m), 1381 (s), 1366 (m), 1323 (m), 1300 (m), 1173 (m), 1152 (w), 1144 (w), 1061 (m), 1034 (m), 986 (m), 970 (m), 887 (m), 874 (m), 816 (w), 723 (w), 627 (w), 554 (m).
HRMS:	(ESI-TOF); m/z calcd. for $C_{28}H_{44}O_3Na^+$ [M+Na] ⁺ : 451.3183, found: 451.3192.
opt. act.:	$[\alpha]_D^{26} = +50.0$ ($c = 1.0$, $CHCl_3$).

3 α ,5 α -Cyclo-5 α -ergost-7-ene-6,22,23-trione (**S2**)

m.p.:	154–156 °C (CH_2Cl_2).
TLC:	$R_f = 0.26$ (<i>n</i> hexane/EtOAc 9:1, <i>v/v</i>).
1H-NMR:	(400 MHz, $CDCl_3$); δ [ppm] = 5.78 (t, $J = 2.3$ Hz, 1H), 3.49 (dq, $J = 10.3, 7.0$ Hz, 1H), 3.29 – 3.22 (m, 1H), 2.27 (ddd, $J = 10.8, 7.7, 2.3$ Hz, 1H), 2.14 – 2.07 (m, 2H), 2.02 – 1.87 (m, 3H), 1.81 – 1.67 (m, 8H), 1.58 – 1.48 (m, 2H), 1.21 – 1.12

(m, 2H), 1.11 – 1.08 (m, 6H), 1.00 (d, J = 7.0 Hz, 3H), 0.92 (d, J = 6.7 Hz, 3H), 0.84 (d, J = 6.9 Hz, 3H), 0.76 (t, J = 4.6 Hz, 1H), 0.74 (s, 3H).

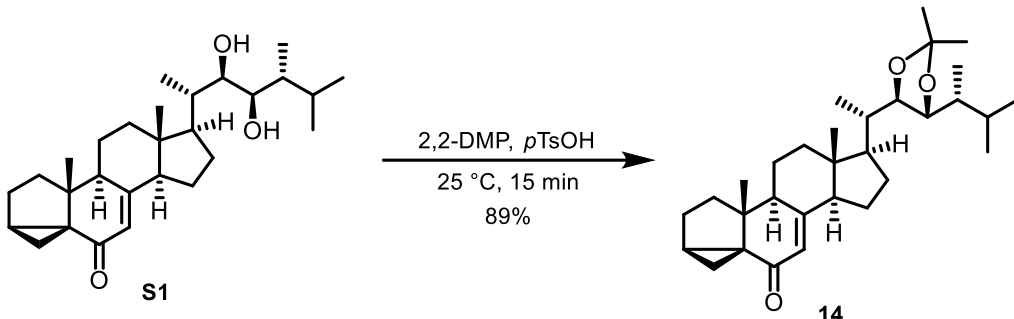
$^{13}\text{C-NMR}$: (101 MHz, CDCl_3); δ [ppm] = 203.5, 202.3, 197.1, 163.3, 124.0, 55.5, 52.1, 45.2, 44.8, 44.4, 43.8, 42.1, 40.9, 39.1, 35.1, 33.9, 29.5, 27.1, 26.9, 23.3, 23.1, 21.4, 19.6, 18.4, 16.4, 13.3, 12.9, 11.7.

IR: $\tilde{\nu}$ [cm^{-1}] = 2963 (m), 2961 (w), 2872 (w), 1703 (s), 1649 (s), 1614 (w), 1454 (m), 1379 (m), 1321 (m), 1302 (m), 1175 (m), 1016 (m), 991 (m), 922 (m), 887 (m), 880 (m), 874 (m), 816 (w), 754 (w), 685 (w), 673 (w), 627 (w), 474 (w).

HRMS: (ESI-TOF); m/z calcd. for $\text{C}_{28}\text{H}_{40}\text{O}_3\text{Na}^+$ [M+Na] $^+$: 447.2870, found: 447.2858.

opt. act.: $[\alpha]_D^{26} = +26.0$ (c = 1.0, CHCl_3).

(22*R*,23*R*)-3*α*,5*α*-Cyclo-5*α*-ergost-7-ene-22,23-[(1-methylethylidene)bis(oxy)]-6-one (14)



To a stirred suspension of diol **S1** (670 mg, 1.56 mmol, 1.0 eq.) in 2,2-dimethoxypropane (15.6 mL) was added *p*-toluenesulfonic acid (14.9 mg, 78.0 μ mol, 0.05 eq.) After stirring for 15 min at 25 °C, the solution was diluted with CH_2Cl_2 (20 mL), washed with sat. aq. NaHCO_3 (10 mL), the organic phase was dried over MgSO_4 , and all volatiles were removed under reduced pressure. Column chromatography (SiO_2 , *n*hexane/EtOAc 6:1, *v/v*) gave enone **14** (649 mg, 1.39 mmol, 89%) as colourless crystals.

m.p.: 170–171 °C (CHCl_3).

TLC: R_f = 0.28 (*n*hexane/EtOAc 6:1, *v/v*).

$^1\text{H-NMR}$: (400 MHz, CDCl_3); δ [ppm] = 5.79 (t, J = 2.3 Hz, 1H), 3.97 (d, J = 6.9 Hz, 1H), 3.57 (dd, J = 9.4, 6.9 Hz, 1H), 2.30 – 2.22 (m, 1H), 2.18 – 2.07 (m, 4H), 1.99 (tdd, J = 12.3, 8.0, 4.6 Hz, 1H), 1.83 – 1.66 (m, 9H), 1.61 – 1.45 (m, 5H), 1.40 (s, 3H), 1.35 (s, 3H), 1.09 (s, 3H), 1.01 (d, J = 6.5 Hz, 3H), 0.91 (d, J = 6.9 Hz, 3H), 0.81 (d, J = 6.8 Hz, 3H), 0.75 (t, J = 4.7 Hz, 1H), 0.72 (d, J = 6.9 Hz, 3H), 0.67 (s, 3H).

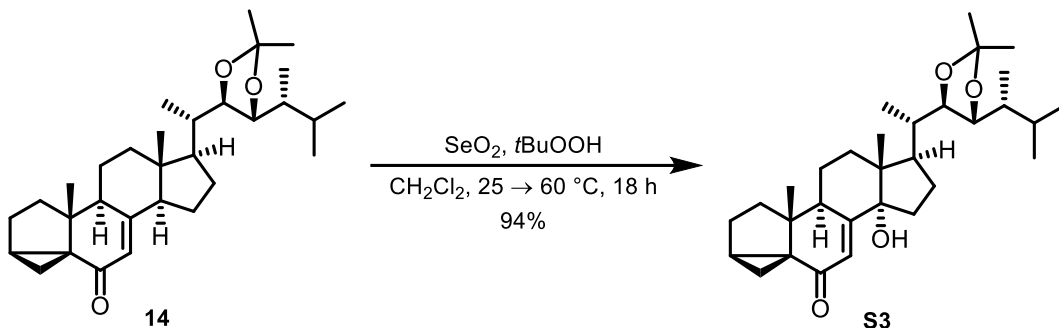
$^{13}\text{C-NMR}$: (101 MHz, CDCl_3); δ [ppm] = 197.3, 164.2, 123.8, 108.2, 82.4, 80.5, 55.9, 53.7, 45.2, 44.5, 43.9, 43.8, 42.1, 39.0, 38.4, 35.1, 33.9, 27.9, 27.53, 27.48, 27.3, 26.9, 23.3, 22.8, 21.3, 19.6, 16.1, 13.3, 13.0, 12.4, 10.0.

IR: $\tilde{\nu}$ [cm^{-1}] = 2955 (m), 2938 (m), 2874 (w), 1649 (s), 1618 (w), 1458 (w), 1377 (s), 1366 (m), 1323 (w), 1304 (m), 1256 (m), 1209 (m), 1182 (m), 1167 (m), 1043 (s), 1032 (m), 999 (m), 988 (w), 922 (w), 891 (m), 872 (m), 816 (w), 716 (w), 629 (w), 507 (w).

HRMS: (ESI-TOF); m/z calcd. for $\text{C}_{31}\text{H}_{48}\text{O}_3\text{Na}^+$ [M+Na] $^+$: 491.3496, found: 491.3508.

opt. act.: $[\alpha]_D^{26} = +68.0$ (c = 1.0, CHCl_3).

(22*R*,23*R*)-14-Hydroxy-3*a*,5*a*-cyclo-5*a*-ergost-7-ene-22,23-[(1-methylethylidene)bis(oxy)]-6-one (**S3**)



To a stirred suspension of SeO_2 (330 mg, 2.98 mmol, 0.5 eq.) in CH_2Cl_2 (5.6 mL) in a pressure vessel was added $t\text{BuOOH}$ (70% aq., 3.3 mL, 23.8 mmol, 4.0 eq.) at 0 °C. After stirring at 25 °C for 15 min, enone **14** (2.79 g, 5.95 mmol, 1.0 eq.) in CH_2Cl_2 (6.9 mL) was added. The vessel was sealed and the mixture was stirred at 60 °C for 18 h. The reaction mixture was allowed to cool to 25 °C and was carefully added to aq. NaHSO_3 (10%, 60 mL) at 0 °C. The mixture was extracted with CH_2Cl_2 (3×80 mL) and the combined organic phases were washed sequentially with sat. aq. NaHCO_3 (50 mL) and brine (50 mL), dried over MgSO_4 , and concentrated under reduced pressure. Column chromatography (SiO_2 , *n*hexane/ EtOAc 5:1 → 4:1, v/v) gave γ -hydroxy enone **S3** (2.71 g, 5.59 mmol, 94%) as a colourless crystalline solid.

m.p.: 209–213 °C (CHCl₃).

TLC: $R_f = 0.23$ (nhexane/EtOAc 4:1, v/v).

¹H-NMR: (400 MHz, CDCl₃); δ [ppm] = 5.99 (d, *J* = 2.6 Hz, 1H), 3.96 (dd, *J* = 6.9, 1.1 Hz, 1H), 3.58 (dd, *J* = 9.4, 6.9 Hz, 1H), 2.78 (td, *J* = 9.1, 2.7 Hz, 1H), 2.35 – 2.27 (m, 1H), 2.27 – 2.19 (m, 1H), 2.11 (ddt, *J* = 10.6, 7.2, 3.8 Hz, 2H), 2.06 – 1.95 (m, 2H), 1.83 (dt, *J* = 8.7, 4.5 Hz, 1H), 1.77 – 1.66 (m, 6H), 1.61 (ddd, *J* = 12.5, 9.0, 6.7 Hz, 3H), 1.53 – 1.44 (m, 1H), 1.39 (d, *J* = 0.8 Hz, 3H), 1.35 – 1.33 (m, 3H), 1.29 (s, 1H), 1.10 (s, 3H), 0.99 (d, *J* = 6.6 Hz, 3H), 0.92 (d, *J* = 7.0 Hz, 3H), 0.82 (d, *J* = 6.8 Hz, 3H), 0.79 (t, *J* = 4.7 Hz, 1H), 0.75 (s, 3H), 0.73 (d, *J* = 7.0 Hz, 3H).

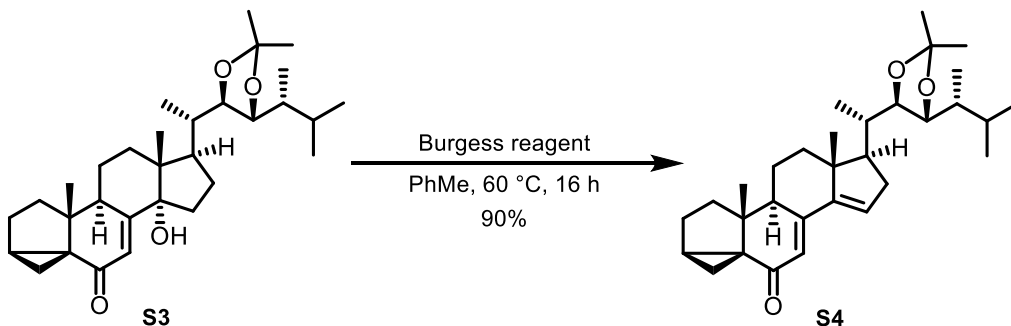
¹³C-NMR: (101 MHz, CDCl₃); δ [ppm] = 198.2, 163.9, 123.5, 108.2, 85.2, 82.5, 80.6, 48.3, 46.5, 45.3, 44.1, 44.0, 38.1, 37.9, 35.7, 33.8, 32.2, 30.7, 27.9, 27.5, 27.3, 26.9, 26.2, 21.9, 21.3, 19.4, 16.2, 15.9, 13.8, 13.2, 10.1.

IR: $\tilde{\nu}$ [cm⁻¹] = 3383 (br, w), 2957 (m), 2938 (m), 2874 (w), 1636 (s), 1456 (w), 1375 (m), 1271 (w), 1215 (w), 1179 (w), 1169 (m), 1144 (w), 1047 (s), 1024 (m), 1001 (w). 881 (s), 864 (m), 827 (w), 814 (w).

HRMS: (ESI-TOF); m/z calcd. for $C_{31}H_{48}O_4Na^+ [M+Na]^+$: 507.3448, found: 507.3460.

opt. act.: $[\alpha]_D^{26} = +110.0$ ($c = 1.0$, CHCl₃).

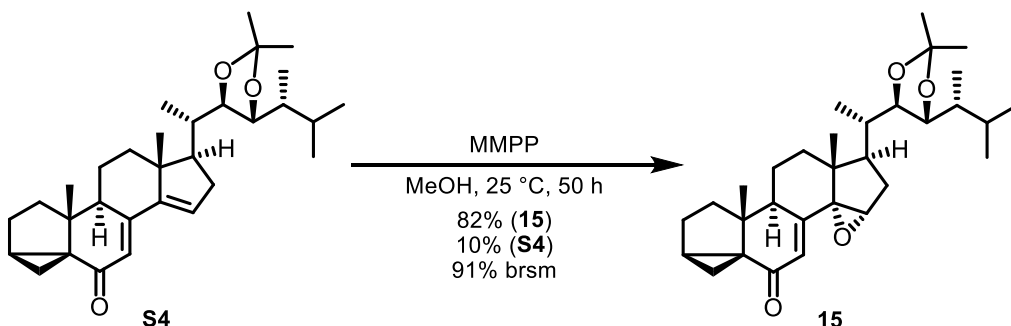
(22R,23R)-3 α ,5-cyclo-5 α -ergosta-7,14-diene-22,23-[(1-methylethylidene)bis(oxy)]-6-one (**S4**)



To a stirred solution of γ -hydroxy enone **S3** (534 mg, 1.10 mmol, 1.0 eq.) in toluene (11.0 mL) was added Burgess reagent^[3] (368 mg, 1.54 mmol, 1.5 eq.). After stirring at 60 °C for 16 h the mixture was allowed to cool to 25 °C, diluted with EtOAc (12 mL), and washed with sat. aq. NaHCO₃ (10 mL). The aqueous layer was extracted with EtOAc (2 \times 15 mL) and the combined organic phases were washed with brine (15 mL), dried over MgSO₄, and concentrated under reduced pressure. Column chromatography (SiO₂, *n*hexane/EtOAc 9:1, *v/v*) gave dienone **S4** (461 mg, 987 μ mol, 90%) as a yellow foam.

- TLC:** R_f = 0.23 (*n*hexane/EtOAc 9:1, *v/v*).
- ¹H-NMR:** (400 MHz, CDCl₃); δ [ppm] = 6.24 (d, J = 2.7 Hz, 1H), 6.05 (dd, J = 3.8, 2.0 Hz, 1H), 3.91 (dd, J = 7.2, 1.4 Hz, 1H), 3.61 (dd, J = 9.4, 7.1 Hz, 1H), 2.61 (ddd, J = 16.1, 7.1, 3.7 Hz, 1H), 2.34 (ddd, J = 12.0, 6.1, 2.7 Hz, 1H), 2.20 – 2.05 (m, 5H), 1.97 (ddd, J = 12.4, 8.2, 4.6 Hz, 1H), 1.83 (dt, J = 8.8, 4.6 Hz, 1H), 1.76 – 1.68 (m, 5H), 1.64 (s, 1H), 1.58 (ddd, J = 9.8, 6.8, 3.1 Hz, 1H), 1.50 (td, J = 13.2, 3.7 Hz, 1H), 1.39 (s, 3H), 1.35 (s, 3H), 1.09 (s, 3H), 1.02 (d, J = 6.5 Hz, 3H), 0.94 (s, 3H), 0.92 (d, J = 7.0 Hz, 3H), 0.82 (d, J = 6.9 Hz, 3H), 0.78 (t, J = 4.8 Hz, 1H), 0.72 (d, J = 7.0 Hz, 3H).
- ¹³C-NMR:** (101 MHz, CDCl₃); δ [ppm] = 197.9, 154.0, 149.7, 128.5, 122.0, 108.1, 82.5, 80.3, 56.2, 46.6, 45.9, 44.1, 43.8, 42.5, 39.2, 36.4, 35.4, 35.1, 33.2, 28.0, 27.5, 27.3, 26.7, 22.1, 21.3, 18.9, 17.1, 16.2, 13.8, 13.0, 10.0.
- IR:** $\tilde{\nu}$ [cm⁻¹] = 2955 (m), 2930 (m), 2870 (m), 1647 (s), 1614 (m), 1595 (w), 1458 (m), 1377 (s), 1366 (s), 1314 (m), 1302 (m), 1250 (m), 1215 (m), 1173 (s), 1128 (m), 1045 (s), 1022 (m), 1001 (m), 887 (m), 822 (m), 505 (w).
- HRMS:** (ESI-TOF); *m/z* calcd. for C₃₁H₄₆O₃Na⁺ [M+Na]⁺: 489.3339, found: 489.3332.
- opt. act.:** $[\alpha]_D^{27} = -170.0$ (*c* = 1.0, CHCl₃).

(22*R*,23*R*)-14,15*a*-Epoxy-3*a*,5*a*-cyclo-5*a*-ergost-7-ene-22,23-[(1-methylethylidene)bis(oxy)]-6-one (**15**)



To a suspension of dienone **S4** (2.26 g, 4.84 mmol, 1.0 eq.) in MeOH (195 mL) was added magnesium bis(monoperoxyphthalate) hexahydrate (80%, 3.89 g, 6.30 mmol, 1.3 eq.). After stirring at 25 °C for 50 h, water (40 mL) was added and MeOH was removed under reduced pressure. Sat. aq. NaHCO₃ (40 mL) was added, and the mixture was extracted with EtOAc (3 \times 100 mL). The combined organic phases were washed sequentially with sat. aq. NaHCO₃ (80 mL) and brine (80 mL), dried over MgSO₄, and concentrated under reduced pressure. Column chromatography (SiO₂, *n*hexane/EtOAc 6:1, *v/v*) gave epoxide **15** (1.91 g, 3.95 mmol, 82%) as a crystalline solid and recovered dienone **S4** (218 mg, 468 μ mol, 10%).

- m.p.:** 186–187 °C (CHCl₃).
- TLC:** R_f = 0.21 (*n*hexane/EtOAc 6:1, *v/v*).
- ¹H-NMR:** (400 MHz, CDCl₃); δ [ppm] = 5.91 (d, J = 2.8 Hz, 1H), 3.88 – 3.82 (m, 2H), 3.56 (dd, J = 9.4, 7.1 Hz, 1H), 2.58 (ddd, J = 11.2, 7.6, 2.7 Hz, 1H), 2.35 (ddd, J = 13.5, 6.7, 0.9 Hz, 1H), 2.09 (td, J = 6.9, 3.3 Hz, 1H), 2.06 – 1.97 (m, 2H), 1.81

(ddd, $J = 11.9, 7.1, 3.9$ Hz, 3H), 1.67 (d, $J = 11.4$ Hz, 5H), 1.59 – 1.48 (m, 2H), 1.42 (ddd, $J = 13.4, 10.2, 1.0$ Hz, 1H), 1.36 (s, 3H), 1.33 (s, 3H), 1.19 – 1.14 (m, 1H), 1.13 (s, 3H), 0.95 (d, $J = 6.5$ Hz, 3H), 0.91 (d, $J = 7.0$ Hz, 3H), 0.84 (s, 3H), 0.80 (d, $J = 6.9$ Hz, 3H), 0.78 (t, $J = 4.6$ Hz, 1H), 0.69 (d, $J = 7.0$ Hz, 3H).

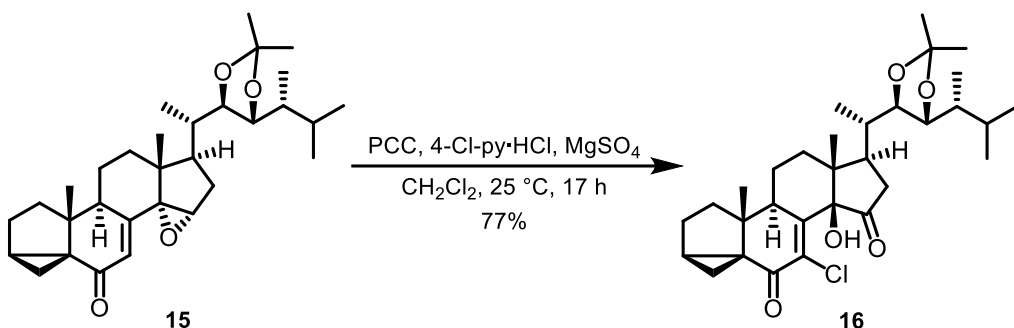
$^{13}\text{C-NMR}$: (101 MHz, CDCl_3); δ [ppm] = 197.3, 156.1, 124.9, 108.2, 81.7, 80.2, 72.0, 59.4, 45.9, 45.7, 44.1, 43.8, 41.1, 40.4, 36.1, 35.7, 33.6, 33.5, 31.3, 27.9, 27.4, 27.3, 26.8, 22.0, 21.3, 19.4, 16.1, 14.5, 13.6, 13.0, 9.9.

IR: $\tilde{\nu}$ [cm^{-1}] = 2957 (m), 2940 (m), 2874 (w), 1655 (s), 1458 (m), 1377 (s), 1366 (m), 1300 (m), 1258 (m), 1207 (m), 1175 (s), 1132 (m), 1043 (s), 1024 (s), 997 (m), 970 (m), 951 (m), 922 (w), 891 (m), 876 (m), 853 (m), 824 (m), 814 (m), 768 (m), 756 (w), 617 (w), 519 (w), 449 (w).

HRMS: (ESI-TOF); m/z calcd. for $\text{C}_{31}\text{H}_{46}\text{O}_4\text{Na}^+ [\text{M}+\text{Na}]^+$: 505.3288, found: 505.3294.

opt. act.: $[\alpha]_D^{30} = -14.0$ ($c = 1.0$, CHCl_3).

(*22R,23R*)-7-Chloro-14*β*-hydroxy-3*α*,5*α*-cyclo-5*α*-ergost-7-ene-22,23-[(1-methylethylidene)bis(oxy)]-6,15-dione (**16**)



To a suspension of pyridinium chlorochromate (1.79 g, 8.29 mmol, 4.0 eq.), 4-chloropyridine hydrochloride (1.87 g, 12.4 mmol, 6.0 eq.), and MgSO_4 (1.79 g) in CH_2Cl_2 (14 mL) was added epoxide **15** (1.00 g, 2.07 mmol, 1.0 eq.) in CH_2Cl_2 (6.5 mL). After stirring at 25 °C for 17 h, the mixture was diluted with Et_2O (25 mL), filtered through Celite® and rinsed with Et_2O (3 × 15 mL). The filtrate was concentrated under reduced pressure and column chromatography (SiO_2 , *n*hexane/EtOAc 6:1, *v/v*) gave α -chloro enone **16** (851 mg, 1.60 mmol, 77%) as a yellow foam.

TLC: $R_f = 0.29$ (*n*hexane/EtOAc 6:1, *v/v*).

$^1\text{H-NMR}$: (400 MHz, CDCl_3); δ [ppm] = 3.82 (d, $J = 7.1$ Hz, 1H), 3.59 (dd, $J = 9.4, 6.9$ Hz, 1H), 3.09 (dd, $J = 11.0, 6.6$ Hz, 1H), 2.81 (dd, $J = 17.6, 6.5$ Hz, 1H), 2.51 – 2.39 (m, 2H), 2.33 (dd, $J = 17.6, 11.4$ Hz, 1H), 2.27 – 2.19 (m, 1H), 2.14 – 2.07 (m, 1H), 2.06 – 1.91 (m, 2H), 1.91 – 1.84 (m, 2H), 1.84 – 1.72 (m, 4H), 1.68 – 1.56 (m, 3H), 1.38 (s, 3H), 1.34 (s, 3H), 1.22 – 1.13 (m, 1H), 1.09 (s, 3H), 1.03 (d, $J = 6.9$ Hz, 6H), 0.92 (d, $J = 7.0$ Hz, 3H), 0.82 (d, $J = 7.0$ Hz, 3H), 0.71 (d, $J = 6.9$ Hz, 3H).

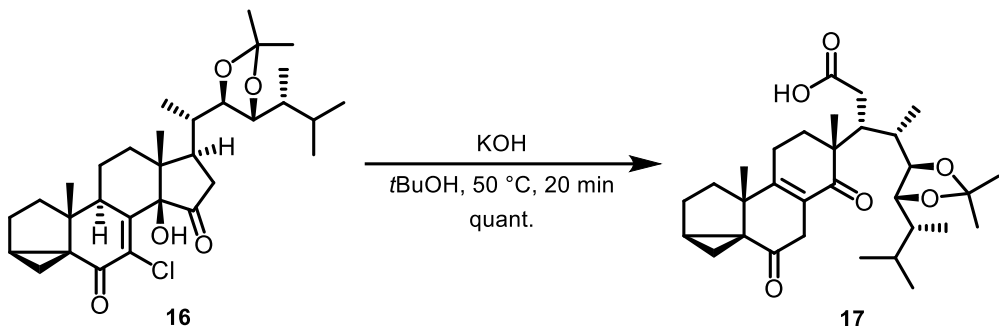
$^{13}\text{C-NMR}$: (101 MHz, CDCl_3); δ [ppm] = 209.2, 189.5, 151.7, 127.5, 108.5, 83.4, 82.3, 80.5, 48.4, 44.7, 43.8, 43.5, 43.0, 42.9, 41.5, 37.0, 35.6, 35.5, 31.3, 27.9, 27.4, 27.3, 27.1, 25.6, 21.2, 20.3, 16.1, 13.9, 13.5, 13.3, 10.1.

IR: $\tilde{\nu}$ [cm^{-1}] = 3400 (br, w), 2959 (m), 2872 (m), 1748 (s), 1676 (s), 1597 (w), 1578 (w), 1456 (m), 1377 (s), 1366 (s), 1294 (m), 1249 (m), 1209 (m), 1165 (m), 1136 (s), 1070 (s), 1020 (s). 995 (s), 957 (m), 897 (s), 872 (m), 833 (m), 822 (m), 725 (m), 658 (m), 600 (m), 538 (m), 505 (m).

HRMS: (ESI-TOF); m/z calcd. for $\text{C}_{31}\text{H}_{45}\text{ClO}_5\text{Na}^+ [\text{M}+\text{Na}]^+$: 555.2848, found: 555.2843.

opt. act.: $[\alpha]_D^{31} = +149.0$ ($c = 1.0$, CHCl_3).

(22*R*,23*R*)-6,14-Dioxo-3*a*,5-cyclo-14,15-seco-5*a*-ergost-7-ene-22,23-[(1-methylethylidene)bis(oxy)]-15-oic acid (**17**)



Finely ground KOH (448 mg, 7.98 mmol, 5.0 eq.) was suspended in *t*BuOH (10.7 mL) and heated to 50 °C. After 10 min at this temperature, α-chloro enone **16** (851 mg, 1.60 mmol, 1.0 eq.) in *t*BuOH (5.3 mL) was added over a period of 5 min and stirring was continued at 50 °C for 20 min. The mixture was allowed to cool to 25 °C, water (20 mL) was added and the pH was adjusted with 1 M HCl to 2. The mixture was extracted with EtOAc (3 × 30 mL) and the combined organic phases were washed with brine (30 mL), dried over MgSO₄, and concentrated under reduced pressure to give carboxylic acid **17** (823 mg, 1.60 mmol, quant.) as a yellow foam which was used in the next step without further purification.

Spectroscopically homogeneous carboxylic acid **17** for analysis was obtained by preparative TLC (*n*hexane/EtOAc/AcOH 1:1:0.01, *v/v/v*).

TLC: $R_f = 0.32$ (*n*-hexane/EtOAc/AcOH 1:1:0.01, v/v/v).

¹H-NMR: (600 MHz, CDCl₃); δ [ppm] = 3.97 – 3.92 (m, 1H), 3.56 (t, *J* = 7.7 Hz, 1H), 3.41 (dd, *J* = 20.8, 1.4 Hz, 1H), 2.85 – 2.78 (m, 2H), 2.52 – 2.46 (m, 2H), 2.35 (dd, *J* = 11.4, 7.3 Hz, 1H), 2.30 (dd, *J* = 17.7, 7.0 Hz, 1H), 2.15 (dt, *J* = 14.1, 4.3 Hz, 1H), 2.10 (dd, *J* = 14.1, 6.8 Hz, 1H), 2.05 (ddp, *J* = 10.5, 6.9, 3.5 Hz, 1H), 1.95 – 1.91 (m, 1H), 1.87 – 1.81 (m, 2H), 1.78 (dd, *J* = 8.2, 4.8 Hz, 1H), 1.75 – 1.68 (m, 2H), 1.54 (ddd, *J* = 7.9, 6.9, 3.5 Hz, 1H), 1.32 (s, 3H), 1.31 (s, 3H), 1.22 (dd, *J* = 12.9, 7.9 Hz, 1H), 1.19 (s, 3H), 1.10 (s, 3H), 1.05 (d, *J* = 7.0 Hz, 3H), 1.01 (t, *J* = 5.0 Hz, 1H), 0.90 (d, *J* = 7.0 Hz, 3H), 0.83 (d, *J* = 6.8 Hz, 3H), 0.80 (d, *J* = 7.0 Hz, 3H).

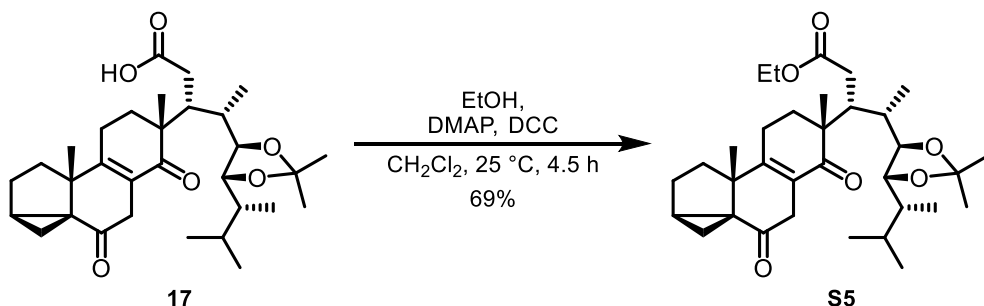
¹³C-NMR: (151 MHz, CDCl₃); δ [ppm] = 208.5, 202.2, 177.2, 158.3, 128.3, 108.3, 82.0, 80.7, 48.0, 47.4, 43.2, 42.5, 40.9, 37.0, 36.9, 34.5, 32.9, 32.4, 30.8, 27.9, 27.5, 27.1, 26.3, 23.3, 22.4, 21.5, 19.6, 16.6, 15.2, 14.7, 10.9.

IR: $\tilde{\nu}$ [cm⁻¹] = 2961 (m), 2934 (m), 2872 (m), 1730 (m), 1697 (s), 1661 (s), 1452 (m), 1427 (m), 1375 (s), 1368 (s), 1277 (m), 1240 (s), 1209 (s), 1171 (s), 1159 (s), 1130 (m), 1096 (m), 1028 (s), 876 (s), 812 (m), 621 (w), 507 (m).

HRMS: (ESI-TOF); m/z calcd. for $C_{31}H_{46}O_6Na^+ [M+Na]^+$: 537.3187, found: 537.3173.

opt. act.: $[\alpha]_D^{26} = +93.0$ ($c = 1.0$, CHCl_3).

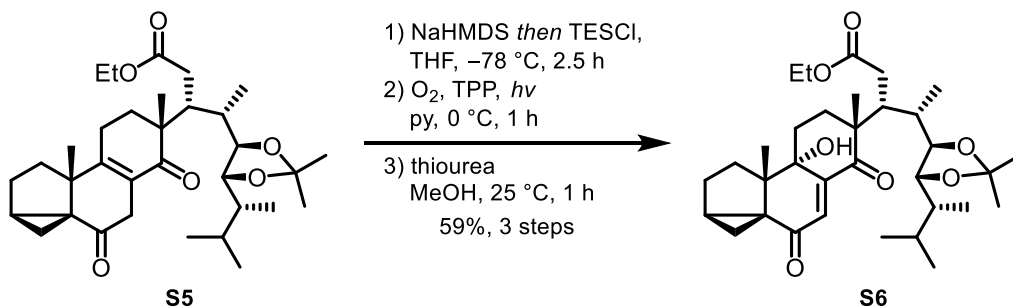
O-Ethyl (22*R*,23*R*)-6,14-dioxo-3*α*,5-cyclo-14,15-seco-5*α*-ergost-8-ene-22,23-[(1-methylethylidene)bis(oxy)]-15-ate (**S5**)



To a stirred solution of acid **17** (1.01 g, 1.95 mmol, 1.0 eq.), *N,N'*-dicyclohexylcarbodiimide (483 mg, 2.34 mmol, 1.2 eq.) and *N,N*-dimethyl-4-aminopyridine (23.8 mg, 195 µmol, 0.1 eq.) in CH₂Cl₂ (19.5 mL) was added EtOH (170 µL, 29.3 mmol, 1.5 eq.). After stirring at 25 °C for 4.5 h, the mixture was filtered through Celite® and rinsed with CH₂Cl₂ (3 × 10 mL). The filtrate was concentrated under reduced pressure and column chromatography (SiO₂, *n*hexane/EtOAc 5:1, v/v) gave ethyl ester **S5** (735 mg, 1.35 mmol, 69%) as a yellow foam.

TLC:	$R_f = 0.23$ (<i>n</i> hexane/EtOAc 5:1, v/v).
¹H-NMR:	(400 MHz, CDCl ₃); δ [ppm] = 4.04 – 3.87 (m, 3H), 3.54 (t, <i>J</i> = 7.7 Hz, 1H), 3.40 – 3.31 (m, 1H), 2.80 (dt, <i>J</i> = 21.0, 3.4 Hz, 1H), 2.71 (dd, <i>J</i> = 17.6, 4.5 Hz, 1H), 2.56 – 2.52 (m, 1H), 2.48 (d, <i>J</i> = 10.7 Hz, 1H), 2.37 – 2.28 (m, 1H), 2.23 (dd, <i>J</i> = 17.6, 7.1 Hz, 1H), 2.19 – 2.01 (m, 3H), 1.94 – 1.68 (m, 7H), 1.53 (td, <i>J</i> = 7.3, 3.4 Hz, 1H), 1.31 (s, 3H), 1.29 (s, 3H), 1.21 (d, <i>J</i> = 7.2 Hz, 3H), 1.18 (s, 3H), 1.08 (s, 3H), 1.04 (d, <i>J</i> = 6.9 Hz, 3H), 1.00 (t, <i>J</i> = 5.0 Hz, 1H), 0.90 (d, <i>J</i> = 6.9 Hz, 3H), 0.85 – 0.76 (m, 6H).
¹³C-NMR:	(101 MHz, CDCl ₃); δ [ppm] = 208.1, 202.4, 173.7, 158.3, 128.1, 108.1, 82.0, 80.7, 60.3, 48.1, 47.3, 43.1, 42.5, 40.5, 36.9, 36.9, 34.4, 32.9, 32.7, 31.1, 27.9, 27.4, 27.1, 26.3, 23.4, 22.3, 21.5, 19.6, 16.6, 15.1, 14.4, 14.3, 10.9.
IR:	ν [cm ⁻¹] = 2961 (m), 2932 (m), 2872 (m), 1730 (s), 1694 (s), 1661 (s), 1632 (w), 1452 (m), 1427 (w), 1377 (s), 1366 (s), 1298 (m), 1250 (m), 1240 (m), 1207 (s), 1180 (s), 1155 (s), 1130 (m), 1096 (m), 1038 (s), 1024 (s), 878 (m), 812 (w), 756 (m), 621 (w), 507 (w).
HRMS:	(ESI-TOF); <i>m/z</i> calcd. for C ₃₃ H ₅₀ O ₆ Na ⁺ [M+Na] ⁺ : 565.3500, found: 565.3500.
opt. act.:	$[\alpha]_D^{26} = +91.0$ (<i>c</i> = 1.0, CHCl ₃).

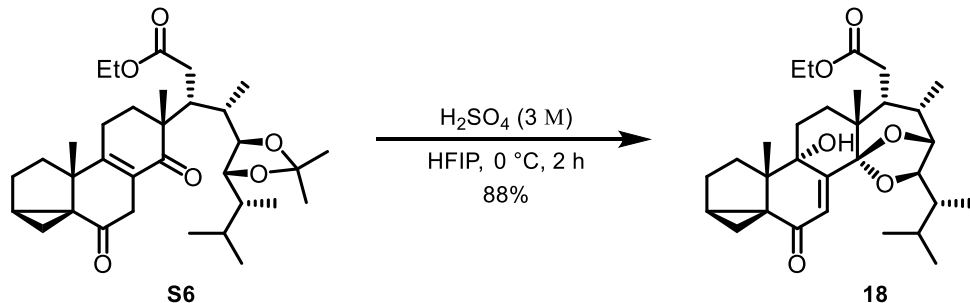
O-Ethyl (22*R*,23*R*)-9*α*-hydroxy-6,14-dioxo-3*α*,5-cyclo-14,15-seco-5*α*-ergost-7-ene-22,23-[(1-methylethylidene)bis(oxy)]-15-ate (**S6**)



To a stirred solution of ethyl ester **S5** (720 mg, 1.33 mmol, 1.0 eq.) in THF (8.8 mL) was added sodium bis(trimethylsilyl)amide (2 M in THF, 800 μ L, 1.59 mmol, 1.2 eq.) at -78°C . After 1.5 h at -78°C , triethylsilyl chloride (450 μ L, 2.65 mmol, 2.0 eq.) was added and the mixture was stirred for an additional 1 h at this temperature. All volatiles were removed under reduced pressure and the crude TES-enol ether was immediately redissolved in pyridine (13.3 mL) and cooled to 0°C . Tetraphenylporphyrin (24.5 mg, 39.8 μmol , 0.03 eq.) was added and the mixture was irradiated (300 W mercury lamp) under a constant flow of oxygen through the solution. After 1 h all volatiles were removed under reduced pressure and the crude endoperoxide was redissolved in MeOH (13.3 mL). Thiourea (505 mg, 6.63 mmol, 5.0 eq.) was added and the suspension was stirred for 1 h at 25°C . To the reaction mixture was added brine (13 mL), the aqueous phase was extracted with EtOAc (3×20 mL), the combined organic phases were washed sequentially with 1 M HCl (2×15 mL), sat. aq. Na_2CO_3 (15 mL), and brine (15 mL), dried over MgSO_4 , and all volatiles were removed under reduced pressure. Column chromatography (SiO_2 , *n*hexane/EtOAc 5:1, *v/v*) gave 9-alcohol **S6** (441 mg, 788 μmol , 59%) as a yellow oil.

TLC:	$R_f = 0.21$ (<i>n</i> hexane/EtOAc 5:1, <i>v/v</i>).
¹H-NMR:	(400 MHz, CDCl_3): δ [ppm] = 6.86 (s, 1H), 4.19 – 4.06 (m, 2H), 3.89 (d, $J = 7.8$ Hz, 1H), 3.45 (t, $J = 8.3$ Hz, 1H), 3.32 (br, 1H), 3.11 (dd, $J = 8.9, 4.7$ Hz, 1H), 2.56 – 2.40 (m, 3H), 2.18 (dd, $J = 14.6, 7.5$ Hz, 1H), 2.12 (d, $J = 13.6$ Hz, 1H), 2.09 – 2.02 (m, 2H), 1.94 (s, 2H), 1.91 (dd, $J = 13.4, 3.3$ Hz, 1H), 1.85 (d, $J = 3.8$ Hz, 1H), 1.79 (dd, $J = 8.4, 4.3$ Hz, 1H), 1.70 (dd, $J = 12.0, 8.6$ Hz, 1H), 1.59 – 1.47 (m, 2H), 1.29 (s, 3H), 1.26 (t, $J = 7.1$ Hz, 3H), 1.11 (s, 3H), 1.09 (s, 3H), 1.08 – 1.04 (m, 6H), 0.87 (d, $J = 6.9$ Hz, 3H), 0.83 (t, $J = 4.9$ Hz, 1H), 0.76 (d, $J = 6.8$ Hz, 3H), 0.71 (d, $J = 7.0$ Hz, 3H).
¹³C-NMR:	(101 MHz, CDCl_3): δ [ppm] = 201.3, 198.4, 173.6, 148.1, 132.0, 108.8, 81.9, 81.0, 74.1, 60.8, 50.0, 49.8, 44.0, 43.8, 43.2, 38.6, 36.9, 33.3, 32.1, 28.3, 27.9, 27.1, 26.5, 26.2, 25.9, 25.0, 22.2, 21.3, 17.8, 16.3, 14.3, 10.8, 10.0.
IR:	$\tilde{\nu}$ [cm^{-1}] = 3464 (w, br), 2961 (m), 2936 (w), 2874 (w), 1732 (m), 1990 (w), 1659 (s), 1655 (s), 1603 (w), 1458 (m), 1377 (s), 1368 (s), 1314 (m), 1252 (m), 1188 (m), 1163 (s), 1123 (m), 1080 (m), 1038 (s), 1007 (s), 916 (w), 893 (m), 874 (m), 810 (w), 766 (w), 756 (w), 569 (w), 507 (w).
HRMS:	(ESI-TOF); <i>m/z</i> calcd. for $\text{C}_{33}\text{H}_{50}\text{O}_7\text{Na}^+$ [M+Na] ⁺ : 581.3449, found: 581.3456.
opt. act.:	$[\alpha]_D^{26} = -61.0$ (<i>c</i> = 1.0, CHCl_3).

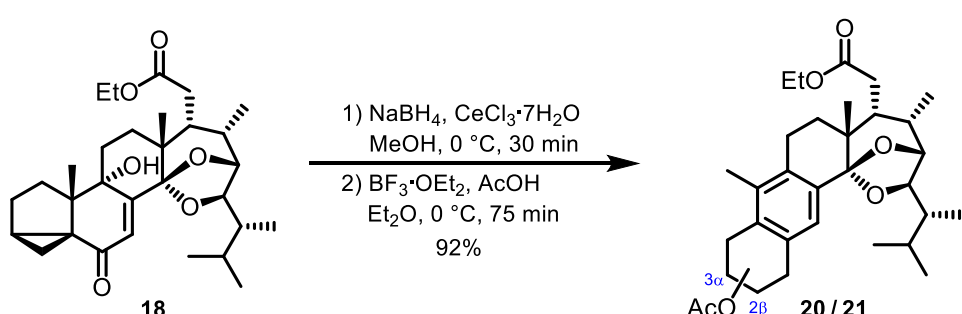
O-Ethyl (22*R*,23*R*)-14 β ,22 β :14 α ,23 β -diepoxy-9 α -hydroxy-6-oxo-3 α ,5-cyclo-14,15-seco-5 α -ergost-7-en-15-ate (**18**)



To a stirred solution of 9-alcohol **S6** (143 mg, 257 μmol , 1.0 eq.) in hexafluoroisopropanol (6.0 mL) was added 3 M H_2SO_4 (1.5 mL) at 0°C . After stirring at 0°C for 2 h, brine (5 mL) was added and the aqueous phase was extracted with CH_2Cl_2 (3×10 mL), the combined organic phases were dried over MgSO_4 , and all volatiles were removed under reduced pressure. Column chromatography (SiO_2 , *n*hexane/EtOAc 6:1, *v/v*) gave intramolecular acetal **18** (113 mg, 226 μmol , 88%) as a yellow oil.

TLC:	$R_f = 0.31$ (nhexane/EtOAc 6:1, v/v).
$^1\text{H-NMR}$:	(400 MHz, CDCl ₃); δ [ppm] = 6.48 (s, 1H), 4.14 (qd, J = 7.1, 1.3 Hz, 2H), 4.06 (d, J = 3.1 Hz, 1H), 3.60 (d, J = 10.0 Hz, 1H), 3.16 (br, 1H), 2.79 (dd, J = 16.9, 9.9 Hz, 1H), 2.68 (td, J = 7.2, 3.2 Hz, 1H), 2.42 – 2.30 (m, 2H), 2.28 – 2.18 (m, 1H), 2.17 – 2.09 (m, 1H), 2.09 – 2.03 (m, 1H), 2.02 – 1.95 (m, 1H), 1.91 (dd, J = 13.8, 4.1 Hz, 1H), 1.78 – 1.62 (m, 4H), 1.45 (ddd, J = 10.2, 6.8, 3.4 Hz, 1H), 1.28 (t, J = 7.1 Hz, 3H), 1.26 – 1.24 (m, 1H), 1.24 – 1.20 (m, 1H), 1.06 (s, 6H), 0.93 (d, J = 7.3 Hz, 3H), 0.81 (d, J = 7.0 Hz, 3H), 0.74 (d, J = 6.9 Hz, 3H), 0.70 (dd, J = 5.2, 4.2 Hz, 1H), 0.64 (d, J = 6.9 Hz, 3H).
$^{13}\text{C-NMR}$:	(101 MHz, CDCl ₃); δ [ppm] = 197.7, 175.2, 153.5, 126.0, 108.1, 81.9, 79.5, 73.7, 60.8, 49.3, 42.9, 42.0, 41.3, 40.4, 37.9, 32.5, 31.5, 31.3, 28.9, 27.7, 27.0, 26.3, 23.2, 22.9, 20.9, 16.5, 16.2, 14.5, 14.3, 10.7.
IR:	$\tilde{\nu}$ [cm ⁻¹] = 3524 (w), 2961 (m), 2932 (w), 2876 (w), 1732 (s), 1661 (s), 1636 (w), 1630 (w), 1458 (w), 1379 (s), 1368 (m), 1314 (m), 1298 (m), 1260 (m), 1231 (s), 1171 (s), 1155 (s), 1109 (m), 1096 (w), 1020 (s), 1007 (s), 982 (s), 926 (s), 903 (s), 874 (m), 754 (s), 665 (w), 631 (m), 503 (m).
HRMS:	(ESI-TOF); m/z calcd. for C ₃₀ H ₄₄ O ₆ Na ⁺ [M+Na] ⁺ : 523.3030, found: 523.3029.
opt. act.:	$[\alpha]_D^{29} = -70.0$ (c = 1.0, CHCl ₃).

O-Ethyl (22*R*,23*R*)-1(10 \rightarrow 6)abeo-14,15-seco-3 α -acetoxy-14 β ,22 β :14 α ,23 β -diepoxy-ergosta-5,7,9-trien-15-ate (**20**)
O-Ethyl (22*R*,23*R*)-1(10 \rightarrow 6)abeo-14,15-seco-2 β -acetoxy-14 β ,22 β :14 α ,23 β -diepoxy-ergosta-5,7,9-trien-15-ate (**21**)



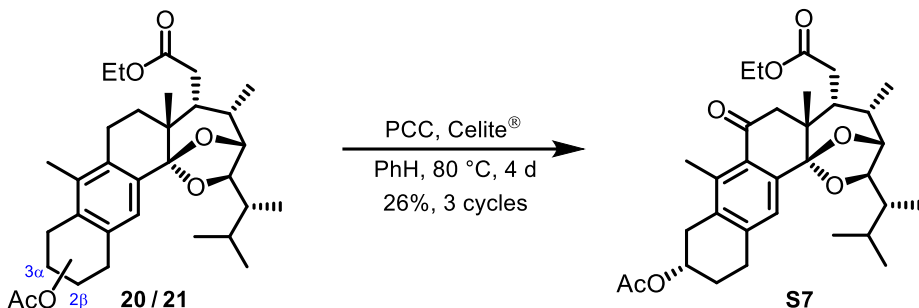
To a solution of intramolecular acetal **18** (220 mg, 438 µmol, 1.0 eq.) in MeOH (4.4 mL) were added CeCl₃·7H₂O (196 mg, 526 µmol, 1.2 eq.) and NaBH₄ (19.9 mg, 526 µmol, 1.2 eq.) at 0 °C. After stirring for 30 min at the same temperature, H₂O (5 mL) was added, the aqueous phase was extracted with CH₂Cl₂ (3 × 10 mL), the combined organic phases were dried over MgSO₄, and all volatiles were removed under reduced pressure. The crude 6,9-diol was redissolved in Et₂O (13.0 mL) and cooled to 0 °C. Acetic acid (5.2 mL) and BF₃·OEt₂ (5.2 mL) were added, and the resulting mixture was stirred at this temperature for 75 min. The mixture was diluted with EtOAc (65 mL) and carefully poured into sat. aq. NaHCO₃ (65 mL). The aqueous phase was extracted with EtOAc (3 × 70 mL), the combined organic phases were washed sequentially with sat. aq. NaHCO₃ (50 mL) and brine (50 mL) and dried over MgSO₄. All volatiles were removed under reduced pressure and column chromatography (SiO₂, nhexane/EtOAc 6:1, v/v) gave an inseparable mixture (2:1, determined by integration of 7-H signals (δ [ppm] 7.18 (major) and 7.22 (minor)) in the ¹H-NMR) of anthrasteroids **20/21** (212 mg, 403 µmol, 92%) as a colourless oil. For chemical separation see paragraph 6.

TLC: $R_f = 0.26$ (*n*-hexane/EtOAc 6:1, v/v).
 $^1\text{H-NMR}$: (400 MHz, CDCl₃); δ [ppm] = See paragraph 6.

¹³C-NMR: (101 MHz, CDCl₃); δ [ppm] = See paragraph 6.

HRMS: (ESI-TOF); m/z calcd. for $C_{32}H_{46}C_6Na^+ [M+Na]^+$: 549.3187, found: 549.3189.

O-Ethyl (22*R*,23*R*)-1(10 \rightarrow 6)abeo-14,15-seco-3 α -acetoxy-14 β ,22 β :14 α ,23 β -diepoxy-ergosta-5,7,9-trien-11-on-15-ate (**S7**)



To a stirred solution of anthrasteroids **20/21** (212 mg, 403 µmol, 1.0 eq.) in benzene (30.5 mL) in a pressure vessel, were added pyridinium chlorochromate (1.56 g, 7.26 mmol, 18.0 eq.) and Celite® (2.54 g). The suspension was heated to 80 °C and stirred at this temperature for 4 d. The mixture was then cooled to 25 °C, filtered over Celite®, and all volatiles were removed under reduced pressure. Column chromatography (SiO_2 , *n*hexane/EtOAc 5:1, *v/v*) gave 11-ketone **S7** (31.8 mg, 58.8 µmol, 15%) as a colourless oil and anthrasteroids **20/21** (111 mg, 210 µmol, 52%) as a yellowish oil. The reisolated starting material was then subjected to the same procedure two more times to give 11-ketone **S7** (56.7 mg, 105 µmol, 26%) as a colourless oil.

TLC: $R_f = 0.20$ (*n*hexane/EtOAc 5:1, *v/v*).

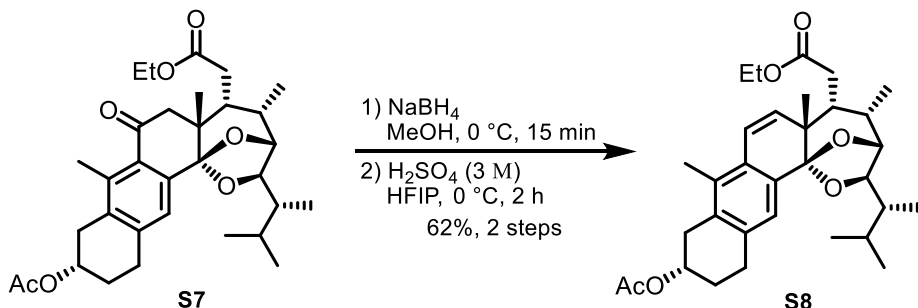
¹H-NMR: (600 MHz, CDCl₃); δ [ppm] = 7.28 (s, 1H), 5.20 (tdd, *J* = 8.3, 5.6, 2.9 Hz, 1H), 4.20 – 4.14 (m, 3H), 3.62 (d, *J* = 10.3 Hz, 1H), 3.13 (d, *J* = 14.0 Hz, 1H), 3.06 (dd, *J* = 17.0, 5.4 Hz, 1H), 2.96 – 2.88 (m, 2H), 2.81 (dd, *J* = 17.1, 9.6 Hz, 1H), 2.76 (dt, *J* = 7.2, 4.0 Hz, 1H), 2.75 – 2.71 (m, 1H), 2.50 (s, 3H), 2.48 – 2.45 (m, 1H), 2.39 (ddd, *J* = 9.9, 6.7, 3.3 Hz, 1H), 2.35 – 2.31 (m, 1H), 2.07 (d, *J* = 0.9 Hz, 3H), 2.05 – 2.03 (m, 1H), 1.92 (tdt, *J* = 12.8, 10.6, 6.6 Hz, 2H), 1.69 (ddd, *J* = 10.1, 6.7, 3.1 Hz, 1H), 1.30 – 1.27 (m, 3H), 1.18 (s, 3H), 0.98 (d, *J* = 7.3 Hz, 3H), 0.87 – 0.85 (m, 3H), 0.74 (d, *J* = 7.0 Hz, 3H), 0.73 – 0.71 (m, 3H).

¹³C-NMR: (151 MHz, CDCl₃); δ [ppm] = 199.7, 174.9, 170.8, 141.4, 139.4, 138.2, 135.1, 129.0, 124.3, 107.7, 82.8, 78.7, 70.1, 60.9, 48.9, 42.4, 42.1, 42.0, 33.0, 31.4, 31.2, 28.1, 27.2, 25.9, 24.5, 21.5, 21.2, 16.9, 15.5, 14.3, 14.3, 10.4.

HRMS: (ESI-TOF); m/z calcd. for $C_{32}H_{44}O_7Na^+ [M+Na]^+$: 563.2979, found: 563.2967.

opt. act.: $[\alpha]_D^{25} = +42.0$ ($c = 1.0$, CHCl_3).

O-Ethyl (22*R*,23*R*)-1(10 \rightarrow 6)abeo-14,15-seco-3 α -acetoxy-14 β ,22 β :14 α ,23 β -diepoxy-ergosta-5,7,9,11-tetraen-15-ate (**S8**)



To a stirred solution of 11-ketone **S7** (22.9 mg, 42.4 µmol, 1.0 eq.) in MeOH (800 µL) was added NaBH₄ (1.9 mg, 50.8 µmol, 1.2 eq.) at 0 °C. After stirring for 15 min at this temperature water (4 mL) was added and the mixture was warmed to 25 °C. The aqueous phase was extracted with EtOAc (4 × 5 mL), the combined organic phases were washed with brine (5 mL) and dried over MgSO₄. The solvent was removed under reduced pressure and the crude 11-alcohol was redissolved in hexafluoroisopropanol (400 µL) and treated with 3 M H₂SO₄ (50 µL) at 0 °C. The mixture was stirred at this temperature for 2 h before adding sat. aq. NaHCO₃ (4 mL). The aqueous phase was extracted with CH₂Cl₂ (3 × 5 mL) and the combined organic phases were dried over MgSO₄. The solvent was removed under reduced pressure and column chromatography (SiO₂, *n*-hexane/EtOAc 6:1, *v/v*) gave 11,12-ene **S8** (13.8 mg, 26.3 µmol, 62%) as a colourless oil.

TLC: $R_f = 0.27$ (*n*hexane/EtOAc 6:1, *v/v*).

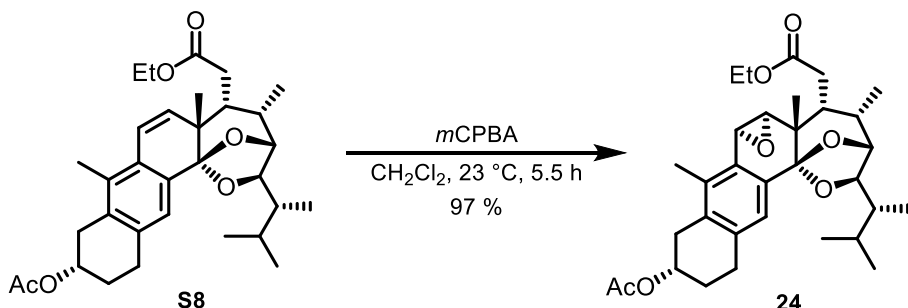
¹H-NMR: (400 MHz, CDCl₃); δ [ppm] = 7.14 (s, 1H), 6.66 (d, *J* = 10.1 Hz, 1H), 5.88 (d, *J* = 10.1 Hz, 1H), 5.24 – 5.14 (m, 1H), 4.21 – 4.15 (m, 3H), 3.65 (d, *J* = 9.5 Hz, 1H), 3.03 (dd, *J* = 16.9, 5.8 Hz, 1H), 2.93 – 2.84 (m, 3H), 2.73 – 2.64 (m, 2H), 2.60 (dd, *J* = 18.0, 4.3 Hz, 1H), 2.46 (q, *J* = 5.9 Hz, 1H), 2.17 (s, 3H), 2.07 (s, 3H), 2.03 – 1.98 (m, 1H), 1.94 – 1.84 (m, 1H), 1.77 (tt, *J* = 10.0, 5.0 Hz, 1H), 1.56 (dq, *J* = 6.7, 3.4 Hz, 1H), 1.29 (t, *J* = 7.2 Hz, 3H), 1.12 (s, 3H), 0.97 (d, *J* = 7.3 Hz, 3H), 0.78 (d, *J* = 7.0 Hz, 3H), 0.70 (d, *J* = 6.9 Hz, 3H), 0.66 (d, *J* = 6.9 Hz, 3H).

¹³C-NMR: (101 MHz, CDCl₃); δ [ppm] = 175.9, 170.9, 135.1, 134.9, 133.0, 132.2, 130.7, 129.1, 122.2, 121.8, 108.7, 82.7, 77.8, 70.6, 60.7, 43.7, 41.9, 40.6, 33.1, 32.4, 31.2, 27.6, 27.5, 26.2, 23.8, 21.6, 21.3, 16.0, 14.4, 14.3, 14.0, 10.4

HRMS: (ESI-TOF): m/z calcd for $C_{32}H_{44}O_6Na^+ [M+Na]^+$: 547.3030, found: 547.3021.

opt. act.: $[\alpha]_D^{30} = +9.0$ ($c = 1.0$, CHCl_3).

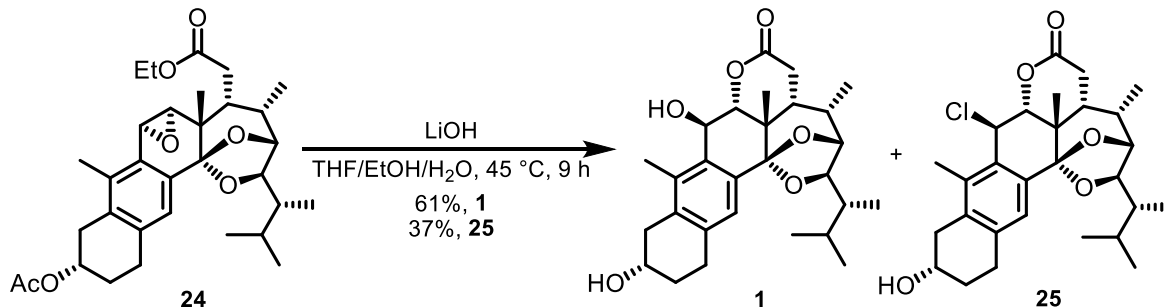
O-Ethyl (22*R*,23*R*)-1(10 \rightarrow 6)abeo-14,15-seco-3 α -acetoxy-11 α ,12 α :14 β ,22 β :14 α ,23 β -triepoxy-ergosta-5,7,9-trien-15-ate (**24**)



To a stirred solution of 11,12-ene **S8** (3.4 mg, 6.48 µmol, 1.0 eq.) in CH₂Cl₂ (130 µL) was added *meta*-chloroperoxybenzoic acid (2.2 mg, 9.72 µmol, 1.5 eq.) at 25 °C. After 5.5 h the mixture was diluted with CH₂Cl₂ (4 mL) and washed with sat. aq. Na₂S₂O₃ (3 mL). The aqueous phase was extracted with CH₂Cl₂ (3 × 5 mL), the combined organic phases were washed with sat. aq. NaHCO₃ (5 mL) and dried over MgSO₄. The solvent was removed under reduced pressure and column chromatography (SiO₂, *n*hexane/EtOAc 3:1, v/v) gave epoxide **24** (3.4 mg, 6.29 µmol, 97%) as a colourless oil.

TLC:	$R_f = 0.28$ (<i>n</i> hexane/EtOAc 3:1, v/v).
¹H-NMR:	(400 MHz, CDCl ₃); δ [ppm] = 7.23 (s, 1H), 5.23 – 5.15 (m, 1H), 4.20 – 4.12 (m, 4H), 3.67 (d, $J = 9.6$ Hz, 1H), 3.41 (d, $J = 4.4$ Hz, 1H), 3.30 (dd, $J = 17.7, 6.2$ Hz, 1H), 3.03 (dd, $J = 16.9, 5.5$ Hz, 1H), 2.86 (s, 1H), 2.74 – 2.58 (m, 4H), 2.34 (s, 3H), 2.07 (s, 3H), 2.03 – 1.98 (m, 1H), 1.92 – 1.79 (m, 2H), 1.62 (s, 1H), 1.56 (ddd, $J = 9.9, 6.9, 3.1$ Hz, 1H), 1.28 (t, $J = 7.1$ Hz, 3H), 0.98 (d, $J = 6.9$ Hz, 6H), 0.78 (d, $J = 7.0$ Hz, 3H), 0.70 (d, $J = 4.8$ Hz, 3H), 0.69 (d, $J = 4.7$ Hz, 3H).
¹³C-NMR:	(101 MHz, CDCl ₃); δ [ppm] = 175.8, 170.9, 136.7, 136.1, 133.3, 132.7, 128.6, 123.6, 106.2, 82.4, 78.3, 70.4, 60.7, 59.1, 47.6, 42.0, 40.8, 40.8, 33.1, 31.4, 31.2, 27.6, 27.5, 26.0, 22.4, 21.6, 21.4, 15.9, 14.5, 14.4, 13.7, 10.3.
HRMS:	(ESI-TOF); <i>m/z</i> calcd. for C ₃₂ H ₄₄ O ₇ Na ⁺ [M+Na] ⁺ : 563.2979, found: 563.2986.
opt. act.:	[\mathcal{α}]_D^{30} = -32.0 (c = 1.0, CHCl ₃).

Asperfloketal A (**1**) and 11-Chloro asperfloketal A (**25**)



To a stirred solution of epoxide **24** (3.0 mg, 5.55 µmol, 1.0 eq.) in a mixture of THF/EtOH/H₂O (1:1:1, 110 µL) was added LiOH (0.7 mg, 27.7 µmol, 5.0 eq.). The solution was heated to 45 °C and stirred at this temperature for 9 h. H₂O (2 mL) was added and the solution was acidified with 1 M HCl (3–4 drops) till precipitation occurred. CH₂Cl₂ (1 mL) was added, the aqueous phase was extracted with CH₂Cl₂ (3 × 2 mL), and the combined organic phases were dried over MgSO₄. The solvent was removed under reduced pressure and column chromatography (SiO₂, *n*hexane/EtOAc 1:1 → 0:1, v/v) gave asperfloketal A (**1**) (1.6 mg, 3.40 µmol, 61%) as an amorphous colourless solid and 11-chloride **25** (1.0 mg, 2.05 µmol, 37%) as a colourless oil.

Asperfloketal A (**1**)

TLC:	$R_f = 0.25$ (EtOAc).
¹H-NMR:	(600 MHz, CDCl ₃); δ [ppm] = 7.17 (s, 1H), 5.14 (d, $J = 4.4$ Hz, 1H), 4.59 (d, $J = 1.7$ Hz, 1H), 4.19 (d, $J = 3.5$ Hz, 1H), 4.11 (dd, $J = 11.1, 8.5, 5.4, 3.2$ Hz, 1H), 3.65 (d, $J = 10.5$ Hz, 1H), 3.08 – 3.02 (m, 1H), 2.86 (q, $J = 6.2$ Hz, 2H), 2.80 – 2.73 (m, 2H), 2.56 (dd, $J = 16.7, 8.2$ Hz, 1H), 2.51 (dd, $J = 18.3, 13.2$ Hz, 1H), 2.27 (s, 3H), 2.24 (dt, $J = 9.4, 2.9$ Hz, 1H), 2.07 – 2.00 (m, 1H), 1.94 (d, $J = 5.8$ Hz, 1H), 1.82 (td, $J = 7.0, 3.0$ Hz, 1H), 1.79 – 1.73 (m, 1H), 1.62 (ddd, $J = 10.2,$

6.8, 3.1 Hz, 2H), 1.30 (s, 3H), 1.04 (d, J = 7.3 Hz, 3H), 0.78 (d, J = 7.1 Hz, 3H), 0.69 (d, J = 6.8 Hz, 3H), 0.63 (d, J = 6.9 Hz, 3H).

$^{13}\text{C-NMR}$: (151 MHz, CDCl_3); δ [ppm] = 171.7, 137.4, 136.7, 135.6, 131.1, 130.9, 123.5, 106.1, 83.4, 82.8, 78.0, 68.0, 67.9, 41.9, 37.9, 37.0, 35.7, 31.4, 30.3, 28.2, 28.1, 25.7, 22.5, 21.1, 15.4, 14.8, 13.2, 10.2.

HRMS: (ESI-TOF); m/z calcd. for $\text{C}_{28}\text{H}_{38}\text{O}_6\text{Na}^+ [\text{M}+\text{Na}]^+$: 493.2561, found: 493.2548.

opt. act.: $[\alpha]_D^{27} = -24.0$ (c = 0.5, CHCl_3).

11-Chloro asperfloketal A (25)

TLC: R_f = 0.31 (*n*hexane/EtOAc 1:1, *v/v*).

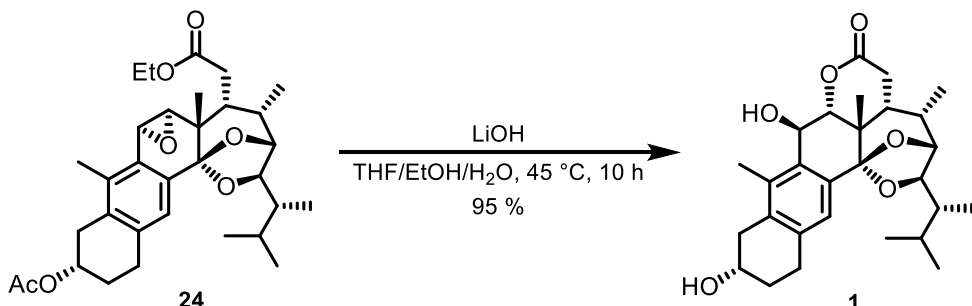
$^1\text{H-NMR}$: (500 MHz, CDCl_3); δ [ppm] = 7.18 (s, 1H), 5.43 (d, J = 1.6 Hz, 1H), 4.88 (d, J = 1.5 Hz, 1H), 4.21 (d, J = 3.5 Hz, 1H), 4.18 – 4.10 (m, 1H), 3.62 (d, J = 10.5 Hz, 1H), 3.07 (ddd, J = 16.6, 5.6, 1.5 Hz, 1H), 2.87 (dd, J = 7.8, 5.3 Hz, 2H), 2.81 – 2.74 (m, 2H), 2.56 (dd, J = 16.7, 8.5 Hz, 1H), 2.50 (dd, J = 18.3, 13.2 Hz, 1H), 2.30 (s, 3H), 2.27 (dq, J = 9.4, 3.2 Hz, 1H), 2.05 (dddd, J = 10.4, 6.6, 5.8, 3.2 Hz, 1H), 1.81 – 1.70 (m, 2H), 1.61 (ddt, J = 10.2, 6.8, 2.9 Hz, 2H), 1.44 (s, 3H), 1.04 (d, J = 7.3 Hz, 3H), 0.77 (d, J = 7.1 Hz, 3H), 0.68 (d, J = 6.8 Hz, 3H), 0.62 (d, J = 6.9 Hz, 3H).

$^{13}\text{C-NMR}$: (151 MHz, CDCl_3); δ [ppm] = 170.8, 138.1, 137.4, 135.8, 131.4, 128.4, 123.5, 105.7, 84.0, 82.8, 77.9, 68.0, 54.4, 41.8, 37.6, 37.1, 36.2, 31.4, 30.3, 28.4, 28.1, 25.7, 23.3, 21.1, 16.1, 14.8, 13.2, 10.2.

HRMS: (ESI-TOF); m/z calcd. for $\text{C}_{28}\text{H}_{37}\text{O}_6\text{ClNa}^+ [\text{M}+\text{Na}]^+$: 511.2222, found: 511.2225.

opt. act.: $[\alpha]_D^{27} = +25.3$ (c = 0.4, CHCl_3).

Asperfloketal A (1)



To a stirred solution of epoxide **24** (3.4 mg, 6.29 μmol , 1.0 eq.) in a mixture of THF/EtOH/H₂O (1:1:1, 130 μL) was added LiOH (0.8 mg, 31.4 μmol , 5.0 eq.). The solution was heated to 45 °C and stirred at this temperature for 10 h. H₂O (2 mL) was added and the solution was acidified with 0.1 M H₂SO₄ till precipitation occurred. CH₂Cl₂ (1 mL) was added, the aqueous phase was extracted with CH₂Cl₂ (3 \times 2 mL), and the combined organic phases were dried over MgSO₄. The solvent was removed under reduced pressure and preparative TLC (SiO₂, EtOAc) gave asperfloketal A (**1**) (2.8 mg, 5.95 μmol , 95%) as an amorphous colourless solid.

4 NMR Comparison

Table 1 NMR comparison of natural asperfloketal A (**1**) and synthetic material.

#	¹ H-NMR		¹³ C-NMR	
	natural	synthetic	natural	synthetic
1	2.86 m	2.86 q (5.9)	28.2	28.2
2	1.76 m, 2.04 m	1.76 m, 2.03 m	31.4	31.4
3	4.13 m	4.12 dddd (9.7, 8.4, 5.4, 3.2)	68.0	68.0
4	2.57 dd (16.6, 8.3), 3.07 dd (16.6, 5.4)	2.56 dd (16.7, 8.3) 3.05 ddd (16.7, 5.4, 1.4)	37.0	37.0
5	---	---	136.8	135.6
6	---	---	135.7	136.8
7	7.17 s	7.17 s	123.5	123.5
8	---	---	131.1	130.9
9	---	---	130.8	131.1
10	---	---	137.4	137.4
11	5.13 brs	5.14 brs	68.0	67.9
12	4.60 d (1.7)	4.60 d (1.7)	83.3	83.4
13	---	---	35.7	35.7
14	---	---	106.0	106.1
15	---	---	171.7	171.7
16	2.77 dd (18.3, 3.2), 2.52 dd (18.3, 13.2)	2.76 m 2.51 dd (18.3, 13.2)	28.2	28.2
17	2.25 ddd (13.3, 6.5, 2.9)	2.24 dq (9.3, 3.2)	37.9	37.9
18	1.30 s	1.30 s	22.5	22.5
19	2.31 s	2.28 s	15.5	15.4
20	2.76 m	2.76 m	30.3	30.3
21	1.04 d (7.3)	1.04 d (7.3)	13.2	13.2
22	4.19 d (3.5)	4.19 d (3.5)	82.8	82.8
23	3.65 d (10.5)	3.65 d (10.5)	78.0	78.0
24	1.62 m	1.61 td (7.0, 3.5)	41.9	41.9
25	1.82 m	1.82 td (7.0, 3.0)	25.7	25.7
26	0.63 d (6.8)	0.63 d (6.9)	14.8	14.8
27	0.78 d (7.1)	0.78 d (7.3)	21.1	21.1
28	0.69 d (6.8)	0.69 d (6.8)	10.2	10.2

All chemical shifts are reported in ppm. Coupling constants are given in parentheses and are reported in Hz. m = centered multiplet. All spectra were measured in CDCl₃ and are referenced to the residual solvent peak at δH = 7.26 ppm and δC = 77.16 ppm as done in the original isolation report.^[1] ¹H-NMR spectra were recorded at 500 MHz. ¹³C-NMR spectra were recorded at 151 MHz. Blue highlights indicate reassessments to the original isolation report (see paragraph 5).

5 Correction of original ^{13}C -NMR assignments from isolation report

Some assignments of signals in the original isolation report and our analysis differ slightly. The assignment of C5 and C9 in the ^{13}C -NMR spectrum can be supported by ^1H - ^{13}C -HMBC experiment which confirms that the signals at 135.6 ppm and 131.1 ppm correspond to those atoms (Figure 1). Further analysis shows, while the signal at 131.1 ppm correlates with 11-CH and 12-CH, no correlation with the signal at 135.6 ppm can be observed (Figure 2). Also, a fairly strong correlation of the signal at 135.6 ppm with 4-CH₂ can be seen and a weaker one with 3-CH. Only a very weak correlation of the signal at 131.1 ppm can be observed with 4-CH₂. This leads us to believe, that the original assignment by the isolators is switched and the signal at 131.1 ppm should be assigned to C9 and the signal at 135.6 ppm to C5.

For the assignments of C6 and C8 the signals at 130.9 ppm and 136.8 ppm can be identified. While the signal at 136.8 ppm correlates with 1-CH₂ and 2-CH₂, no such correlation can be seen with the signal at 130.9 ppm (Figures 3 and 4). It is not possible to confirm a correlation between the signal at 130.9 ppm and for instance 11-CH due to overlapping correlations, but due to the process of elimination, we are confident that the signal at 136.8 ppm should be assigned to C6, while the signal at 130.9 ppm should be assigned to C8.

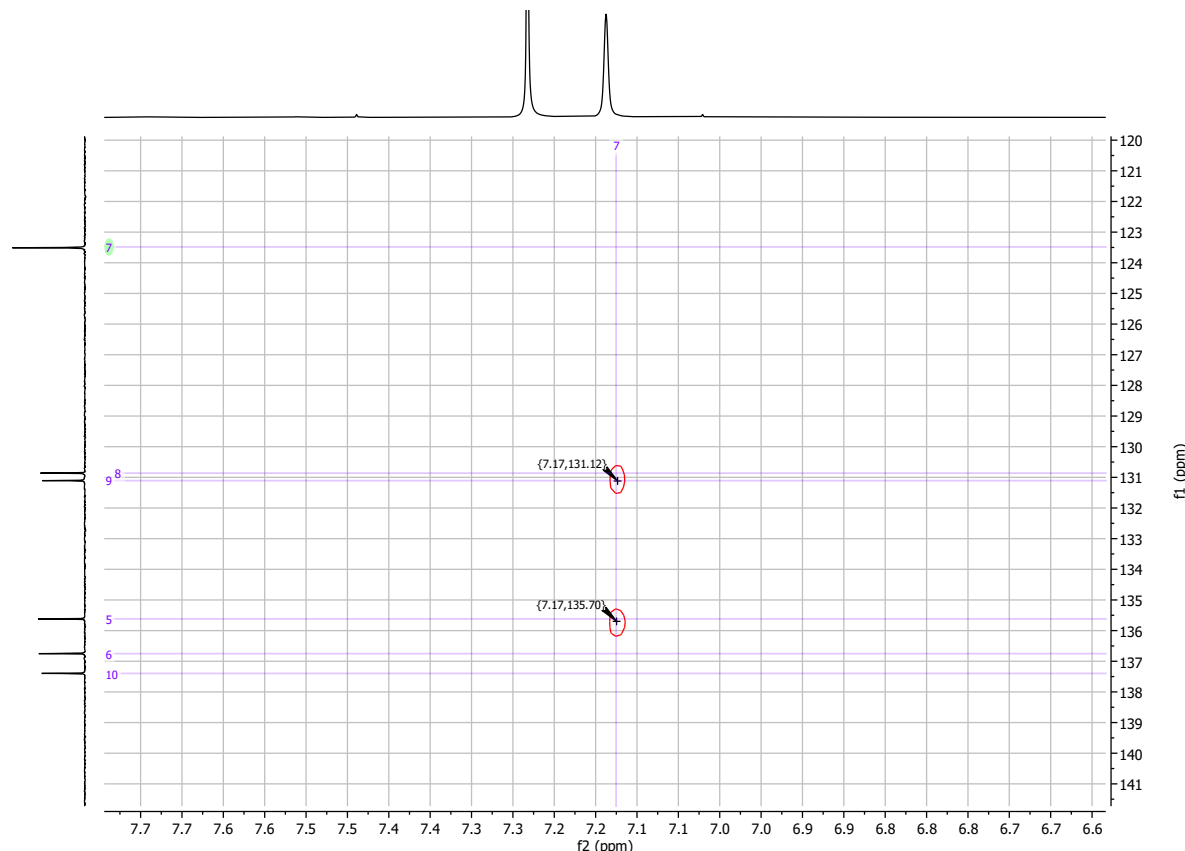


Figure 1: ^1H - ^{13}C -HMBC spectrum of asperfloketal A (**1**) (detail 1).

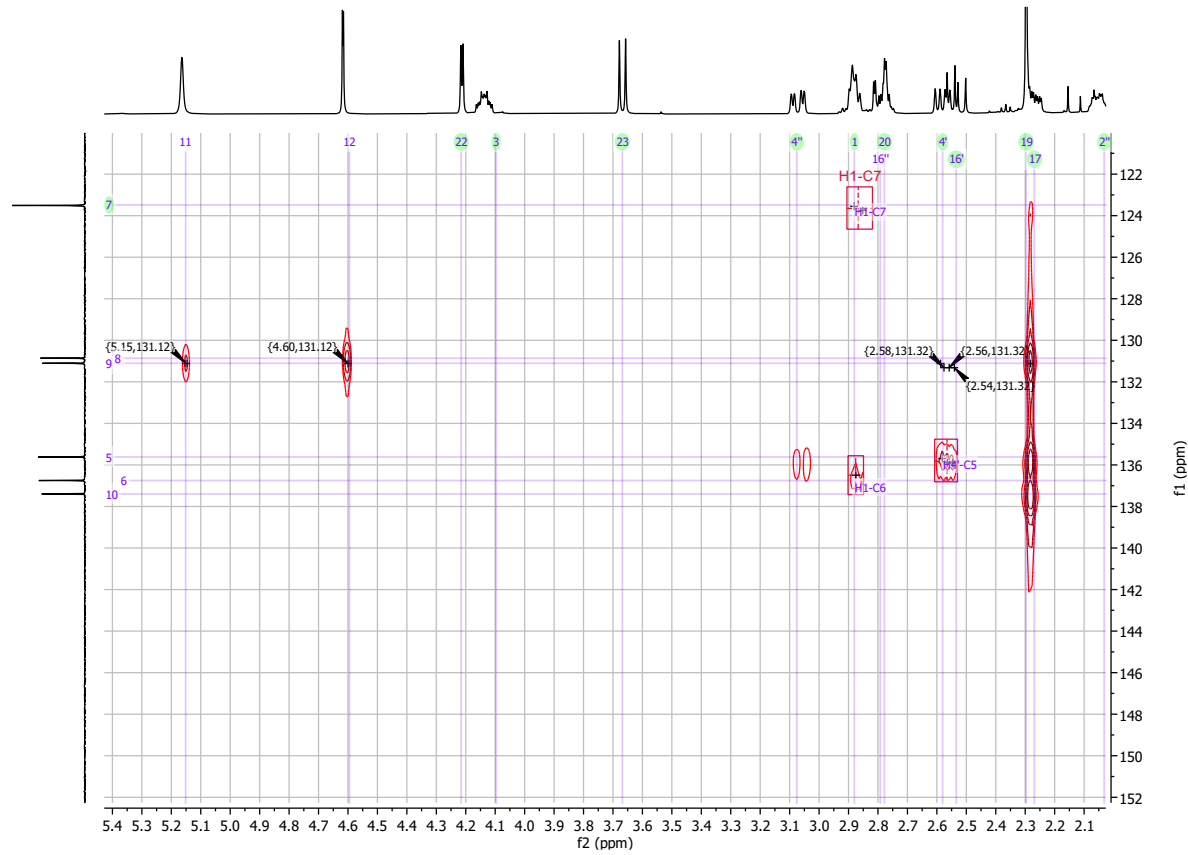


Figure 2: ^1H - ^{13}C -HMBC spectrum of asperfloketal A (1) (detail 2).

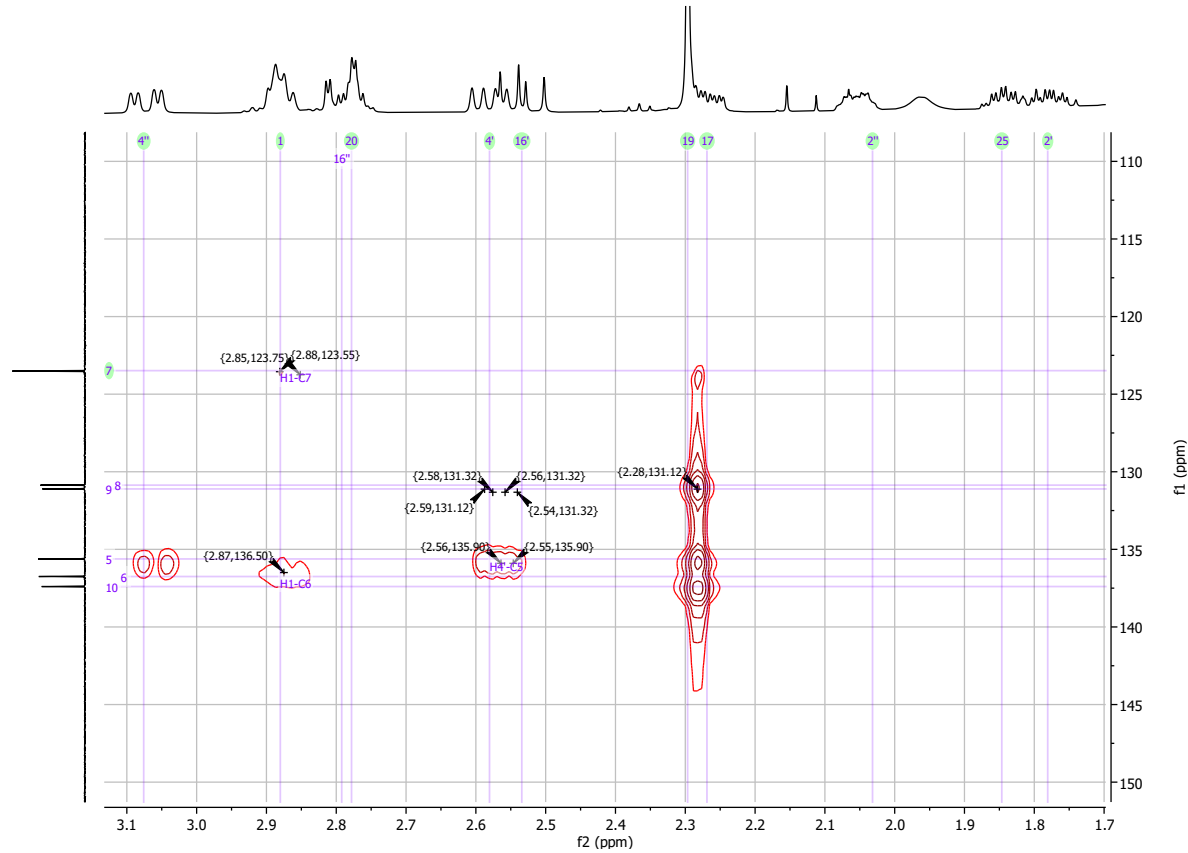


Figure 3: ^1H - ^{13}C -HMBC spectrum of asperfloketal A (1) (detail 3).

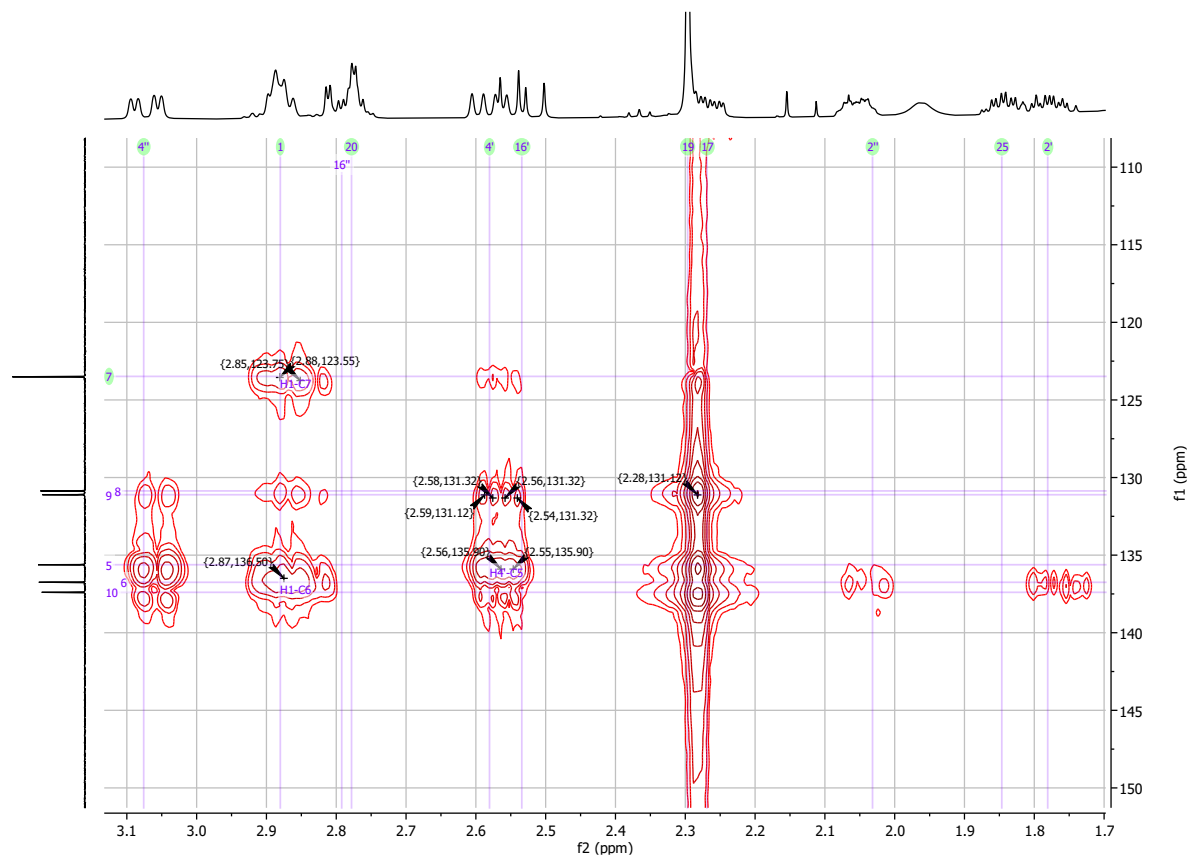
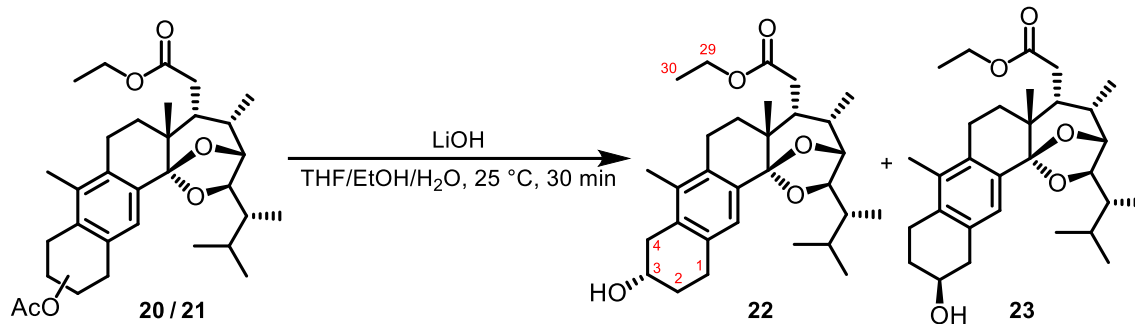


Figure 4: ¹H-¹³C-HMBC spectrum of asperfloketal A (**1**) (detail 4).

6 Characterization of mixture 20/21



The mixture of **20/21** was not separable by standard methods. To confirm the presence of both, the 3 α **22** and 2 β **23** compound, we selectively deprotected the acetyl group [procedure same as **24** \rightarrow **1**, @25 °C, stopped after 30 min (TLC indicates only deprotection of acetate, but not of ethyl ester)] and then separated the mixture by preparative TLC (SiO₂, toluene:Et₂O 3:1, v/v).

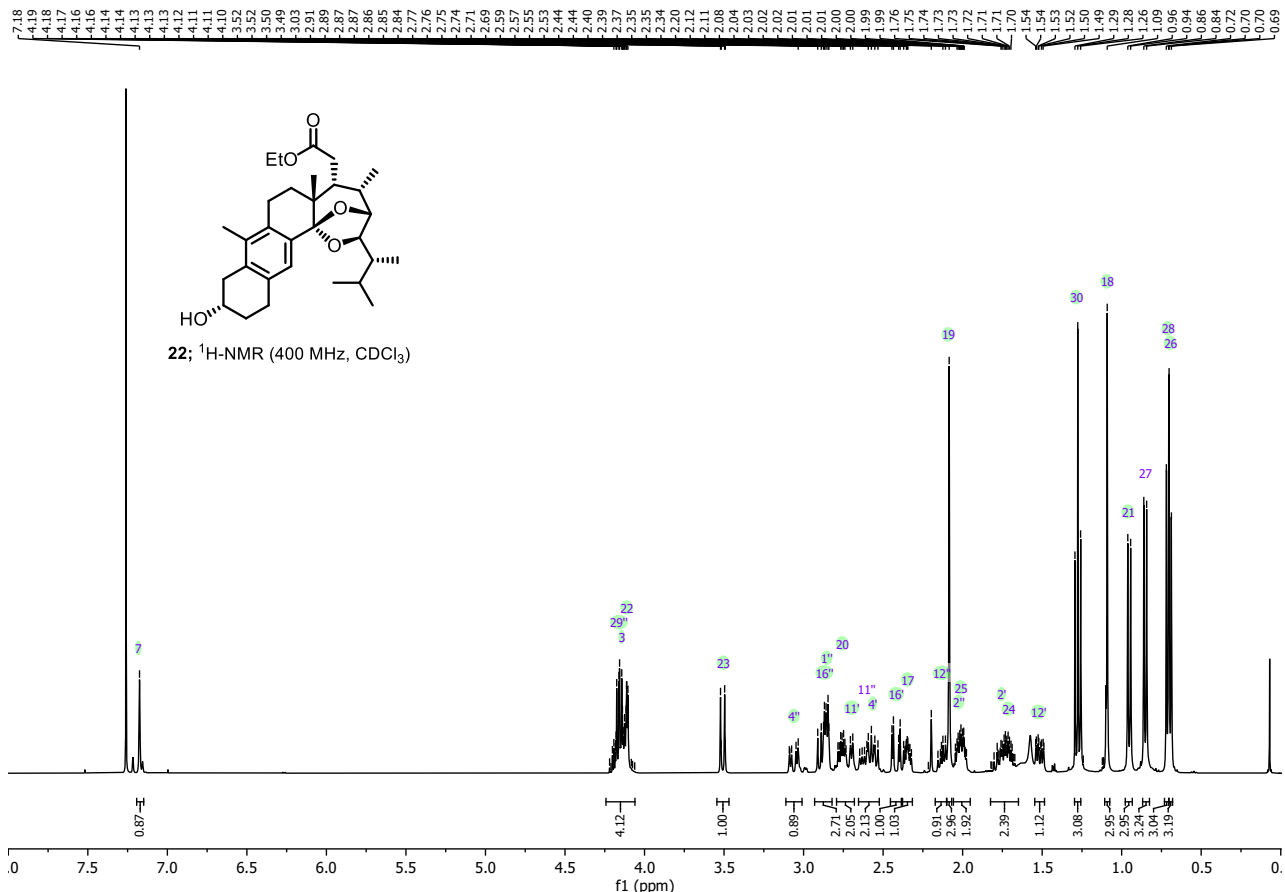
Acetylation of alcohols **22** and **23** was performed under standard conditions (Ac₂O (4.0 eq.), NEt₃ (6.0 eq.), DMAP (0.1 eq.) in CH₂Cl₂ (0.4 M) @ 25 °C for 2 h).

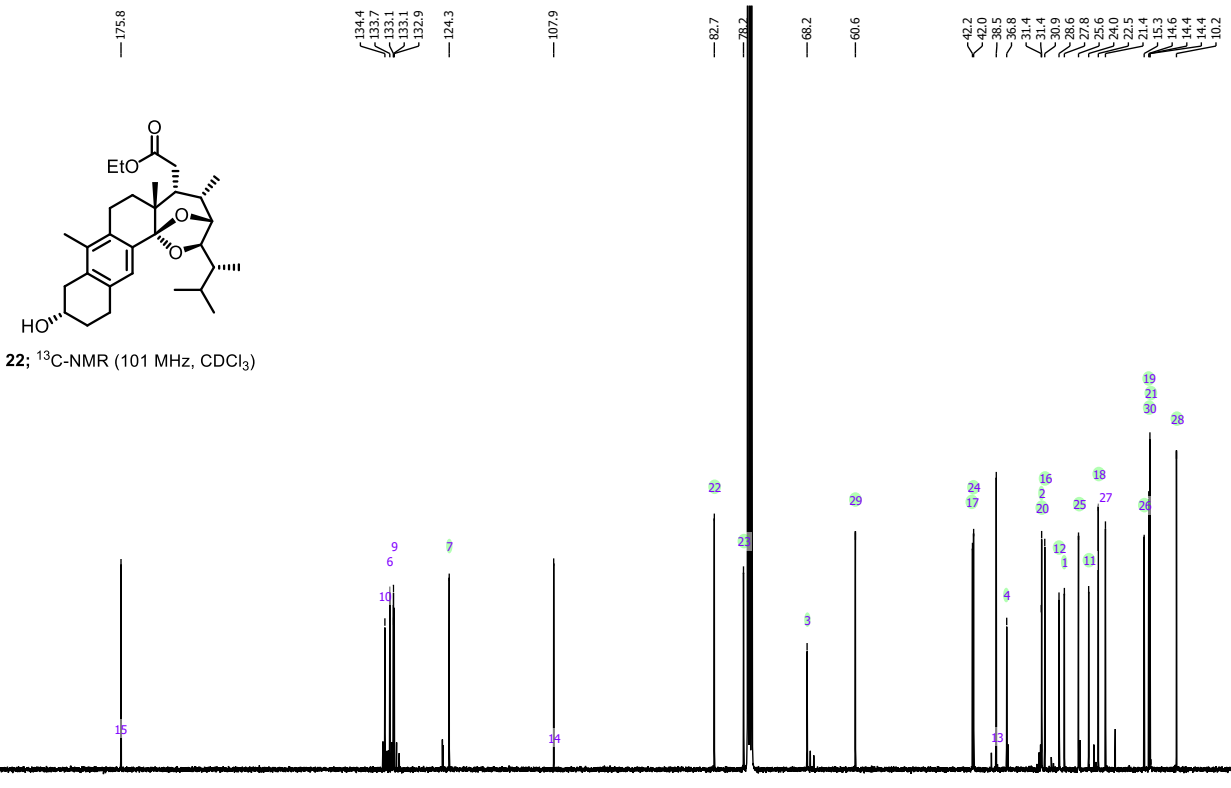
Table 2 NMR comparison of 3 α -alcohol **22** and 2 β -alcohol **23**.

#	3 α -alcohol 22	¹³ C-NMR	2 β -alcohol 23	¹³ C-NMR
1	2.87 m	27.8	2.86 m, 2.52 dd (16.6, 8.8)	36.3
2	2.01 m, 1.74 dddd (17.2, 10.1, 8.3, 5.4)	31.4	4.09 m	67.9
3	4.14 m	68.2	2.10 m, 1.74 m	31.4
4	3.06 dd (16.8, 5.6), 2.59 m	36.8	2.86 m, 2.64 ddd (17.1, 10.4, 6.1)	25.7
5	---	not assignable	---	134.3
6	---	133.7	---	132.1
7	7.18 s	124.3	7.20 s	125.4
8	---	not assignable	---	132.7
9	---	132.9	---	133.2
10	---	134.4	---	134.2
11	2.74 m, 2.59 m	24.0	2.57 m	23.2
12	2.13 m, 1.51 ddd (12.7, 6.0, 1.8)	28.6	2.10 m, 1.51 m	28.6
13	---	38.5	---	38.5
14	---	107.9	---	107.9
15	---	175.8	---	175.8
16	2.87 m, 2.42 dd (17.0, 3.8)	30.9	2.86 m, 2.42 dd (17.0, 3.8)	30.9
17	2.35 m	42.2	2.35 m	42.2
18	1.09 s	22.5	1.10 s	22.5
19	2.08 s	14.6	2.19 s	19.9
20	2.74 m	31.4	2.77 td (7.1, 3.2)	31.5

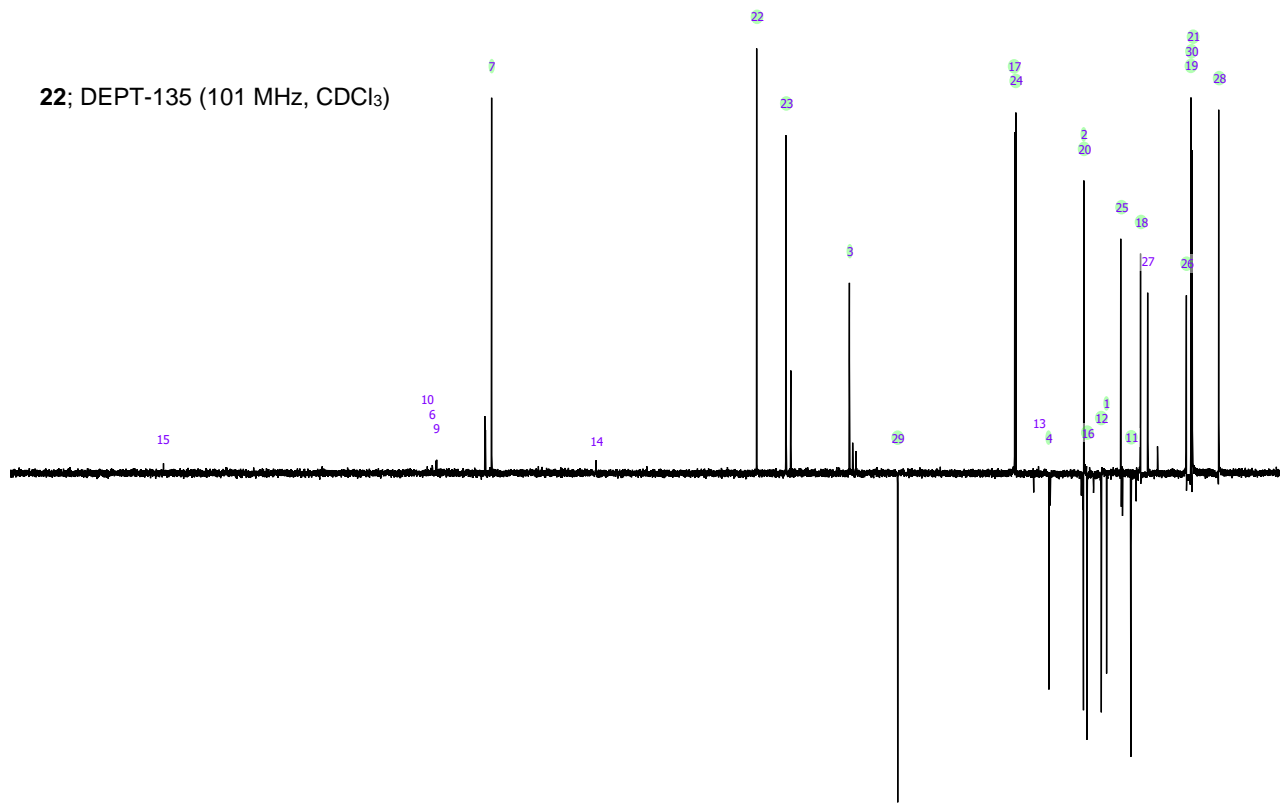
21	0.95 d (7.3)	14.4	0.95 d (7.3)	14.4
22	4.14 m	82.7	4.12 d (3.2)	82.7
23	3.51 dd (10.4, 1.7)	78.2	3.50 d (10.4)	78.1
24	1.74 dddd (17.2, 10.1, 8.3, 5.4)	42.0	1.74 m	42.0
25	2.01 m	25.6	1.99 pd (7.0, 2.8)	25.6
26	0.69 d (5.7)	15.3	0.70 d (6.8)	15.3
27	0.85 (7.0)	21.4	0.85 (7.1)	21.3
28	0.71 d (5.7)	10.2	0.71 d (6.9)	10.2
29	4.14 m	60.6	4.16 dddd (14.3, 10.2, 7.2, 3.6)	60.6
30	1.28 t (7.1)	14.4	1.27 (7.2)	14.4

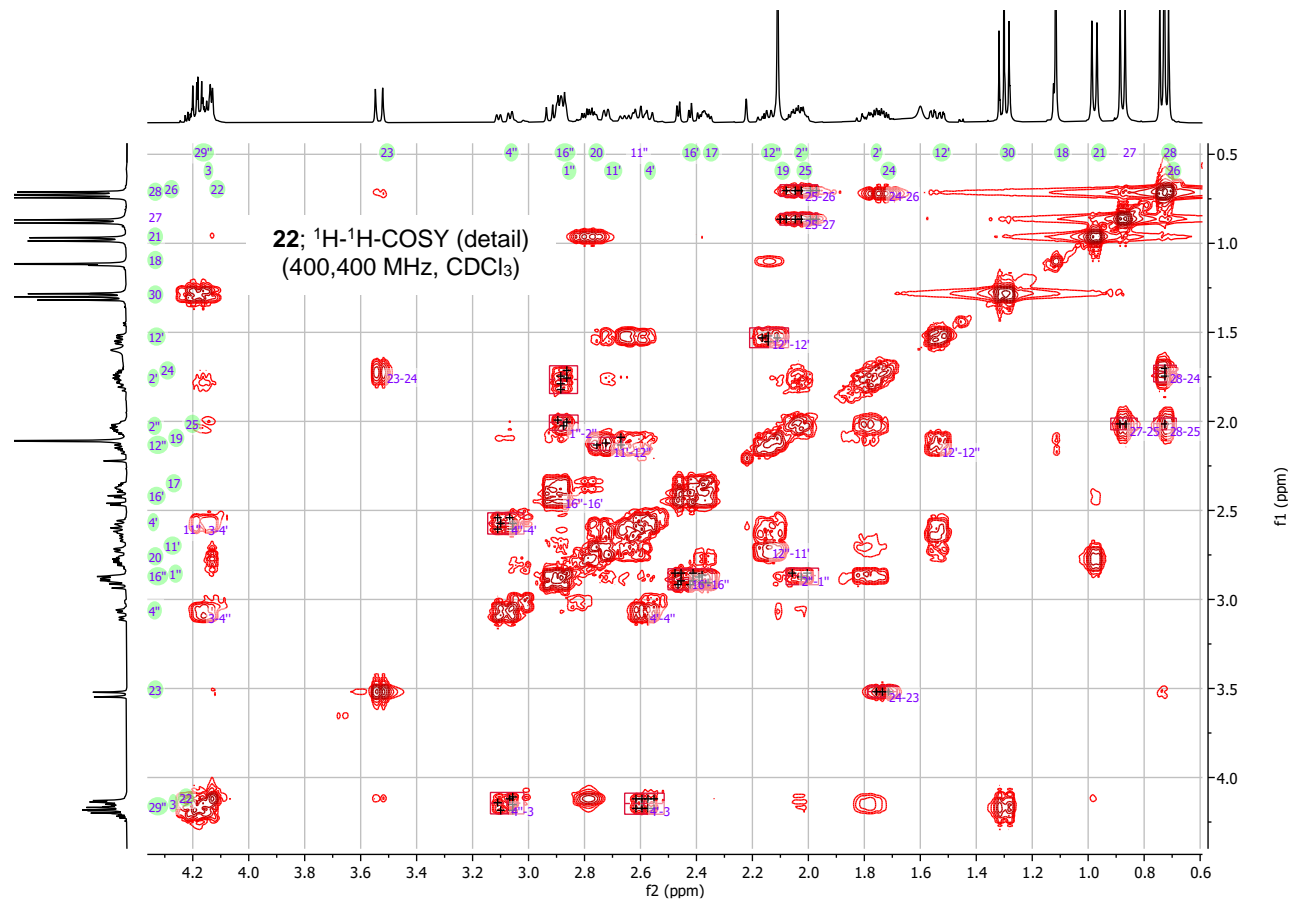
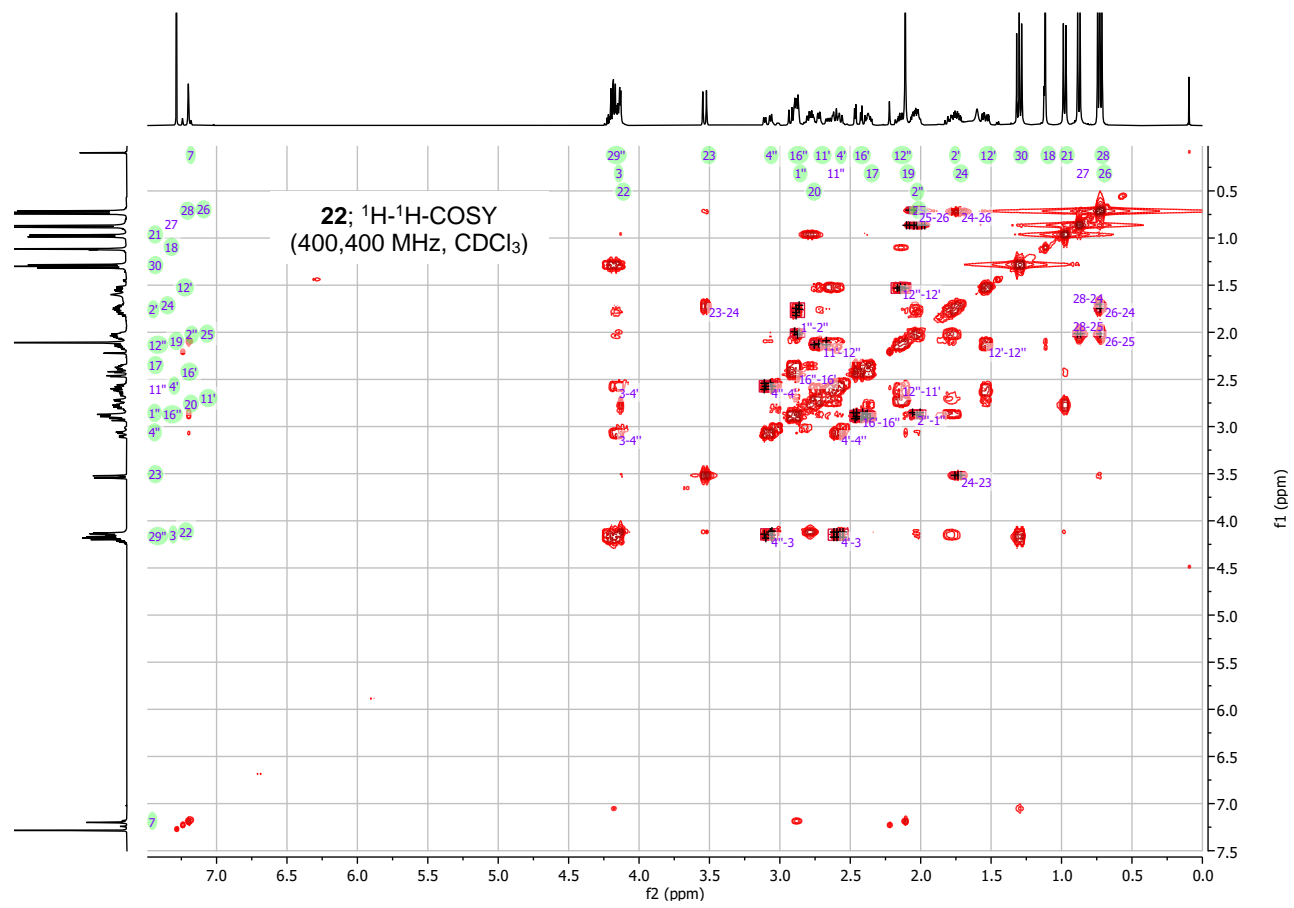
All chemical shifts are reported in ppm. Coupling constants are given in parentheses and are reported in Hz. m = centered multiplet. All spectra were measured in CDCl_3 and are referenced to the residual solvent peak at $\delta\text{H} = 7.26$ ppm and $\delta\text{C} = 77.16$ ppm. $^1\text{H-NMR}$ spectra were recorded at 400 MHz and 500 MHz. $^{13}\text{C-NMR}$ spectra were recorded at 101 MHz and 151 MHz.

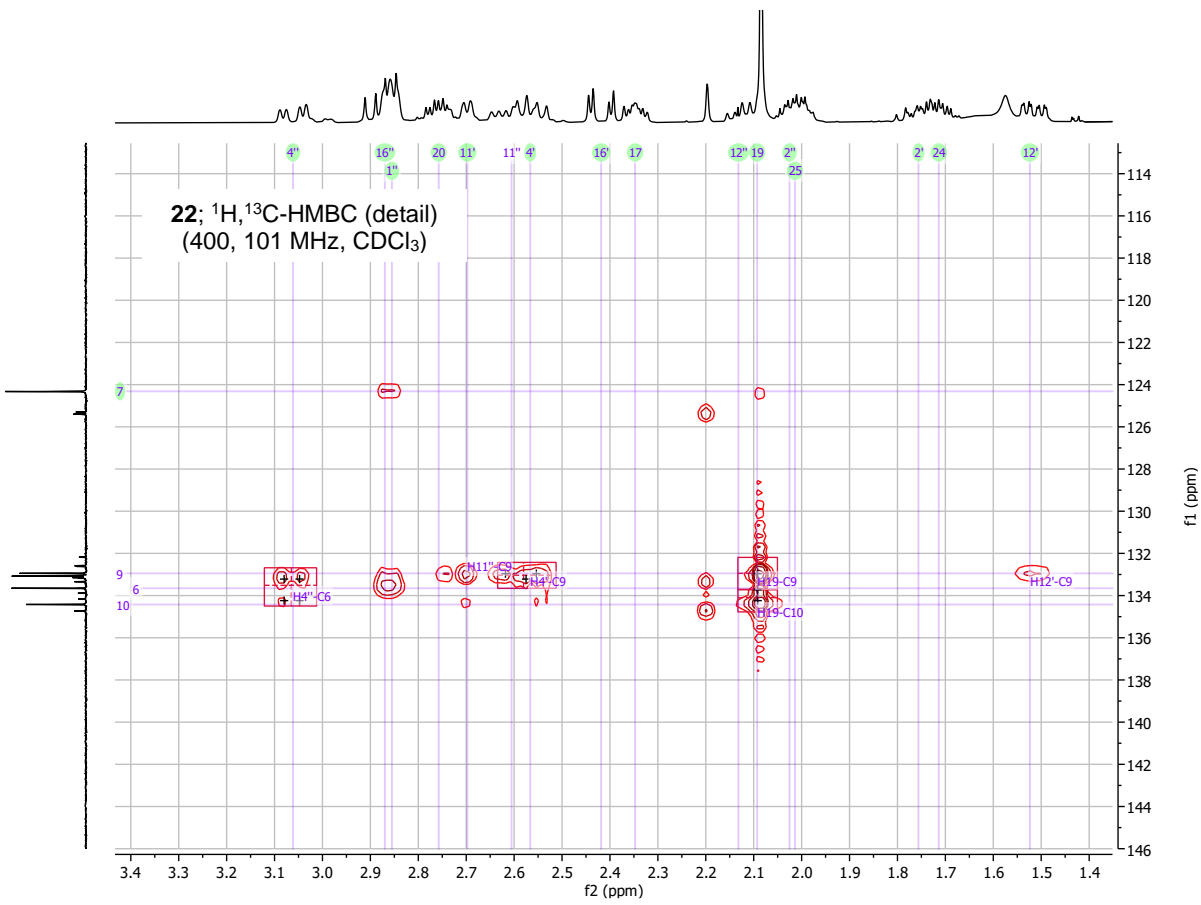
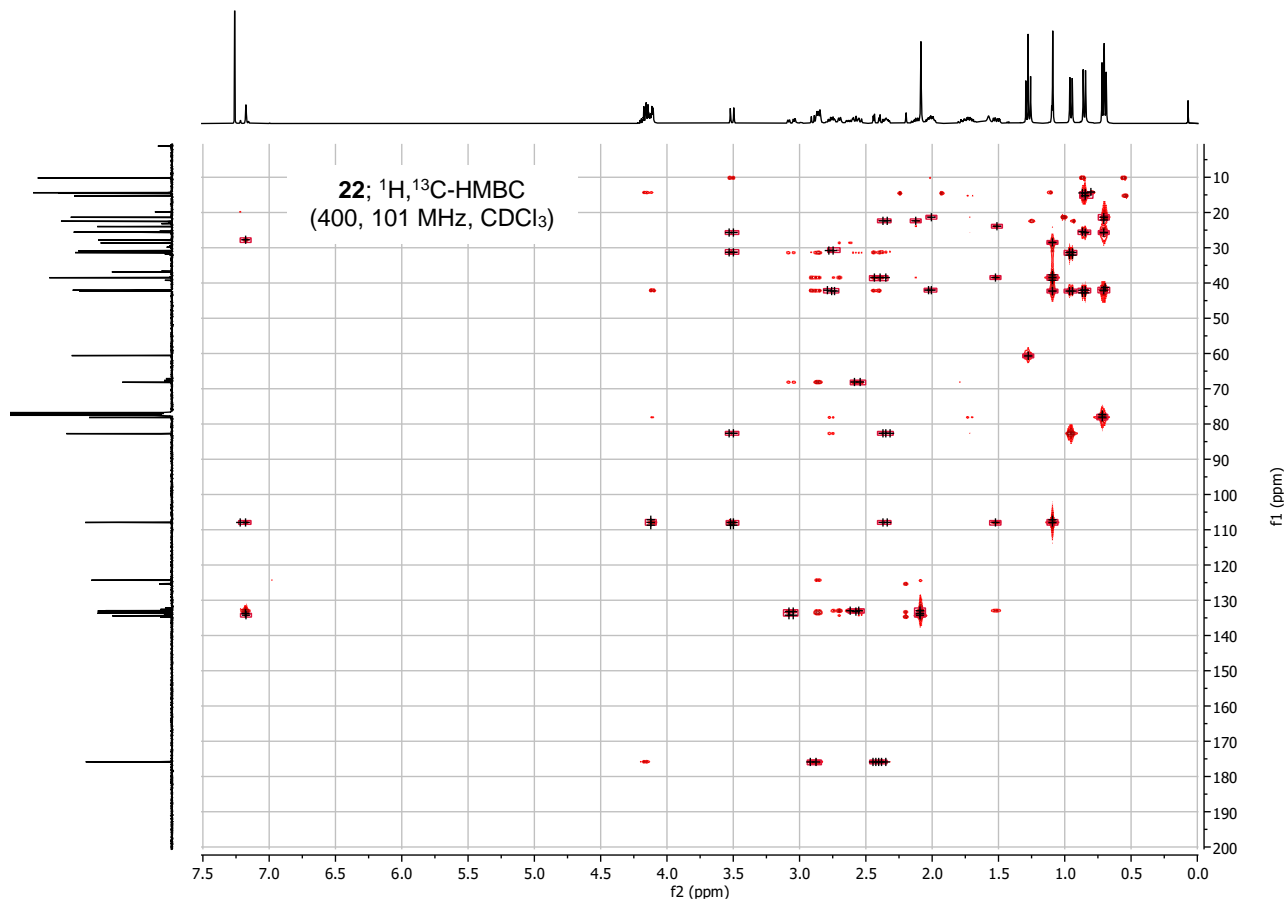


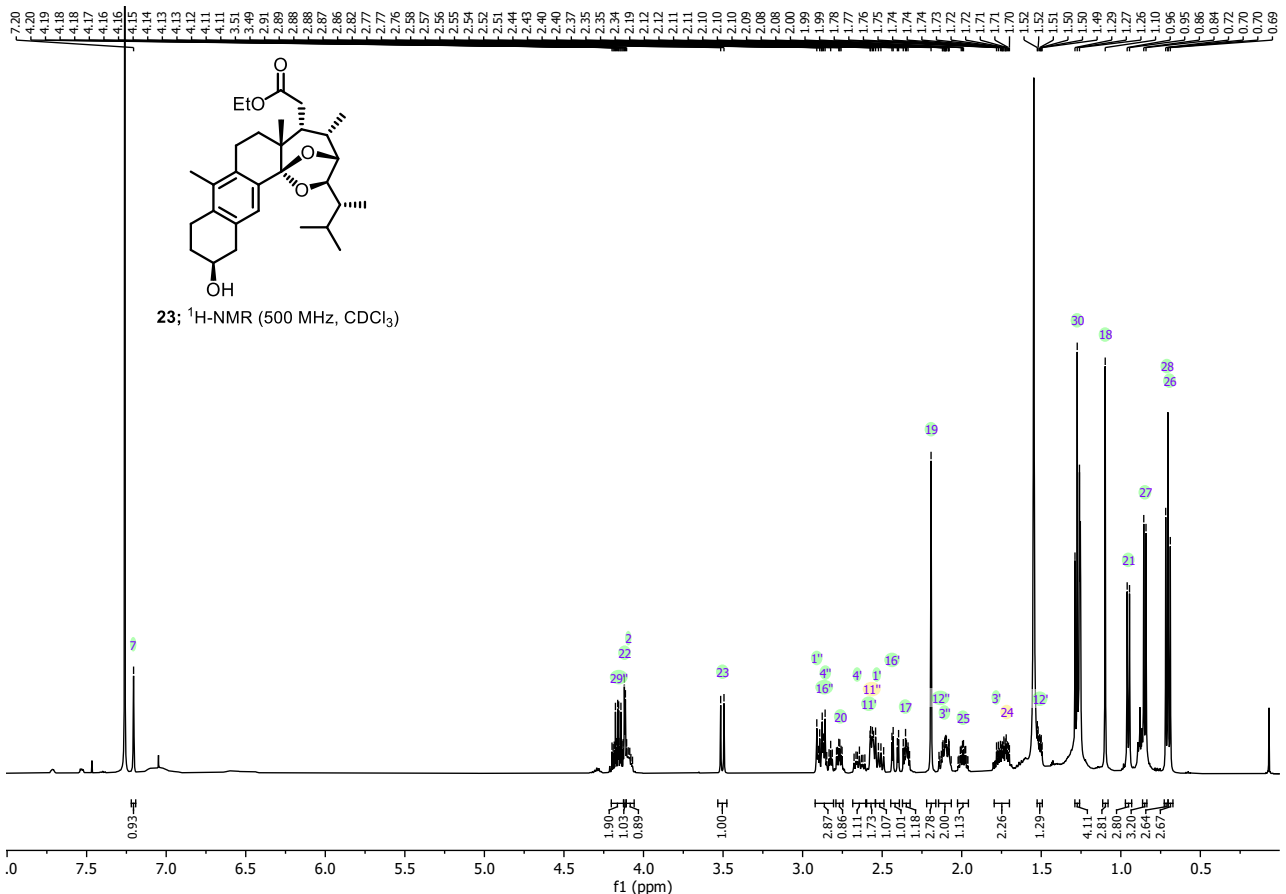
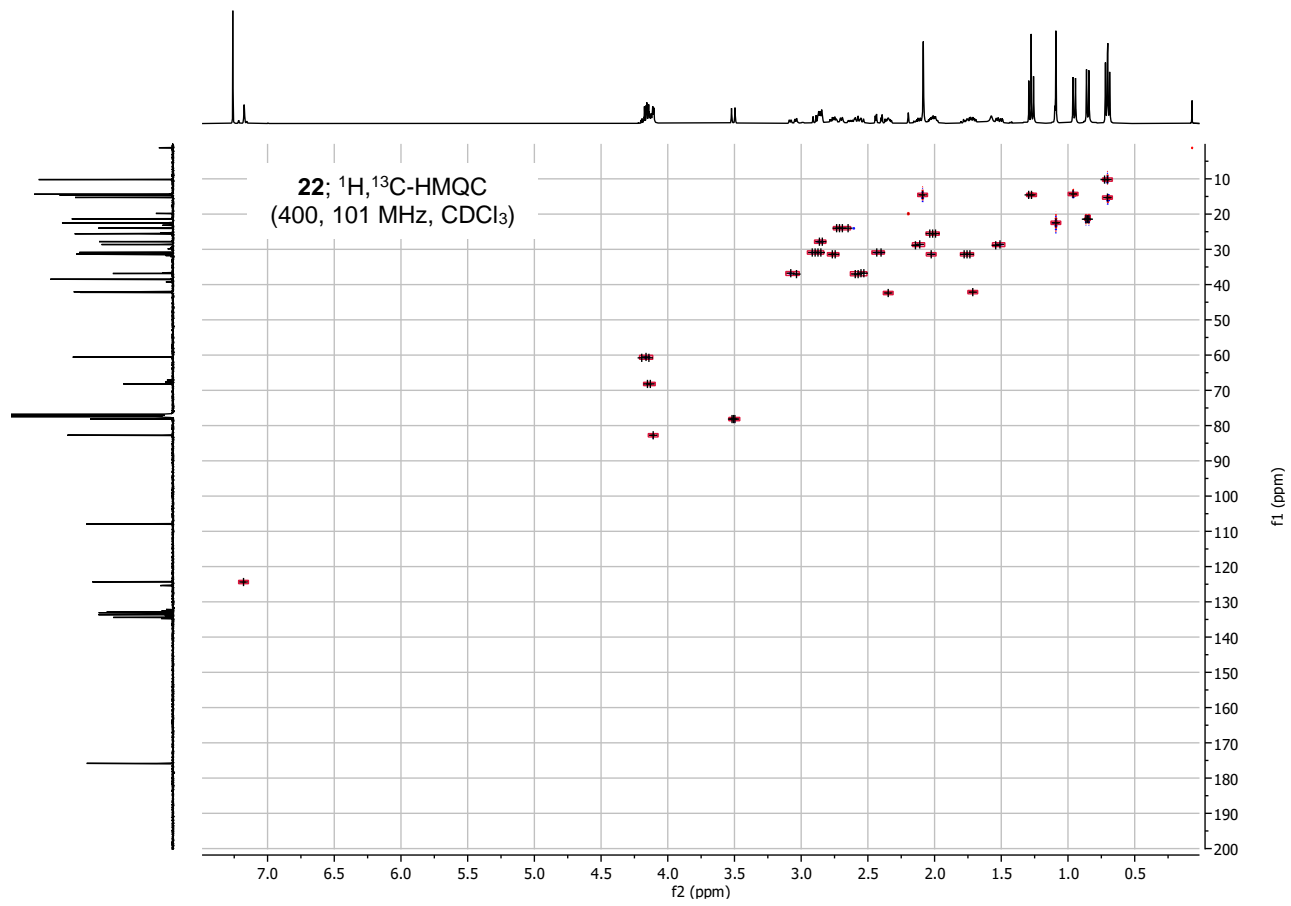


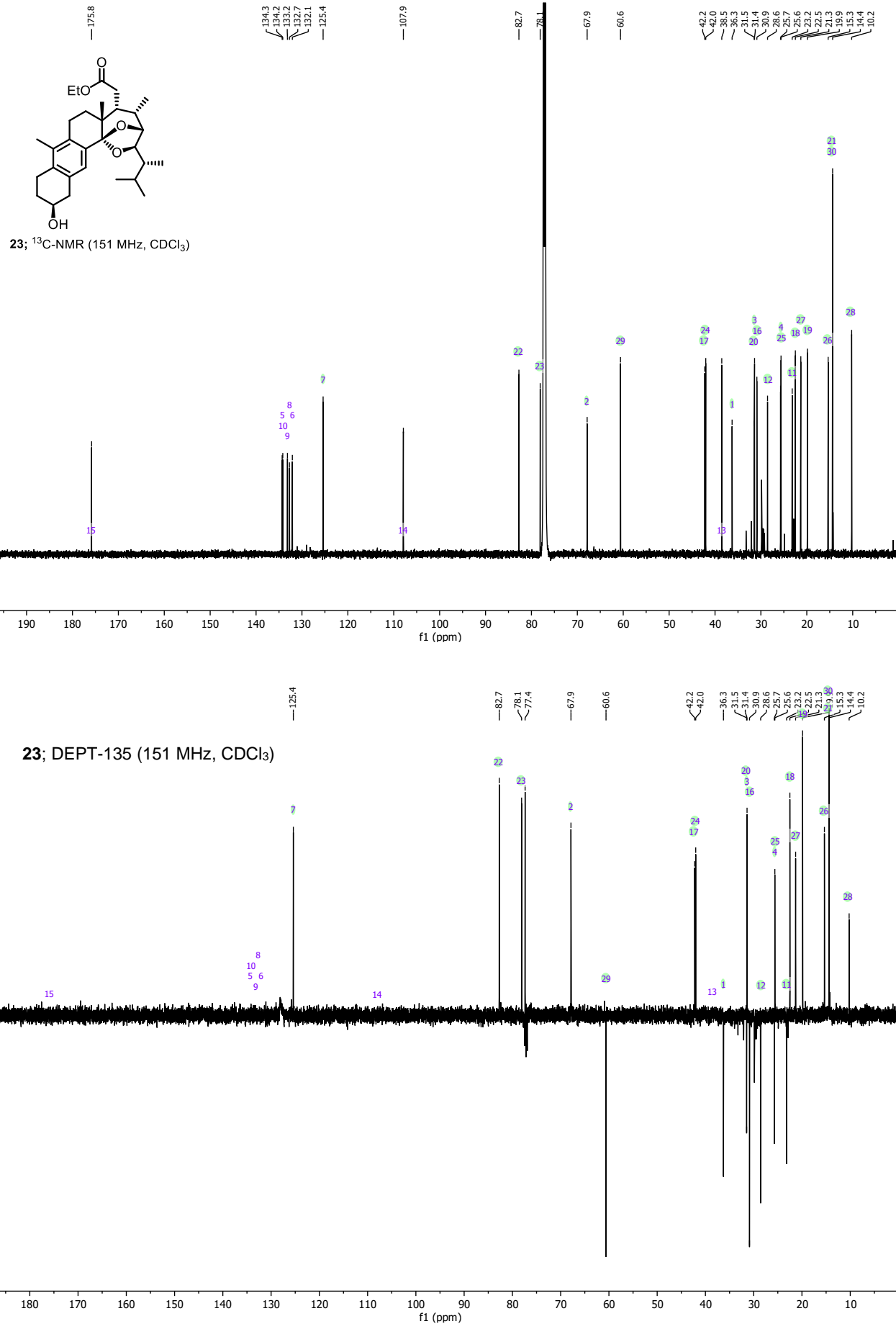
22; DEPT-135 (101 MHz, CDCl₃)

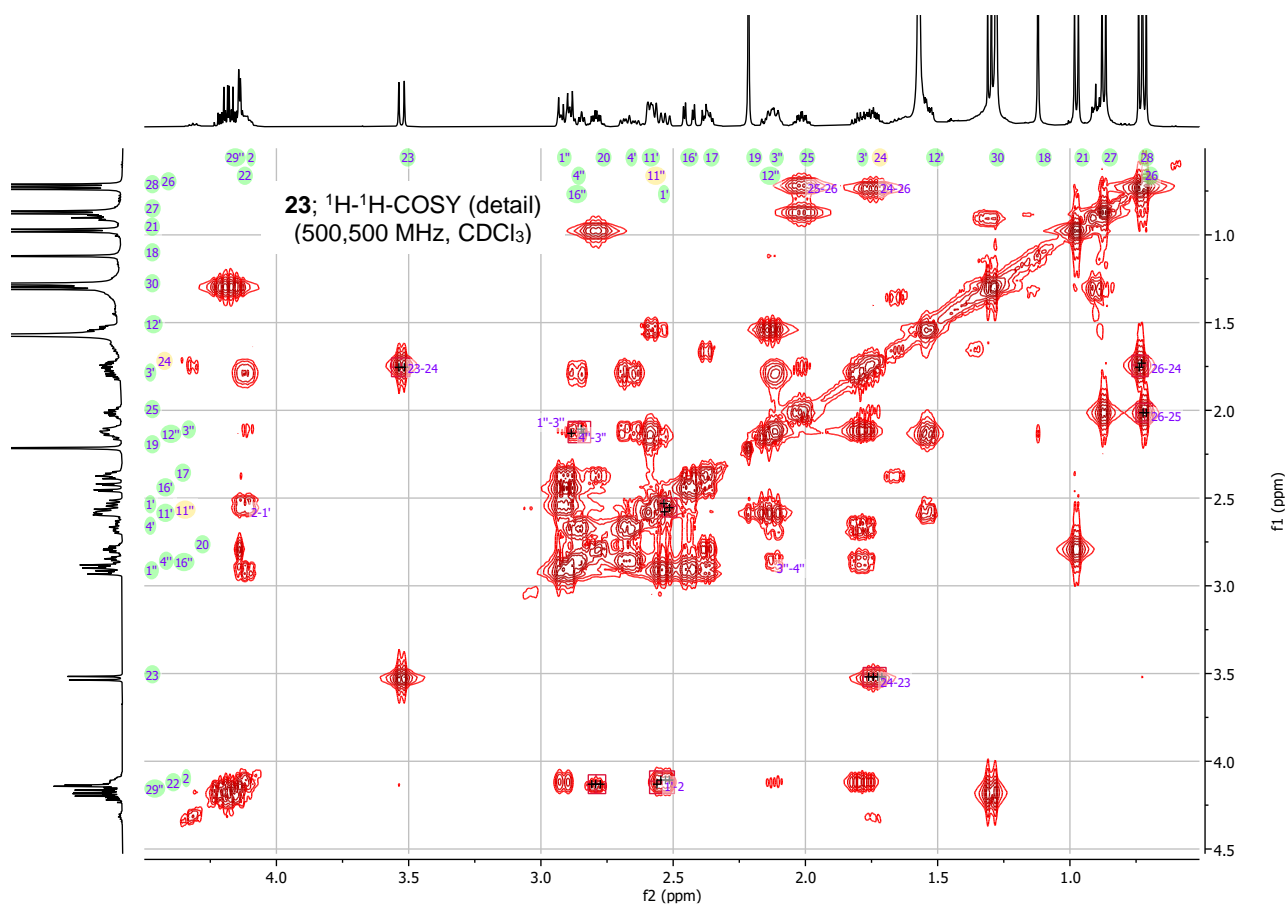
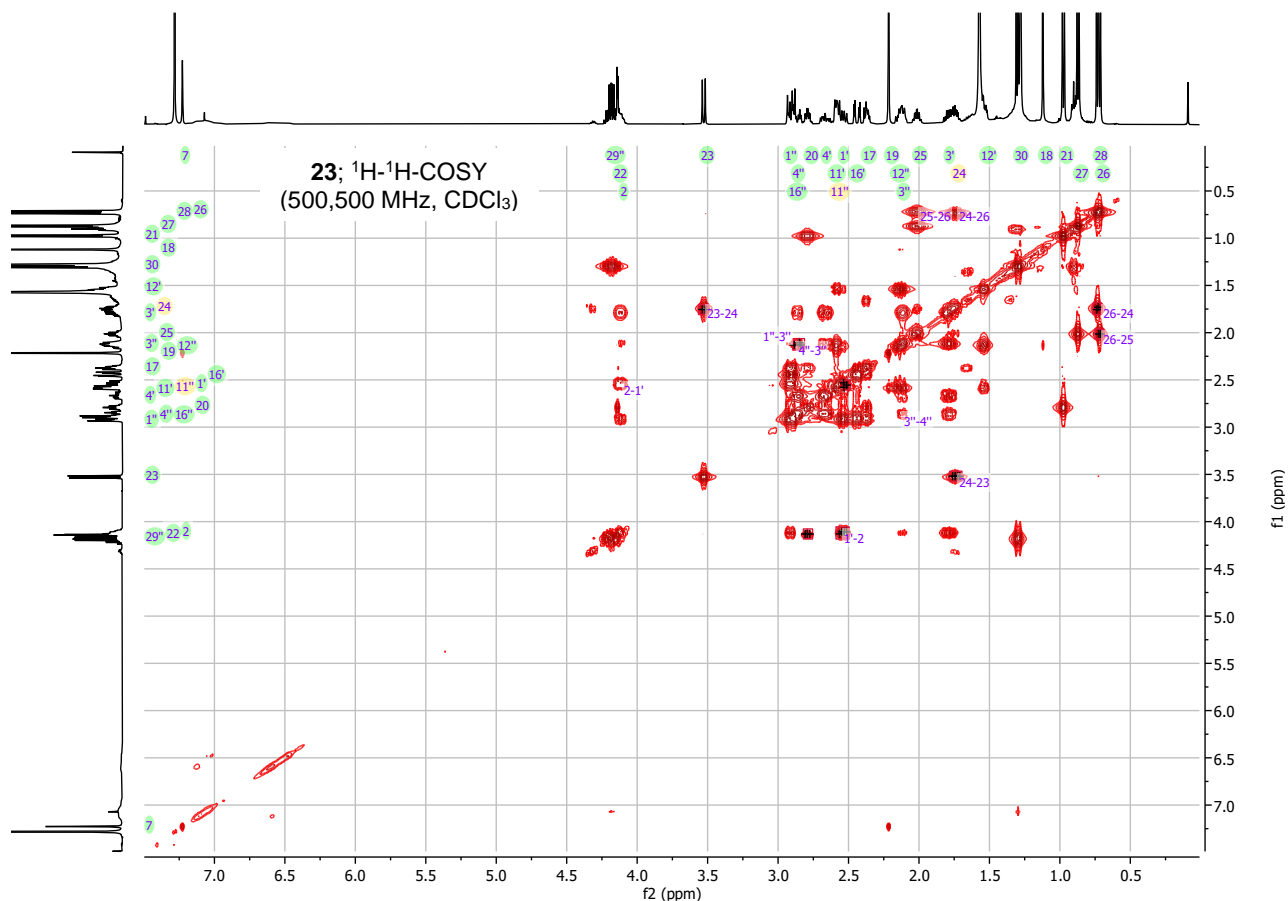


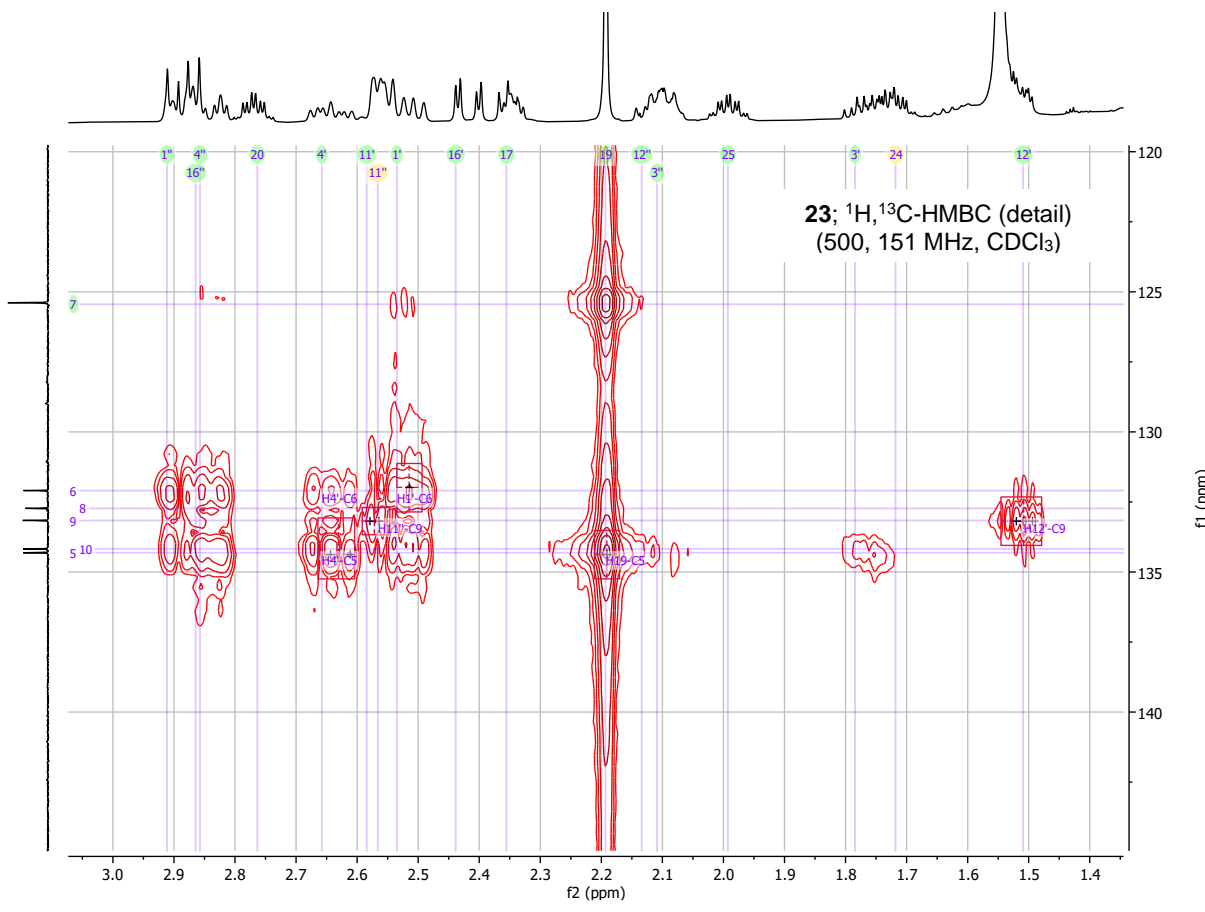
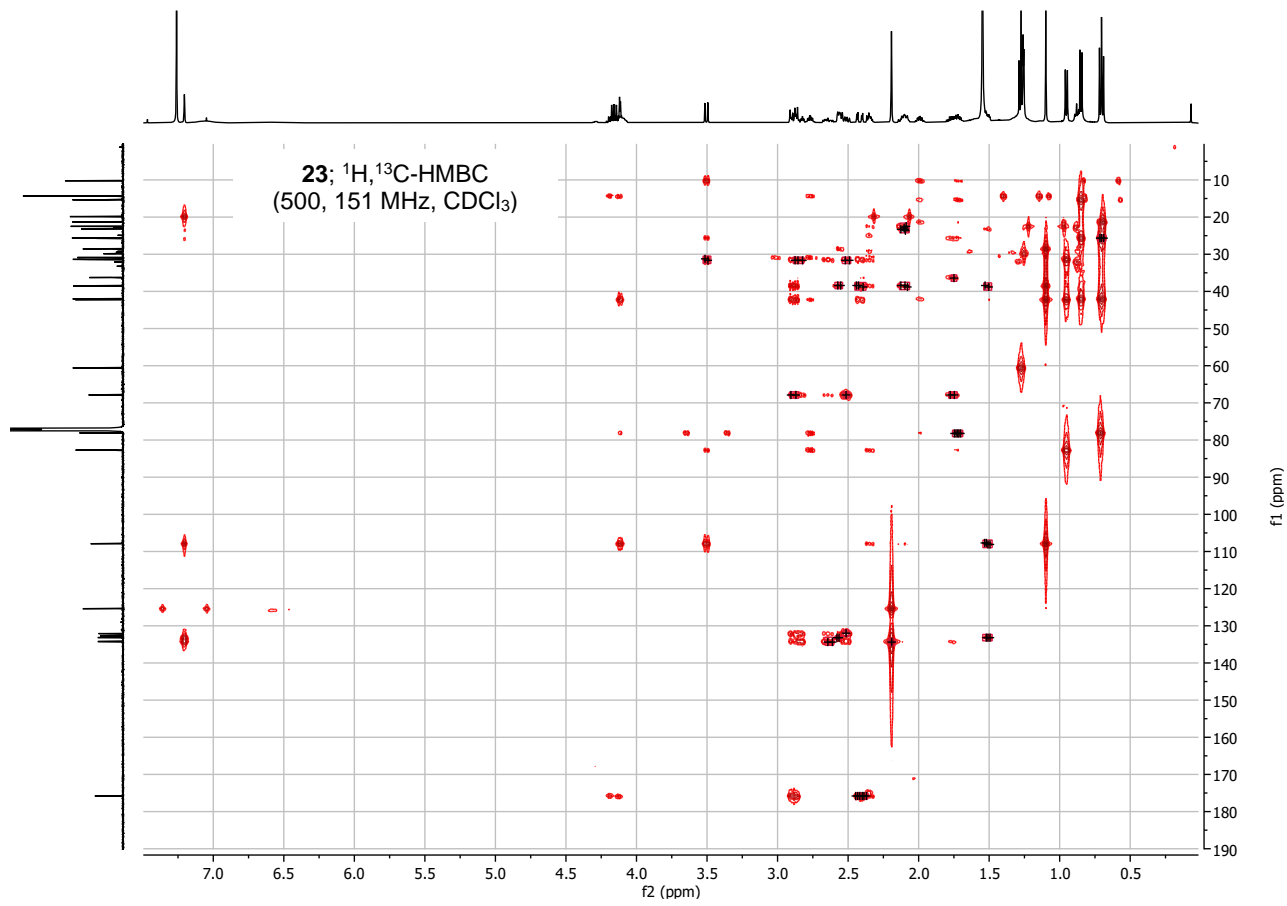


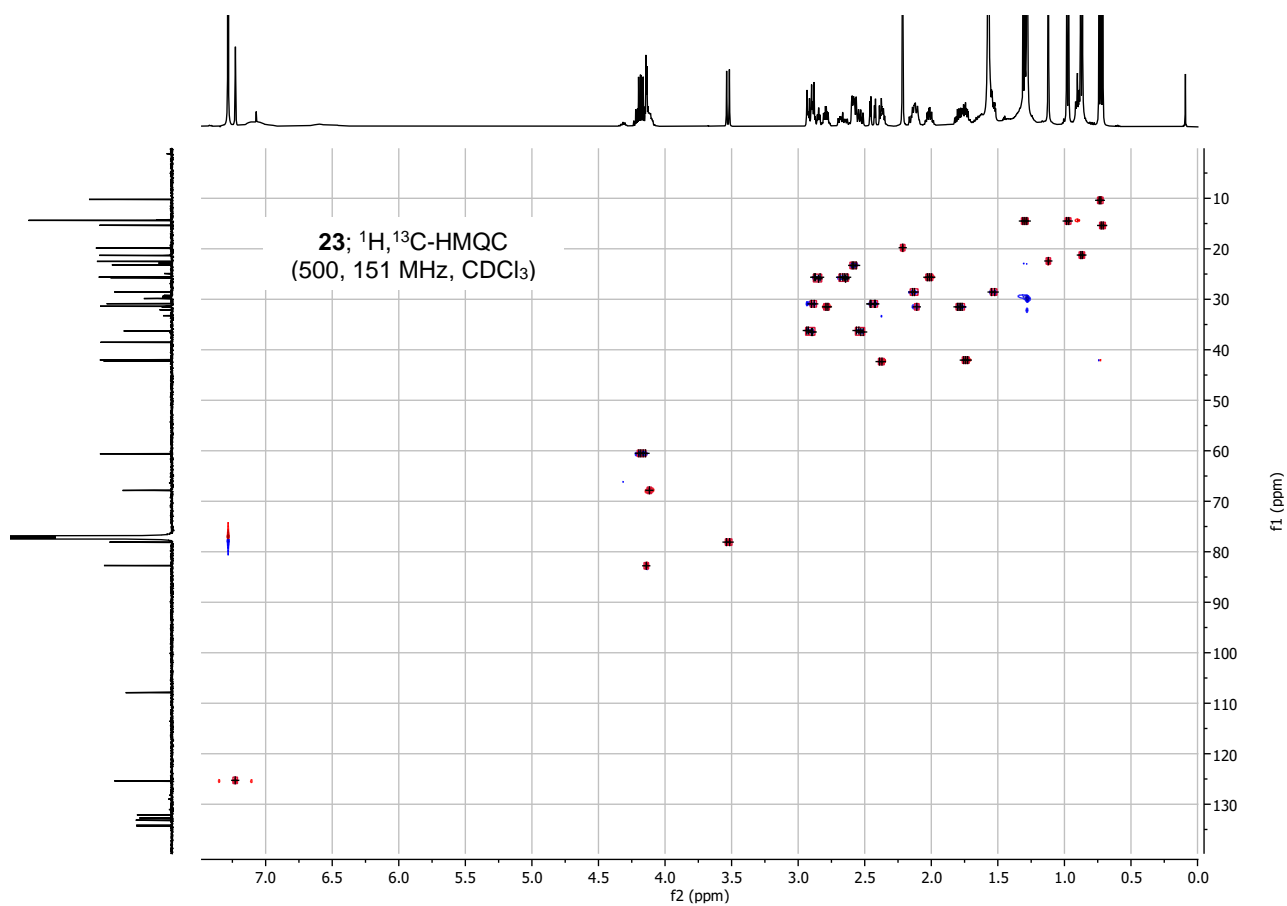
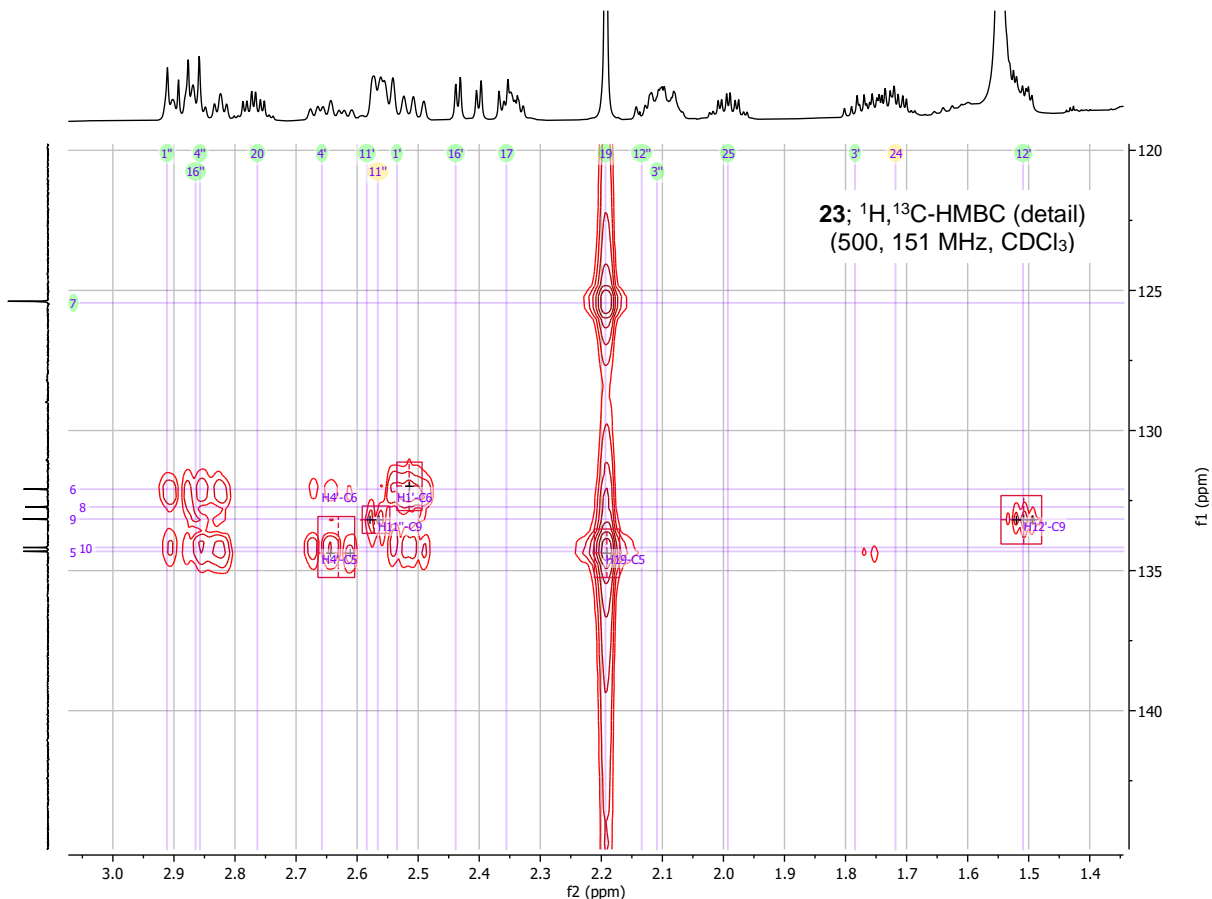


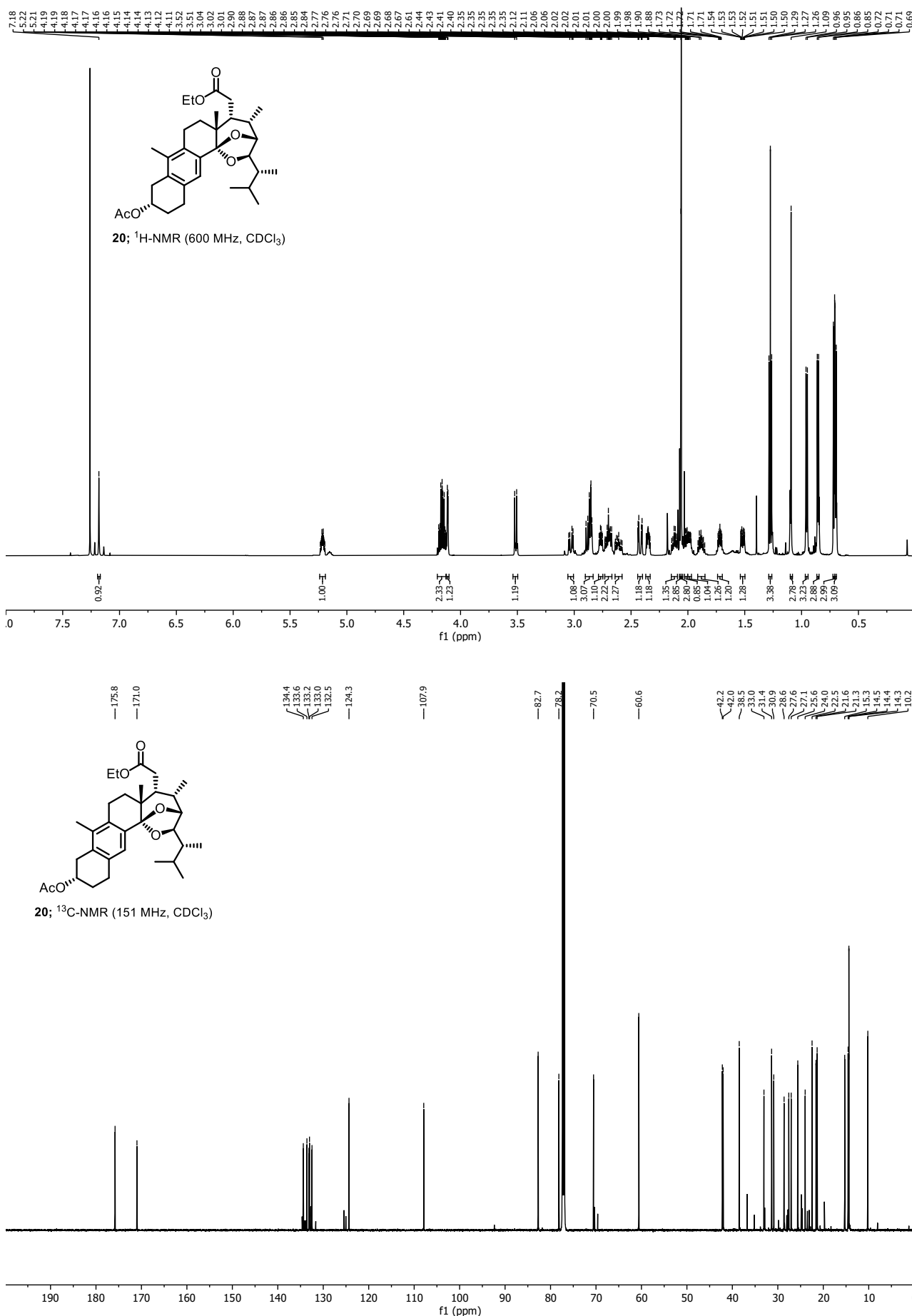


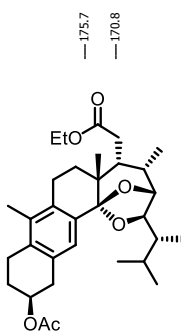
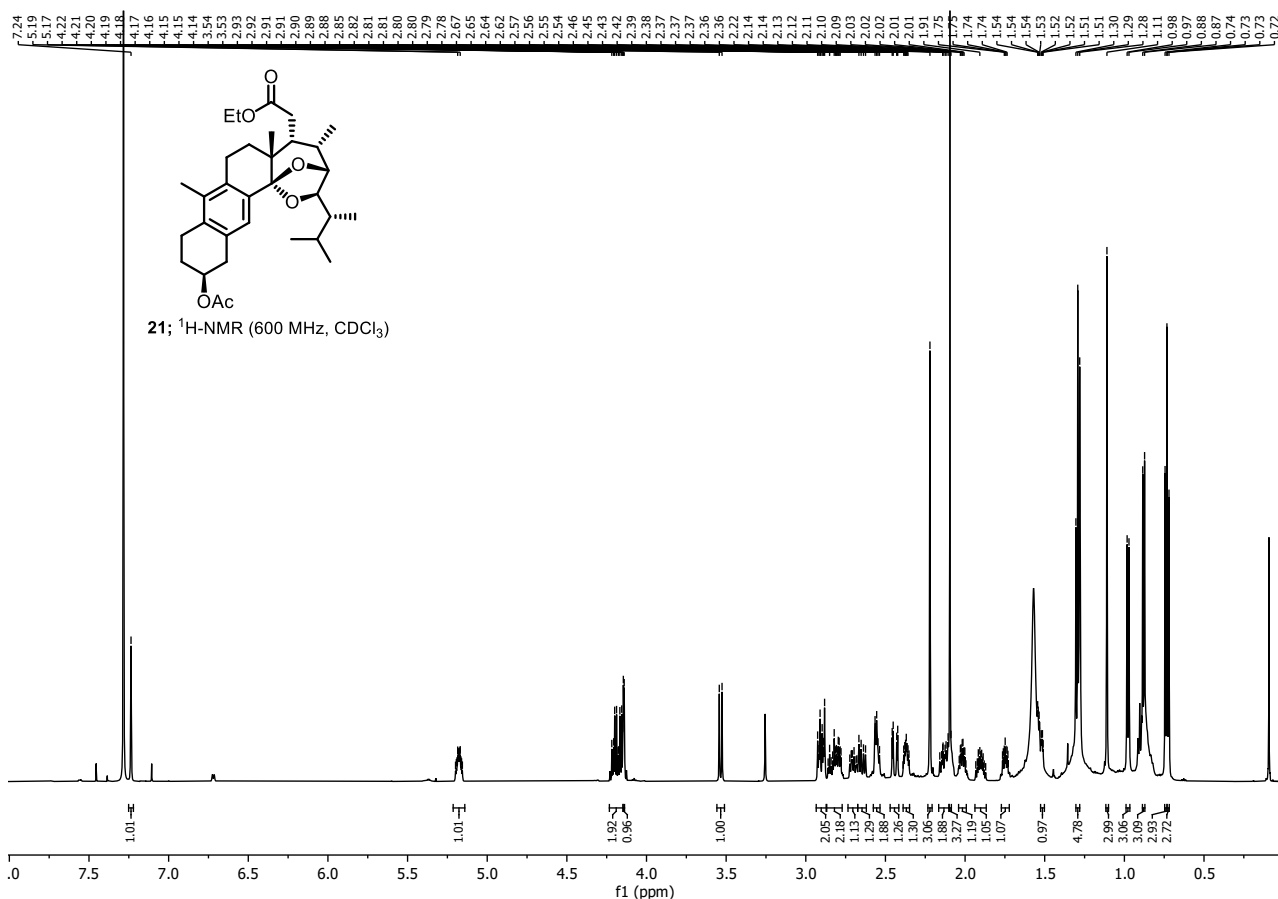




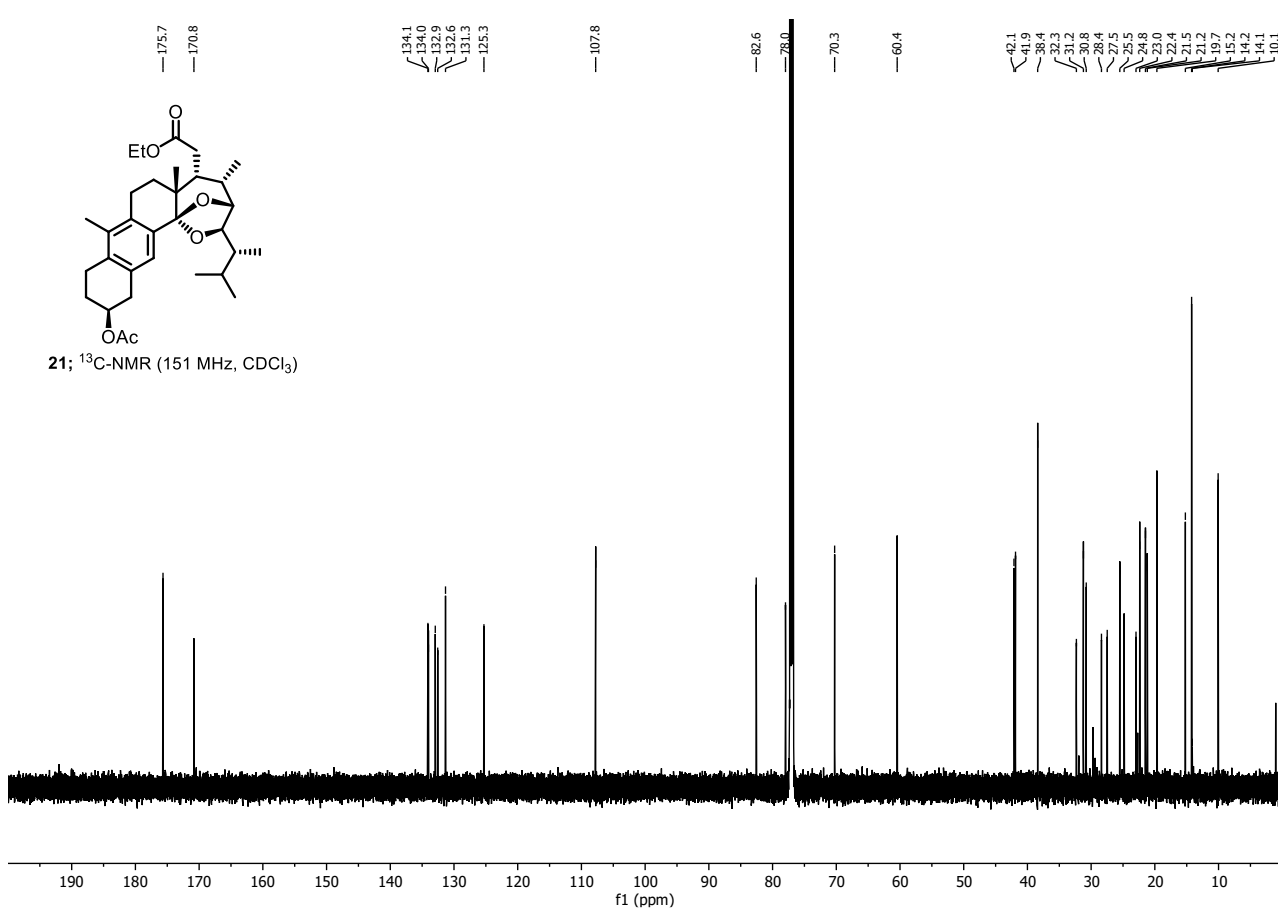


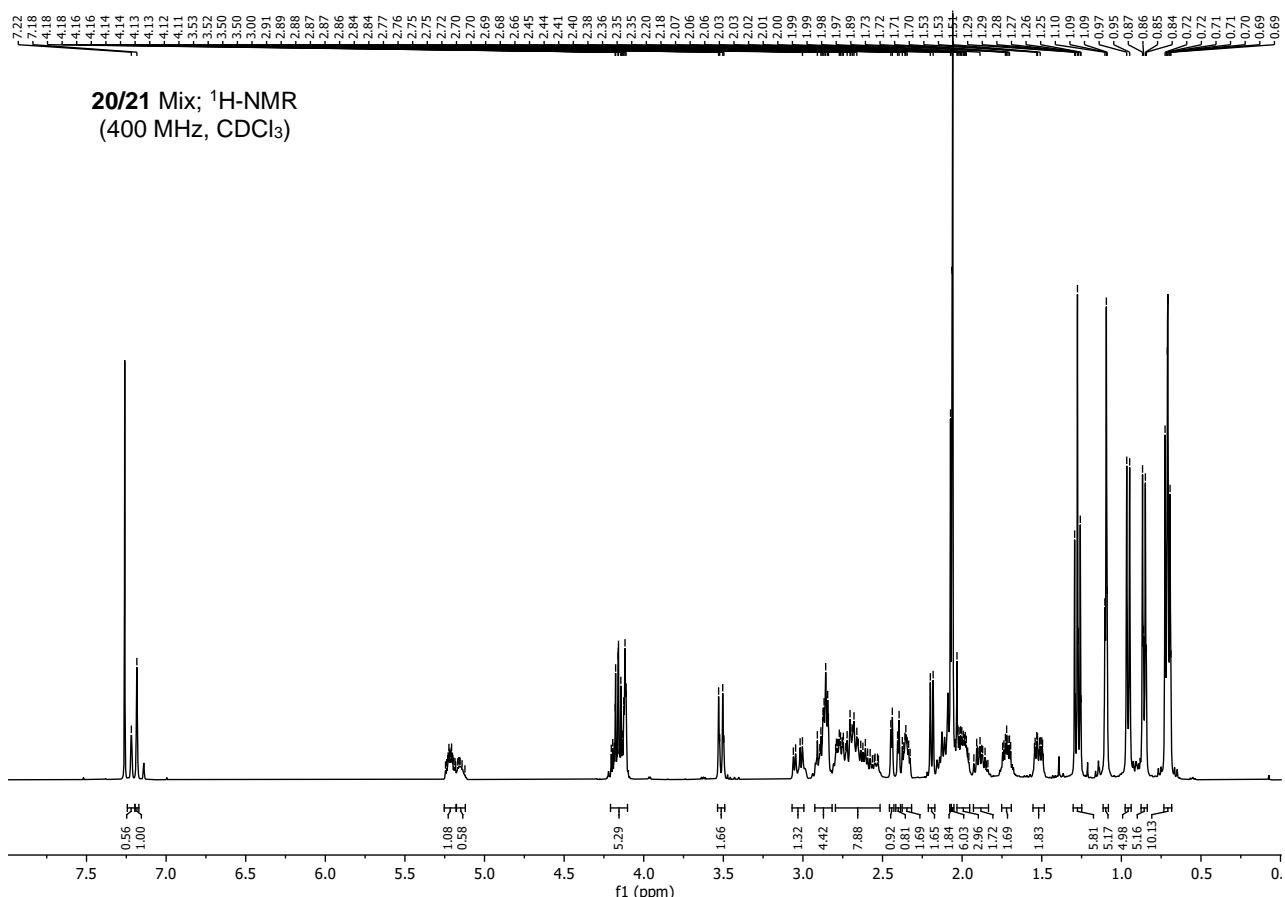




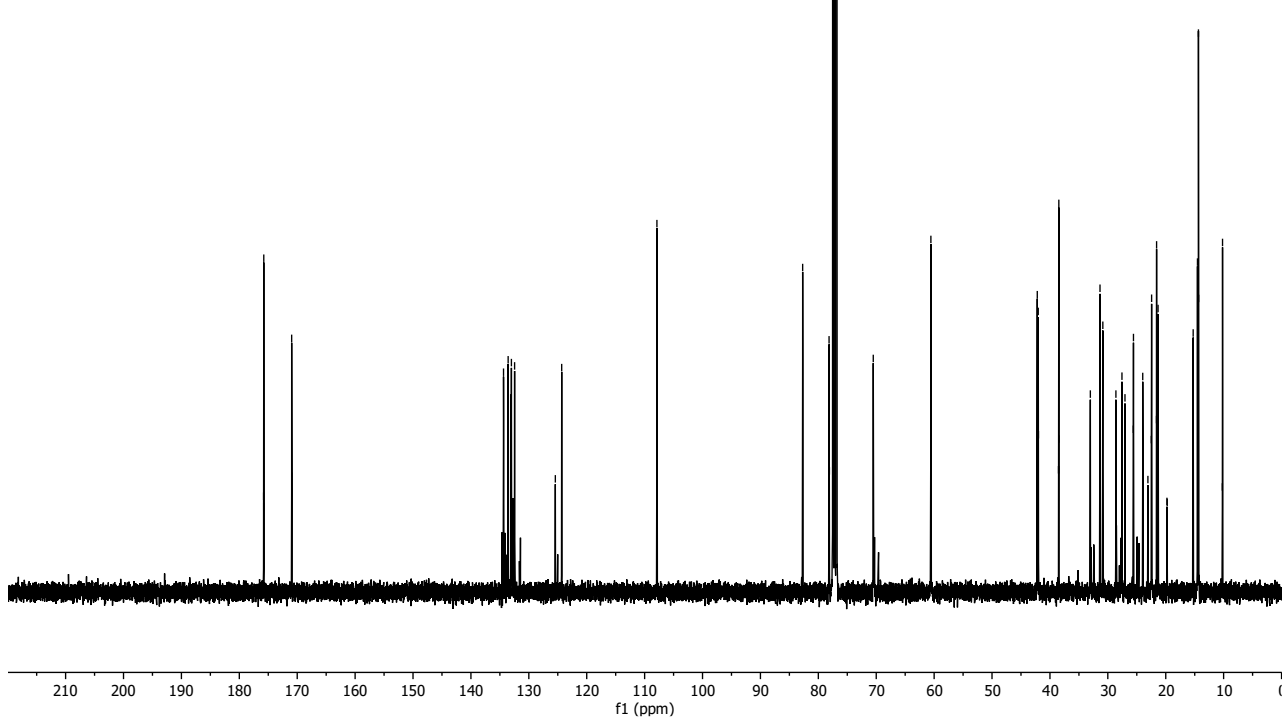


21; ^{13}C -NMR (151 MHz, CDCl_3)





20/21 Mix; ^{13}C -NMR
(101 MHz, CDCl_3)



O-Ethyl (22*R*,23*R*)-1(10→6)abeo-14,15-seco-3 α -acetoxy-14 β ,22 β :14 α ,23 β -diepoxy-ergosta-5,7,9-trien-15-ate (**20**)

¹H-NMR: (600 MHz, CDCl₃); δ [ppm] = 7.18 (s, 1H), 5.24 – 5.19 (m, 1H), 4.16 (dqd, J = 11.0, 7.1, 3.5 Hz, 2H), 4.11 (d, J = 3.1 Hz, 1H), 3.52 (d, J = 10.4 Hz, 1H), 3.03 (dd, J = 17.0, 5.5 Hz, 1H), 2.90 – 2.83 (m, 3H), 2.77 (td, J = 7.1, 3.1 Hz, 1H), 2.73 – 2.67 (m, 2H), 2.61 (ddd, J = 17.4, 11.9, 6.0 Hz, 1H), 2.42 (dd, J = 17.0, 3.9 Hz, 1H), 2.35 (tdd, J = 8.9, 4.0, 2.1 Hz, 1H), 2.12 (dt, J = 12.4, 6.2 Hz, 1H), 2.06 (s, 3H), 2.06 (s, 3H), 2.01 (dd, J = 6.9, 2.9 Hz, 1H), 2.00 – 1.97 (m, 1H), 1.91 – 1.85 (m, 1H), 1.72 (ddd, J = 10.2, 6.8, 2.9 Hz, 1H), 1.52 (ddd, J = 12.8, 6.1, 1.7 Hz, 1H), 1.27 (t, J = 7.1 Hz, 3H), 1.09 (s, 3H), 0.95 (d, J = 7.3 Hz, 3H), 0.86 (d, J = 7.1 Hz, 3H), 0.71 (d, J = 6.8 Hz, 3H), 0.70 (d, J = 7.0 Hz, 3H).

¹³C-NMR: (151 MHz, CDCl₃); δ [ppm] = 175.8, 171.0, 134.4, 133.6, 133.2, 133.0, 132.5, 124.3, 107.9, 82.7, 78.2, 70.5, 60.6, 42.2, 42.0, 38.5, 33.0, 31.4, 30.9, 28.6, 27.6, 27.1, 25.6, 24.0, 22.5, 21.6, 21.3, 15.3, 14.5, 14.4, 14.3, 10.2.

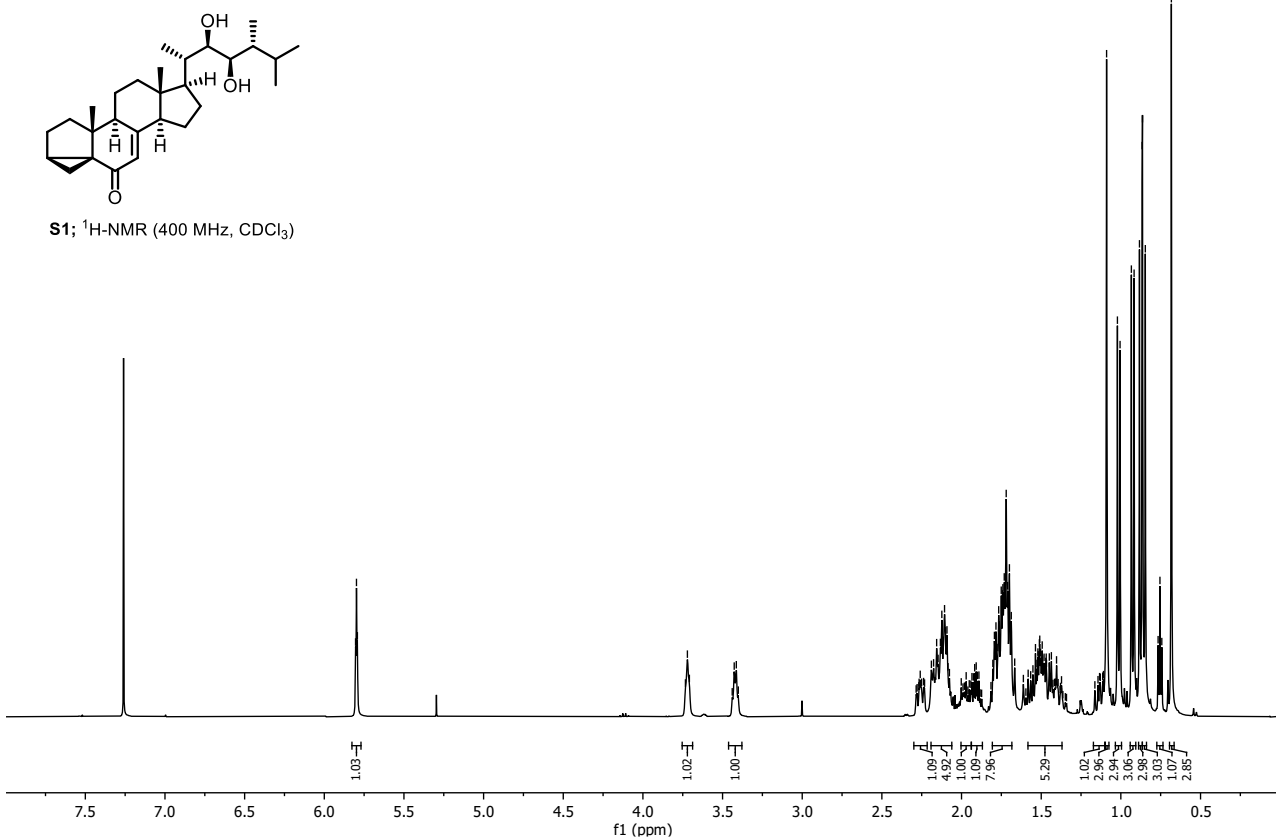
O-Ethyl (22*R*,23*R*)-1(10→6)abeo-14,15-seco-2 β -acetoxy-14 β ,22 β :14 α ,23 β -diepoxy-ergosta-5,7,9-trien-15-ate (**21**)

¹H-NMR: (600 MHz, CDCl₃); δ [ppm] = 7.24 (s, 1H), 5.21 – 5.14 (m, 1H), 4.23 – 4.15 (m, 2H), 4.14 (d, J = 3.2 Hz, 1H), 3.53 (d, J = 10.4 Hz, 1H), 2.93 – 2.87 (m, 2H), 2.87 – 2.77 (m, 2H), 2.74 – 2.67 (m, 1H), 2.65 (dd, J = 16.9, 8.0 Hz, 1H), 2.55 (dd, J = 10.8, 5.9 Hz, 2H), 2.44 (dd, J = 17.0, 3.8 Hz, 1H), 2.37 (ddd, J = 10.1, 6.9, 3.8 Hz, 1H), 2.22 (s, 3H), 2.17 – 2.10 (m, 2H), 2.10 (s, 3H), 2.02 (ddd, J = 9.8, 7.0, 3.6 Hz, 1H), 1.90 (dtd, J = 12.5, 9.5, 5.7 Hz, 1H), 1.75 (ddd, J = 10.1, 6.8, 2.9 Hz, 1H), 1.52 (dd, J = 5.0, 2.7 Hz, 1H), 1.29 (t, J = 7.2 Hz, 3H), 1.11 (s, 3H), 0.98 (d, J = 7.3 Hz, 3H), 0.88 (d, J = 7.1 Hz, 3H), 0.74 (d, J = 7.0 Hz, 3H), 0.73 (d, J = 6.7 Hz, 3H).

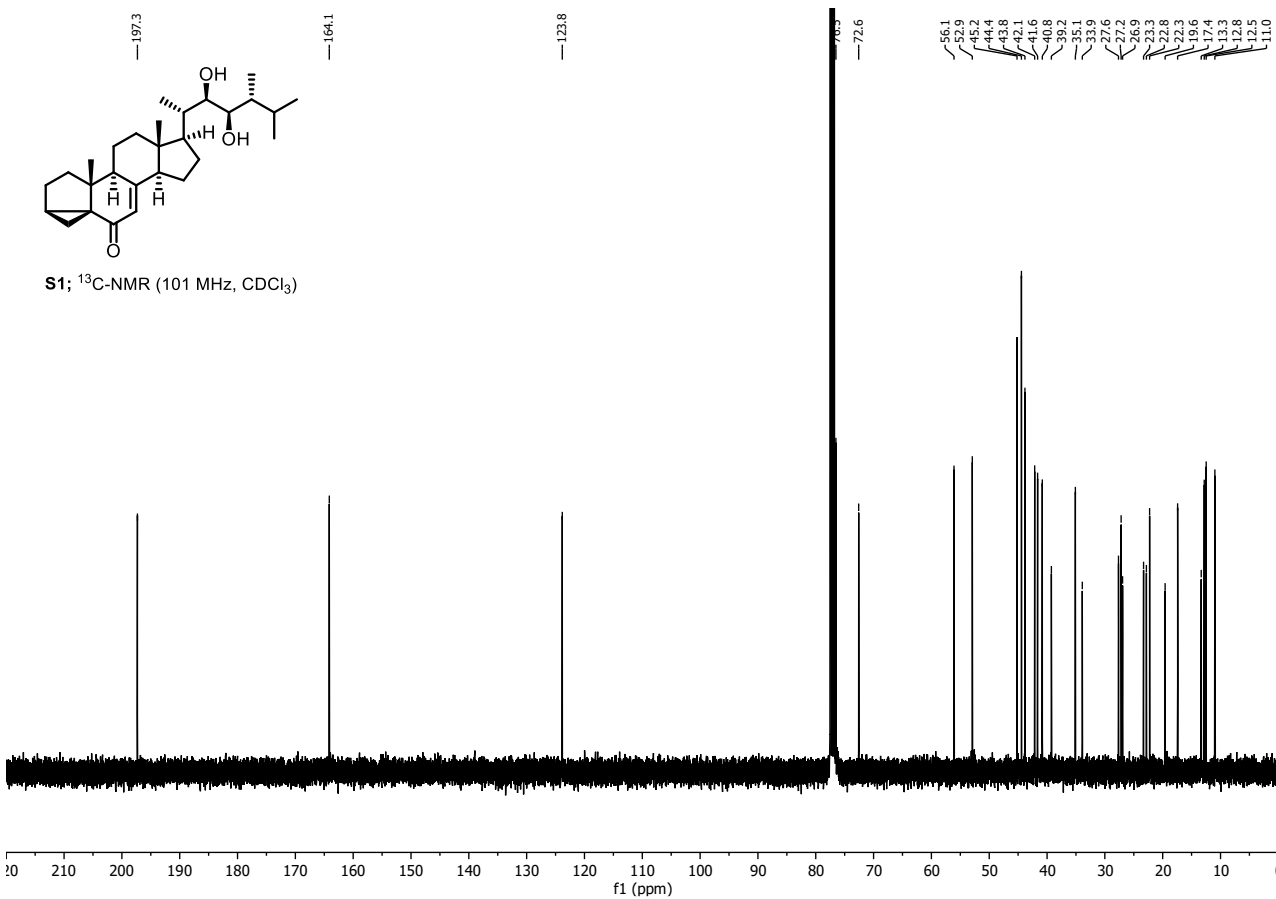
¹³C-NMR: (151 MHz, CDCl₃); δ [ppm] = 175.7, 170.8, 134.1, 134.0, 132.9, 132.6, 131.3, 125.3, 107.8, 82.6, 78.0, 70.3, 60.4, 42.1, 41.9, 38.4, 32.3, 31.2, 30.8, 28.4, 27.5, 25.5, 24.8, 23.0, 22.4, 21.5, 21.2, 19.7, 15.2, 14.2, 14.1, 10.1.

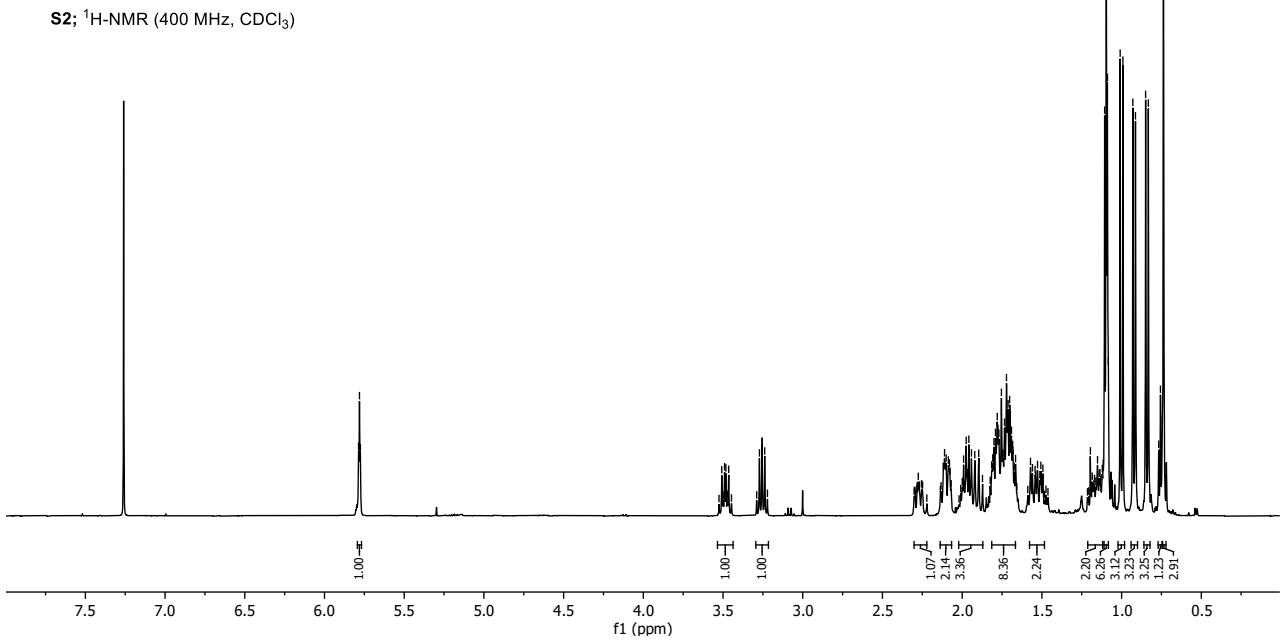
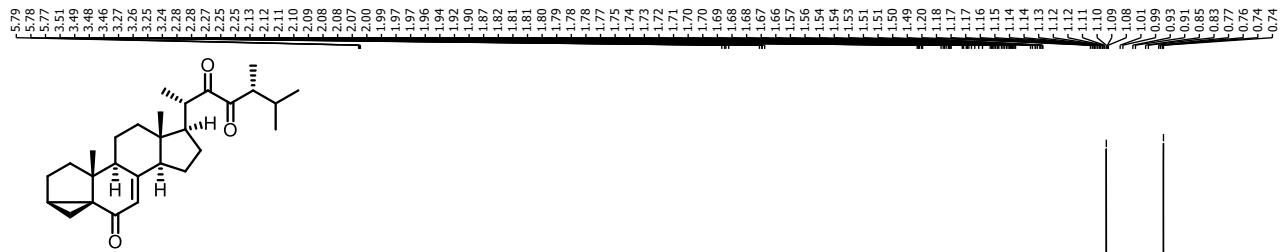
7 NMR Spectra

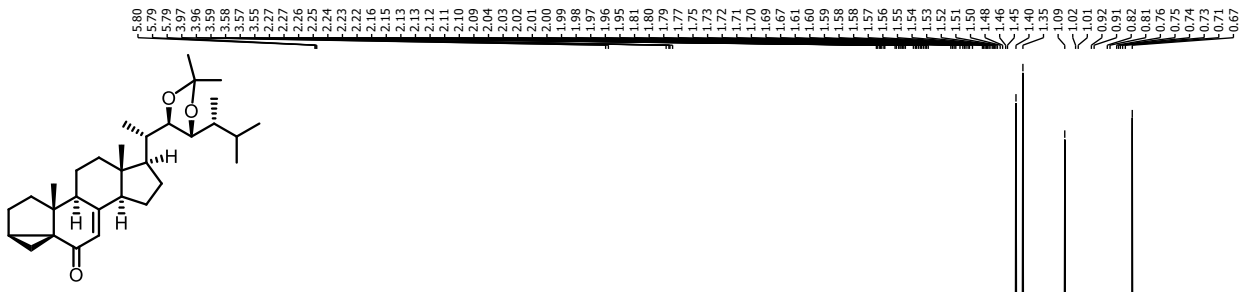
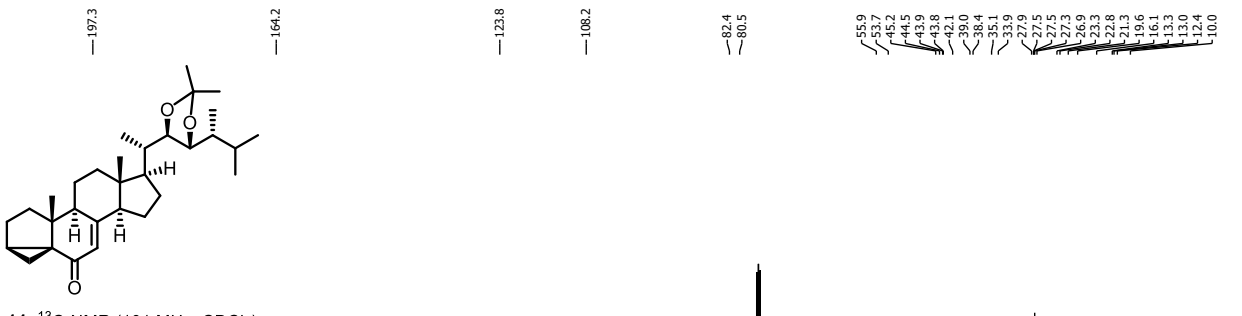
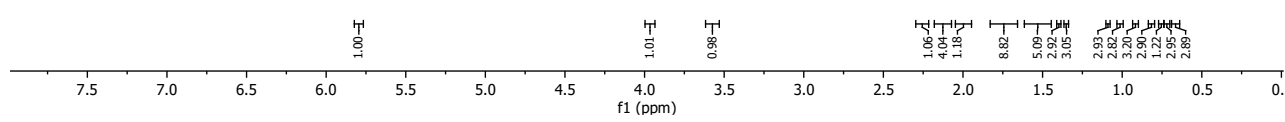
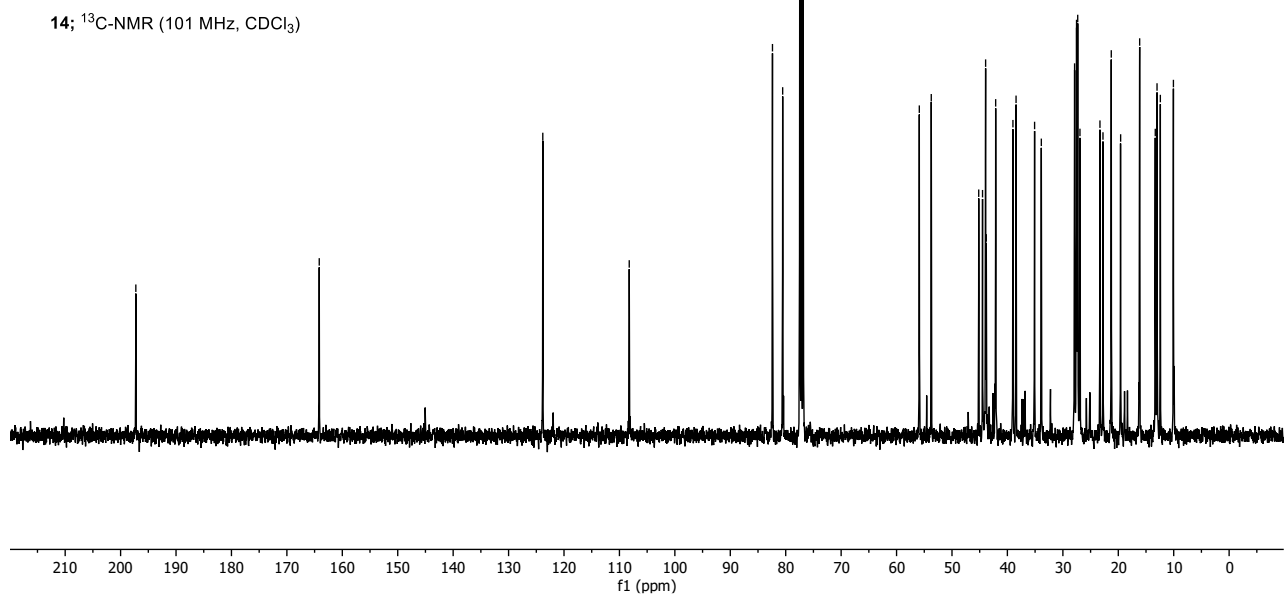
S1; ^1H -NMR (400 MHz, CDCl_3)

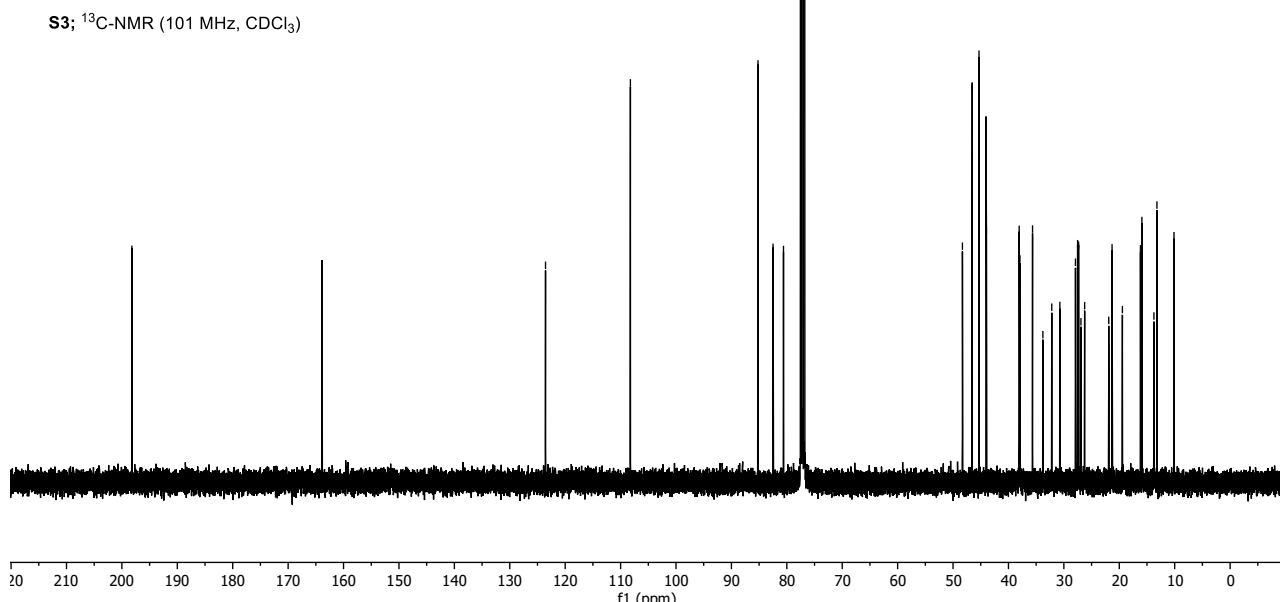
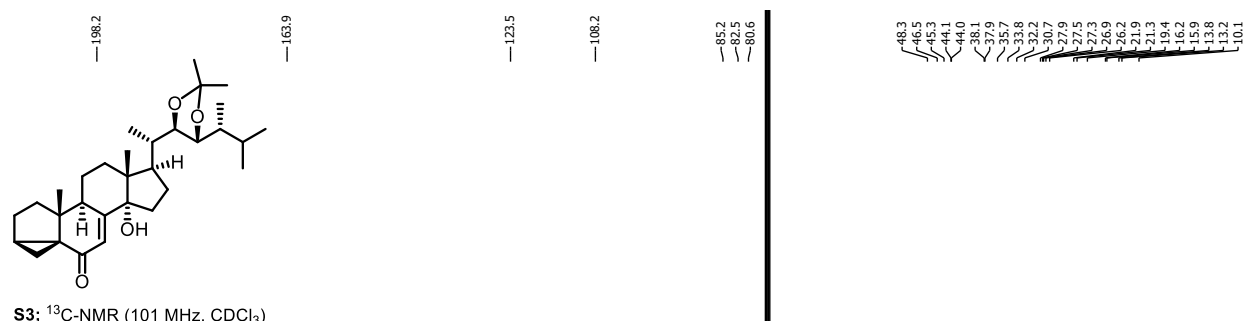
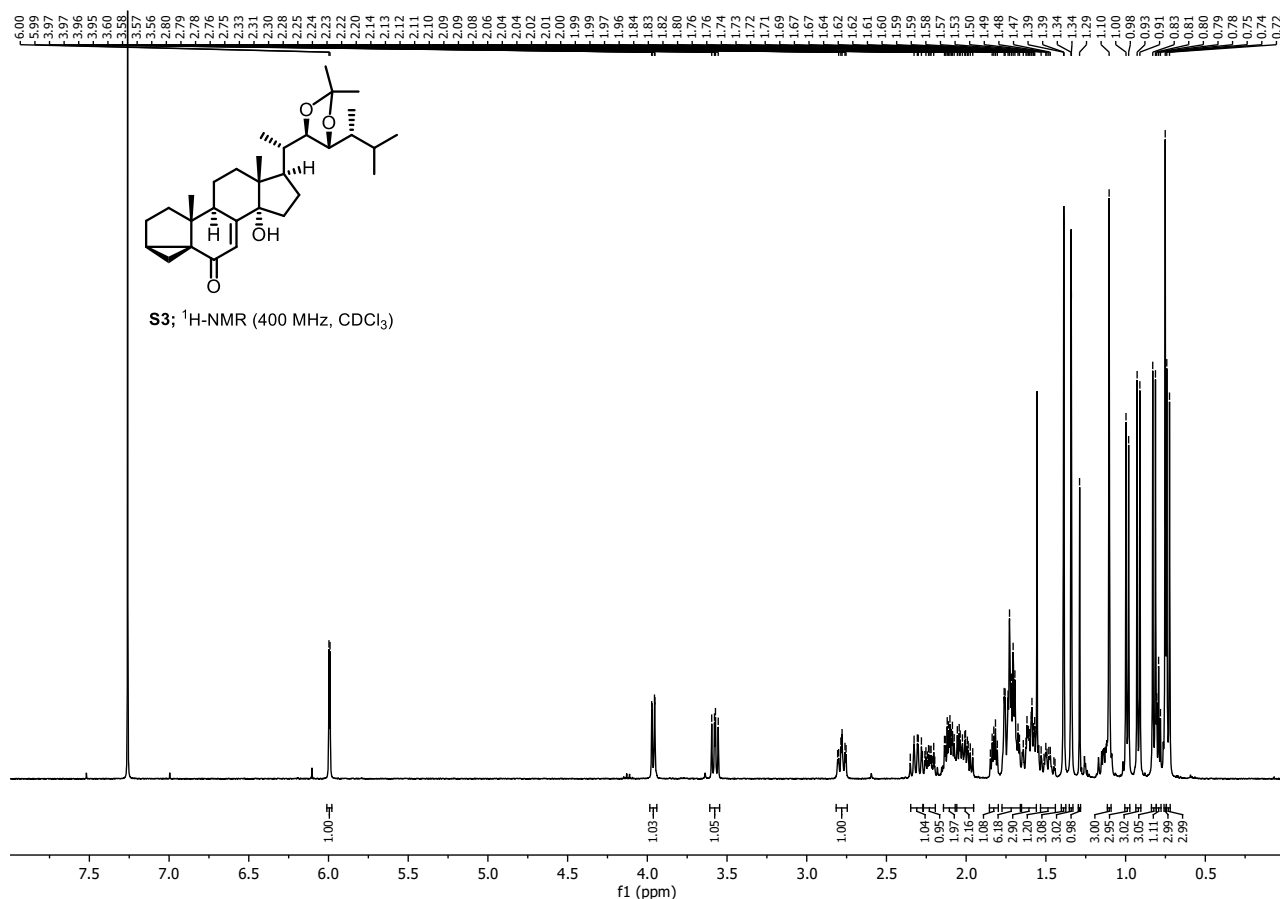


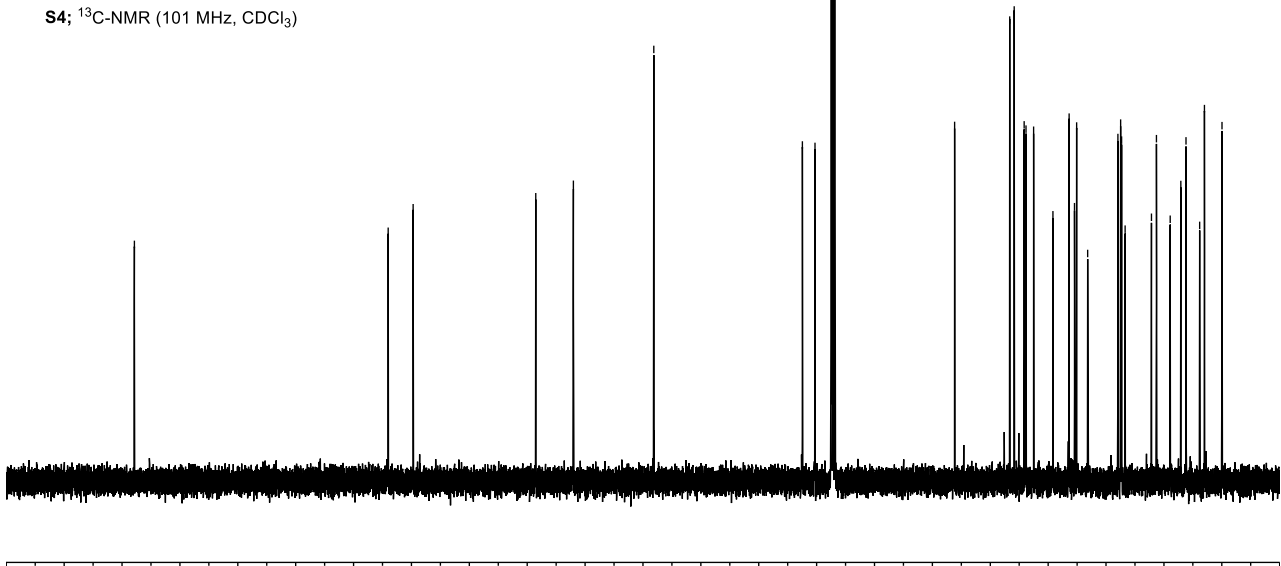
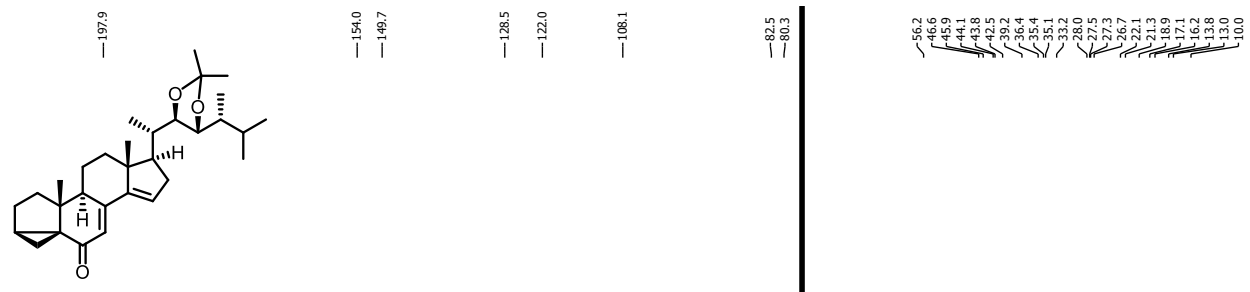
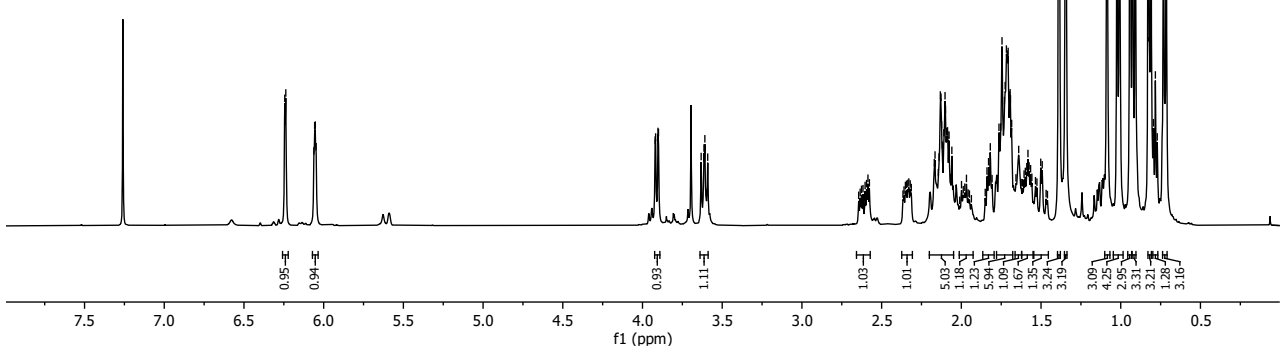
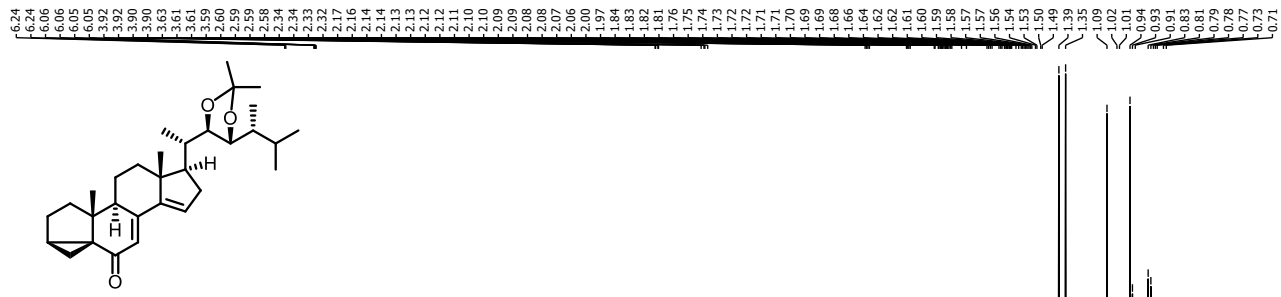
S1; ^{13}C -NMR (101 MHz, CDCl_3)

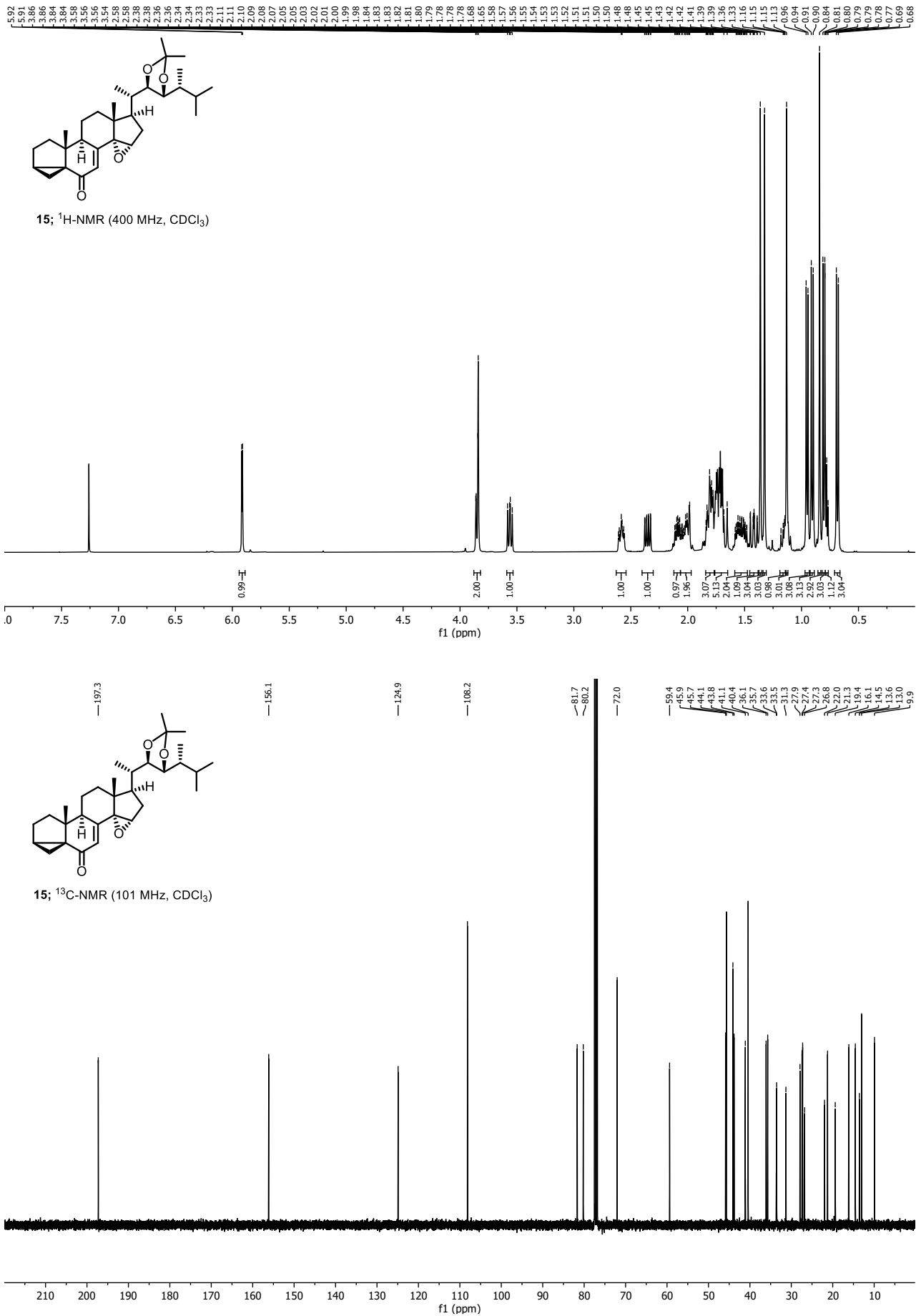


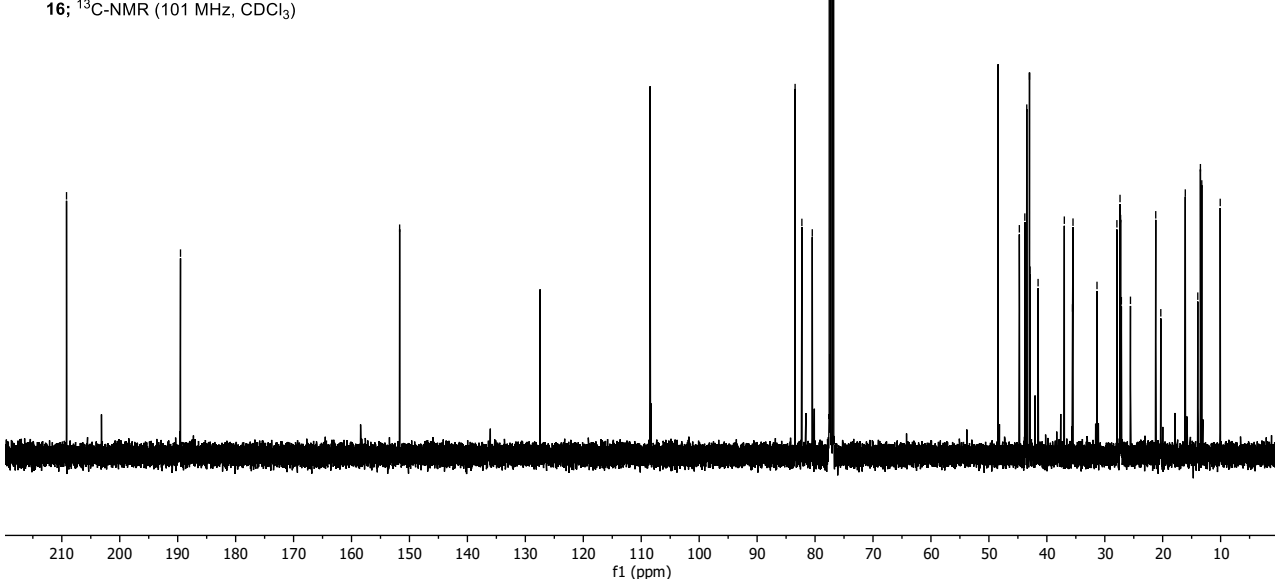
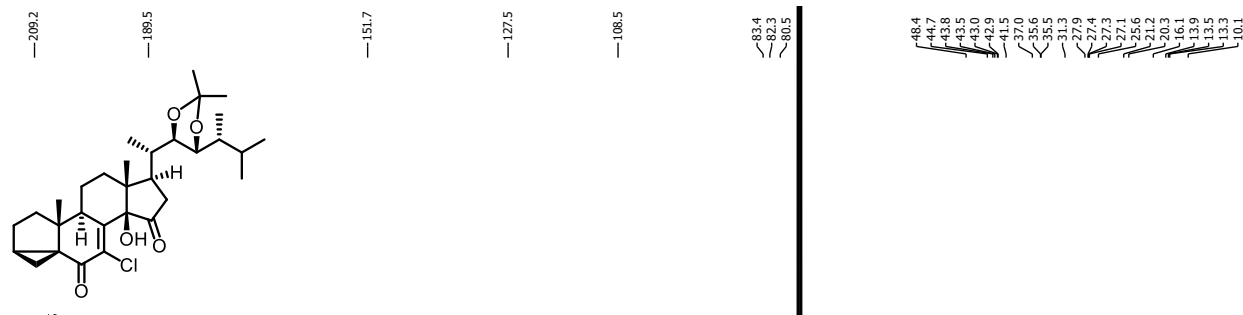
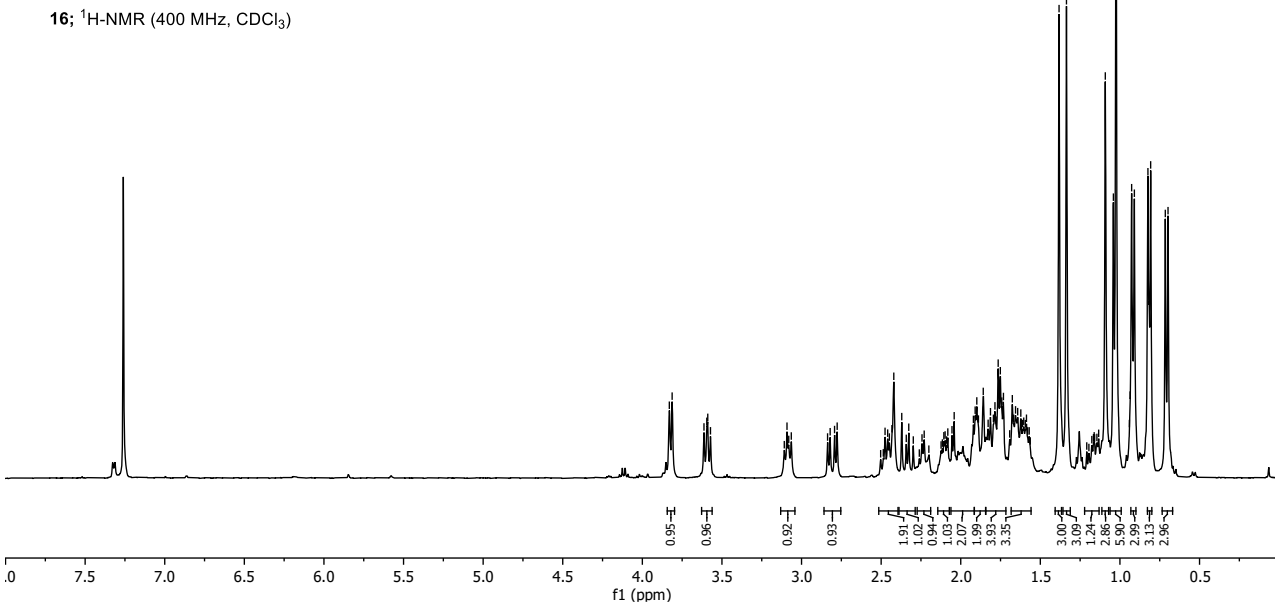
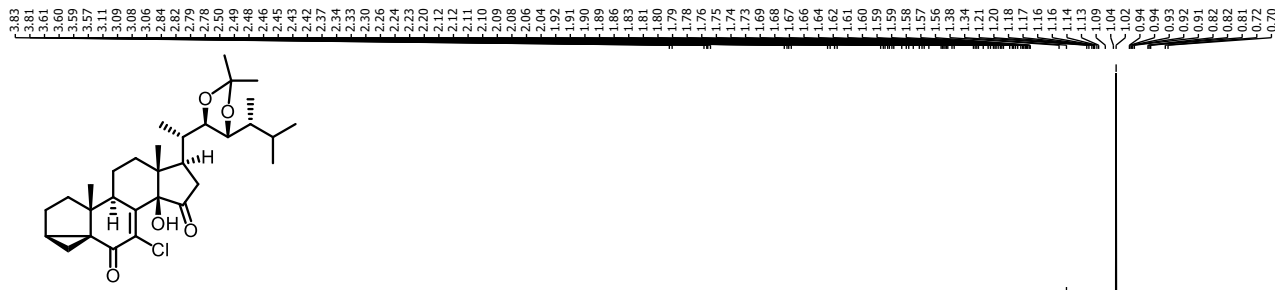


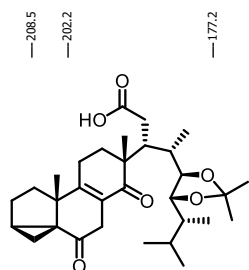
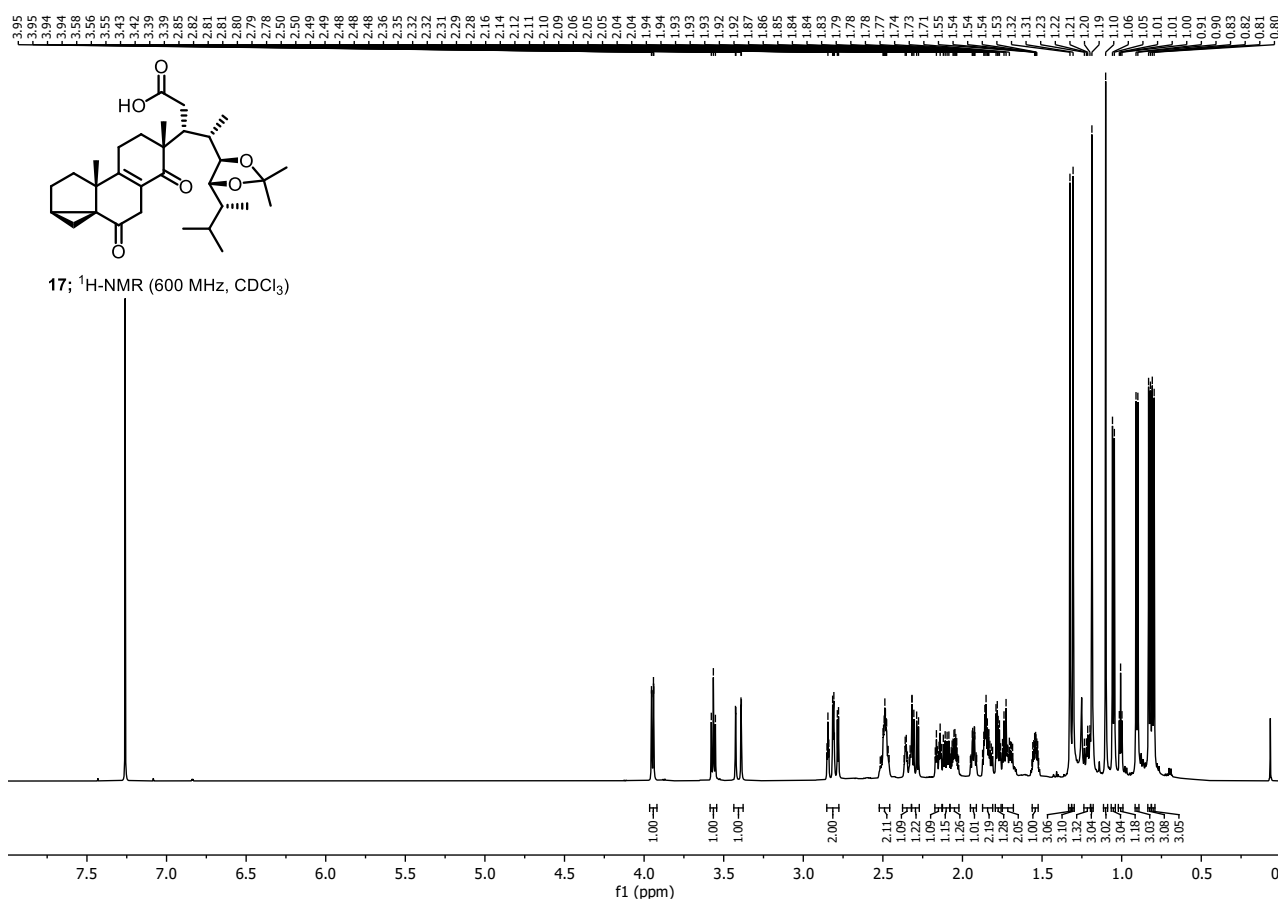
14; ¹H-NMR (400 MHz, CDCl₃)14; ¹³C-NMR (101 MHz, CDCl₃)



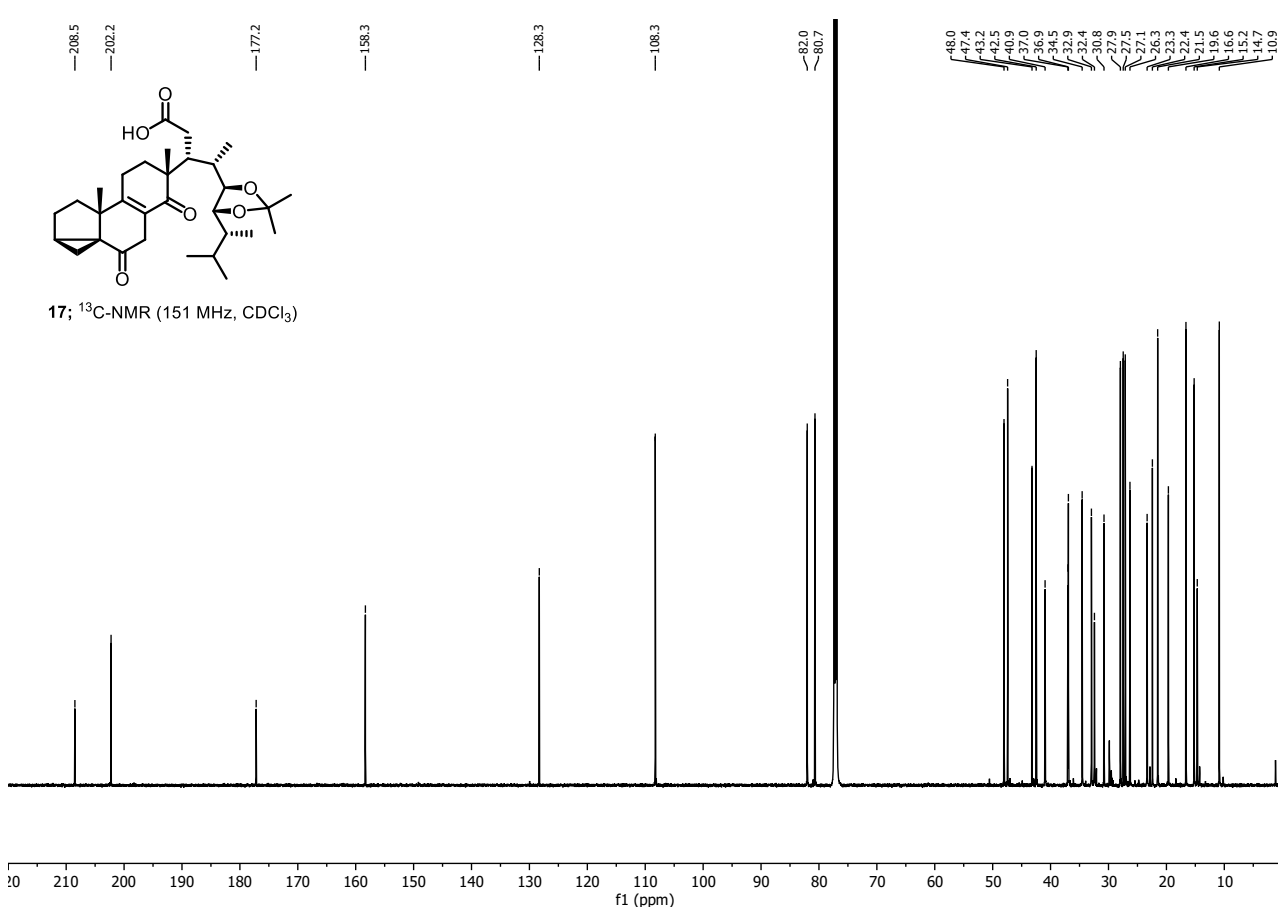


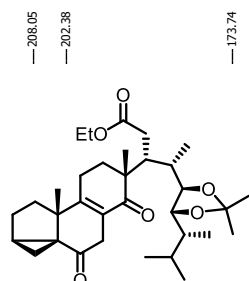
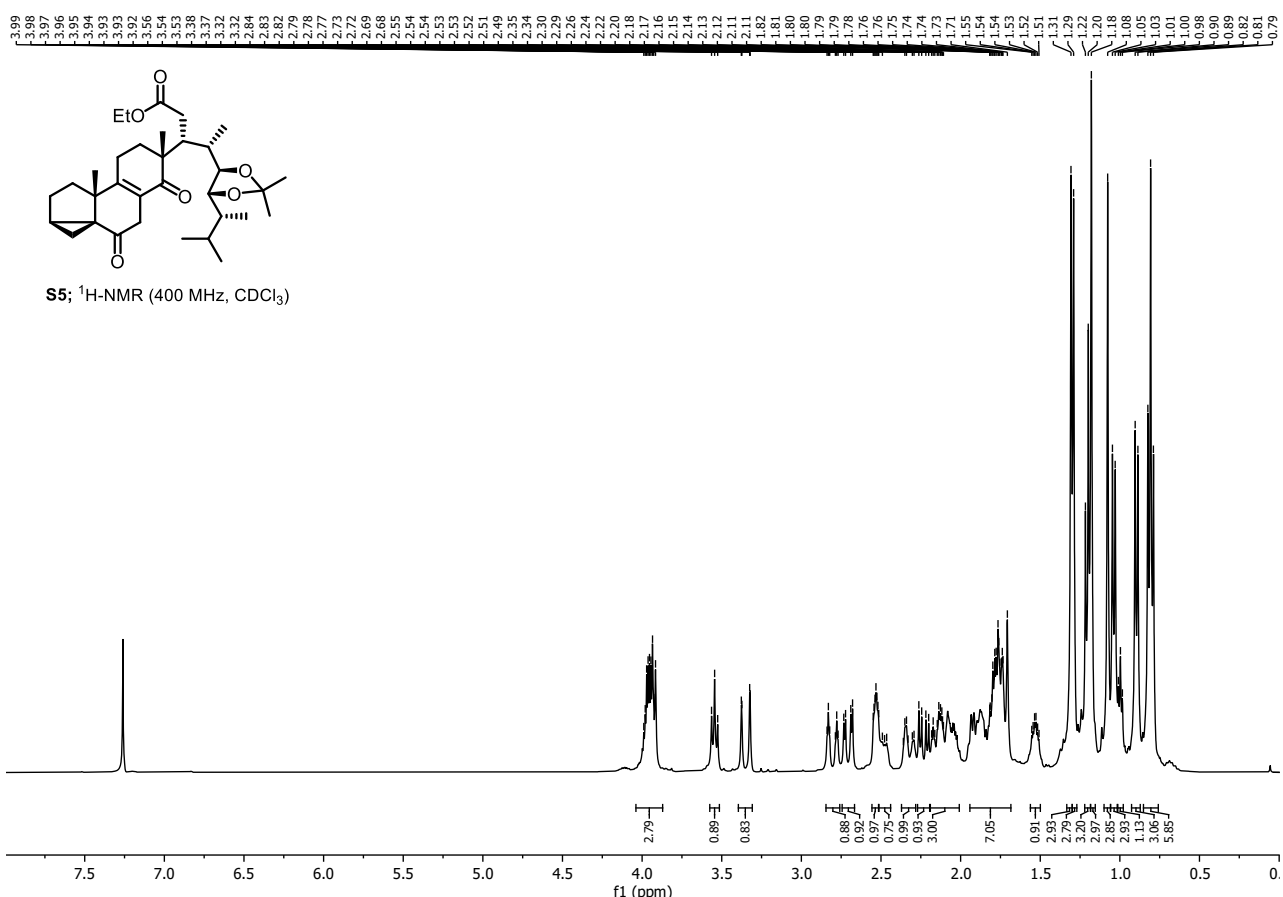




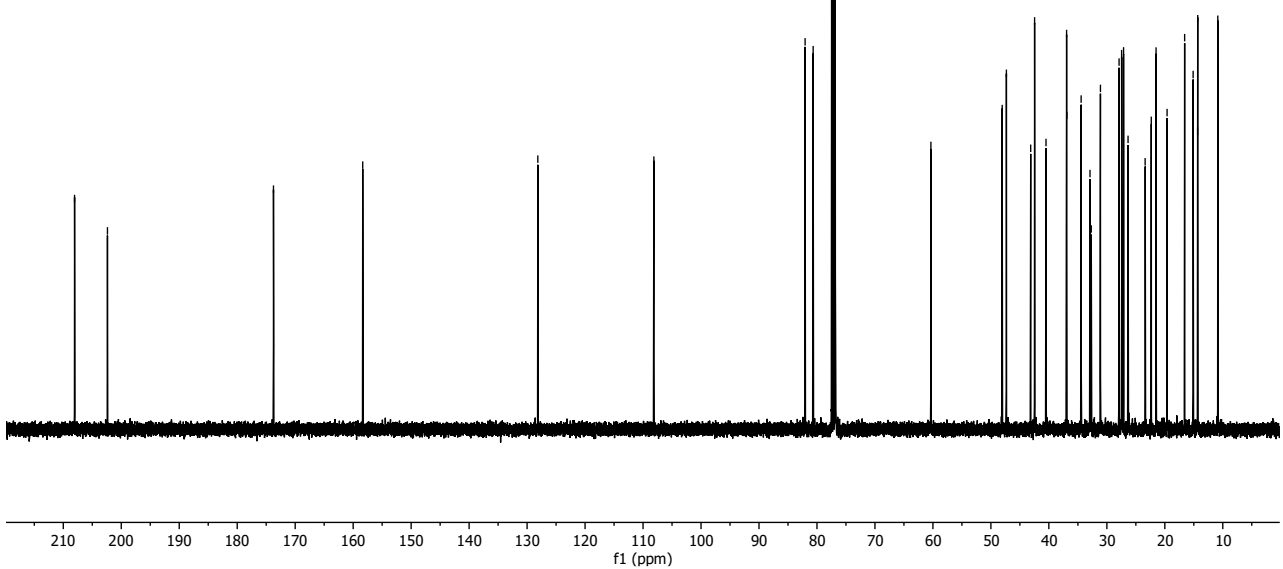


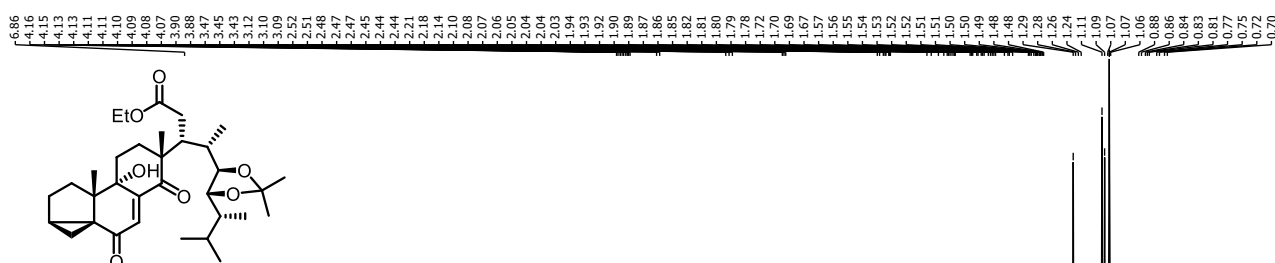
17; ^{13}C -NMR (151 MHz, CDCl_3)



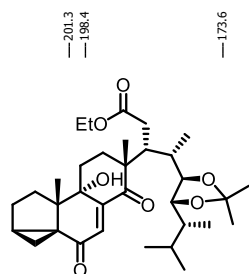
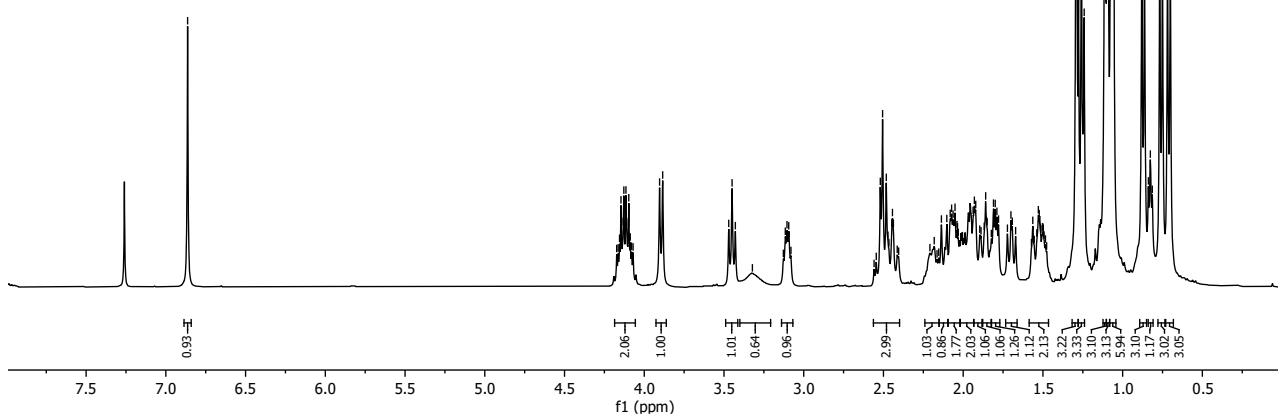


S5: ^{13}C -NMR (101 MHz, CDCl_3)

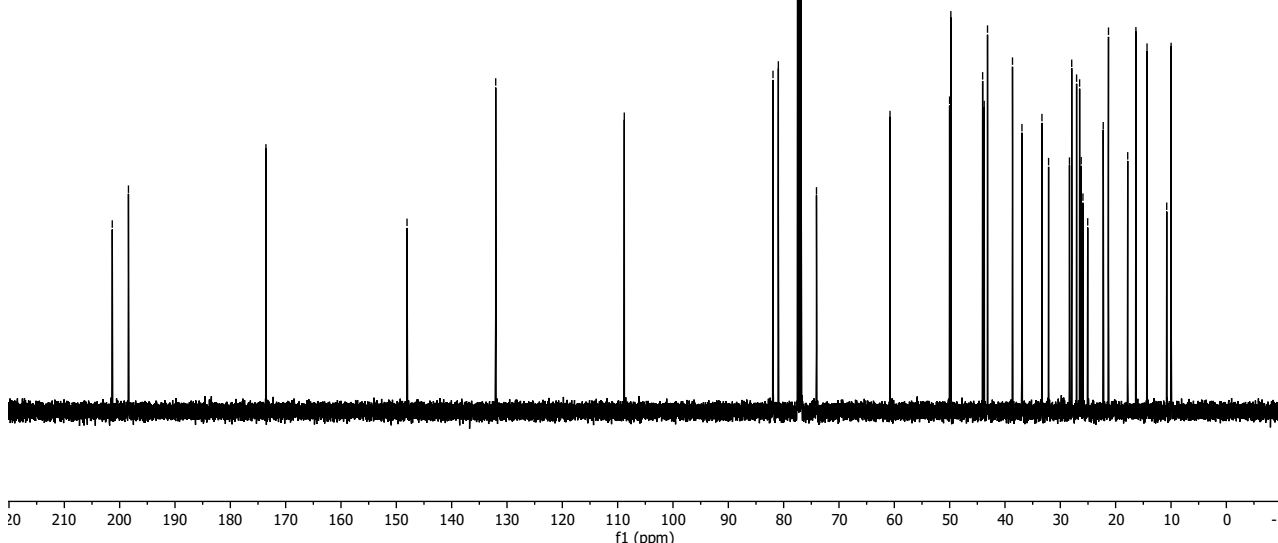


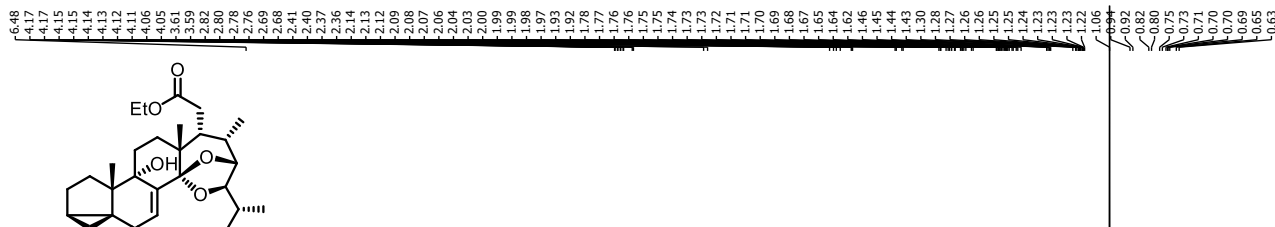


S6; ^1H -NMR (400 MHz, CDCl_3)

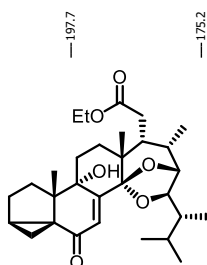
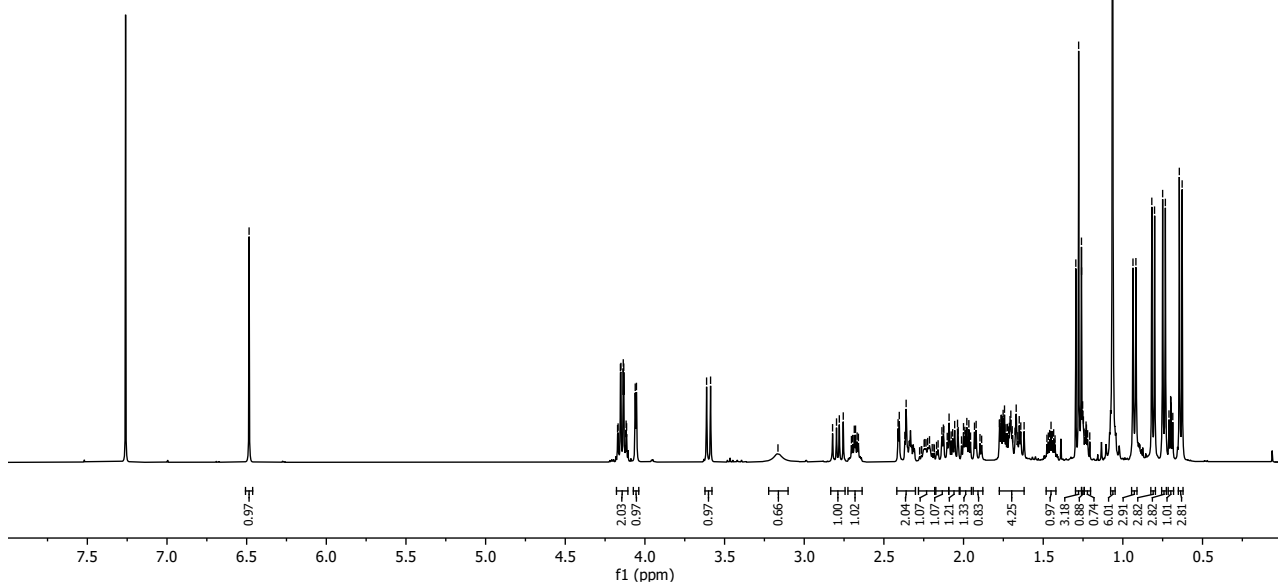


S6; ^{13}C -NMR (101 MHz, CDCl_3)

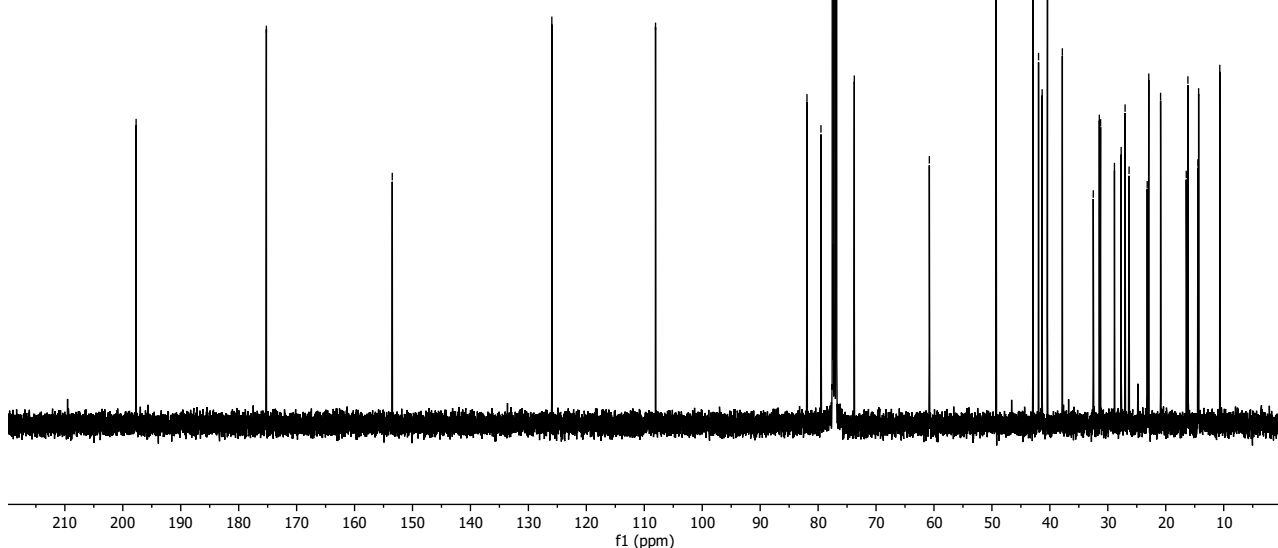


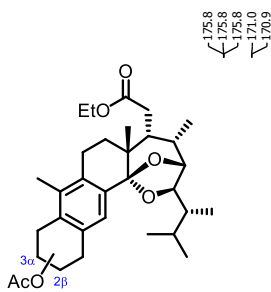
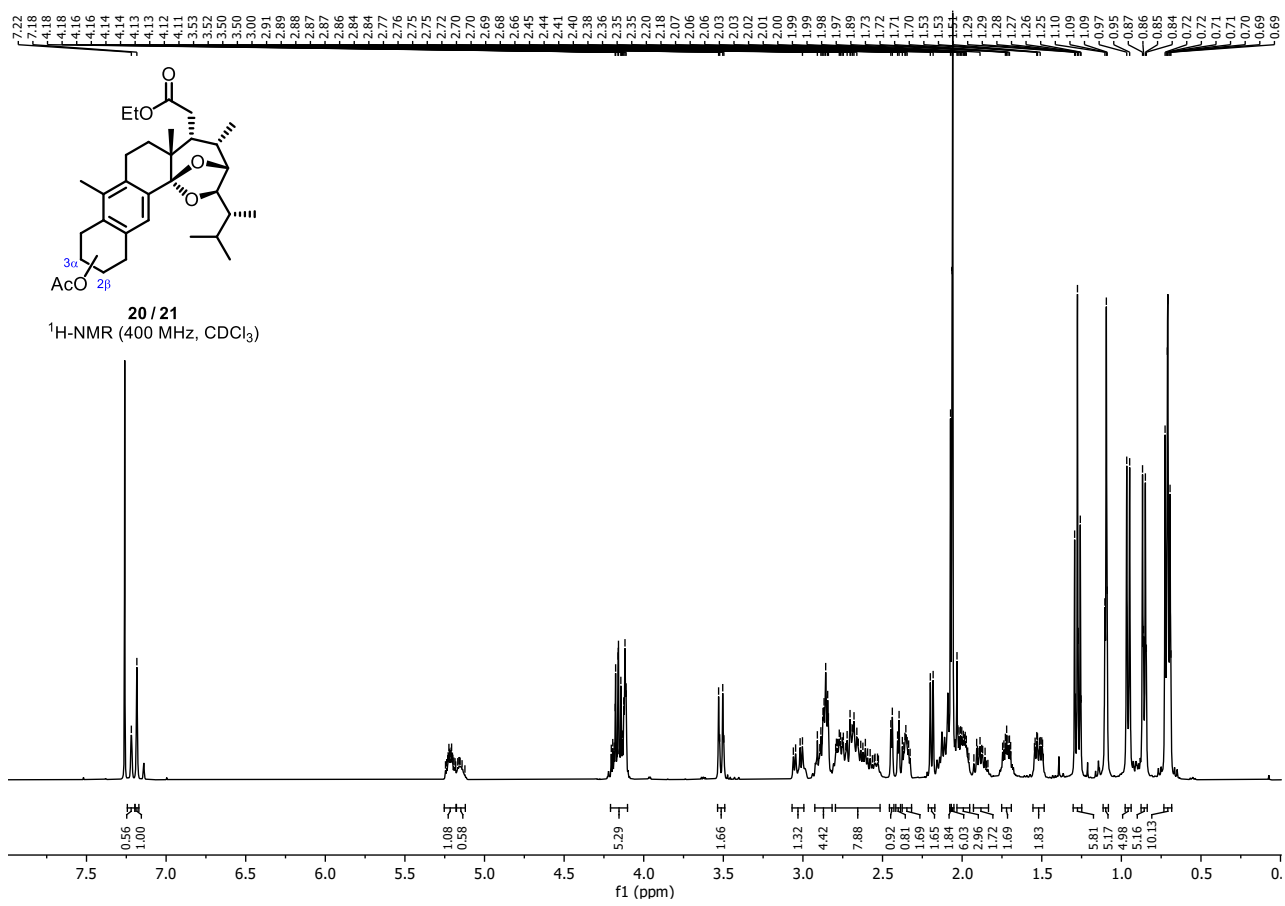


18; $^1\text{H-NMR}$ (400 MHz, CDCl_3)

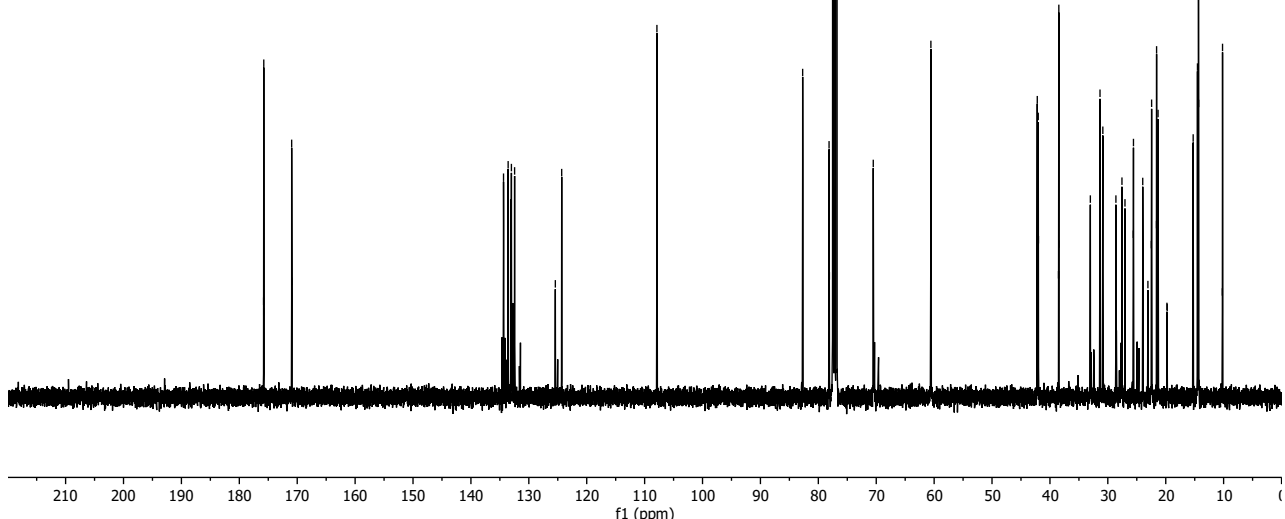


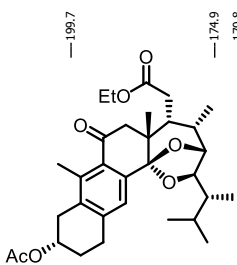
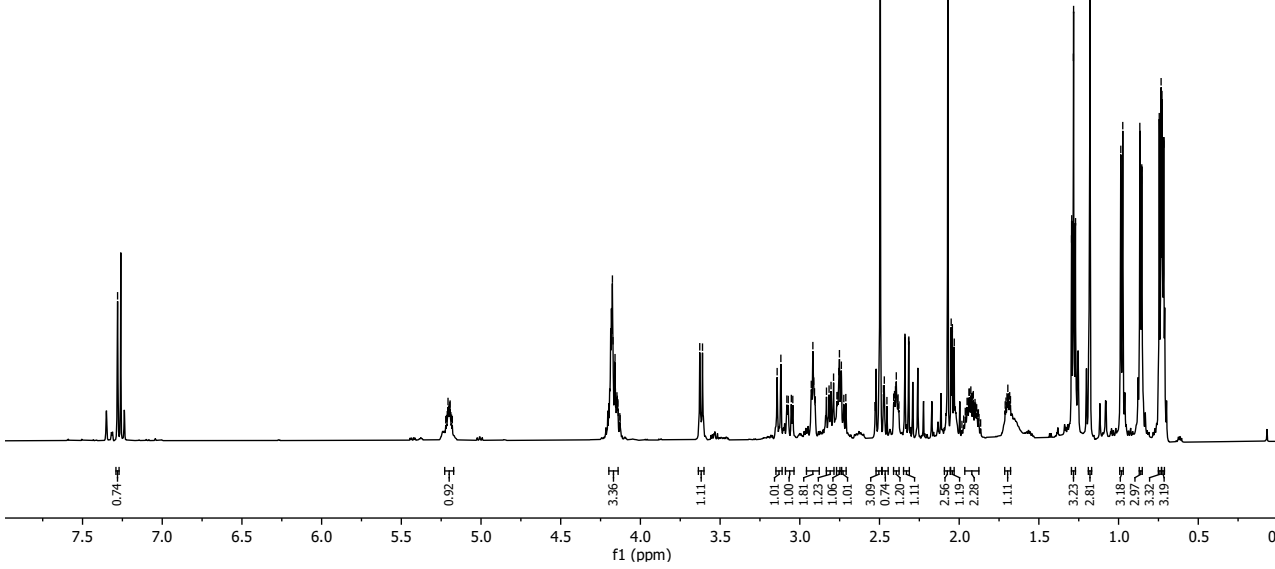
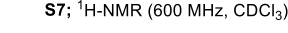
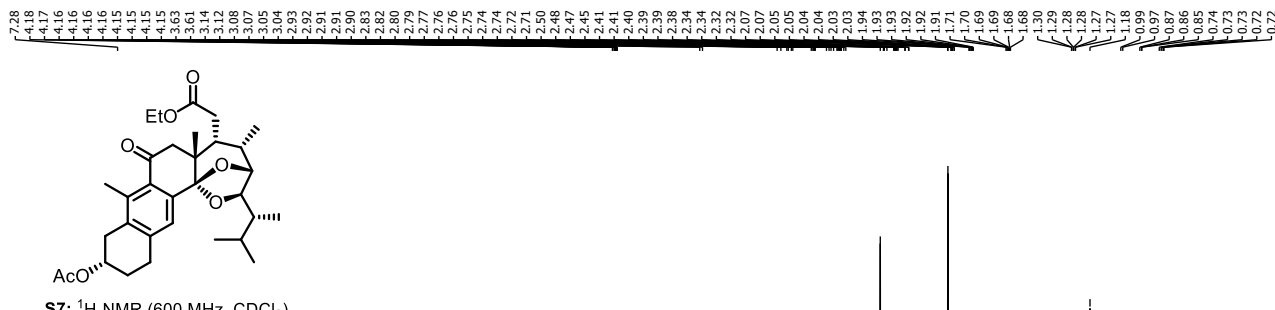
18: ^{13}C -NMR (101 MHz, CDCl_3)



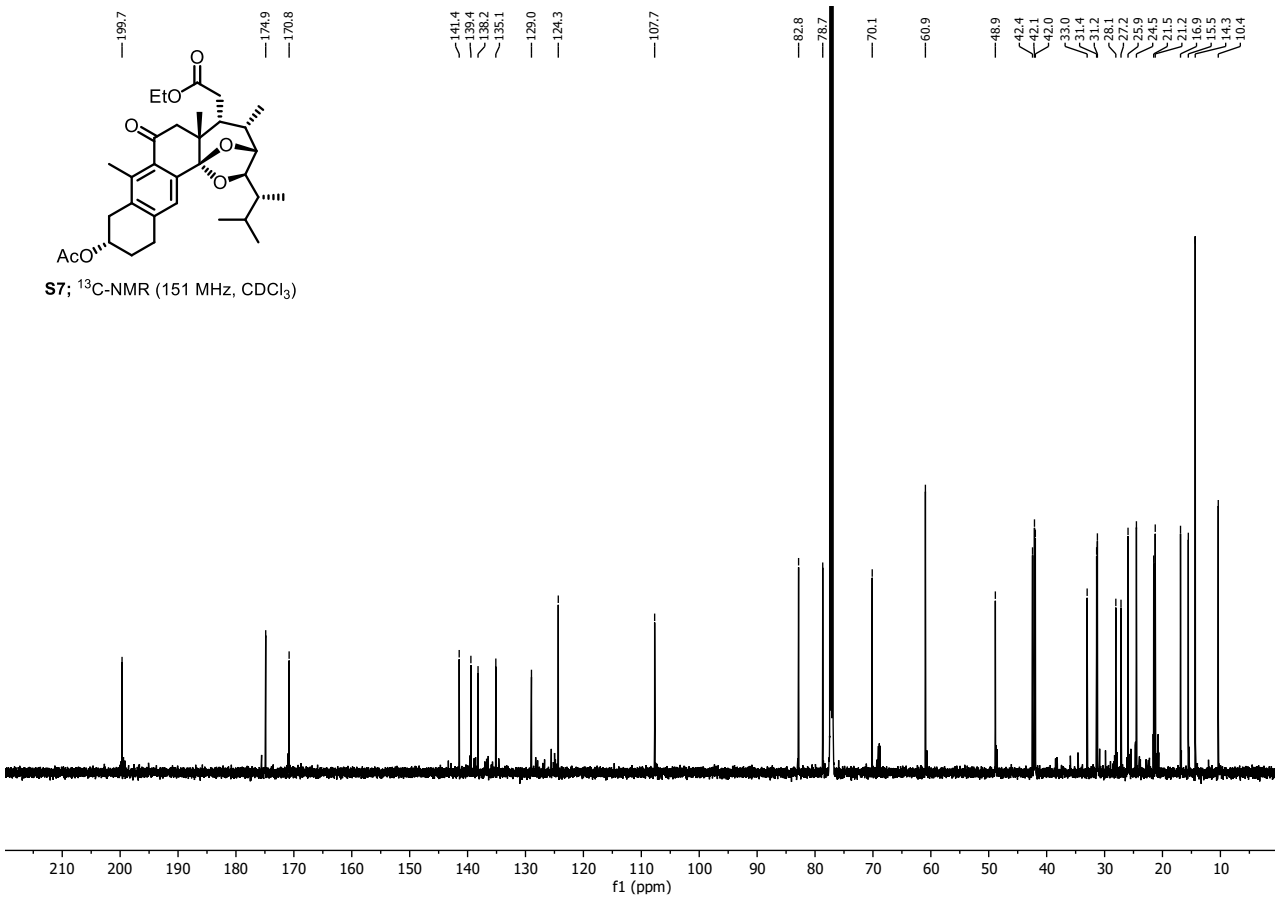


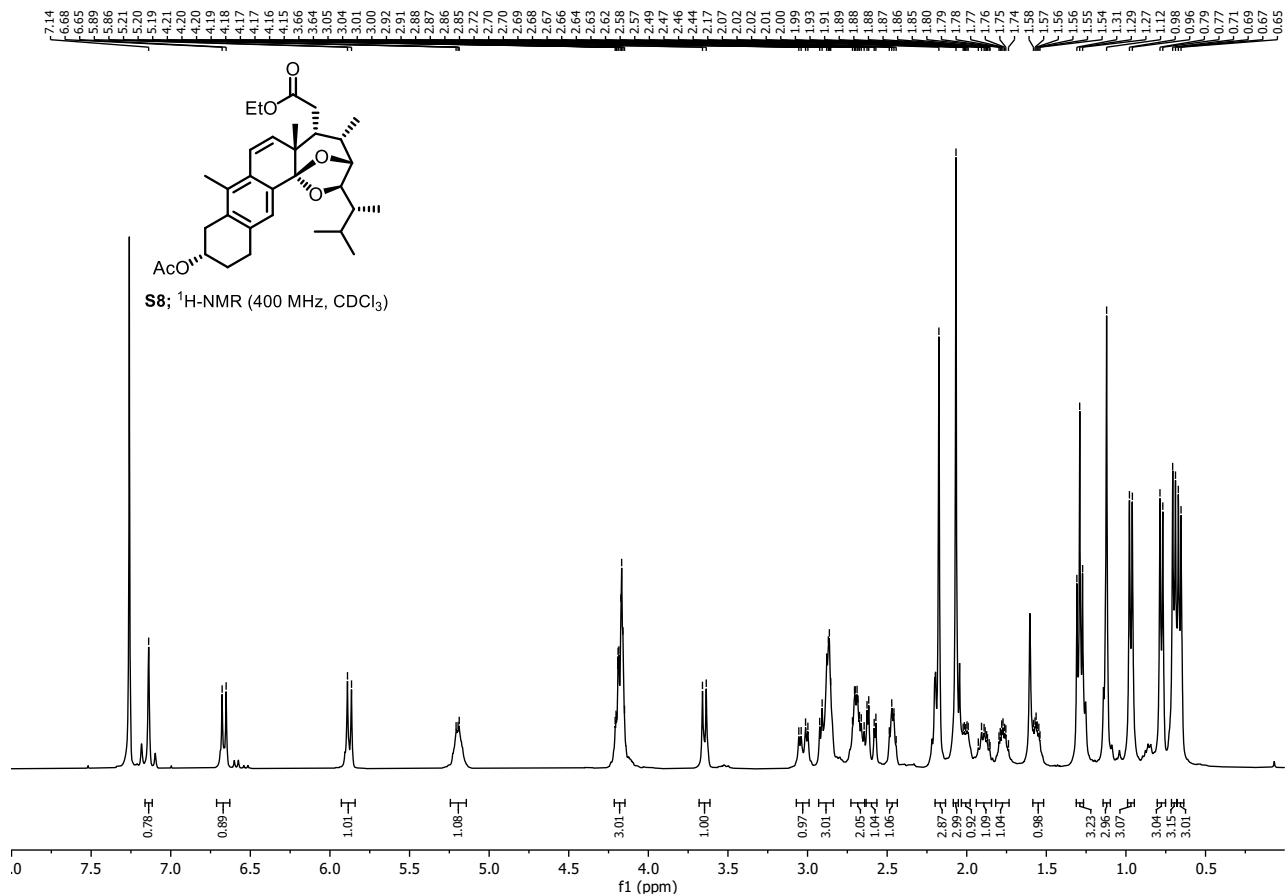
20 / 21

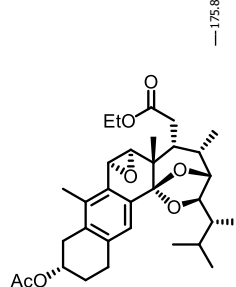
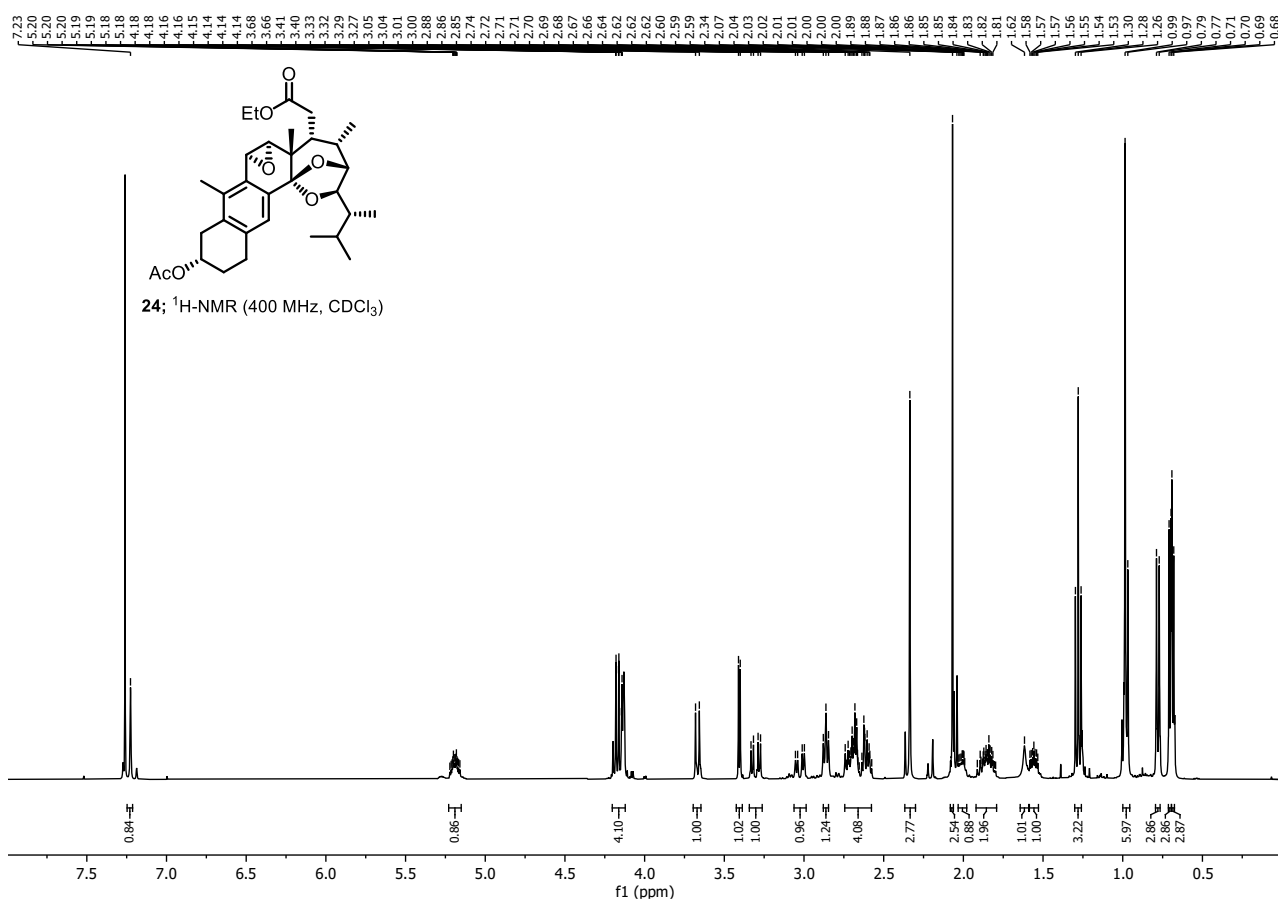




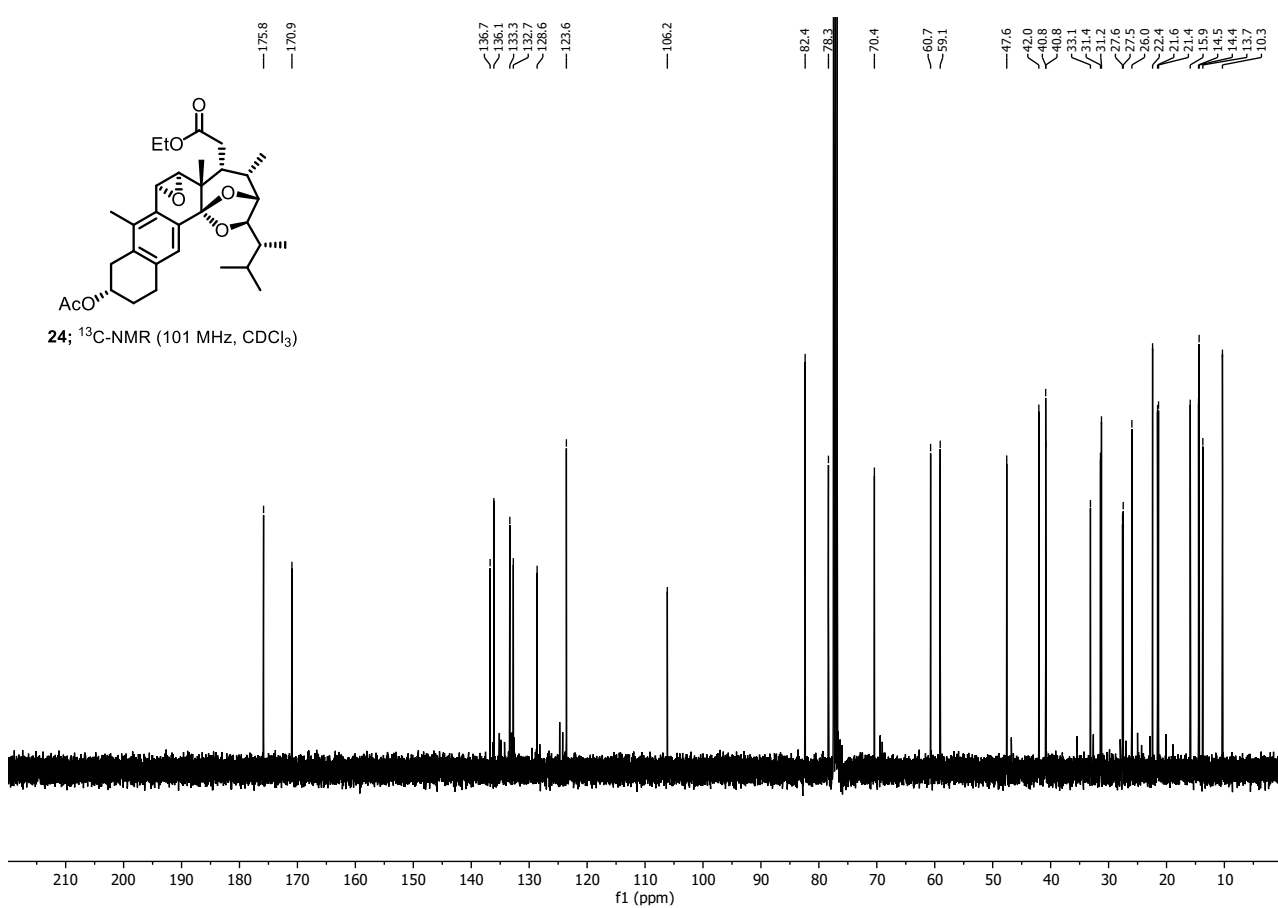
S7; ^{13}C -NMR (151 MHz, CDCl_3)

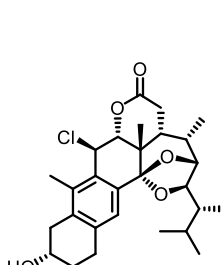
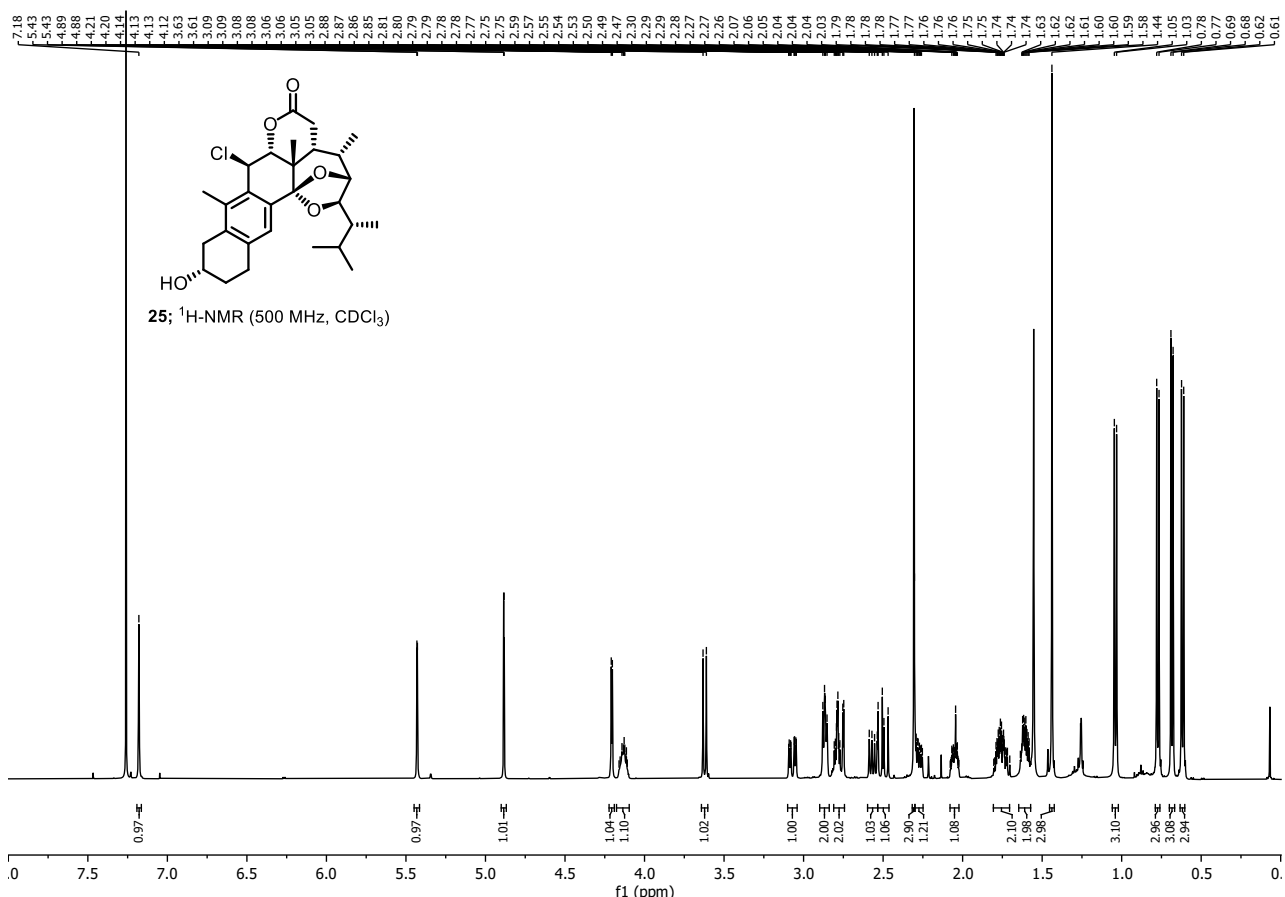




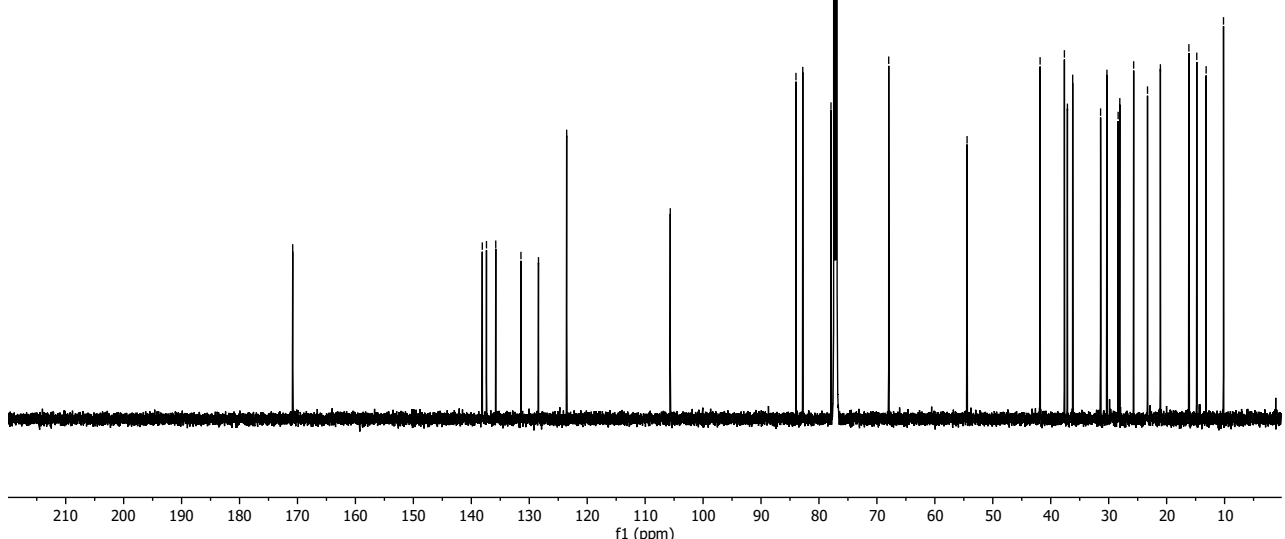


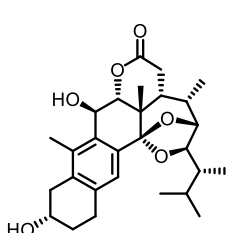
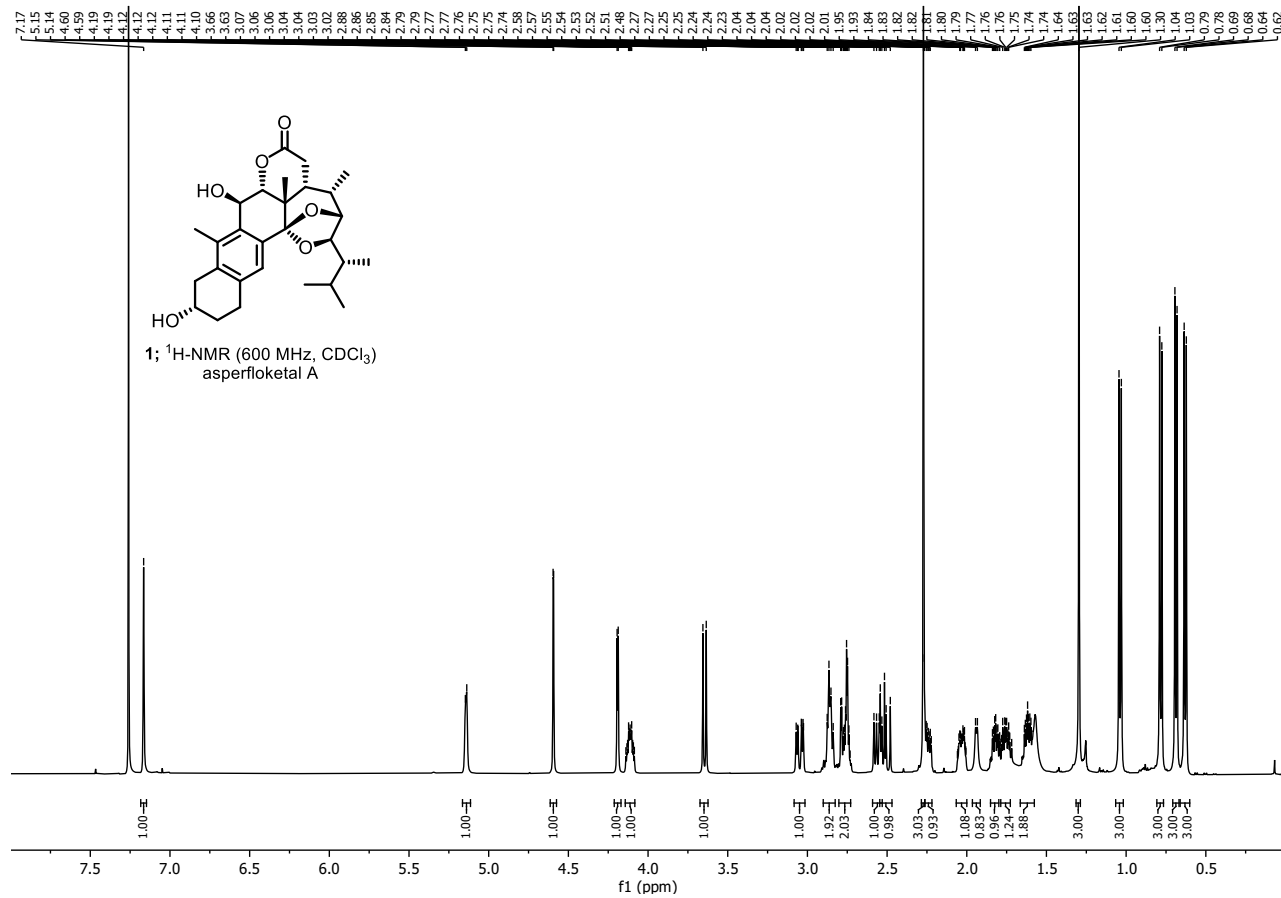
24; ^{13}C -NMR (101 MHz, CDCl_3)



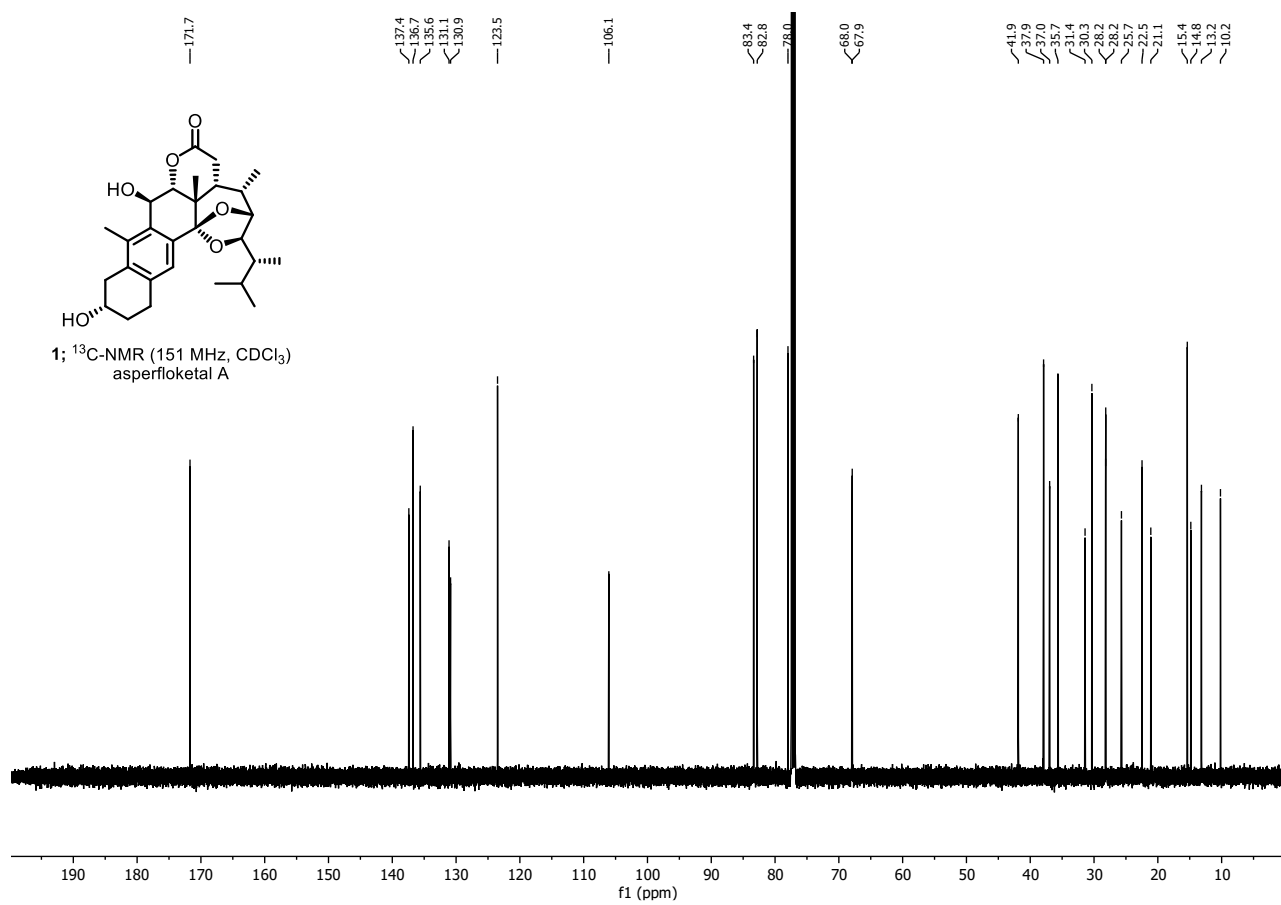


25; ^{13}C -NMR (151 MHz, CDCl_3)

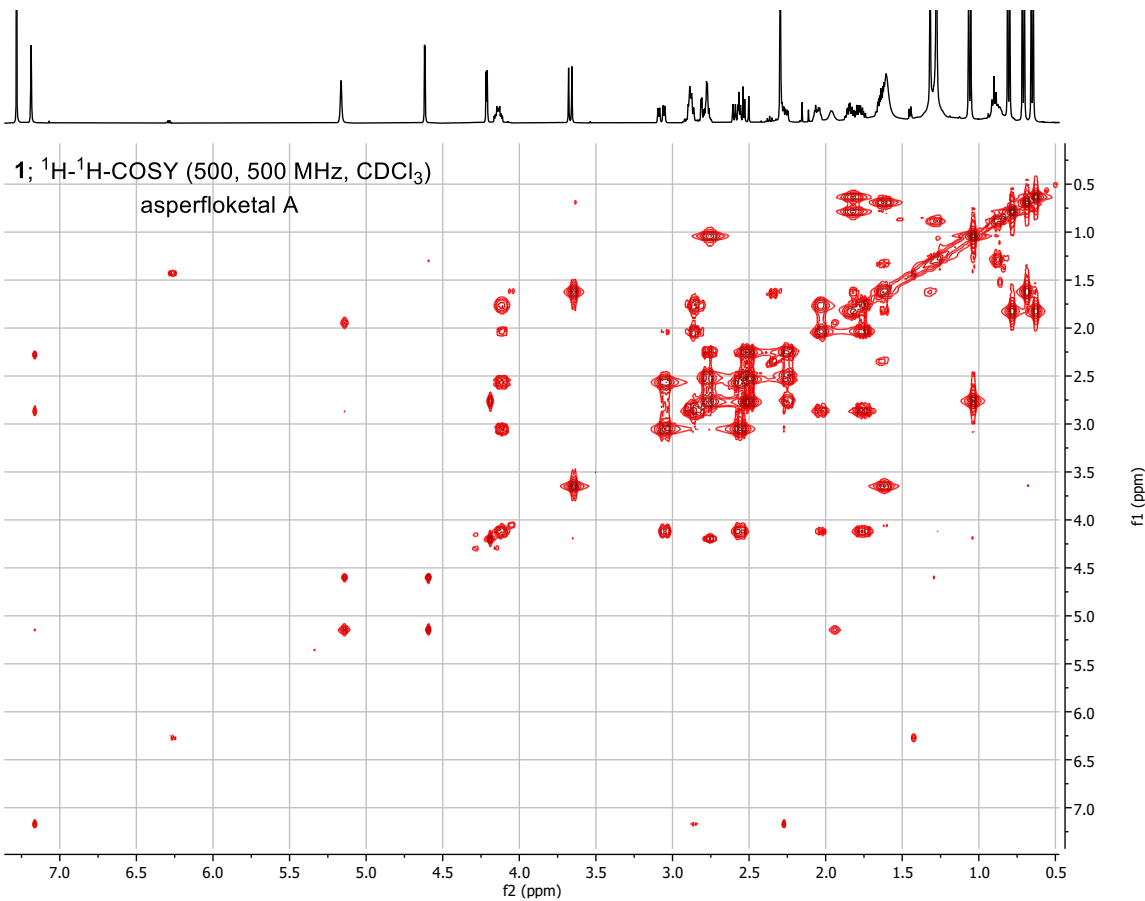
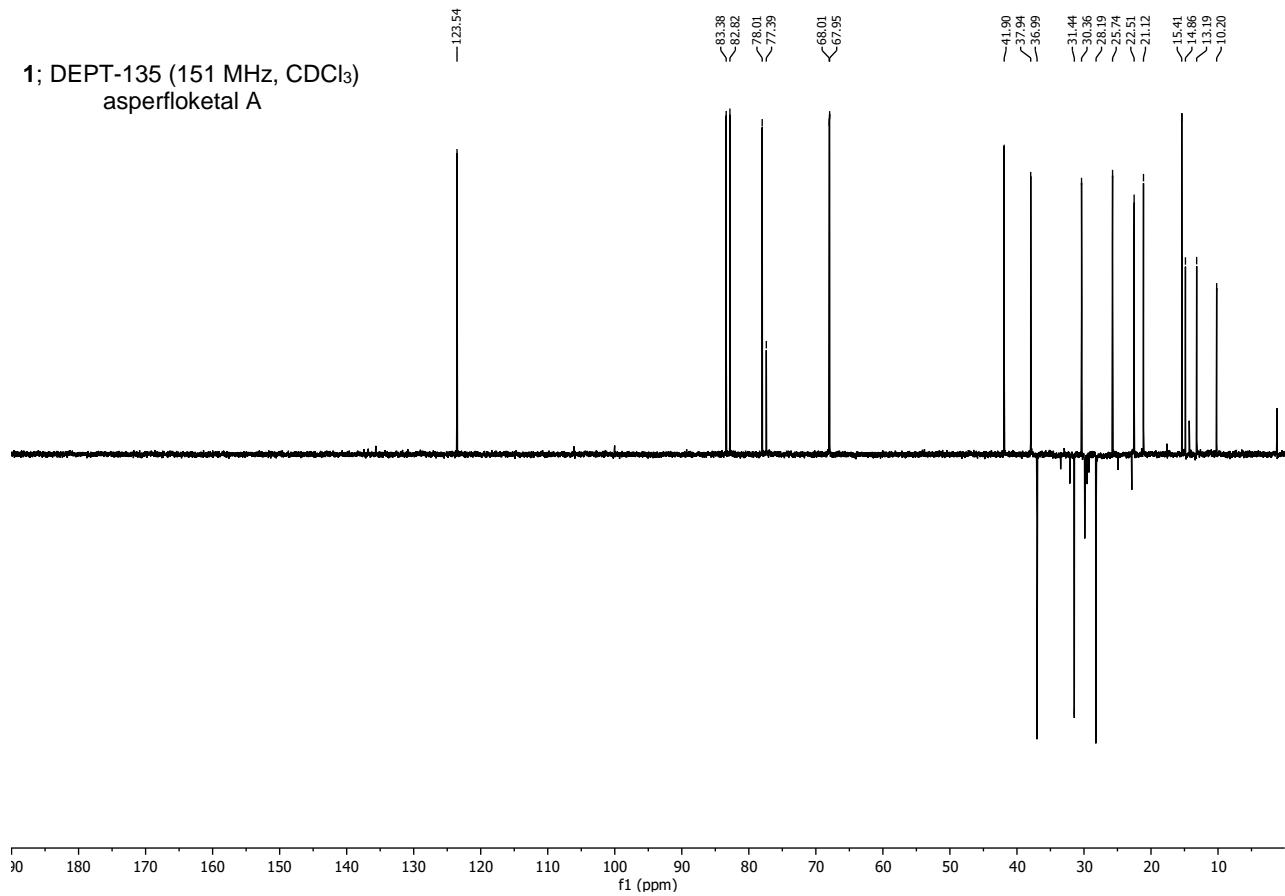


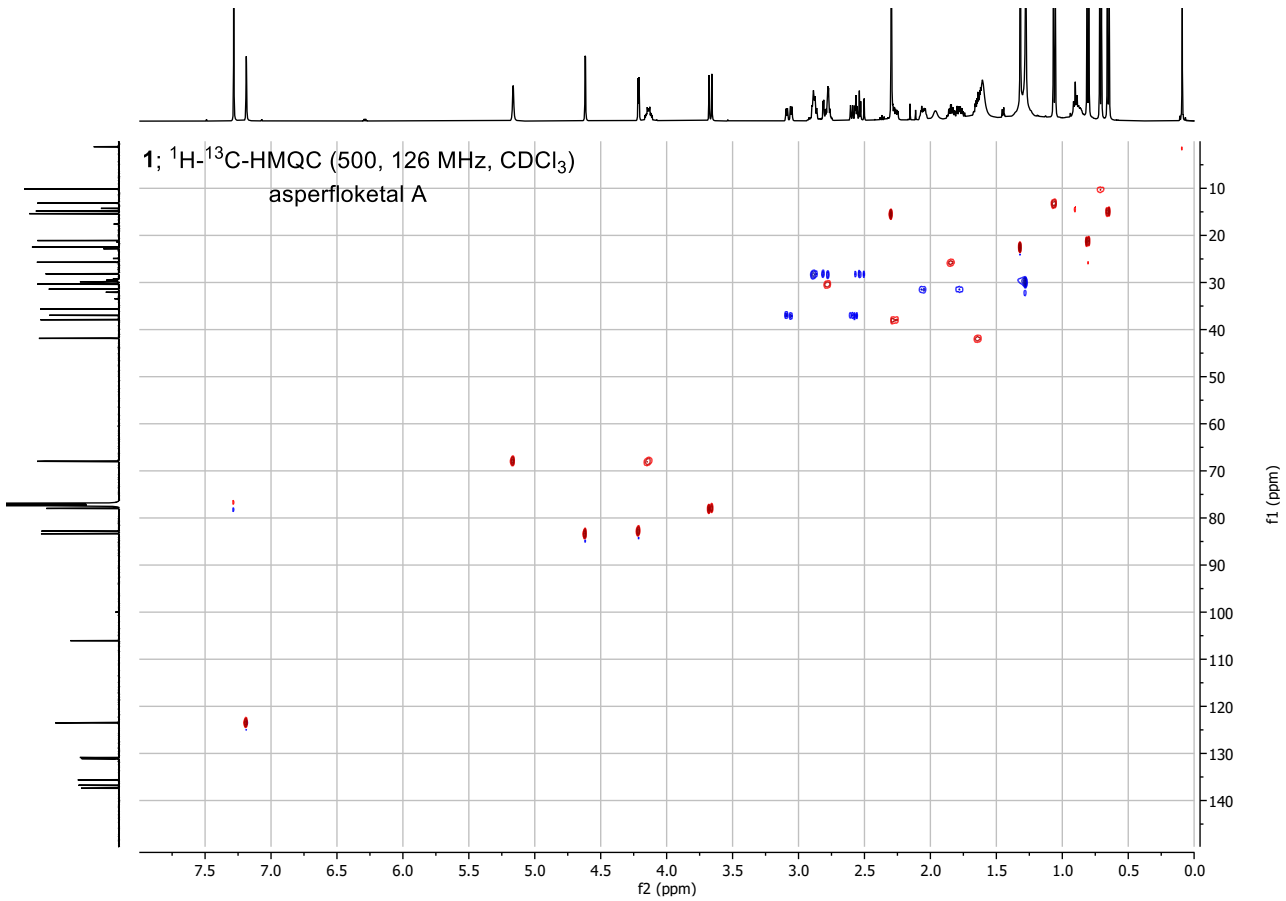
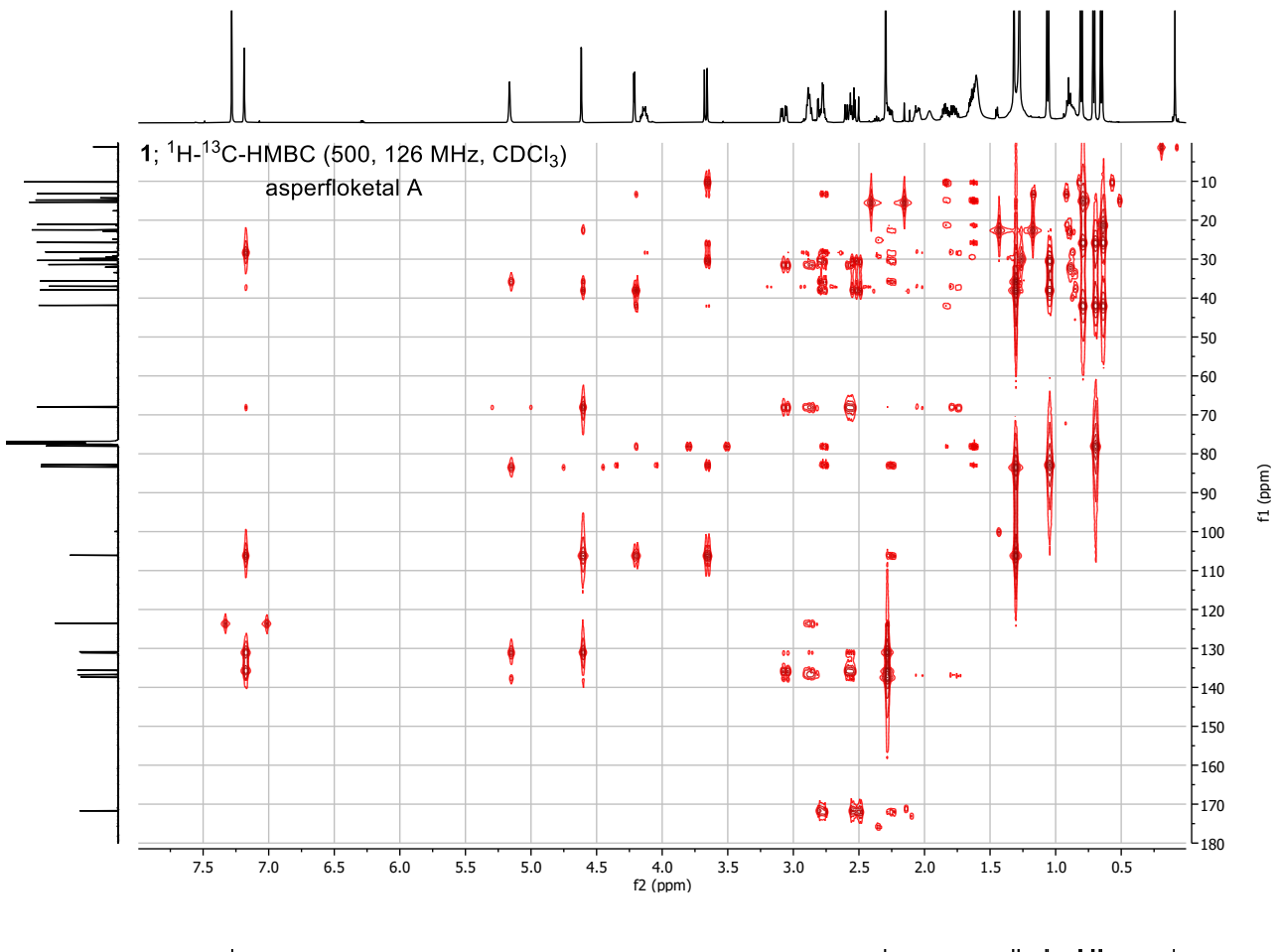


1; ^{13}C -NMR (151 MHz, CDCl_3)
asperfloketal A



**1; DEPT-135 (151 MHz, CDCl_3)
asperfloketal A**





References

- [1] Jiao, F.-R.; Gu, B.-B.; Zhu, H.-R.; Zhang, Y.; Liu, K.-C.; Zhang, W.; Han, H.; Xu, S.-H.; Lin, H.-W. Asperflokets A and B, the First Two Ergostanes with Rearranged A and D Rings, *J. Org. Chem.* **2021**, *86*, 10954–10961.
DOI: <https://doi.org/10.1021/acs.joc.0c02049>
- [2] The Sharpless ligand was prepared as described in: Jacobsen, E. N.; Markó, I.; Mungall, W. S.; Schroeder, G.; Sharpless, K. B. Asymmetric dihydroxylation via ligand-accelerated catalysis, *J. Am. Chem. Soc.* **1988**, *110*, 1968–1970.
DOI: <https://doi.org/10.1021/ja00214a053>
- [3] Burgess reagent was prepared as described in: Burgess, E. M.; Penton, H. R.; Taylor, E. A.; Thermal reactions of alkyl N-carbomethoxysulfamate esters, *J. Org. Chem.* **1973**, *38*, 26–31.
DOI: <https://doi.org/10.1021/jo00941a006>

Title:

Biogenetic space-guided synthesis of rearranged terpenoids

Type of authorship:

First Author

Type of article:

Feature Article

Share of work:

70% Mykhaylo Alekseychuk

30% Philipp Heretsch

Contribution to the publication:

The topic for this review was chosen by Mykhaylo Alekseychuk and Philipp Heretsch.

The natural products discussed were chosen by Mykhaylo Alekseychuk.

The manuscript was written by Mykhaylo Alekseychuk and and eddited by Philipp Heretsch.

Journal:

Chemical Communications

5-Year-impact factor:

5.553 (Academic Accelerator)

Date of publication:

10.05.2023

Number of citations:

0

DOI:

10.1039/D3CC01009K

PubMed-ID:

37162324

Reproduced from M. Alekseychuk and P. Heretsch, *Chem. Commun.* **2023**, 59, 6811–6826. with permission from the Royal Society of Chemistry.

This article is an open access article distributed under the terms and conditions of the Creative Commons Attribution Unported (CC BY 3.0) license.



Cite this: *Chem. Commun.*, 2023,
59, 6811

Received 28th February 2023,
Accepted 24th April 2023

DOI: 10.1039/d3cc01009k

rsc.li/chemcomm

Biogenetic space-guided synthesis of rearranged terpenoids

Mykhaylo Alekseychuk and Philipp Heretsch *

Natural product chemistry is constantly challenged by newly discovered, complex molecules. Elements of complexity arise from unprecedented frameworks, with a large amount of densely packed stereogenic centres and different functional groups along with a generally high oxidation state. As a prime example, rearranged triterpenoids possess all these elements. For their total synthesis, a limit of what is considered sensible in terms of steps and yield is frequently reached. As an alternative, semisynthetic approaches have gained a great amount of attention in recent years. In this featured article, we present our and others' contributions towards the development of efficient and economic syntheses of complex terpenoid natural products and elaborate on the underlying rationale of biogenetic space-guided synthetic analysis.

Introduction

The synthesis of complex natural products has shaped the field of organic chemistry. In the last few decades, total synthesis, a discipline deemed mature by some, has started to evolve beyond what has been coined the “age of feasibility”. The focus has shifted from making a molecule at any cost to providing answers to the pressing demand for sustainable, facile and concise routes even to the most complex targets.¹

Institute of Organic Chemistry, Leibniz Universität Hannover, Schneiderberg 1B, 30167 Hannover, Germany. E-mail: philipp.heretsch@oci.uni-hannover.de



Mykhaylo Alekseychuk

Mykhaylo Alekseychuk was born in Lviv, Ukraine, in 1997. He studied chemistry at Freie Universität Berlin gaining experiences in total synthesis of alkaloids and steroids along the way and graduated in 2020 with a master's thesis in the field of semisynthesis of rearranged steroids under the supervision of P. Heretsch. Right after, he joined the Heretsch group as a PhD student continuing his work on the semisynthesis of rearranged terpenoids completing the syntheses of spirochensilide A and B and asperfloketal A, both highlighted in this review.

Facilitating and streamlining access to the most complex natural products requires an understanding of nature's ways to biosynthesise these structures, *i.e.*, of their biogenesis. Biomimetic syntheses can then provide routes which frequently outperform conventional synthetic planning.² In the absence of a plausible biogenesis proposal, this strategy is not accessible, though.

Our group and others have recently engaged in the synthesis of highly oxidised and rearranged triterpenoid natural products. In this review, we would like to highlight in several



Philipp Heretsch

Philipp Heretsch was born in Lippstadt, Germany, in 1982. He obtained his PhD degree from Universität Leipzig (supervisor: A. Giannis) in 2009. After a postdoctoral stay with K. C. Nicolaou at The Scripps Research Institute, La Jolla, California, and at Rice University, Houston, Texas, he was appointed assistant professor at Freie Universität Berlin in 2015. Since 2022 he has been a full professor at Leibniz Universität Hannover. Philipp Heretsch has been working on the total synthesis of natural products since the beginning of his career. His group is now pursuing framework reconstruction strategies for the synthesis of terpenoids and alkaloids, guided by biosynthetic hypotheses.



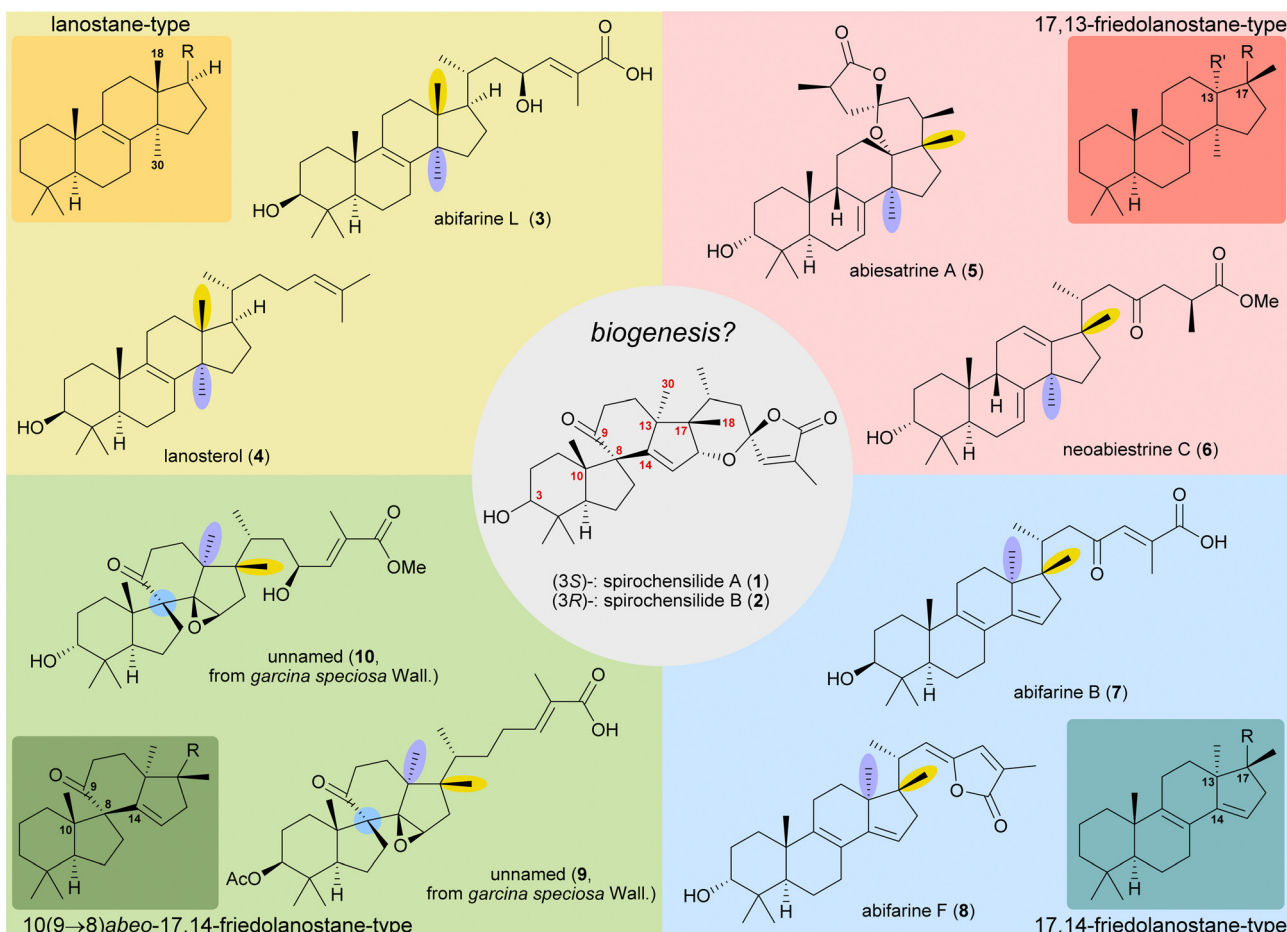


Fig. 1 Natural products with related carbon frameworks in our biogenetic space-guided analysis towards spirochensilide A (1) and B (2).

examples the rationale of biogenetic space-guided analysis, which we followed during our endeavours.

Thus, rigorously applying the following steps greatly helped to narrow down a synthetic problem. Accordingly, the chemical space around the natural product to be accessed is analysed. Co-isolated products as well as related natural products from close and more distant producing organisms are identified and then evaluated for a potential biosynthetic connection. Like assembling a puzzle, by putting these structural hints together, one can gather ideas on how nature may perform the relevant manipulations to transform a member of the standard repertoire of secondary metabolites into the natural product in question. In this analysis, unprecedented structural motifs, especially reconnections within the skeletal framework, are identified in a stepwise manner, with the intermediates being either already known isolated entities or those constituting anticipated natural products.

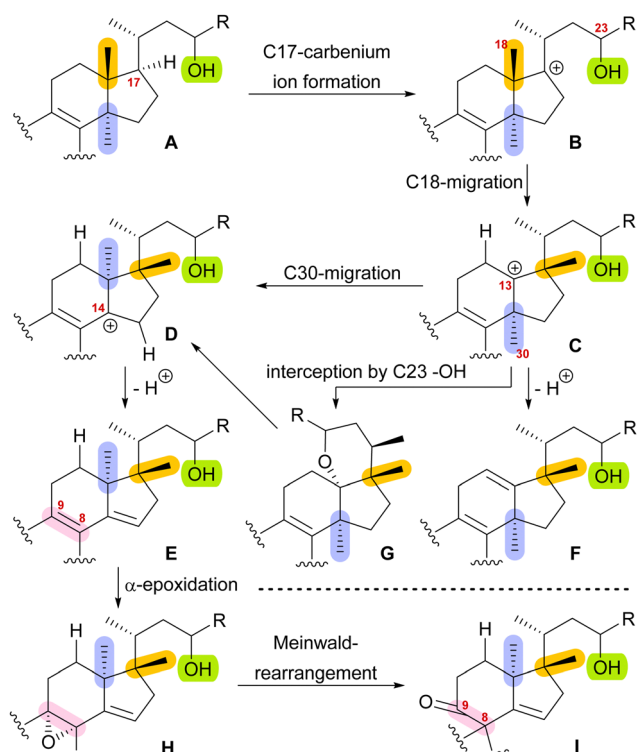
When this process of biogenetic space-guided analysis has provided a sensible biogenesis proposal, we set out to prove this hypothesis by chemically emulating the steps. If correct, replication of the key steps can be realised by chemical means (*i.e.*, biomimetically), employing the anticipated reactivity, and, thereby, supporting the biogenesis hypothesis. As a result of this process, not only the natural product, but also structurally

related natural products *en route* to the final target can be obtained. Since the other intermediates encountered in the process all resemble the target structure to a certain degree, studying the structure–activity relationships (SARs) is another potential advantage and can provide answers to the question “which structural characteristics are necessary to provide a respective biological function?”

Spirochensilide A and B

The concept of biogenetic space-guided analysis is best demonstrated in the example of our synthesis of spirochensilide A (1) and B (2). These lanosterol-derived triterpenes were isolated by the group of Li and co-workers in 2015 from the Chinese fir *Abies chensiensis*.³ They feature a rearranged 10(9 → 8)abeo-17,14-friedolanostane-type carbon backbone with a spiro[4.5]decane and a 1,6-dioxaspiro[4.5]decene-motif (Fig. 1). Thus, the methyl groups 18 and 30 which reside at C13 and C14 in the lanostane skeleton have both moved by one carbon, to C14 and C17, respectively. Spirochensilide A (1) and spirochensilide B (2) differ in the stereoconfiguration at C3, with spirochensilide A (1) being the major isolated diastereomer.





Scheme 1 Proposed biosynthetic steps for the formation of $10(9 \rightarrow 8)$ abeo-17,14-friedolanostanes based on biogenetic space-guided analysis.

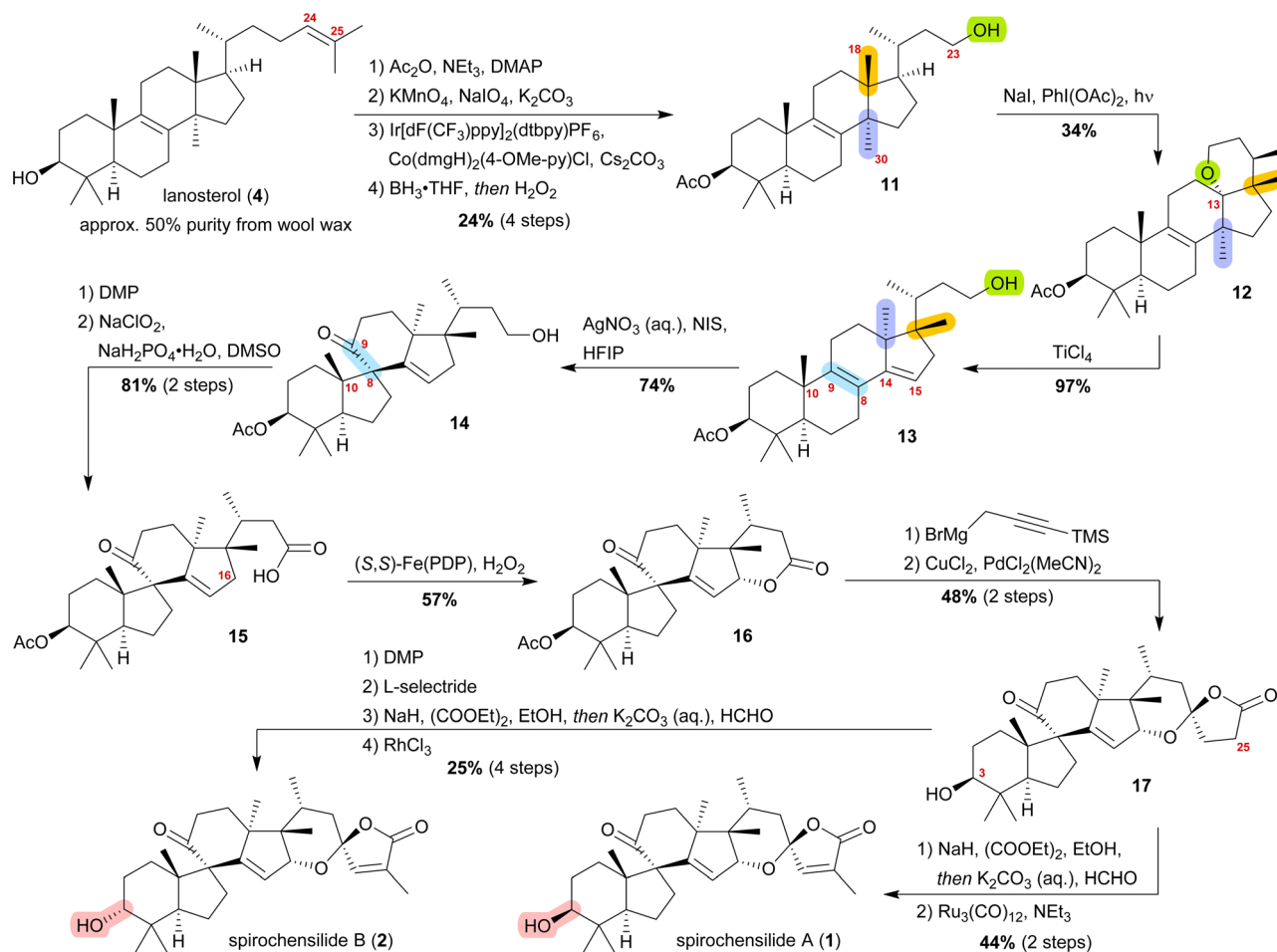
The first total synthesis of spirochensilide A (**1**) was published in 2020 by Yang and co-workers⁴ with a Meinwald rearrangement⁵ and a Pauson–Khand reaction as key steps and proceeded in 27 linear steps from geranyl acetate. We first encountered the spirochensilides as potential targets for semi-synthesis in 2019 and were instantly intrigued by their interesting structure, so we decided to take a deeper look into a plausible biosynthesis. During our investigation, we identified abifaraines⁶ and abiesatrides,⁷ two classes of natural products containing 17,14-friedolanostane-type or 17,13-friedolanostane-type carbon backbones, respectively, isolated from other species of the *Abies* genus, *i.e.*, *Abies fargesii* for abifaraines and *Abies georgei* Orr for abiesatrides (Fig. 1). Thus, in abifarine L (**3**) the standard lanostane framework is still unaffected, while abiesatrine A (**5**) and neoabiestrine C (**6**)⁸ are 17,13-friedolanostanes and abifarine B (**7**) and abifarine F (**8**) have a 17,14-friedolanostane carbon backbone, indicating that the shifts of the 18 and 30 methyl groups may occur in a stepwise and not concerted manner. When looking further into related natural products, we also noticed yet unnamed steroids **9** and **10**, among others, displaying an $10(9 \rightarrow 8)$ abeo-motif and, at the same time, migrated 18 and 30 methyl groups.⁹ We reasoned, the 17,14-friedolanostane carbon backbone may be a prerequisite for the later formation of the $10(9 \rightarrow 8)$ abeo-motif, especially since no isolated natural products solely possessing the $10(9 \rightarrow 8)$ abeo-motif, but without shifted methyl groups could be found. Extensive experiments by the isolators of the spirochensilides on lanostane-derived 8,9-epoxides to effect a Meinwald rearrangement, and thus forge the spiro-motif, failed, further supporting our assumption.³

With this hypothesis, we proposed a biosynthetic pathway for the 17,14-friedolanostane framework, as found in spirochensilide A (**1**) and B (**2**) (Scheme 1):¹⁰ Formation of a carbenium ion at C17 **B** is followed by a Wagner–Meerwein rearrangement of the 18-Me group from C13 to C17. The so-obtained carbenium ion at C13 **C** can then either undergo a second Wagner–Meerwein rearrangement of the 30-Me group from C14 to C13 to give cation **D** followed by proton elimination to yield diene **E** or directly lose a proton to give the 12,13-double bond in **F**, as in neoabiestrine C (**6**). Nucleophilic interception by the C23 OH-group can, as a third alternative, give tetrahydropyran **G**, as in abiesatrine A (**5**). This tetrahydropyran could, at a later point, also be reopened to regenerate the carbenium ion at C13 **C** and facilitate the 30-Me rearrangement. Diene **E** could then selectively be epoxidised from the α -face at the 8,9-double bond to give epoxide **H**, which could then rearrange in a Meinwald rearrangement to give the $10(9 \rightarrow 8)$ abeo-17,14-friedolanostane framework **I**.

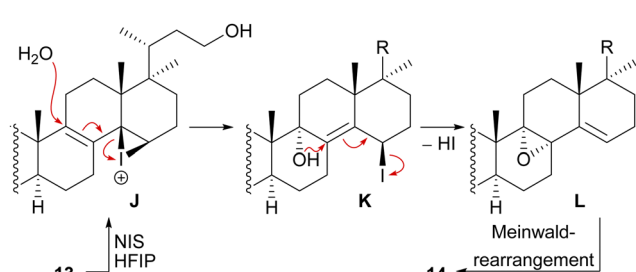
We decided to plan our synthesis around these rearrangements and employ lanosterol (**4**) as a starting material. To access the desired carbenium species in the unfunctionalised C17 position and without introducing a leaving group beforehand, we envisioned a radical process taking advantage of the distal hydroxyl moiety at C23, present, *e.g.*, in unnamed natural product **10**, and use it for an H-atom transfer (HAT) process. Thus, acetylation of the C3-alcohol and Lemieux–von Rudloff oxidative scission¹¹ of the side chain gave the 24-carboxylic acid (structure not shown), which was consecutively subjected to a photocatalytic decarboxylative elimination¹² to give the terminal olefin which was then converted into the desired C23-alcohol **11** in a hydroboration/oxidation reaction (Scheme 2). The use of NaI, PhI(OAc)₂ and light from a 45W CFL lamp gave the corresponding alkoxy radical which underwent 1,5-HAT.¹³ A radical-polar crossover then furnished the carbenium ion, which induced the Wagner–Meerwein rearrangement of the 18-Me group. Interestingly, and as predicted as a third alternative (*vide supra*), the alcohol at C23 then intercepted the C13 carbenium ion and formed tetrahydropyran **12**. This product was readily transformed into the desired 17,14-friedolanostane **13** by the addition of TiCl₄. Using so-obtained diene **13**, epoxidation attempts only gave the $14\beta,15$ -epoxide instead of the required $8\alpha,9$ -epoxide. This reactivity could be exploited by the formation of a fleeting $14\beta,15$ -iodonium ion **J** employing *N*-iodosuccinimide (NIS), AgNO₃ and H₂O (Scheme 3). Under these conditions, presumably, an intramolecular S_N2' reaction gave the desired $8\alpha,9$ -epoxide **L** which instantly rearranged to give the $10(9 \rightarrow 8)$ abeo-motif. The choice of solvent (hexafluoroisopropanol, HFIP) was critical for this reaction, as all other solvents tested led mostly to decomposition or, and only when the C23-alcohol was protected, to very low yields (3–14%).

The primary alcohol at C23 of $10(9 \rightarrow 8)$ abeo compound **14** was then oxidised to carboxylic acid **15** using Dess–Martin periodinane (DMP) followed by Pinnick oxidation. Lactone **16** was formed in the following step by allylic oxidation using the White–Chen catalyst.¹⁴ The 1,6-dioxaspiro[4.5]decene system was then installed in a two-step procedure. First, addition of





Scheme 2 Semisyntheses of spirochensilide A (**1**) and B (**2**) by Heretsch and co-workers. ppy = 2-phenylpyridine, dtbpy = 4,4'-di-tbutyl-2,2'-bipyridine, dmgh = dimethylglyoximate, (S,S)-PDP = (−)-2-((S)-2-((S)-1-(pyridin-2-ylmethyl)pyrrolidin-2-yl)pyrrolidin-1-yl)methyl)pyridine.



Scheme 3 Mechanistic details of the iodonium-induced epoxidation of **13**.

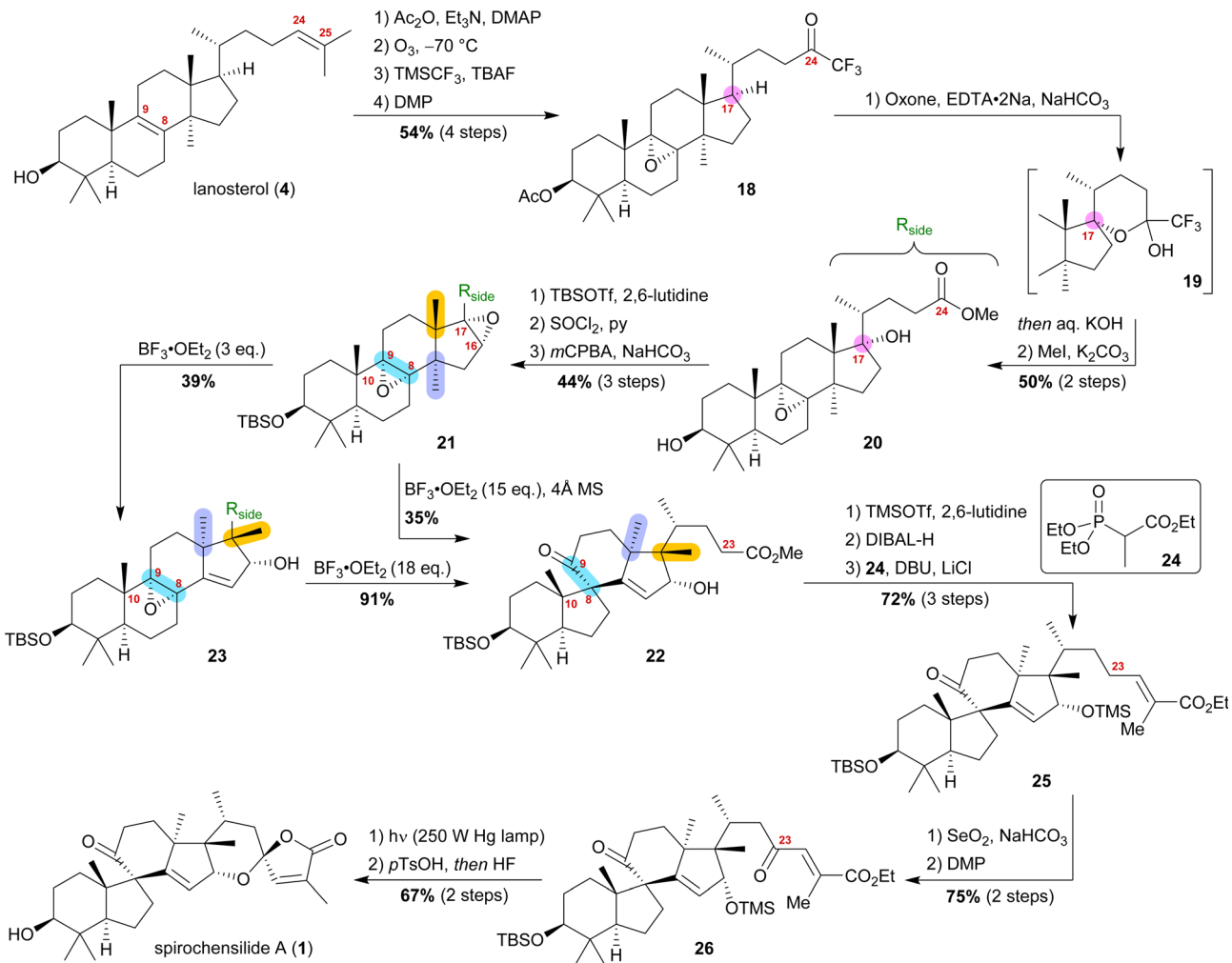
silylated propargylmagnesium bromide to lactone **16** and simultaneous deprotection of the acetate at C3, followed by cyclisation of the hemiacetal using PdCl₂(MeCN)₂/CuCl₂ to afford lactone **17**, was carried out. To complete the synthetic access to spirochensilide A (**1**), introduction of an exomethylene group in the α -position of the lactone and subsequent double bond isomerisation were necessary. For spirochensilide B (**2**), before the last two steps were carried out, first, the stereoconfiguration of the C3 alcohol of **17** had to be inverted by oxidation and diastereoselective reduction.

The synthesis of spirochensilide A (**1**) was, thus, completed in 13 steps from lanosterol (**4**), which, in comparison to the total synthesis by Yang and co-workers (27 steps), highlights the main advantage of semisynthesis over total synthesis.^{4,10}

A few months after we reported our synthesis, a second semisynthetic approach was published by the group of Deng.¹⁵ Following a similar synthetic approach, they arrived at the same conclusion, *i.e.*, the Wagner–Meerwein rearrangements most likely have to precede the Meinwald rearrangement to render the latter possible. As their synthesis still differs from our approach, we here present a second example of a biogenetic space-guided analysis.

Starting from lanosterol (**4**), the C3 alcohol was acetylated, and then ozonolysis at $-78\text{ }^\circ\text{C}$ led to the epoxidation of the 8,9-double bond while concomitantly cleaving the 24,25-double bond to provide an aldehyde, which was then converted to trifluoromethyl ketone **18** by reaction with TMSCF₃ and subsequent oxidation with DMP (Scheme 4). The use of oxone and NaHCO₃ initiated a dioxirane-mediated¹⁵ formation of hemiacetal **19**, which was then hydrolysed to give C17 alcohol and C24 acid. Methylation in a consecutive step using MeI gave methyl ester **20**. During this transformation, the acetate at C3





Scheme 4 Semisynthesis of spirochensilide A (**1**) by Deng and co-workers.

was removed and reprotection of the thus-obtained 3-hydroxyl group as a TBS-ether became necessary.

Elimination of the alcohol at C17 and epoxidation of the so-generated double bond then furnished $16\alpha,17$ -epoxide **21**. This epoxide was then rearranged to $10(9 \rightarrow 8)$ abeo- $17,14$ -friedolanostane **22** when treated with 15 eq. of $\text{BF}_3\text{-OEt}_2$. The authors further investigated this reaction and were able to perform the Wagner–Meerwein cascade without the consecutive Meinwald rearrangement by using only 3 eq. of $\text{BF}_3\text{-OEt}_2$. So-obtained epoxide **23** could then undergo Meinwald rearrangement when treated with excess $\text{BF}_3\text{-OEt}_2$. This competition experiment proved the order of rearrangements and further supported our results. Protection of the C16 alcohol of $10(9 \rightarrow 8)$ abeo- $17,14$ -friedolanostane **22** as a TMS-ether allowed for side chain extension *via* selective reduction of the methyl ester to the aldehyde using DIBALH and subsequent Horner–Wadsworth–Emmons reaction with propanoate **24** to give allylic ester **25**. Riley oxidation at C23 and oxidation of the so-formed alcohol using DMP gave ketone **26**. Finally, photoisomerisation of the $24,25$ -double bond was performed with subsequent TMS-deprotection under acidic conditions, leading to an intramolecular hemiacetalisation/lactonisation

cascade and, thus, generating the dioxaspiro[4.5]decene motif. The addition of HF deprotected the C3 alcohol to yield spirochensilide **A** (**1**) in a total of 17 steps.¹⁵

Both syntheses show the power of biogenetic space-guided synthetic planning arriving at more step-efficient approaches (13 steps [Heretsch],¹⁰ 17 steps [Deng]¹⁵) in comparison to the total synthesis (27 steps [Yang]⁴).

Strophasterol A and penicillitone

The synthesis of strophasterol A (**27**) is another example of biogenetic space-guided synthetic planning published by our group.¹⁶ In addition, it also furnished a versatile $14,15$ -secosteroid platform, applicable for the syntheses of several other $14,15$ -secosteroids as recently showcased in our syntheses of penicillitone (**28**)¹⁷ and asperflokal A (**54**)¹⁸ (*vide infra*).

Strophasterols A–D (**27**, **32–34**) were first isolated from *Stropharia rugosoannulata* in 2012 by Kawagishi and co-workers,¹⁹ while strophasterols E (**35**) and F (**36**) were discovered later in 2019 by the group of Kikuchi from *Pleurotus eryngii*.²⁰ Especially,



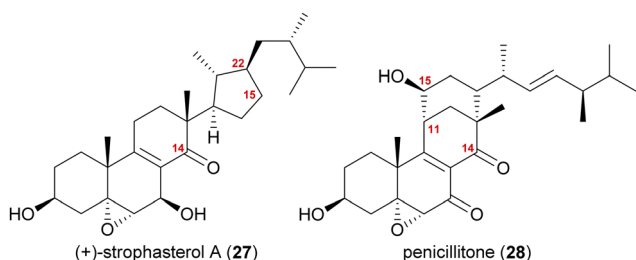


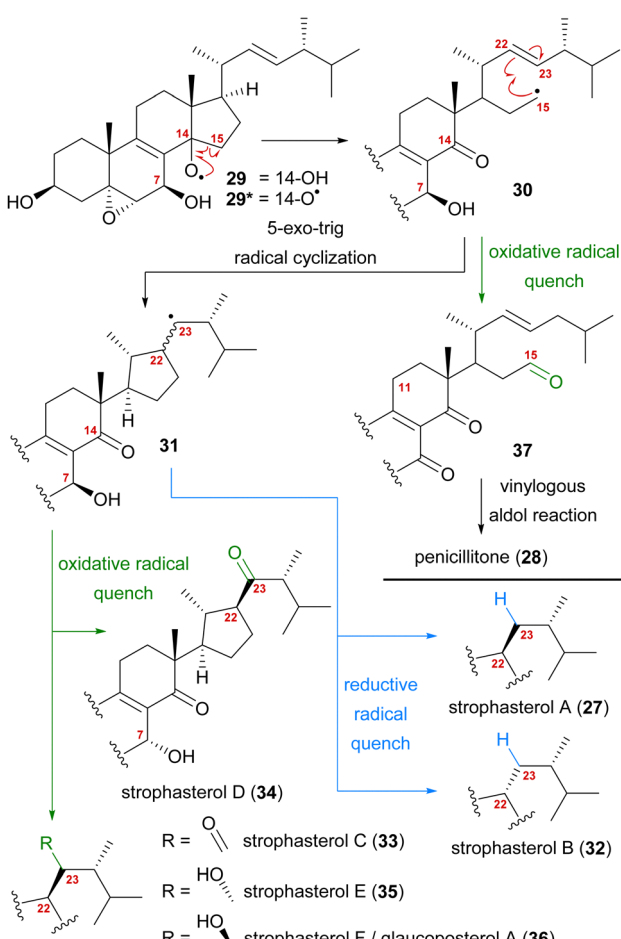
Fig. 2 Structures of strophasterol A (27) and penicillitone (28).

strophasterol A (27) gained attention due to its mitigating effects on Alzheimer's disease.

A first look at the connectivity of the carbon framework indicated a cleavage of the C14–C15-bond with C15 being reconnected to side chain C22 forming a five-membered ring (Fig. 2). In combination with the oxidation level of C23 (methylene or carbonyl), a radical cyclisation mechanism may be operative in the formation of this motif (Scheme 5). Analysis of the co-isolated natural products from *Stropharia rugosoannulata* furnished highly oxidised steroid 29 with a C14 alcohol and the A and B rings functionalised in a similar manner as in

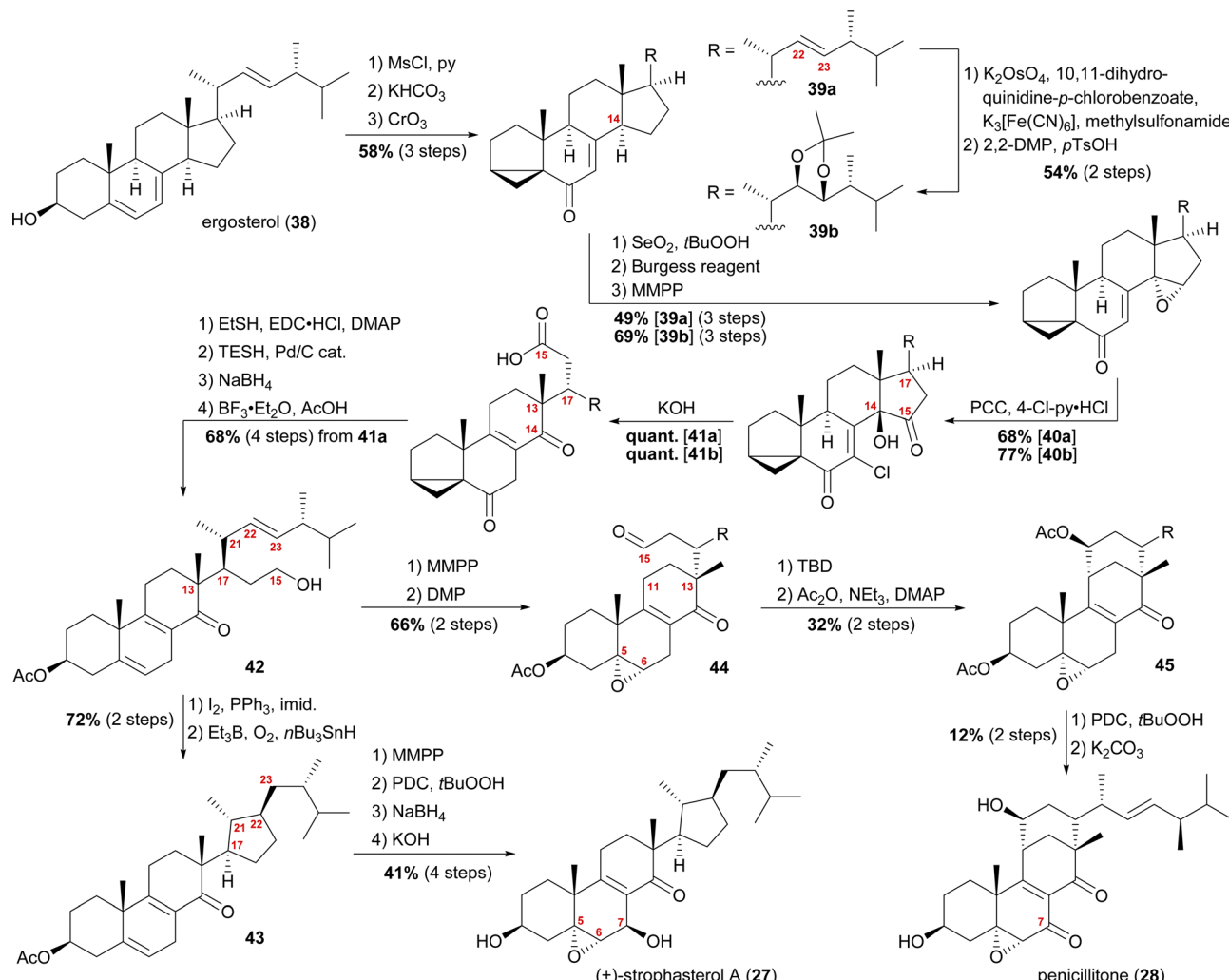
strophasterols.¹⁹ Building upon this information, we initially proposed 29 to be a biosynthetic precursor in which an alkoxy radical 29* would be formed from the C14 alcohol. This alkoxy radical could then initiate a β -scission of the C14,15-bond resulting in ketone 30 with a radical at C15. The latter would react in the 5-exo-trig radical cyclisation to furnish cyclopentane 31 with a radical at C23. A reductive quench of this radical would lead to either strophasterol A (27) or B (32), while an oxidative quench could lead to the formation of strophasterols C–F (33–36). Assuming an oxidative quench could also happen with the C15 radical 30, the formation of aldehyde 37 became a possibility. This aldehyde could react in an intramolecular vinylogous aldol reaction to furnish structurally related penicillitone (28). Penicillitone (28) was first isolated in 2014 by Wei and co-workers from *Penicillium purpurogenum* and was very recently synthesised for the first time by our group.^{17,21}

When we tried performing a radical-mediated 14,15 cleavage on a model substrate, however, we instead observed selective cleavage of the C13–C14-bond which was the starting point for our synthetic efforts towards dankasterone A (68) and B (69), as well as swinhoeisterol A (70) and periconiastone A (71), as will be discussed later. Although we chemically disproved the first step of our proposed radical biosynthetic pathway for this particular model system, a radical 14,15 cleavage may still be operative in a more closely related system and enzymatic environment, though. Our synthesis of strophasterol A commenced with the access to 14,15-steroid platform 41. Starting from ergosterol (38), masking the diene in the B ring was achieved by the formation of i-steroid 39a (Scheme 6).²² Towards the synthesis of asperflokal A (*vide infra*), dihydroxylation and acetonide protection in the side chain was performed on the same i-steroid 39a. From there, the transformations towards the 14,15-seco platforms were identical for both, the 22,23-bishydroxy- and the Δ^{22} -compounds, with slightly higher yields being obtained for the 22,23-diols, possibly due to the absence of an additional, potentially reactive, double bond. In the next step, i-steroids 39a/39b were oxidised at C14 using Riley conditions; the alcohol was then eliminated with the Burgess reagent and the resulting 14,15-double bond was reacted with magnesium monoperoxypythalate (MMPP) to selectively give 14 α ,15-epoxides 40a/40b. Oxidation with pyridinium chlorochromate (PCC) and 4-chloropyridinium chloride gave α -chloro enones 41a/41b, which underwent 14,15-cleavage by treatment with KOH.¹⁶ Mechanistic insights into this two-step transformation can be found in our recent report on the synthesis of asperflokal A (54).¹⁸ Acid 41a was then reduced to the C15-alcohol by first forming the corresponding thioester with ethanethiol and subsequent treatment with triethylsilane under Pd(0)-catalysis.²³ Reduction of the C6-oxo moiety and unmasking of the i-steroid using AcOH/BF₃·OEt₂ gave alcohol 42. Conversion of the primary hydroxyl at C15 to the corresponding iodide and subsequent treatment with Et₃B, nBu₃SnH and oxygen²⁴ provided the intended cyclisation product 43 as a single diastereomer. With the core structure in place, epoxidation of the 5,6-double bond, allylic oxidation at C7 followed by reduction to



Scheme 5 Initially proposed biosynthetic pathway towards strophasterols A–F (27, 32–36) and penicillitone (28) based on the 14,15-cleavage of co-isolated alcohol 29.





Scheme 6 Semisyntheses of strophasterol A (27) and penicillitone (28) by Heretsch and co-workers. $\text{TBD} = 1,5,7\text{-triazabicyclo}(4.4.0)\text{dec-5-ene}$.

the alcohol and, finally, deprotection of the acetate at C3 concluded the first synthesis of strophasterol A (27) in 18 steps from ergosterol (38). Against initial assumptions, the allylic oxidation at C7 did not take place in the bisallylic system 43, but was only successful after epoxidation of the 5,6-double bond.

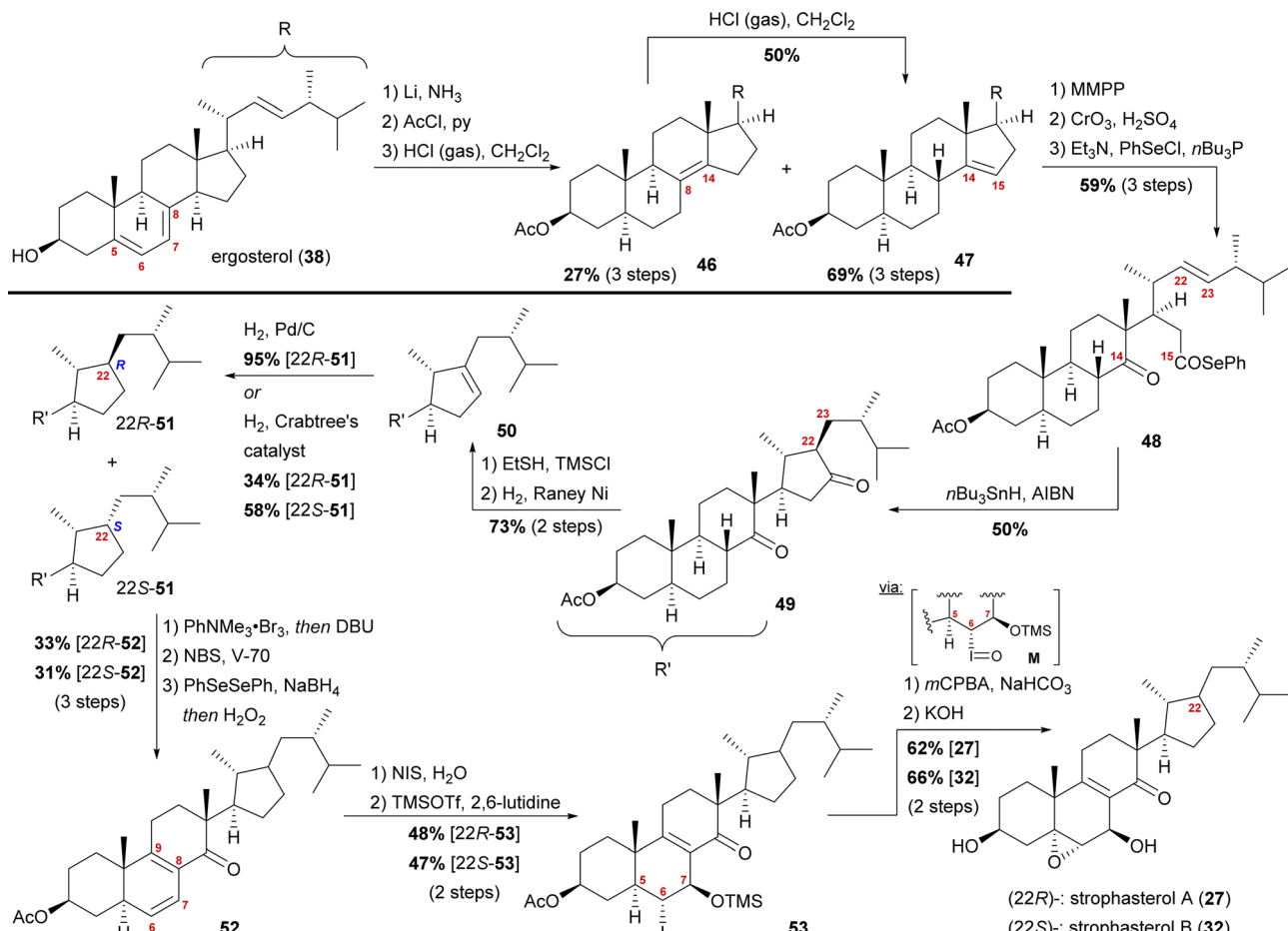
Going back to alcohol 42, epoxidation of the 5,6-double bond using MMPP followed by oxidation of the C15 hydroxyl with DMP gave an aldehyde, which, under basic conditions (1,5,7-triazabicyclo(4.4.0)dec-5-ene, TBD), reacted *via* an intramolecular vinylogous aldol reaction with C11 to yield the penicillitone framework 45. When screening different bases, it turned out that only TBD was capable of facilitating the aldol reaction, presumably due to its ability to coordinate in the transition state.²⁵ The synthesis of penicillitone (28) was then completed by acetate protection of so-generated C15 hydroxy steroid 45, oxidation at C7, and, finally global deprotection.¹⁷

The group of Kuwahara later published a second semisynthetic approach towards strophasterol A (27) as well as strophasterol B (32) (Scheme 7).²⁶ Following their initial studies,

optimisation of their cyclisation step allowed them to synthesise strophasterols A–F (27, 32–36) in 2017–2020.^{26–28} Additionally, their work provided proof for the identity of glaucoposterol A and strophasterol F (36).²⁸

Starting with ergosterol (38), the first goal was the cleavage of the C14–C15-bond. Therefore, the reduction of the 5,6-double bond under Birch conditions, protection of the C3 hydroxyl as an acetate, and isomerisation of the 7,8-double bond were performed. The latter reaction yielded both the 8,14-double bond isomer 46 as the minor product and the 14,15-double bond isomer 47 as the major product, with 46 being convertible into 47 under the same conditions. The 14,15-double bond was then cleaved by epoxidation and oxidative cleavage with CrO_3 and H_2SO_4 giving the corresponding carboxylic acid, which was then reacted with PhSeCl to give selenoester 48. Using Boger's acyl radical formation method,²⁹ selenoester 48 was treated with $n\text{Bu}_3\text{SnH}$ and AIBN to give cyclopentanone 49. Formation of thienoel ether using ethanethiol and TMSCl and subsequent desulphurisation with RANEY® nickel selectively gave cyclopentene 50, which was then hydrogenated to give selectively





Scheme 7 Semisyntheses of strophasterol A (27) and B (32) by Kuwahara and co-workers. V-70 = 2,2'-azobis(4-methoxy-2,4-dimethylvaleronitrile).

either 22*R*-cyclopentane **51** (Pd/C, H₂) or a 1.7:1 mixture of 22*R*-**51**:22*S*-**51**-cyclopentanes when using Crabtree's catalyst. Both 22*R*-**51** and 22*S*-**51** could then be transformed to strophasterol A (**27**) or B (**32**) using analogous conditions. Thus, α -bromination at C8 with concomitant *in situ* dehydrobromination was performed giving the 8,9-double bond isomer. Allylic bromination at C7 was accomplished using *N*-bromosuccinimide (NBS) and 2,2'-azobis(4-methoxy-2,4-dimethylvaleronitrile) (V-70).³⁰ Dehydrobromination turned out to be non-trivial, requiring first transformation of the bromide into a selenide and subsequently an oxidative elimination to give diene **52**. This procedure could be performed as a one-pot sequence. The 6,7-double bond was then regioselectively transformed in a halohydrin reaction to furnish the 6 α -iodo-7 β -hydroxy moiety, which was TMS-protected in the following step, giving iodide **53**. When treated with *m*-chloroperbenzoic acid (*m*CPBA), the 5 α ,6-epoxide was formed by first oxidation of the iodide to iodosyl **M**, elimination of the latter giving the 5,6-double bond, which, in turn, was epoxidised by *m*CPBA.³¹ Finally, global deprotection under basic conditions gave strophasterol A (**27**) or B (**32**), respectively, in a total of 17 steps each. The route of Kuwahara, thus, proves a similar radical cyclisation to be competent to forge the desired cyclopentyl motif. Towards this goal, a 14,15-secosteroid is traversed, potentially allowing access to penillitone, and, thus pointing at a biogenetic relation.

Asperfloketal A

The asperfloketals A (**54**) and B (**55**) are two anthrasteroids isolated in 2020 by Han, Xu, Lin and co-workers from *Aspergillus flocculosus* 16D-1, a fungus isolated from the marine sponge *Phakellia fusca*.³² These two regioisomeric natural products only differ in the position of the hydroxyl in the A ring, which prompted our interest in their biogenesis as well as in the biosynthetic formation of anthrasteroids itself (Fig. 3). Their complex rearranged skeletons include nine contiguous stereogenic centres (ten total), a ketal motif and a cleaved C14–C15-bond.

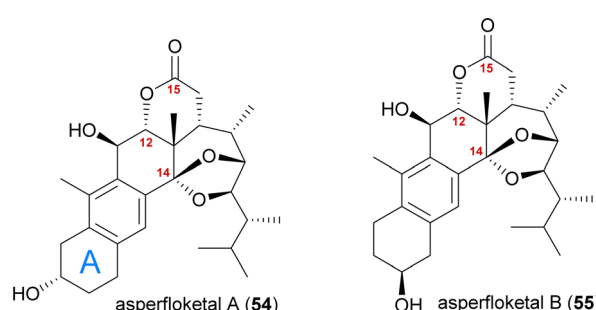


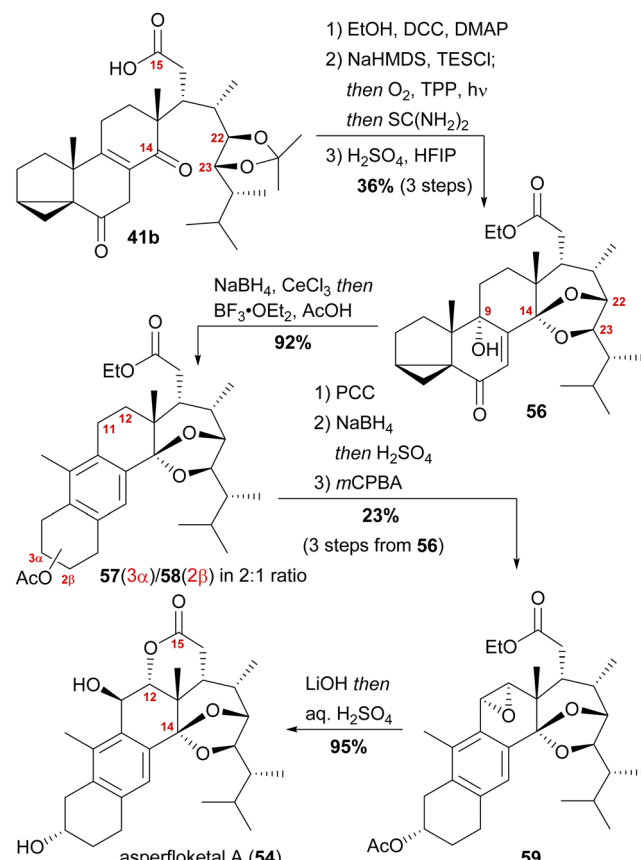
Fig. 3 The asperfloketals A (**54**) and B (**55**).



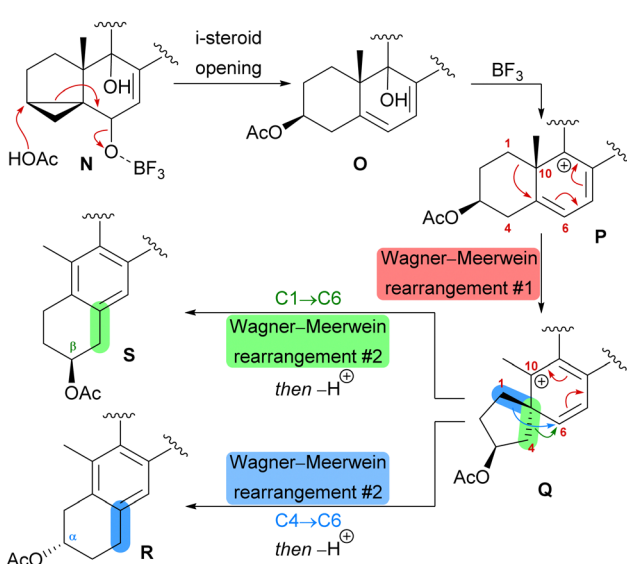
When looking at all anthrasteroids isolated from natural sources until 2020, it became evident that only structures with a 3α -OH-group in the A ring had been reported, and no examples of anthrasteroids with a 2β -OH-group existed, with asperfloketal B (antrasteroid numbering is different from steroid numbering, see Scheme 8) being the first reported.³³ The isolators proposed a dehydration event taking place, which would be followed by rehydration to transform asperfloketal A (54) into asperfloketal B (55).³²

The first synthetic anthrasteroids were obtained in 1954.³⁴ As a proposed mechanism for their formation from steroid starting materials, two consecutive Wagner–Meerwein rearrangements giving first a $1(10 \rightarrow 5)$ -abeo-framework Q and then the $1(10 \rightarrow 5)$, $1(5 \rightarrow 6)$ -diabeo-steroid R (Scheme 8, blue pathway) were discussed.³⁵ Historically, rather harsh conditions were used for this rearrangement, often leading to low yields of the 3α -product (R), elimination of the alcohol and no 2β -product (S).^{35,36} Our initial intuition for an attempted chemical emulation of the anthrasteroid rearrangement required a substrate possessing a hydroxy group at C9 (as in O) to allow for milder conditions in the rearrangement. To account for the formation of both regioisomeric asperfloketals, we furthermore speculated that the C4–C5-bond in Q could migrate instead of the C1–C5-bond. Thus, in a mechanistic bifurcation event, both anthrasteroids could be formed from the same intermediate, which would also constitute a more straightforward biogenetic route. Further analysis of the asperfloketal framework revealed the C14–C15-bond to be cleaved oxidatively with the C14 oxo moiety forming the intramolecular ketal with a 22,23-diol in the process, while the carboxylic acid would connect to C12, and thus, yield the required lactone.

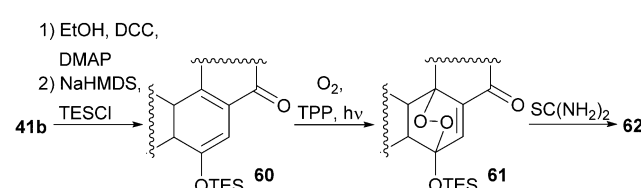
With our previously synthesised 14,15-seco steroid platform, an additional dihydroxylation/acetonide protection step in position 22,23 (Scheme 6, 39 \rightarrow 39b) was the starting point for the chemical emulation of the anthrasteroid rearrangement.¹⁸ Ketone 41b could, thus, be obtained in 10 steps. Then, the carboxylic acid



Scheme 9 Semisynthesis of asperfloketal A (54) by Heretsch and co-workers.



Scheme 8 Proposed biomimetic anthrasteroid rearrangement mechanism.

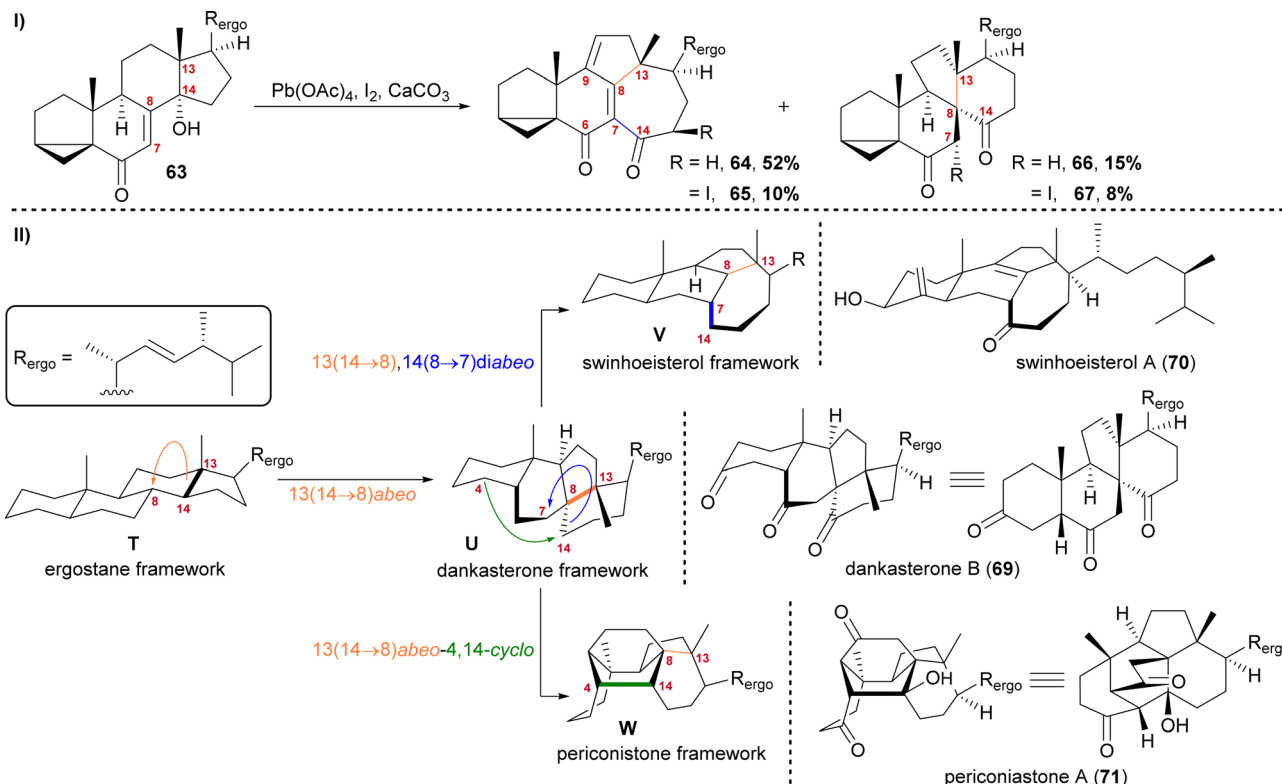


Scheme 10 Mechanistic details of 41b.

was masked as an ethyl ester, and the hydroxy moiety at C9 was introduced by formation of silyl enol ether 60, [4+2]-addition of oxygen to the so-obtained diene and cleavage of the endoperoxide 61 (Scheme 9 and Scheme 10).

Finally, intramolecular transketalisation was accomplished by using aq. H_2SO_4 in HFIP. Enone 56 was then reduced to the allylic alcohol and treated with $BF_3\cdot OEt_2$ in acetic acid to give the rearranged anthrasteroids 57/58, by first unmasking the 5,6-double bond (Scheme 8, N \rightarrow O) and then generating the carbocation at C9 (Scheme 8, P). To our delight, this reaction sequence gave two products in excellent yields, which after extensive 2D NMR analysis turned out to be the regioisomeric anthrasteroid rearrangement products in a 2:1 (57:58) ratio. From there, oxidation at the benzylic C11, reduction and elimination and, finally, epoxidation, selectively gave 11α , 12-epoxide 59. Global deprotection then yielded asperfloketal





Scheme 11 I: Alkoxy radical initiated framework rearrangement. II: Biogenetic space-guided analysis of dankasterone B (69), swinhoeisterol A (70) and periconiastone A (71).

A (54) in 18 steps from ergosterol (38). We assume the final cyclisation of the lactone to proceed by first opening of the epoxide through a benzylic $\text{S}_{\text{N}}2$ reaction with hydroxide to give the $11\beta,12\alpha$ -diol, followed by transesterification during acidic work-up. When using aq. HCl instead of aq. H_2SO_4 for the acidic work-up, we could also observe the formation of 11β -chloro asperfloketal A (not shown) as a side-product, supporting this mechanistic rationale.

Dankasterone A and B, periconiastone A and swinhoeisterol A

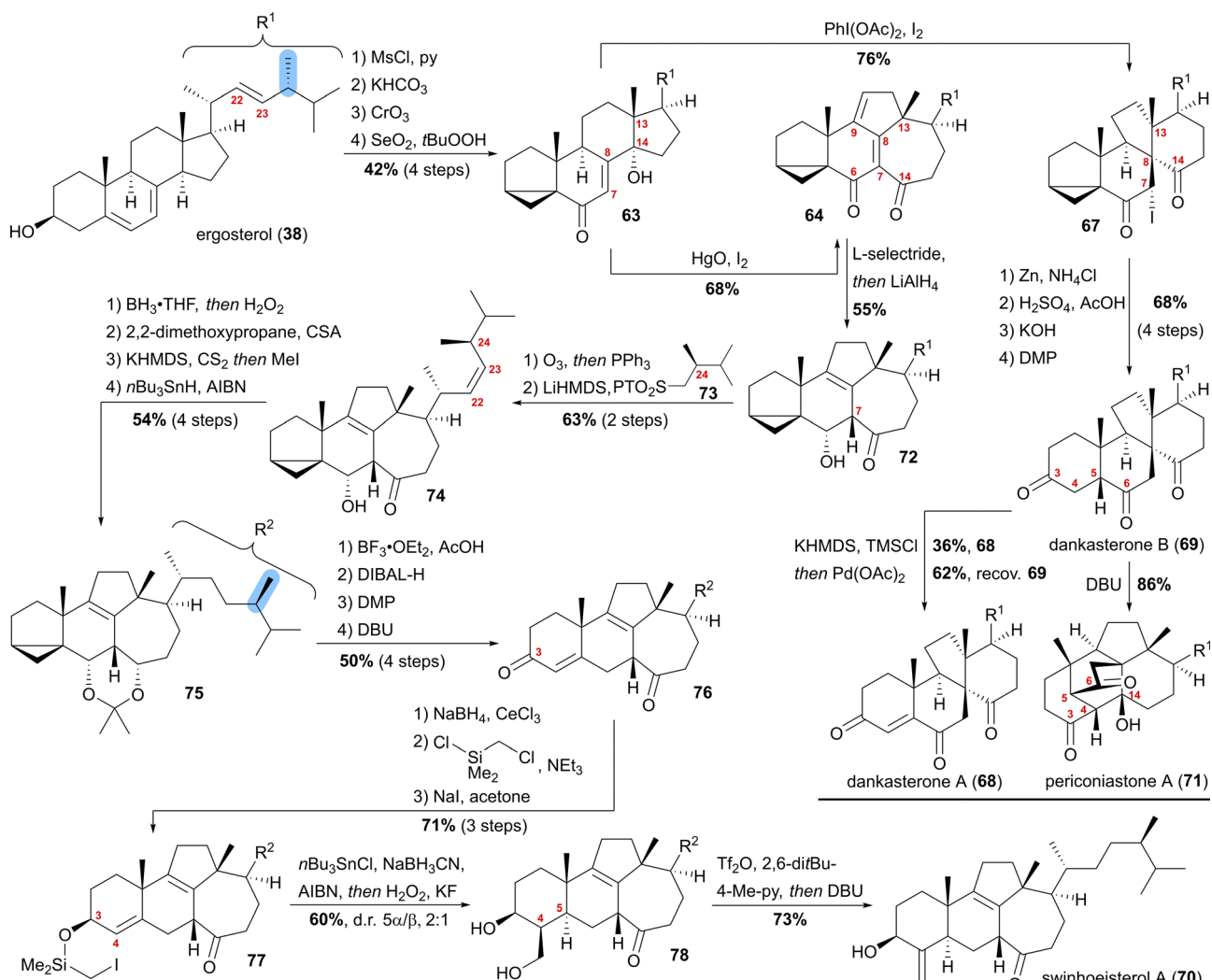
The first natural products of this group to be isolated were dankasterone A (68) in 1999 from the *Halichondria* sponge-derived fungus *Gymnascella dankaliensis* by Amagata, Minoura, Numata and co-workers,³⁷ followed by dankasterone B (69) in 2007 from the same fungus and by the same group.³⁸ Seven years later, Riccio, Bifulco, Gerwick, Zhang and co-workers were able to isolate swinhoeisterols A (70) and B (not shown) from the marine sponge *Theonella swinhonis*.³⁹ More recently, peroniastone A (71) was isolated in 2019 by Liu, Hu, Zhang and co-workers from the endophytic fungus *Periconia* sp. TJ403-rc01.⁴⁰

We first started investigating this group of natural products when looking for a radical 14,15-scission approach towards the synthesis of strophasterol A (27)¹⁶ using a hydroxy group at C14 63 to initiate the scission. When generating the corresponding alkoxy radical, a mixture of ketone 66/67 and dienone 64/65 was

formed (Scheme 11-I).^{41,42} While 66 and 67 possessed the $13(14 \rightarrow 8)$ abeo-framework U, as it can be found in dankasterone A (68) and B (69), 64 and 65 possessed the $13(14 \rightarrow 8), 14(8 \rightarrow 7)$ diabeo-framework V which corresponds to swinhoeisterol A (70) (Scheme 11-II). When investigating the mechanism of formation of both products, we realised the structural connection between the dankasterones and the swinhoeisterols, a suspicion further deepened by the geographical proximity of their respective places of isolation, *i.e.*, the Sea of Japan and the South China Sea, respectively.^{37–39} Thus, the rearrangement might proceed through the dankasterone framework U as an intermediate. As an integral part of the transformation of the dankasterone into the swinhoeisterol framework V, we assume a Dowd–Beckwith rearrangement.⁴³ The proposed radical mechanism can be found in our original report. While this project was already in progress, the structure of peroniastone A (71) was published. An intramolecular aldol reaction was proposed for the formation of the C4–C14-bond to give the $13(14 \rightarrow 8)$ abeo-4,14-cyclo framework W, directly from dankasterone B (69).

Our synthesis started from ergosterol (38), which, after i-steroid formation and allylic oxidation, gave previously reported alcohol 63 (Scheme 12). Upon subjecting this alcohol to (diacetoxiodo)benzene and iodine treatment, selective formation of α -iodide 67 possessing the dankasterone skeleton was observed in good yields. Deiodination with zinc, opening of the i-steroid with H_2SO_4 in acetic acid, followed by deprotection





Scheme 12 Semisyntheses of dankasterone A (68) and B (69), swinhoeisterol A (70) and periconiastone A (71) by Heretsch and co-workers.

of the partially acetate-protected mixture led, after oxidation of the 3-hydroxy moiety with DMP, to dankasterone B (69) in only 9 steps from ergosterol (38). To transform dankasterone B (69) into dankasterone A (68), Saegusa–Ito oxidation of the corresponding silyl enol ether was performed, giving a separable mixture of dankasterone A (68) and reisolated dankasterone B (69).

To put the biosynthesis hypothesis of periconiastone A (71) to a test, we then investigated the propensity of 69 to undergo an intramolecular aldol addition between C4 and C14. Thus, diazabicycloundecene (DBU) was employed as a base, which indeed gave periconiastone A (71) as a single diastereomer and in an excellent yield. When trying to selectively synthesise the swinhoeisterol framework from alcohol 63, instead of (diacetoxyiodo)benzene, mercuric oxide and iodine were employed to give dienone 64 with complete selectivity and good yields. To reduce undesired reactivity when introducing the required side chain with a (24*R*)-configured methyl group, first, the diene in 64 was reduced in a 1,6-fashion with L-selectride. Subsequently, and in the same pot, LiAlH₄ was used to reduce the C6

oxo-moiety to give 6 α -alcohol 72 with an 8,9-double bond. With compound 72 in hand, regioselective ozonolysis of the 22, 23-double bond was performed, followed by Z-selective Julia–Kocienski olefination with sulfone 73, which was prepared in six-steps from (*R*)-Roche ester.⁴⁴ To circumvent epimerisation at C24, a reactivity observed when hydrogenation of 74 was attempted with Pd or Pt and H₂, hydroboration/oxidation was performed to yield mostly the 23-hydroxy-isomer and no detectable epimerisation at C24, while concomitantly the oxo-moiety at C14 was reduced. Protection of the 6 α ,14 α -diol as an acetonide followed by Barton–McCombie deoxygenation of the 23-hydroxy moiety then gave acetonide 75. When treated with $\text{BF}_3 \cdot \text{OEt}_2$ in acetic acid, the acetonide was deprotected, while at the same time, opening of the i-steroid gave the C3 acetate and a 5,6-double bond. Non-basic deprotection of this acetate with DIBALH, global oxidation of the alcohols to the corresponding ketones, and finally, DBU mediated 5,6-double bond isomerisation gave enone 76. To introduce the missing exomethylene group at C4 and to generate the correct stereoconfiguration at C5, the enone was reduced under Luche conditions giving the



β -allylic alcohol, which was silylated using (chloromethyl)chlorodimethylsilane (product not shown). The Finkelstein reaction yielded iodide 77, which in the presence of AIBN, n Bu₃SnCl and NaBH₃CN underwent a Nishiyama–Stork radical cyclisation⁴⁵ to give a dimethyl oxasilolane. Subjecting the latter to Tamao's conditions⁴⁶ gave diol 78. Elimination of the primary alcohol by triflation, followed by the addition of DBU, then completed the first synthesis of swinhoeosterol A (70) in 21 steps from ergosterol (38).

These divergent syntheses of dankasterones A (68) and B (69), periconiastone A (71) and swinhoeosterol A (70) are valuable examples of a biosynthetic proposal to connect seemingly unrelated natural products and discovering and exploring novel reactivity.⁴¹ Only by careful analysis of the migration events needed to (formally) convert ergosterol into swinhoeosterol, the intermediacy of the dankasterone and periconiastone natural products was realised. The former served as a mechanistic bifurcation point and helped to emulate chemically the reaction cascade to arrive at the swinhoeosterol class of natural products. The effortlessness by which these rearrangements could be realised under radical conditions further points to a possible radical nature of these transformations during their biogenesis.

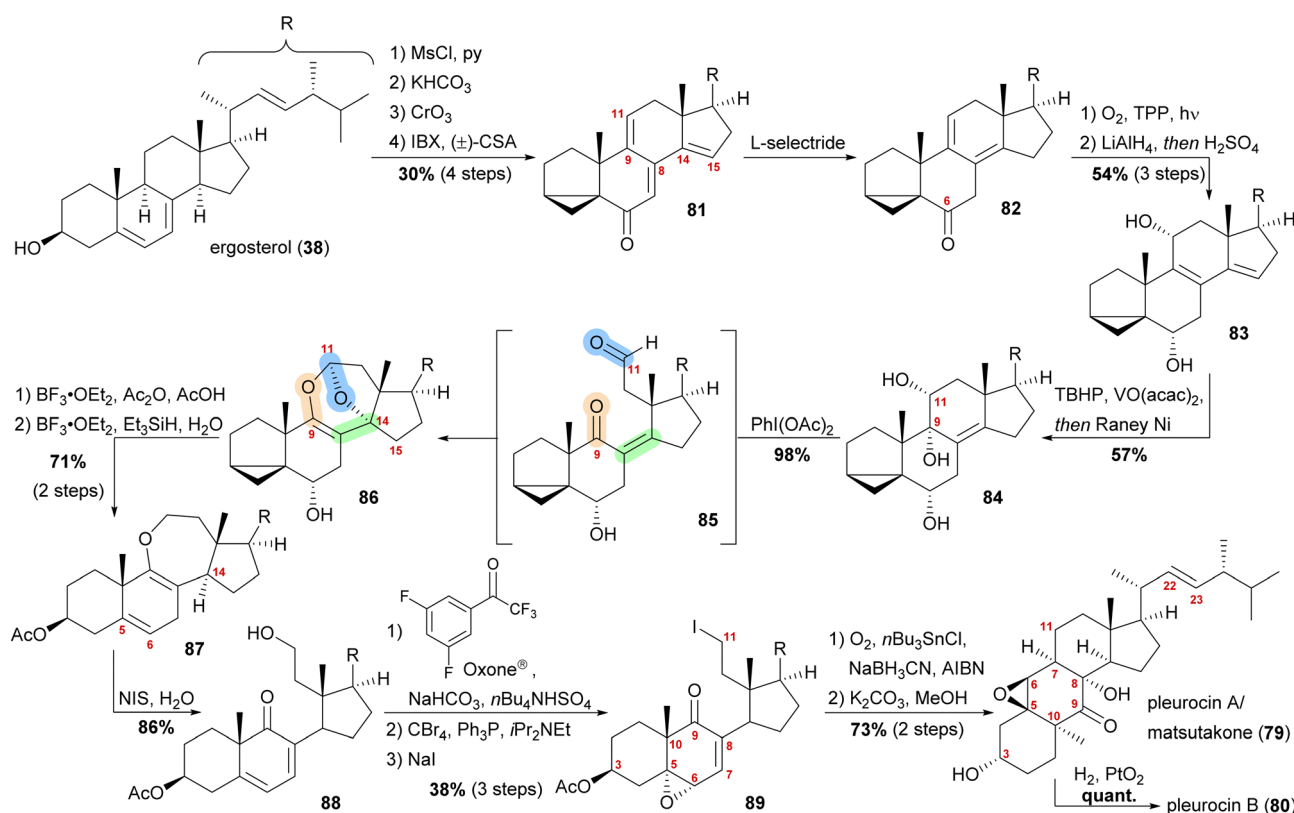
Pleurocin A/matsutakone and pleurocin B

Two representatives of the group of 11(9 \rightarrow 7)abeo steroids are the natural products pleurocin A/matsutakone (79) and

pleurocin B (80), with pleurocin B (80) being the 22, 23-dihydro-derivative of the former. The two names pleurocin A and matsutakone (79), respectively, can be traced back to the almost simultaneous isolation reports by the groups of Feng and Liu from *Tricholoma matsutake*⁴⁷ and by Tanaka and co-workers from *Pleurotus eryngii*⁴⁸ in 2017. Pleurocin B (80) was co-isolated together with pleurocin A (79) from *Pleurotus eryngii*.

While both groups independently put forward biosynthetic proposals of polar mechanisms for the C9–C11-bond cleavage and the C7–C11-bond formation reaction, a closer look at the structure and functional group distribution convinced us that a 6-*endo*-trig radical cyclisation, initiated by a C11 based radical in a molecule such as 89 (*vide infra*), followed by trapping of oxygen by a C8-centred radical could better explain the formation of the natural products from a similar biosynthetic precursor. To test this hypothesis, the synthesis of a 9, 11-secosteroid platform from ergosterol (38) was attempted first.⁴⁹

By forming the i-steroid 39a from ergosterol and treating the latter with 2-iodoxybenzoic acid (IBX) and camphorsulfonic acid (CSA), tetraene 81 was generated (Scheme 13).⁵⁰ While studying this reaction, it became clear that first, the 14, 15-double bond was introduced, followed by the 9,11-double bond, as no conditions were found to selectively generate the 9,11-double bond. Conjugate reduction with L-selectride gave 1,3-cyclohexadiene 82 which readily reacted *via* an [4+2]



Scheme 13 Semisyntheses of pleurocin A/matsutakone (79) and pleurocin B (80) by Heretsch and co-workers.

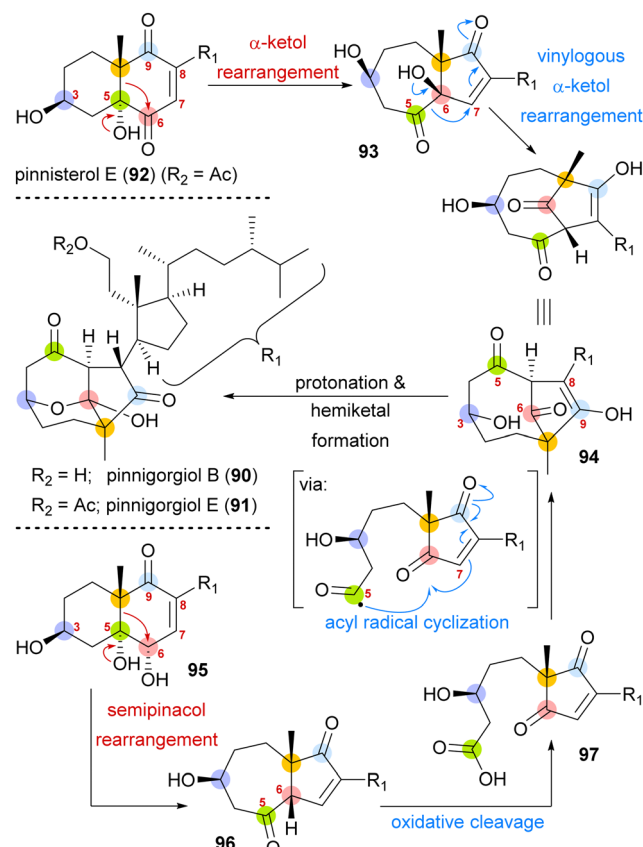


addition with singlet oxygen in the presence of TPP to provide the corresponding endoperoxide (not shown). Treatment of the latter with LiAlH₄ reductively cleaved the endoperoxide while also reducing the C6 oxo moiety, resulting in 11 α ,14 α -diol. Under strongly acidic work-up conditions, elimination of the C14 hydroxyl moiety could be observed, resulting in the formation of diene **83**. Regio- and diastereoselective epoxidation of the 8,9-double bond, followed by immediate vinylogous reductive opening by addition of RANEY® nickel, gave the desired 9 α ,11 α -diol **84**, leaving the 22,23-double bond unscathed in the process. The cleavage of the C9–C11-bond was then achieved by addition of (diacetoxyiodo)benzene, presumably giving aldehyde **85**, which then underwent an intramolecular dioxa-[4+2]-cycloaddition to form oxepane acetal **86**. Treatment of the latter with BF₃OEt₂ and acetic anhydride in acetic acid unmasked the i-steroid and also initiated β -elimination of H15, forming the 14,15-double bond while opening the tetrahydrofuran to the corresponding lactol acetate (not shown). Ionic reduction of C11 with Et₃SiH and BF₃OEt₂ as well as reduction of the extended enolate 14,15-double bond under the same conditions then provided enol ether **87**. Hydrolysis of the enol ether was achieved by subjecting the molecule to aqueous NIS, which presumably first gave a 9,10-iodonium ion, which was then hydrolysed to yield an α -iodo ketone. Elimination of this α -iodide introduced the 7,8-double bond in **88**. Regio- and stereoselective epoxidation of the 5,6-double bond was then achieved by *in situ* generated dioxirane from 2,2,2,3',5'-pentafluoroacetophenone.⁵¹ The C11 hydroxy moiety was converted stepwise into iodide **89** through the intermediacy of a bromide. The stepwise conversion was necessary as a direct conversion of the hydroxy moiety to the iodide **89** under Appel-type conditions led to the deoxygenation of the epoxide. To complete the synthesis, the required C11-centered radical was formed by using Nakamura's conditions (1.5 eq. of O₂, NaBH₃CN as a stoichiometric reductant and catalytic amounts of AIBN and *n*Bu₃SnCl).⁵² This oxidative radical cyclisation was followed by deacetylation to give pleurocin A/matsutakone (**79**) as a single diastereomer. Hydrogenation of the 22,23-double bond of the latter also provided pleurocin B (**80**) in quantitative yield.⁴⁹

Pinnigorgiols B and E

Pinnigorgiol B (**90**) and pinnigorgiol E (**91**), the 11-acetyl derivative of the former, were both isolated in 2016 by Sung and co-workers from a Taiwanese gorgonian coral *Pinnigorgia* species.⁵³ In addition, pinnisterol E (**92**) was isolated, which is assumed to be the biosynthetic precursor, and thus, became key to devising a synthetic access (*vide infra*).

Pinnigorgiol B (**90**) has a tricyclo[5.2.1.1]decane framework and a γ -diketone moiety structurally resembling related aplysiasecosterol A (not shown) which was isolated in 2015⁵⁴ and synthesised in 2018 by the group of Li.⁵⁵ Pinnigorgiol B is both a 9,11-seco and a 5(6 \rightarrow 7),6(5 \rightarrow 10)diabeo steroid. We chose to highlight the approach by Gui and co-workers, as it is an impressive example of a semisynthesis taking into consideration the (hypothetical) biogenesis.⁵⁶

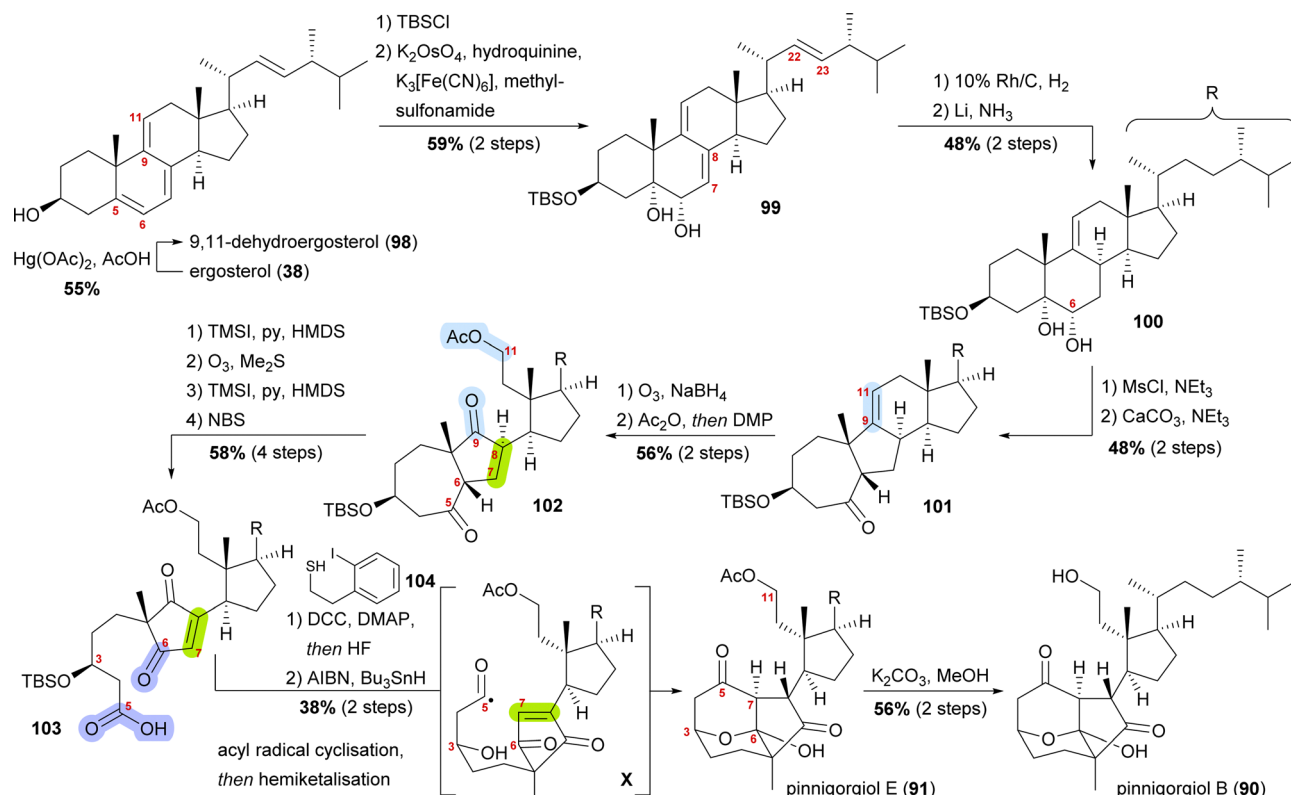


Scheme 14 Proposed biosynthetic pathway towards pinnigorgiol B (**90**) and E (**91**) from pinnisterol E (**92**) and reactivity-based synthesis plan by Gui and co-workers.

A biosynthetic proposal by Kigoshi and Kita envisioned an α -ketol rearrangement taking place in co-isolated pinnisterol E (**92**) to yield α -hydroxy ketone **93**, which then could react in a second, this time vinylogous α -ketol rearrangement, to yield the key diketone **94** (Scheme 14). As diketone **94** should be transformed into the natural product under acidic catalysis, Gui defined **94** as a key intermediate to their approach. When analysing α -hydroxy ketone **93**, they found reports of structurally similar systems undergoing an undesired, facile C10 migration from C6 to C5. To circumvent this problem, they opted to develop a stepwise approach: starting with *syn*-diol **95** and accessing diketone **96** in a semipinacol rearrangement.⁵⁷ Subsequent oxidative cleavage of the C5–C6-bond should give acid **97**, which then could be transformed to the same key diketone **94** through an acyl radical cyclisation.

Starting from ergosterol (**38**), Treibs conditions were used to introduce a 9,11-double bond (**98**, Scheme 15).⁵⁸ Next, the C3 hydroxyl was protected as a TBS ether and the 5,6-double bond was regio- and diastereoselectively dihydroxylated to furnish diol **99**. Hydrogenation over rhodium on carbon selectively reduced the 22,23-double bond, while Birch reduction could then be employed to selectively reduce the 7,8-double bond to obtain **100**, leaving only the 9,11-double bond unchanged. Extensive studies were performed to arrive at this desired outcome. Mesylation of the C6 hydroxyl allowed for subsequent





Scheme 15 Semisyntheses of pinnigorgiol B (87) and E (88) by Gui and co-workers.

semipinacol rearrangement and gave ketone 101.⁵⁹ Ozonolysis of the 9,11-double bond followed by reductive work-up gave the corresponding diol, which was then selectively acetylated at C11 and then oxidised at C9 to provide diketone 102. Regioselective formation of silyl enol ether⁶⁰ from the C5 oxo moiety, followed by ozonolysis of the enol ether subsequently gave acid. The 7,8-double bond was then introduced by the regioselective formation of silyl enol ether from the C6 oxo moiety and subsequent reaction with *N*-bromosuccinimide. Acid 103 was transformed into the corresponding thioester with thiol 104, and the TBS ether was removed. Treatment with AIBN and Bu_3SnH generated the desired acyl radical X,⁶¹ which, in an 8-*exo*-trig cyclisation followed by direct hemiketalisation, gave pinnigorgiol E (91). Hydrolysis of acetate then gave pinnigorgiol B (90), completing a 16-step synthesis from ergosterol (38).

Conclusions

In this review, we outlined the advantages of rigorously following biogenetic space-guided analysis to access complex terpenoid natural products in a semisynthetic fashion. Thus, by evaluating the structural space of co-isolated and related natural products, insights into the biosynthetic transformations and their order can be gained. With a general scheme for the possible biogenesis of the natural product in question, a chemical synthesis can then be planned and reduced to practice, thus elucidating innate reactivity, generating hypothesised intermediates and accessing anticipated natural products. This

approach has, in our and other hands, helped to streamline synthetic routes, allowed access to additional related natural products *en route* and most importantly, provided chemical support for the biogenetic hypotheses. During the case studies presented in this review, we have encountered on several occasions that polar reactions were not sufficient in accessing the desired natural products and their intermediates, but rather an intricate interplay of radical and polar reactivity was necessary to successfully reduce a synthetic plan to practice. Especially the further development of radical and radical-polar crossover logic is a current pursuit of our group.

Author contributions

Mykhaylo Alekseychuk wrote the original draft. Philipp Heretsch supervised the writing process and edited the manuscript.

Conflicts of interest

The authors declare no competing financial interest.

Acknowledgements

Financial support for this work was provided by the European Research Council (ERC Consolidator Grant “RadCrossSyn”), Deutsche Forschungsgemeinschaft (Heisenberg-Program HE 7133/8-1) and Boehringer Ingelheim Stiftung (plus3 perspectives



program). We would like to thank our former and current group members who worked on the projects highlighted here (Sinan C. A. Adrian, Maximilian G. Bauer, Dr Fenja L. Duecker and Dr Robert C. Heinze). Finally, we would like to thank an unknown reviewer for his/her valuable comments.

Notes and references

- 1 (a) T. Gaich and P. S. Baran, *J. Org. Chem.*, 2010, **75**, 4657–4673; (b) P. S. Baran, *J. Am. Chem. Soc.*, 2018, **140**, 4751–4755; (c) F. Reuß and P. Heretsch, *Angew. Chem., Int. Ed.*, 2020, **59**, 10232–10234.
- 2 For recent examples, see: (a) Y. Wang, W. Ju, H. Tian, W. Tian and J. Gui, *J. Am. Chem. Soc.*, 2018, **140**, 9413–9416; (b) G. Xu, M. Elkin, D. J. Tantillo, T. R. Newhouse and T. J. Maimone, *Angew. Chem., Int. Ed.*, 2017, **56**, 12498–12502; (c) M. Schmid and D. Trauner, *Angew. Chem., Int. Ed.*, 2017, **56**, 12332–12335; (d) R. Liffert, A. Linden and K. Gademann, *J. Am. Chem. Soc.*, 2017, **139**, 16096–16099; (e) F. Bartels, Y. J. Hong, D. Ueda, M. Weber, T. Sato, D. J. Tantillo and M. Christmann, *Chem. Sci.*, 2017, **8**, 8285–8290; (f) A. Y. Hong and B. M. Stoltz, *Angew. Chem., Int. Ed.*, 2014, **53**, 5248–5260; (g) A. Giannis, P. Heretsch, V. Sarli and A. Stössel, *Angew. Chem., Int. Ed.*, 2009, **48**, 7911–7914 For reviews, see: (h) P. D. Brown and A. L. Lawrence, *Nat. Prod. Rep.*, 2017, **34**, 1193–1202; (i) M. Baunach, J. Franke and C. Hertweck, *Angew. Chem., Int. Ed.*, 2015, **54**, 2604–2626; (j) M. Razzak and J. K. de Brabander, *Nat. Chem. Biol.*, 2011, **7**, 865–875; (k) M. C. de La Torre and M. A. Sierra, *Angew. Chem., Int. Ed.*, 2004, **43**, 160–181.
- 3 Q.-Q. Zhao, Q.-Y. Song, K. Jiang, G.-D. Li, W.-J. Wei, Y. Li and K. Gao, *Org. Lett.*, 2015, **17**, 2760–2763.
- 4 X.-T. Liang, J.-H. Chen and Z. Yang, *J. Am. Chem. Soc.*, 2020, **142**, 8116–8121.
- 5 J. Meinwald, S. S. Labana and M. S. Chadha, *J. Am. Chem. Soc.*, 1963, **85**, 582–585.
- 6 W. Wu, X. Chen, Y. Liu, Y. Wang, T. Tian, X. Zhao, J. Li and H. Ruan, *Phytochemistry*, 2016, **130**, 301–312.
- 7 X.-W. Yang, S.-M. Li, L. Wu, Y.-L. Li, L. Feng, Y.-H. Shen, J.-M. Tian, J. Tang, N. Wang, Y. Liu and W.-D. Zhang, *Org. Biomol. Chem.*, 2010, **8**, 2609–2616.
- 8 Y.-L. Li, Y.-X. Gao, X.-W. Yang, H.-Z. Jin, J. Ye, L. Simmons, N. Wang, A. Steinmetz and W.-D. Zhang, *Phytochemistry*, 2012, **81**, 159–164.
- 9 (a) L. M. M. Vieira, A. Kijjoa, R. Wilairat, M. S. J. Nascimento, L. Gales, A. M. Damas, A. M. S. Silva, I.-O. Mondranondra and W. Herz, *J. Nat. Prod.*, 2004, **67**, 2043–2047; (b) L. M. M. Vieira, A. Kijjoa, R. Wilairat, M. S. J. Nascimento, L. Gales, A. M. Damas, A. M. S. Silva, I.-O. Mondranondra and W. Herz, *J. Nat. Prod.*, 2005, **68**, 969–970.
- 10 M. Alekseychuk, S. Adrian, R. C. Heinze and P. Heretsch, *J. Am. Chem. Soc.*, 2022, **144**, 11574–11579.
- 11 (a) X. Chen, X. Shao, W. Li, X. Zhang and B. Yu, *Angew. Chem., Int. Ed.*, 2017, **56**, 7648–7652; (b) R. U. Lemieux and E. von Rudloff, *Can. J. Chem.*, 1955, **33**, 1701–1709.
- 12 X. Sun, J. Chen and T. Ritter, *Nat. Chem.*, 2018, **10**, 1229–1233.
- 13 E. A. Wappes, S. C. Fosu, T. C. Chopko and D. A. Nagib, *Angew. Chem., Int. Ed.*, 2016, **55**, 9974–9978.
- 14 M. S. Chen and M. C. White, *Science*, 2007, **318**, 783–787.
- 15 (a) D. Yang, M.-K. Wong, X.-C. Wang and Y.-C. Tang, *J. Am. Chem. Soc.*, 1998, **120**, 6611–6612; (b) X. Long, J. Li, F. Gao, H. Wu and J. Deng, *J. Am. Chem. Soc.*, 2022, **144**, 16292–16297.
- 16 R. C. Heinze, D. Lentz and P. Heretsch, *Angew. Chem., Int. Ed.*, 2016, **55**, 11656–11659.
- 17 M. Bauer and P. Heretsch, *Synthesis*, 2023, **55**, 1322–1327.
- 18 M. Alekseychuk and P. Heretsch, *J. Am. Chem. Soc.*, 2022, **144**, 21867–21871.
- 19 J. Wu, S. Tokuyama, K. Nagai, N. Yasuda, K. Noguchi, T. Matsumoto, H. Hirai and H. Kawagishi, *Angew. Chem., Int. Ed.*, 2012, **51**, 10820–10822.
- 20 T. Kikuchi, M. Isobe, S. Uno, Y. In, J. Zhang and T. Yamada, *Bioorg. Chem.*, 2019, **89**, 103011.
- 21 J. Xue, P. Wu, L. Xu and X. Wei, *Org. Lett.*, 2014, **16**, 1518–1521.
- 22 T. C. Morris and P. A. Patil, *J. Org. Chem.*, 1993, **58**, 2338–2339.
- 23 T. Fukuyama, S. C. Lin and L. Li, *J. Am. Chem. Soc.*, 1990, **112**, 7050–7051.
- 24 K. Nozaki, K. Oshima and K. Uchimoto, *J. Am. Chem. Soc.*, 1987, **109**, 2547–2549.
- 25 (a) C. Ghobril, C. Sabot, C. Mioskowski and R. Baati, *Eur. J. Org. Chem.*, 2008, 4104–4108; (b) P. Hammar, C. Ghobril, C. Antheaume, A. Wagner, R. Baati and F. Himo, *J. Org. Chem.*, 2010, **75**, 4728–4736.
- 26 S. Sato, Y. Fukuda, Y. Ogura, E. Kwon and S. Kuwahara, *Angew. Chem., Int. Ed.*, 2017, **56**, 10911–10914.
- 27 S. Sato and S. Kuwahara, *Org. Lett.*, 2020, **22**, 1311–1315.
- 28 S. Sato, Y. Taguchi and S. Kuwahara, *Tetrahedron*, 2020, **76**, 131129.
- 29 D. L. Boger and R. J. Mathvink, *J. Org. Chem.*, 1992, **57**, 1429–1443.
- 30 T. G. Back and N.-X. Hu, *Tetrahedron Lett.*, 1992, **33**, 5685–5688.
- 31 (a) J. Lee, J. Oh, S. Jin, J.-R. Choi, J. L. Atwood and J. K. Cha, *J. Org. Chem.*, 1994, **59**, 6955–6964; (b) T. L. Macdonald, N. Narasimhan and L. T. Burk, *J. Am. Chem. Soc.*, 1980, **102**, 7760–7765.
- 32 F.-R. Jiao, B.-B. Gu, H.-R. Zhu, Y. Zhang, K.-C. Liu, W. Zhang, H. Han, S.-H. Xu and H.-W. Lin, *J. Org. Chem.*, 2021, **86**, 10954–10961.
- 33 (a) H. Koshino, T. Yoshihara, S. Sakamura, T. Shimanuki, T. Sato and A. Tajimi, *Phytochemistry*, 1989, **28**, 771–772; (b) S. Kosemura, S. Uotsu and S. Yamamura, *Tetrahedron Lett.*, 1995, **36**, 7481–7482; (c) T. Nakada and S. Yamamura, *Tetrahedron*, 2000, **56**, 2595–2602; (d) X. Luo, F. Li, P. B. Shinde, J. Hong, C.-O. Lee, K. S. Im and J. H. Jung, *J. Nat. Prod.*, 2006, **69**, 1760–1768; (e) X.-H. Liu, F.-P. Miao, X.-R. Liang and N.-Y. Ji, *Nat. Prod. Res.*, 2014, **28**, 1182–1186; (f) D. Wakana, T. Itabashi, K.-I. Kawai, T. Yaguchi, K. Fukushima, Y. Goda and T. Hosoe, *J. Antibiot.*, 2014, **67**, 585–588.
- 34 W. R. Nes and E. Mosettig, *J. Am. Chem. Soc.*, 1954, **76**, 3182–3186.
- 35 W. R. Nes, J. A. Steele and E. Mosettig, *J. Am. Chem. Soc.*, 1958, **80**, 5230–5232.
- 36 (a) W. R. Nes, *J. Am. Chem. Soc.*, 1956, **78**, 193–198; (b) W. R. Nes, R. B. Kostic and E. Mosettig, *J. Am. Chem. Soc.*, 1956, **78**, 436–440; (c) O. Tanaka and E. Mosettig, *J. Am. Chem. Soc.*, 1963, **85**, 1131–1133; (d) K. Tsuda, R. Hayatsu, J. A. Steele, O. Tanaka and E. Mosettig, *J. Am. Chem. Soc.*, 1963, **85**, 1126–1131.
- 37 T. Amagata, M. Doi, M. Tohgo, K. Minoura and A. Numata, *Chem. Commun.*, 1999, 1321–1322.
- 38 T. Amagata, M. Tanaka, T. Yamada, M. Doi, K. Minoura, H. Ohishi, T. Yamori and A. Numata, *J. Nat. Prod.*, 2007, **70**, 1731–1740.
- 39 J. Gong, P. Sun, N. Jiang, R. Riccio, G. Lauro, G. Bifulco, T.-J. Li, W. H. Gerwick and W. Zhang, *Org. Lett.*, 2014, **16**, 2224–2227.
- 40 W. Gao, C. Chai, Y. He, F. Li, X. Hao, F. Cao, L. Gu, J. Liu, Z. Hu and Y. Zhang, *Org. Lett.*, 2019, **21**, 8469–8472.
- 41 F. L. Duecker, R. C. Heinze and P. Heretsch, *J. Am. Chem. Soc.*, 2020, **142**, 104–108.
- 42 F. L. Duecker, R. C. Heinze, S. Steinhauer and P. Heretsch, *Chemistry*, 2020, **26**, 9971–9981.
- 43 (a) P. Dowd and W. Zhang, *Chem. Rev.*, 1993, **93**, 2091–2115; (b) A. L. J. Beckwith, D. M. O’Shea and S. W. Westwood, *J. Am. Chem. Soc.*, 1988, **110**, 2565–2575; (c) A. L. J. Beckwith, D. M. O’Shea, S. Gerba and S. W. Westwood, *Chem. Commun.*, 1987, 666–667; (d) P. Dowd and S. C. Choi, *J. Am. Chem. Soc.*, 1987, **109**, 6548–6549.
- 44 V. S. Yakimchuk, V. V. Kazlova, A. L. Hurski, R. G. Savchenko, S. A. Kostyleva, V. N. Zhabinskii and V. A. Khripach, *Steroids*, 2019, **148**, 82–90.
- 45 (a) G. Stork and M. Kahn, *J. Am. Chem. Soc.*, 1985, **107**, 500–501; (b) H. Nishiyama, T. Kitajima, M. Matsumoto and K. Itoh, *J. Org. Chem.*, 1984, **49**, 2298–2300.
- 46 K. Tamao, N. Ishida and M. Kumada, *J. Org. Chem.*, 1983, **48**, 2120–2122.
- 47 Z.-Z. Zhao, H.-P. Chen, B. Wu, L. Zhang, Z.-H. Li, T. Feng and J.-K. Liu, *J. Org. Chem.*, 2017, **82**, 7974–7979.
- 48 T. Kikuchi, Y. Horii, Y. Maekawa, Y. Masumoto, Y. In, K. Tomoo, H. Sato, A. Yamano, T. Yamada and R. Tanaka, *J. Org. Chem.*, 2017, **82**, 10611–10616.
- 49 R. C. Heinze and P. Heretsch, *J. Am. Chem. Soc.*, 2019, **141**, 1222–1226.
- 50 K. C. Nicolaou, Y.-L. Zhong and P. S. Baran, *J. Am. Chem. Soc.*, 2000, **122**, 7596–7597.
- 51 W. Li and P. L. Fuchs, *Org. Lett.*, 2003, **5**, 2853–2856.
- 52 M. Sawamura, Y. Kawaguchi and E. Nakamura, *Synlett*, 1997, 801–802.
- 53 Y.-C. Chang, L.-M. Kuo, J.-H. Su, T.-L. Hwang, Y.-H. Kuo, C.-S. Lin, Y.-C. Wu, J.-H. Sheu and P.-J. Sung, *Tetrahedron*, 2016, **72**, 999–1004.



Lebenslauf

Mykhaylo Alekseychuk

Master of Science (M.Sc.)

Geboren am 21.11.1997 in Lwiw (Ukraine)

Deutsche Staatsangehörigkeit

Ausbildung

	Promotionsstudium
Juni 2021 – August 2023	Institut für Organische Chemie der Leibniz Universität Hannover Arbeitsgruppe Prof. Dr. Philipp Heretsch
Okt. 2020 – Mai 2021	Promotionsstudium Institut für Chemie und Biochemie der Freien Universität Berlin Arbeitsgruppe Prof. Dr. Philipp Heretsch
März 2019 – Sep. 2020	Masterstudium – M. Sc. Chemie Institut für Chemie und Biochemie der Freien Universität Berlin
Okt. 2015 – Feb. 2019	Bachelorstudium – B. Sc. Chemie Institut für Chemie und Biochemie der Freien Universität Berlin
Sep. 2009 – Juni 2015	Allgemeine Hochschulreife – Abitur Hermann-Ehlers-Gymnasium

Stipendien

Okt. 2020 – Dez. 2020	Dahlem Research School (DRS) Promotionsstipendium
-----------------------	---

Wissenschaftliche Präsentationen (außerhalb)

April 2023	Kurzvortrag 35. Irseer Naturstofftage, DECHEMA, Kloster Irsee, Deutschland
April 2023	Poster 35. Irseer Naturstofftage, DECHEMA, Kloster Irsee, Deutschland.

Veröffentlichte Publikationen

3. „Biogenetic space-guided synthesis of rearranged terpenoids.“

M. Alekseychuk, P. Heretsch, *Chem. Commun.*, **2023**, 59, 6811–6826.

2. „Chemical Emulation of the Biosynthetic Route to Anthrasteroids: Synthesis of Asperfloketal A.“

M. Alekseychuk, P. Heretsch, *J. Am. Chem. Soc.* **2022**, 144, 21867–21871.

1. „Biogenesis-Inspired, Divergent Synthesis of Spirochensilide A, Spirochensilide B, and Abifarane B Employing a Radical-Polar Crossover Rearrangement Strategy.“

M. Alekseychuk, S. Adrian, R. C. Heinze, P. Heretsch, *J. Am. Chem. Soc.* **2022**, 144, 11574–11579.